

NAT'L INST OF STAND & TECH R.I.C.



A11104 062606

NATIONAL BUREAU OF STANDARDS &
TECHNOLOGY
Research Information Center
Gaithersburg, MD 20899 /

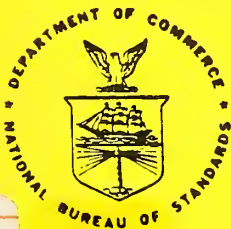
NBSIR 88-3753

9th Joint Panel Meeting of the UJNR Panel on Fire Research and Safety

Nora H. Jason
Barbara A. Houston

U.S. DEPARTMENT OF COMMERCE
National Bureau of Standards
National Engineering Laboratory
Center for Fire Research
Gaithersburg, MD 20899

April 1988



Stimulating America's Progress
1913-1988

U.S. DEPARTMENT OF COMMERCE
NATIONAL BUREAU OF STANDARDS

OC
100
J56
8803753
1988
C.2

Research Information Center
National Bureau of Standards
Gaithersburg, Maryland 20899

NBSIR 88-3753

**9TH JOINT PANEL MEETING OF THE
UJNR PANEL ON FIRE RESEARCH AND
SAFETY**

NBSC

QC100

, US6

NO. 88-3753

1988

C. 2

Nora H. Jason
Barbara A. Houston

U.S. DEPARTMENT OF COMMERCE
National Bureau of Standards
National Engineering Laboratory
Center for Fire Research
Gaithersburg, MD 20899

April 1988

U.S. DEPARTMENT OF COMMERCE, C. William Verity, *Secretary*
NATIONAL BUREAU OF STANDARDS, Ernest Ambler, *Director*

NINTH JOINT PANEL MEETING
OF THE UJNR PANEL ON
FIRE RESEARCH AND SAFETY

Joint with Combustion Toxicity and 6th Expert Meeting of the
U.S.-Japan-Canada Cooperative Research Group on Toxicity of Combustion
Products from Building Materials and Interior Goods

May 4-8, 1987
Factory Mutual Research Corporation
Norwood, Massachusetts

TABLE OF CONTENTS

	<u>Page</u>
Agenda.....	vii
List of Members (Japan).....	xiv
List of Members (U.S.).....	xvi
List of Combustion Toxicity Participants.....	xviii
Group Photograph.....	xix
 OPENING SESSION.....	 1
 FIRE AND SMOKE PHYSICS.....	 3
Progress Reports:	
Fire and Smoke Physics in Japan.....	4
Fire and Smoke Physics in the U.S.....	8
Forced Smolder Propagation in a Horizontal Fuel Layer and the Transition to Flaming Combustion.....	13
Wood Ignition and Pyrolysis.....	24
Deterministic Properties of Turbulent Diffusion Flames from Low Q* Fires.....	41
Transient Combustion in a Turbulent Fire.....	50
Numerical Simulation of Early Stage of a Compartment Fire by Field Model.....	63
Critical Discussion on Fire Development.....	73
Radiation from Diffusion Flames-Smoke Point.....	83
Effect of Radiant Flux on Smoke Emission.....	100
The Distribution of Soot in Large Buoyant Diffusion Flames.....	111
Predicting Capability of a Multiroom Fire Model.....	113
 RISK, HAZARD, AND EVACUATION.....	 130
Progress Reports:	
Fire Risk Analysis Methods in the U.S.....	131
Risk, Hazard and Evacuation in Japan.....	136
Discussion.....	138
A Method of Fire Risk Analysis--Estimation of Life Risk in Buildings.....	139
Discussion.....	145
Response Surface Approximation of a Fire Risk Analysis Computer Code.....	146
Discussion.....	155
An Engineering Fire Protection Design Assessment System.....	157
Discussion.....	170
Basic Structure of the Evacuation Safety Design Method.....	172
Discussion.....	188
Fire Risk Evaluation Method for Multi-Occupancy Building.....	189
Discussion.....	201
An Evacuation Model for the Use in Fire Safety Designing of Buildings.....	203
Discussion.....	218
A Summary of the Assumptions and Limitations in Hazard I.....	219
Discussion.....	229

	<u>Page</u>
FIRE TOXICITY AND CHEMISTRY.....	231
Progress Reports:	
Fire and Toxicity Chemistry in Japan.....	232
Fire Toxicity and Chemistry Research in the U.S.....	235
Canadian Overview.....	238
Incapacitation of Mice Exposed to Gases in Full-Scale Fire Tests.....	240
Determination of the Kinetic Parameters and the Heat of Combustion of the Volatiles for Wood.....	257
Correlation for the Generation of Carbon Monoxide in Small- and Large-Scale Fires.....	267
RISK, HAZARD, AND EVACUATION (CONT.).....	279
EXITT - A Simulation Model of Occupant Decisions and Actions in Residential Fires.....	280
Discussion.....	292
Emotional Instability in Fire Smoke -- Experiment of Human Behavior in Smoked Filled Corridor.....	294
Discussion.....	304
Large Fires and Nuclear Winter.....	305
Discussion.....	311
OPEN TECHNICAL SESSION.....	313
FMRC Sprinkler Research.....	314
Discussion.....	324
Progress in Modeling Sprinkler Performance.....	325
Combustion Behaviour of Building Materials Using a Model Box with Air Supplied System.....	336
Fire Induced Flow in a Clean Room with Downward Vertical Laminar Flow.....	357
FIRE TOXICITY AND CHEMISTRY (CONT.).....	367
Toxicological Effects of Different Time Exposures to the Fire Gases: CO or HCN or to CO Combined with HCN or CO ₂	368
Discussion.....	384
Toxic Gas Test by the Several Pure and Mixture Gases.....	386
Discussion.....	396
Strategy of Fire Suppression by Using Fire Retardants.....	397
Discussion.....	404
Studies on the Toxicity of Smoke Containing Hydrogen Chloride.....	405
Discussion.....	416
Toxic Gases from Combustion of Wood Treated with Retardants.....	417
Discussion.....	427
Bench- and Full-Scale Toxicity Tests of FRP Furniture.....	428
Discussion.....	441
Evolution of Toxic Gases from Experimental Fires in an Existing Building.....	443
Discussion.....	454
Human Effects of Poisonous Gases Generated During Fire - Especially, Presence of HCN and CO.....	455

	<u>Page</u>
A Proposed Method for the Simultaneous Analysis of HCN and NO _x in Fire Gases.....	461
Discussion.....	469
Evaluation of Combustion Toxicity from Various Materials Using a New Testing Apparatus.....	470
Discussion.....	488
A Review of the Five-Year Cooperative Program on Smoke Toxicity.....	490
Panel Discussion.....	493
OPEN TECHNICAL SESSION (CONT.).....	495
Characterization of Flame Spread Over PMMA Using Holographic Interferometry Sample Orientation Effects.....	496
Discussion.....	508
A Numerical Study of Periodic Alternating Flow of Fires.....	509
CLOSING SESSION.....	519
Discussion.....	520
Resolutions	
Closing Addresses	
Author's Index.....	527

AGENDA
9th UJNR PANEL ON FIRE RESEARCH AND SAFETY
MAY 4-8, 1987
NORWOOD, MASSACHUSETTS

Saturday, May 2

Japanese arrive; no activities.

Sunday, May 3

Early P.M.: Planning Meeting (Delegation Chairmen)
 Selection of Session Chairmen
 Plans for 10th UJNR
3:00 Tour of Boston and Quincy Market

Monday, May 4

9:00 Opening Ceremonies
 Call to order by Dr. Jack E. Snell, U.S. Chairman
 Welcoming Remarks by Mr. John A. Love, President of Factory Mutual
 Engineering and Research
 Remarks and Introductions of U.S. Panel Members by Dr. Jack E.
 Snell
 Remarks and Introductions of Japanese Panel Members by Mr. Akira
 Takahashi

9:40 Election of Officers
 Approval of Proceedings of the 8th Panel Meeting
 Approval of Agenda for the 9th Panel Meeting
 Election of Session Chairmen
 Appointment of Resolution Committee
 Other Business

9:50 Group Photograph

FIRE AND SMOKE PHYSICS - (Chairman: John de Ris)

10:00 Y. Hasemi, Progress Report - Japan

10:15 E. Zukoski, Progress Report - U.S.

10:30 Refreshment Break

10:45 T.J. Ohlemiller, "Forced Smolder Propagation in a Horizontal Fuel
 Layer and the Transition to Flaming Combustion" (delivered by
 T. Kashiwagi)

11:30 A. Atreya and H. Emmons, "Wood Ignition and Pyrolysis"

12:15 Lunch

Chairman: Makoto Tsujimoto

1:30 Y. Hasemi and M. Nishihata, "Deterministic Properties of Turbulent Diffusion Flames from Low Q^* Fires"

2:15 H. Baum and R. Rehm, "Transient Combustion in a Turbulent Fire"

3:00 Refreshment Break

3:15 T. Yoshikawa, J. Mashige, T. Joh, and O. Sugawa, "Numerical Simulation of Early Stage of a Compartment Fire by Field Model"

4:00 T. Hirano, "Critical Discussion on Fire Development"

4:45 Adjourn

Tuesday, May 5

- 8:00 Depart for FMRC West Gloucester Facility
- 9:30 Tour FMRC West Gloucester Facility
- 11:30 Lunch
- 12:30 Return to FMRC Norwood

PARALLEL SESSIONS

A. FIRE AND SMOKE PHYSICS (cont.) - (Chairman: Patrick J. Pagni)

- 1:30 J. de Ris, "Radiation from Diffusion Flames-Smoke Point"
- 2:15 G. Mulholland, V. Henzel, and V. Babrauskas, "Effect of Radiant Flux on Smoke Emission"
- 3:00 Refreshment Break
- 3:15 E. Zukoski, "The Distribution of Soot in Large Buoyant Diffusion Flames"
- 4:00 K. Nakamura, "Predicting Capability of a Multiroom Fire Model"
- 4:45 Adjourn

Evening: Cocktails and Formal Dinner at FMRC

B. RISK, HAZARD, AND EVACUATION - (Chairman: Harold E. Nelson)

- 1:30 J. Hall, Progress Report - U.S.
- 1:45 T. Tanaka, Progress Report - Japan
- 2:00 M. Tsujimoto, "A Method of Fire Risk Analysis--Estimation of Life Risk in Buildings"
- 2:45 Refreshment Break
- 3:00 M. Brandyberry and G. Apostolakis, "Response Surface Approximation of a Fire Risk Analysis Computer Code"
- 3:45 H. Nelson, "An Engineering Fire Protection Design Assessment System"
- 4:30 Adjourn

Evening: Cocktails and Formal Dinner at FMRC

Wednesday, May 6

PARALLEL SESSIONS

B. RISK, HAZARD, AND EVACUATION (cont.) - (Chairman: James G. Quintiere)

9:00 T. Tanaka, "Basic Structure of the Evacuation Safety Design Method"

9:45 A. Sekizawa and T. Jin, "Fire Risk Evaluation Method for Multi-Occupancy Buildings"

10:30 Refreshment Break

10:45 K. Takahashi and T. Tanaka, "An Evacuation Model for the Use in Fire Safety Designing of Buildings"

11:30 R. Bukowski, "A Summary of the Assumptions and Limitations in HAZARD 1"

12:15 Lunch

1:30 Tour of FMRC Laboratories

Evening: Light Supper
Fenway Park: Major League Baseball
Boston Red Sox vs. Oakland Athletics

A. FIRE TOXICITY AND CHEMISTRY - (Chairman: Toshisuke Hirano)

9:00 H. Suzuki, Progress Report - Japan

9:15 R. Gann, Progress Report - U.S.

9:30 T. Harmathy, Progress Report - Canada

9:45 T. Tanaka and M. Yoshida, "Incapacitation of Mice Exposed to Gases in Full-Scale Fire Tests"

10:30 Refreshment Break

10:45 W. Parker, "Determination of the Kinetic Parameters and the Heat of Combustion of the Volatiles for Wood"

11:30 A. Tewarson, "Correlation for the Generation of Carbon Monoxide in Small- and Large-Scale Fires"

12:15 Lunch

1:30 Tour of FMRC Laboratories

Evening: Light Supper
Fenway Park: Major League Baseball
Boston Red Sox vs. Oakland Athletics

Thursday, May 7

PARALLEL SESSIONS

- B. RISK, HAZARD, AND EVACUATION (cont.) - (Chairman: John R. Hall, Jr.)
- 9:00 B. M. Levin, "EXITT - A Simulation Model of Occupant Decisions and Actions in Residential Fires"
- 9:45 T. Jin and T. Yamada, "Emotional Instability in Fire Smoke-- Experiment of Human Behavior in Smoke Filled Corridor"
- 10:30 Refreshment Break
- 10:45 G. Carrier, "Large Fires and Nuclear Winter"
- 11:30 General Discussion
- 12:15 Lunch
- B. OPEN TECHNICAL SESSION - (Chairman: Hiroaki Suzuki)
- 1:30 C. Yao, "FMRC Sprinkler Research"
- 2:15 D. Evans, "Progress in Modeling Sprinkler Performance"
- 3:00 Refreshment Break
- 3:15 F. Saito and M. Yoshida, "Combustion Behaviour of Building Materials Using a Model Box with Air Supplied System"
- 4:00 O. Sugawa, Y. Oka and H. Hotta, "Fire Induced Flow in a Clean Room with Downward Vertical Laminar Flow"
- 4:45 Adjourn
- Evening: Reception and Dinner at NFPA and Tour of Facilities

Thursday, May 7 (cont.)

A. FIRE TOXICITY AND CHEMISTRY (cont.) - (Chairman: Takeyoshi Tanaka)

- 9:00 B.C. Levin et al., "Toxicological Effects of Different Time Exposures to the Fire Gases: CO or HCN or to CO Combined with HCN or CO₂"
- 9:45 T. Sakurai, "Toxic Gas Test by the Several Pure and Mixture Gases"
- 10:30 Refreshment Break
- 10:45 T. Hirano and I. Nakaya, "Strategy of Fire Suppression by Using Fire Retardants"
- 11:30 G. Hartzell, A. Grand, and W. Switzer, "Studies on the Toxicity of Smoke Containing Hydrogen Chloride"
- 12:15 Lunch
- Chairman: Richard G. Gann
- 1:30 T. Hirata and S. Kawamoto, "Toxic Gases from Combustion of Wood Treated with Retardants"
- 2:15 A. Kim and Y. Tsuchiya, "Bench- and Full-Scale Toxicity Tests of FRP Furniture"
- 3:00 Refreshment Break
- 3:15 T. Morikawa, E. Yanai and T. Nishina, "Evolution of Toxic Gases from Experimental Fires in an Existing Building"
- 4:00 Y. Tsuda and Y. Nishimaru, "Human Effects of Poisonous Gases Generated During Fire - Especially, Presence of HCN and CO"
- 4:45 R. Curtis and Y. Tsuchiya, "A Proposed Method for the Simultaneous Analysis of HCN and NO_x in Fire Gases"
- 5:30 Adjourn
- Evening: Reception and Dinner at NFPA and Tour of Facilities

Friday, May 8

PARALLEL SESSIONS

A. FIRE TOXICITY AND CHEMISTRY (cont.) - (Chairman: Raymond Friedman)

9:00 S. Yusa, "Evaluation of Combustion Toxicity from Various Materials Using a New Testing Apparatus"

9:45 Panel Discussion: A Review of the Five-Year Cooperative Program on Smoke Toxicity; R. Gann, H. Suzuki, and Y. Tsuchiya

10:30 Adjourn

B. OPEN TECHNICAL SESSION (cont.) - (Chairman: James G. Quintiere)

9:00 A. Ito and T. Kashiwagi, "Characterization of Flame Spread Over PMMA Using Holographic Interferometry Sample Orientation Effects"

9:45 K. Satoh, "A Numerical Study of Periodic Alternating Flow of Fires"

10:30 Adjourn

10:45 CLOSING CEREMONIES

12:00 Lunch

LIST OF MEMBERS (JAPAN)

Panel Members

Mr. Akira Takahashi (Japanese Chairman)
Director General
Building Research Institute
Ministry of Construction

Dr. Hiroaki Suzuki
Head, Smoke Control Division
Environment, Design and Fire Department
Building Research Institute
Ministry of Construction

Dr. Takeyoshi Tanaka
Chief Research Member
Testing and Evaluation Department
Building Research Institute
Ministry of Construction

Dr. Yuji Hasemi
Chief Research Member
Smoke Control Division
Environment, Design and Fire Department
Building Research Institute
Ministry of Construction

Dr. Tadahisa Jin
Head, The Second Research Division
Fire Research Institute
Fire Defense Agency
Ministry of Home Affairs

Mr. Tokio Morikawa
Chief, Combustion Section
The First Research Division
Fire Research Institute
Fire Defense Agency
Ministry of Home Affairs

Dr. Toshimi Hirata
Chief Research Member
Forestry and Forest Products Research Institute
Ministry of Agriculture, Forestry and Fisheries

Prof. Makoto Tsujimoto
Department of Architecture
Faculty of Engineering
University of Nagoya

Associate Members

Prof. Toshisuke Hirano
Department of Reaction Chemistry
Faculty of Engineering
University of Tokyo

Dr. Saburo Horiuchi
Chairman, Japanese Association of
Fire Science and Engineering

Dr. Yukio Tsuda
Department of Legal Medicine
School of Medicine
Yokohama City University

Dr. Osami Sugawa
Center for Science and Technology
Science University of Tokyo

Mr. Toshiro Sakurai
Japanese Association of Fire Science and Engineering
(Research Institute of Marine Engineering)

Mr. Kiyoshi Takahashi
Japanese Association of Fire Science and Engineering
(Technical Research Division, Fujita Corporation)

Mr. Kazuhito Nakamura
Japanese Association of Fire Science and Engineering
(Design Division, Shimizu Constructing Co., Ltd.)

Ms. Tomoko Joh
Japanese Association of Fire Science and Engineering
(Century Research Center)

Mr. Masashi Yoshida
Research Member
Testing and Evaluation Department
Building Research Institute
Ministry of Construction

Current NBS Visiting Scientist

Dr. Ai Sekizawa
Branch Chief Research Member
The Third Research Division
Fire Research Institute
Fire Defense Agency
Ministry of Home Affairs
(June 1986/1987, Visiting Scientist at NBS)

LIST OF MEMBERS (U.S.)

Panel Members

Dr. Jack E. Snell (U.S. Chairman)
Director, Center for Fire Research
National Bureau of Standards

Dr. Richard G. Gann (CFR Coordinator)
Chief, Fire Measurement and Research Division
Center for Fire Research
National Bureau of Standards

Dr. Takashi Kashiwagi (Secretary)
Polymer Combustion Research
Fire Measurement and Research Division
Center for Fire Research
National Bureau of Standards

Dr. Raymond Friedman (retired)
Vice President of Research
Factory Mutual Research Corporation

Mr. Harold E. Nelson
Center for Fire Research
National Bureau of Standards

Prof. Patrick J. Pagni
Vice Chairman, Department of Mechanical
Engineering
University of California, Berkeley

Dr. John de Ris
Factory Mutual Research Corporation

Prof. Edward E. Zukoski
Division of Engineering and
Applied Sciences
California Institute of Technology

Dr. James G. Quintiere
Chief, Fire Science and Engineering Division
Center for Fire Research
National Bureau of Standards

Dr. John R. Hall, Jr.
Director, Fire Analysis Division
National Fire Protection Association

Honorary Members

Prof. Howard Emmons (retired)
Division of Applied Science
Harvard University

Prof. Hoyt C. Hottel (retired)
Department of Chemical Engineering
Massachusetts Institute of Technology

Associate Members

Prof. Arvind Atreya
Division of Engineering Research
Michigan State University

Dr. Gordon E. Hartzell
Head, Department of Fire Technology
Southwest Research Institute

Dr. Archibald Tewarson
Factory Mutual Research Corporation

Prof. George Apostolakis
Mechanical, Aerospace and Nuclear
Engineering Department
University of California, Los Angeles

Mr. Cheng Yao
Manager, Applied Research Department
Factory Mutual Research Corporation

Prof. George Carrier
Division of Applied Sciences
Harvard University

Dr. Howard R. Baum
Center for Fire Research
National Bureau of Standards

Dr. Barbara C. Levin
Center for Fire Research
National Bureau of Standards

Dr. Bernard M. Levin
Center for Fire Research
National Bureau of Standards

Combustion Toxicity Participant

Dr. Yoshi Tsuchiya
Division of Building Research
National Research Council of Canada



9th Joint Panel Meeting

UJNR Panel on Fire Research and Safety

UJNR Mutual Research Corporation

May 4, 1987



OPENING SESSION

Opening Session

Dr. Richard Gann, Coordinator for the 9th UJNR Panel Meeting, opened the joint session by welcoming the delegation to the Factory Mutual Research Corporation. He then introduced Mr. John Love, President of Factory Mutual Engineering and Research for opening remarks. Dr. Jack Snell, Director, Center for Fire Research, and Mr. Akira Takahashi, Director General, Building Research Institute, introduced the United States and Japanese panel members.

The Combustion Toxicity and 6th Expert Meeting of the U.S.-Japan-Canada Cooperative Research Group on Toxicity of Combustion Products from Building Materials and Interior Goods was held in conjunction with the 9th UJNR Panel Meeting. The Combustion Toxicity meeting was called Fire Toxicity and Chemistry and took place on Wednesday, Thursday and Friday, May 6, 7 and 8, 1987.

Selection of the Chairmen for the sessions was made. The Panel voted unanimously to make the following individuals session chairmen:

Fire and Smoke Physics	J. de Ris P. Pagni	M. Tsujimoto
Risk, Hazard, and Evacuation	H. Nelson J. Hall	J. Quintiere
Fire Toxicity and Chemistry	T. Hirano R. Gann	T. Tanaka R. Friedman
Open Technical Session	H. Suzuki	J. Quintiere

The minutes of the 8th Joint Panel Meeting in Tsukuba were approved and will be printed in the Proceedings to be published by the Japanese delegation.

The agenda for the week was reviewed and approved. Procedural details for the sessions were discussed.

The opening session adjourned after the above-mentioned discussions were completed. The group photograph was taken.

FIRE AND SMOKE PHYSICS SESSION

PROGRESS REPORT ON FIRE AND SMOKE PHYSICS IN JAPAN

Yuji Hasemi
Building Research Institute

INTRODUCTION

Studies on fire and smoke physics reported after the previous UJNR Joint Meeting held in Tsukuba are reviewed. The following journals and preprints are referred to for this purpose except for those essentially reported at this or the previous meeting.

- a) Transactions of Architectural Institute of Japan(AIJ).
- b) Bulletin of Japanese Association of Fire Science and Engineering(JAFSE).
- c) Proceedings of the Annual Meeting of AIJ.
- d) Proceedings of the Annual Meeting of JAFSE.
- e) Fire Science and Technology.

The studies introduced in this report may be classified into the following research areas; the review will be made on the basis of this classification.

- i) analysis or observation of overall behaviors of enclosure fires.
- ii) dynamics of turbulent diffusion flames.
- iii) flame spread.
- iv) experiments and calculation of smoke layer formation process in a huge enclosure.
- v) application of fire modeling to specific problems.

STUDIES ON OVERALL BEHAVIOR OF ENCLOSURE FIRES

Influence of the location of fuels on the behavior of an enclosure fire was studied experimentally by Takeda(1,2) using 0.40m and 0.25m cube model enclosures with PMMA slabs as the fuel on the floor, the wall and the ceiling. He reported that burning rate is somewhat lower with the fuel on the wall than on the floor, and for the fuel on the ceiling, stable combustion was obtained only for small openings($A\sqrt{H} \lesssim 0.006m^{5/2}$). He also reported the overall behavior of PMMA fires in a model enclosure with two openings, one window and one doorway,(3) and proposed a concept of "equivalent ventilation parameter" to explain the burning rate based on the opening conditions. He also compared "floor combustion" with "wall combustion" in this experiment, and reported that the behavior of the smoke flowing out of openings is very different between these two conditions; the smoke flew out from only one opening at floor fire and it flew out from the two openings in the case of wall fires.

While in these reports, he reported an oscillatory combustion in enclosure fires, Nitta has tried to explain this oscillation by showing that an oscillation equation can be derived from the equations of energy and momentum conservation for the fire enclosure(4). In this theory, the oscillation is attributed essentially to the interaction among the ventilation rate, enclosure temperature and pressure difference on the opening rather than the change of oxygen or fuel gas concentrations in the combusting field.

DYNAMICS OF TURBULENT DIFFUSION FLAMES

Oscillatory behavior is also well known in turbulent diffusion flames. Matsubara and Satoh of FRI(5,6) have tried to examine an idea of fluiddynamic mechanism for this kind of oscillation. Matsubara assumed an interaction between the buoyancy and the inductive power within the flame leading to the generation of the oscillation; he made numerical calculations on the plumes from a "ring" heat source using a field model, and obtained a mushroom-shaped convection above the heat source. Satoh examined the influence of small fluctuation on the behavior of a turbulent plume by using UNDSAFE, and obtained a frequency-heat release rate relationship somewhat close to the conventional experimental relationships obtained in enclosure fires.

Fire whirl is another characteristic fluiddynamic phenomenon in relation with turbulent diffusion flames. Hasemi(7) has solved the basic equations describing incompressible fire whirls, and obtained the distributions of temperature and velocity as a function of external circulation. The calculated velocity field is very close to the experiments of Emmons and Mayle.

FLAME SPREAD

Studies concerned with flame spread in fire situation have been reported by Takeno, Kitaoka and Hirano(8) and Terai and Kato(9,10,11).

Takeno et al made measurements of flame spread and temperature distribution using a 0.4m x 1.2m fuel tray containing glass beads and kerosene to simulate a flame spread along a ground soaked with combustible liquid(8). They reported that the flame spread velocity along the fuel surface in this situation is considerably smaller than for a combustion along the liquid surface; this reduction suggests the dissipation of the Marangoni effect in their experiments. They also reported that the temperature distribution within the fuel bed is somewhat close to that generally observed in a flame spread along a combustible solid.

Terai et al have reported a calculation model of the combustion on a combustible floor to predict flame spread from material properties of the floor, assuming very stage of an enclosure fire(9). Their model is essentially based on heat transfer taking account of radiation from flame to fuel surface and its surroundings as well as heat conduction within the combusting solid, and for the two-dimensional calculation of the temperature rise of the surrounding surface of a flame, they have applied the integral equation method(10). More recently, they have measured heat transfer within and in the surroundings of a turbulent diffusion flame to obtain necessary properties for this model, and finally compared some aspects between the experiments and their model(11). While there is still considerable difference between their calculation and experiments, their work is valuable to know what component process should be studied to predict fire spread in relatively early fires.

FIRE AND SMOKE IN LARGE ENCLOSURE

Studies on fire and smoke control in a large enclosure have been getting popular in Japan, probably due to the growing interest on the construction of air-supported structures. Katsuno et al(12,13), Tanaka et al(14), Nagasawa et al(15) and Akeno et al(16) reported full-scale and model experiments while there are still many papers reporting smoke-layer calculations.

Katsuno et al reported an outline of full-scale fire experiments using the former Kuramae Kokugikan Smo Arena conducted in 1984(12,13); the space was approximately 6000m² in area and 32m high and the experiments using methanol and clothings as fuels have provided basic data on the general behavior of fire and smoke, and effectiveness of sprinklers and smoke venting in a large structure. They reported that the observed smoke layer height is

close to the calculation based on Thomas' entrainment model with empirical correction of Tsujimoto.

Tanaka et al developed an analytical calculation model of smoke formation process in a large structure with/without forced venting(14, Part I), and compared this theory with experiments with methanol as the fuel at the full scale fire test laboratory of BRI, 27m x 20m in plan and 20m high(14, Part II). They reported that the theory is very close to the experimental smoke layer height, if the lower bound of smoke layer in experiment is defined as the height at the discontinuous change of temperature and smoke density. They also made smoke layer measurements using a few Tsukuba Expo. pavilions before their destruction, and compared the results with the model(16). However, in some of the pressure measurement, the reported interior pressure was always lower than the exterior one; this suggests some difficulties in simultaneous pressure measurement around such a large structure.

Nagasawa et al reported model experiments on smoke layer formation process in a 20m long and 60m high air-supported structure using its 1/50 reduced model(15). They controlled heat release rate at the anticipated fire source for the conservation of the Archimedes number, and reported that the resulted smoke layer height is close to a calculation based on Zukoski's entrainment model.

SPECIFIC PROBLEMS

Hamada et al have reported some experimental aspects of flame from line burner flowing along a surface composed of wall and ceiling(17), and represented flame length and the distribution of temperature rise along a flame as functions of Q , for a line fire. Their result shows that the flame height relationship is close to Hasemi's correlation for wall fires while their experiment was made not only on a wall. They reported that their excess temperature along the ceiling is considerably higher than the experimental relationship without wall reported by Heskestad.

Mizuno et al(18) have observed burning behavior of upholstered furnitures using BRI's calorimeter, and reported their calorific properties; reported calorific potential of two different mattresses with urethane foam was 14.7MJ/kg and 12.8MJ/kg. Heat release rate measured by oxygen consumption method was almost proportional to the mass loss rate measured with load cells from very early stage to fully developed combustion.

Yamada et al have measured temperature, velocity, CO_2 concentration and smoke particles of smoke in an approximately 20m long, 2.5m high corridor with 15.2kW propane line burner as the fuel(19). Their concern is to obtain some criteria for the formation of two layers, since the formation of "clean" layer in the lower part of a corridor is an important condition for evacuation in fire. They suggest, from the vertical distribution of smoke particles at several distance, the existence of some recirculation within the ceiling layer in very far region from the fire source.

Hasemi et al have derived a simple method to estimate material properties concerned to ignitability from ignitability tests on the basis of the concept ignition as a result of rise of surface temperature to ignition temperature due to external radiation(20). Estimated ignition temperature and thermal inertia are very close to the values obtained by other independent methods for industrial materials such as PMMA and particle board, however for wood, the estimated properties using the data from many institutions are somewhat different from conventional method; the discrepancy is probably due to the influence of moisture within the specimens.

Mima et al reported some experimental results on the movement of smoke generated from smoke candles in a vertical laminar clean room(21). As estimated naturally, the measured smoke density distribution suggests that the diffusion of smoke within a laminar clean room is very insignificant.

REFERENCES

- 1 Takeda,H., "Scale modeling of enclosure fire with PMMA as the fuel," (d), 1986.
- 2 Takeda,H., "Experimental investigation of PMMA compartment fire," (e), No.1, 1985.
- 3 Takeda,H., "Wall fire behavior in the dual opening compartment," (e), No.1,2, 1986.
- 4 Nitta,K., "A study on oscillatory fire," (c), 1986.
- 5 Matsubara,Y., "A study on the oscillatory behavior in pool fires," (d), 1986.
- 6 Satoh,K., "Numerical study on the oscillatory behavior of fire plumes," (d), 1986.
- 7 Hasemi,Y., "Deterministic modeling of flame-cored fire whirls," (a), No.356, 1985.
- 8 Takeno,K., Kitaoka,M., and T.Hirano, "Flame spread along a ground soaked with combustible liquid," (d), 1985.
- 9 Terai,T., and Kato,T., "Calculation of the temperature rise at early stages of enclosure fires," (d), 1985.
- 10 Terai,T., and Kato,T., "On calculation of floor temperature rise by integral equations," (c), 1986.
- 11 Terai,T., Private communication, 1987.
- 12 Katsuno,H., Torii,S., Kunimoto,Y., and Kawasaki,K., "Fire experiments using the former Kuramae Kokugikan Smo Arena," (d), 1985.
- 13 Katsuno,H., Ishikawa,K., and Murakami,K., "Smoke behavior in a large structure," (d), 1985.
- 14 Tanaka,T., and Yanama,T., "Smoke control in large spaces, Part I,II," (c), 1985, or (e), No.1, 1985.
- 15 Nagasawa,Y., and Sakamoto,K., "Scale model studies on smoke movement in an air-supported structures, Part I,II", (c), 1985.
- 16 Akeno,T. Tanaka,T., Yamana,T., Takahashi,K., and Nakamura,K., "Smoke venting experiments at Tsukuba Expo. pavilions, Part I-III," (c), 1986.
- 17 Hamada,T., Kato,T., "Flow characteristics of flames along a surface composed of vertical wall and ceiling," (d), 1985.
- 18 Yamanaka,K., Mizuno,T., and Kawagoe,K., "A study on calorific property of upholstered items," (c), 1986.
- 19 Yamada,T., and Jin,T., "Experimental study of fire smoke mixing process in a building," (c), 1986.
- 20 Hasemi,Y., and Yoshida,M., "A simple estimation method of ignitability of interior-lining materials," (c), 1986.
- 21 Mima,T., Ui,K., and Ishii,T., "Experimental study on smoke diffusion in vertical laminar clean room," (c), 1986.

* The symbols (a)-(e) denote the journals or preprints as follows.

- (a): Transactions of Architectural Institute of Japan(AIJ), in Japanese.
- (b): Bulletin of Japanese Association of Fire Science and Engineering(JAFSE), in Japanese.
- (c): Proceedings of the Annual Meeting of AIJ, in Japanese.
- (d): Proceedings of the Annual Meeting of JAFSE, in Japanese.
- (e): Fire Science and Technology, in English.

SUMMARY REPORT
FIRE AND SMOKE PHYSICS SESSION

E. E. ZUKOSKI
Mechanical Engineering and Jet Propulsion
California Institute of Technology
Pasadena California 91125

ABSTRACT

A brief summary is given of some recent developments in the area of fire and smoke physics.

1. INTRODUCTION

I have chosen a few topics which interest me and are relevant to fire and smoke physics to review here. The selection of topics and papers is a rather personal one and certainly is not exhaustive.

2. FIRE-PLUME MODELING

The dependence of the length of diffusion flames on parameters such as fuel flow rate and burner diameter indicate that there are three regimes of behavior for these flames, see Zukoski (1985). These observations strongly suggest that other properties of these flames will also differ in these regimes and that the regimes should be used in discussing other data sets.

For example, when the the heat release per unit area of the fuel bed is very small and the flame height is less than the burner diameter, regime I, the flame is composed of a number of independent flamelets. The flame height is less than the burner diameter. It appears to scale with the square of the heat release rate per unit area and is independent of the total heat release rate or burner diameter. For larger heat release rates per unit area, regime III, the flamelets merge to form a single well-defined structure. The flame height is larger than 3 burner diameters and scales with the total heat release but is independent of the burner diameter. The important parameter in fixing this transition appears to be the ratio of flame height to burner diameter, Z_f/D , and the transition occurs as this ratio increases from 1 and 3.

In both of these regimes, the initial momentum flux of the fuel is negligible compared with the change in momentum flux in the plume generated by buoyancy forces. When the initial momentum flux is larger than the buoyancy generated momentum flux in the flame, a third regime is observed in which the flame length scales with the burner diameter and is independent of the total heat release. Flame lengths in this regime are typically 50 to 200 burner diameters. The transition to this regime occurs when the flow changes from a buoyancy controlled to a momentum controlled flow.

As the heat release increases, the transition between regimes I and III is completed when the heat release parameter Q^* is near one. (Here Q^* is defined as $[Q] / [\rho]_o C_p o T_o (-gD) D^2$]; and ρ_o , T_o , $C_p o$ are the density, specific heat and temperature of the ambient fluid; D is the burner diameter; g , the acceleration of gravity. The Q^* parameter has been shown to correlate flame length data for a wide range of fuels in regime III and apparently also, in the transition regime II. Its usefulness as a correlation parameter for regime I has not been verified and it is not the correct parameter to use in predicting the transition between regime III and V.

The selection of the appropriate parameters to use in describing these regimes and the clarification of the flow in regime I are important issues, I believe.

3. INTERNAL STRUCTURE OF THE FIRE PLUME

Processes which occur within the fire plumes discussed above are very complex and the high level of fluctuations and high temperatures make very difficult the accurate measurement of velocity, composition, and temperature. However, recent measurements have given us some additional information concerning the flow in the flame itself. Interesting results are reported by Miake-Lye and Toner (1986), and in a series of papers by Gore and Faeth, e.g., Gore and Faeth (1986).

In the work of Miake-Lye and Toner, discussed in more detail later in this meeting, a laser beam was directed through a large diffusion flame and the light scattered from soot was observed with photodiode array camera. The diffusion flames studied covered the range $0.2 < Q^* < 3.0$ and hence were in regime II and the edge of III in the scheme discussed above. The presence of soot was assumed to be a marker for a diffusion flame for this fuel-air system. The most interesting result obtained in the study was that soot and hence diffusion flames were observed to be present at points within the outer boundary of the diffusion flame more than 40% of the time. Thus the interior of the flame is a very complex region which contains geometrically complex regions which are either fuel or air rich and which are separated by diffusion flames. This result has interesting implications when the radiation from flames is considered.

The experiments of Gore and Faeth clarify the influence of radiation on the reactions in turbulent diffusion flames and suggest that some of the simple models used to describe these flames are not applicable when radiation from the soot removes a large part of the heat added by the combustion process.

4. CHEMICAL REACTIONS IN FLAMES

The chemical species formed in diffusion flames include the primary constituents, water and carbon dioxide, but also a wide range of trace species, some of which are toxic and hence of great interest in the study of accidental fires. The most prevalent of these toxic species is carbon monoxide which is found in the species produced in most accidental fires and is toxic over short periods of exposure at levels greater than 0.1%.

Combustion in Air: In a recent series of papers, Tewarson (1986) and DeRis (1985) have published the results of a long series of tests on the

properties of a wide range of fuels. They report, among other properties, the species produced when the fuel is pyrolyzed in an inert atmosphere and then burned in a laminar diffusion flame in air. The results show that the fraction of the carbon in the fuel which becomes carbon monoxide or soot in the combustion products varies very strongly with the chemistry of the fuel. They propose a correlation for many of these products based on the soot point for a laminar diffusion flame in which the products of pyrolysis are used as the fuel. These results can be used to predict the amounts of a wide range of species which are present in the products of diffusion flames burning in air.

Combustion in Two-Layer Systems: In many accidental fires, the supply of oxygen can be greatly reduced in the upper part of the fire room. For example, when a large diffusion flame is present in a room fire, a two-layer situation may develop in which an upper layer contains the products of combustion and the lower unvitiated air. As the fire develops, the upper part of the flame may gradually extend into the upper vitiated-layer, due to the growth of the fire and the thickness of the upper layer, while the lower part of the flame will still be surrounded by unvitiated air. In situations of this type, the concentration of oxygen in the upper layer may be reduced to a small value and this almost inert gas will be strongly entrained into the fire-plume which extends into the upper layer.

Under these circumstances, the chemical species formed by the fire may be quite different from those found in the products of diffusion flames burning in unvitiated air. Studies of this situation were first made by Cetegen et al (1984) for natural gas diffusion flames. A large hood was used to collect the products of combustion and to model the upper layer. By varying the spacing between the lower edge of the hood and the burner, the amount of air entrained into the fire plume could be varied over a wide range and the fuel-air ratio of the mixture entering the hood could easily be changed from 0.0 to 2.5 times the stoichiometric value.

Work with this apparatus was extended by Lim (1984) and Miake Toner (1986), and Beyler (1983) carried out similar studies of a wide range of fuels in a smaller hood. The interface in this apparatus was less well-defined and mixing was not as complete.

In these experiments, several important results were observed. First, the flame continues to burn in the vitiated gas contained within hood, even when the separation between the burner and the lower edge of the hood was a small fraction of the burner diameter. In this situation, no oxygen remained in the upper layer and most of the flame was above the interface. The heat released by the fire under these circumstances was determined from measured values of the species present in the hood, and it was found to be no more than ten percent less than the theoretical heat release. The theoretical value was based on an equilibrium calculation for the flow of fuel and entrained air into the fire plume and transported into upper layer. See Toner (1986).

Second, as long as there was more than 5% mole fraction of oxygen within the hood, the products of combustion were close to their equilibrium values and were quite similar to those suggested by Tewarson. However, when the mixture ratio for the gas entering the hood was above the stoichiometric value, the oxygen mole fraction was reduced to less than 1% and

concentrations of the chemical species observed in the hood were far from their equilibrium values for the mixture of elements involved and for the gas temperatures observed.

The measured mole fractions of the species present in the products were well correlated by the mixture ratio of fuel and air entering the upper layer in the hood, see Beyler (1983), but were independent of the residence time of the gas or the temperature of the gas within the upper layer. Observed temperatures covered the range, $200 < T < 900$ K, see Lim (1985) and Toner (1986). These results suggest that the reaction in the flame are quenched by the entrainment of inert gas into the flame at temperatures above 900 K.

The mole fractions of species observed in the upper layer are roughly similar to those observed in samples withdrawn from points within the flame zone of diffusion flames and averaged over long periods of time.

The observed mole fractions were found by Beyler to be a sensitive function of the fuel chemistry. The concentration of carbon monoxide in the gas within the upper layer were as high as 2 to 6% when the mixture ratio entering the hood was greater than 1.5 times the stoichiometric value. These concentrations are high enough to be almost instantly lethal and hence fires of the type discussed here are very potent sources of toxic gases.

Third, Beyler (1983) found that the products of reaction in the upper layer would become flammable with air when the fuel-air ratios of the gas entering the hood were high, e.g., around 2.2 times stoichiometric for methane. He was able to develop a model for prediction of the flammability limits for a wide range of fuels.

As a final note, when the flammability limit was reached, burning started on the interface and the products formed there were hotter than the gas within the hood. This gravitationally unstable mass of hot gas was observed by Lim to cause the gas within the hood to turn over rapidly. This process may be one of the causes for "flashover."

Combustion in Vitiated Atmosphere: Products produced when the entire flame is surrounded by a vitiated atmosphere are much closer to equilibrium values and, because the flammability limit is reached when the concentration of oxygen is reduced to values not much less than 10 mole percent, the nonequilibrium values of concentrations which were found in the two layer case are not observed here. A recent study of flammability limits, Lockwood (1986), indicates that the flammability limit is better correlated by a limiting adiabatic flame temperature than by the oxygen index method.

REFERENCES

Beyler, Craig Lynn, (1983) "Development and Burning of a Layer of Products of Incomplete Combustion Generated by a Buoyant Diffusion Flame," PhD thesis, Harvard University, Cambridge, Mass., Sept.

Cetegen, B. M., Zukoski, E. E., and Kubota, T., (1984) "Entrainment in the Near and Far Field of Fire Plumes", Combustion Science and Technology, Vol. 39, pp. 305-331.

de Ris, John, "A Scientific Approach to Flame Radiation and Material Flammability," presented at the Eighth U.S.-Japan Panel on Fire Research and Safety, Tsukuba, Japan, May 1985.

Gore, J. P. and Faeth, G. M., (1986) "Structure and Spectral Radiation Properties of Turbulent Ethylene/Air Diffusion Flames," The Twenty-First Symposium (International) on Combustion, Munich, August.

Lim, Christopher, (1984) "I. Mixing in Doorway Flows, II. Entrainment in Fire Plumes," AE Degree Thesis, CIT, June.

Miake-Lye, Richard C. and Toner, Stephen J., (1987) "Laser Soot-Scattering Imaging of a Large Buoyant Diffusion Flame," Combustion and Flame 67: pp. 9-26.

Tewarson, Archibald, (1986) "Prediction of Fire Properties of Materials Part I: Aliphatic and Aromatic Hydrocarbons and Related Polymers," Technical Report for NBS, Center for Fire Research, July.

Toner, Stephen J., (1986) "Entrainment, Chemistry and Structure of Fire Plumes," PhD Degree Thesis, CIT, June.

Zukoski, E. E., (1985) "Fluid Dynamic Aspects of Room Fires," Fire Safety Science - Proceeding of the First International Symposium 1985 Howard W. Emmons Invited Lecture, pp. 1-30.

FORCED SMOLDER PROPAGATION IN A HORIZONTAL FUEL LAYER
AND THE TRANSITION TO FLAMING COMBUSTION*

Thomas J. Ohlemiller
Center for Fire Research
National Bureau of Standards
Gaithersburg, MD 20899

Abstract

It is well known that a smoldering fuel responds to an increased oxygen supply by becoming faster and hotter until, eventually, flames erupt. This sequence is examined quantitatively for thick horizontal layers of a permeable fuel, i.e., cellulosic insulation with air flowing over the top surface. Two configurations are possible, forward and reverse smolder; both are investigated experimentally. The influence of combustion retardants is also examined; these include boric acid, a smolder retardant, and borax, a flaming retardant. Both prevent the transition to flaming in the absence of adjacent flammable material but are less effective in its presence. The overall response of these various fuel mixtures and configurations suggests that both kinetics and oxygen supply rate (not the latter alone) play substantial roles in dictating smolder response to an air flow. Keywords: air flow, cellulosic materials, flaming, insulation, retardants, smoldering.

1. INTRODUCTION

Cellulosic insulation of the type investigated here is made from recycled paper products, mostly newsprint. When properly ground to a finely fibrous form, such products become an excellent thermal insulation. The inherent combustibility of the base material (essentially wood) must be controlled, however, by the addition of combustion retardants and by adherence to installation practices that keep the insulation away from heat sources. When heated sufficiently even retarded insulation may smolder (1).

Smoldering insulation becomes an immediate life threat when and if it undergoes a transition into flaming combustion. For the usual attic type of installation, this is most likely to be caused by air flowing over or through the smoldering combustion zone as a result of winds impinging on the structure. Such winds may directly penetrate various attic vents or induce flow to/from rooms below the attic via ceiling holes around devices such as recessed light fixtures, vent fans, etc. It is clearly desirable to lessen the tendency of a smoldering insulation material to transition into flaming in such a manner.

There have been two previous studies of smoldering horizontal fuel layers in the presence of flowing air with some observations on the appearance of flaming. Palmer [2] examined the behavior of wood and grass dusts in layers up to 6 cm thick with air velocities up to 8 m/s; the configuration was quite similar to that used here but the bulk densities were 2-3 times higher except for the case of cork dust. The presence of flaming was noted but not examined

*Work sponsored by the Department of Energy, Building Thermal Envelope Systems and Materials Program

in any detail. Leisch [3] examined the behavior of grain kernel fragments, grain and wood dust in 20 cm layers at air velocities up to 19 m/s. In this case the fuel layer was set into the bottom of the flow tunnel so that its top surface was initially flush with the tunnel floor. Flames were noted, under some conditions, to appear and to be trapped in the surface depression left by the smoldering process.

The present study was undertaken to look at the impact of both smolder and flaming retardants on the forced flow smolder and flaming transition process. Further details and discussion can be found in Ref. 11.

2. EXPERIMENTAL APPARATUS AND PROCEDURE

A flow tunnel, illustrated in Fig. 1, was constructed for the purpose of examining the behavior of a smoldering insulation layer subjected to a flow of air over its surface. The tunnel provides a straight test section 115 cm long, 20.3 cm wide and 56 cm high; it is constructed from Marinite board. Air is drawn through the tunnel by a centrifugal fan at the downstream end; the speed of the fan can be varied to give flow velocities from 0.3 to 5.0 m/s. The flow velocity is uniform over the central cross-section of the tunnel to within $\pm 2\%$, as measured by an air velocity probe. Sidewall boundary layer effects do not appear to influence the central 50% of the tunnel over the majority of the length of the region where the insulation layer is placed. The sample thus behaves, to a large degree, as though it is in a steady wind blowing parallel to its top surface. The boundary layer on the top surface of the sample grows from the tunnel inlet. From the peak flow velocity and the longitudinal distance to the downstream end of the bed, one would infer that the boundary layer is laminar in all cases. However, the fuel bed surface is rough due to its particulate nature and to its uneven shrinkage during smoldering; this introduces local separation in numerous places and, in effect, causes a mildly turbulent boundary layer. This can be seen when smoke is being generated by the smolder process.

The leading and trailing edges of the insulation bed are ramped at an angle of 35° to lessen flow separation effects. The intersection of the upstream ramp with the top surface is always smoothed and rounded before a test by pressing down the insulation. The downstream intersection was not so treated and the flow is always fully separated from there onward (downstream).

Flow velocity is measured continually during a test with a Sierra Instruments Model 615 MHT air velocity meter*. The placement of the meter probe is ahead of the sample bed where the tunnel cross-section has its full 56 cm height so the flow velocity over the top of the bed is about 20% higher than that recorded by the meter. The velocity values reported here are for the full cross-section height. The local cross-section above the sample varies as it smolders and shrinks; the tunnel was made 56 cm high to keep the corresponding variation in flow velocity within 20%.

*Certain commercial equipment, instruments, or materials are identified in this paper in order to adequately specify the experimental procedure. Such identification does not imply recommendation or endorsement by the National Bureau of Standards, nor does it imply that the materials or equipment identified are necessarily the best available for the purpose.

Unretarded insulation from a commercial manufacturer is fully conditioned to 50% relative humidity at 21-24°C. It is weighed out and then fluffed by hand within a plastic bag to remove all clumps. It is packed in two stages, as uniformly as possible, into a pan that imposes the shape and size shown in Fig. 1. The bulk density was the maximum achievable with hand packing, 0.08-0.10 g/cm³; this spread of values results from a varying tendency of the material to expand upward after it is removed from the packing pan. The same range of bulk density for the organic portion of the insulation is used when the material is retarded. The combustion retardants (boric acid and 10 mol borax) were usually reagent grade but NF grade was used in a few tests. In all cases the material is through 200 mesh. It is mixed with the insulation in sufficient quantity to give a final product that is 15% by weight retardant. Uniform dispersion is achieved by two hours of mixing on a roller mill. Thereafter all procedures are the same as with the unretarded material. After placement in the flow tunnel, the vertical sides of the insulation bed are in contact with either 1.27 cm Marinite board or 1.27 cm white pine board. The sample width is thus reduced to 17.8 cm. The bottom of the sample is always in contact with 1.27 cm Marinite board. Thermocouples (chromel/alumel in a 0.050 cm diameter stainless steel sheath) are inserted laterally into the insulation bed so that the junction is at centerline mid-depth; three thermocouples are used, symmetrically placed about the sample center with a nominal separation of 10 cm from one to the next.

The insulation layer can be ignited to smoldering on either end to produce propagation in the same direction as the air flow (forward smolder) or in the opposite direction (reverse smolder). The igniter is a 1.3 mm diameter electrical heater formed into a zig-zag pattern 8 cm long x 13 cm wide so that it uniformly ignites the full width of the insulation bed. It is slipped under the desired end of the bed, raised to 375°C and left in place for up to one hour. During ignition the air flow velocity through the flow tunnel is 0.15-0.30 m/s; it is raised to the desired test value (and subsequently held constant) only after the smolder front on the top surface of the bed approaches the top end of the ramp portion.

The progress of the smolder front is easily visible on the top of the bed since it changes the insulation from a light gray to a dark black color. A motor-driven, 35 mm camera, viewing the top of the bed through a window in the top of the flow tunnel, monitors the smolder front progress by taking pictures at precisely-timed intervals (typically 10 min.). It also views ruled index marks of 1.27 cm spacing on both sides of the bed. The photos are magnified after a test and used to compute the smolder front velocity along the top of the bed. Smolder velocity at mid-depth is inferred from the thermocouples via their spacing and the time between 250°C isotherms.

3. RESULTS AND DISCUSSION

The smolder velocities given in the following figures are all derived from the successive photos of the top surface of the fuel bed. The average value derived from the three imbedded thermocouples generally agreed with this value within 5 to 10% (and frequently closer). However, the two successive values derived from the thermocouples almost always showed some acceleration of the smolder front at the mid-depth of the bed. In contrast, the top surface photos rarely showed any clear-cut acceleration or deceleration. Evidently the smolder front was slowly changing shape as it moved through the bed; this effect was not large enough to obscure any of the trends discussed here.

3.1 Behavior of Unretarded Insulation

Reverse smolder. Reverse smolder tests (propagation in direction opposite to air flow) were run with two different batches of unretarded material. Figure 2 shows the measured smolder velocity as a function of air flow velocity. There is no significant difference in smolder velocity behavior between these two batches of material for this smolder mode. Both exhibit only the same weak acceleration of the smolder rate with increased air flow velocity; the smolder velocity increases by 67% as the air velocity goes from 0 to 5 m/s.

The batch 1 material exhibited a type of localized flaming phenomenon also seen with this material in forward smolder; here it appeared at air flow velocities greater than 4 m/s. At random intervals blue flames (CO burning) appeared in residual char on top of the bed lasting up to 2 minutes and spreading up to 10 cm through the residual char before extinguishing. They never spread up to the leading edge of the smolder front on the top surface of the bed where flaming based on pyrolysis products rather than CO could be established. This flaming phenomenon was not viewed as a true transition from smoldering to flaming.

Thus, no true transition occurred in reverse smolder over the range of air velocities achievable with the present apparatus. For this reason, coupled with the relatively weak response of smolder velocity to air velocity in reverse smolder, it was concluded that the reverse smolder mode represents a distinctly lesser hazard than forward smolder (see below); it was not pursued further with regard to combustion retardant effects.

Forward smolder. Figure 2 also shows the forward smolder behavior of the same two batches of unretarded insulation material. Here the differing batches exhibit a qualitatively similar smolder velocity response but there are significant quantitative differences. Most of the quantitative differences in forward smolder velocity between batch one and batch two material are probably due to differences in bulk density; the batch two material was, in most cases, packed to a bulk density about 20% greater than for batch one. From stoichiometric considerations with an oxygen supply rate-limited process [1], one expects an increase in bulk density to cause a comparable decrease in smolder velocity. In addition, above a critical air flow velocity, batch 1 exhibited the CO flames in confined holes in the char, as discussed above; batch 2 did not.

Flaming development from forward smolder. Both batches, at air flow velocities between 2 and 2.5 m/s, exhibit a true transition to flaming combustion in that flames appear which move onto virgin fuel, consuming self-generated pyrolysis vapors. The CO flames in the char are not a necessary precursor to the initiation of pyrolysis vapor flames since they did not occur with batch 2 material. The pyrolysis-vapor flames typically originated in a cavity-like depression or step formed just to the char side of the leading edge of the smolder front on the top surface. Such a depression was formed rather erratically, evidently by the combination of char shrinkage and consumption. The interior surface of such cavities could be seen to glow just prior to flaming ignition. Evidently the concave structure facilitated locally higher temperatures due to decreased radiative losses; these structures may also have facilitated flaming ignition by allowing local build-up of

a flammable gas mixture and by providing a flame-holding region. The complexity of these details implies that modeling of the transition process will be difficult at best.

The pyrolysis-vapor flames originated at a local region (1-2 cm wide) along the leading edge of the smolder front, spread laterally across the leading edge quite quickly (f 1 sec), then spread downstream over the virgin portion of the fuel bed. The spread is spatially erratic and transient. Since the cellulosic insulation material is made ultimately from wood, it is a good char former. Thus, a flame cannot be permanently stabilized on the exposed top surface of the insulation bed; the build-up of only 2-3 mm of char slows the evolution of pyrolysis vapors to the point where the flame blows off. The flame thus at first spreads rapidly over a large area of the virgin fuel then falls back to regions that provide a flame holder function. Slight depressions in the top surface of the virgin fuel area where flow separation occurs provide temporary anchor points until the char again becomes too thick (after about 1-2 minutes); the flame then dies but it frequently will have initiated smoldering in the local region where it temporarily persisted. The longest-lived flames (up to about 5 min.) are anchored at the original leading edge of the smolder front where the smolder process provides pre-heated fuel and a supplementary source of pyrolysis vapors. Since the smolder process consumes fuel at a much slower rate than the flames, it too ultimately becomes inadequate as an anchor and the flames extinguish. The smolder process continues, its geometry distorted by new initiations downstream; after a variable-time interval, the whole process of flaming ignition, spread and extinction is repeated with spread occurring only on areas of fuel not previously charred.

Mechanism of forward/reverse smolder differences. The differing responses of forward and reverse smolder to increasing air flow pose interesting mechanistic questions. It has not yet been possible to explore these in great depth but some information has been obtained. It should be noted that Palmer [2] also saw such differences though he did not pursue their cause.

Once a smoldering process is past the initiation stage, it has generally been accepted that its rate is controlled by the rate of oxygen supply [2,4,5, 6]. Here again there would seem to be room for such an interpretation. In forward smolder the air flow impinges on the upward ramping surface of the char; in reverse smolder the flow over the char is separated as is apparent from the smoke behavior. One expects better oxygen transfer to the char in the forward smolder case.

Mass transfer measurements. In view of the considerable surface roughness here, it was decided that direct measurements of the local mass transfer rates were desirable. The technique chosen, evaporation of a subliming solid (camphor), has been used in the past mainly to infer local heat transfer rates from local mass transfer rate measurements [7]. Unretarded cellulosic insulation beds were smoldered in both forward and reverse configurations (1.95 m/s air flow velocity) and then quickly extinguished with nitrogen after the top of the smolder wave progressed over about two-thirds of the length of the fuel bed. Pre-weighed flakes of camphor (approximately 1 cm square, $1\frac{1}{2}$ - $2\frac{1}{2}$ mm thick, with tape covering the bottom surface) were placed at several lateral and longitudinal positions on the top surface of the char. A given set of camphor flakes was exposed to a fixed air flow velocity over the extinguished fuel bed surface for a period up to four hours; the weight loss

from each flake was then sufficient to permit a weighing accuracy of 1-2%. From the weight loss, the flake area and the vapor pressure of camphor, one can compute the effective local mass transfer coefficient [7].

The variation with position on the char surface is not very great ($\leq 35\%$ on the forward smolder case from approximately 23 cm behind the leading edge of the smolder front to approximately 6 cm in front of it). This variation was not pursued extensively because it is small enough to be of secondary importance. Of greatest interest is the behavior near the leading edge of the smolder front; this has the greatest bearing on smolder propagation rate. The difference there in mass transfer coefficients is only about 25-30% whereas the smolder velocities can differ by a factor of two. In addition, smolder in the two configurations shows differing air velocity dependencies while the dependency of the mass transfer coefficient is essentially independent of configuration. Furthermore, despite the slightly larger coefficient in the forward configuration, depletion of oxygen in the boundary layer over the preceding char probably leads to a slower oxygen transport rate near the leading edge in the forward case; the reverse case does not exhibit this oxygen depletion. Thus, one is led to conclude that oxygen transport alone cannot account for the forward/reverse differences.

Probable source of the forward/reverse smolder differences. The leading edge region of the smolder front is subject to the greatest heat losses. It loses heat by conduction and radiation into surrounding virgin fuel; it also radiates from its top surface to the cold surroundings. In reverse smolder this region also may suffer a net convective heat loss to the air flowing over the surface, in spite of the flow separation. (Note that the convective heat transfer coefficients will behave the same as the mass transfer coefficients.) Certainly the virgin fuel just ahead of the leading edge of the reverse smolder front (prior to flow separation) suffers a convective heat loss because the air passing over it is at room temperature. In contrast, forward smolder provides a configuration that preheats the air flow as it approaches the leading edge of the smolder front; one expects a net convective heat input to the char just upstream of the leading edge of the smolder front as well as to the downstream virgin fuel not yet charred. In fact the top surface temperature profile at 2 m/s shows that in the forward smolder case, the drying of water from the insulation is pushed several centimeters ahead of the smolder reaction zone by the convective heat input. Drying is immediately in front of the reaction zone for reverse smolder.

In view of these considerations and the observed smolder behavior, we hypothesize that the leading edge region of the smolder front is kinetically-limited, particularly with regard to char oxidation, not oxygen supply rate-limited (the remainder of the smolder front is oxygen supply rate-limited, as is usually assumed). A kinetically-limited region will be highly responsive to temperature (and additives, see below) and thus to the net heat flux; it will be only weakly responsive to an enhanced oxygen flux.

Consider the forward smolder case first, in view of this hypothesis. An increased air flow directly increases the heat transfer coefficient from the char-heated air to the leading edge region causing some acceleration there. Furthermore the increased air flow first impinges on the oxygen supply rate-limited portion of the char oxidation zone upstream of the leading edge region. There it accelerates the char oxidation rate, raising the local

surface temperature and thereby heats the air further. This hotter air in turn transfers more heat to the leading edge region enhancing its acceleration. This occurs in spite of the fact that the enhanced char oxidation depletes more oxygen from the heated air in the boundary layer (which probably overrides the increased mass transfer coefficient). If the leading edge of the smolder front can thus move forward more and more rapidly due to the forward transport of reaction heat by the gas, the remaining portion of the smolder front (the oxygen supply limited portion) can keep up by adjusting its shape (length) to assure that the oxygen supply rate per unit length of smolder front is sufficient.

Accelerating char oxidation closer and closer to the leading edge of the smolder zone puts a heat source of increasing strength and temperature in closer proximity to the virgin fuel. The top surface temperature profile at 2 m/s shows that the forward smolder mode supports a temperature gradient parallel to the surface that is $2^{1/2}$ x greater than in the reverse smolder case. Ultimately the accelerated char oxidation at the leading edge leads to the development of the concave structures, described above, which ignite pyrolysis vapors to flaming.

The reverse smolder case might at first be expected to go slower with increased air velocity on the basis of the preceding heat transfer considerations. In fact, Palmer [2] did find one material (cork dust) that smoldered more slowly with increased air velocity above about 3 m/s in the reverse smolder configuration; many of his materials showed a constant reverse smolder velocity with increased air flow velocity above about 1 to 2 m/s, though they accelerated at lower air velocities. Here, Fig. 2 shows only a slow but steady increase of reverse smolder velocity. Evidently here the increased convective heat loss from the leading edge region is more than compensated by other changes. The oxygen supply rate-limited region beyond the leading edge (downstream) responds to the increased oxygen supply by getting hotter as in the forward smolder case. The separated flow, with its attendant flow reversal, helps move some of this heat up toward the leading edge. Conduction and radiation through the fuel bed do so also. Furthermore, the leading edge char zone is 50% thicker in the reverse case, lessening heat losses. The net summation of the increased inputs of heat to the leading edge region is evidently sufficient to outweigh the increased convective loss from the top surface. The present arguments suggest that any model of the effects seen must describe the gas phase above the fuel as well as the fuel bed itself, since their coupling is a key feature of the observed behavior.

It is interesting to note that the multi-dimensional nature of the smolder propagation process studied here provides a new balance of processes distinctly different than in one-dimensional smolder with similar materials [8]. The overall results are considerably different: in one-dimensional smolder, forward propagation is much slower than reverse propagation; here the opposite is found to be true.

3.2 Behavior of Retarded Insulation

Both boric acid, a smolder inhibitor, and borax, a flaming inhibitor, were tested separately for their influence on forced flow smolder (forward configuration) and the transition process. Figure 3 summarizes the results. It is apparent that they differ drastically in their influence on the smolder

rate. In the absence of any adjacent wood, they appear to be equally effective in preventing flaming, i.e., neither permitted the appearance of flaming at air velocities up to about 5m/s, the maximum value achievable with the present apparatus. (In the presence of flammable wood sidewalls, much of this effectiveness was lost; see Ref. 11.)

Thermal analysis (TG/DSC; 5°C/min in air) of the three material compositions used here revealed that, as with pure cellulose (9), the retardants act mainly on the char oxidation process. Boric acid substantially slows the rate of heat release from this process but borax, a char oxidation promoter, appears to have only weak effect on this material, which already contains plenty of catalytic metal ions (10, 11).

The striking differences in smolder velocities at equal air velocities in Fig. 3 are once again a demonstration that external oxygen supply rate alone does not dictate smolder velocity. The preceding arguments about the importance of the leading edge of the smolder zone again apply here. If it is kinetically-limited as hypothesized, it is sensitive to catalysts and inhibitors of the char oxidation process. Thus boric acid slows the propagation by inhibiting char oxidation in the leading edge region. By slowing down, the thermal wave becomes thicker and the heat losses to the virgin fuel decrease. The char oxidation process becomes less complete thereby insulating itself beneath the char residue, cutting heat losses still further [1]. By covering itself with such an insulating layer, the char oxidation zone interposes an additional series resistance to oxygen transport that makes it less sensitive to changes in external air flow velocity. Because of these interacting effects, quantitative prediction of the net effect of a given change in char oxidation rate, for example, requires a detailed model of the entire two-dimensional system.

Borax, as noted, causes some acceleration of the char oxidation process. The acceleration is small relative to the unretarded case and the smolder velocities are only slightly greater. There is, however, no transition to flaming here. The leading edge of the smolder front thus moves faster with further air flow increases, becomes thinner and is able to tolerate the increased heat losses that this implies. The remaining portion of the smolder wave must adjust its shape to assure a sufficient oxygen supply rate so that it can keep up. It has practically no "cover" between the char reaction zone and the external air flow (only a 1-2 mm quenched skin of char on the top of the fuel bed) and so it is highly responsive to changes in the external air flow velocity.

The reaction zone length is stretched out in the borax case by about 40% to about 37 cm from about 27 cm for boric acid. Thus not only does the borax case assure its reaction zone a higher oxygen supply rate by remaining close to the top surface of the fuel bed, it also stretches out the reaction zone at a more shallow angle to facilitate a greater supply rate per unit length of reaction front.

The failure of the transition to flaming to occur with either retardant is presumably due to differing causes. For boric acid, the infrared TV viewing the top surface makes it apparent that the surface is much cooler than the unretarded (or borax) case. Thus it is probable that, for nearly all of the air flow range, the temperature was insufficient to ignite a flammable mixture of pyrolysis products even if it existed above the fuel bed surface. The

situation is evidently changing at flow velocities above 4.5 m/s since the smolder velocity begins to accelerate; this is discussed somewhat in Ref. 11.

In view of the minor effect that borax has on the thermal analysis behavior, its success in suppressing flaming is surprising. That is, it does not appear to act by promoting char formation as it does with cellulose since the amount of char in thermal analysis is about the same as for unretarded material. Its mode of action is not presently known; it could be an indirect effect such as a failure to facilitate formation of the intermittent cavity-like depressions at the leading edge of the smolder front (absence of these was noted with borax present). Recall that these were the source of flaming ignition in the unretarded case.

4. SUMMARY AND CONCLUSIONS

For a given insulation composition, there is a large difference in response between a smolder wave moving in the same direction as the accompanying air flow (forward smolder) or in the opposite direction (reverse smolder). Reverse smolder of an unretarded insulation showed only a weak increase in velocity as the air flow increased; no transition to flaming was seen at air velocities up to 5 m/s. Forward smolder of the same insulation was accelerated considerably more, and, at air velocities in the range 2 - 2 1/2 m/s, flames developed which spread over the uncharred material ahead of the smolder zone. These differing responses are not due solely to differences in oxygen transfer rate to the smoldering fuel. They are qualitatively consistent with the idea that the leading edge of the smolder front is kinetically-limited and is therefore sensitive to the differences in convective heat transfer implicit in forward and reverse configurations. The overall smolder wave is thus partially kinetically-controlled (leading edge region) and partially oxygen transport-controlled (bulk of wave behind leading edge).

Borax and boric acid assert their influence, at least in part, through the kinetically-controlled leading edge region by accelerating (borax) or slowing (boric acid) the char oxidation kinetics. By slowing the char oxidation kinetics to the point of incomplete char consumption, boric acid also manages to slow the oxygen supply rate to the trailing portion of the smolder wave making it less responsive to changes in air flow velocity. This partial suppression of char oxidation is lost at sufficiently high air velocities and a very hot smolder process is generated. Nevertheless, boric acid suppresses flaming up to at least 5 m/s. Borax does also, even though it somewhat accelerates the smolder propagation process; its mode of flaming suppression is not clear.

Actual installations of cellulosic insulation almost invariably juxtapose layers of the material with wooden structural supports. The wood, of course, contains no retardants. When wooden sidewalls are included in the forced-flow smolder apparatus there is no significant impact on the critical velocity for appearance of flaming with unretarded insulation. However, the benefits of borax are completely lost; the glowing insulation smolder zone that does not itself transition to flaming ignites the adjacent wood at essentially the same air velocity as is seen with unretarded insulation. The benefits of boric acid are reduced but not lost when wooden sidewalls are present; the critical air flow velocity for appearance of flames drops from above 5 m/s to about 3-3/4 m/s. Since borax and boric acid are usually used together, it is

probable that the combination offers less margin of improvement than boric acid alone. From this and the rather weak effect that boric acid has on increasing the minimum temperature for initiation of smoldering in cellulosic insulation, one sees that there is a continuing need for more effective smolder retardants.

4. REFERENCES

- [1] Ohlemiller, T., "Smoldering Combustion Hazards of Thermal Insulation Materials", National Bureau of Standards, NBSIR 81-2350, August 1981.
- [2] Palmer, K., "Smoldering Combustion in Dusts and Fibrous Materials", Combust. Flame 1 (1957) 129.
- [3] Leisch, S., "Smoldering Combustion in Horizontal Dust Layers", Ph.D. Thesis, University of Michigan Dept. of Aerospace Engineering, Nov. 1983.
- [4] Moussa, N., Toong, T.-Y. and Garris, C., "Mechanism of Smoldering of Cellulosic Materials:", Sixteenth Symposium (International) on Combustion, The Combustion Institute, Pittsburg (1977) p. 1447.
- [5] Summerfield, M., Ohlemiller, T. and Sandusky, H., "A Thermophysical Mathematical Model of Steady-Draw Smoking and Predictions of Overall Cigarette Behavior", Combust. Flame 33 (1978) p. 263.
- [6] Ohlemiller, T., Bellan, J. and Rogers, F., "A Model of Smoldering Combustion Applied to Flexible Polyurethane Foams", Combust. Flame 36 (1979) p. 197.
- [7] Eckert, E. and Goldstein, R., Measurements in Heat Transfer, 2nd ed., McGraw-Hill (Hemisphere Publishing Corp.), Washington, DC (1976) p. 407 ff.
- [8] Ohlemiller, T. and Lu'cca, D., "An Experimental Comparison of Forward and Reverse Smolder Propagation in Permeable Fuel Beds", Combust. Flame 54 (1983) 131-147.
- [9] Shafizadeh, F., Bradbury, A., De Groot, W. and Aanerud, T., "Role of Inorganic Additives in the Smoldering Combustion of Cotton Cellulose", Ind. Eng. Chem., Prod. Res. Dev. 21 (1982) p. 97.
- [10] McCarter, R., "Smoldering Combustion of Wood Fibers: Cause and Prevention", J. Fire Flamm. 9 (Jan. 1978) p. 119.
- [11] Ohlemiller, T., "Forced Smolder Propagation and the Transition to Flaming in Cellulosic Insulation", National Bureau of Standards NBSIR 85-3212, Oct. 1985.

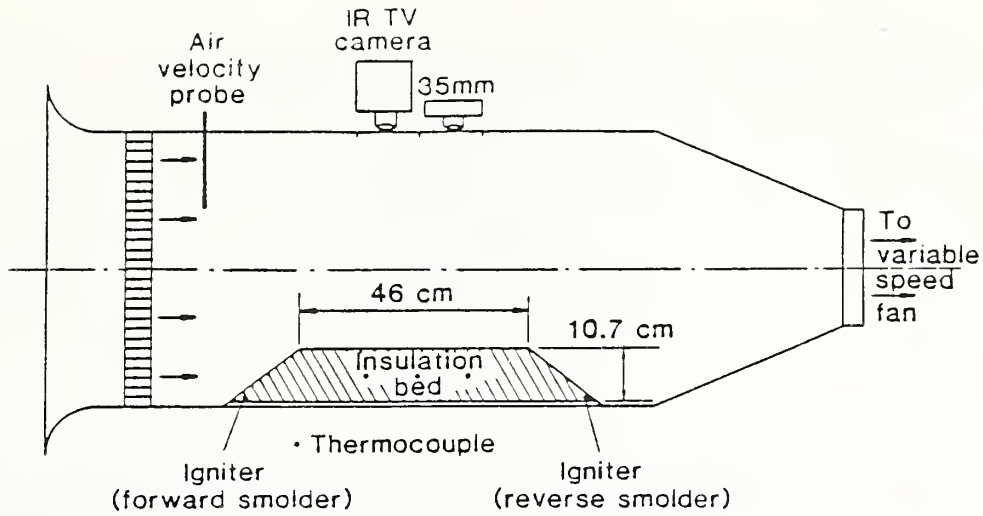


Figure 1 Schematic of flow tunnel apparatus for study of smolder propagation with flow over the fuel bed. Flow tunnel cross-section is 20.3 cm wide by 56 cm high.

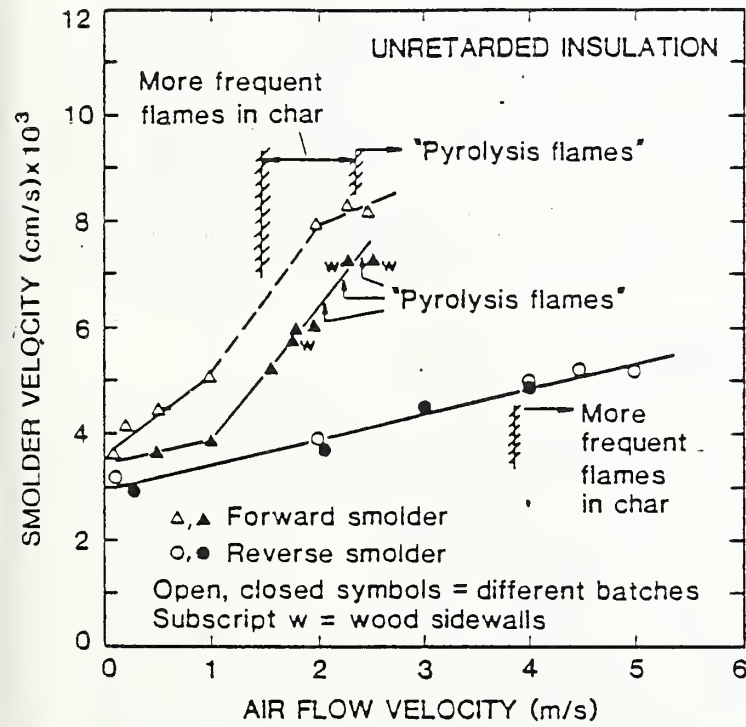


Figure 2 Measured effect of air velocity on smolder velocity of air flowing over the fuel bed in both forward and reverse configurations.

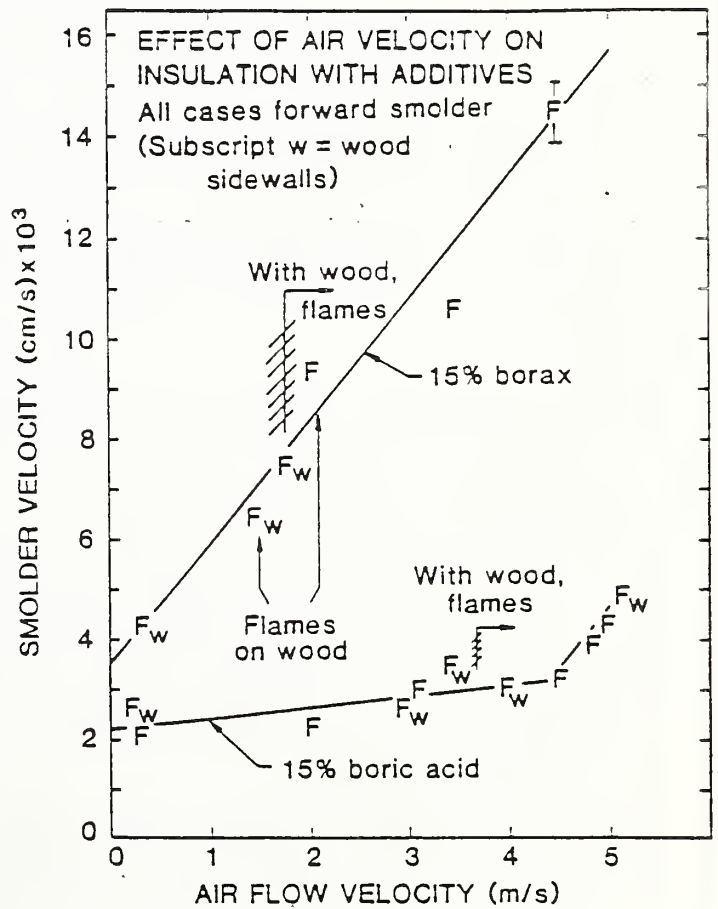


Figure 3 Measured effect of air velocity on smolder velocity of two compositions with additives; all results are for forward smolder mode. Flames appeared only when wood sidewalls were present.

Wood Ignition and Pyrolysis

ARVIND ATREYA
Mechanical Engineering Department
Michigan State University
and
HOWARD W. EMMONS
Division of Applied Sciences
Harvard University

ABSTRACT

In this study piloted ignition and pyrolysis of wood are investigated both experimentally and theoretically with the intention of understanding the various chemical and physical processes that are involved. Accurate measurements of surface temperature and evolved mass flux were made under well controlled external radiation conditions and time for sustained ignition was noted. It was found that even small quantities of adsorbed moisture (4% dry weight) has a very noticeable effect on both evolved mass flux and heat flux. Good agreement between the measured and calculated mass flux was obtained by using surface temperature instead of incident heat flux as the boundary condition. Discrepancies between the measured and calculated incident heat flux was found to be due to exothermic gas phase reactions with oxygen. These exothermic gas phase reactions eventually lead to spontaneous ignition. The effects of various terms in the energy equation were also evaluated by comparison of the theoretical model with the experimental results. It was found that the controversial heat of pyrolysis is small and can be neglected. Internal convective heat transfer by volatiles and variation of thermal properties with temperature were also found to be small effects. Piloted ignition was found to occur in the kinetically controlled pyrolysis regime. A simplified formula for fuel mass flux was also developed.

1. INTRODUCTION

Wood and other cellulosic materials, such as cotton and paper products, form the bulk of the fuels in many fires. These materials, when heated to a sufficiently high temperature, undergo thermal decomposition or pyrolysis to produce combustible gases and char. These combustible gases mix with the surrounding air to produce a flammable mixture which ignites either spontaneously or with the help of an external flame or a spark. Once a flame is established in the gas-phase, further thermal decomposition of the solid occurs to produce the fuel which feeds the flame. The fuel production rate under flaming conditions is often called the burning rate. Thus, study of pyrolysis of cellulosic materials is of considerable importance for determining both the critical conditions at ignition and the subsequent burning rate. This paper presents an experimental and theoretical investigation into pyrolysis and ignition of wood.

Pyrolysis of thick samples of wood involves both the physics of heat and mass transfer and the kinetics of thermal decomposition. Studies of decomposition chemistry have been performed on thermally thin samples [1-6] to avoid complications caused by heat and mass transfer processes. Kinetic parameters for overall apparent decomposition reactions have been obtained from these studies. For thermally thick samples of wood, heat and mass transfer processes have also been studied with varying degrees of sophistication. Theoretical models from purely thermal [7-8] (with infinite rate decomposition kinetics) to fairly detailed numerical [9-12] (with finite rate decomposition kinetics) are available in the literature. Experimentally, mass evolution rate

and temperatures at various locations in the thick solid have been measured for different incident heat fluxes. Some investigators [13-15] have also measured density profiles inside the solid using radiographic techniques.

Despite this substantial volume of information, large discrepancies in the interpretation of data on pyrolysis of wood still exist. The best example of these discrepancies is seen in the reported values of the heat of decomposition, which is usually determined by comparing a theoretical model with the experimental results. The reported heats of thermal decomposition vary greatly from significantly endothermic [-180 cal/gm; Kung's [10] Re-analysis of Bamford et al's [9] data] to significantly exothermic [+444 cal/gm; Shivadev and Emmons [3]]. Some variation in this global property is to be expected because the composition of the products of pyrolysis is not fixed. But, a variation as wide as reported seems due to our lack of understanding. The net result is that the fuel production rate (required for both ignition and burning rate) as a function of heat input rate, cannot, as yet, be reliably predicted.

2. EXPERIMENTS

In an attempt to understand the pyrolysis and ignition process, well controlled small scale experiments were performed on horizontal samples of various woods. The samples (8 cm x 8 cm x 1.9 cm) were pre-dried in an oven at 105°C for 5 to 8 hours and then allowed to cool over anhydrous CaSO₄ in a desiccator. These experiments were conducted in air using the apparatus shown in Fig. 1. The water-cooled plate was suddenly removed, exposing the instrumented sample to a constant incident heat flux. Incident heat flux was also continuously monitored by using an off-center radiometer calibrated against the heat flux at the center. The temperature of the electrical radiant heater, as measured by an infrared pyrometer, was about 1200K, which is representative of fire radiation [16].

For the pyrolysis experiments, front and back surface temperatures and the weight loss were measured as a function of time. The H₂ pilot flame and the 4 RPM motor were not used during these experiments. For the ignition experiments, a small (2 mm dia.) pilot flame was periodically lowered to within a millimeter of the sample surface and then quickly removed. The time required for sustained ignition was noted and for some cases surface temperature was also measured. The sample was slowly rotated (at 4 RPM) to avoid overheating a single spot on the wood surface by repeated trials.

In these experiments, weight loss of the sample was measured by a sensitive weighing table (resolution ± 0.001 gm) and surface temperature by a specially fabricated film thermocouple in order to increase the contact area (see Ref. 17 for further details). Temperature measurements with the film thermocouple were very repeatable (within $\pm 3^\circ\text{C}$) and the physical contact remained excellent even during charring. The data was collected by a microcomputer and the mass flux was obtained by a polynomial spline fit to the weight loss data. Several experiments, at different levels of incident heat flux (1.5 to 4.0 W/cm²), were conducted for each kind of wood for both ignition and pyrolysis. The results of three pyrolysis experiments and corresponding numerical calculations (to be described later) are shown in Figures 2a, 2b, and 2c for maple and Figures 3a, 3b, and 3c for vertical grain white pine [VGP]. Results of other pyrolysis experiments are summarized elsewhere [18]. The results of piloted ignition experiments are shown in Figures 4 and 5.

The mass flux curves shown in Figures 2a and 3a do not start at the origin. This is partly due to the disturbance in weight measurement caused by a sudden removal of the cooling plate and primarily due to the desorption of absorbed moisture, because no appreciable decomposition of wood is expected to start at surface temperatures lower than 540K. The high heat flux tests [#8 in Fig. 2a

and #7 in Fig. 3a] had to be terminated due to the occurrence of spontaneous ignition. These tests were also terminated at the first visible signs of surface combustion or glowing. Often none or very little ash was observed on the surface of the sample at the end of the test, although considerable cracking of char had occurred.

The mass flux at ignition, shown in Figure 5, was calculated using measured surface temperature for a moisture-free slab. The model used for these calculations is described below.

3. THEORETICAL MODELS OF WOOD PYROLYSIS

The data obtained in this study, provides a useful basis for developing a predictive model for pyrolysis of wood. The existing models of wood pyrolysis [9-12] have numerically explored the effect of various parameters and terms of the equations that were used, but only a few comparisons were made with the experimental results. In the present study, data from at least eight different experiments for each wood is compared with the model to evaluate the effect of various parameters. An attempt is made to understand the effect of various chemical and physical processes occurring during the pyrolysis of wood with the help of experimental data and mathematical models.

3.1 Decomposition Kinetics

The experimental data of Figures 2a and 3a clearly shows that the mass flux initially increases, reaches a maximum and then slowly decreases with time. A qualitative comparison with purely thermal pyrolysis temperature models [7,8] (which predict that for large times the mass flux decays as the square root of time) suggest that diffusion of heat is the controlling mechanism for large times. This is because heat has to diffuse through the thick char layer to reach the reaction zone. However, in the initial stages of pyrolysis the exposed surface of the solid produces most of the volatile mass flux. Thus, surface boundary condition and decomposition kinetics are expected to play a dominant role for small times. Therefore, for a theoretical model to be valid for both large and small times it must include both heat and mass transfer and decomposition kinetics. A relevant question is: How much chemical detail needs to be included to explain the observed behavior? Due to the complex decomposition chemistry, most kinetic studies (on both thermally thin and thick samples of wood) have been limited to the determination of the activation energy (E) and frequency (A), in the following single overall decomposition reaction:

$$\frac{\partial \rho_s(t)}{\partial t} = -(\rho_s(t) - \rho_f) A \exp(-E/RT(t)), \quad (1)$$

The values of E and A obtained by various authors from experiments on thermally thin samples of wood or cellulose fall into two distinct groups. The first group can be approximately represented by $E \approx 30$ Kcals/gm mole and $A \approx 10^8$ /sec, and the second group by $E \approx 54$ Kcals/gm mole and $A \approx 10^{17}$ /sec. A closer examination of the reported results show that experiments for the first group were conducted in air and for the second groups in an inert atmosphere. This is consistent with Shafizadeh [6] work which confirmed that pyrolysis proceeds faster in air than in inert atmosphere.

Kinetic parameters obtained from thermally thick samples seem to agree with those obtained from small samples in air, even though some experiments [15,19] were conducted in nitrogen flow. This apparent discrepancy is resolved by Lewellen et al's [20] results for pyrolysis of α -cellulose in helium. They found that reaction rates for a heating rate of 400°C/sec at 1 atm pressure were higher than those at 10,000°C/sec at 0.0005 atm pressure. Thus, greater the

residence time of the pyrolysis products in the cellulose matrix, higher is the reaction rate. This suggests that increased residence time of the pyrolysis products in thick samples enhances the reaction rate in a manner perhaps similar to that by oxygen in small samples. Lewellen et al [20] also showed that char is not a primary product of the pyrolysis of cellulose. In their experiments, there was not leftover char. Results of other investigators [6,21,22] show that char yield depends on the temperature exposure history of the sample. It increase with decrease in decomposition temperature and also with the duration of sample exposure to lower temperatures. Hence, char yield would vary with depth for thick samples. To account for variation in char yield Madorsky [23], Broido [24] and Shafizadeh [6] have suggested a competing two reaction mechanism (dehydration and depolymerization) for cellulose pyrolysis based on the results of experiments on small samples.

All these results can be combined into a likely decomposition mechanism shown in Fig. 6. In large samples, it is possible that levoglucosan pyrolyzes as it travels through the hot char matrix [12,15]. Since, the chemical structure and products of pyrolysis of levoglucosan are very similar to cellulose, steps B and C of Fig. 6 are probably very similar. This would explain why large samples showed a behavior similar to that of small samples pyrolyzing in air. Thus for large samples, char-forming (or dehydration) reactions are expected to dominate. The extent to which non-char-forming (or depolymerization) reactions occur in real fire situations, however, is not negligible. This is evident from the variable char yield obtained by Atreya [18] and Lee, et. al. [15] for wood. Thus, for correctness, the likely overall decomposition scheme suggested in Figure 6 should be used. However, due to the lack of appropriate kinetic data, Equation (1) is used and char yield (or ρ_f) is assumed to be a constant. As can be seen from Table 1, for vertical grain pine (VGP), two different char yields had to be assumed to obtain agreement with the experimental results. Higher char yield for lower temperature experiments is consistent with the work on small samples [22].

3.2 Desorption of Moisture

Another noticeable effect in the mass flux data shown in Figures 2a and 3a is that it quickly rises to about 0.2 mg/cm sec and that the duration of its stay at this level decreases with increased incident heat flux. It was found that this is due to desorption of moisture.

Moisture is held in wood in three ways [25]: (i) Free or adsorbed water present in the cell cavities. (ii) Adsorbed moisture, which can be up to 30% by weight and is a few molecules thick layer held by hydrogen bonds. This layer is monomolecular at about 5% adsorbed moisture. Wood under normal conditions contains about 12% moisture. (iii) Water of constitution, which is a part of the cellulose molecule. When wood is heated different types of moisture are released gradually with no distinction between them. The term "dry wood" is an arbitrarily defined standard (such as 24 hours at 105°C over phosphorous pentoxide). Theoretically, wood may be considered "dry" when all the adsorbed moisture and none of the water of constitution is extracted. Experimentally, it is not possible to extract all the adsorbed moisture without thermally degrading wood. Thus even though the samples used for the experiments were predried, some moisture flux is to be expected. This will significantly affect the ignition process.

In a theoretical formulation, moisture which is not a part of the molecule (i.e., adsorbed moisture) must be considered as a separate specie because the temperature dependence of its production rate is different from the rest of the pyrolysis products. This is evident from Figures 2a and 3a. Thus, in the

present formulation, the rate of desorption is assumed to follow a first order Arrhenius expression, viz.,

$$\frac{\partial \rho_m}{\partial t} = -A_m \rho_m \exp(-E_m/RT). \quad (2)$$

The kinetic constants ' E_m ' and ' A_m ' along with the heat of desorption ' Q_m ' were determined by best fit of this theoretical model to data from separate low heat flux experiments (details are given in Ref. 18). Surface temperatures was always below 450 K to assure that only moisture desorption and no decomposition occurred. Values of these constants, so obtained, are listed in Table 1. The only remaining unknown in Equation (2) is the absolute value of the initial concentration of adsorbed moisture. Since there is no way of determining this value, it had to be assumed. Due to similar conditioning of all the samples prior to the test, a fixed value was assumed for a kind of wood.

3.3 Conservation of Mass

If all the volatiles that are generated by thermal degradation and desorption of moisture are convected out, then conservation of mass requires:

$$\frac{\partial M_g}{\partial x} = \frac{\partial \rho_s}{\partial t} + \frac{\partial \rho_m}{\partial t} \quad (3)$$

where ' x ' is the depth inside the solid, with $x=0$ as the top and $x=L$ as the bottom surface of the solid. M_g is the outward mass flux of volatiles, being positive in the negative x -direction.

3.4 Conservation of Energy

Equations (1) to (3) are considered essential in order to explain the experimental results shown in Figures 2a and 3a. The extent of detail required for energy balance cannot, similarly, be determined by inspection. Thus, ignoring kinetic energy of volatiles and work done by gravity and pressure, energy balance is written as:

$$\begin{aligned} & (\rho_a c_{pa} + \rho_c c_{pc} + \rho_m c_{pm}) \frac{\partial T}{\partial t} - \frac{\partial}{\partial x} \left[k_s \frac{\partial T}{\partial x} \right] + \left[\frac{\rho_a}{\rho_w} \right] M_g \frac{\partial H_g}{\partial x} \\ & - \frac{\partial \rho_s}{\partial t} \left[-Q + \left[H_a - H_c \frac{\rho_f}{\rho_w} \right] / \left[1 - \frac{\rho_f}{\rho_w} \right] - H_g \right] \\ & - \frac{\partial \rho_m}{\partial t} (Q_m + H_m - H_g) , \end{aligned} \quad (4)$$

The symbols are defined in the nomenclature.

In Equ. (4), the left hand side is the increase in enthalpy of unpyrolyzed active material, char, and moisture in the elemental volume. Terms on the right hand side are: (i) influx of energy due to conduction, (ii) energy convected out by volatile gases assumed to be in good thermal contact with the solid, (iii) net heat required to produce a unit mass of pyrolysis gases (positive when endothermic), and (iv) net heat required to evaporate a unit mass of moisture. Here ρ_a and ρ_c are instantaneous densities of unpyrolyzed active material and char. At any instant, $\rho_s(x,t) = \rho_a(x,t) + \rho_c(x,t)$, hence at $t=0$, $\rho_s = \rho_a$ and

at $t \rightarrow \infty$, $\rho_s = \rho_f$. For the fixed char yield ($-\rho_f/\rho_w$) ρ_s is linearly related to ρ_a by;

$$\rho_s(t, x) = \left[1 - \frac{\rho_f}{\rho_w} \right] \rho_a(t, x) + \rho_f \quad (5)$$

To simulate energetic effects due to cracking of char, convective heat transfer between the volatiles and the solid matrix is not permitted for those elemental slabs where $\rho_s = \rho_f$ (i.e. $\rho_a = 0$) and is completely retained for those elemental slabs where $\rho_s = \rho_w = \rho_a$. For intermediate elements convective heat transfer is gradually turned off.

Following Tamanini [11], the thermal conductivity (k_s) was assumed to be linearly related to density as,

$$k_s = \frac{\rho_a}{\rho_w} k_a + \frac{\rho_c}{\rho_f} k_c + \frac{\rho_m}{\rho_w} k_m, \quad (6)$$

where k_a and k_c were treated as linear functions of temperature [$k = k^* + k^*(T - T_\infty)$] and k_m was assumed to be a constant. Also, specific heat (C_p) was assumed to linearly vary with temperature as: $C_p(T) = C_p^* + C_p^*(T - T_\infty)$. The property values for maple and VGP are summarized in Table 1.

3.5 Numerical Calculations and Boundary Conditions

The Equations (1), (2), (3) and (4) along with variable properties defined by Eqs. (5) and (6) were numerically solved by using the Crank-Nicolson method to express the finite difference form of the derivatives (details are given in Ref. 18) Tamanini's [11] computer code (SPYVAP) was modified to include energetics, kinetics, and changes in physical properties due to desorption of moisture, to simulate cracking, and to include the blowing correction in the convective heat transfer coefficient.

Finally boundary conditions must be carefully selected for comparison with experiments. Previous investigators [10,11,12] have used the experimentally prescribed incident heat flux as the boundary condition for the exposed surface. This, however, results in interpretation of theoretical results due to: (i) spectral absorptance of the solid surface relative to the spectral quality of the incident radiation [27], (ii) changes in surface radiative properties during decomposition, (iii) absorption of incident radiation by the decomposition products [28], and (iv) exothermic surface reactions. The net effect is that the boundary conditions no longer correspond to the experiments. These uncertainties were eliminated in this work by using the measured surface temperatures (Fig. 2c and 3c) instead of incident heat flux. Thus, only the solid phase decomposition process was modeled. Incident heat flux required to obtain the measure temperature was also calculated and compared with the experimental value. Figures 2a and 3a show a comparison between measured and calculated mass flux for three different experiment on maple and VGP and Figures 2b and 3b show the corresponding comparison for incident heat flux. In these figures 'dots' are measured values and solid lines are the results of numerical calculations. The values of 'E' and 'A' (see Table 1) were chosen to obtain the best fit between the theory and the data for all eight experiments. The best

fit of 'E' and 'A' are in good agreement with those reported in the literature [2].

Similar calculations were performed to determine the critical fuel mass flux at ignition. Measured surface temperatures (Fig. 4) were used as boundary conditions and the time required for sustained flaming was plotted on the calculated mass flux. The results of these calculations are shown in Figure 5. Note that the average fuel mass flux at ignition is in good agreement with the literature [9] value of 0.25 mg/cm sec. Also note that moisture was not included in these calculations for purposes of comparison with literature values. Moisture content for these experiments was low (estimated - 4% by weight). However, higher moisture content is expected to have a significant effect on both time to ignition and mass flux at ignition.

4. DISCUSSION OF RESULTS

The agreement between the calculated and measured mass flux (Figures 2a and 3a) seems reasonable given the complexities of the process. The measured and calculated incident heat fluxes (Figures 2b and 3b) do not, however, agree equally well over the entire domain. This implies that the production rate of fuel can be correctly predicted if the experimental surface temperature history is used. In other words, the solid phase decomposition process is correctly modeled. Hence, the effect of various terms in the energy equation (Equ. 4) can now be evaluated.

The third term on the RHS of Equ. 4 is the net heat required to produce a unit mass of pyrolysis gases. Ignoring the temperature dependence of the specific heats for the purposes of discussion this term may be expressed as:

$$\left[C_{pw}^{\circ} - C_{pc}^{\circ} \left(\frac{\rho_f}{\rho_w} \right) - C_{pg}^{\circ} \left(1 - \frac{\rho_f}{\rho_w} \right) \right] (T - T_{\infty}) / \left(1 - \frac{\rho_f}{\rho_w} \right) - Q$$

For representative values of the specific heats ($C_{pw}^{\circ} = 0.33$; $C_{pc}^{\circ} = 0.17$ and $C_{pg}^{\circ} = 0.26$ cal/gm), the quantity on the left hand side is always positive and for a constant char yield of 21% it is 0.113 cal/gm°C. Hence, this term is the difference between the heat of pyrolysis (Q) at the reference temperature (T_{∞}) and the stored energy released when a unit mass of pyrolysis gases are generated. Figure 7 shows that the net energy required decreases with increase in temperature. The numerical values in Fig. 7 were calculated by using a dynamic TGA curve from Browne and Tang [21]. Thus, for $Q = 30$ cal/gm (endothermic) pyrolysis at temperatures greater than 285°C would appear net exothermic. For $Q = +60$ cal/gm, the crossover from net endothermic to net exothermic takes place at temperatures above 500°C. For the TGA curve shown, pyrolysis is essentially complete at temperatures below 450°C, so that the entire pyrolysis process would appear endothermic.

It is interesting to note (for $Q = +40$ cal/gm, crossover at 372°C) that as the heating rate increases, a greater portion of decomposition would take place at higher temperatures. This would tend to make the decomposition process net exothermic. On the other hand, increasing the heating rate would reduce the char yield, resulting in a lower slope of the energy release line. This would shift the point crossover from endothermic to exothermic towards higher temperatures. Hence, a compensating effect. From this discussion it is evident that it is not possible to explain the large endothermic or exothermic effects reported in the literature. Furthermore, it can be mathematically shown [12,18] that a large exothermic heat of pyrolysis (≥ 250 cal/gm) would lead to a thermal runaway; a phenomena that has not been observed.

In an attempt to resolve the controversy about the magnitude and sign of the heat of pyrolysis of wood, calculations for $Q = 30, 0.0$ and -30 cal/gm were compared with the data for all eight experiments on maple and VGP. It was found that the best overall agreement was obtained by using 0.0 cal/gm. Figures 2a and 2b show such a comparison for maple and Figures 3a and 3b for VGP. Thus it seems that the controversial heat of pyrolysis is too small and can be ignored. This considerably simplifies the energy equation. The entire term multiplying $\partial \rho_s / \partial t$ in Equ. 4 can be neglected, because the heat of pyrolysis 'Q' is small and the other terms are of comparable magnitudes and opposite sign (Fig. 7).

Contrary to the heat of pyrolysis, desorption of even small quantities of moisture has a very noticeable effect. This is represented by the last term in Equ. 4. Figures 2a and 2b show the effect of small amounts of moisture for Experiment #1 on maple. The dashed lines are the result of calculation for 0% moisture. The corresponding calculation with 4% moisture is shown by the solid line. For expt. #1, using 0% moisture resulted in poor agreement between the calculated and measured mass flux up to 200 sec. and the corresponding effect on the heat flux was about $0.4W/cm^2$.

The second term on the RHS of Equ. 4 is the heat carried away by volatiles while traveling through the solid. For the calculations shown by solid lines in Figures 8a and 8b, this term was set equal to zero. The results indicate that the heat exchange between the volatiles and the hot solid matrix is not a major effect and is further diminished by the loss of intimate contact due to the cracking of char.

The effect of temperature dependence of the thermal conductivity and the specific heat is shown by dashed lines in Figures 8a and 8b. The agreement with the data was the worst for large times (or temperatures). It is interesting to note that the temperature dependence of thermal properties and the heat transfer to volatiles have an opposite effect on volatile mass flux, though the magnitude of the former is somewhat greater. For the case when heat is not convected out by the volatiles, more heat is retained in the interior to generate fuel gases. For the case when thermal properties do not increase with temperature, less heat is conducted into the solid thus reducing the evolved mass flux. The two effects are therefore mutually compensating.

The next most noticeable result is that the agreement between calculated and measured mass flux is quite reasonable, but the heat flux required to obtain the measured surface temperature (which was used as the boundary condition) agrees well up to a certain time and then deviates considerably from the measured values (Fig. 3b.). This suggests that the theoretical modeling has ignored some very important phenomena which must occur at the surface. A closer examination of the experimental data shows that (i) the deviation in the required heat flux occurs slightly before the peak of the mass flux curves (Fig. 3a and 3b), (ii) the inflection points in the measured surface temperature curves (Fig. 3c) correspond to the deviation in the required heat flux, (iii) for high heat flux cases (expt. #8 of Fig. 2a and expt. #7 of Fig. 3a), spontaneous ignition occurred at about this temperature. These observations suggest that the gas phase reactions, that eventually lead to spontaneous ignition, have started at this instant. For low heat flux cases, thermal runaway to spontaneous ignition did not occur because of heat loss to the surface and due to the attenuation in the fuel supply rate by the formation of char. Thus, if exothermic gas phase reactions that supply additional heat to the fuel surface do indeed take place, then the gas temperature slightly above the surface must be higher. Figures 9 confirms this hypothesis. Other investigators [29] have also reported similar inflection points in their surface temperature measurements. To further confirm this hypothesis the experiments need to be repeated in an inert atmosphere.

From these results it is very tempting to conclude that a large variation (endo-exothermic) observed in the heat of pyrolysis of wood may be either due to the desorption of moisture or to the exothermic gas phase reactions with oxygen and that the actual heat of pyrolysis is quite small and can be ignored. Note that if incident heat flux rather than surface temperature was used as a boundary condition, then the only way to account for additional heat would be by assuming exothermic heat of pyrolysis.

These results are also in agreement with the decomposition kinetics suggested in Fig. 6. Depolymerization reaction A in Fig. 6 is due to scission of CO bonds and is highly endothermic [23]. Dehydration reactions B and C are not expected to be exothermic, except in the presence of oxygen. Hence, it is likely that the observed high exothermicity is due to the oxidation of the pyrolysis products. As described earlier (Fig. 7), physical arguments based on temperature dependency of the enthalpy of the pyrolysis products can not account for the large endo-exothermic effects reported in the literature.

Finally, from Figure 5 we note that piloted ignition occurs on the initial rise of the mass flux curves--a domain where surface boundary condition and decomposition kinetics play a dominant role. The heat flux boundary condition at the surface is given by:

$$-k \left. \frac{\partial T}{\partial x} \right|_{x=0} = \epsilon \left[F - \sigma (T_s^4 - T_\infty^4) - h (T_s - T_\infty) \right] = f, \quad (7)$$

where f is the flux into the solid.

From Equations (1) and (3) assuming 0% moisture and small changes in density (i.e. $\rho_s \approx \rho_w$) we obtain the fuel mass flux as:

$$\dot{m}'' = A (\rho_w - \rho_f) \int_0^L \exp(-E/RT) dx \quad (8)$$

Since, a thin surface layer produces this mass flux, $T(x,t)$ may be approximated by:

$$T(x,t) = T_s(t) \left[1 - \frac{xf(t)}{kT_s} \right]. \quad (9)$$

Substituting Equ. (9) in Equ. (8), integrating, and taking the lowest order term of the asymptotic expansion for large E , we obtain:

$$\dot{m}'' = A (\rho_w - \rho_f) \left(\frac{kT_s}{f} \right) \left(\frac{RT_s}{E} \right) e^{-E/RT_s}. \quad (10)$$

Where, the upper limit of integration, L , was replaced by: $(T_s - T_\infty) k/f$. Using Equ. (10), volatile mass flux can be calculated from the knowledge of measured surface temperature shown in Figure 4. Results of such calculations for incident heat flux of 2.84 W/cm^2 are shown in Figure 5 by the dashed curve. Given the approximations used in deriving Equ. (10), the agreement with a more detailed calculation is excellent. Thus, Equ. (10) provides a useful relationship between the critical surface temperature and critical fuel mass flux at ignition.

5. CONCLUSIONS

In this study, pyrolysis and ignition of wood was investigated both experimentally and theoretically. A phenomenological picture that emerges from this work is shown in Fig. 10. The heat required for the decomposition reaction was found to be small and can be ignored in the energy balance (Equ. 4). On the other hand, desorption of even small quantities of moisture was found to significantly effect the energetics of the pyrolysis process. The experiments also demonstrate the existence of exothermic gas phase reactions when pyrolysis occurs in the presence of oxygen. These exothermic reactions eventually lead to spontaneous ignition. However, more experiments under well controlled atmosphere are needed to rule out the possibility of simultaneous exothermic surface reactions.

The theoretical model developed for pyrolysis of wood with moisture, successfully explains the experimental results. This model, however, is incomplete because the char yield is a priori assumed rather than predicted. In this model, using surface temperature rather than heat flux, as a boundary condition, permits the separation of the phenomena occurring in the gas phase from those occurring in the solid phase. A comparison of the experimental and theoretical results shows that the internal convective heat transfer by volatiles and variation of transport properties with temperature are small effects.

The results of piloted ignition are consistent with previous work and the pyrolysis model. It was found that ignition occurs prior to significant formation of char i.e. in the kinetically controlled pyrolysis regime. A simplified formula for fuel mass flux derived for this regime agrees well with more detailed calculations. This formula also provides a relationship between the critical fuel mass flux and critical surface temperature at ignition.

ACKNOWLEDGEMENTS

The first author is especially indebted to Professor G.F. Carrier for several helpful suggestions. This work was supported by the Center of Fire Research, National Bureau of Standards.

NOMENCLATURE

A	- Frequency factor (1/sec)
C _p	- Specific heat (cal/gm°C)
k	- Thermal conductivity (cal/gm°C sec)
h	- Heat transfer coefficient/ε
L	- Thickness of the sample
E	- Activation Energy (kcal/gm mole)
ε	- Emissivity (=absorptivity) of the surface
R	- Gas constant (Kcal/gm mole K)
F	- Prescribed incident heat flux
T	- Temperature (°K)
σ	- Stefan-Boltzmann constant
m"	- Outward mass flux (-M _g at x=0) mg/cm ² sec
t	- Time (sec)
x	- Distance; x=0, top surface; x=L, bottom surface of the sample (cm)
ρ	- Density based on original volume (gm/cm ³)
α	- Thermal diffusivity (cm ² /sec)

- M_g - Outward mass flux of volatile gases (water vapor and decomposition products)
- H - Thermal sensible specific enthalpy $\left(- \int_{T_\infty}^T C_p(T) dT \right)$
- Q - Endothermic heat of decomposition of wood for a unit mass of volatiles generated (cal/gm), at ambient temperature.
- Q_m - Heat of moisture desorption (cal/gm) at ambient temperature.

SUBSCRIPTS

- ∞ - Ambient
- s - Solid (unpyrolyzed wood and char), surface
- w - Dry virgin wood before pyrolysis has started, i.e., at $t=0$
- c - Char (instantaneous value)
- g - Volatile gases (water vapor and decomposition products)
- a - Unpyrolyzed active material (instantaneous value)
- f - Final value after pyrolysis has completed, i.e., at $t \rightarrow \infty$
- m - Adsorbed moisture
- p - Pyrolysis

SUPERSSCRIPTS

- \circ - Constant value
- $*$ - Temperature coefficient

REFERENCES

1. Tang, W.K.: Effect of Inorganic Salts of Pyrolysis of Wood, Alpha-Cellulose, and Lignin, Determined by Dynamic Thermogravimetry, U.S. Forest Service Research Paper, FPG71, Forest Products Laboratory, Madison, Wisconsin, (1967).
2. Roberts, A.F.: Combustion and Flame, 14, 261 (1970).
3. Shivadev, U.K. and Emmons, H.W.: Combustion and Flame, 22, 223, (1974).
4. Min, K.: Combustion and Flame, 30, 285 (1977).
5. Hileman, F.D., Wojcik, L.J., Futrel, J.M., and Einhorn, I.N.: Thermal Uses and Properties of Carbohydrates and Lignins, Academic Press, New York, p. 49 (1976).
6. Shafizadeh, F.: Chemistry of Pyrolysis and Combustion of Wood, Int'l Conference on Residential Solid Fuels, Oregon Graduate Center, Portland, Oregon (1981).
7. Kanury, M.A.: J. of Fire and Flammability, Vol 2, 191 (1971).
8. Delichatsios, M.A., and de Ris, J.: Analytical model for the pyrolysis of charring materials, Fall Technical Meeting, Eastern Section, 68 (1983).
9. Bamford, C.H., Crank, J., and Malan, D.H.: Proc. Cambridge Phil. Soc. 42, 166 (1946).
10. Kung, H.C.: Combustion and Flame, Vol 18, 185 (1972).

11. Tamanini, F.: The third full-scale bedroom fire test of the Home Fire Project Vol. II--Analysis of test Results, Technical Report, Factory Mutual Research Corp., Norwood, MA, 107 (1976).
12. Kansa, E.J., Perlee, H.E., and Chaiken, R.F.: Combustion and Flame 29, 311 (1977).
13. Kanury, A.M.: Thermal Decomposition Kinetics of Charring Polymeric Solids, FM Research Corporation Report 19721-4 (1971).
14. Nolan, P.F., Brown, D.J., and Rothwell, E.: 14th Symposium (Int'l) on Combustion, 1143, The Combustion Inst., (1973).
15. Lee, C., Chaiken, R.F., and Singer, J.M.: 16th Symposium (Int'l) on Combustion, 1459, The Combustion Inst., (1976).
16. Markstein, G.H." 18th Symposium (Int'l) on Combustion, The Combustion Institute, 537, (1981).
17. Atreya, A., Carpentier, C., and Harkleroad, J., "Effect of Sample Orientation on Piloted Ignition and Flame Spread," Accepted for publication in The First International Symposium on Fire Safety Science, 1985.
18. Atreya, A., Pyrolysis, ignition and fire spread on horizontal surfaces of wood, Ph.D. Theses, Harvard University, Cambridge, (1983).
19. Roberts, A.F., and Clough, G.: 9th Symposium (Int'l) on Combustion, 158, The Combustion Inst., (1963).
20. Lewellen, P.C., Peters, W.A., and Howard, J.B.: 16th Symposium (Int'l) on Combustion, 1471, The Combustion Inst., (1976).
21. Browne, F.L., and Tang, W.K.: Fire Res. Abs. and Rev., 4, 76 (1962).
22. Broido, A., and Nelson, M.A.: Combustion and Flame, 24, 263 (1975).
23. Madorsky, S.L.: Thermal Degradation of Organic Polymers, Robert E. Krieger Publishing Company, Huntington, New York (1975).
24. Broido, A.: Thermal Uses and Properties of Carbohydrates and Lignins, Academic Press, N.Y. 1976).
25. Stamm, A.J.: Wood and Cellulose Science, The Ronald Press Company, New York (1964).
26. Hodgmann, C.D., Weast, R.C., and Selby, S.M.: Handbook of Chemistry and Physics, Chemical Rubber Publishing Co., Cleveland (1960).
27. Wesson, H.R., Welker, J.R., and Slipevich, C.M.: Combustion and Flame, 16, 303 (1971).
28. Kashiwagi, T.: Fire Safety Journal, 3, 185, (1981).
29. Quintiere, J., Harkleroad, M. and Walton, D., Combustion Science Technology, Vol. 32 67-89, (1983).

TABLE 1

THE FOLLOWING CONSTANTS WERE USED IN THE ANALYSIS OF PYROLYSIS

DATA FOR MAPLE AND VGP

Activation energy 'E'	= 30 Kcals/gm mole (best fit parameter)
Pre-exponential factor 'A'	= 2.5×10^8 l/sec (best fit parameter)
Heat of pyrolysis 'Q'	= -30; 0.0; 30 cal/gm (variable under study) (positive when endothermic)
* Thermal conductivity ' k_w '	= $4 \times 10^{-4} + 0.29 \times 10^{-6} (T-T_0)$ cal/cm sec K (Ref. 1)
* Thermal conductivity ' k_c '	= $1.7 \times 10^{-4} + 0.29 \times 10^{-6} (T-T_0)$ cal/cm sec K (Ref. 16)
Density of wood ' ρ_w '	= 0.676 gm/cm ³ (measured)
Char yield ' ρ_c/ρ_w '	= 0.24 (assumed constant)
Specific heat of wood ' C_{pw} '	= $0.35 + 0.36 \times 10^{-4} (T-T_0)$ cal/gm K (Ref. 16)
Specific heat of wood ' C_{pc} '	= $0.17 + 0.48 \times 10^{-4} (T-T_0)$ cal/gm K (Ref. 24)
Specific heat of gasses ' C_{pg} '	= $0.25 + 0.43 \times 10^{-4} (T-T_0)$ cal/gm K (Ref. 24)
Activation energy for adsorbed moisture ' E_m '	= 10.5 Kcals/gm mole (Ref. 1)
Pre-exponential factor for adsorbed moisture ' A_m '	= 4.50E+3 l/sec (Ref. 1)
Heat of moisture desorption ' Q_m '	= 574 cal/gm (Ref. 1)

THE FOLLOWING CONSTANTS WERE DIFFERENT FOR VGP

Activation energy 'E'	= 28 Kcals/gm mole (best fit parameter)
Pre-exponential factor 'A'	= 1.0×10^8 l/sec (best fit parameter)
Heat of pyrolysis 'Q'	= 0.0 cal/gm (assumed)
* Thermal conductivity ' k_w '	= $6.30 \times 10^{-4} + 0.29 \times 10^{-6} (T-T_0)$ cal/cm sec K (Ref. 1)
* Thermal conductivity ' k_c '	= $1.4 \times 10^{-4} + 0.29 \times 10^{-6} (T-T_0)$ cal/cm sec K (assumed)
Density of wood ' ρ_w '	= 0.326 gm/cm ³ (measured)
Char yield ' ρ_c/ρ_w '	= 0.32 (best fit for expt. numbers 1, 2 & 3) 0.25 (best fit for expt. numbers 4, 5, 6, 7 & 8)
Specific heat of wood ' C_{pw} '	= $0.33 + 0.36 \times 10^{-4} (T-T_0)$ cal/gm K (Smithsonian Tables)

*The temperature dependence was estimated by a simple resistance model with intra-void radiation.

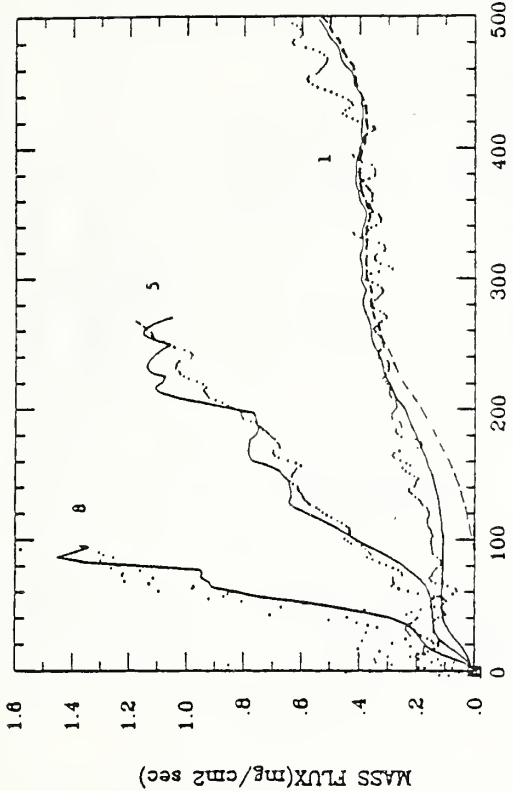


Fig. 2a {Pyrolysis of Maple with moisture} TIME(sec)

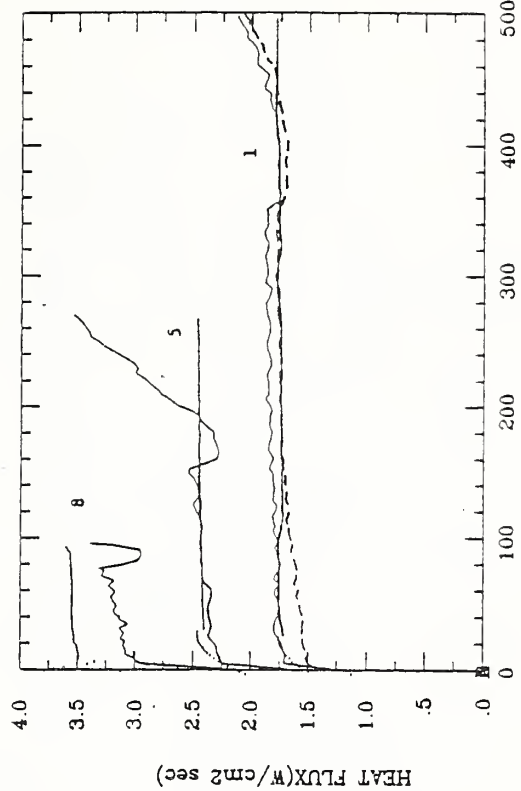


Fig. 2b {Pyrolysis of Maple with moisture} TIME(sec)

Fig. 2a, b A comparison of measured and calculated mass flux and incident heat flux for three experiments on maple. Dots--data; solid lines--calculations; Q--0.0, 4% moisture. Expt. #1: Dashed lines for 0% moisture.

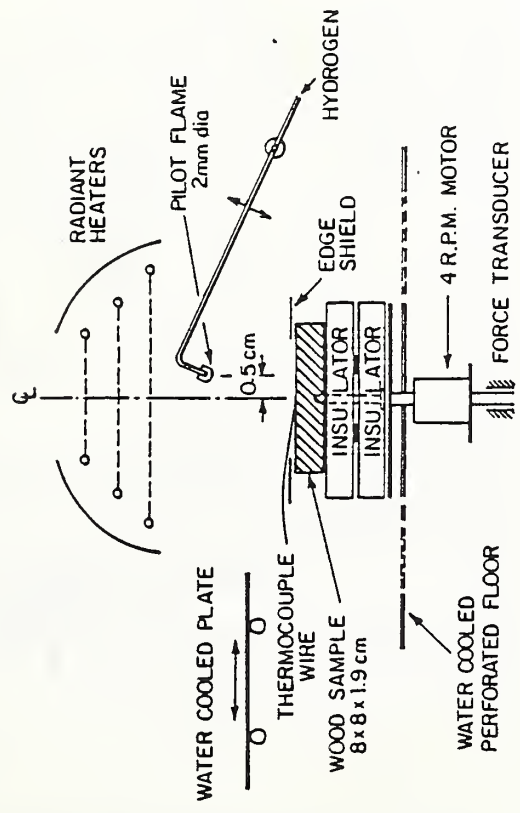


Fig. 1 Schematic of experimental apparatus.

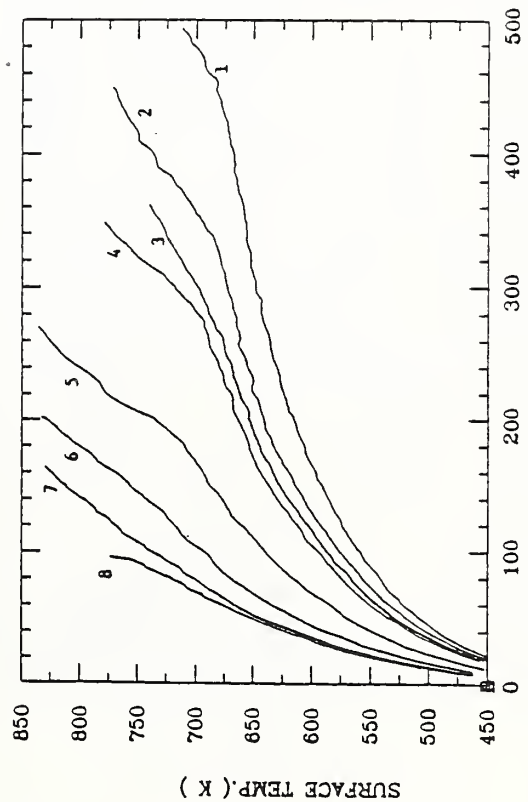


Fig. 2c {Surface temperature for Maple} TIME(sec)

Measured surface temperatures for all 8 experiments on maple.

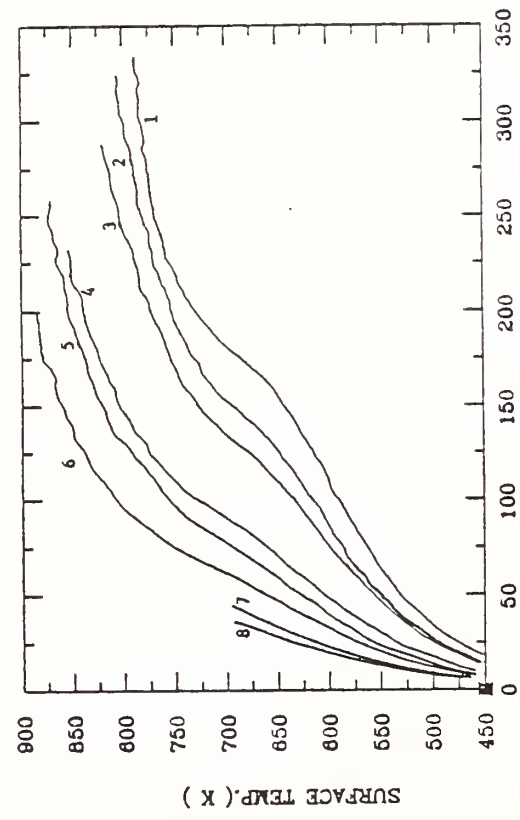


Fig. 3c {Surface temperature for V.G.Pine | TIME(sec)
Measured surface temperatures for all 8 experiments on VGP.

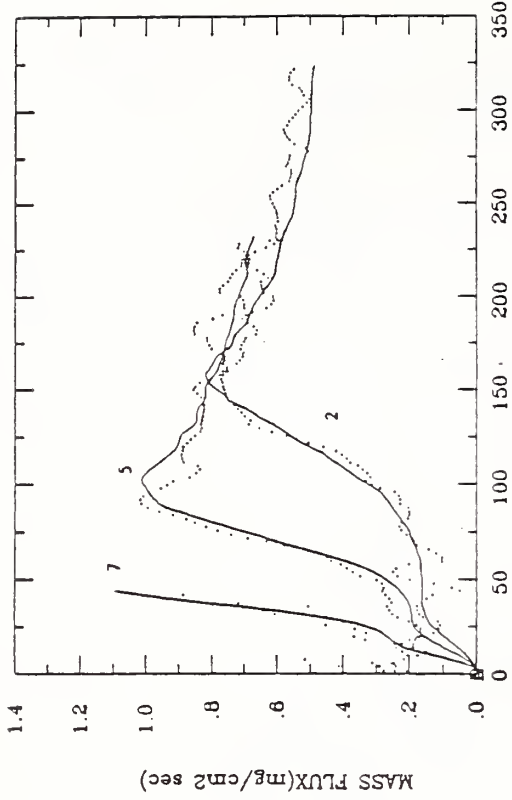


Fig. 3a {Pyrolysis of V.G.Pine with moisture} TIME(sec)

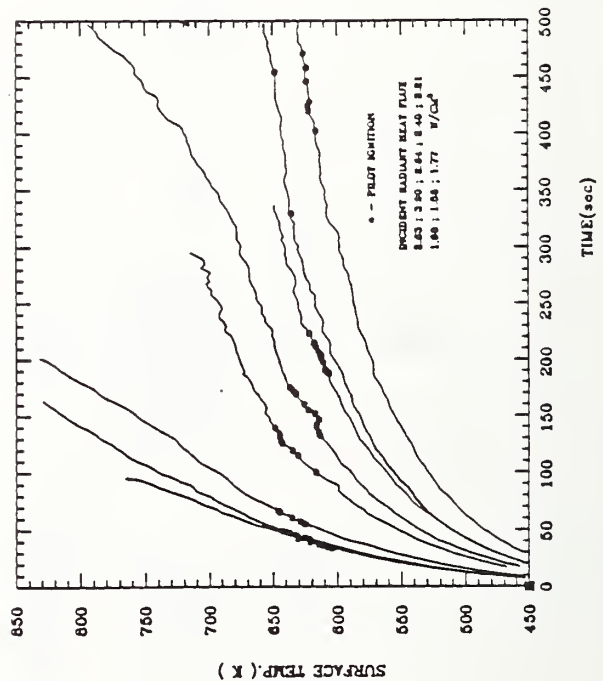


Fig. 4 Measured surface temperatures for piloted ignition.

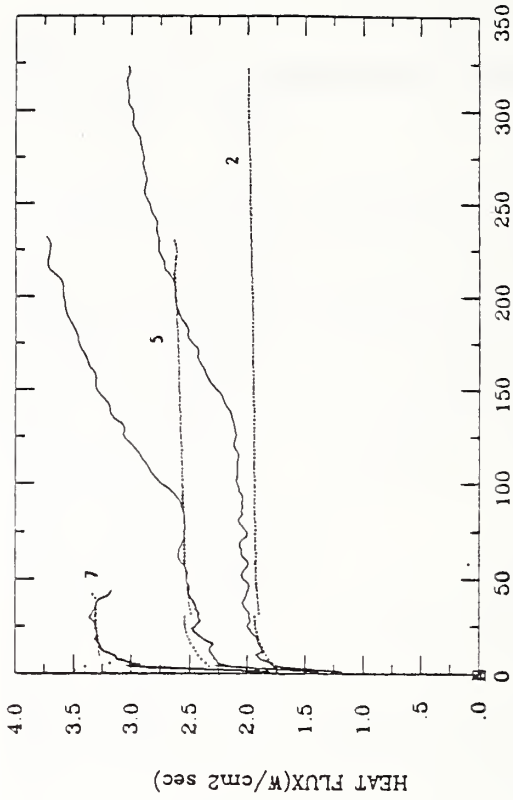


Fig. 3b {Pyrolysis of V.G.Pine with moisture} TIME(sec)

Fig. 3a,b A comparison of measured and calculated mass flux and incident heat flux for three experiments on VGP. Dots--data; solid lines--calculations; Q=0.0; 6% moisture.

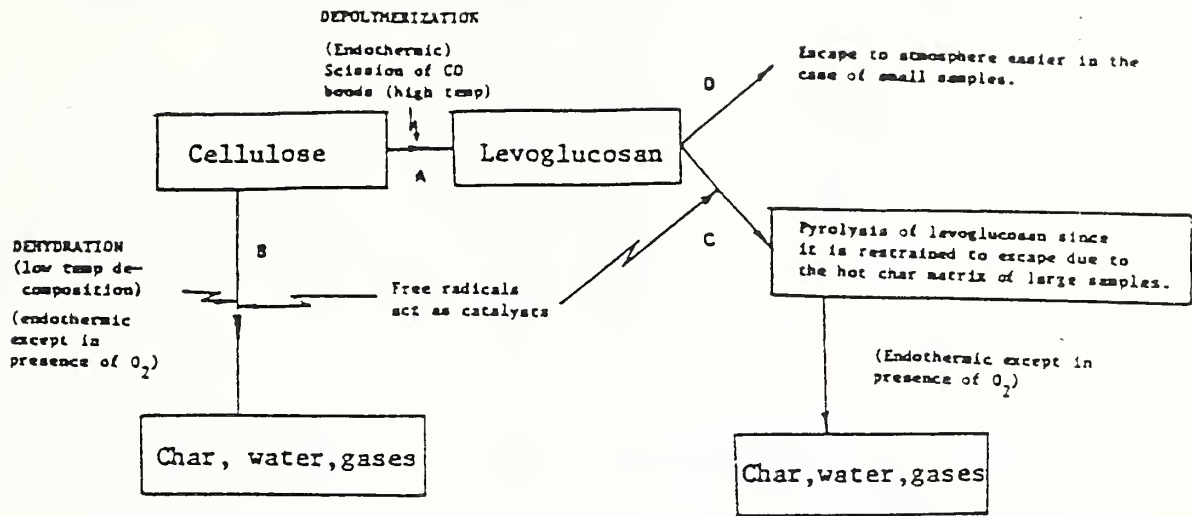


Fig. 6 Decomposition kinetics.

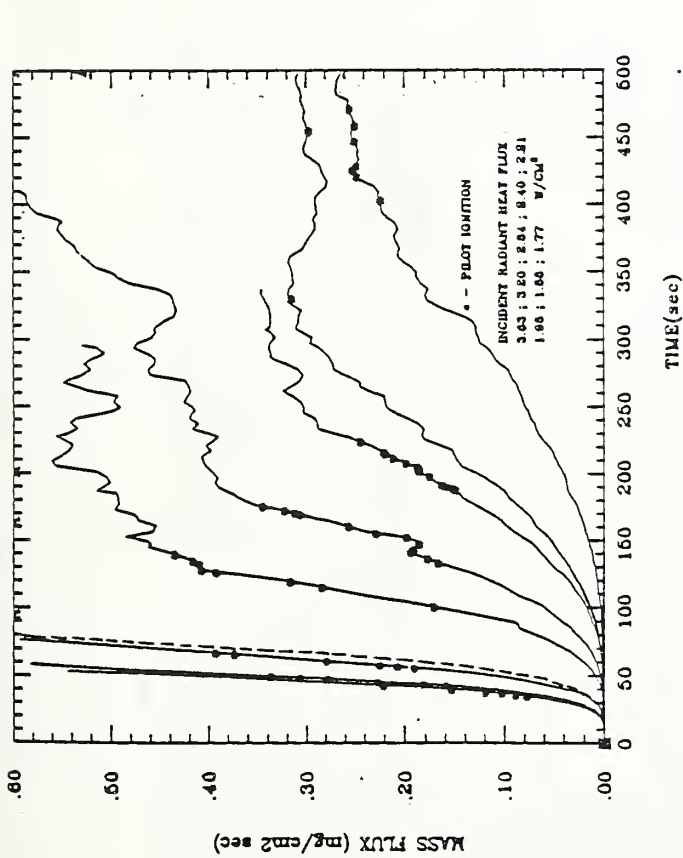


Fig. 5 Calculated fuel mass flux for piloted ignition. Dashed line: fuel mass flux from Equation (10)

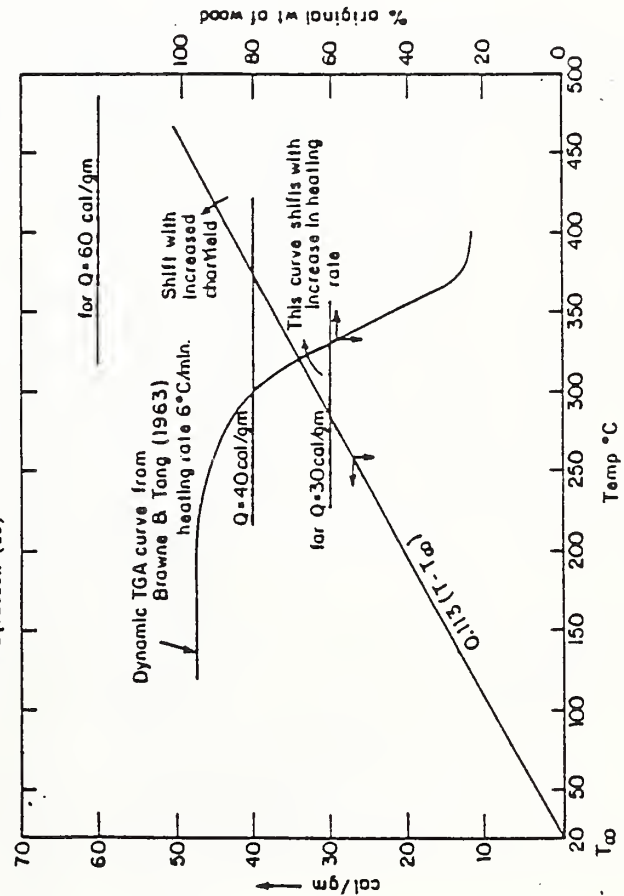


Fig. 7 Decomposition energetics.

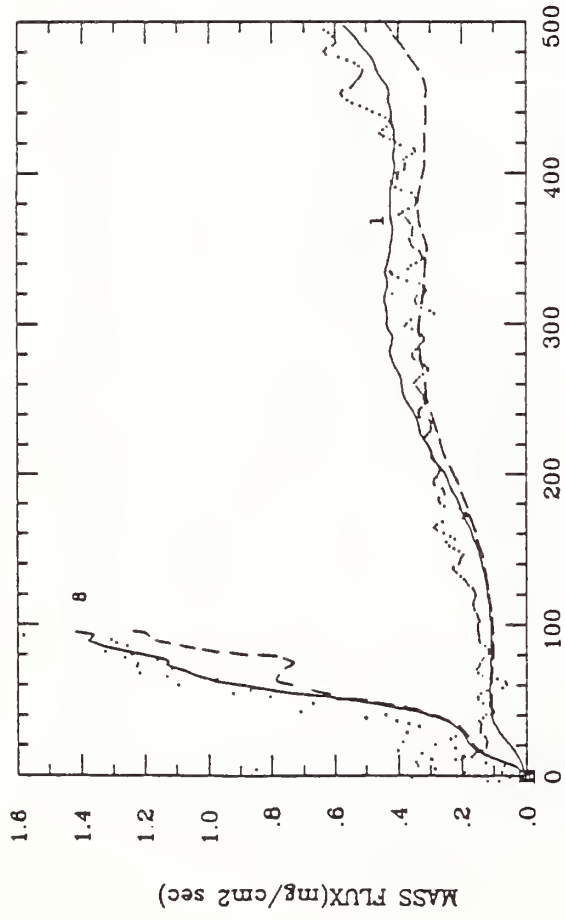


Fig. 8a {Pyrolysis of Maple with moisture} TIME(sec)

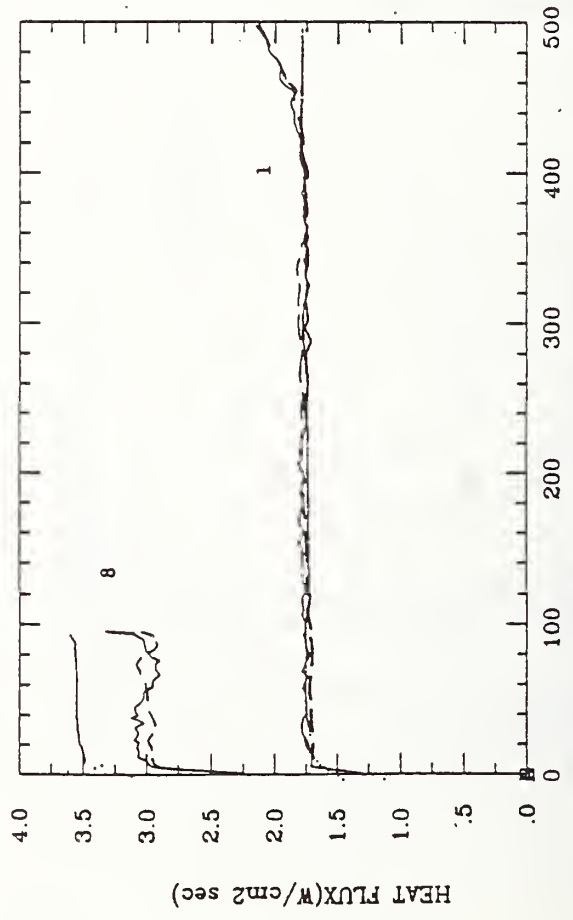


Fig. 8b {Pyrolysis of Maple with moisture} TIME(sec)

Fig. 8a,b Effects of internal heat transfer by volatile end temperature dependent properties on mass and heat flux. Q=0.0; 4) moisture; Dots--data; solid lines--no internal heat transfer; dashed lines--not temperature dependent properties.

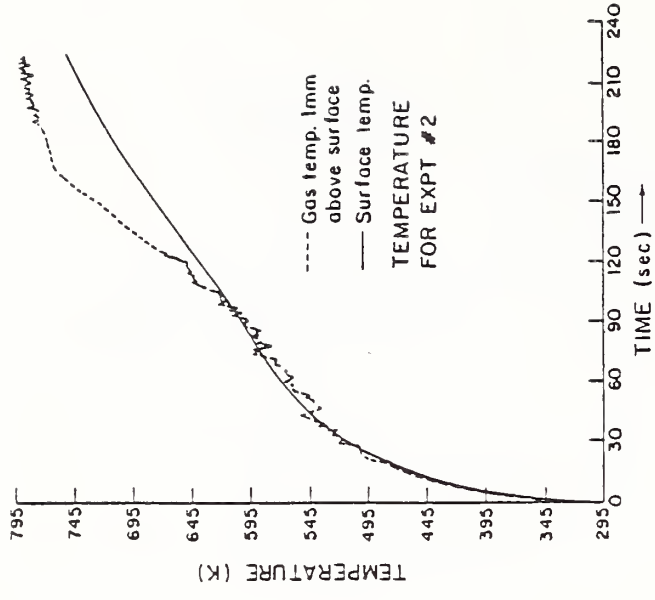


Fig. 9 Surface and gas temperatures for VGP.

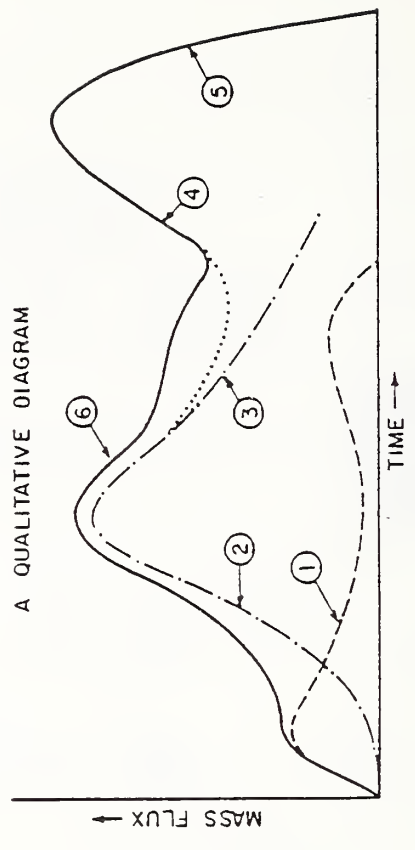


Fig. 10 Pyrolysis of a finite slab of wood with moisture, insulated at the back and in an inert atmosphere. 1) Mass flux due to desorption of moisture. 2) Kinetically controlled pyrolysis. 3) Diffusion controlled pyrolysis (semi-infinite mode). 4) Rise due to the insulated back boundary. 5) Final fall due to consumption of all reactants. 6) The composite curve.

DETERMINISTIC PROPERTIES OF TURBULENT DIFFUSION FLAMES FROM LOW Q^* FIRES

Yuji Hasemi
Building Research Institute
Ministry of Construction

Mitsuru Nishihata
Center for Fire Science and Technology
Science University of Tokyo

INTRODUCTION

Turbulent diffusion flames are generally a major element in the development of a fire. In the early stages of a building fire, flames have a role to preheat the surfaces of the whole enclosure by radiation and to drive hot gas to the ceiling layer. Also in urban or wildland fires, flame radiation and confluence of individual flames into a huge flame have a significance not only for the development of fire but also the generation of difficulties of fire suppression.

Practical properties concerning these aspects of fire safety have been studied for various purposes(1-6). Dimensional analysis of the flame geometry has established the dependence of the ratio of flame height to fuel size on $Q/D^{5/2}$, and its significance has been often represented by a dimensionless heat release rate $Q^* = \rho C T g^{1/2} D^{5/2}$ or some other parameter representing an essentially same implication(4-6,10); temperature, velocity and entrainment in the turbulent plume above a flame have been also found to be influenced by the flame geometry, and its significance in the application of point source theory, location of virtual source, has been correlated with Q^* or flame height(7-10). While low Q^* fires are still probable both in building fires and in mass fires(9-11), in most of the experiments heat release rate has been chosen to generate a flame height considerably greater than the characteristic fuel size, i.e. $Q^* \gg 0.1$. Sand-wick experiments by Wood et al(12) provide only available data to have a peep of the practical properties in the $Q^* \leq 0.1$ regime. The dimensional analysis expects a dependence of flame height only on the heat release rate per unit area, Q/D^2 , in the low Q^* regime(1), and earlier experimental works seem to show this tendency(10,12); however there is still considerable discrepancy and scattering among the relevant experimental data. Also for the properties of the upper plume region, the concept of virtual source is expected to fail in the limit of low Q^* fires, since low Q^* fires must be essentially closer to a flat heat source with finite area rather than a point source.

The difficulty in the experiments on low Q^* fires is essentially the necessity of relatively large fuel and therefore a huge experimental facility. Since Wood et al's data still seem to show some instability probably due to the use of sand wicks, accumulation of experimental data on low Q^* fires using various fuels is important as a basis for predicting their practical properties.

The purpose of this paper is to report some characteristic behaviors of low Q^* fires obtained from experiments using a large porous refractory burner, which may allow a more controllable and stable combustion even in the low Q^* regime than any other conventional fuels do.

EXPERIMENTAL DESCRIPTION

The experiments were conducted primarily using a porous square burner of 1.0m with propane as the fuel, and supplementary experiments were made using 0.20m and 0.50m square burners to study some source-size dependence of the flame properties.

The burners were filled with ceramic beads of approximately 8mm diameter, and the height of their surfaces was approximately 0.5m above the floor of a laboratory, 27m by 20m in plan and 27m high without artificial floor surround at the level of the burner exits. Anticipating that burner exit velocity would become less uniform by reducing the fuel supply, plumbing inside the 1.0m burner was carefully made; the burner surface appeared to be covered with flames for every experiment reported in this paper.

Observations were made on the geometry of visible flames (general shape and height) and centerline temperature.

Visible flame was observed by eyes and monitored by a video camera during each experiment. Since the general shape of flame was found to change dramatically by the operation of fuel supply rate during a preparatory test using the 1.0m burner, the shape of flame was carefully observed. Data of the height of flame tips were obtained from observation of the videotape; the reported values of flame height are the average of the data observed for more than 3 minutes at the intervals of 1 s.

Temperature measurements were made using 0.20m diameter chromel-alumel thermocouples. The time constant of the temperature measurement system is approximately 10 s. No corrections have been made for the radiation and conduction losses from the junction of each thermocouple. To eliminate the influence of accidental sway of the flame, temperature was monitored at each height not only just above the center of each burner but also at 4 different points 5cm apart from the center. The reported values of temperature are the average of the centerline temperatures at the interval of 10 s over 3 minutes while the centerline temperature was higher than those at any other points.

RESULTS

Flame Geometry

The general shape of flame in the very low Q^* regime was apparently quite different from that in the regimes of conventional studies (mostly $Q^* > 0.1$). For $Q < 43\text{kW}$ ($Q^* < 0.039$) of the 1.0m burner, fire was broken into flamelets of approximately same height distributed over the burner surface. At $Q = 43\text{kW}$ ($Q^* \approx 0.039$), flamelets along the burner sides starts to join together to build "filmy" flames, and at approximately $Q = 130\text{kW}$ ($Q^* = 0.11$), small flametips starts to appear above the filmy flame. Figure 1 shows a

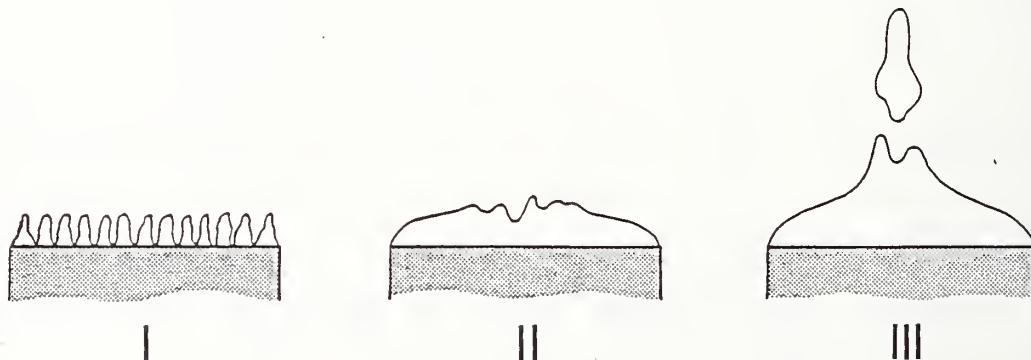


Figure 1 Shapes of flames

brief sketch of the characteristic flame shapes for these 3 regimes. The filmy flames in the region II, looked like a combusting boundary layer above a horizontal flat plate under forced convection. Similar transition of the flame shape was also seen for the 0.50m burner, while the transition from flamelets to filmy flames was somewhat ambiguous at the 0.20m burner. Figure 2 summarizes the Q-D relationships at these transitions; it is noteworthy that the critical heat release rate for the transition from filmy fire to the appearance of flametips is almost proportional to the square of the characteristic fuel size, and practically represented as

$$(Q/D^2)_{crit} = 140 \text{ (kW/m}^2\text{)} \quad (1)$$

The slope representing the transition from individual flamelets to filmy flames seem to be somewhat less steeper than this while the slope itself is not yet clear.

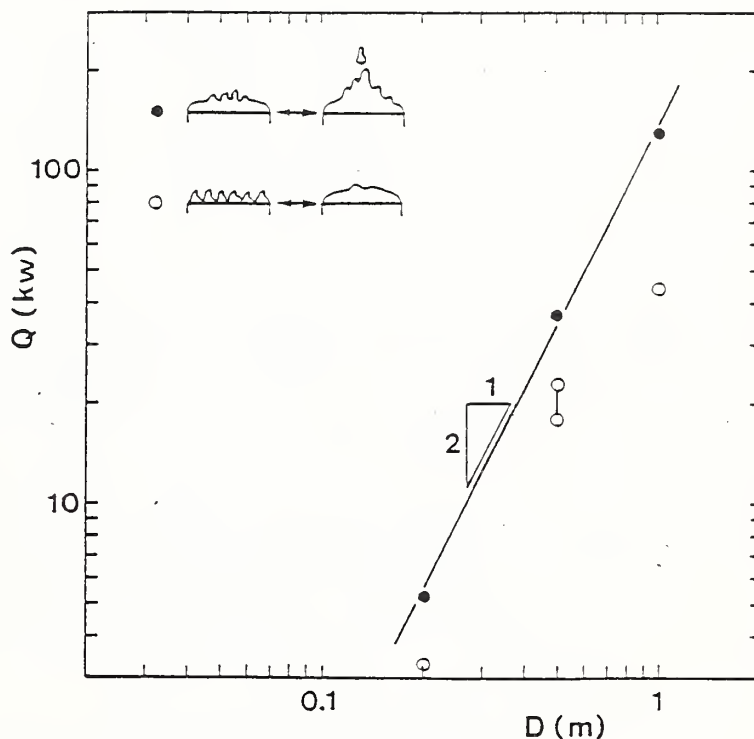


Figure 2 Heat release rate vs. characteristic fuel size at the transition of flame shape

Results of flame height measurements are summarized in Figure 3 and compared with results from earlier works. While the flame height data for $L_f/D < 0.5$ or $Q < 0.1$ are generally scattered, it is evident at each experiment that the slope tends to become sharper in the low L_f/D regime. For $Q < 43\text{kW}$ of the 1.0m burner and for $Q < 23\text{kW}$ of the 0.50m burner, the expression $L_f/D \approx Q^{2/3}$ or $L_f \approx (Q/D^2)^{2/3}$ may be adequate, while L_f/D seems to be proportional to Q for $Q \geq 130\text{kW}$ of the 1.0m burner and for $Q \geq 35\text{kW}$ of the 0.50m burner, and the slope between these two regimes is somewhat less steeper than the both regimes. This gentle slope in the very low Q regime is one significant result which has not been reported in relevant previous reports(10,12). Interestingly, these divisions of the regimes are corresponding to the division for general flame shape as shown in Figure 2.

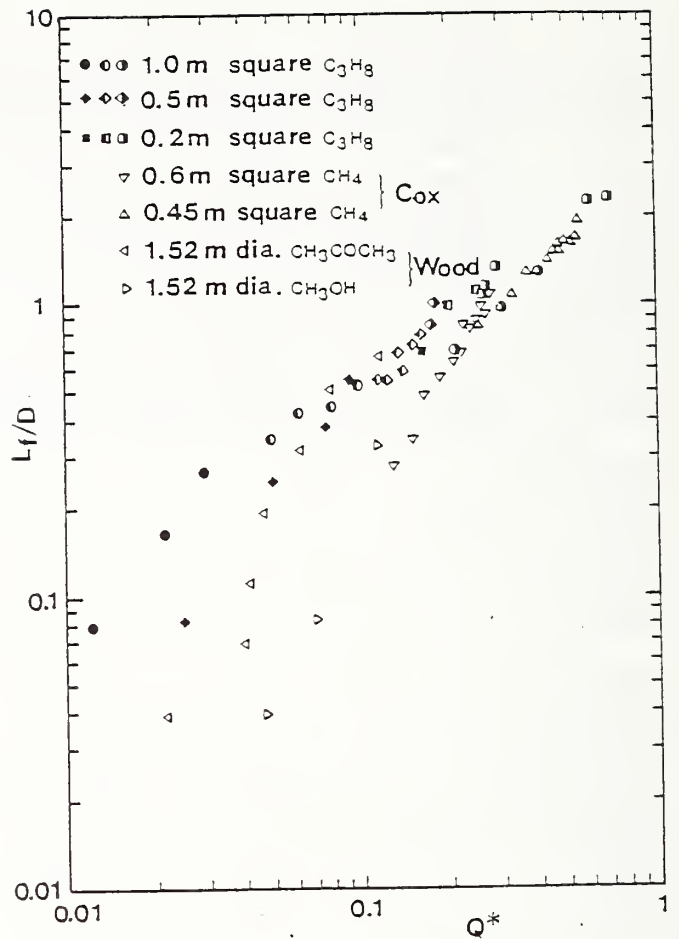


Figure 3 Normalized flame height vs. Q^*
 Characters depicting the regimes in Figure 1 (●◆■: regime I,
 ○◆□: regime II, ○◆△: regime III)

Centerline Temperature

Figure 4 shows the centerline excess temperatures for the 1.0m burner as a function of the height from the burner surface normalized by $Q_*^{2/5} D$; the centerline excess temperatures are somewhat scattered, while they tend to cluster around one curve obtained in previous experiments for around unity of $Q_*^{2/5}$. Since the slopes of most of the data in the figure are evidently less steeper than $-5/3$ while most of the temperature measurements were made above the visible flames, the concept of virtual source was applied to adjust the slope to $-5/3$ as shown in Figure 5. The adjusted data are divided into two groups; one includes only the data from $Q_* > 0.039$, namely the regimes II and III, and the other comes from those on $Q_* < 0.039$ fires. The data on the regimes II and III are scattering around the line obtained in the previous paper(9), whereas the other data are considerably lower than the previous results; this may suggest that the concept of virtual source would fail in the regime I. The centerline excess temperatures for the 0.50m burner are also shown as a function of both $z/Q_*^{2/5} D$ and $(z+\Delta z)/Q_*^{2/5} D$ in Figures 6 and 7. The difference of the regime I and the other in Figure 7 is less significant than in Figure 5. However, the centerline temperature in the regime I is still lower than those in the other regimes.

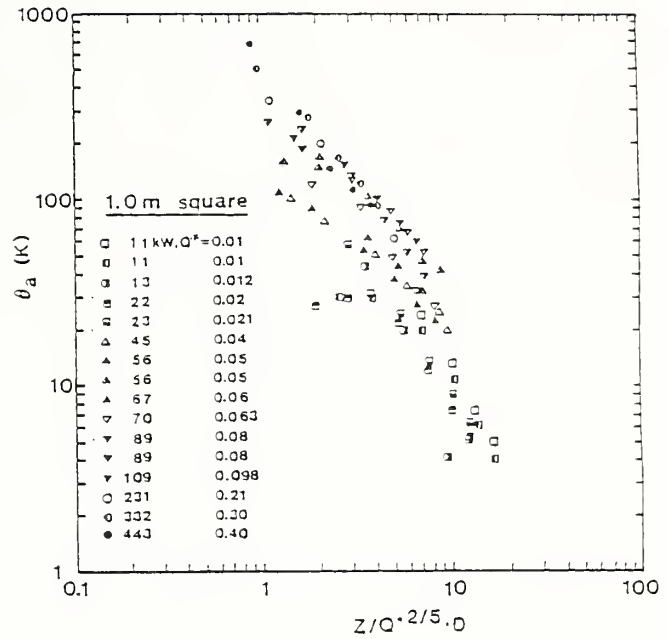


Figure 4 Centerline excess temperature vs. normalized height(1.0m burner)
 Characters depict the regimes in Figure 1(□:regime I,△▽:regime II,
 ○:regime III).

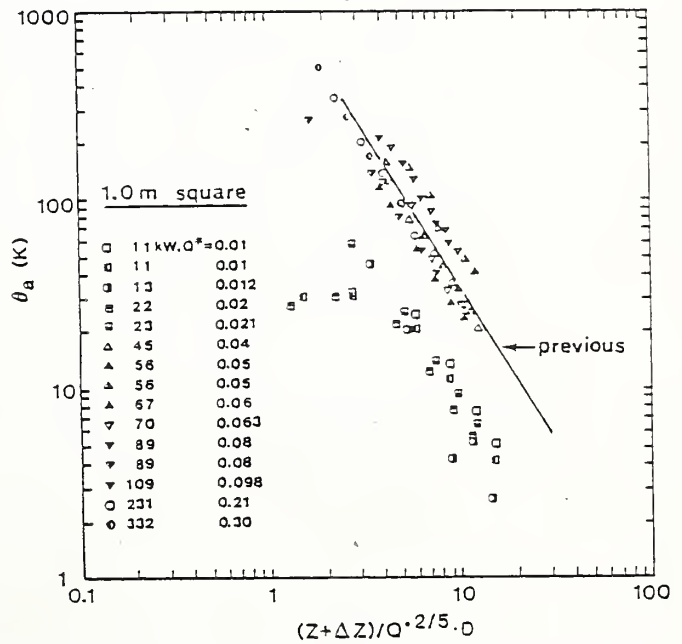


Figure 5 Centerline excess temperature vs. normalized height from virtual
 source(1.0m burner)
 Characters depict the regimes in Figure 1(□:regime I,△▽:regime II,
 ○:regime III).

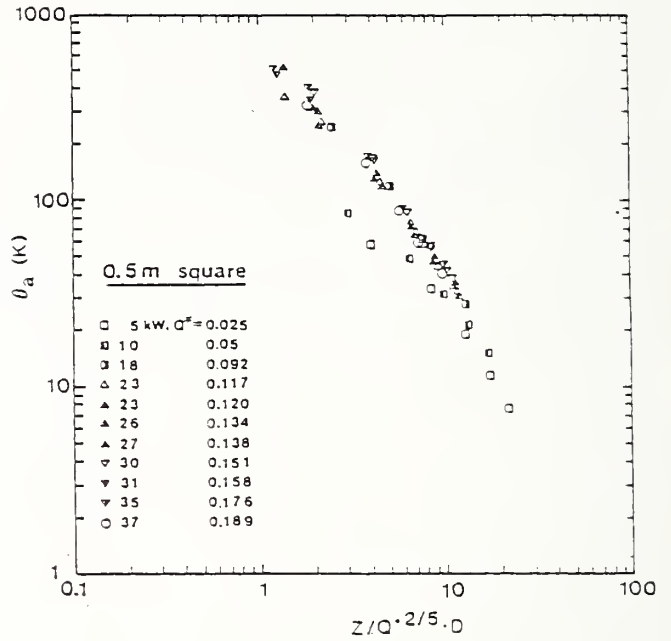


Figure 6 Centerline excess temperature vs. normalized height(0.50m burner)
 Characters depict the regimes in Figure 1(□:regime I,△▽:regime II,
 ○:regime III).

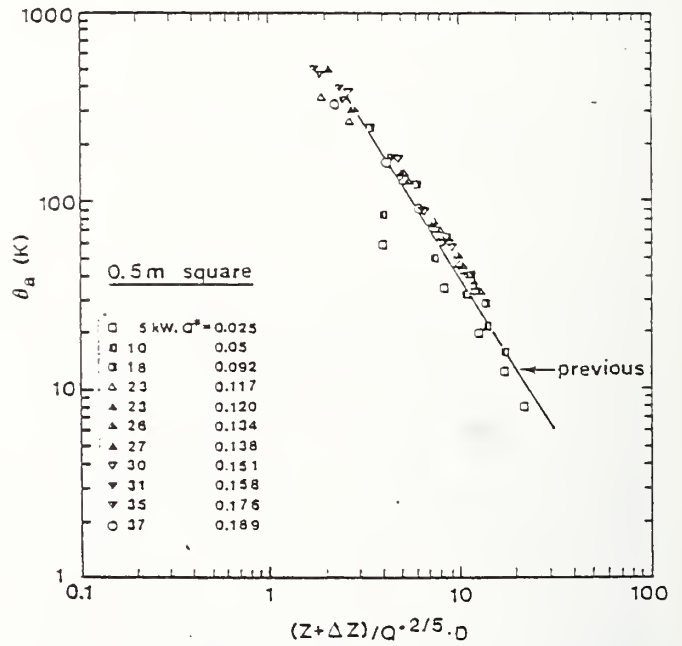


Figure 7 Centerline excess temperature vs. normalized height from virtual
 source(0.50m burner)
 Characters depict the regimes in Figure 1(□:regime I,△▽:regime II,
 ○:regime III).

The location of the virtual source thus obtained is summarized in Figure 8; its depth tends to become lower with decrease of Q^* for $Q^* > 0.039$, and apparently it turns to rise in the regime I. The virtual source locations for $Q^* \geq 0.1$ seems consistent with previous experimental works(7-9); however, for the regime II, the location is considerably lower than the expected value from the previous experiments, and in the regime I, the location is scattered around 0.

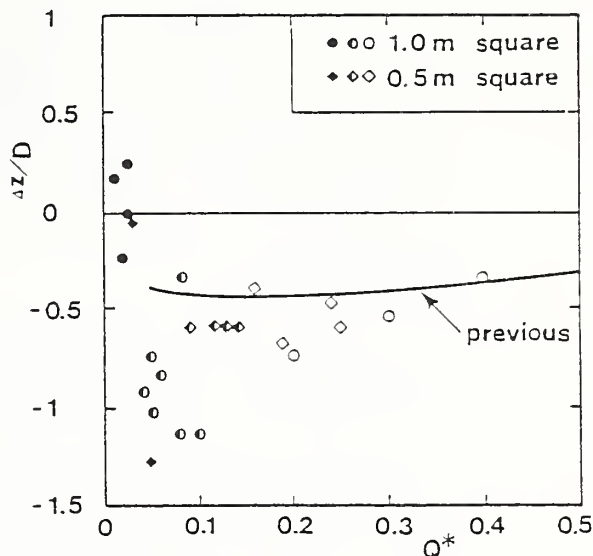


Figure 8 Location of virtual source vs. Q^*
 Characters depict the regimes in Figure 1 (●◆:regime I, ○◇:regime II, ○○:regime III).

DISCUSSIONS

The present experiments seem to show that the $L_f \propto (Q/D^2)^2$ relationship holds for very low Q fires, in the regime I of Figure 1 or 2, as anticipated from previous dimensional studies(1,10,11). However, there is still considerable discrepancy in the flame height between the 1.0m and 0.50m burners, and the transition from the regime I to II does not seem to be governed by Q^* . Controlling mechanism of these transitions are important from the viewpoint of fire safety; in a room fire, the difference of regimes implies a significant difference of preheating of surrounding combustibles by the flame, and, in a mass fire, this transition may provide some information concerning the criticality for the confluence of individual flames into a gigantic flame which is attributed to one mechanism leading to a great loss as seen at The Kanto Earthquake Fire(1923).

The following is an exploratory discussion to seek a responsible mechanism for these criticalities based on the dimensional relationships obtained in the present experiments, while it should be noted in advance that different mechanisms may induce one identical dimensional relationship and there is still some possibilities of other mechanisms leading to the criticalities.

One possible cause for these transitions is the criticality of oxygen supply by entrainment. At the upper bound of the regime II for the 1.0m burner, the filmy flame appeared to cover the whole surface of the burner, and therefore the appearance of flametips is attributed to the lack of oxygen supplied onto the burner surface. Actually the heat release rate at this criticality is proportional to the burner surface area, D^2 , as seen in Figure 2, and it is expected that there is a critical available oxygen or fresh air rate per unit fuel surface area. Using the general value of reaction heat per unit mass of air for usual natural fuels(2700kJ/kg, see Ref.13), the critical

available entrained air, M, per unit area based on the above hypothesis is estimated as

$$M/D^2 = 0.052 \text{ (kg/m}^2\text{)} \quad (2)$$

The transition from individual flamelets to a filmy fire must be related more to the entrainment through the circumference of the fuel surface, since the nature of this criticality is somewhat "local" in the sense that a filmy flame starts to develop along the margin of a fuel and gradually takes the place of flamelets in the central part of the burner by the increase of Q. If this criticality depends on the heat release rate per entrainment through the circumference, Q/D may be a primary parameter characterizing this criticality; this mechanism is worth studying since the power of D representing Q at this criticality in Figure 2 is somewhat close to 1.

CONCLUSIONS

Some experimental observations on low Q^* fires are reported. The following conclusions can be drawn.

- 1 Flame behavior can be classified into 3 regimes according to the shape of the flame.
- 2 For $Q/D^2 = 140 \text{ kW/m}^2$, flametips are observed above a continuous flame, and flame height is proportional to $2/3$ power of heat release rate.
- 3 For very low Q , fire is broken into individual flamelets, and flame height is apparently proportional to $(Q/D^2)^{2/3}$. In this regime, the concept of virtual source fails evidently.
- 4 There is a transition regime between the above two regimes. In this regime, fire looks like a combusting boundary layer under forced convection. The dependence of flame height on heat input is less significant than in either of the two regimes. The concept of virtual source seems to hold in this region.
- 5 Experiments using larger fuels is encouraged to develop a model to predict the practical properties of low Q fires.

ACKNOWLEDGEMENTS

The authors are indebted to Mr. Jun'ichi Izumi, research associate of BRI from Mitsui Homes Co., for the assistance in the experiments. The authors are also grateful to Mr. Hideo Matsumoto of BRI who fabricated the major apparatus for the experiments. His effort to build a large uniform burner is gratefully appreciated.

TERMINOLOGY

C	specific heat of air
D^p	characteristic fuel size
L_f	flame height
M_f	entrained air
Q^*	heat release rate
Q	dimensionless heat release rate defined as $Q/\rho_o T_o g^{1/2} D^{5/2}$
T	absolute temperature
g	gravitational acceleration
ρ	density

suffix

o . ambient air
crit criticality

REFERENCES

- 1 Thomas, P.H., Webster, C.T., and Raftery, M.M., "Some Experiments on Buoyant Diffusion Flames," *Combustion and Flame*, Vol.5, 1961, pp.359-367.
- 2 McCaffrey, B.J., "Purely Buoyant Diffusion Flames: Some Experimental Results," NBSIR-79-1910, 1979.
- 3 Cox, G., and Chitty, R., "A Study of the Deterministic Properties of Unbounded Fire Plumes," *Combustion and Flame*, Vol.39, 1980, pp.191-209.
- 4 Zukoski, E.E., Kubota, T., and Cetegen, B., "Entrainment in Fire Plumes," *Fire Safety Journal*, Vol.3, 1980/81, pp.107-121.
- 5 Hasemi, Y., and Tokunaga, T., "Deterministic Modeling of Unconfined Turbulent Diffusion Flames," *Transactions of ASME, Journal of Heat Transfer*, Vol.108, 1986, pp.882-888.
- 6 Heskestad, G., "Luminous Heights of Turbulent Diffusion Flames," *Fire Safety Journal*, Vol.5, 1983, pp.103-108.
- 7 Cetegen, B.M., Zukoski, E.E., and Kubota, T., "Entrainment and Flame Geometry of Fire Plumes," NBS-GCR-82-402, 1982.
- 8 Heskestad, G., "Virtual Origins of Fire Plumes," *Fire Safety Journal*, Vol.5, 1983, pp.109-114.
- 9 Hasemi, Y., and Tokunaga, T., "Flame Geometry Effects on the Buoyant Plumes from Turbulent Diffusion Flames," *Fire Science and Technology*, Vol.4, 1984, pp.15-26.
- 10 Cox, G., and Chitty, R., "Some Source-dependent Effects of Unbounded Fires," *Combustion and Flame*, Vol.60; 1985, pp.219-232.
- 11 Zukoski, E.E., "Fluid Dynamic Aspects of Room Fires," *Proc. First International Symposium on Fire Safety Science*, 1985, pp.1-30.
- 12 Wood, B.D., Blackshear, P.H., and Eckert, E.R.G., "Mass Fire Model: An Experimental Study of the Heat Transfer to Liquid Fuel Burning from a Sand-filled Pan Burner," *Combustion Science and Technology*, Vol.4, 1971, pp.113-129.
- 13 Huggett, C., "Estimation of Heat release by Means of Oxygen Consumption Measurements," *Fire and Materials*, Vol.4, No.2, 1980, pp.61-65.

TRANSIENT COMBUSTION IN A TURBULENT FIRE

Howard R. Baum
Ronald G. Rehm
Center for Fire Research
National Bureau of Standards
Gaithersburg, Maryland 20899, USA

ABSTRACT

A mathematical model of the local transient diffusion flame generated by a mixing in a turbulent eddy is presented. It is intended ultimately as a computational "molecule" to be imbedded in the authors existing numerical simulation of large scale fire driven flows. The model consists of a three dimensional strain-vortex field which exactly satisfies the constant property Navier Stokes equations, a convection diffusion equation for the mixture fraction which determines the thermodynamic quantities, and a potential flow determined by the conservation of mass. The properties of the model are explained and its relevance to turbulent combustion are illustrated by sample results.

1. INTRODUCTION

The purpose of this paper is the presentation of a mathematical model of gas phase combustion appropriate for use in a field equation simulation of enclosure fires. It is therefore necessary to summarize briefly how such simulations are performed. Typically, the enclosure containing the fire is divided into a large number of rectangular cells. Within each cell the laws expressing the conservation of mass, momentum, and energy in each cell are represented in an approximate algebraic form so that a single value for the velocity, temperature, and pressure is associated with each cell at any instant of time. Given a set of values for these quantities at any instant of time, the conservation laws then determine their values a small interval of time later. Thus, for a prescribed initial state and room geometry, the evolution of the gaseous properties in the room can be predicted.

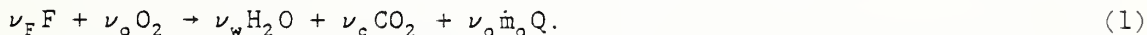
Clearly, the accuracy with which such a simulation can be carried out depends strongly upon the number of cells that can be employed in the calculation. Using modern numerical techniques on current generation vector computers, it is quite feasible to employ roughly 10^5 computational cells and several thousand time intervals. Figure 1 shows a sample time frame from a calculation performed by the authors (1). The motion is followed by seeding the flow with thousands of point particles which originated in the fire. The $(40)^3$ grid used means that the minimum length scale in the computation is 7.5 cm. While this is adequate to resolve the largest scales of the turbulent fire induced flow, the diffusion controlled combustion phenomena characteristic of fires typically evolve on sub-millimeter scales. Indeed, the flow in figure 1 was calculated by replacing the fire with a prescribed heat source.

In order to study the combustion itself, it is necessary to abandon a grid fixed in space. Instead, attention is focused on the fuel, since only in the vicinity of the fuel can combustion occur. Each of the point particles is now taken to represent a fixed mass of fuel. The location of each blob of fuel at each instant of time is determined by tracking the particles trajectory through the large scale flow. If the rate of heat release of each fuel parcel can be determined as a function of its local environment for each instant of time; then the composite heat release rate of all the fuel parcels represents the desired replacement for the prescribed heat release currently employed. In order to determine the rate of heat release of an individual fuel blob, it is necessary to change the scale of the analysis and consider in detail how it burns. (See fig. 1).

2. MODEL FORMULATION

The combustion process viewed on the scale of an individual fuel parcel contains three essential ingredients: First, the molecular mixing of fuel and oxidizer and consequent release of heat; second, a local flow field on the scale of the fuel parcel characteristic of turbulence, to enhance the molecular mixing; finally, a mechanism whereby the flow is modified by the combustion process.

To address the first point we consider a highly idealized reaction between a fuel F and oxygen leading to "perfect" combustion denoted by the reaction



Here, ν_i are the stoichiometric coefficients for the overall reaction and Q is the energy released per unit mass of oxygen consumed. While such a model is hopeless as a description of the real combustion chemistry, and says nothing about the resulting carbon balance between soot, CO, and CO₂ it is a useful starting point for the mixture fraction concept. This concept can be generalized to permit real combustion chemistry to be incorporated (2). We further assume that all species diffuse according to Ficks law with equal diffusion coefficients D, and that the Lewis Number of the mixture is unity. Then, in a frame of reference moving with the fuel parcel, the species mass fractions Y_i and temperature T obey the following conservation equations:

$$\rho C_p \left\{ \frac{\partial T}{\partial t} + \vec{u} \cdot \nabla T \right\} - \nabla \cdot (\rho D \nabla T) = \dot{q} \quad (2)$$

$$\rho \left\{ \frac{\partial Y_i}{\partial t} + \vec{u} \cdot \nabla Y_i \right\} - \nabla \cdot (\rho D \nabla Y_i) = \dot{m}_i$$

The quantities \dot{q} and \dot{m}_i in equations (2) are the rate of heat released and mass consumed for each species respectively per unit volume, while \vec{u} is the fluid velocity and ρ the density.

We are now in a position to introduce the mixture fraction variable. The stoichiometry given by equation (1) implies the following relationships between \dot{q} , \dot{m}_i , the stoichiometric coefficients ν_i , and the molecular weight m_i :

$$\dot{m}_F/\nu_F m_F = \dot{m}_O/\nu_O m_O = -\dot{q}/Q\nu_O m_O = \dot{m}_W/\nu_W m_W = \dot{m}_C/\nu_C m_C$$

These relationships allow all of eqs. (2) to be collapsed to a single equation for the mixture fraction Z , defined as:

$$Z \equiv (\beta - \beta^\infty)/(\beta^I - \beta^\infty) \quad (3)$$

Here β is any of the quantities conserved in the reaction

$$\begin{aligned} \beta_1 &= Y_F/\nu_F m_F - Y_O/\nu_O m_O \\ \beta_2 &= C_p T/Q + Y_O \\ \beta_3 &= Y_{n_2} ; \beta_4 = Y_F/\nu_F m_F + Y_W/\nu_W m_W \\ \beta_5 &= Y_W/\nu_W m_W - Y_C/\nu_C m_C = 0 \end{aligned} \quad (4)$$

The quantity β^∞ denotes the value of the conserved quantity in the ambient environment seen by the individual fuel parcel; this value is ultimately determined from the large scale flow calculation. The quantity β^I is the initial value of β at the instant the fuel parcel is injected into the gas phase from the burning object. The result is that all of equations (2) can be replaced by a single equation and initial conditions for the mixture fraction Z .

$$\rho \left\{ \frac{\partial Z}{\partial t} + \vec{u} \cdot \nabla Z \right\} = \nabla \cdot (\rho D \nabla Z) \quad (5)$$

$$\begin{aligned} Z(o, \vec{r}) &= 1 && \text{in fuel} \\ Z(o, \vec{r}) &= 0 && \text{otherwise} \end{aligned}$$

The connection between Z and the physical variables is completed by adding an equation for the gas and the fast chemistry assumption to equations (3) and (4). The equation of state is assumed to have the form:

$$\rho T = \rho_\infty T_\infty \quad (6)$$

The fast chemistry assumption means that fuel and oxidizer cannot coexist. Thus, the quantity β , represents fuel for $Z > Z_s$, the flame sheet value of the mixture fraction, and oxidizer for $Z < Z_s$. Requiring that fuel and oxidizer vanish at the flame sheet readily yields the flame sheet temperature T_s and mixture fraction Z_s as:

$$Z_s = (Y_o^a / \nu_o m_o) (Y_F^i / \beta \nu_F m_F + Y_o^a / \nu_o m_o)^{-1} \quad (7)$$

$$T_s = T_\infty + \frac{Q}{C_p} (Y_F^i + (\nu_F m_F / \nu_o m_o) Y_o^a)^{-1}$$

The state relationships between Y_i , T , ρ , and Z are shown schematically in fig. 2. While the sketch applies only to the idealized reaction given in eq. (1), Bilger (2) has pointed out that laminar flame data can be used to generate a realistic set of state relations that are applicable to turbulent flows. Faeth (3) has exploited this idea to predict the structure and radiation from turbulent buoyant jets. Pagni (4) has used variables equivalent to Z in his analysis of excess pyrolyzate.

Next, we consider an appropriate description of the local flow field on the scale of the fuel parcel. In a frame of reference moving with the large scale fluid motion, it is always possible to express the local velocity \vec{u} as a combination of a solenoidal (vortex-induced) velocity \vec{v} and an irrotational flow derived from a potential ϕ .

$$\vec{u} = \vec{v} + \nabla\phi \quad (8)$$

$$\nabla \cdot \vec{v} = 0 \quad ; \quad \nabla \times \vec{v} = \vec{\omega}$$

The vortex induced velocity field is assumed to be a transient vortex stretched by imposed strain field (5). The geometry of this strain-vortex field is illustrated in fig. 3. This geometry is known to be characteristic of the velocity field in an individual turbulent eddy. In fact, it can be shown that the smallest length scale in this model emerges naturally as Kolmogoroff scale (5).

The vortex induced velocity field is an exact solution of the constant property Navier-Stokes equations. If v_x , v_r , and v_θ are relatively the axial, radial, and swirl components of the solenoidal velocity field, the Navier-Stokes equations have solutions of the form:

$$\begin{aligned} v_x &= \alpha x; \quad v_r = -\alpha r/2; \quad v_\theta = \Omega r_o W(r,t) \\ r &= r_o r; \quad t = (\alpha)^{-1} t \end{aligned} \quad (9)$$

Here α is the imposed strain rate; Ω the initial vorticity, and r_o the initial radius of the vortex. The intensification and collapse of the vortex induced swirl are shown in figure 4 for a local Reynolds number $\alpha r_o^2 / \nu$ of 500.

Finally, we consider the feedback of the energy release on the flow field. This consists of two parts. First, the heat released from the fuel parcels acts as a distributed heat source for the large scale fluid motion; altering the density field and thus changing the buoyancy forces which drive the large scale flow. Second, the expansion due to the heat addition generates a

potential field which alters the local velocity on a small scale. Since attention is focused on the local flow field on the scale of the individual fuel parcel, we consider the second part.

To proceed, note that the conservation of mass can be written in the form:

$$\left\{ \frac{\partial \rho}{\partial t} + \vec{u} \cdot \nabla \rho \right\} + \rho \nabla \cdot \vec{u} = 0 \quad (10)$$

Now recall that all thermodynamic variables can be related uniquely to the mixture fraction variable Z . Using this fact together with the velocity decomposition given by eq. (8) in eq. (10), an equation for the velocity potential ϕ is obtained. The solution to this equation is:

$$\phi = J + \frac{Q}{\rho_a C_p T_a} \left(\frac{\nu_o m_o}{\nu_F m_F} Y_F^I + Y_o^a \right) \frac{\rho_s D_s}{4\pi} \int_{z=z_s} ds n_k \frac{\partial Z}{\partial y_k} \frac{1}{|\vec{x} - \vec{y}|}$$

$$J = \frac{Q}{\rho_a C_p T_a} Y_F^I \frac{\nu_o m_o}{\nu_F m_F} \int_0^z \rho(Z) D(Z) dZ \quad ; \quad 0 \leq Z \leq Z_s \quad (11)$$

$$J = \frac{-Q}{\rho_a C_p T_a} Y_o^a \int_0^z \rho(Z) D(Z) dZ \quad ; \quad Z_s \leq Z \leq 1$$

The physical content of eq. (11) is that the flow induced by the local heat addition consists of two parts. The contribution denoted by J is the heat flux conducted away from the flame sheet towards either the ambient gas or the interior of the fuel parcel. The formulae differ on either side of the flame sheet because the conduction heat flux vector is discontinuous at the flame sheet itself. The discontinuity arises because in the fast chemistry limit, the chemical heat release is confined to the flame sheet, a (possible multiply connected) surface characterized by the mixture fraction taking on the value Z_s given by eq. (7). The remaining contribution to the portion ϕ is the direct effect of the heat addition. The integral involves the mixture fraction gradient evaluated at the flame sheet, integrated over the entire reaction surface. Although the two contributions give rise to comparable velocities, the velocity gradients associated with the heat flux are much larger, and these terms are much more important in coupling the velocity field to the heat release.

3. ANALYSIS AND DISCUSSION

The combustion model may now be summarized as follows: The gasified fuel is to be represented by a large number of distinct parcels, which interact with and modify their local environments. The rate of heat release q_p for each fuel parcel may be computed as:

$$q_p = -Q \left(\frac{\nu_o m_o}{\nu_F m_F} Y_F^I + Y_o^o \right) \rho_s D_s \int \phi ds n_k \frac{\partial Z}{\partial x_k} \quad (12)$$

In order to evaluate this formula, it is necessary to solve for Z. This requires a solution to eq. (5), with the velocity field expressed by eqs. (8), (9), and (11). Since the potential flow (eq. (11)) itself involves Z, and the density ρ as well as the diffusivity D are both functions of Z, the resulting system is highly non-linear. Moreover, the intense mixing induced by the vortex field leads to an extremely convoluted interface across which the fuel and oxidizer diffuse. The remainder of this paper discusses how these difficulties may be approached and a solution for the mixture fraction obtained.

The starting point for the analysis is equation (5). Since $\rho(Z)$ and $D(Z)$ are non-differentiable functions of the mixture fraction, it is more convenient to work with a modified mixture fraction $F(Z)$, defined by:

$$F(Z) = \int_0^Z \rho(Z)D(Z)dZ / \int_0^1 \rho(Z)D(Z)dZ \quad (13)$$

The function $F(Z)$ varies within the range $0 \leq F \leq 1$, and is constant with value F_s , say, along the flame sheet. The velocity potential can be written as:

$$\begin{aligned} \phi &= \phi_s + K_+ F(Z) ; & 0 \leq F \leq F_s \\ \phi &= \phi_s - K_- F(Z) ; & F_s \leq F \leq 1 \end{aligned} \quad (14)$$

Here, ϕ_s denotes the contribution of the surface integral over the flame sheet in eq. (11), while the constants K_+ and K_- are given by:

$$K_+ = \frac{Q}{\rho_o C_p T_o} Y_F^I \frac{\nu_o m_o}{\nu_F m_F} \int_0^1 \rho(Z)D(Z)dZ \quad (15)$$

$$K_- = \frac{Q}{\rho_o C_p T_o} Y_o^o \int_0^1 \rho(Z)D(Z)dZ$$

The mixture fraction equation can now be rewritten in terms of F in the form:

$$\begin{aligned} \frac{\partial F}{\partial t} + (\vec{v} + \nabla \phi_s) \cdot \nabla F + K_+ (\nabla F)^2 &= D \nabla^2 F ; & 0 \leq F \leq F_s \\ \frac{\partial F}{\partial t} + (\vec{v} + \nabla \phi_s) \cdot \nabla F - K_- (\nabla F)^2 &= D \nabla^2 F ; & F_s \leq F \leq 1 \end{aligned} \quad (16)$$

The function F and its first derivative are continuous across the flame sheet for times $t > 0$, while the initial conditions for F are identical with those for Z (see equation (5)).

To proceed, it is necessary to approximate the diffusion coefficient D by a constant value, which will for the present taken to be the flame sheet value, D_s . We also note that at high Reynolds numbers the vortex induced velocity \vec{v} is both larger in magnitude and has much steeper gradients than the heat release potential flow $\nabla\phi_s$. This contribution to the potential flow is henceforth neglected. Given these simplifications, it is possible to reduce equations (16) to a single constant property linear equation without further approximation. We introduce a new dependent variable, the pseudo-mixture fraction G defined as follows:

$$\begin{aligned} G &= a_+ + b_+ \exp(-K_+ F/D_s) ; 0 \leq F \leq F_s \\ G &= a_- + b_- \exp(K_- F/D_s) ; F_s \leq F \leq 1 \end{aligned} \quad (17)$$

The quantities a_+ , a_- , b_+ , and b_- are chosen so that the continuity of F and ∇F at the flame sheet implies continuity of G and ∇G there. We also require that G vanishes with F and that $G=1$ when $F=1$. This leads to a simple linear system of algebraic equations which will not be displayed here. The more important result is that equations (16) collapse to the single linear equation

$$\begin{aligned} \frac{\partial G}{\partial t} + (\vec{v} \cdot \nabla) G &= D_s \nabla^2 G \\ G(0, r) &= 1 \text{ in Fuel} \\ G(0, r) &= 0 \text{ otherwise.} \end{aligned} \quad (18)$$

At this point the issue of non-linearity has been dealt with; and we turn to the effect of mixing by the vortex. This had been studied by Marble (6), Karagozian and Marble (7), and Lundgren (8) within the context of an inviscid flow field. Here, we indicate an alternative approach which allows for viscous effects and can handle a variety of fuel geometries (5). The solution for the stretched vortex flow represented by equations (9) can be used to generate a set of Lagrangian cylindrical coordinates ξ , ρ , ϕ ; analogous to the cylindrical coordinates x , r , θ illustrated in figure 3. The transformation is defined by the relations

$$\begin{aligned} \xi &= \hat{x} \exp(-\hat{t}) \\ \rho &= \hat{r} \exp(\hat{t}/2) \\ \phi &= \theta - (\Omega/\alpha\epsilon) \psi(\rho, \tau) \\ \psi(\rho, \tau) &= (\rho)^{-1} \int_0^\tau V(\rho, \tau) d\tau \end{aligned} \quad (19)$$

$$\tau = \epsilon [\exp(\hat{t}) - 1]$$

$$\hat{w} = \exp(\hat{t}/2) V(\rho, \tau)$$

$$\epsilon = \nu / \alpha r_0^2$$

Note that the quantity ϵ is the reciprocal of the local Reynolds number which sets the local viscous length scale in the vortex flow defined in equation (9).

The introduction of Lagrangian coordinates transforms equation (18) into the form:

$$\frac{\partial G}{\partial \tau} = \frac{1}{S_c} \left\{ (1 + \tau/\epsilon)^{-3} \frac{\partial^2 G}{\partial \xi^2} + \frac{1}{\rho} \frac{\partial}{\partial \rho} \left(\frac{\rho \partial G}{\partial \rho} \right) + \frac{D_{\phi\phi}}{\rho^2} \frac{\partial^2 G}{\partial \phi^2} \right. \\ \left. - (\Omega/\alpha\epsilon) \left[\frac{1}{\rho} \frac{\partial}{\partial \rho} \left\{ \left(\frac{\rho \partial \psi}{\partial \rho} \right) \frac{\partial G}{\partial \phi} \right\} + \frac{\partial \psi}{\partial \rho} \frac{\partial^2 G}{\partial \rho \partial \phi} \right] \right\} \quad (20)$$

Here, S_c is the Schmidt number ν/D , and $D_{\phi\phi}$ is the effective azimuthal diffusivity in Lagrangian cylindrical coordinates given by:

$$D_{\phi\phi} = +1(\Omega/\alpha\epsilon)^2 \left(\frac{\partial \psi}{\partial \rho} \right)^2 \quad (21)$$

Equations (20) and (21) are very important in understanding the role of vorticity in turbulent combustion. Note that in Lagrangian coordinates there is no advection by definition, but the diffusion is now both anisotropic and inhomogeneous. In the absence of diffusion ($S_c \rightarrow \infty$) G would not change from its initial state in these coordinates. Thus, the mixing process is contained in the transformation given by equations (19). As an example, the evolution of a cross section of an initially spherical parcel of fluid due to vortex mixing is shown in figure 5. The shape in Lagrangian coordinates in the absence of diffusion remains a circle displaced from the center of the vortex.

The diffusion itself is strongly enhanced by the vortex induced strain. Figure 6 shows the quantity $(\Omega/\alpha\epsilon)$ plotted versus the Lagrangian radial coordinate ρ for the velocity field $(\partial\psi/\partial\rho)$ displayed in figure 4. Recall that the local Reynolds number is 500 in this calculation. Even for this relatively modest Reynolds number, figure 6 and equation (21) show that in the region of most intense vorticity, the azimuthal diffusivity is enhanced by a factor of over 10^3 relative to its value in the absence of eddy motion. The final stage of the analysis exploits this directionality to obtain a solution for the pseudo-mixture fraction G .

The solution proceeds in two parts. Although a formal result can be obtained for any initial shape of fuel parcel, we restrict attention at present to a sphere of radius R_0 displaced from the center of the vortex as shown in figure 7. Then, in the absence of the vortex (i.e. strain only), the diffusion equation can be readily solved in the form:

$$G = \frac{S_c}{2\tau} \int_0^{R_0} d\lambda \lambda J(\lambda, \xi - a) \exp \left\{ \frac{-S_c}{4\tau} (\hat{\rho}^2 + \lambda^2) \right\} I_0 (S_c \lambda \hat{\rho} / 2\tau)$$

$$J = \frac{1}{2} \left\{ \operatorname{erf} \left[\left(\frac{S_c}{4f} \right)^{1/2} (\xi - a + \sqrt{R_0^2 - \lambda^2}) \right] + \operatorname{erf} \left[\left(\frac{S_c}{4f} \right)^{1/2} (a - \xi + \sqrt{R_0^2 - \lambda^2}) \right] \right\} \quad (22)$$

$$\hat{\rho} = (\rho^2 - 2b \rho \cos \phi + b^2)^{1/2}$$

$$f(\tau) = \tau(1 + \tau/2\epsilon)/(1 + \tau/\epsilon)^2$$

Here, a and b are parameters describing the displacement of the sphere from the center of symmetry of the strain field. Denote this solution by G ($\Omega=0$). Now this solution can always be expanded in a Fourier series in the form

$$G(\Omega = 0) = \sum_{n=-\infty}^{\infty} \exp(in\phi) \hat{G}_n(\rho, \xi, \tau). \quad (23)$$

Although the Fourier coefficients G_n can obviously be expressed as an integral, in practice it is undoubtedly much more efficient to apply the Fast Fourier Transform (FFT) algorithm to tabulated values of $G(\Omega=0)$ directly. In any event, once values of G_n have been obtained, a further analysis of equation (20) shows that in the large Schmidt number large Reynolds number limit (5), the solution to the full equation becomes:

$$G = \sum_{n=0}^{\infty} \exp(in\phi) \hat{G}_n(\rho, \xi, \tau) \zeta_n(\rho, \tau) \quad (24)$$

$$\zeta_n = \exp\{-n^2 (S_c)^{-1} (\Omega/\alpha\epsilon)^2 \int_0^{\tau} \left(\frac{\partial \psi}{\partial \rho} \right)^2 d\tau\}$$

Physically, the solution states that the vortex free solution is appropriate in any region not yet caught up in the vortex. However, once the vortex passes thru any region of space, the azimuthal diffusion dominates all else. This effect is weakly modulated by the remaining anisotropy in the strain induced (vortex-free) diffusion. The large Schmidt number limit is not appropriate in a formal sense for gaseous mixtures. However, in the analogous case of heat transfer, Lighthill (9) has shown that the large Prandtl number limit, while even less appropriate for gases, in fact yields a very accurate approximation for boundary layer heat transfer in gases. It is also worth

noting that equation (24) contains as special cases all previous results (6), (7), (8) in the absence of viscous effects on the flow field.

4. CONCLUDING REMARKS

The mathematical combustion model whose formulation and analysis is outlined above, is but one ingredient required in a comprehensive simulation of fires in enclosures. The roles of radiation and soot particulate formation have yet to be addressed. These phenomena are also crucial to an understanding of fire growth processes, since the radiative feedback to burning surfaces provides the energy needed to gasify the fuel in the first place. However, it is necessary to begin somewhere; and if the gas phase combustion can be adequately predicted by models like that described above, then a useful basis for more complete studies will be in place.

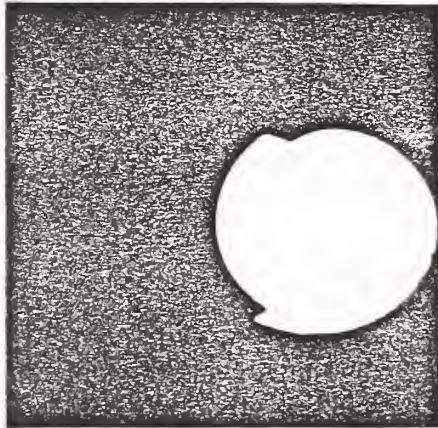
5. ACKNOWLEDGEMENT

This work was supported by the Air Force Office of Scientific Research under Contract #ISSA-87-0018.

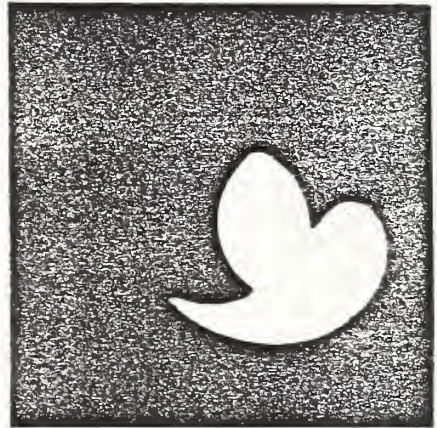
6. REFERENCES

- (1) Baum, H.R. and Rehm, R.G.: *Combustion Science and Technology* 40, p. 55, 1984.
- (2) Bilger, R.W.: "Turbulent Reacting Flows" (P.A. Libby and F.A. Williams, Eds.) p. 65, Springer-Verlag, 1980.
- (3) Jeng, S-M., Lai, M-C., and Faeth, G.M.: *Combustion Science and Technology* 40, p. 41, 1984.
- (4) Pagni, P.J. and Shih, T.M.: "Sixteenth Symposium (International) on Combustion", p. 1329, The combustion Institute, 1976.
- (5) Baum, H.R., Corley, D.M., and Rehm, R.G.: *Twenty First International Symposium on Combustion*, The Combustion Institute (In Press).
- (6) Marble, F.E.: "Recent Advances in the Aerospace Sciences" (C. Casci, Ed.), p. 395, Plenum, 1985.
- (7) Karagozian, A.R. and Marble, F.E.: *Combustion Science and Technology* 45, p. 65, 1985.
- (8) Lundgren, T.S.: *Phys. Fluids* 40, p. 1641, 1985.
- (9) Lighthill, M.J.: *Proc. Roy. Soc. A* 202, p. 359, 1950.

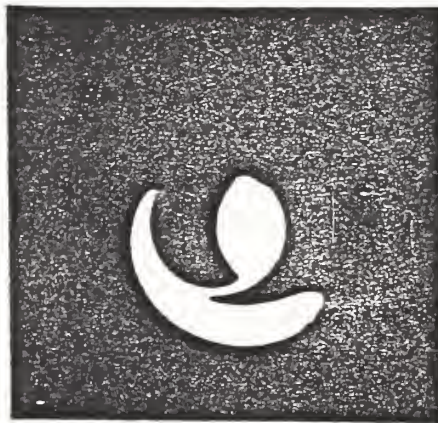
$\varepsilon = .002 \quad \hat{\Omega} = 2. \quad \text{TIME} = 0.10$



$\varepsilon = .002 \quad \hat{\Omega} = 2. \quad \text{TIME} = 0.50$



$\varepsilon = .002 \quad \hat{\Omega} = 2. \quad \text{TIME} = 1.0$



$\varepsilon = .002 \quad \hat{\Omega} = 2. \quad \text{TIME} = 1.5$



Figure 5. Mixing of initially spherical fuel parcel by vortex displaced one half radius from center. Local Reynolds number 500, vorticity/strain ratio 2.

Buoyant Convection and Combustion Models

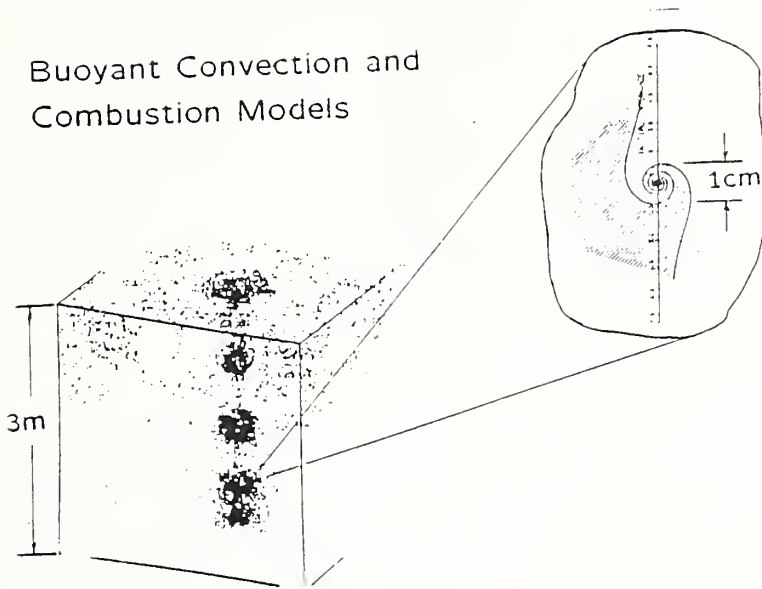


Figure 1. Relationship of buoyant convection and combustion models

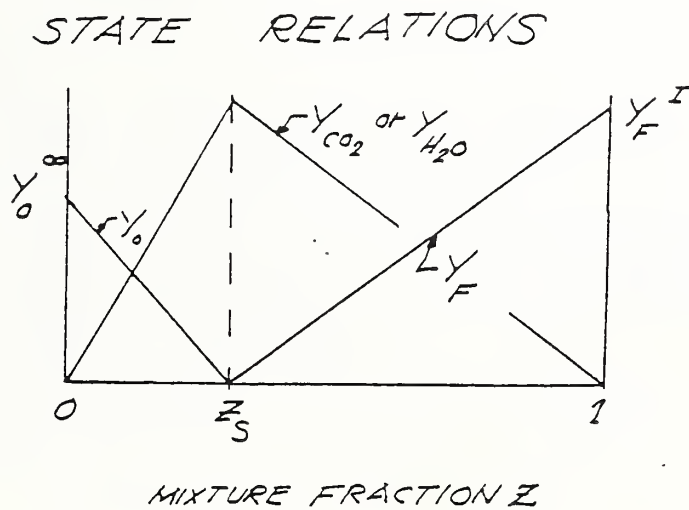


Figure 2. Sketch of state relationships between dependent variables and Z

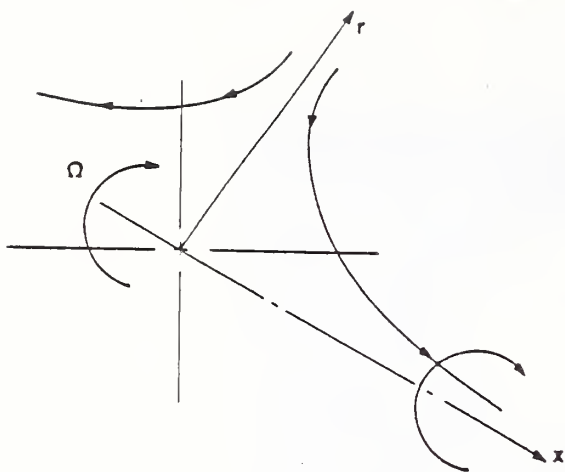


Figure 3. Vortex-Stain field geometry

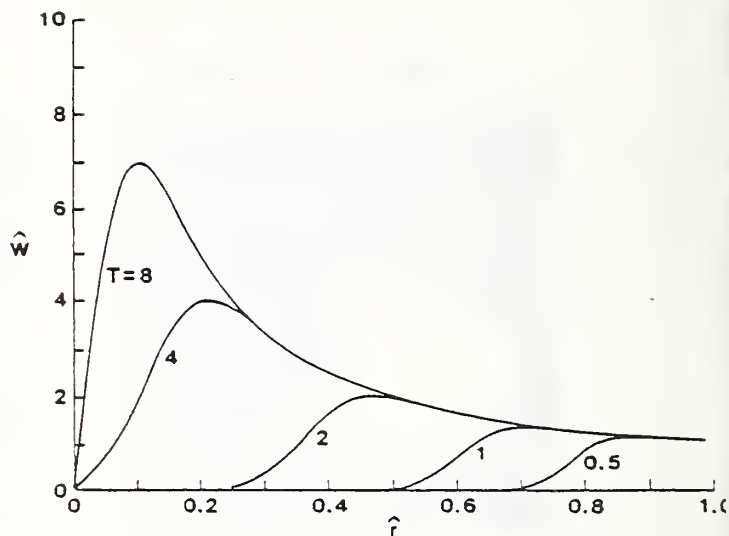


Figure 4. Swirl velocity in vortex

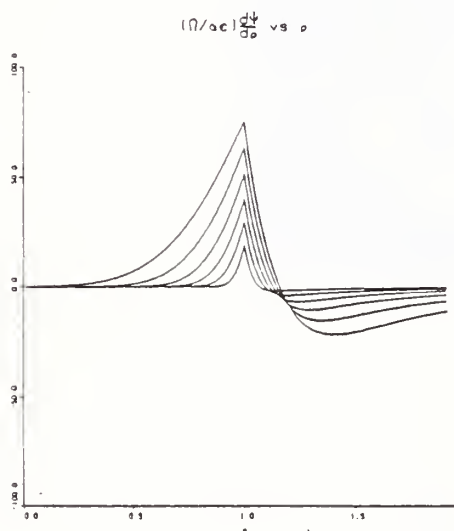


Figure 6. Diffusivity enhancement function

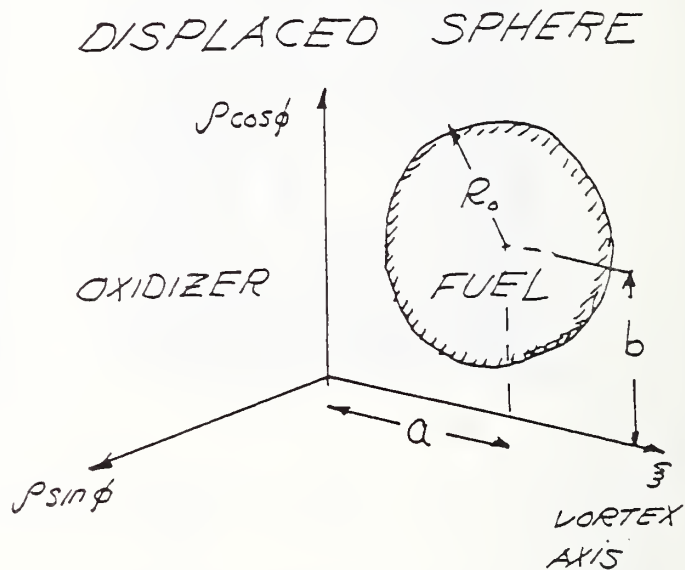


Figure 7. Spherical fuel parcel geometry

Tomoaki YOSHIKAWA ^{a)}, Junji MASHIGE ^{b)},
Tomoko JŌ ^{b)}, and Osami SUGAWA ^{c)}

- a) Japan Meteorological Agency, Meteorological Research Institute,
1-1, Nagamine Yatabe-cho, Tukuba, Ibaraki, 305, Japan
- b) Century Research Center Corporation
3-6-2, Nihonbashi Honcho, Chuo-ku, Tokyo, 103, Japan
- c) Department of Architecture, Faculty of Science and Technology,
Center for Fire Science and Technology,
Science University of Tokyo,
Yamazaki 2641, Noda City, Chiba, 278, Japan

ABSTRACT

We improve the field-equation model previously proposed in 1984 ¹⁾ by the inclusion of the mechanism of ignition by radiation, and the behavior of smoke particles. We apply this extended field-equation model in analysis for the fire conditions, and compare those with experiments. Our calculated values such as a temperature, velocities of gas and smoke concentration reasonably agree with the experiments.

1. THE BASIC EQUATIONS FOR THE FIELD EQUATION MODEL

Let us write the following basic equations and programs for the fluid dynamics based on the techniques that has been developed from 1982 to 1984 ^{1) 2)}

- Equation of momentum,

$$\frac{\partial \bar{\rho} \bar{u}_i}{\partial t} + \frac{\partial \bar{\rho} \bar{u}_i \bar{u}_j}{\partial x_j} = - \frac{\partial \bar{p}}{\partial x_i} + \frac{\partial \bar{\sigma}_{ij}}{\partial x_j} - \left[\frac{\partial (\bar{\rho} \bar{u}_i \bar{v})}{\partial x_i} + \left\{ \frac{\partial (\bar{\rho} \bar{u}_i \bar{v})}{\partial x_i} + \frac{\partial (\bar{\rho} \bar{u}_j \bar{v})}{\partial x_j} \right\} \right] - \delta_{ij} \bar{\rho} \bar{v} \quad (1)$$

- Equation of continuity,

$$\frac{\partial \bar{\rho}}{\partial t} + \frac{\partial \bar{\rho} \bar{u}_i}{\partial x_i} = 0 \quad (2)$$

- Equation of energy,

$$\bar{\rho} \frac{\partial \bar{h}}{\partial t} + \frac{\partial \bar{\rho} \bar{u}_i \bar{h}}{\partial x_i} = Q + \frac{D\bar{P}}{Dt} + \frac{\partial}{\partial x_i} (K \frac{\partial \bar{T}}{\partial x_i}) - \left[\frac{\partial \bar{\rho} \bar{h} \bar{v}}{\partial t} + \frac{\partial (\bar{\rho} \bar{u}_i \bar{h} \bar{v})}{\partial x_i} \right] \quad \text{where } K = \bar{q} \bar{v} L \quad \bar{h} = C_p \bar{T} \quad (3)$$

- Equation of transport and turbulent energy,

$$\frac{\partial \bar{\rho} \bar{q}}{\partial t} + \frac{\partial \bar{\rho} \bar{u}_i \bar{q}}{\partial x_i} = \frac{\partial}{\partial x_i} (\bar{\rho} K \frac{\partial \bar{q}}{\partial x_i}) + \nu \frac{\partial^2 \bar{q}}{\partial x_i^2} + g K \frac{\partial \bar{p}}{\partial x_j} - \bar{\rho} \bar{c} + K \frac{\partial \bar{u}_i}{\partial x_j} \left(\frac{\partial \bar{\rho} \bar{u}_i}{\partial x_j} + \frac{\partial \bar{\rho} \bar{u}_j}{\partial x_i} \right) \quad (4)$$

- Equation of gas transport,

$$\frac{\partial \bar{\rho} \bar{a}}{\partial t} + \frac{\partial \bar{\rho} \bar{u}_i \bar{a}}{\partial x_i} = \frac{\partial}{\partial x_i} \left(K \frac{\partial \bar{\rho} \bar{a}}{\partial x_i} - \bar{J}_{a_i} \right) + \bar{\phi}_a \quad (5)$$

- Equation of state,

$$\bar{p} = \bar{\rho} R \bar{T} \quad (6)$$

The basic idea of the chemical reaction and the radiation is the same as in the previous study²⁾. However we develop the subroutines which describe, accurately and in detail, the actual condition of a fire (such as named of the behavior of smoke particle, the estimation of the combustion rate relating to the oxygen concentration, the ignition of the wall and etc).

2. THE EXTENDED FIELD-EQUATION MODEL

2.1. CALCULATION OF THE SMOKE CONCENTRATION

The amount of the smoke generation can be calculated by the extended field-equation model with the combustion rate and smoke generation coefficient. In the extended equation model, the movement of gas and smoke is described by (5) and,

$$\frac{\partial \bar{C}_s}{\partial t} + \frac{\partial \bar{C}_s \bar{u}_i}{\partial x_i} = \frac{\partial}{\partial x_i} \left(\lambda \frac{\partial \bar{C}_s}{\partial x_i} \right) + \bar{q} \quad (7)$$

\bar{C}_s : smoke concentration in terms of extinction coefficient (1/m),
 $C_s = C/V$

C : amount of smoky corpuscule per unit volume,

V : Volume of the space filled with smoke (m³),

C_{so} : concentration of smoke generation,

K : smoke generation coefficient,

ΔW : weight of combustion(kg),

RB : combustion rate,

$K \cdot RB$: amount of smoke generation per unit time.

The definition of C_s is

$$C_s = 1/L \text{ LOGe}(100/T), \quad (8)$$

L : beam length(m),

T : transmissivity (%).

Smoke generation coefficient C can be expressed as,

$$C = C_s \cdot V. \quad (9)$$

But because of the relations:

$$C = k \Delta W, \quad (10)$$

K : smoke generation coefficient,

ΔW : Weight of combustion (kg).

Therefore the generation rate of smoke, C can be represented as,

$$C = k \Delta W,$$

where ΔW is combustion rate. As the output, $C_s = C/V$ is more useful and easier to understand the diffusion condition of smoke.

The amount of smoke generated from fire source is denoted by C which is advecting and diffusing to other mesh cells. $C(C_s \cdot V)$ should be deemed as the number per unit volume. If the smoke inside the room does not leak, the total amount of smoke produced by that time is written as $\int_0^t K \Delta W dt$ which is equal to the total amount of smoke $\sum C_i = \sum C_s v_i$. The order of magnitude of C_s concentration is about 0~30. The maximum value 30 corresponds to the situation when the flash over occurs.

2.2. ESTIMATION OF GENERATION RATE OF ENERGY DUE THE OXYGEN CONCENTRATION

The oxygen concentration inside a flaming cell and the generation rate of energy should be related.

Therefore, if the oxygen concentration inside the flaming cell is positive, the generation rate of energy of the calorie produced per unit volume can be calculated.

When the oxygen concentration inside the flaming cell is negative, the volume of calorie due to the amount of oxygen obtained from the flaming object should be described as the generation rate of energy in the flaming cell. Now negative concentration shows the amount of the lack of oxygen.

We show following basic equation.

① When the oxygen concentration is positive,

$$\text{HEATS} = \text{RB} * \text{QPER} / (\Delta x)^3, \quad (11)$$

HEATS : a generation rate of energy per unit hour and volume inside a flaming cell (Kcal/m³/sec),
 RB : speed of combustion (kg/sec)
 QPER : a generation rate of energy per unit mass (Kcal/Kg),
 ΔX : size of mesh (m).

② When the oxygen concentration is negative,

$$\begin{aligned} \text{HEATS} &= (\text{number of mol of oxygen in a flaming object}) \\ &* (\text{generation rate of energy per 1 mol of oxygen}) / (\Delta x)^3 \\ &= \text{RB} * \text{WP}(3) / \text{O2MOL} * \text{HATUO2} / (\Delta X)^3, \end{aligned} \quad (12)$$

HEATS : a generation rate of energy per unit hour and volume inside a flaming cell (kcal/m³/sec),
 WP(3) : proportion of oxygen mass in a flaming object,
 O2MOL : mass of oxygen 1 mol (kg),
 HATUO2: released calorie volume when oxygen 1 mol is consumed.

2.3. IMPROVEMENT OF THE TEMPERATURE CALCULATION ON THE SURFACE OF WALL

The temperature of wall surface by radiation is calculated by using the semi-infinite thick wall hypothesis.

The basic equation for this process is described as

$$\begin{aligned} T_1(t) - T_0 &= \int_0^t Q_1(\tau) \phi(t - \tau) d\tau \\ &= \sum_{i=1}^n Q_i \phi_{n-i} \Delta t \end{aligned} \quad (13)$$

T_1 : temperature of surface of wall at the time t sec
 T_0 : temperature of outside surface of wall (from actual measurement)
 $Q_1(t)$: radiation energy that the surface of wall obtains at the time t sec (Kcal/m² · sec : watt/cm²)
 ϕ : inditial response of surface temperature to heat input when T=t sec, weight of getting calorie volume from t- Δt to t
 $\phi_i(t - \tau_i) = 2 * (\sqrt{t - \tau_i + \Delta t_i} - \sqrt{t - \tau_i}) / \sqrt{\pi k \rho c}$ (14)

Q_i : the i th receiving calorie.
 ϕ_{n-i} : the i th weight function
 , for the n th computation.
 K : thermal conductivity.
 ρ : density of material of wall.
 C : specific heat of material of wall.

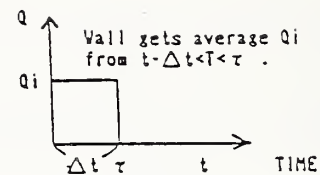


Fig 1. Conception of Q_i

2.4. IGNITION OF WALL

When the temperature of the wall surface reaches the pyrolysis temperature, the ignition is assumed to take place. Then heat flux to the wall surface is assumed to be consumed in vaporization at the wall material.

The algorithm is described by the following 3 equations,

$$\textcircled{1} \quad SW' = mv * HV \quad (15)$$

SW' : heat flux to the wall surface (Kcal/m²sec),
 ΔH_v : latent heat (Kcal/kg) (In case of Oak, $\Delta H_v = 1341.5$ Kcal/kg),
 mv : total volume of generating gas at unit time per unit area (kg/m²sec).

$$\textcircled{2} \quad mO_2 = mv * wp(3) \quad (16)$$

mO_2 : total generating volume of O_2 per unit time (kg/m²sec),
 $WP(3)$: mass % of O_2 in the generating gas from wall
 ($WP(3)$ depends on a substance).

$$\textcircled{3} \quad HEATW = mO_2 * \Delta x^2 / O_2MOL * HATUO_2 \quad (17)$$

$HEATW$: generating energy rate per unit time and unit volume at the cell bordering on the wall,
 O_2MOL : mass of 1 mol oxygen (kg/mol),
 $HATUO_2$: releasing calorie when 1 mol of oxygen is consumed (Kcal/mol).

3. SIMULATION OF THE FULL-SCALE FIRE.

3.1 INPUT DATA FOR THE COMPUTATION

For the simulation of the full-scale fire in 1985, we calculate 2 examples. In order to confirm the reliability of our model, we replaced the subroutine which reasonably describes the combustion rate as shown in Fig2-1 and Fig2-2. The input data of the computation is shown in Table 1 and Table 2.

TABLE 1. CONDITION OF TWO COMPUTATION

	CASE1	CASE2
Room Size (x,y,z)	(2.97m,1.89m,1.89m)	(2.97m,1.89m,1.89m)
Door (width,height)	(0.81m,1.35m)	(0.81m,1.35m)
Mesh size	0.27m	0.27m
Fire source	3 mesh cells on the floor of central interior part	9 mesh cells on the floor of left interior part
Fuel	Alcohol (CH ₃ OH)	Crib
Combustion rate per 1 grid	$RB=0.00147/82.5t^2$ $(0<t<82.5)$ $RB=0.00147$ $(82.5<t)$	$RB=0.14/82.5^2/*t^2/15/9$ $(0<t<82.5\text{sec})$ $RB=((0.35/31.5)t-0.776$ $)/15/9$ $(82.5<t<114\text{sec})$ $RB= [-(0.24/96/96)(t-$ $114)^2+0/49] /15/9$ $(114<t)$
X-axis TIME (min) Y-axis RB per 15 sec (kg/15sec)		
Energy release per unit mass	4600 kcal/kg	3600 kcal/kg
Energy per O ₂ 1mol	410KJ=97.9kcal	410KJ=97.9kcal
Composition of Combusting articles	[C] 37.5% [H] 12.6% [O] 49.9% [not burning ratio] 0%	[C] 43.5% [H] 5.2% [O] 38.3% [not burning ratio] 13%
Smoke generation coefficient	—	0.05
Model	<p>Fig2-1</p>	<p>Fig2-2</p>

TABLE 2. Composition of the wall wood used in case 2

	fireproof board	Plywood
Thermal conductivity (kcal/msecdeg)	$(0.060+0.0009\theta)/3600$	2.667×10^{-5}
Density (kg/m ³)	400	588
Specific heat (kcal/kgdeg)	0.2	0.38
Time step of wall temperature computation (sec)	1	10
Latent heat(kcal/kg)		1313.9
O ₂ in wall wood (%)		38.3

Remark) θ : temperature of wall wood(° C)

3.2. RESULT OF THE COMPUTATION.

CASE1

In Figure3, we show the distribution patterns of the temperature, the atmospheric pressure variation and O₂ concentration at the vertical section of $y=0.945m$ and the horizontal section under the ceiling of $z=1.755m$. The patterns of every element shows results at steady state. And this is not significantly different from the results of our previous work. However, as for the temperature and the O₂ concentration, our present results show that the temperature level increase and lower part of the O₂ concentration spread.

The atmospheric vectors are obtained for the region of the vertical section of $y=0.945m$ and $x=1.485m$ and the horizontal section of $z=0.945m$, $1.755m$. Figure4 shows result at the steady state (90 sec). In the region of the vertical section, the vertical stream forms the convective circulation which keeps the balance at the lower part of the center of the room. We observed the strongest stream 1.5m/s just above the fire source. Our extended field equation model predicts the strong gush out 1.2m/s under the hanging wall at the entrance, and the inflow jet (1.2m/s) in the domain along the bottom of the region of the entrance. The distribution patterns on the horizontal planes do not show any significant difference comparing with our previous result.

Although the calculation of the time variation of each element was done at all meshes, we demonstrate the temperature, the atmospheric pressure, the turbulent energy and diffusion coefficient at 3 points from A to C, and O₂ concentration at the 4 points including the heat source D.

Temperature (Figure5) becomes steady at 90sec and follows well the rising of the combustion power. The temperature is 470° k under the ceiling and falls at the the middle point B between the ceiling and the entrance and further the temperature falls at the upper part of the door C. But the difference of the temperature between A and C is only 20° k. Since the hot gas is thick and advection is fast, the decrease of the temperature caused by diffusion is very small. The pressure deviation is also sensi-

tive to the change of the combustion and it becomes steady at about 90sec. The level of the pressure is considerably low at the ceiling A, and it is equivalent to the value at the middle point B and the upper part of the entrance C.

The pressure inversion at B and C (so-called a jet effect) did not occur(Figure6). Also the change of the turbulent energy (Figure7) and the diffusion coefficient (Figure8) are consistent with the tendency of the temperature and the atmospheric pressure. At the ceiling A all of the two quantities are larger than the ones at other places, and they become comparable at the entrance C and the middle B. Although, we do not observe the inversion of turbulent energy and diffusion coefficient at steady state our results of Figure6 suggests that the inversion would appear at the time from 10 sec to 20sec. We expect the gush out associated with the inversion.

The O_2 concentration decreases to about 18% at the heat source D but the O_2 concentration decreases only 2% near the door at A~C.(Figure 9)

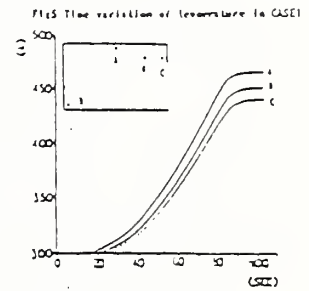
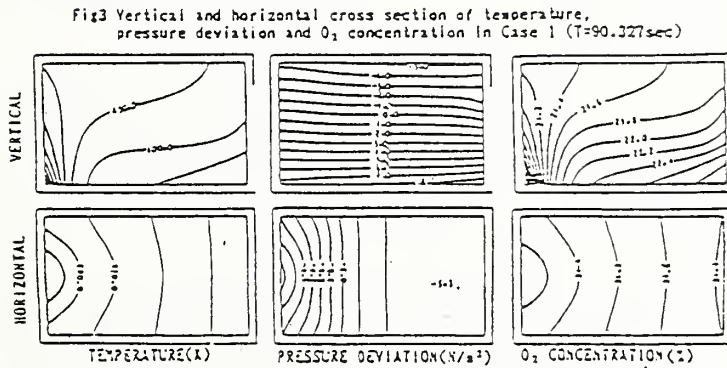
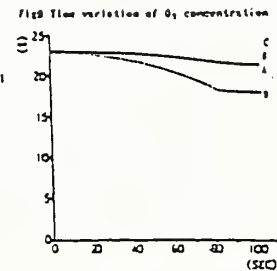
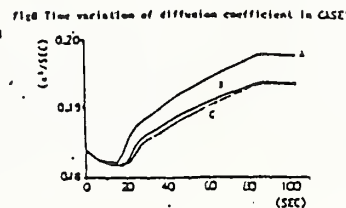
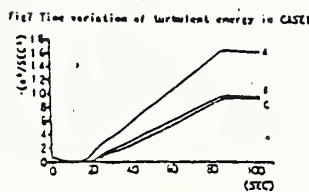
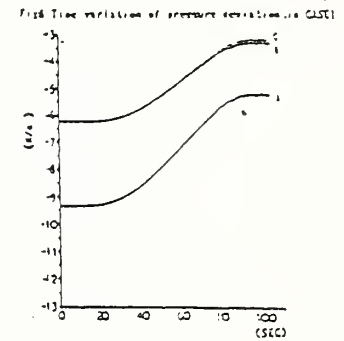
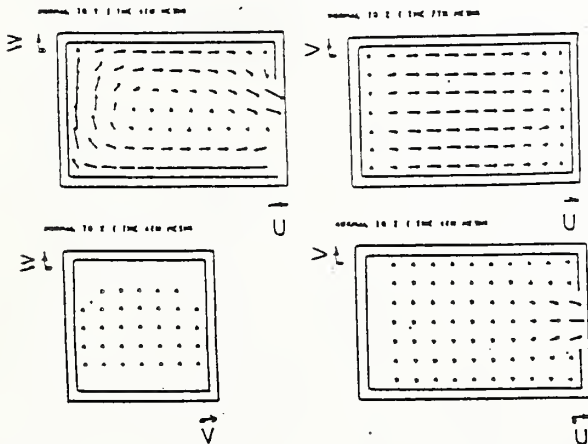


Fig4 vertical and horizontal cross section of flow field in CASE1
1 unit vector shows 1.0m/sec (T=90.327sec)



CASE2

Supposing that a wooden furniture (example, a desk) is placed at a corner of a room, we calculate until the combustion peak.

The distribution of the temperature, the pressure deviation, the O_2 concentration and the smoke concentration are described in a planimetric map (vertical section of $y=0.675m$, $z=1.755m$). Figure 10 shows the distribution of each element at the combustion peak excluding the smoke concentration. Comparing with the results of the case1, the temperature is $100^\circ K$ higher under the ceiling and $50^\circ K$ higher at the upper part of the entrance. The pressure deviation shows almost the same level as in the case1 around 60 sec but both of the pressure deviation under the ceiling and at the floor of the entrance increase about $1N/m^2$ at 90sec, which indicates the increase of the pressure. The O_2 concentration of case2 is similar to that of case1, but it is 1% higher approximately. The decrease of concentration was less significant than the increase of the temperature. This is because of follows different quantities between case1 and case2, namely the place of the heat source, the mesh area for the heat source and furthermore combustion rate.

The distributions of the smoke concentration at 30, 60, 90 sec are shown in Figure 11. We describe that it is all concentrated on the heat source inside the cell at the beginning, and it diffuses to the middle part of the entrance. Finally it gets higher than the one at the center of the room.

The movement of gas is shown for the vertical section of $y=0.675m$, the vertical section of $x=1.485m$ and the horizontal plane of $z=0.945m$, $z=1.755m$. Figure 12 describes the flow condition of the combustion peak. Since the fire source is placed at left side of the back cell, the unsymmetrical pattern appears. A right revolving vortex appears even on the vertical section $x=1.485m$. The velocity has the maximum of $2.0m/s$ above the heat source and $1.8m/s$ at the upper part of the entrance.

We notice that a circulating flow (faster than $1m/s$) which forms a circulation from the lower part of the entrance to the heat source and heads to the upper part of the entrance just under the ceiling.

The time variation of the temperature, the atmospheric pressure variation, the turbulent energy, the diffusion coefficient are the same as in case1. We show their values at the point of A~C and the oxygen concentration at the point of A~D. The temperature (Figure 13) rises hastily and rises over $700^\circ K$ just beneath the ceiling after 80 sec. The atmospheric pressure variations (Figure 14) decrease at every points and get closer, which means that the pressure of whole cell tends to be higher. The turbulent energy and the diffusion coefficient (Figure 15, Figure 16) are rising hastily at the combustion peak. Also, at around 20 sec, the turbulence of the entrance slightly exceeds the under-ceiling and the turbulence becomes bigger as it gets closer to the fire source and the condition of the local compression, so-called the entrance jet is not seen. The O_2 concentration (Figure 17) is 14% at the source, and 22% from the under-ceiling to the entrance.

Fig10 Vertical and horizontal cross section of temperature, pressure deviation and O₂ concentration in Case 2 (T=90.981sec)

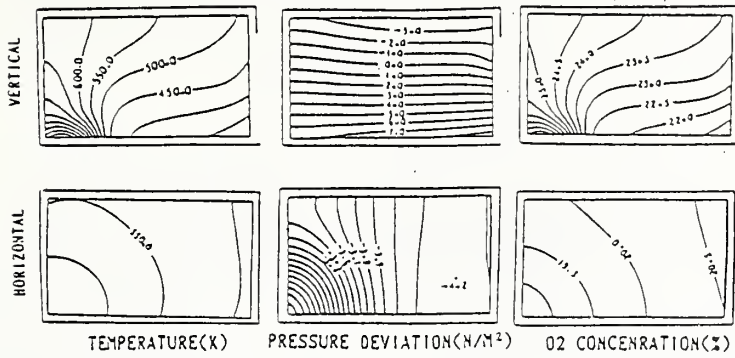


Fig11 Vertical and horizontal cross section of soake concentration

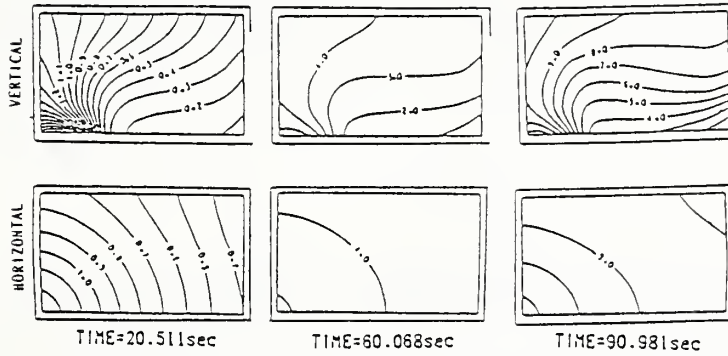


Fig12 vertical and horizontal cross section of flow field in CASE2
1 unit vector shows 1.0m/sec (T=90.981sec)

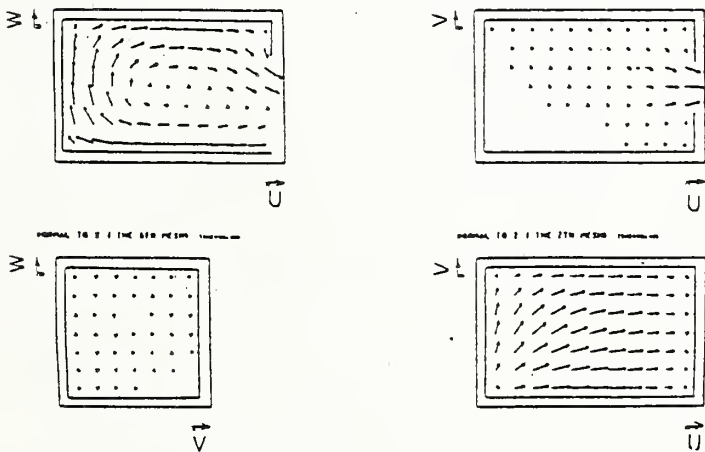


Fig13 Time variation of temperature in CASE2

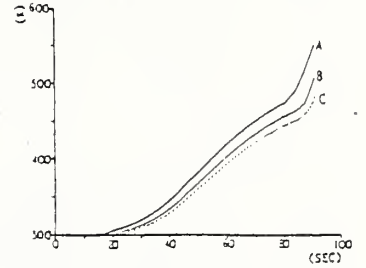


Fig14 Time variation of pressure deviation in CASE2

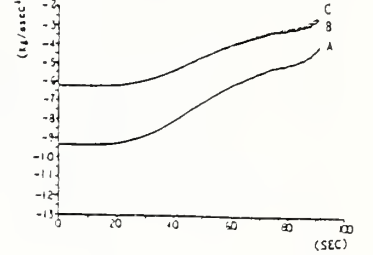


Fig15 Time variation of turbulent energy in CASE2

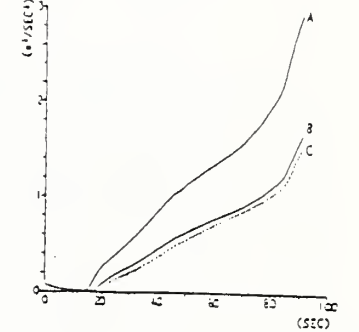


Fig16 Time variation of diffusion coefficient in CASE2

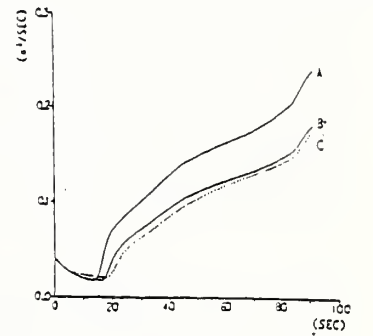
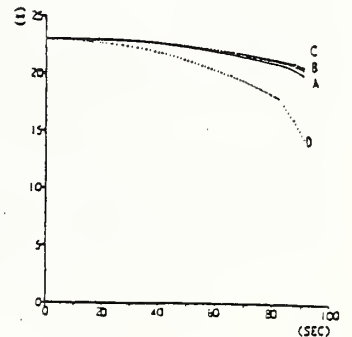


Fig17 Time variation of O₂ concentration



The temperature of the wall attaching to the furniture is higher than 600° k, and approximately 360° k at the opposite side, and 550° k at the ceiling above the heat source and 760° k at the floor just under the furniture.

5. RESULT

We check the reliability of our model by using the same size room and the same combustion rate as the ones of the experiments. As for the temperature under the ceiling, the gas velocities at the entrance and the O_2 concentration under the ceiling, we obtained the reasonable values. But we could not compare the time of the wall ignition, since the experimental of the time of the wall ignition was not available at that moment.

We will calculate the time of wall ignition by our extended model with the result of the new experiment. And we will add a new model which describes the situation when the door or window open suddenly by some accident.

REFERANCE

- 1) Takeshi Handa, K.Kawagoe, T.Yoshikawa, J.Mashige, T.Joh: Numerical simulation of early stage of a compartment fire, Fire Science and Technology, Vol.4, No.2, 91, 1984.
- 2) Hasemi Y.: Numerical calculation of the natural convection in the compartment, BRI Research Paper, No.69, 1977.

CRITICAL DISCUSSION ON FIRE DEVELOPMENT

Toshisuke HIRANO

Department of Reaction Chemistry, Faculty of Engineering
The University of Tokyo
7-3-1 Hongo, Bunkyo-ku, Tokyo 113

ABSTRACT

A discussion has been made on the basic knowledge to be needed for the understanding and prediction of fire development. It is pointed out that for only limited cases, fire development can be predicted by presently available data. Further, the prediction of fire development required for the assessments of various fire hazards and the improvement of fire protection engineering is discussed, and the need of a stochastic expression is emphasized.

1. INTRODUCTION

Every fire hazard assessment is more or less based on the prediction of fire development. For the evaluation of evacuation time, the rate of fire development and the smoke behavior during fire development are needed. For the recommendation of fireproof materials, the difference of ignitabilities or flame spread rates under the conditions of fire development should be interpreted. For other types of fire hazard assessments, also the prediction of some aspects of fire development would be required. Thus, a clear understanding of fire development seems to be essential to reduction of the damages to be caused by fires.

In the prediction of fire development, a model is used, the quality of which depends on the amount of knowledge of phenomena, and the reliability of the predicted results apparently depends on the accuracies of available data. The data usually used to predict fire development are concerning various phenomena, such as ignition, flame spread, smoldering, burning zone behavior, fire plume, smoke behavior, heat release, radiation, convection, ventilation, and so on. These data have been accumulated by a number of previous studies[1-9]. The data concerning some of these phenomena are sufficient for the prediction of fire development, while those concerning other phenomena are insufficient.

For the last decade, a number of excellent computer programs for the prediction of fire behavior have been established. Consequently, an accurate prediction of fire development seems possible if needed data are available and initial and boundary conditions are given[10-14]. Furthermore, even if the prediction were accurate enough, the predicted result for a set of initial and boundary conditions would be only an example. In general, it is doubtful that the predicted result is for the most probable fire development, which is really required for fire hazard assessments[15-17].

The objective of this paper is to indicate needed data for the prediction of fire development under arbitrary conditions, and to reveal the necessity of appropriate prediction methods to explore the most probable phenomena. The discussion presented in this paper will give us future problems to be solved in fire research.

2. NEEDED KNOWLEDGE ON FIRE DEVELOPMENT

Figure 1 shows a block diagram representing the processes of fire development. For the understanding or prediction of fire development, knowledge of each phenomenon in Figure 1 is indispensable. Basically, our knowledge of a phenomenon should be based on presently available data concerning it, so that to understand fire development to a further extent, the accumulation of available data is necessary. In this section, the data to accumulate urgently are discussed.

Ignition is the first process at fire occurrence. A large number of studies have been carried out on this subject[1-3,6,8], and the mechanisms of various types of ignition have been revealed. Also, quantities representing ignition characteristics, such as ignition temperature, minimum ignition energy, and ignition delay time, have been evaluated or measured. The results of theoretical and experimental studies on this subject were summarized in several review papers[1-3,6,8]. A large number of data are available.

However, if the initial and boundary conditions are actual ones, the ignition characteristics will be not always predictable. It will be found hard to predict the phenomenon that the ignition delay time at radiative ignition depends on the orientation of the irradiated combustible material surface as shown in Figure 2. Such a difficulty is attributable to lack of data on the solid combustible ignition under natural convection. This example seems to indicate that more data are needed for ignition under various initial and boundary conditions. At present, the ignition process under actual conditions is not always predictable. This may be the reason why the ignition process is not considered in the practical prediction of fire development.

The next stage of fire development is flame spread. Flame spread under various conditions have been examined and appropriate models have been proposed[3,4]. The results of previous studies on this subject have been summarized in several review papers[3,4,6,7]. The mechanisms of various types of flame spread have been explored and a large number of data have been accumulated. The studies on this subject seem to be at the most advanced stages among those on the subjects concerning fire development.

In spite of the accumulation of a large number of data and advanced stages of studies, many ambiguities remain as yet. Flame spread under particular conditions is not always predictable. In the case shown in Figure 3, the flame spread rate depends on the both characteristics of liquid and porous solid bed and no reasonable model for the prediction of flame spread rate has been proposed. This example implies that the flame spread rate over a material with complicated characteristics is hardly predictable. The parameters to be considered in addition to the material characteristics for the prediction of the flame spread are the thickness, convection, radiation, surface orientation, and thermal properties of the material. Although the effects of these parameters on the flame spread have been studied extensively, more data on particular types of flame spread seem insufficient for the understanding or prediction of flame spread under arbitrary conditions.

Smoldering and smoldering-flaming transition are important phenomena to understand early stages of fires as pointed out in the previous paper [6]. However, available data concerning this subject are only a few. The smoldering-flaming transition is a subject to be urged to study because the processes of fire development following to it depend on it. Another important problem is to examine the relation between the product composition and ambient conditions under which smoldering occurs. Very likely to

the flame spread, almost the same parameters affect the smoldering, such as the thickness, convection, radiation orientation, and physical and chemical properties of the material.

The rate of the combustion product generation must be the knowledge indispensable for fire modeling. However, little effort has been made to predict it in a practical case when a piece of furniture, wall, ceiling, or floor is burning. Although needed data are on those various types of burning zone behavior, most previous studies on the modeling of burning zone behavior have concerned with pool burning[5].

Pool burning behavior is closely related to the fire intensity in a room and greatly affects the fire plume and smoke behavior. The rate of burning depends not only on the burning zone size but also on its configuration. However, very few data are available on the pool burning of the configuration other than circular although in an actual fire the burning zone configuration is not circular. Further, the burning rate in a small size pool should be distributed on the burning zone surface, so that the burning rate at the center would be different from that near the leading edge of the spreading flame.

The fire plume and gas flow inside a compartment are the subject convenient for the computer simulation, so that many studies have been performed on the prediction of these phenomena by using high-speed computers[7]. Consequently, a number of excellent programs for the prediction of the fire plume behavior have been established. However, the programs applicable to the prediction of fire induced gas flows in a large size compartment are still very few. The effect of the mixing inside the high temperature zone should be considered as pointed out in the previous papers[6,7]. The gas flow behavior in a long corridor or tunnel is also the problem to be solved because it is very important for the fire prevention and protection activities. This problem seems to be worth to investigate, although it is not easy one including the heat transfer between the flowing gas and the wall.

3. IDEAL PREDICTION OF FIRE DEVELOPMENT

If the understanding of phenomena concerning fires were complete, a quantity H representing fire hazards would be evaluated under a given set of initial and boundary conditions, i.e., H would be given by an equation as follows:

$$H = f(t, x_1, x_2, x_3, y_1, y_2, \dots, z_1, z_2, \dots), \quad (1)$$

where t is the time, x_1, x_2, x_3 are the distances along the coordinates representing each point in the space, y_1, y_2, \dots the initial conditions, and z_1, z_2, \dots are the boundary conditions. In these conditions, the values representing the material characteristics and space structure under consideration must be included.

For an ideal case when f is given as a simple function of a variable w , a critical value w_c of w can be found by assuming the value of f_c that is a criterion of the safe and danger (Figure 4). For a practical case, the situation is different. The requirement for fire hazard assessments should be not to find such a criterion but to find the optimum conditions to minimize the total expense E for fires (Figure 5). E is the sum of the loss L to be caused by fires and the cost C of fire protection, and both L and C should be related to f , i.e.,

$$E = L + C = T_1(f) + T_2(f), \quad (2)$$

where $T_1(f)$ and $T_2(f)$ are equal to L and C , respectively, expressed using the transformation equations relating L and C to f .

The optimum value of a quantity w of the initial and boundary conditions ($y_1, y_2, \dots, x_1, x_2, \dots$) to minimize E can be found to solve the following partial differential equation,

$$\partial E / \partial w = \partial(T_1(f)) / \partial w + \partial(T_2(f)) / \partial w. \quad (3)$$

The value w_0 that is w to minimize E as shown in Figure 5 is eventually required for fire protection engineering.

The effort to obtain w_0 is equivalent to that to design for the optimum fire protection. However, to do so is impossible because complete understanding of phenomena concerning fires is unconceivable, so that the details of the function f cannot be expected to determine. Further, available data are not always appropriate to deduce E as mentioned in the previous section. What we can do at present is to propose a model represented by an approximate equation f_a instead of f and to estimate an approximate value w_{a0} instead of w_0 on the basis of our knowledge on fire development.

f_a to be deduced from any one of presently available models is a function of time and space by which fire hazards can be predicted under a given set of initial and boundary conditions. This may be a reason why the predicted results are not satisfactorily coincide with those expected by other persons. The initial and boundary conditions assumed in a prediction seem to be different from those assumed in other prediction. In actual cases, however, the initial and boundary conditions are variant, so that f_a based on a presently available model seem not suitable to find w_{a0} .

The difficulty to find w_{a0} on the basis of the predicted results is partly attributable to the uncertainty of selection of a set of initial and boundary conditions. It is not easy to find a suitable set of conditions among a large number of conceivable sets of conditions. For example, there may not be generally acceptable reasons to decide the conditions of opening and flammability. Both conditions obviously depend on the human behavior, weather, and other known and unknown factors. In these situations, each condition should be expressed stochastically [18,19], and the concept of the most probable condition is acceptable.

It may be recognized that there is a set of limiting conditions under which the circumstances are kept to be safe against fires. These limiting conditions are required for the fire protection engineering such as the evacuation planning, detector development, building design, and development of the technique for fighting fires. Each limiting condition may not be determined uniquely and should be expressed stochastically, too.

For the hazard assessments, a specific value of f_c representing a criterion of the hazard and the mathematical expression of a function f_a should be required. In the mathematical expression of f_a based on the stochastic expression of the initial and boundary conditions, the relations of these conditions to the fire development phenomena should be adopted. Since the conditions are expressed stochastically, stochastic data of phenomena concerning fire development should be required.

4. FUTURE RESEARCH ON FIRE DEVELOPMENT

In order to predict fire development in an appropriate accuracy, the initial and boundary conditions to be assumed for the prediction of each phenomenon should be given as accurate as necessary. Even if the initial

and boundary conditions were given accurately, the phenomenon cannot be predicted without an excellent model and a large number of data. Further, knowledge of fire development is indispensable for the prediction. This situation can be easily seen from the fact that only a few persons can predict the aspects from the time being under ignitable conditions to ignition although such aspects are very important information.

As discussed in Section 2, a large number of data under various conditions are needed. Important are the fundamental studies to accumulate accurate and useful data. The test methods of material for fire protection are also very important to understand the properties of materials during fires. Also, it is desirable that the material properties under various fire conditions can be inferred from the results of tests.

Other important discussion made in Section 3 is that by the prediction to be required for the fire protection engineering, the limiting values should be derived from the data expressed stochastically. Thus, data should be accumulate to stochastically express the physical or chemical characteristics of fire development. Also, a model is required, based on which a stochastic expression of the function f_a is possible.

The probability density function g_{vk} of flame spread rate V_f under a certain set of conditions can be expressed as shown in Figure 6(a). If the probability p_k of circumstances under the kth set of conditions is known as well as g_{vk} , then g_v is given as follows:

$$g_v = \sum_{k=1}^n p_k g_{vk}, \quad (4)$$

where n is the conceivable number of the sets of conditions, and g_v is supposed to be expressed as shown in Figure 6(b). Further, the burning zone area A_b can be calculated on the basis of g_v and is supposed to be expressed as shown in Figure 6(c).

The data needed in the above process to evaluate A_b are those on flame spread rate under various sets of conditions and p_k , although both requirements are not easy to satisfy. Although the data to be required for the prediction of other phenomena will be much more hard to obtain, we have to make an effort to satisfy the requirements for the prediction really needed for fire hazard assessments.

REFERENCES

1. Kanury, A. M., "Ignition of Cellulosic Solids - A Review," Fire Research Abstracts and Reviews, 14, pp. 24-52(1972).
2. N.F.P.A., "National Fire Codes," Vol. 13, NFPA(1979).
3. Akita, K. and Hirano, T., "Ignition of PMMA and Flame Spread over Its Surface," Saigai-no-Kenkyu, 11, pp. 291-297(1980).
4. Fernandez-Pello, A. C. and Hirano, T., "Controlling Mechanisms of Flame Spread," Combustion Science and Technology, 32, pp. 1-31(1983).
5. Orloff, L., "Simplified Radiation Modeling of Pool Fires," Eighteenth Symposium(International) on Combustion, pp. 549-561, The Combustion Institute, Pittsburgh(1981).
6. Hirano, T., "Combustion Phenomena at Early Stages of Fires," Proceedings of the Eighth Joint Panel Meeting UJNR Panel on Fire Research and Safety, pp. 214-227, Building Research Institute, Ministry of Construction, Japanese Gov.(1985).
7. Zukoski, E. E., "Fluid Dynamic Aspects of Room Fires," Fire Safety Science, Proceedings of the First International Symposium, pp. 1-30,

- Hemisphere, Washington(1986).
8. Emmons, H. W., "The Needed Fire Science," *ibid*, pp. 33-53.
 9. Friedman, R., "Some Unsolved Fire Chemistry Problems," *ibid*, pp. 349-359.
 10. Emmons, H. W., "The Prediction of Fires in Building," Seventeenth Symposium(International) on Combustion, pp. 1101-1111, The Combustion Institute, Pittsburgh(1979).
 11. Wakamatsu, T. and Hasemi, Y., "Progress in Fire Growth Modeling in Japan," Proceedings of the Eighth Joint Panel Meeting UJNR Panel on Fire Research and Safety, pp. 125-135, Building Research Institute, Ministry of Construction, Japanese Gov.(1985).
 12. Rockett, J. A. and Morita, M., "The NBS/Harvard Mark VI Multi-Room Fire Simulation," NBSIR 85-3281, U. S. Department of Commerce, National Bureau of Standards(1986).
 13. Mitler, H. E. and Rockett, J. A., "How Accurate is Mathematical Fire Modeling?" NBSIR 86-3459, U. S. Department of Commerce, National Bureau of Standards (1986).
 14. Tanaka, T., "Present Status of Building Fire Modeling and Review; Parts 1 & 2," Journal of the Japanese Association of Fire Science and Engineering, 36, pp. 1-5(Vol. 5); pp. 1-9(Vol. 6)(1986).
 15. Seeger, P. G.(Session Chair),"People-Fire Interactions," Fire Safety Science, Proceedings of the First International Symposium, pp. 495-590, Hemisphere, Washington(1986).
 16. Fitzgerald, R. W.(Session Chair),"Translation of Research into Practice," *ibid*, pp. 591-676.
 17. Kersken-Bradley, M.(Session Chair),"Statistic, Risk, and System Analysis," *ibid*, pp. 941-1056.
 18. Morishita, Y., "A Stochastic Model on Fire Spread-A trial for Evaluation of Fire Spread Risk," Proceedings of the Eighth Joint Panel Meeting UJNR Panel on Fire Research and Safety, pp. 35-42, Building Research Institute, Ministry of Construction, Japanese Gov.(1985).
 19. Lin, W-C. T. and Williamson, R. B., "The Use of Probabilistic Networks for Analysis of Smoke Spread and the Egress of People in Buildings," Fire Safety Science, Proceedings of the First International Symposium, pp 953-962, Hemisphere Washington(1986).

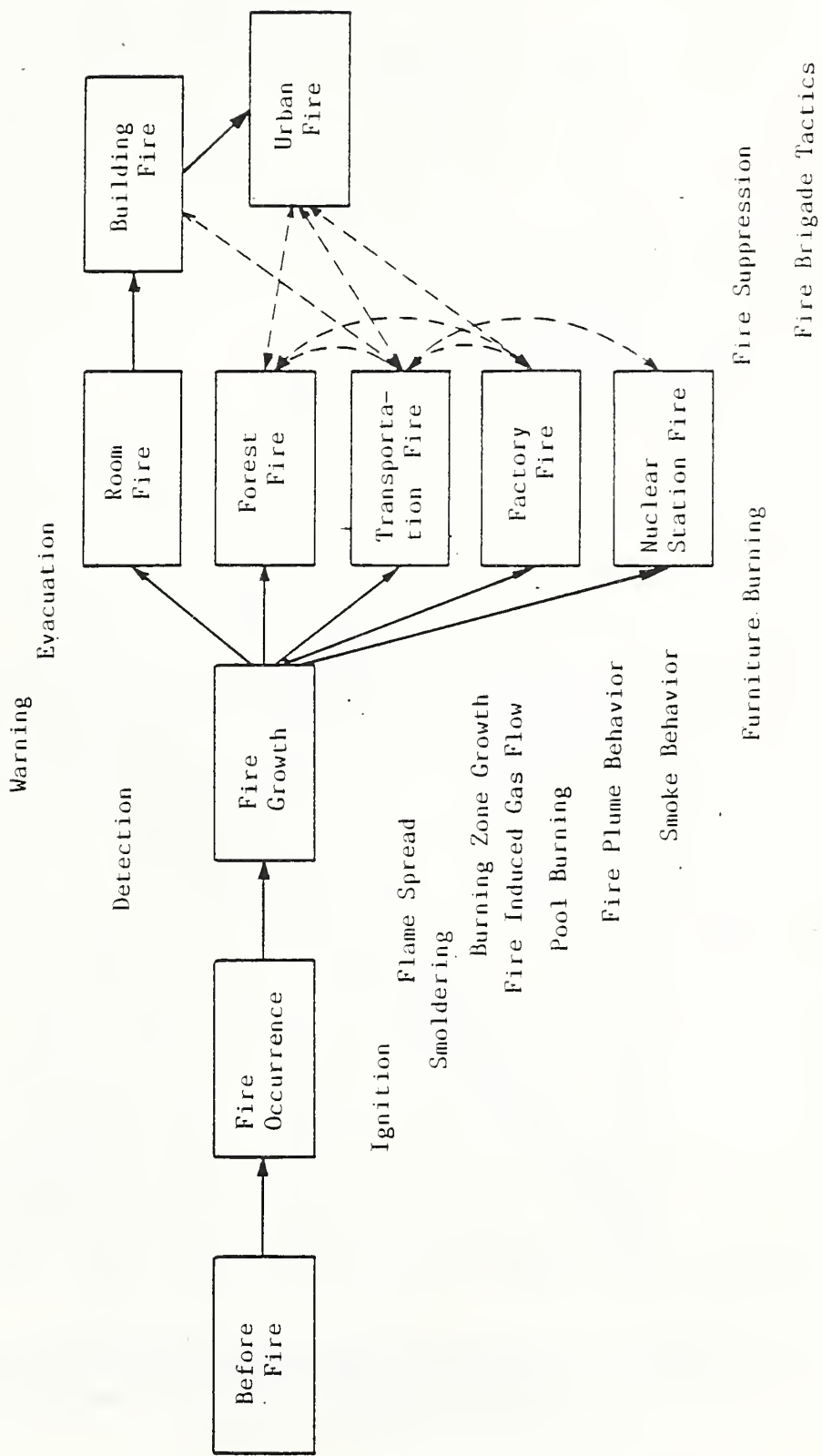


Figure 1. A block diagram of fire development.

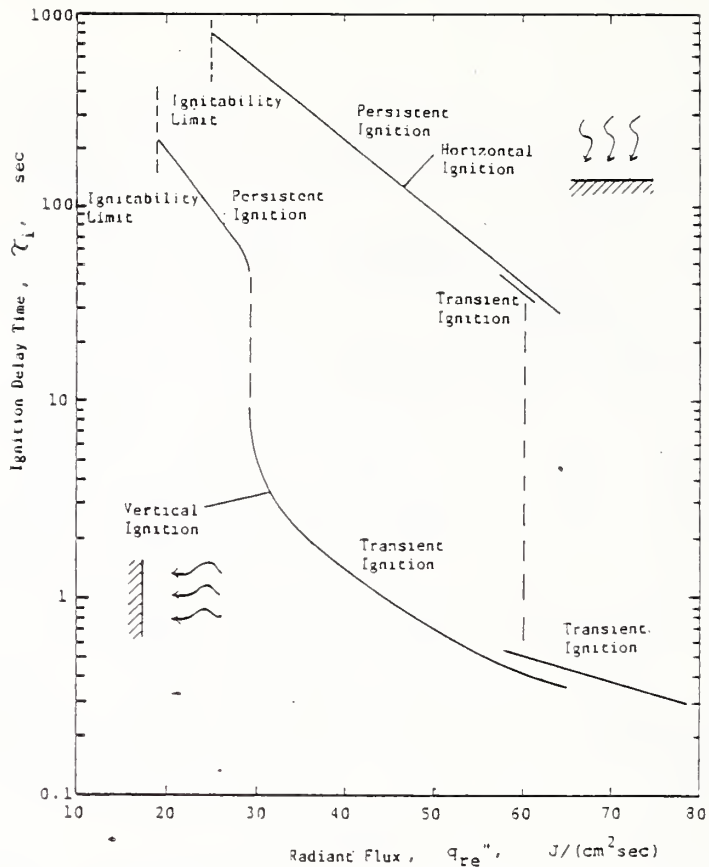


Figure 2. Ignition delay times at radiative heating of horizontal and vertical PMMA surfaces.

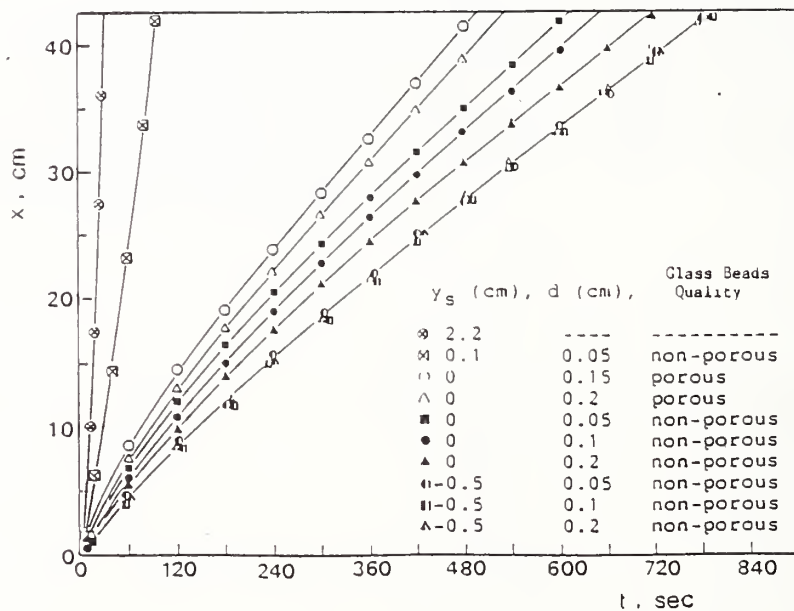


Figure 3. Position-time (x-t) diagrams representing the movements of leading flame edges. y_s : distance from the bead layer surface to kerosene surface; d : bead diameter.

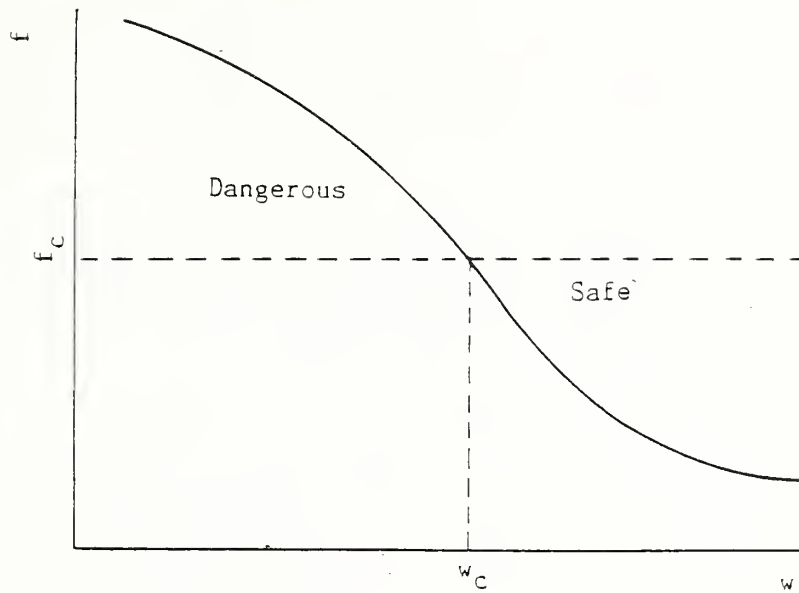


Figure 4. An illustrative example of the variation of f .

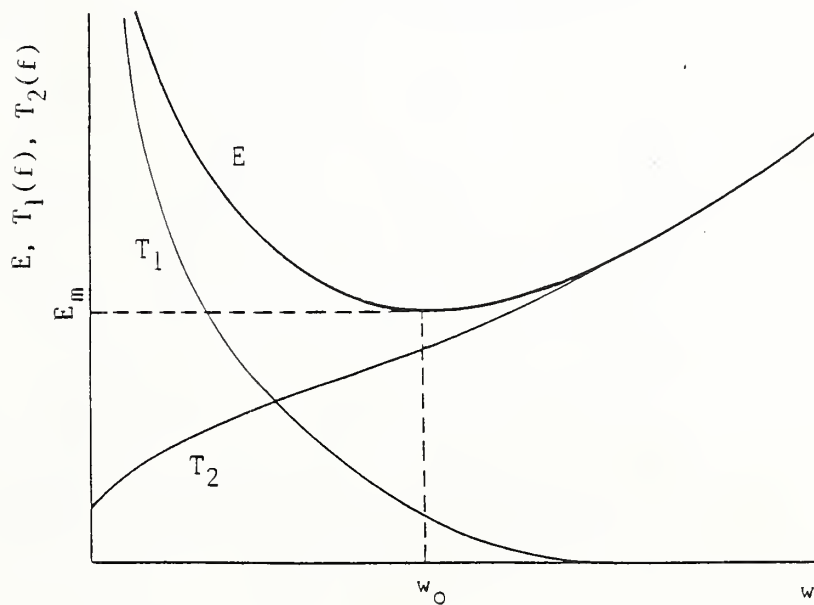


Figure 5. Illustrative examples of the variations of $T_1(f)$, $T_2(f)$, and E .

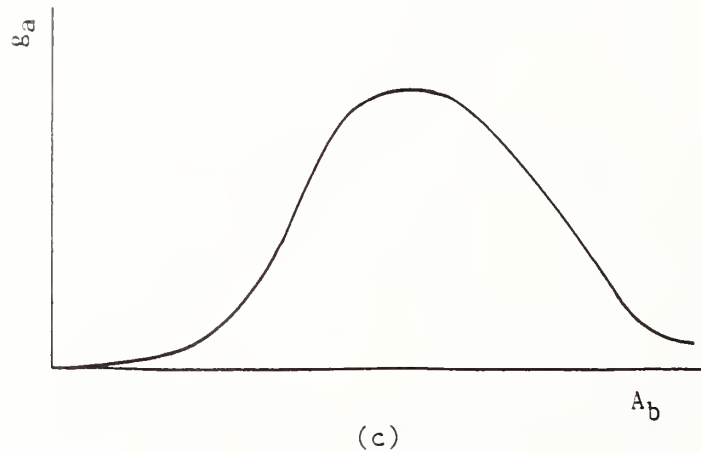
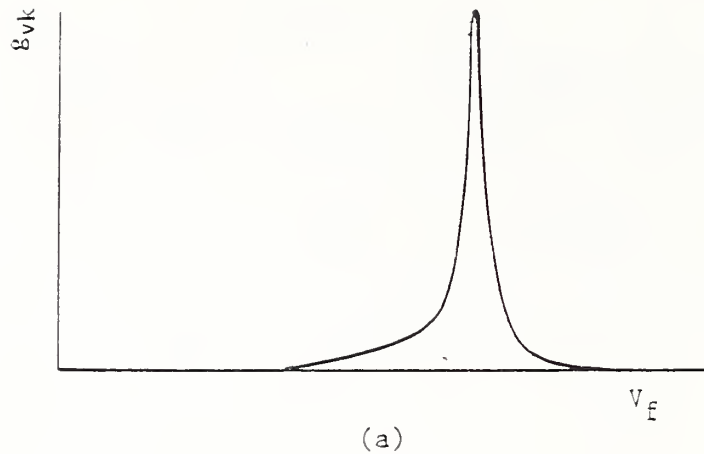


Figure 6. Probability density functions(p.d.f.) of flame spread rate V_F and burning area A_b . (a) the p.d.f. of V_F under the k th set of conditions; (b) the overall p.d.f. of V_F ; (c) the overall p.d.f. of A_b .

RADIATION FROM DIFFUSION FLAMES-SMOKE POINT

John de Ris
Factory Mutual Research Corporation

9th Joint Panel Meeting of the
UJNR Panel on Fire Research and Safety
May 4-8, 1987

ABSTRACT

A wide-range of experiments provide extensive empirical evidence that the laminar smoke-point value of a fuel provides a fundamental chemical measure of a fuel's propensity to radiate and release hazardous products of combustion from turbulent flames. It is also shown that the parameter $1/(B_c+1)$ correlates the overall flame radiation from turbulent ethane wall fires. In addition wall-fire flame radiation measurements versus height show that the flame radiation increases proportional to height in the lower fuel-rich portion of the flames. This simple proportionality is attributed to the absence of soot oxidation in the lower flame region.

INTRODUCTION

The flammability of a material is strongly influenced by its flame radiation. At hazardous fire scales the radiative heat-feedback from the flames to the pyrolyzing fuel surface is generally significantly greater than the convective heat-feedback. Fuels which release a greater fraction of their chemical energy in the form of thermal radiation (rather than convection) are generally more hazardous, because it is easier for radiation to return to the pyrolyzing surface. At present, the two principal impediments to predicting fire heat release rates and upward fire spread rates - namely solving the flammability problem - are: 1) our lack of scientific knowledge of flame radiation, and 2) the absence of some practical test method for evaluating the flame radiation from materials of interest. In general, the relative importance of flame radiation increases with fire scale, so that it is impractical to assess a material's flame radiation using conventional small-scale rate-of-heat-release test apparatus which, by imposing significant levels of external radiation (to simulate large-scale combustion conditions), overpower any direct flame radiation measurement. Instead, we shall have to become more clever in our search for a practical method for measuring flame radiation.

This requires, however, a deeper scientific understanding of flame radiation which is the subject of much of Factory Mutual's current flammability research.

SMOKE-POINT CORRELATIONS

About four years ago Markstein¹ discovered that the radiant fraction from buoyant turbulent fuel-jet flames burning in air is directly correlated by the fuel's laminar smoke-point flame-height, as shown in Figure 1. The radiant fraction itself from a buoyant turbulent fuel-jet is quite insensitive to the overall flame size or (heat release rate) when the heat release rate is above a few kilowatts. The smoke-point is defined as the maximum flame height for which a laminar "candle-like" flame just does not emit soot from its flame tip. The smoke-point of a fuel characterizes its tendency to produce soot. Fuels with long smoke-point heights produce less soot than fuels with short smoke-point heights. The smoke-point is a rather easy measurement to make for liquid or gaseous fuels for which one can manually adjust the flame height by controlling the rate of fuel supply to the flame whose height is proportional to the chemical heat release rate. In retrospect, Markstein's discovery is not surprising because flame radiation comes predominantly from the soot formed in the flame. For a given fuel burning in a small laminar buoyant "candle-like" flame beneath its smoke-point height, the peak concentration of soot is proportional to the flame residence time which, in turn, is proportional to the square root of the flame height. By changing the height of a laminar flame, one controls its flow residence time, τ_{res} , and its corresponding Damköhler number τ_{res}/τ_{chem} which controls the influence of the flame chemistry. As the laminar flame-height increases, it loses an increasing fraction of its chemical heat-release in the form of radiation until the soot at the flame tip is cooled below its critical oxidation temperature and unburnt soot is released from the flame-tip as a result of radiative extinction. Markstein¹ has shown that for hydrocarbon fuels burning in air at their smoke-point condition, about 30% of their chemical energy is released in the form of radiation. For turbulent buoyant flames, as distinct from a laminar flames, the turbulent microscale flow time (e.g. Kolmogorov time $\tau \sim [\nu\delta/u^3]^{1/2}$) controls the final combustion processes and is relatively insensitive to the overall fire heat release rate; so that those hydrocarbon fuels whose turbu-

lent buoyant flames (burning in air) release more than 30% of their energy in the form of radiation (such as propylene) also tend to release copious amounts of smoke; whereas, those hydrocarbon fuels which release less than 30% of their energy in the form of radiation (such as propane) tend to release relatively little smoke from buoyant turbulent flames.

In a related study Tewarson² measured the chemical energy fraction actually released, χ_A , as well as the fraction of convective heat release, χ_C , from small turbulent pool fires for a variety of (noncharring) solid and liquid fuels indicated in Figure 2. From these two measurements he inferred the fraction of radiative heat release, χ_R , by difference. He also measured the associated laminar smoke-point flame heights by vaporizing the various fuels in an electrically-heated Erlenmeyer flask. As can be seen in Figure 2, his correlation of radiative fraction for condensed fuels is almost identical to Markstein's correlation for gaseous fuels. In addition Tewarson² found that the smoke-point also correlates the release of smoke, carbon monoxide and unburned hydrocarbons for the same wide range of fuel types.

In another study on the blockage of radiative heat transfer to the base of large (38 cm and 76 cm diameter) pool fires Markstein⁴ found that the peak centerline soot concentration is also correlated by the smoke-point for gaseous fuels. Finally Kent⁵ very recently has shown that the fuel smoke-point correlates the peak soot concentration in pure momentum driven (e.g. forced convective) turbulent fuel-jet diffusion flames for both aromatic and aliphatic fuels burning in air. Thus, we now have extensive empirical evidence that the laminar smoke-point value of a fuel provides a fundamental chemical measure of a fuel's propensity to radiate and release hazardous products of combustion from turbulent diffusion flames. This result can now guide the development of a practical flame-radiation test method.

We note here that all the above empirical correlations involved burning pure fuels in air with similar adiabatic flame temperatures and stoichiometric mass ratios of ambient oxidant to supplied fuel. To obtain a more general and deeper scientific understanding we need to extend our knowledge to: fuel mixtures, fuels diluted with inerts such as N_2 , fuels diluted with products of combustion such as CO_2 and H_2O which can chemically oxidize soot, and oxidants having significantly enhanced or depleted oxygen concentrations as compared to normal air. While such studies are of obvious intellectual interest in pro-

viding a more firmly based scientific understanding of flame-radiation, they can also yield important practical dividends. For example, we know that flame radiation increases much more strongly than convective heat transfer with ambient oxygen concentration. It is thus likely that by performing standard rate-of-heat release tests in different ambient oxygen concentrations, one may be able to separately identify the radiant fraction of a burning material and thus determine its expected flammability at large scale. Such a determination will require a firmer basic scientific understanding of flame radiation. Presently, FMRC researchers are exploring this possibility by measuring the increase in flame radiation with ambient oxygen concentration for various fuels in both laminar and turbulent flames. We will report on these results at the next UJNR meeting.

WALL-FIRE COMBUSTION MODELING

Figure 3 shows the classical Shvab-Zeldovich conception of a diffusion flame, where fuel diffuses toward the flame from the right and oxygen diffuses in from the left. The flame position is determined by the stoichiometric ratio, S , of the mass of oxidant mixture required to react with unit mass of fuel mixture. It is presumed that both fuel and oxidant cannot exist instantaneously at the same position; because if this were not the case, the lesser reactant (either fuel or oxidant) would be immediately consumed by the dominant reactant, thereby eliminating the lesser reactant. For diffusion flames the chemical reaction rates are much faster than diffusion rates, so that the overall rate of combustion is determined by diffusion of reactants into the flame. For the Shvab-Zeldovich conception of a diffusion flame the rate of heat release is proportional to the rate of reactant diffusion into the flame. If one assumes that the diffusivities of the various species are the same and also equal to the thermal diffusivity, then the peak flame temperature is equal to the adiabatic stoichiometric equilibrium flame temperature for the reactants provided they are completely consumed and there is no loss of energy by radiation. One can mathematically show that the above theoretical conception holds for both steady and transient as well as laminar and turbulent diffusion flames.

In reality, diffusion flame chemistry is considerably more complicated. Fuel and oxygen molecules do not simply combine to form products with an

associated release of heat. Instead, numerous chemical intermediates are formed and then consumed. Nevertheless, both theory⁶ and experiment⁷ show that the concentrations of all major species as well as lesser species such as carbon monoxide and molecular hydrogen (to a certain extent) can be correlated by a mixture fraction variable such as

$$\xi = \frac{S Y_F + 1 - Y_O/Y_{O\infty}}{S + 1}$$

which is neither created nor destroyed by the chemical reactions. This type of mixture fraction variable has the particular advantage of yielding straight lines in diagrams for species concentrations in those regions where a particular species does not undergo chemical reaction. This allows one to use geometrical constructs for interpreting flame relationships.

One can readily extend this simple Shvab-Zeldovich description to diffusion flames having incompleteness of combustion and release of heat by radiation, provided one assumes that: 1) a fixed fraction, $1 - \chi_A$, of the supplied fuel does not participate in the chemical reaction and acts like an inert associated with the incompleteness of combustion, and 2) that a fixed fraction, χ_R , of the theoretical (e.g. total) heat of combustion immediately leaves the flame zone in the form of radiation. These assumptions lead to the following definition of convective B-number

$$B_c = \frac{\dot{m}''}{\dot{q}_c''} \left[\frac{\Delta H_c (\chi_A - \chi_R)}{S \chi_A} - C_p (T_S - T_\infty) \right]$$

where \dot{q}_c'' is the convective heat transfer rate to the fuel surface and \dot{m}'' is the mass transfer of fuel from the surface. Here ΔH_c is the theoretical net heat of combustion, T_S is the surface temperature and T_∞ is the ambient reference temperature associated with the definition of ΔH_c .

The dotted lines in Figure 3 show the temperature (or to be more precise, the sensible enthalpy) profiles versus mixture fraction for fuel supplied from a fuel-jet ($B_c = \infty$ or $\dot{q}_c'' = 0$). If instead the same fuel is introduced to the fire from a pyrolyzing wall with a mass transfer rate \dot{m}'' and having a resultant convective heat feedback rate \dot{q}_c'' then the actual fuel concentration observed immediately adjacent to the fuel surface is reduced by the factor $B_c / (B_c + 1)$ as indicated in Figure 3. This reduction comes from the back diffusion of pro-

ducts of combustion which, while not actually being absorbed by the wall, nevertheless are present at the wall surface with a total concentration $1/(B_c+1) = 1-B_c/(B_c+1)$ adjacent to the fuel surface. Finally the introduction of a cooler (or less hot) fuel surface can cause a reduction in the flame temperature (or sensible enthalpy) as suggested in Figure 3.

These theoretical considerations suggest that the introduction of a pyrolyzing fuel surface providing a mass transfer, \dot{m}'' , and receiving a convective heat feedback, \dot{q}_c'' , should be equivalent (from a Shvab-Zeldovich viewpoint) to supplying the flames from a fuel-jet supplying fuel at a concentration of $B_c/(B_c+1)$ together with products of stoichiometric combustion with a total concentration of $1/(B_c+1)$, all at a temperature equal to the surface temperature, T_S . By so doing the buoyant turbulent fuel-jet should replicate the conditions at the fuel surface. By using this procedure one hypothetically also replicates the full detailed fuel decomposition chemistry as the fuel heats up while diffusing toward the flame surface. We are currently setting up an experiment at FMRC with NBS sponsorship to test this hypothesis by measuring the radiant fraction from fuel jets suitably diluted with same fuel's products of stoichiometric combustion generated in an auxiliary burner. We anticipate that the addition of gaseous H_2O and CO_2 to the fuel supply will reduce the soot formation through both a reduction of the flame temperature as well as by chemically enhancing the soot oxidation through increased concentrations of H_2O and CO_2 which are known to augment soot oxidation at high temperatures.

WALL-FIRE FLAME RADIATION MEASUREMENTS

Markstein³ has recently performed a series of flame radiation measurements using a 38 cm wide by 1.83 m high wall burner producing two-dimensional flames through use of 15 cm deep side-walls to prevent sideways inflow. Most of the measurements involved use of a series of three 22 cm high water-cooled sintered-metal gas panels supplying ethane fuel-gas to the flames at a controlled mass transfer rate, \dot{m}'' . A water-cooled heat transfer plate was present above the sintered-metal gas burners. Measurements were also made for ethane supplied from a narrow slot burner at the base of the wall to simulate the case of $B_c \rightarrow \infty$ (or $\dot{q}_c''=0$). For each fire the total heat feedback rate to each wall section was measured by measuring the temperature rise (i.e. heat absorption

rate) of the cooling-water. Two types of flame radiation measurements were performed. One used a wide-angle radiometer to record the total flame radiation emitted by the fire; while the other used a scanning slit-radiometer to record the flame emission versus height. Since the boundary layer flames were optically thin, it was assumed in all cases that half the flame radiation returned to the wall and the other half radiated out into the laboratory away from the wall. The convective heat transfer back to the wall was inferred for each panel section by comparing the measured total heat feedback with the associated radiative component by integrating the scanning radiometer measurements over the corresponding panel section.

We are presently replacing the wall burner because it is only suitable for using relatively non-sooty fuels such as ethane. We are also considerably improving the spatial resolution of the scanning radiometer. Thus the measurements discussed here should be regarded as preliminary. Nevertheless, they are rather interesting and can serve to guide the development of upward fire spread models.

Figure 4 shows the total radiant fraction, χ_R , from the wall flames plotted against $1/(B_c+1)$ which we showed in the previous section is the total concentration of combustion products (chiefly H_2O , CO_2 and N_2) at the wall surface. One sees that the radiant fraction decreases linearly with increasing presence of combustion products. We also see that $1/(B_c+1)$ provides a reasonable correlating parameter which was anticipated by the theoretical arguments of the previous section.

The radiant fraction for the slot burner was 19%, independent of the flame height or fuel supply rate. This 19% fraction should be compared to the radiant fraction of 21% measured for ethane buoyant turbulent fuel-jets burning in the open without an adjacent water-cooled wall. Thus the presence of the water-cooled wall over the entire length of the wall flames results in only a slight reduction in their radiant emission. Apparently, the overall emission from the flames is much more sensitive to how the fuel is supplied to the fire than any subsequent convective cooling by an adjacent wall surface.

Figure 9 shows the observed flame height as interpreted by the scanning radiometer when the flame radiation dips below a certain arbitrarily chosen threshold value. The flame heights seem to correlate reasonably well with the heat release rate per unit burner width, $(\dot{Q}')^{2/3}$, as suggested by the theory

based on dimensional analysis for a turbulent line-fire. These threshold flame height measurements do not appear to be sensitive to the pyrolysis zone heights.

We obtain a rather different perspective when we examine the actual radiant flux distribution measurements shown in Figures 5 through 8. All these flux distribution curves are very well correlated by: 1) normalizing the height, z , in the abscissa by $L_f = 0.17(\dot{Q}')^{1/2}$ where the flame radiation goes to zero, and 2) normalizing the flux distribution, $\dot{q}_R''(z)$ in the ordinate by $\chi_R \dot{Q}' / L_f$ so that the area under each curve is exactly equal to one-half; since only one-half of the total flame radiation returns to the wall surface. Alternative correlations of radiant flux distributions using the conventional $L_f \sim (\dot{Q}')^{2/3}$ were much poorer. This surprised us. However, we note that the prediction that $L_f \sim (\dot{Q}')^{2/3}$ is based on arguments relating to the rate of chemical heat release. Here we are, instead, considering measurements of flame radiation which is not expected to be locally proportional to the rate of chemical heat release. In fact, from other studies⁸, we know that most of the chemical energy from turbulent diffusion flames is released considerably earlier than the radiative energy. The soot is formed where the majority of the chemical heat release occurs, and then continues to radiate until it is completely oxidized in the upper flame region of soot oxidation.

DISCUSSION OF THE WALL RADIANT FLUX DISTRIBUTIONS

Examining Figure 5 for the slot burner more closely we see that

$$\frac{d\dot{q}_R''(z)}{dz} = \frac{\chi_R \dot{Q}'}{L_f^2} m = \frac{\chi_R}{(0.17)^2} m$$

where the initial slopes of the curves, m , are effectively the same in all cases. This initial slope seems to depend only on χ_R and be independent of both heat release per unit flame width, \dot{Q}' and the number of burners. In this region the flame is fuel-rich so that the rate of chemical heat release depends only on the rate of turbulent air entrainment into the flame as established by Delichatsios⁹. It typically takes about fifteen mass units of air to react stoichiometrically with unit mass of fuel. As each clump of air is engulfed into the flame in this lower region, it is soon "eaten up" by the excess fuel. Because of the large stoichiometric mass ratio, S , both the

diffusion flame and fuel immediately penetrate into the air clump. The soot which is formed cannot diffuse because its enormous molecular weight causes it to have zero diffusivity. This soot is left behind in a hydrocarbon-rich gas where it cannot be oxidized. The subsequent Lagrangian evolution of this soot volume cloud follows almost identically to the original entrained air clump volume evolution. Thus, we expect the rate of soot formation to be proportional to the rate of combustion in the lower flame region, while the rate of soot oxidation is probably negligible in this same lower region. The rate of combustion per unit area, as established by Delichatsios⁹, is proportional to the upward velocity $\bar{u} z^{1/2}$, so that the accumulative upward flow of soot at a given height is proportional to $z^{3/2}$ or

$$\bar{\rho} \bar{u} \bar{Y}_S \delta \sim z^{3/2}$$

where $\bar{\rho}$ is the mean gas density, \bar{Y}_S is the mean soot mass concentration and δ is the effective boundary layer thickness. Dividing by \bar{u} we have the amount of soot per unit wall area

$$\bar{\rho} \bar{Y}_S \delta \sim z$$

which is proportional to $\dot{q}_R''(z)$ in the lower flame region. In this lower region the local rate of combustion per unit area

$$\dot{q}_{\text{chem}}'' \sim \bar{u} z^{1/2}$$

so that the local radiant fraction

$$\chi_R(z) = \frac{\dot{q}_R''(z)}{\dot{q}_{\text{chem}}''(z)} \sim z^{1/2}$$

which starts at low values near the base of the flame and thus causes little initial flame cooling by radiation in this lower flame region, and consequently, the effective flame radiation temperature T_R remains roughly constant, so that the flame radiation should initially be proportional to the amount of soot per unit flame area. Thus, we have arrived at a plausible heuristic explanation for why $\dot{q}_R''(z) \sim z$ in this lower region.

Continuing our attention on Figure 5, one might guess that most of the original fuel is consumed around the radiation peak occurring at 30% of L_f . At this point the combustion gases may be predominantly N_2 , CO , H_2 , H_2O and CO_2 as well as soot. As the soot is depleted the radiant heat flux $\dot{q}_R''(z)$ will decrease. Since ethane is a nonsmoky fuel, essentially all the soot will be consumed because there is not enough soot to induce radiant extinction of the flame with concomitant release of smoke and CO . Thus, the relatively steep decline in radiation and the relatively small final decay tail of $\dot{q}_R''(z)$ might have been anticipated. One might further speculate here that more sooty fuels such as propylene will have considerably slower declines in radiation and longer final decay tails.

Examining the remaining profiles in Figures 6, 7 and 8, one sees approximately the same initial rise in their fuel-rich regions near the base. Here the rate of fuel supply is independent of z and the rate of combustion is again initially proportional to $z^{1/2}$, so that we again anticipate an initial fuel-rich region. However, at least for the low mass transfer rates of Figure 8 with its three panels, the fuel-rich region should be much shorter and the flame presumably soon becomes limited by the fuel supply at a lower height. Once the initial fuel-rich region is eliminated, the soot that is formed from further fuel supply from the wall is probably speedily oxidized resulting in a local radiant fraction which is more constant with height. Such speculations may be useful for: suggesting possible future experiments, further ways of correlating the data or hopefully stimulating more rigorous theoretical arguments.

Finally for completeness we show in Figure 10 a cross plot of the threshold flame length measurements against the formula $L_f = 0.17 (\dot{Q})^{1/2}$ which gave the superior radiant flux distribution correlations. Clearly the threshold which was used to determine the flame heights in Figure 9 is rather high. The data seem to correlate on a parallel line which suggests that the possibility that the present scanning radiometer data may lead to additional parallel lines for other threshold values.

NOMENCLATURE

B	$\frac{\dot{m}''}{(\dot{q}_R'' + \dot{q}_C'')} \left[\frac{\Delta H_c}{S} - C_p (T_s - T_\infty) \right], [-].$
B _C	$\frac{\dot{m}''}{\dot{q}_C''} \left[\frac{\Delta H_c (\chi_A - \chi_R)}{S \chi_A} - C_p (T_s - T_\infty) \right], [-].$
ΔH_c	Fuel heat of combustion [E/M].
l_s	Smoke-point height, [L].
\dot{m}''	Mass flux, [M/L ² t].
$\dot{q}_R''(z)$	Radiant heat flux to wall, [E/L ² t].
$\dot{q}_C''(z)$	Convective heat flux to wall, [E/L ² t].
\dot{q}_{chem}''	Chemical heat release rate per unit wall area [E/L ² t].
\dot{Q}'	Heat release rate per unit wall length, [E/Lt].
\dot{Q}'_R	$\chi_R \dot{Q}'$, [E/Lt].
S	Stoichiometric air-to-fuel mass ratio [-].
T_s	Surface temperature, [θ].
T_∞	Ambient temperature, [θ].
\bar{u}	Upward gas velocity, [L/t].
\bar{Y}_s	Soot mass fraction, [-].
z	Height, [L].
δ	Boundary layer thickness, [L].
ν	Kinematic viscosity, [L ² /t].
$\bar{\rho}$	Gas density, [M/L ³].
ξ	Mixture fraction, [-].
χ_A	Actual heat release rate fraction, [-].
χ_C	Convective heat release rate fraction, [-].
χ_R	Radiative heat release rate fraction, [-].
τ_{res}	Microscale flow time, [t].
τ_{chem}	Characteristic chemical time, [t].

REFERENCES

1. Markstein, G.H.: "Relationship Between Smoke-Point and Radiant Emission from Buoyant Turbulent and Laminar Diffusion Flames," Twentieth Symposium (International) on Combustion, The Combustion Institute, Pittsburgh, PA (1981).
2. Tewarson, A.: "Prediction of Fire Properties of Materials, Part I: Aliphatic and Aromatic Hydrocarbons and Related Polymers," FMRC Tech. Rept. J.I. OK3R3.RC-070(A), Factory Mutual Research, Norwood, MA (July 1986).
3. Markstein, G.H.: "Radiation Emission from Wall Fires," Fall Technical Meeting, Eastern Section, The Combustion Institute, Philadelphia, PA, Nov. 4-6, 1985. Also private communication.
4. Markstein, G.H.: "Measurements on Gaseous-Fuel Pool Fires with a Fiber-Optic Absorption Probe," Comb. Sci. and Tech., 39, 215-33, (1984).
5. Kent, J.H.: "Turbulent Diffusion Flame Sooting- Relationship to Smoke-Point Tests," Comb. and Flame, 67, 223-233 (1987).
6. Miller, J.A., Kee, R.J., Smooke, M.D., and Grear, J.R.: "The Computation of the Structure and Extinction Limit of a Methane-Air Stagnation Point Diffusion Flame," Western States Section, The Combustion Institute, Paper WS5/CI 84-10, 1984.
7. Bilger, R.W.: "Reaction Rates in Diffusion Flames," Comb. and Flame, 30 277-284, (1977).
8. Tamanini, F.T.: "Direct Measurement of the Longitudinal Variation of Burning Rate and Product Yield In Turbulent Diffusion Flames," Comb. and Flame 51, 231-243 (1983).
9. Delichatsios, M.A.: "A Simple Algebraic Model for Turbulent Wall Fires," Twenty-First Symposium (International) on Combustion, The Combustion Institute, Pittsburgh, PA, 1987.

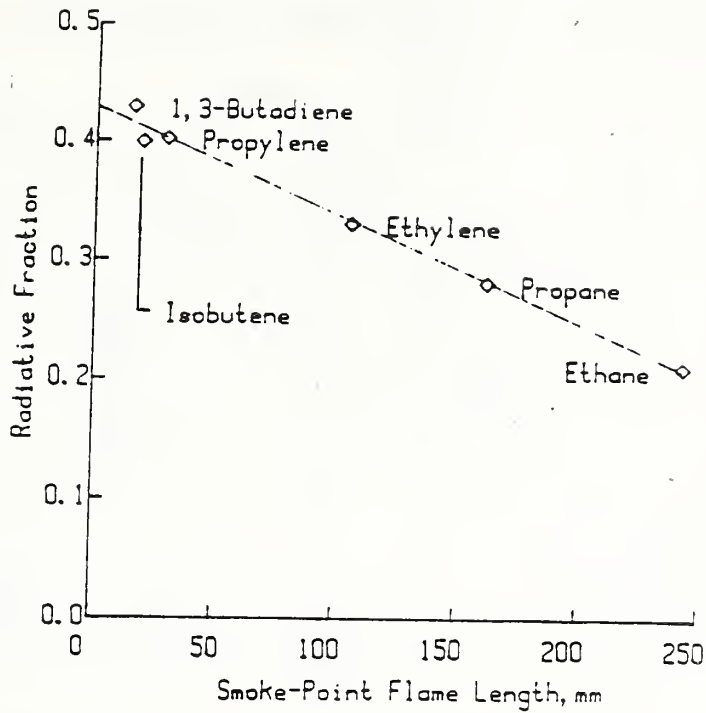


Figure 1: Correlation of radiative fraction, χ_R , for buoyant turbulent fuel-jet flames vs. laminar smoke-point flame height l_s for gaseous fuels having similar flame temperatures. Ref. 1.

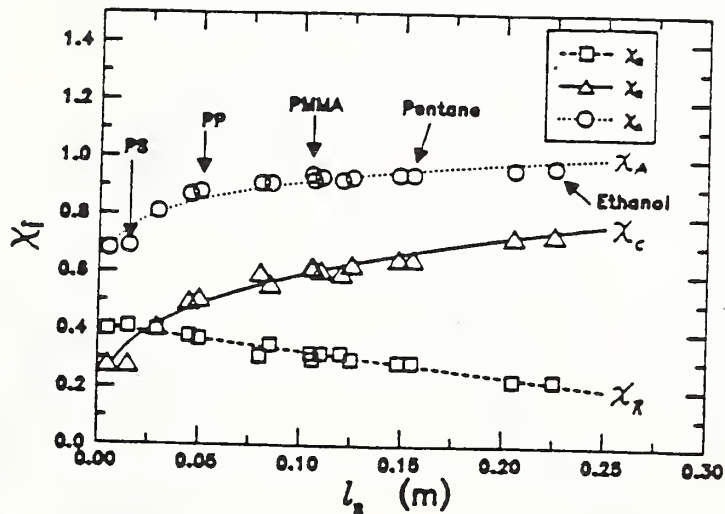


Figure 2: Correlation of actual heat release fraction, χ_A , convective heat release fraction, χ_C , and radiative heat release fraction, χ_R , from small turbulent pool fires vs. measured laminar smoke-point flame height for various noncharring solid and liquid fuels. Ref. 2.

DIFFUSION FLAME COMBUSTION MODEL

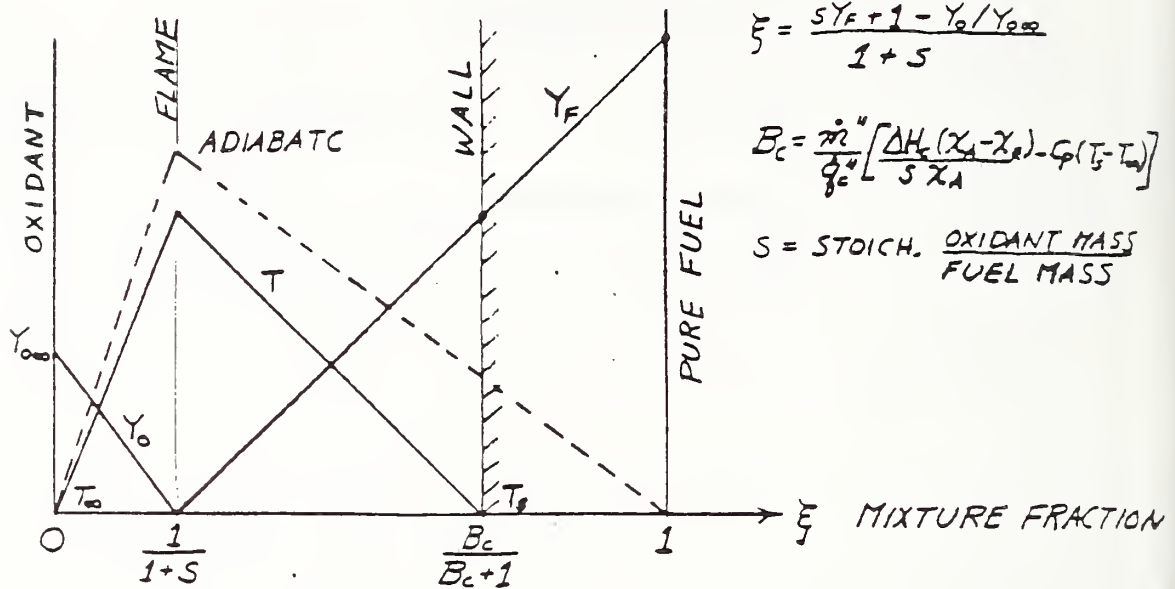


Figure 3: Schvab-Zeldovich diffusion-flame combustion model for turbulent wall fires showing how the presence of the wall reduces the supplied fuel concentration and temperature in the gas-phase at the wall. Here ξ is the normalized conserved mixture fraction and B_c is the convective mass transfer driving force.

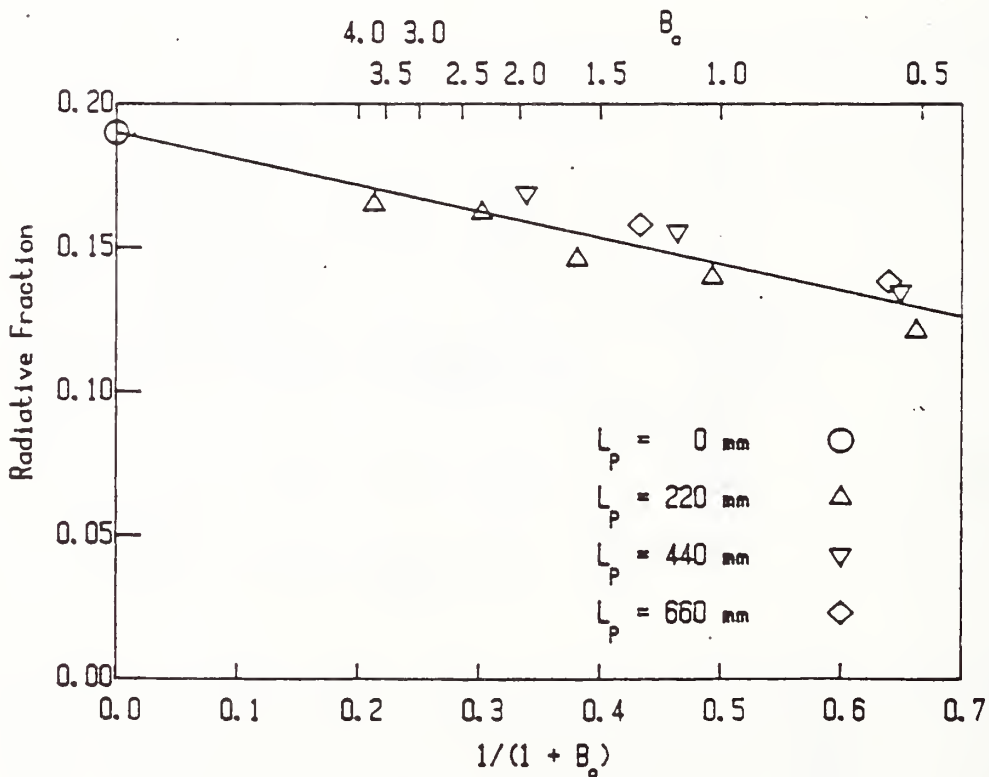


Figure 4: Corresponding correlation of the overall flame radiative fraction from two-dimensional turbulent ethane wall-fires vs. $1/(1+B_c)$ which is the fraction of combustion products present at the fuel supply surface. Ref. 3.

ETHANE WALL FIRES

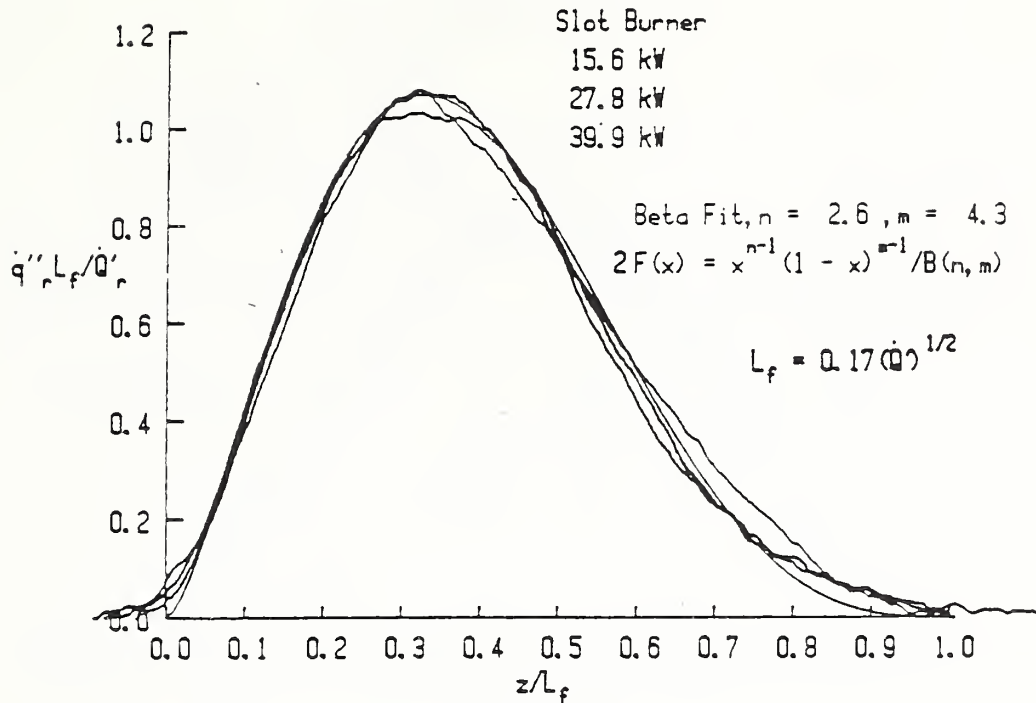


Figure 5: Correlation of the normalized local flame radiant heat release \dot{q}''_r vs. normalized height for ethane released from a slot at the base of a 38 cm. wide wall-burner with side walls. The radiant distribution correlates best for $L_f = (\dot{Q}')^{1/2}$. Ref. 3.

ETHANE WALL FIRES

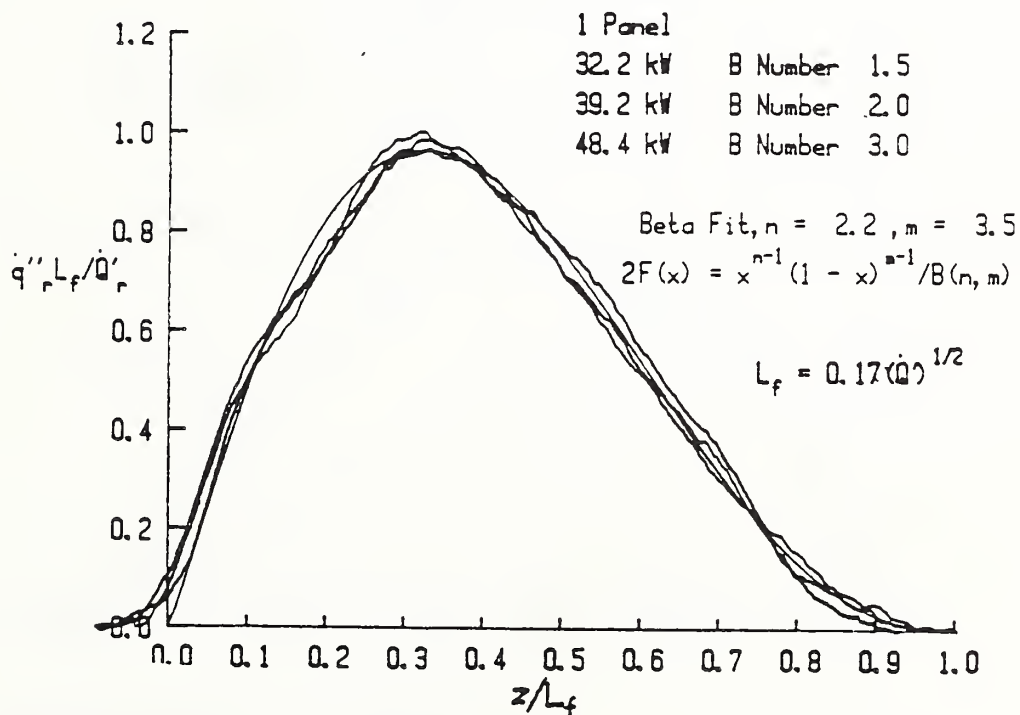


Figure 6: Correlation of the normalized local flame radiant heat transfer, \dot{q}''_r vs. normalized height for ethane released from a single panel (22 cm. high by 38 cm. wide) in the wall burner with side walls for three different total B-numbers. Ref. 3.

ETHANE WALL FIRES

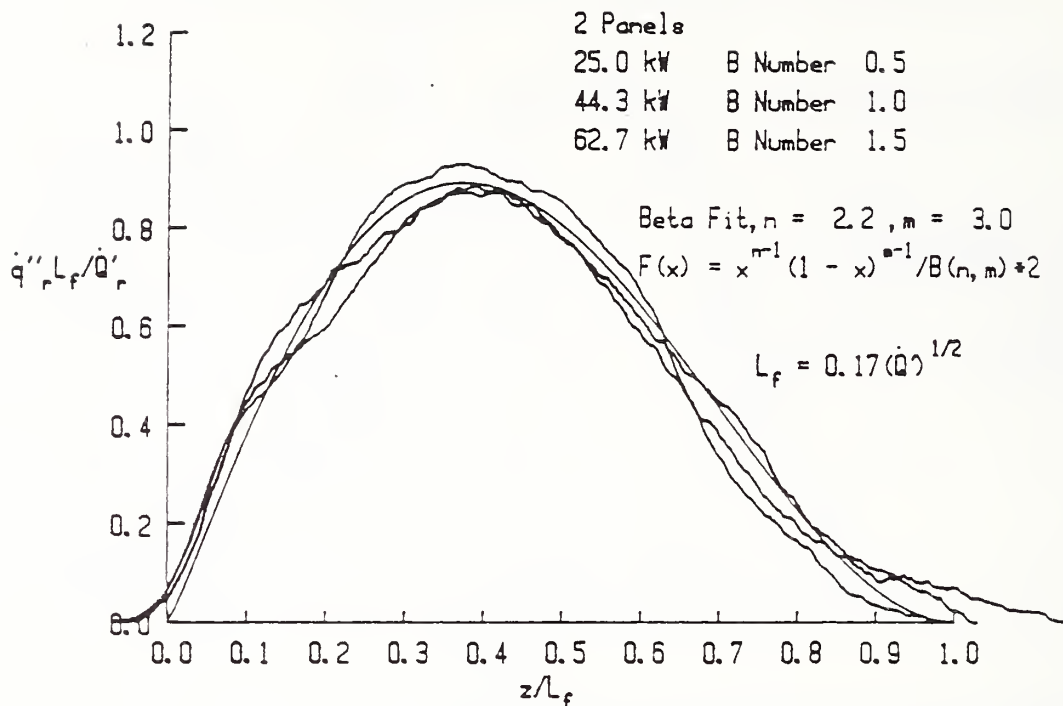


Figure 7: Correlation of the normalized local flame radiant heat transfer, \dot{q}''_r vs. normalized height for ethane released from two panels (44 cm. high by 38 cm. wide) in a wall burner with side walls for three different total B-numbers. Ref. 3.

ETHANE WALL FIRES

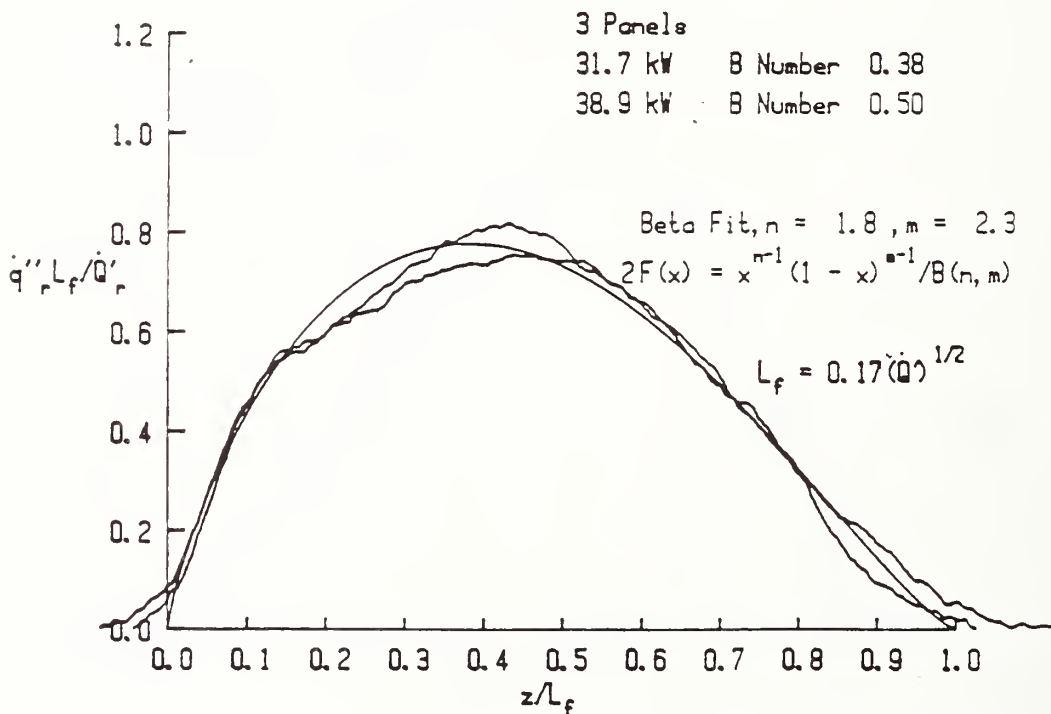


Figure 8: Correlation of the normalized local flame radiant heat transfer, \dot{q}''_r vs. normalized height for ethane released from three panels (66 cm. high by 38 cm. wide) in a wall burner with side walls for two different total B-numbers. Ref. 3.

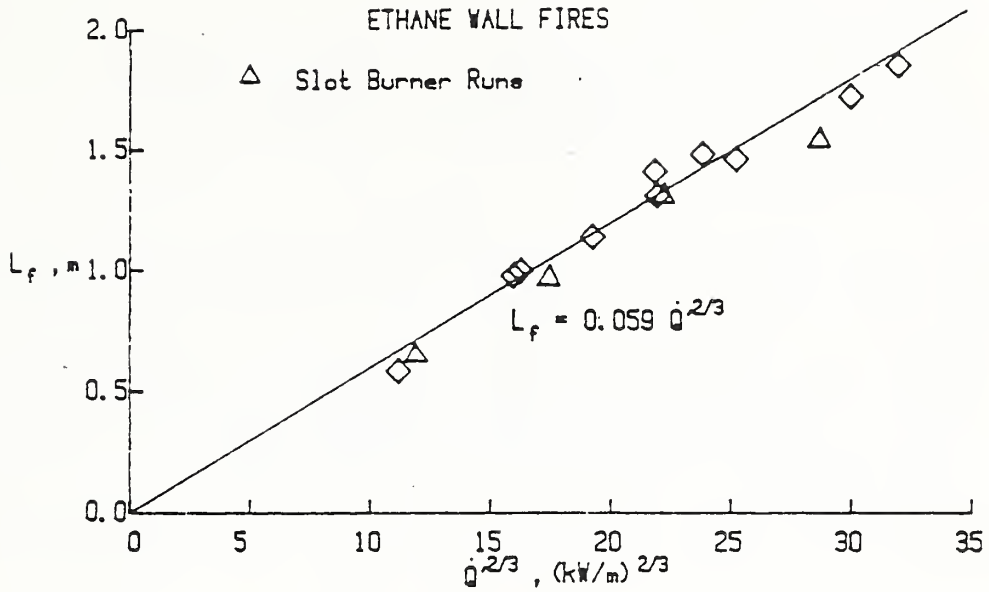


Figure 9: Correlation of flame heights L_f interpreted from a fixed finite threshold for \dot{q}_R'' versus traditional $(Q')^{2/3}$. Note the slight data curvature. Ref. 3.

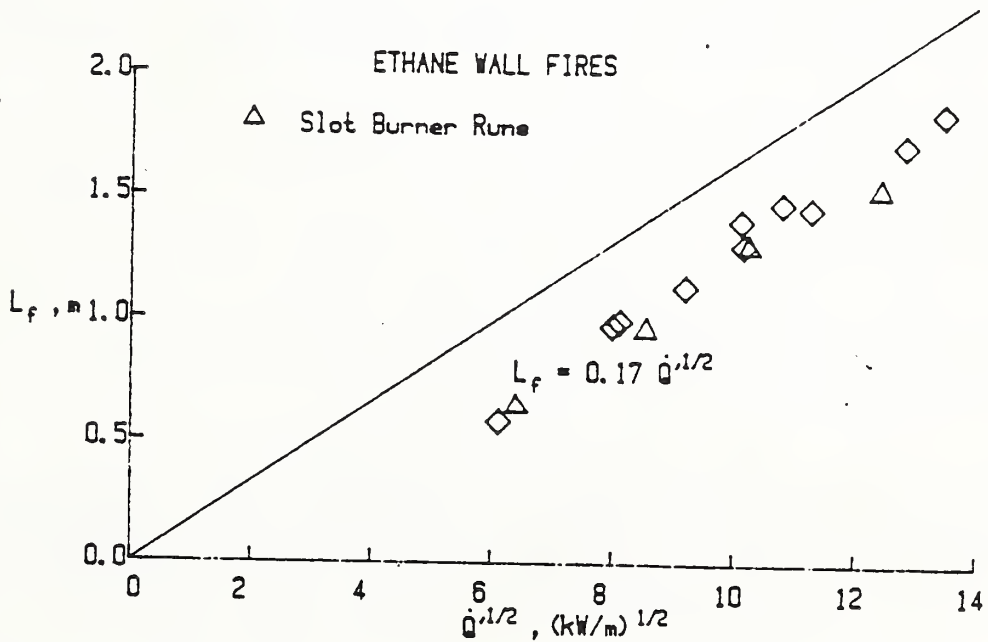


Figure 10: Correlation of the flame heights L_f interpreted from a fixed finite threshold for \dot{q}_R'' versus $(Q')^{1/2}$. The line $L_f = 0.17 (Q')^{1/2}$ is from the $\dot{q}_R'' = 0$ values fitting the complete \dot{q}_R'' profiles shown in Figures 5-8. Ref. 3.

Effect of Radiant Flux on Smoke Emission

G. W. Mulholland, V. Henzel¹, V. Babrauskas
National Bureau of Standards
Gaithersburg, Maryland 20899, USA

ABSTRACT

Smoke emission and the light extinction coefficient are measured for propane, heptane, PMMA, wood, Prudhoe Bay crude oil, and rigid polyurethane in the Cone Calorimeter for radiant fluxes up to 100 kW/m². By increasing the specific burning rate in the Cone Calorimeter to match the burning rate in a large scale test, a good correlation is obtained between the smoke properties obtained with the Cone and the same properties obtained in large scale tests. Time-resolved data are obtained for both smoke concentration and the optical extinction coefficient. For wood, it was found that soot emission increases during the later part of the burn while the optical properties remain constant.

1. INTRODUCTION

An important element in assessing the hazard of a fire is the smoke emission. Smoke from a developing fire will affect the visibility of escape routes. At the present time there is a limited amount of information regarding emission and optical properties of smoke as a function of material burning and fire scale. While there have been some small scale studies on smoke emission (Bankston *et al.* [1], Tewarson [2]) for construction materials and materials found in buildings and houses, there is no general correlation allowing one to predict the smoke emission for a large scale fire based on small scale results.

The study reported here was motivated by the observation [1,2] that the burning rate of a fuel can have a pronounced effect on the smoke emission. The hypothesis to be tested is that, for a given fuel, the smoke emission is primarily controlled by the burning rate per unit area for the case of overventilated burning. The dependence of smoke emission upon the burning rate, however, may vary from fuel to fuel. In our study the smoke emission is measured as a function of burning rate for a number of fuels and the results compared with large scale free burn results. The burning rate is varied by changing the radiant flux to the sample.

2. SMOKE MEASUREMENTS

The most rudimentary smoke quantity is the smoke yield, ϵ , which is defined as the mass of smoke aerosol generated per mass of fuel consumed. This quantity is determined by a mass flux method and by a carbon balance method. The key measurements in the flux method are the measurement of the mass of smoke

¹Nuclear Research Center Negev, Beer-Sheva 84 190, Israel.

collected on a filter, the mass loss of the fuel, the air flow rate to the filter, and the total flow rate in the stack. The carbon balance method is based on the measurement of the carbon-containing combustion products including CO_2 , CO , and smoke aerosol. A standard 47 mm filter holder with glass fiber filters and a tapered element oscillating microbalance (TEOM) were used for filter collection. The TEOM contains a removable filter element at the end of an oscillating hollow rod, and the mass deposited on the filter is determined from the change in the frequency of the rod. A nominal flow rate of 2 l/min is maintained through the filter. The TEOM is virtually the only commercial instrument capable of providing time-resolved information on smoke emission for high concentrations of sooty smoke.

One of the principal optical properties of interest is the specific extinction area, on fuel-pyrolysates basis, σ_F . For a flow system such as the Cone Calorimeter, σ_F is obtained from the measurement of the extinction coefficient, k , for a He-Ne laser beam (633 nm) transmitted through the flowing smoke.

$$\sigma_F = k / (\dot{m}_F / \dot{V}) \quad , \quad (1)$$

where \dot{m}_F is the fuel mass loss rate and \dot{V} is the volumetric flow rate through the duct. As a heuristic example, a value of $1 \text{ m}^2/\text{g}$ for σ_F means that if the smoke produced by one gram of fuel were collected over a 1 m^2 area, the light incident on this area would be blocked (intensity reduced by a factor e). Another optical property of interest is the specific extinction area, on soot-mass basis, σ_S , defined by

$$\sigma_S = k / m_S \quad ; \quad (2)$$

where m_S is the mass concentration of smoke. The quantity σ_S is an intrinsic property of the smoke depending on the wavelength of light, the optical properties of the smoke, and on the size distribution of the smoke. The quantities σ_F and σ_S are related through the equation

$$\sigma_F = \epsilon \sigma_S \quad . \quad (3)$$

3. EXPERIMENTAL PROCEDURE

The smoke emission measurements were performed in the Cone Calorimeter developed by Babrauskas [3]. The conical radiant source shown in Fig. 1 provides a uniform radiant flux over the 100 cm^2 sample for radiant fluxes up to 100 kW/m^2 . After a warmup period for the radiant source to reach steady state, the sample is inserted and ignited via a spark. The smoke aerosol and combustion gases rise through the conical heater into the exhaust hood and are sampled from a horizontal section of pipe as indicated in Fig. 1. The fuel burning rate is monitored with a load cell and, from monitoring the O_2 consumption in the exhaust gases, the heat release rate of the fuel is determined [4]. Both the incident and transmitted laser beam are monitored with photodiodes to achieve the high level of precision in the determination of the percent transmission necessitated by the 10 cm path length. The gases sampled include CO , CO_2 , O_2 , and H_2O .

A square cross section diffusion burner (2.35 cm edge length) was used for burning propane. Both the heptane and Prudhoe Bay crude oil were burned in a 8.5 cm diameter cylindrical vessel made of glass. The wood, PMMA, and rigid polyurethane were in the form of square samples measuring 10 cm on an edge with a thickness of about 2.5 cm.

Large scale fires up to 350 kW were also studied with a large scale version of the Cone Calorimeter but without an external radiant flux. The apparatus has a maximum flow of about 2 m³/s through a 2.4 m by 2.4 m collection hood located 2.4 m above the floor. As indicated in Fig. 2, the smoke from the fire is mixed by a tripper plate and then sampled 5 duct diameters downstream by an isokinetic probe. The filter collection system allows sequential collection of three filter samples over the course of a burn and is designed to minimize particle loss by heating the sampling lines and filters to the stack temperature. As in the Cone, gas analysis and light extinction measurements were performed.

4. RESULTS

The effect of the external radiant flux on the specific light extinction coefficient, σ_f , is shown in Fig. 3 for propane, PMMA, and wood. Propane is unique, because the burning rate is not effected by the radiant flux. It is set by the fuel flow rate, which has a value of about 3 l/min for all four tests. The value of σ_f for propane combustion increases by about a factor of three as the radiant flux is increased from 30 to 100 kW/m². With increasing radiant flux, the smoke emission doubles as indicated in Table 1. The value obtained for ϵ by the flux and carbon balance method agree to about 10 - 20 % for all materials. Only the values obtained by the flux method are reported in Table 1. Most entries in Table 1 correspond to an average of more than one test. Propane is the simplest case, since the external radiant flux affects the flame processes but not the generation rate of the fuel vapor. For all the other fuels, the external radiant flux affects both the generation rate of fuel vapor and the flame processes.

The mass burning rate of PMMA is approximately tripled by increasing radiant flux from 25 to 100 kW/m²; however, in this case both the smoke yield and σ_f are relatively insensitive to the radiant flux. The results are also insensitive to the sample orientation.

For the case of red oak, the smoke measurements are difficult at low fluxes because of the low smoke production. The uncertainty in σ_f is approximately ± 0.005 , which is comparable in magnitude to the observed value at the lowest radiant flux (see Fig. 3). Both the smoke yield and the specific extinction coefficient increase by almost a decade with increasing radiant flux. The major peaks in the specific extinction coefficient mirror the same peaks seen in the burning rate. The time dependence of ϵ shown in Fig. 4 also has a similar shape, though in this case there is a high level of noise. The enhanced burning at the later stage apparently results from reduced conductive heat loss when the thermal "wave" propagates through the entire sample. As has been reported by Bankston *et al.* [1], the smoke generation is greater if the sample is burning in a horizontal rather than vertical orientation.

Heptane was the only fuel that exhibited a decrease in smoke emission with an increase in the radiant flux. The mass burning rate of heptane increases more rapidly with increasing radiant flux than the other fuels because of the higher vapor pressure of heptane. It was noted that for the heptane fires there was more pronounced boiling at the higher fluxes and also that the heat release rate was several times larger than for the other fuels. It is not known whether the decrease in smoke emission is a result of more efficient combustion in the flame at the higher radiant fluxes or a result of the high temperature in the exhaust system. For the other liquid fuel, Prudhoe Bay crude oil, the smoke emission was found to be relatively insensitive to the burning rate.

As discussed above, the specific extinction coefficient, σ_s , is an intensive property of the smoke. The average value for each fuel is in the range 8 to 12 for the Cone data. The range in the average value of σ_s for the same fuels in the large scale experiments, 8-9, is much less. The collection conditions are more variable in the Cone experiments, with stack temperatures ranging from 100°C to 400°C compared to 50°C to 175°C for the large scale experiments. Also, the sampling system is isokinetic with the gas and wall temperature matched for the large scale apparatus; whereas, for the Cone the temperature of the smoke decreases by as much as several hundred degrees before reaching the filter element. The large difference between the gas temperature and the temperature of sampling duct is expected to lead to significant particle deposition resulting from thermophoresis.

The quantity σ_s is relatively constant as a function of time for burning wood as indicated in Fig. 5; even though both ϵ and σ_f increase significantly in the later stage of the burn. This result suggests that the optical properties of the soot remain relatively constant during the burn even though the soot emission is increasing.

The results for the large scale burns are compared with the Cone results for comparable burning rates in Table 2. The comparison for propane is somewhat artificial, because the burning rate is controlled by the gas flow rate and not by the external radiant flux. The lowest fuel flow rate for the large scale burner corresponds to the flame just barely covering the entire burner surface. It is an interesting coincidence that there is an abrupt increase in smoke emission with increasing fuel flow rate in the large scale experiments and a similar size increase in smoke emission with increasing radiant flux in the Cone.

The most reliably measured quantity for comparing large and small scale results is σ_f , since smoke deposition in the filter sampling line does not effect this measurement. The large and small scale results in units of m^2/g respectively are: heptane 0.086 vs 0.078, Prudhoe Bay crude oil 0.96 vs 1.01, rigid polyurethane 0.79 vs 0.89, and wood 0.034 vs 0.028. The average percent difference is about 12%, which is similar to the expected experimental uncertainty. The largest difference is for wood. In this case, the large scale measurements were made with sugar pine and the small scale with red oak. In the other cases, identical materials were used at both scales. It is also

found that there is good agreement in the smoke emission values for the large and small scale experiments for the same burning rates.

One limitation of this method for intercomparing small and large scale tests is the determination of the burning rate per area for complex structures such as cribs. We roughly estimated the effective burning area of the crib to be half of the total surface area of all the individual pieces. The factor of two reduction takes into account the limited burning of undersurfaces, the physical overlap of the individual pieces, and radiation shielding of lower pieces by upper pieces. Also, for the wood, we have taken an average of the vertical and horizontal results for the cone measurements.

5. DISCUSSION

Experimental results support a good correlation between small and large scale smoke emission results for the same specific burning rate. A demonstration of the general validity/utility of this approach must await measurements on a wider range of materials including composites and a more reliable way to estimate the burning area for complex structures.

Qualitatively, there are three ways in which large scale fires differ from small fires: the burning rate, the flame radiation, and the fluid flow. Applying an external radiant flux to a small sample enables one to match the burning rates for small and large scale and to mimic to some extent the larger fraction of radiant energy in the large fire, but not to reproduce the vigorous turbulent mixing of a large scale fire. Data are needed at fire scales up to at least 5 MW to determine the significance of the fluid flow in the plume and radiant feedback in regard to the small scale correlation.

Data from studies by Tewarson [2] and by Bankston et al. [1] are included in Table 2. It is seen that there is good agreement in the values of ϵ for PMMA, but that Tewarson's value of ϵ for heptane is a factor of two greater than our largest value. Also, the combustion efficiency reported by Tewarson, 0.93, is less than observed in this study.

Bankston et al. [1] report more than a two-fold decrease in smoke emission for wood as the radiant flux is increased from 25 kW/m² to 50 kW/m², while we observe about a factor of two increase. The difference may result from our collecting smoke only after flaming combustion begins, while Bankston et al. [1] may have also collected "pyrolysis smoke" produced before ignition occurred. It is known that the smoke yield from wood during pyrolysis is much greater than during flaming combustion.

Bard and Pagni [5] have proposed a method for estimating the maximum conversion of fuel carbon to soot based on the measurement of the maximum volume fraction of soot within the flame. As a comparison, the maximum yields obtained with the cone are 0.016 for PMMA and 0.013 for wood compared to Bard and Pagni's prediction of 0.024 for PMMA and about 0.018 for wood [5].

The values of σ_s obtained with the Cone ranged from 8 - 12 m²/g and from 8-9 m²/g for the large scale. Seader and Einhorn [6] obtained a mean value of 7.6 m²/g based on measurements on several plastics and wood in a chamber using

a polychromatic light source. Neuman and Steciak [7] obtain values of 10.3, 10.3, and 10.5 m²/g for σ_s based on flaming combustion of heptane, douglas fir, and PMMA, respectively. The measurements were made at $\lambda=633$ nm, which is essentially identical to the wavelength used in our study. These results are consistent with the statement that σ_s for soot is independent of the fuel, though systematic differences among laboratories remain to be resolved.

5. ACKNOWLEDGEMENTS

The authors gratefully acknowledge Nelson Bryner and William Twilley for assisting in obtaining and reducing the smoke data.

6. REFERENCES

- [1] Bankston, C. P., Zinn, B. T., Browner, R. F., and Powell, E. A., Aspects of the Mechanisms of Smoke Generation by Burning Materials, Combustion and Flame, 41, 273-292 (1981).
- [2] Tewarson, A., Prediction of Fire Properties of Fuels, Twenty-First Symp. (Intl.) on Combustion, The Combustion Institute, Pittsburg, 563-570(1986).
- [3] Babrauskas, V., Development of the Cone Calorimeter - A Bench-scale Heat Release Apparatus Based on Oxygen Consumption (NBSIR 82-2611), [U.S.] Nat. Bur. Stand. (1982).
- [4] Huggett, C., Estimation of Rate of Heat Release by Means of Oxygen Consumption Measurements, Fire and Materials, 4, 61-65 (1980).
- [5] Bard, S., and Pagni, P. J., Spatial Variation of Soot Volume Fractions in Pool Fire Diffusion Flames, First Symp. (Intl.) on Fire Safety Science, C. E. Grant and P. J. Pagni, ed. New York, Hemisphere Pub., 361-369 (1986).
- [6] Seader, J. D., and Einhorn, I. N., Some Physical, Chemical, Toxicological, and Physiological Aspects of Fire Smokes, Sixteenth Symp. (Intl.) on Combustion, The Combustion Institute, Pittsburg, 1423 -1444 (1977).
- [7] Newman, J. S., and Steciak, J., Characterization of Particulates from Diffusion Flames, Combustion and Flame, 67, 55 - 64 (1987).

Table 1. Smoke Emission measured with the Cone Calorimeter

Fuel	Radiant Flux, kW/m ²	Burning Rate, g/sm ²	Comb. Eff.	Smoke Yield	$\sigma_F, m^2/g$	$\sigma_S, m^2/g$
Propane	0	176	0.98	0.0057	0.019	-
	30	176	-	0.0064	0.038	6.4
	50	176	0.98	0.0087	0.057	7.3
	100	176	-	0.0137	0.127	9.5
n-Heptane	0	10.0	0.99	0.0125	0.089	7.7
	10	24.0	0.94	0.0131	0.083	6.6
	20	31.9	0.97	0.0096	0.072	7.9
	30	58.4	0.99	0.0062	0.050	8.3
	a		0.93	0.027		
Prudhoe Bay crude oil	0	4.5	40.9 ^b	0.098	1.06	11.7
	25	10.7	38.1	0.096	1.01	10.8
	40	18.1	36.9	0.083	1.01	12.5
	50	23.9	35.5	0.084	0.98	11.7
PMMA	25	16.4	0.96	0.0152	0.159	10.9
	50	25.0	0.96	0.0137	0.169	12.5
	75	37.8	0.95	0.0121	0.167	11.3
	100	47.0	0.96	0.0160	0.164	10.8
	a		0.95	0.016		
Red Oak	25, V	8.9	11.8 ^b	0.0010	0.011	-
	25, H	8.3	10.6	0.0020	0.022	11.2
	50, V	11.7	11.3	0.0018	0.025	13.4
	50, H	11.8	10.9	0.0055	0.050	9.0
	75, V	14.7	11.4	0.0033	0.035	11.0
	75, H	14.6	10.8	0.0080	0.094	14.6
	100, V	18.9	11.3	0.0089	0.060	9.3
	100, H	18.7	11.5	0.0129	0.120	9.8
Douglas fir ^c	25			0.025		
	50			<0.01		
Rigid Poly-urethane foam	50	5.3	0.85	0.080	0.89	9.4

V and H refer to the vertical and horizontal orientation of the sample, respectively.

^aResults by Tewarson.

^bAverage heat of combustion, MJ/kg.

^cResults by Bankston et al. for sample 7.5 by 7.5 cm.

Table 2. Comparison of Small and Large Scale Smoke Emission Results

Fuel/Conditions	\dot{Q} , kW	Burning Rate, g/sm ²	Comb. Eff.	Smoke Yield	σ_f , m ² /g	σ_s , m ² /g
<u>Propane</u> , 1 m	110	2.8	1.03 ^a	0.0077	0.049	-
diff. burner	175	4.2	1.11 ^a	0.0168	0.154	8.1
	350	8.6	1.09 ^a	0.0199	0.161	7.8
2.35 cm burner						
0 kW/m ²	4.2	176	0.98	0.0057	0.019	9.9
50 kW/m ²	4.2	176	0.98	0.0087	0.051	7.3
100 kW/m ²	4.2	176	-	0.0137	0.127	9.5
<u>n-Heptane</u> ,						
31 cm pool	70	24.9	0.89	0.0093	0.074	7.3
50 cm pool	240	28.3	0.94	0.0121	0.098	8.2
8.5 cm pool						
10 kW/m ²	7.1	24.0	0.94	0.0131	0.083	6.6
20 kW/m ²	10.0	31.9	0.97	0.0096	0.072	7.9
<u>Prudhoe Bay crude oil</u> ,						
40 cm pool	65	14.3	34.5 ^b	0.090	0.96	9.5
50 cm pool	185	(18.1)		0.085	-	8.7
8.5 cm pool						
25 kW/m ²	2.3	10.7	38.1 ^b	0.096	1.01	10.8
40 kW/m ²	3.8	18.1	36.9	0.083	1.00	12.5
<u>Wood</u>						
Sugar pine						
1 crib	56	8.7 ^c	12.9 ^b	0.0036	0.029	8.5
3 cribs	254	12.6	13.4	0.0042	0.040	9.4
Red oak, 10 cm						
25 kW/m ²	1.0	8.6	11.2 ^b	0.0015	0.017	11.2
50 kW/m ²	1.3	11.8	11.1	0.0037	0.038	11.2
<u>Polyurethane</u> ,						
rigid 1 crib	125	12.0 ^c	0.68	0.085	0.74	9.1
2 cribs	310	14.6	0.68	0.101	0.81	8.5
10 cm 50 kW/m ²	2.5	5.3	0.85	0.080	0.89	9.4

^a The erroneously large combustion efficiency results from an uncertainty in the propane flow calibration.

^b The heat of combustion in MJ/kg.

^c The effective surface area for combustion is taken as half the total surface area of all the individual sticks.

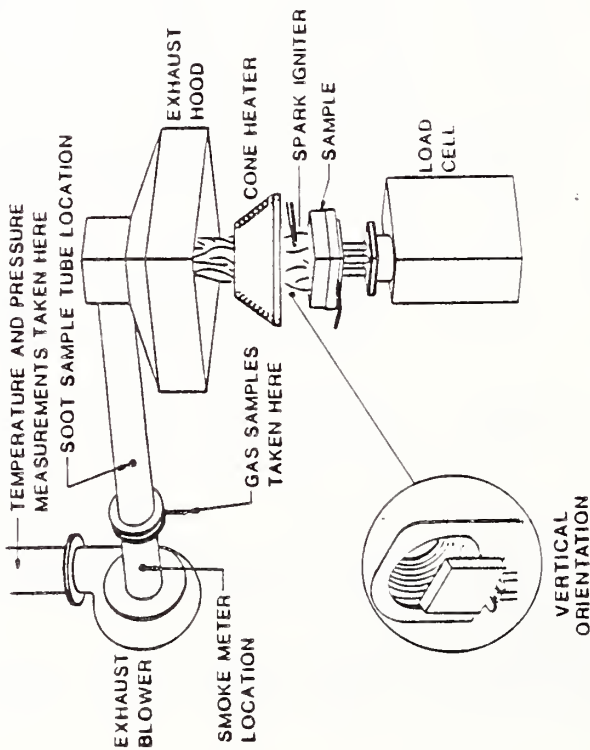


Fig. 1. Conceptual view of small scale test facility

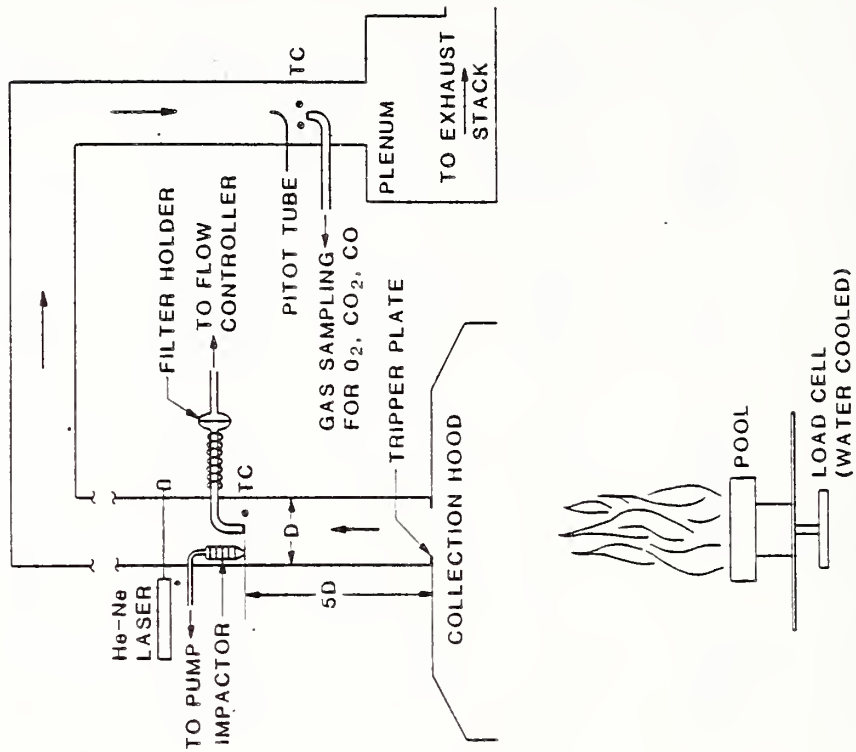


Fig. 2. Large scale facility for monitoring smoke emission/properties.

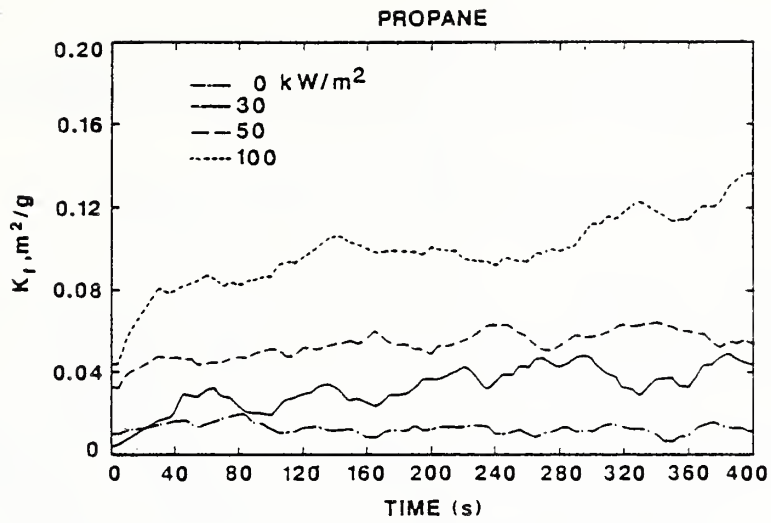


Fig. 3. Specific extinction area, K_f , versus time for radiant fluxes in range 25-100 kW/m^2

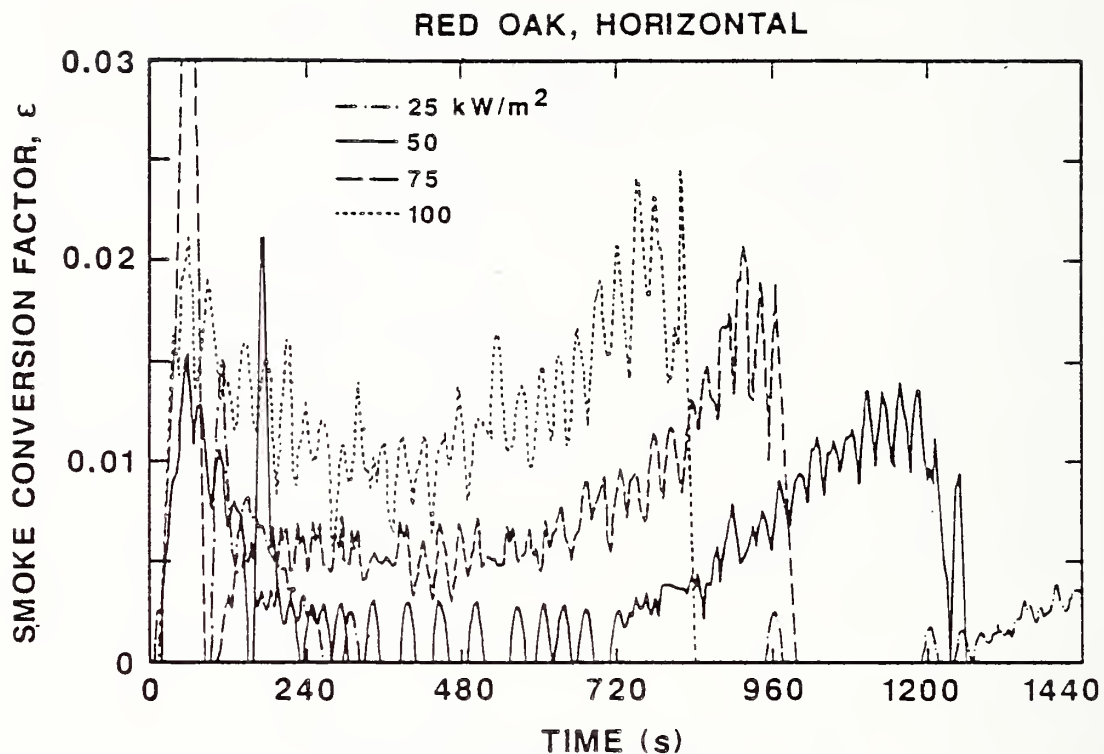


Fig. 4. Smoke conversion factor ϵ versus time

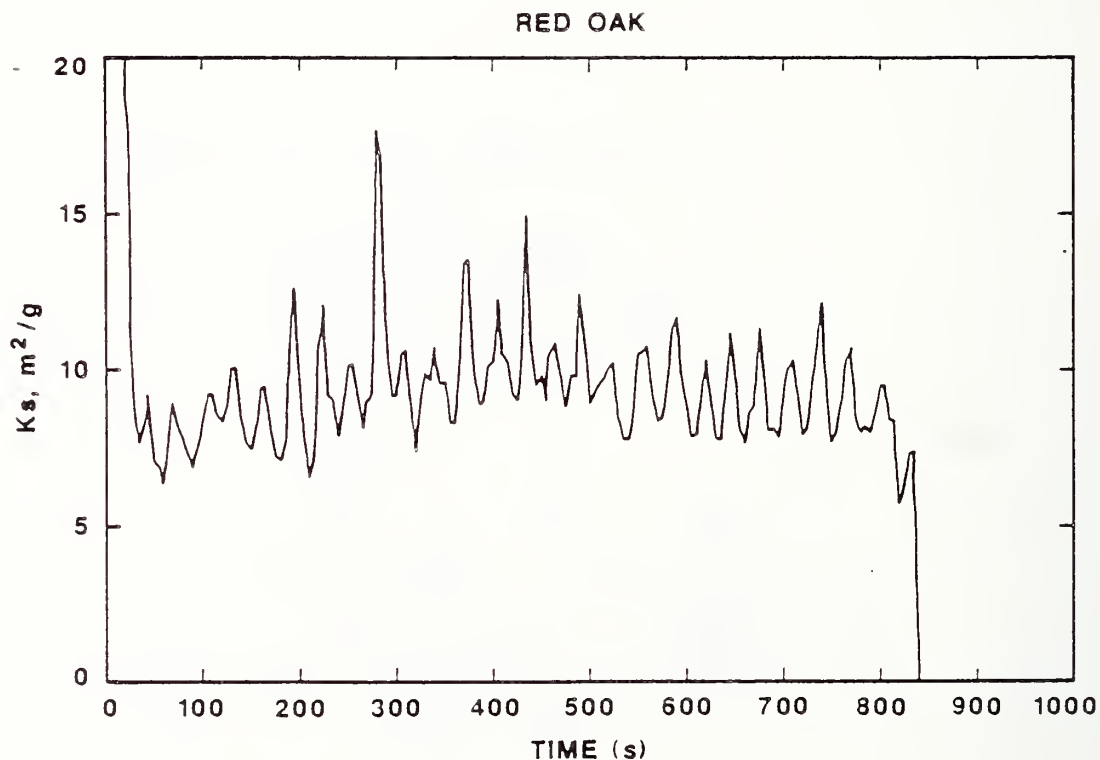


Fig. 5. Specific extinction coefficient K_s versus time for radiant flux of 100 kW/m²

THE DISTRIBUTION OF SOOT IN LARGE BUOYANT DIFFUSION FLAMES

E. E. Zukoski
California Institute of Technology
Pasadena, California 91125

A study is being made of the internal structure of large buoyant fire plumes with a new experimental technique which was developed by R. Miake-Lye and S. J. Toner (1986) following a suggestion by P. Dimotakis. The technique involves the measurement of the light scattered from a narrowly focused argon-ion laser beam by soot which is generated by diffusion flames within the fire plume itself. The beam is directed across the flame and study of the scattered light allows us to measure the distribution of soot within the fire plume. In contrast, photographs taken in light emitted by thermal processes from soot particles allow only the exterior surface of the fire plume to be studied.

The fire plumes used in these studies are methane-air diffusion flames stabilized on a 50 cm diameter burner which utilizes an uncooled bed of glass beads to produce a uniform flow of methane at the burner surface. Flames, with total heat release rates in the range 20 to 200 kW, were chosen for study because other characteristics of these flames have been studied and reported elsewhere, e.g., Cetegen et al (1984). These flames are in the transition regime between flames with height to diameter ratios which are less than one and greater than three and thus are in regime II defined in Zukoski (1986).

In the original experiments, described in Miake-Lye and Toner (1987), the laser beam was passed through the flame in a horizontal direction which intersected a vertical line extending above the center of the burner. Data was obtained for heights which ranged from the surface of the burner to positions several burner diameters above the surface.

Light scattered from the laser beam was filtered to remove the background radiation and then was focused on a 1024 pixel, linear solid-state, RETICON array camera. The array was interrogated at a frequency of 586 hz and the light intensity of each pixel was recorded as a function of the time. The presence of scattered radiation with an amplitude above twice the background radiation level was interpreted to mean that soot was present at that position and time.

In preliminary experiments, we found that at positions where laser light was scattered, visible radiation from soot was present. Because of the rapid cooling of soot particles in the absence of a diffusion flame, visible radiation was assumed to be an indicator of the presence of a diffusion flame. Hence, we expect and assume, in interpreting our data, that scattered radiation is also an indicator of the presence of a diffusion flame.

Thus, if scattered laser light is present at a given point and at a given time, we can reasonably assume that a diffusion flame, complete with fuel on

one side and oxygen on the other, was close to the point under observation at the time of the measurement. In our picture, the fuel and oxygen may be vitiated by combustion products, but both were assumed to be present.

The use of a sheet of laser light would have given us a much more complete picture of the flow, but we were restricted to the beam because we did not have a laser with the power required to produce a sheet with the requisite intensity and by limitations on the data acquisition rate of the camera system used to record the scattered light intensity.

In ongoing experiments, the direction of the beam has been changed to produce a vertical beam which passes through positions which correspond to the centerline of the burner and 5 radial positions extending out to the edge of the 50 cm diameter burner.

The most interesting result of this study has been the discovery that soot is present in very complex and dense patterns within the flame and that it is present between 40 to 60% of the time at all points within the exterior envelope of the fire plume. The exterior envelope here is taken to be the outer surface of the region illuminated by radiation from soot or chemiluminescence. This result has been observed to hold for elevations near the surface of the burner and up to two burner diameters above the burner surface. In our interpretation of the data, these results suggest that diffusion flamelets, separating regions rich in fuel or oxygen, are densely distributed within the exterior envelope of the fire plume. This result can only be true if transport of oxygen from the entrained air throughout the fire plume is very rapid.

We believe that the large structures, shed from the burner in these flames at a frequency of the order of several Hertz, are responsible for this rapid transport and that secondary instabilities which develop on these structures are responsible for the fine details of the diffusion flamelets observed within the flames.

The data being obtained with the vertical orientation of the laser beam will allow us to determine the geometry and celerity of the structures present in the lower part of large diffusion flames and to continue our study of the interior of the fire plume.

This work has been supported by the Gas Research Institute and the Fire Research Center of the National Bureau of Standards.

REFERENCES

Miake-Lye, R. C. and Toner, S. J. (1987), "Laser Soot-Scattering Imaging of a Large Buoyant Diffusion Flame", Combustion and Flame, 67, 9-26.

Cetegen, B.M., Zukoski, E. E. and Kubota, T. (1984), "Entrainment in the Near and Far Field of Fire Plumes", Combustion Science and Technology, 39, 305-331.

Zukoski, E. E. (1985), "Fluid Dynamic Aspects of Room Fires", Proc. of First International Symposium on Fire Safety Science, Hemisphere Publishing Corp, 1986.

PREDICTING CAPABILITY OF A MULTIROOM FIRE MODEL

Kazuhito NAKAMURA

Design Division
Shimizu Construction Corporation
2-16-1 Kyobashi, Chuoh-ku, Tokyo 104

INTRODUCTION

For a performance based fire safety design method of buildings, user friendly computer models to predict smoke transport behavior in buildings is considered to be one of its indispensable elements.

As such prediction models for smoke movement, chiefly two types of zone models have been developed by now, that is, one based on one layer concept and the other based on two layer concept. The former will be convenient to predict smoke movement throughout large scale buildings, high-rise buildings and so on, and the latter is thought to be beneficial when we need to know some more detailed behavior of smoke around the room of fire origin.

However, many of these models, which have been developed primarily for research purpose, will more or less need to be refined for the convenience of design practice as well as for the improvement in accuracy to be used for design purposes. A multiroom smoke movement model (Ref.1), which is based on two layer concept, has been refined from this point of view. The points of refinement include, a) the prediction of lower layer properties, by which stack effect due to the temperature difference between inside and outside of building can be treated, b) capability of dealing with mechanical smoke control, c) time scheduled opening and closing of openings, by which the effects of door opening due to evacuation or window breaking due to fire on smoke movement can be assessed, d) capability of dealing with spaces of complex geometry such as a dome, and e) improvement of stability and speed up in numerical calculation.

Since most of the theoretical aspects of the model are given in Ref.2, this paper focus on the model of the opening jet plume near opening region and some of the features for the convenience of design practices.

OPENING JET PLUME NEAR OPENING

In this model, it is assumed that the plumes originated by fire source and opening jets can penetrate through interfaces of the upper and lower layers, due to which exchanges of mass and heat take place. As a result the method to determine the fraction of mass and heat penetration becomes one of the key points. In the region far away from the source of opening plume, i.e., opening jet, the fraction can be calculated by modeling opening jet plume as vertically rising plumes and assuming Gaussian profiles on the lateral profile of temperature

and vertical velocity in a plume and criterion temperature of penetration (See Appendix 2.).

In the region near an opening, however, simple application of Gaussian profile can cause a problem: i.e. the axis temperature of modeled plume ΔT_a can become higher than the temperature of the opening jet ΔT_j . This is illustrated by the example shown in Fig.2. In this example, an opening jet at 300°C enters a lower layer at 20°C and rises through the layer entraining the air and penetrates into an upper layer at 300°C. In this particular case, the excess temperature on the axis of the modeled plume exceeds the temperature difference between the opening jet and the ambient layer ΔT_j ($=300-20=280$ K) in the region of $Z < 0.72$ m. So, if the criterion temperature for plume penetration is assumed as

$$\Delta T_c = (T_j - T_\infty) / 2 = 140 \text{ [K]}$$

the net heat gain of the upper layer becomes positive in the region of $Z < 0.25$ m as is shown in Fig.2, so that the upper layer is heated while it has to be cooled in reality. Needless to say, this is attributed to the sharp peak of Gaussian profile of the temperature near axis, which is unrealistic in the sense that the plume axis temperature ΔT_a exceeds the opening jet temperature ΔT_j .

It will be more reasonable to consider that an opening jet initially has flat profiles of temperature and velocity, but the profiles collapse as the distance Z increases and eventually turns into Gaussian profiles. Here an interim model is proposed as follows to deal with the penetration in the region near opening.

Let Z_c be the height where the excess temperature of the axis of a plume with a Gaussian profile ΔT_a becomes equal to the temperature difference between the opening jet and the ambient layer ΔT_j . The near region to an opening is defined as the region where $Z < Z_c$. It is assumed that the temperature profile of the off central part of a plume follows Gaussian profile with axis temperature $\Delta T_a'$, and inner part takes flat temperature profile. Similar profile is assumed for the velocity profile being W_a' as the axis velocity of plume. In other words,

$$\frac{\Delta T_a}{\Delta T_a'} = e^{-\beta^2 \eta^2} \quad \text{---(1)}$$

$$\frac{W_a}{W_a'} = e^{-\eta^2} \quad \text{---(2)}$$

where η is the radius in Howarth transformation which corresponds to ΔT_a on the Gaussian temperature profile.

Now, let m_{z1} be the mass flow rate through near axis area ($0 \leq \eta \leq \eta_c$), m_{z2} be the rate through off axis area ($\eta_c \leq \eta$) and m_z be the total mass flow rate, then

$$m_z = m_{z1} + m_{z2} \quad \text{---(3)}$$

$$\begin{aligned} m_{z1} &= 2\pi \int_0^{\eta_c} W_a' e^{-\eta^2} \rho_\infty b^2 \eta d\eta \\ &= \pi W_a' \rho_\infty b^2 e^{-\eta_c^2} \eta_c^2 \quad \text{---(4)} \end{aligned}$$

$$m_{z2} = 2\pi \int_{\eta_d}^{\infty} W_0' e^{-\eta^2} \rho_{\infty} b^2 \eta d\eta$$

$$= \pi W_0' \rho_{\infty} b^2 e^{-\eta_d^2} \quad \text{---(5)}$$

Similarly, for the rate of heat flow through near and off axis regions, we have

$$Q = Q_1 + Q_2 \quad \text{---(6)}$$

$$Q_1 = 2\pi c_p \int_0^{\eta_d} \Delta T_0' e^{-\beta^2 \eta^2} w_0' e^{-\eta^2} \rho_{\infty} b^2 \eta d\eta$$

$$= \pi c_p w_0' \rho_{\infty} b^2 \Delta T_0' e^{-(1+\beta^2)\eta_d^2} \eta_d^2 \quad \text{---(7)}$$

$$Q_2 = 2\pi c_p \int_{\eta_d}^{\infty} \Delta T_0' e^{-\beta^2 \eta^2} w_0' e^{-\eta^2} \rho_{\infty} b^2 \eta d\eta$$

$$= \frac{\pi c_p W_0' \rho_{\infty} b^2}{1+\beta^2} \Delta T_0' e^{-(1+\beta^2)\eta_d^2} \quad \text{---(8)}$$

From Eqs.(1)-(8) and (A3), η_d can be obtained as follows:

$$\eta_d^2 = \frac{1 - \frac{1}{1+\beta^2} \left(\frac{Z+Z_0}{Z_0} \right)^{5.3}}{\left(\frac{Z+Z_0}{Z_0} \right)^{5.3} - 1} \quad \text{---(9)}$$

Using η_d^2 , the rate of mass penetrating through a layer interface is given as follows:

$$m_{p \rightarrow n} = m_z - 2\pi \int_{\eta_{\Delta T_c}}^{\infty} w_0' e^{-\eta^2} \rho_{\infty} b^2 \eta d\eta$$

$$= m_z - \pi w_0' \rho_{\infty} b^2 e^{-\eta_{\Delta T_c}^2}$$

$$= m_z \left\{ 1 - \frac{1}{1+\eta_d^2} e^{-(\eta_d^2 - \eta_{\Delta T_c}^2)} \right\} \quad \text{---(10)}$$

where $\eta_{\Delta T_c}^2$ is the radius in Howarth transformation which corresponds to threshold temperature of penetration ΔT_c . And the penetration rate of heat is given as

$$Q_p = Q - 2\pi c_p \int_{\eta_{\Delta T_c}}^{\infty} \Delta T_0' e^{-\beta^2 \eta^2} w_0' e^{-\eta^2} \rho_{\infty} b^2 \eta d\eta$$

$$= Q - \pi c_p W_0' \rho_{\infty} b^2 \Delta T_0' \frac{e^{-(1+\beta^2)\eta_{\Delta T_c}^2}}{1+\beta^2}$$

$$= Q \left\{ 1 - \frac{1}{1+(1+\beta^2)\eta_d^2} e^{(1+\beta^2)(\eta_d^2 - \eta_{\Delta T_c}^2)} \right\}$$

$$= Q k \quad \text{---(11)}$$

where

$$k = 1 - \frac{1}{1+(1+\beta^2)\eta_d^2} e^{(1+\beta^2)(\eta_d^2 - \eta_{\Delta T_c}^2)} \quad \text{---(12)}$$

So, it follows that the penetration model near opening has been obtained.

It should be kept in mind, however, that this theory is not perfect but of a compromised nature since the total mass flow rate have to be calculated using Eqs.(A1),(A2), i.e., the equations for the flow rate for far field region of plume with virtual point heat source as a adjusting parameter.

1. Treatment of Mechanical Smoke Control System

For the convenience of evaluating efficiencies of smoke control by means of air handling system, this computer model has incorporated a feature to make it possible to deal with smoke control system to some extent.

The method employed in this model is rather simple : The air supply rate or smoke exhaust rate with time is given by the user in terms of volume flow rate as input data and converted into mass flow rate by the code. The mass rate of air given to each layer as the result of air supply is determined at each time step considering the height of the air inlet relative to the height of the layer interface. Similar consideration is taken to determine the mass rate of gases removed from each layer by mechanical exhaustion.

2. Opening and Closing of Openings

In the course of evacuation, condition of opening in a building may change. For example, doors in a building may be opened or closed by evacuees or others, natural smoke vents may be opened to let smoke go out, and fire doors may be closed automatically or manually for confinement of fire. And these changes of opening conditions, of course, greatly affect the movement of smoke in the building. So a feature is incorporated so that the calculation can be made under changing conditions of openings when the time schedules of openings are specified by users as input data.

3. Treatment of spaces of complex shape

Although most of building spaces have rectangular or other simple shapes, the number of spaces which have somewhat complex shape cannot be neglected in particular in case of high ceiling spaces or large scale spaces. This model can deal with such complex spaces by modeling a complex space as a stack of rectangular space units.

SAMPLE CALCULATIONS

In the followings, the results of three sample calculations are shown to demonstrate the computation capability of the present model.

1. Smoke Filling in Large Scale Space

A series of field experiments for smoke behavior were conducted using the pavilions of the international exposition held in Tsukuba, 1985, taking advantage of the time lag between the closing of the fair and the pulling down of the pavilions.

Of the pavilions in which fire experiments were run, the pavilion that had been used for USSR's exhibitions was a large scale space with a saddle back roof as is shown in Fig.5. Its floor area was 2,000 m² and the height of the roof ridge was

19.2 m. As the smoke control measure, a mechanical smoke exhaustion system consisting of five smoke vents, a duct and a fan with the capacity of 1,000 m³/h was installed according to the Building Standard Law of Japan.

Methanol in the six trays arranged together on the center of the floor was used as the fire source. Its heat release rate is estimated as about 2,400 kW.

The predicted and measured results of the temperature and the interface height of the upper layer are shown in Fig.6 for the cases with and without mechanical smoke exhaustion. The layer interface heights of the experiments were determined from the thermocouple readings using the same method as is used by Cooper et al (Ref.5), and the space is modeled as the stack of seven rectangular space unit for the calculation.

The predicted smoke layer height for no mechanical ventilation case agrees comparatively well with the measured results although a trivial difference is observed at the initial stage.

On the other hand, while the predicted layer height for mechanical smoke ventilation case is higher than for no mechanical ventilation by one meter, no meaningful difference can be observed between the experimental layer heights for the two cases. The reasons why the effect of mechanical smoke exhaustion did not appear on the smoke layer heights may be attributed partly to the possible infiltration of outdoor air to the smoke layer through invisibly small openings on the wall of the pavilion and partly to the possible large mixing of the smoke with air as it travels down to the edge of the space after having impinged on the roof.

The predicted layer temperatures are consistently higher than the measured. The position of thermocouple trees may have some relation on this difference, but the convective heat transfer model may be responsible too. While the predicted temperature difference is small between the cases with and without mechanical exhaustion, the measured temperature difference is significant between the two cases. It is suspected that because an exhaustion vent was located right above the fire source, the gas in the plume, which is hotter than the layer average, were exhausted effectively.

2. Mechanical Smoke Exhaustion at Office Space

Of the Tsukuba Expo. '85 pavilions used for the series of the experiments, IBM pavilion was provided with a mechanical smoke exhaustion system at its office area in compliance with The Building Standard Law. The office area used for the experiments consisted of an office with 51 m. and a corridor of 1.75 m wide and 30 m long as is shown in Fig.7. The ceiling height of this area was 2.7 m. One of the mechanical smoke vents were located at a corner of the office and the other at the end of the corridor and could exhaust smoke at the rate of 0.9 m³/s and 1.3 m³/s, respectively.

The fire source was placed at the center of floor of the office. The fuel was methanol and the size of the source was 0.9 m x 0.9 m. The heat release rate is estimated as 320 kW.

The predicted and the experimentally observed behavior of the smoke layers are shown in Fig.9 for the case with mechani-

cal exhaustion, at the office and the corridor, and the case without mechanical exhaustion. The figures schematically illustrates the section of area and the left hand side and the right hand side represents the office and the corridor, respectively. The experimental temperature rise in the smoke layers in Fig.9 were obtained by thermocouple readings and are shown by the shades of different thickness according to the temperature.

In the prediction, the corridor was divided into two parts because it was considerably long and had a turn at the middle.

In the case of no mechanical ventilation, the predicted layer temperatures are somewhat higher than those measured, but generally speaking, the agreement of the predicted and experimentally obtained layer behavior can be said fair. In the case when the mechanical ventilation operated, both the prediction and the experiment demonstrate that the smoke can be effectively exhausted from the spaces by the smoke control system.

3. Prediction of Smoke Movement in a Model Building

Prediction was attempted for the smoke movement for a eight story model building with an atrium. The building consists of an atrium of which size is 20 m x 20 m x 32 mH and two rooms of 10 m x 20 m x 3 mH on each floor. And on 3rd through 8th floor, two fire shutters, 5 m x 3 mH each, are installed on each opening facing to the atrium. On the top of the wall of the atrium is a natural smoke vent of 12 m wide and 1 m high, and on each floor an air supply fan with capacity 4 m³/s is equipped.

The calculation was run under the scenario described as follows:

<u>time</u>	<u>event</u>
before 0 sec.	the outdoor and indoor temperature were 30°C and 20°C respectively
0 sec.	fire breaks out on the floor of the atrium (heat release rate increase linearly from zero to reach 5 MW at 300 sec. and then levels off)
60 sec.	detects fire, evacuation starts throughout the building a window is opened at the office on 7th floor
120 sec.	the fire shutters on each floor close but on 5th and 6th floor one of the two failed to close due to some trouble.
125 sec.	mechanical air supply fan switches on 6th floor
270 sec.	the natural vent opens at the top of the atrium

The results of the prediction are shown in Fig.10. This

calculation for predicting the 600 seconds of fire took about 100 seconds of CPU time by BRI computer (FACOM M-380Q).

CONCLUDING REMARKS

We acknowledge that the models on the entrainment of door-jet or the penetration of plumes are not based on very solid understanding of the phenomena, so we may have to be careful when we apply the model extensively to various problems. However, perfect models are not necessarily available in many other areas of engineering either, in particular when complex problems have to be dealt with.

It is obvious that engineering tools to predict fire behavior can help rationalize fire safety measures of buildings even if they are not perfect. In this sense, many of the existing models can be used in practical issues if sufficient attentions are paid on their limitations.

As for the present model, it is evaluated that with the introduction of partial penetration model of opening jets, the model is refined so that predict smoke movement in building can be predicted reasonably well without giving contradictory results, although it does not seem so good in predicting convective heat transfer. Also, the model is equipped with several features which are thought to be beneficial for design purposes.

The model still needs improvements on many respects, such as convective heat transfer, lateral smoke propagation along corridors, smoke behavior in narrow vertical shafts and so on, so we would like to continue its refinements absorbing better understandings on these phenomena as they grow.

References

1. Tanaka, T., "A Model of Multiroom Fire Spread", NBSIR 83-2718(1983), NBS
2. Nakamura, K. and Tanaka, T., "Refinement of A Multiroom Fire Spread model", The 2nd ASME-JSME Meeting on Thermal Engineering (1987), Hawaii
3. Cetegen, B.M., Zukoski, E.E. and Kubota, T., "Entrainment and Flame Geometry of Fire Plumes", NBS-GCR-87-402(1982), NBS
4. Tanaka, T., "A Proposed Model of the Behavior of Plumes in Two Layer Models", 8th UJNR Joint Panel Meeting on Fire Safety (1985), BRI, Japan
5. Cooper, L.Y., Harkleroad, M., Quintiere, J. and Rinkinen, W., "An Experimental Study of Upper Layer Stratification in Full-Scale Multiroom Fire Scenarios", Journal of Heat Transfer Nov. 1982, Vol.104

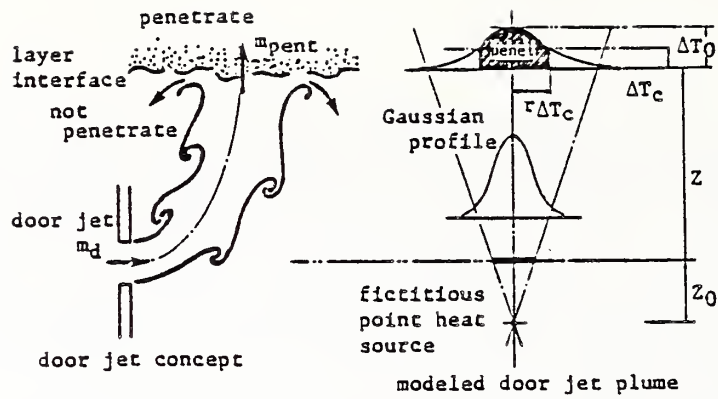
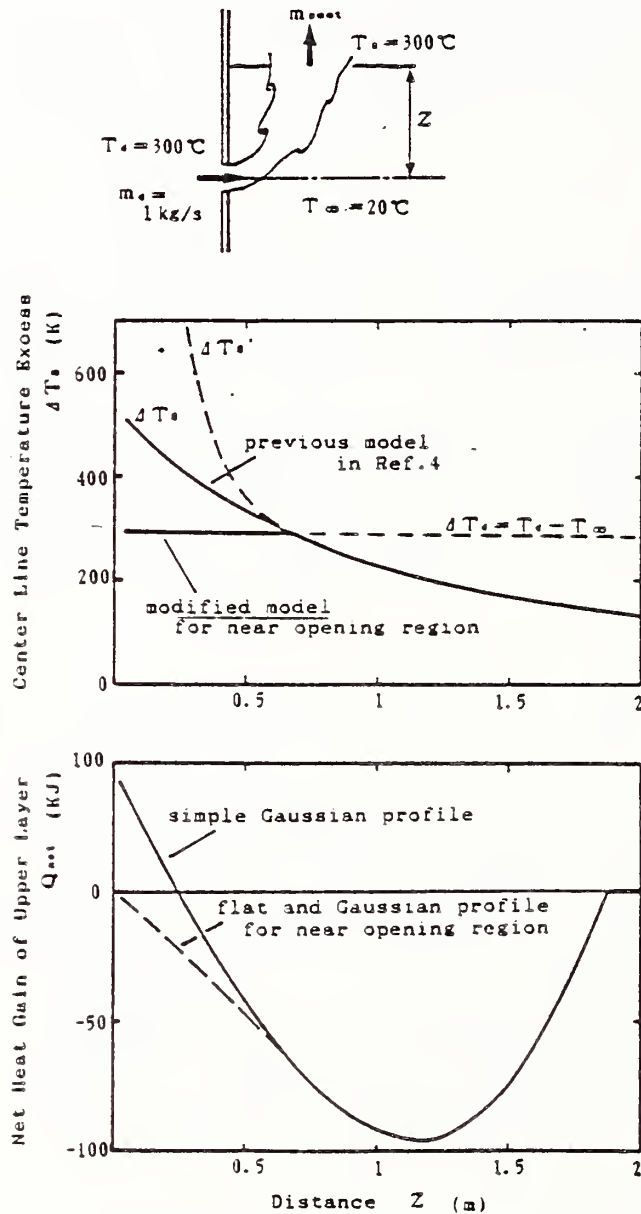


Fig.1 Modeling of door jet plume penetration



note)

$$Q_{u,net} = q - c_p T_c m_{p,net}$$

$$= c_p (T_\infty - T_c) m_{p,net} + k Q$$

Fig.2 Effect of Modified Temperature and Flow Profile Near Opening Region

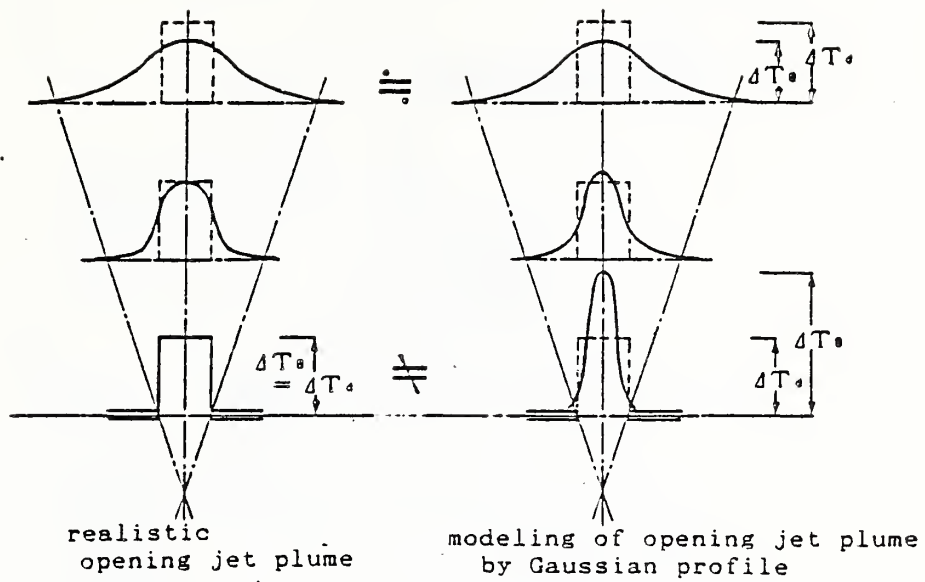


Fig.3 Limitation of Modeling of opening jet plume by Gaussian Profile

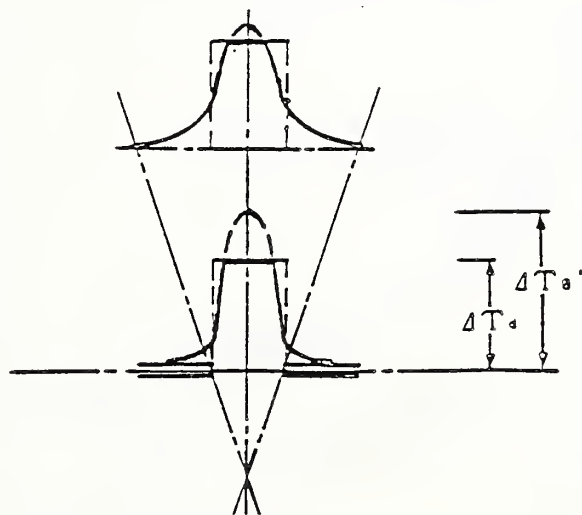


Fig.4 Model of Temperature profile Near Opening Region

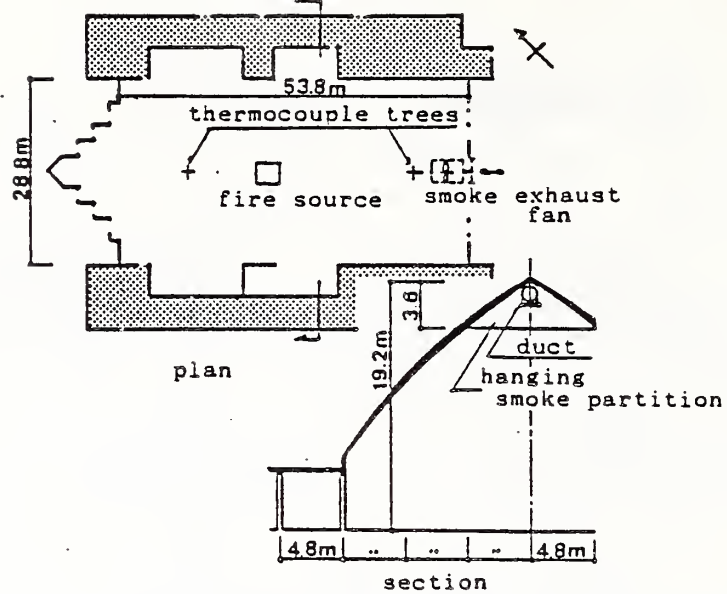


Fig.5 Exhibition Hall of USSR Pavilion

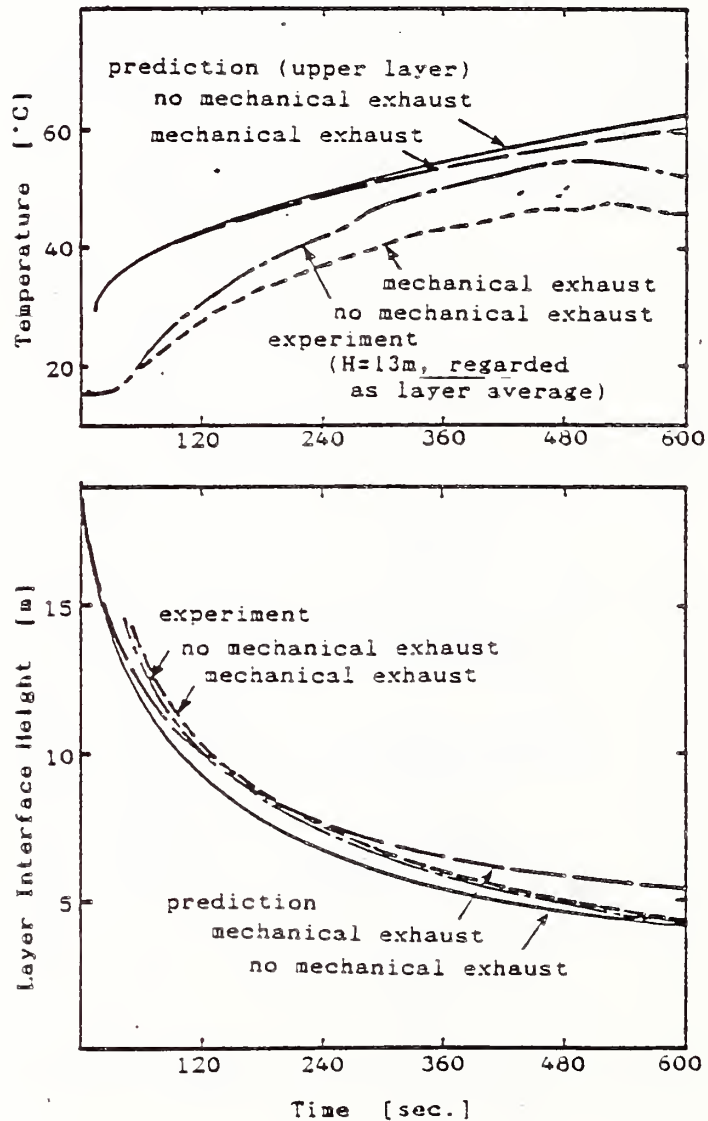


Fig.6 Predicted and Experimented Results of Experiments in USSR pavilion

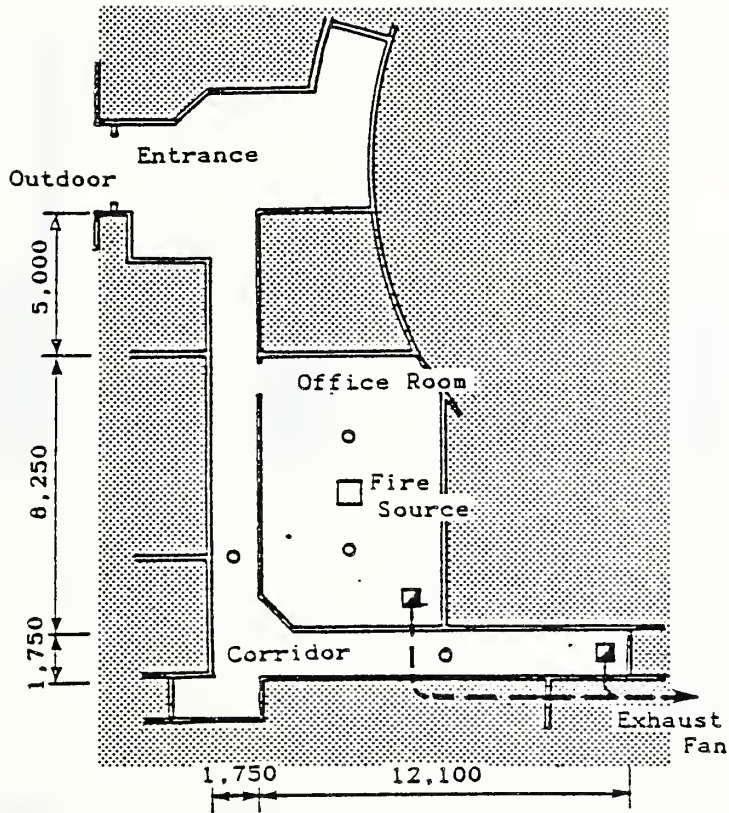
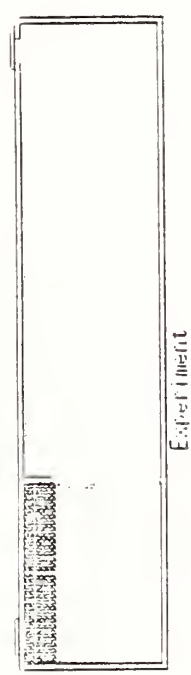
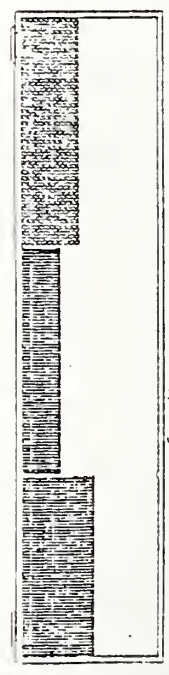


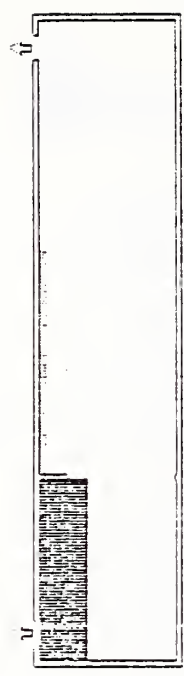
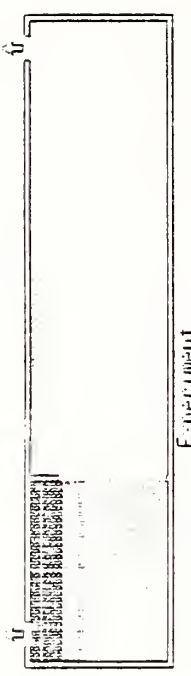
Fig.7 Area for the Experiments in IBM Pavilion



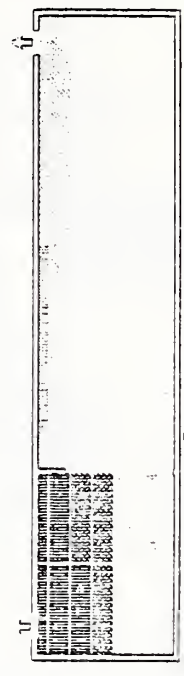
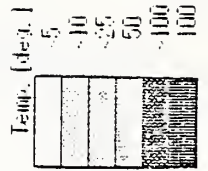
Exp. No. : 1000 Time = 1000 sec.



Exp. No. : 1000 Time = 1000 sec.



Exp. No. : 1000 Time = 1000 sec.



Exp. No. : 1000 Time = 1000 sec.

Fig. 8 Predicted and Experimental Results of Smoke Behavior in IBM Pavilion

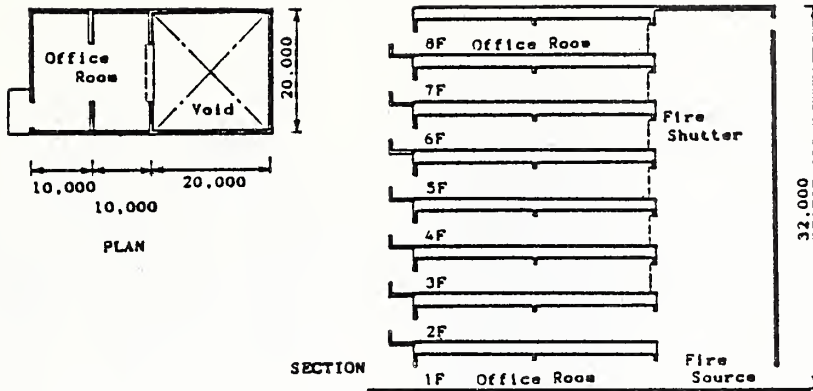
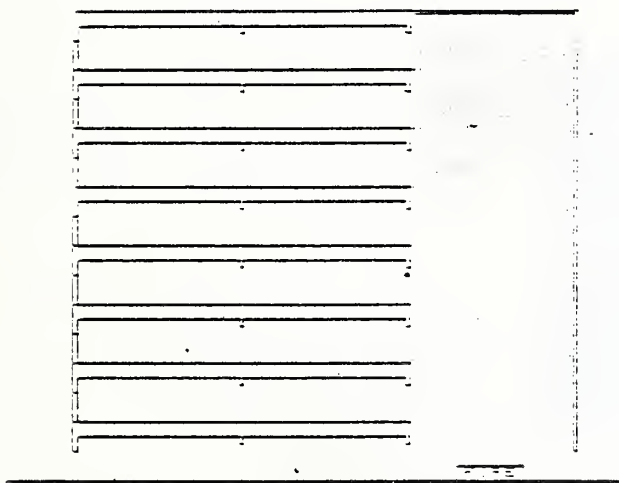
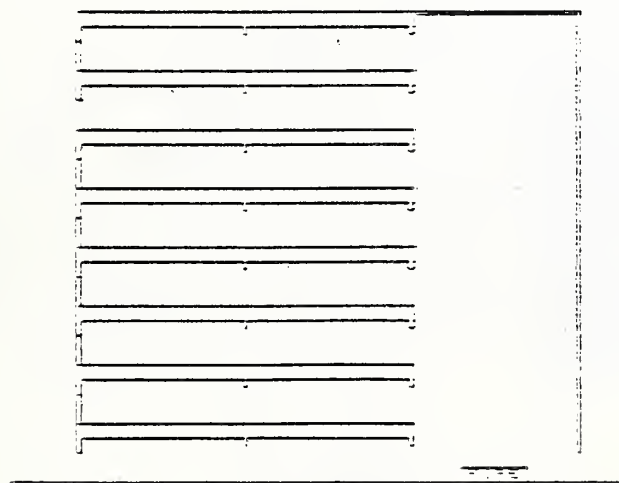
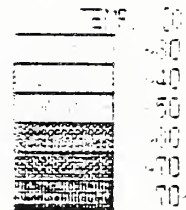


Fig.9 Outline of 8 story Model Building



Time = 60 sec.

A thin smoke layer at less than 30 °C begins to fill the atrium.



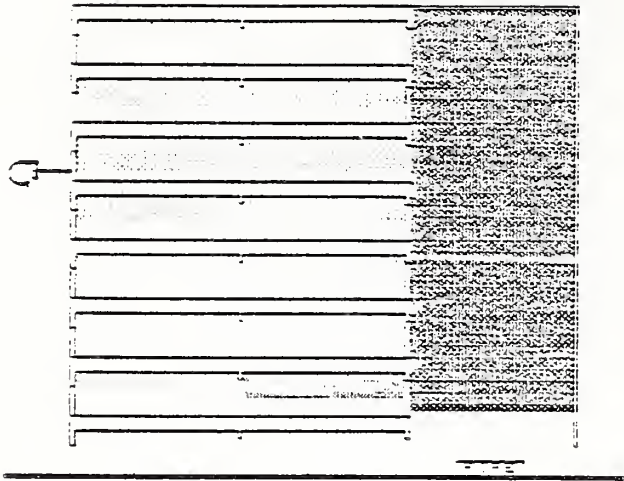
Time = 120 sec.

The temperatures of smoke layers are not yet very high but smoke begins to enter the rooms on each floors. On 7th floor, the smoke layers expands by mixing with the air flowing into the building through the opened window.

Right after this point, fire shutters are closed, but one of the two shutters on 5th and 6th floors remain open due to trouble.

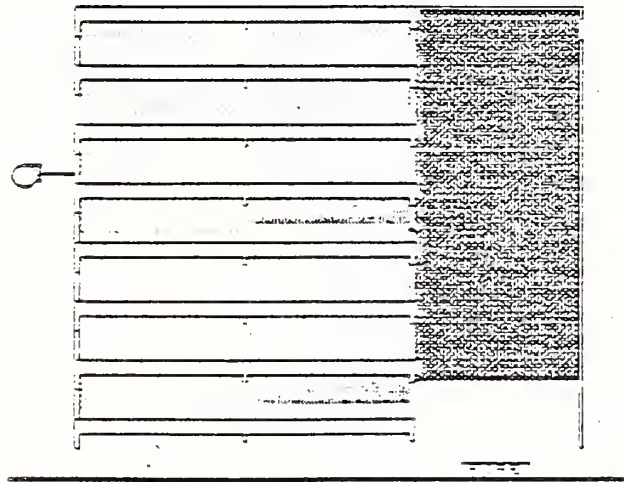
At 125 sec., mechanical air supply on 6th floor is switched on.

Fig.10 Smoke Layer Behavior in 8 story Model Building



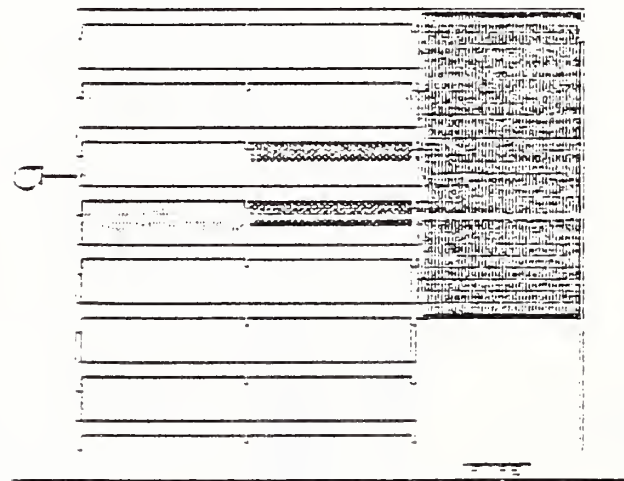
Time = 240 sec.

The smoke layer in the atrium descends to near the bottom and the layer temperature rises to more than 50 °C. The floors of which shutters are closed are kept comparatively safe, although some infiltration of smoke exists. On the floors of which fire shutters are not closed, significant amount of smoke fills the rooms.



Time = 300 sec.

The smoke is gradually removed from the atrium through the natural vent.



Time = 600 sec.

Hazardous condition develops on 5th and 6th floors, when the fire shutters failed to close, but the temperature of 6th floor is somewhat lower than that of 5th floor thanks to the mechanical air supply.



Fig.10 cont'd

Appendix 1. Outline of the Model

The concept of the model is schematically illustrated by Fig.A1. This model assumes that opening jets behave just as fire plumes and partially penetrate through layer interfaces. Zone equations of this model are summarized as follow:

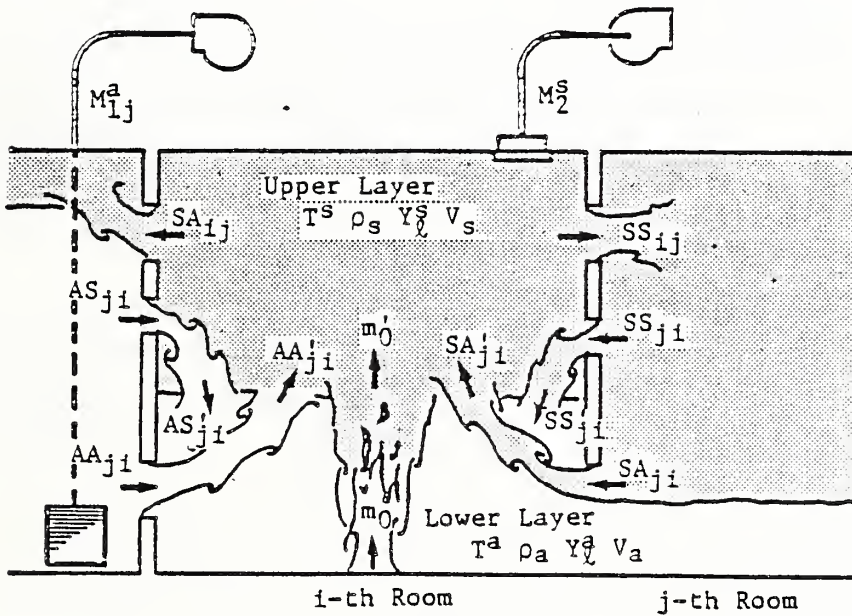


Fig.A1 Concept of the Two layer Zone Model

Upper Layer Temperature

$$\begin{aligned} \frac{d}{dt} T_1^* &= \frac{1}{c_p \rho_{s1} V_{s1}} (\Delta H m_{s1}^* + q^*_{net,1}) \\ &+ \frac{1}{\rho_{s1} V_{s1}} [m_{s1}^* (T_1^* - T_1^*) + k^* m_{s1} (T_0 - T_1^*) \\ &+ (1 - k^{1*}) M_1^* (T_1 - T_1^*) + M_1^{*'} (T_1^* - T_1^*) + k^{1*} M_1^* (T_1 - T_1^*) \\ &+ \sum_j \{ (1 - k^{5j}) SS_{j1} (T_{j1}^* - T_1^*) + SA'_{j1} (T_1^* - T_1^*) + k^{5j} SA_{j1} (T_{j1}^* - T_1^*) \\ &+ (1 - k^{6j}) AS_{j1} (T_{j1}^* - T_1^*) + AA'_{j1} (T_1^* - T_1^*) + k^{6j} AA_{j1} (T_{j1}^* - T_1^*) \}] \end{aligned}$$

Lower Layer Temperature

$$\begin{aligned} \frac{d}{dt} T_0^* &= \frac{1}{c_p \rho_{s0} V_{s0}} (\Delta H m_{s0}^* + q^*_{net,0}) \\ &+ \frac{1}{\rho_{s0} V_{s0}} [(1 - k^*) m_{s0} (T_0 - T_0^*) \\ &+ M_1^{*'} (T_1^* - T_0^*) + k^{1*} M_1^* (T_1 - T_0^*) + (1 - k^{1*}) M_1^* (T_1 - T_0^*) \\ &+ \sum_j \{ SS'_{j0} (T_1^* - T_0^*) + k^{5j} SS_{j0} (T_{j1}^* - T_0^*) + (1 - k^{5j}) SA_{j0} (T_{j1}^* - T_0^*) \\ &+ AS'_{j0} (T_1^* - T_0^*) + k^{6j} AS_{j0} (T_{j1}^* - T_0^*) + (1 - k^{6j}) AA_{j0} (T_{j1}^* - T_0^*) \}] \end{aligned}$$

Mass Fraction of Species 1 within upper layer

$$\begin{aligned} \frac{d}{dt} Y_{11}^* &= \frac{1}{\rho_{s1} V_{s1}} [\tau_1 m_{s1}^* + m_{s1}^* (Y_{11}^* - Y_{11}^*) + k^* m_{s1} (Y_{10} - Y_{11}^*) \\ &+ (1 - k^{1*}) M_1^* (Y_{11} - Y_{11}^*) + M_1^{*'} (Y_{11}^* - Y_{11}^*) + k^{1*} M_1^* (Y_{11} - Y_{11}^*) \\ &+ \sum_j \{ (1 - k^{5j}) SS_{j1} (Y_{11}^* - Y_{11}^*) + SA'_{j1} (Y_{11}^* - Y_{11}^*) + k^{5j} SA_{j1} (Y_{11}^* - Y_{11}^*) \\ &+ (1 - k^{6j}) AS_{j1} (Y_{11}^* - Y_{11}^*) + AA'_{j1} (Y_{11}^* - Y_{11}^*) + k^{6j} AA_{j1} (Y_{11}^* - Y_{11}^*) \}] \end{aligned}$$

Mass Fraction of Species 1 within lower layer

$$\begin{aligned} \frac{d}{dt} Y_{10}^* &= \frac{1}{\rho_{s0} V_{s0}} [\tau_0 m_{s0}^* + (1 - k^*) m_{s0} (Y_{10} - Y_{10}^*) \\ &+ M_1^{*'} (Y_{11}^* - Y_{10}^*) + k^{1*} M_1^* (Y_{11} - Y_{10}^*) + (1 - k^{1*}) M_1^* (Y_{11} - Y_{10}^*) \\ &+ \sum_j \{ SS'_{j0} (Y_{11}^* - Y_{10}^*) + k^{5j} SS_{j0} (Y_{11}^* - Y_{10}^*) + (1 - k^{5j}) SA_{j0} (Y_{11}^* - Y_{10}^*) \\ &+ AS'_{j0} (Y_{11}^* - Y_{10}^*) + k^{6j} AS_{j0} (Y_{11}^* - Y_{10}^*) + (1 - k^{6j}) AA_{j0} (Y_{11}^* - Y_{10}^*) \}] \end{aligned}$$

Upper Layer Volume

$$\begin{aligned} \frac{d}{dt} V_{s1} &= \frac{1}{c_p \rho_{s1} T_1^*} (\Delta H m_{s1}^* + q^*_{net,1}) \\ &+ \frac{1}{\rho_{s1} T_1^*} [k^* m_{s1} T_0 + (m_{s1}^* - k^* m_{s1}) T_1^* \\ &+ (1 - k^{1*}) M_1^* T_1 - (M_1^{*'} - k^{1*} M_1^*) T_1^* - k^{1*} M_1^* T_1 + (M_1^{*'} - k^{1*} M_1^*) T_1^* - T_1^* M_2^* \\ &+ \sum_j \{ (1 - k^{5j}) SS_{j1} T_1^* - (SS'_{j1} - k^{5j} SS_{j1}) T_1^* + k^{5j} SA_{j1} T_1^* + (SA'_{j1} - k^{5j} SA_{j1}) T_1^* \\ &+ (1 - k^{6j}) AS_{j1} T_1^* - (AS'_{j1} - k^{6j} AS_{j1}) T_1^* + k^{6j} AA_{j1} T_1^* + (AA'_{j1} - k^{6j} AA_{j1}) T_1^* \\ &- (SS_{j1} + SA_{j1}) T_1^* \}] \end{aligned}$$

Pressure Balance Equation

$$\begin{aligned} \Delta H (m_{s1}^* + m_{s0}^*) + q^*_{net,1} + q^*_{net,0} \\ + c_p [T_0 m_{s1} + T_1 (M_1^* + M_1^*) - T_1^* M_2^* - T_0^* M_2^* \\ + \sum_j \{ T_{j1}^* (SS_{j1} + SA_{j1}) + T_1^* (AS_{j1} + AA_{j1}) - T_1^* (SS_{j1} + SA_{j1}) - T_1^* (AS_{j1} + AA_{j1}) \}] = 0 \end{aligned}$$

Appendix 2. Formation of Plumes (Ref.2)

The flow rate of fire plume is calculated using the formulas developed by Zukoski et al(Ref.3). Opening jet plumes are modeled as vertical thermal plumes and to calculate the flow rate of the plumes at the height of Z, the equation of plume flow rate for far field region by Zukoski et al(Ref.3) is also applied.

Fictitious point heat source is assumed at a certain distance below an opening jet. The distance is given as

$$Z_0 = \left\{ \frac{m_d}{0.21 \left(\frac{g \rho_\infty^2}{c_p T_\infty} \right)^{1/3} Q^{1/3}} \right\}^{3/5} \quad \text{---(A1)}$$

where

$$Q = c_p |T_d - T_\infty| m_d \quad \text{---(A2)}$$

where T_d and T_∞ are the temperature of opening jet and the ambient layer, and m_d is the mass flow rate of opening jet. With the use of Z_0 , m_z is also expressed as

$$m_z = m_d \left(\frac{Z + Z_0}{Z_0} \right)^{5/3} \quad \text{---(A3)}$$

Gaussian profile is assumed on the vertical velocity of plume, then the mass penetration rate through a layer interface is given as

$$m_{\text{penet}} = \begin{cases} m_z (1 - e^{-\eta^2 \Delta T_c}) & (\Delta T_c < \Delta T_d) \\ 0 & (\Delta T_c \geq \Delta T_d) \end{cases} \quad \text{---(A4)}$$

where η is plume radius in Howarth transformation. With as the critical temperature for penetration, $\eta^2 \Delta T_c$ is defined as

$$\eta^2 \Delta T_c = -\frac{1}{\beta^2} \ln \left(\frac{\Delta T_c}{\Delta T_d} \right) \quad \text{---(A5)}$$

where ΔT_d and ΔT_c are given as

$$\Delta T_d = \left(\frac{T_\infty}{g c_p \rho_\infty^2} \right)^{1/3} Q^{1/3} (Z + Z_0)^{-5/3} \quad \text{---(A6)}$$

$$\Delta T_c = c (T_s - T_d) \quad \text{---(A7)}$$

In Eq.(A7), c is a constant to be determined empirically.

Similar consideration is applied on the penetration of heat to yield:

$$q_{\text{penet}} = \begin{cases} C_o T_\infty m_{\text{penet}} + k Q & (\Delta T_c < \Delta T_d) \\ 0 & (\Delta T_c \geq \Delta T_d) \end{cases} \quad \text{---(A8)}$$

where

$$k = 1 - e^{-(1+\beta^2) \eta^2 \Delta T_c} \quad \text{---(A9)}$$

RISK, HAZARD, AND EVACUATION SESSION

Progress in Fire Risk Analysis Methods

JOHN R. HALL, JR.
Fire Analysis Division
National Fire Protection Association
Quincy, Massachusetts 02269, USA

ABSTRACT

Progress in the development of fire risk analysis methods in the USA since the Eighth UJNR Panel is described. There are several approaches being pursued in parallel, involving different points of emphasis and differing relationships with the rest of fire safety science.

1. INTRODUCTION

Fire risk analysis in the USA has progressed along several different tracks since the Eighth UJNR Panel in 1985. There are three principal research approaches that may be defined by differences in emphasis. One approach is favored by the nuclear power industry, the chemical industry, and other economic sectors where the risks to be analyzed typically are defined by a single building or facility. The second approach is favored by U.S. government regulatory agencies that must review regulatory proposals affecting large parts of the general public. The third approach is now being developed for use on fire risk evaluations of products and furnishings in buildings.

2. FIRE RISK IN TECHNICALLY COMPLEX FACILITIES

Nuclear power plants in the USA are required to have probabilistic risk assessments as part of the requirements for licensing. The model typically used is a fault tree in which an undesirable outcome is analyzed in terms of the logical and probabilistic relationships among events that can produce or prevent it. Fault tree analysis is flexible enough to include both mechanical and human factors. The measure of risk is an overall probability of failure, where failure might be defined as a fire sufficiently severe to damage the safety components preventing core meltdown in a nuclear facility.

Because the emphasis is on measurement of the probability side of the probability/severity duality that defines risk, most research on this approach also addresses aspects of probability estimation. The most sophisticated treatment of uncertainty, for example, is found in this track. Using Bayesian statistical methods, involving prior probability distributions and rules for incorporating fire experience data, the model-builder estimates not just a value for the possibility of each event but a whole distribution for the values that that probability might take.

This also involves close attention to the process of weighing evidence. A recent paper by Ali Mosleh and George Apostolakis addressed techniques for modeling levels of confidence in experts giving expert estimates.¹ Imprecise evidence on the probability of detection was addressed in a related paper by Nathan Siu and George Apostolakis.²

To make this approach useful for decision-makers, the concept of acceptable risk is needed and reduces to an acceptable probability of failure. Modelers have devoted considerable effort to establishing conceptual bases for defining acceptable risk, generally in terms of such natural reference points as unavoidable risk or the risk associated with current practices or codes.

Professor Apostolakis of the University of California at Los Angeles and his students are among the leading developers of theory in using this approach. He will speak later in this session and provide more details. Because this is the approach most firmly grounded in the US standards system and most widely required by law, it is the most frequently applied version of fire risk assessment in the USA today.

2. FIRE RISK IN REGULATORY AGENCIES

US government regulatory agencies increasingly are expected to analyze the costs and benefits of proposed regulations. When the anticipated benefits involve reductions in fire risk, the model they use involves a probability distribution over outcomes of measured severity. This can involve the use of the decision tree format developed by Howard Raiffa and others. Probability estimation is a major element of this approach, but unlike the previous approach, this approach places equal emphasis on techniques for measuring outcome severity. Outcomes are not classified simply as failures or successes but are defined by the degree of loss of life, health, or property. The overall risk measure is therefore an expected loss.

This approach leans heavily on the methods of economics. It therefore emphasizes such techniques as the reduction of several future years of forecast costs and losses to equivalent present values and the development of a dollar figure for the value of saving a statistical life, that is, reducing the expected number of deaths by one. A recent example in simple form is work done by the National Fire Protection Association for the Cigarette Safety Act Technical Study Group.³ In this study, a baseline of current fire losses involving cigarette ignitions was created. Statistical models then were developed to project those losses. Laboratory test results on the ignitability of different types of mattresses and upholstered furniture and the ignition propensities of different types of cigarettes were incorporated into probabilistic models, which produced parameters for use in the statistical projections. Full-scale decision trees were not needed, but the basic modeling format was of this second type.

Unlike the first approach, this second approach tends to address fire problems in which a large quantity of data on real fires exists. This reduces the uncertainty in the probability estimates.

There seems to be little development of new theory specific to fire risk analysis now under way in this approach. However, this approach represents the most common approach to risk analysis generally in the USA and therefore benefits from fundamental work being done on the general models. Most of the current theoretical work addresses not the technical points of estimating benefits but rather the related issues of

transforming expected outcomes into values embodying preferences. An example of this is the ongoing research on factors influencing risk aversion which, in simplified terms, is the tendency of most people to be willing to pay more to avoid the chance of an unpleasant outcome than the expected loss would seem to justify. For example, we might be willing to pay \$400 to avoid a one-third chance of having a fire that would damage property worth \$1,000.

3. FIRE RISK ASSESSMENT METHOD FOR PRODUCTS

The third approach is the subject of a major US research effort, now in its first year, that is building a fire risk assessment method around a core consisting of computerized models of the physics of fire development, the biochemistry of toxic impact, and behavioral models of human actions in fire. The other two modeling approaches use historical fire experience, defined in statistical terms, as much as possible. They address the physics and chemistry of fire primarily as sub-analyses that permit the estimation of particular probability and severity parameters. This new third approach places the physics of fire at the center of the model, using the HAZARD 1 method, which Richard Bukowski will discuss later.

This approach works by subdividing the possible varieties of fire into a set of scenario classes. Each scenario class is associated with a probability of occurrence, typically derived from historical fire data. Each scenario class also is associated with a reference or benchmark scenario. That is, a much more specifically defined class of fires is taken from the larger scenario class, a sub-class with enough definition to serve as a case for study by the hazard models and the human behavior models. The latter models produce an expected number of deaths for that case, and that is taken to be the expected number of deaths per fire for any fire in that scenario class. Then the probability of the scenario class provides the weighting of that death rate value in the overall risk measure.

This method involves a careful balance between the high level of detail required by the hazard and human behavior models and the low level of detail available in the data bases that provide probabilities. If the scenario classes are too detailed, then the hazard model results clearly will be appropriate to the entire class, but there may be very high uncertainty in the estimates of the probability of the class. If the scenario classes are not detailed enough, the probabilities may have high confidence, but there may be low confidence that the benchmark scenario truly represents the average scenario for the class.

Most of the theoretical work therefore involves the development of crosswalks between data bases and models. For example, the many varieties of items that can be involved in fire are grouped into a manageable number of classes defined by at most three or four values of each of several key physical parameters--rate of rise in rate of heat release, ease of secondary ignition by a flaming heat source, peak heat release rate. This permits the hazard model to be run on reference items that represent classes defined by those physical parameters. Similar techniques are used to address other needed crosswalks between data and models.

The models can be tested by evaluating how well they reproduce historical experience in terms of deaths per fire. The research is being conducted by the National Bureau of Standards Center for Fire Research, the National Fire Protection Association, and Benjamin-Clarke Associates. A report on the model is due in August 1987.

4. THE FUTURE OF FIRE RISK MODELING

It is expected that the third approach will see a rapid rise in use once it becomes available. (The project to develop, test, and disseminate it will be completed in August 1989.) This new approach will satisfy the demand for a model that permits explicit calibration in terms of real fires, explicit modeling of new products, and extensive use of all other branches of fire safety science. The rise in use of this model may be constrained, however, in areas where legal requirements have already created a presumption in favor of one of the other two approaches or in situations where fast, inexpensive analysis is required, because the third approach will not be fast or inexpensive, at least as it now appears. (By comparison, the first approach and particularly the second approach can be done with different levels of detail, permitting trade-offs of informational detail, precision, accuracy and completeness against speed and affordability.) Over the longer term, all three approaches are likely to borrow ideas and methods from each other, because their different focuses are in many ways complementary.

REFERENCES

1. "The Assessment of Probability Distributions from Expert Opinions with an Application to Seismic Fragility Curves," Ali Mosleh and George Apostolakis, Risk Analysis, Volume 6, Number 4 (December 1986), pp. 447-461.
2. "Modeling the Detection Rates of Fires in Nuclear Plants: Development and Application of a Methodology for Treating Imprecise Evidence," Nathan Siu and George Apostolakis, Risk Analysis, Volume 6, Number 1 (March 1986), pp. 43-59.
3. "Final Report: Expected Changes in Fire Damages from Reducing Cigarette Ignition Propensity," John R. Hall, Jr., NFPA Report to Technical Study Group of Cigarette Safety Act of 1984, August 29, 1986.
4. Also appearing recently in the literature as an example of the first approach: "Comparative Fire Risk Study of PCB Transformers," Raymond F. Boykin, Mardiros Kazarians, and Raymond A. Freeman, Risk Analysis, Volume 6, Number 4 (December 1986), pp. 477-488.

PROGRESS REPORT ON RISK, HAZARD AND EVACUATION IN JAPAN

by

Takeyoshi TANAKA

Building Research Institute
Ministry of Construction

INTRODUCTION

In the area of research on the analyses of risk and hazards and on human behavior concerning fire, it seems like the most important topics in Japan are the completion of the two research projects carried out by Ministry of Construction and Fire Defence Agency, respectively. So, it will be proper to focus this progress report primarily on these two projects rather than comprehensively covers the researches going on in Japan.

1. FIRE SAFETY DESIGN METHOD OF BUILDINGS

The research project: Fire Safety Design Method of Buildings was started by Ministry of Construction in fiscal 1982 and carried out through the end of fiscal 1986. The primary motivation of the project was to provide building designers with a design method of fire safety for buildings usable as an alternative to the Building Standard Law and its associated orders, which are basically specification standards and whose structure has considerably lost integrity since it has been basically unchanged for some 40 years.

In the Fire Safety Design Method, the objectives of fire safety for buildings, which are abstractly and inclusively described in Article 35 of the law, are expressed in more concrete form. Performance standards are introduced as long as possible and beneficial as the technical standards for fire safety measures of buildings. The performance based technical standards consist of Fire Safety Standards and Standard Fire and Occupants Conditions. In principle, any design of building is supposed to be accepted as long as the design satisfy the fire safety standards under the standard fire and occupants conditions.

Since the prediction methods for various aspects of fire behavior are indispensable to actually operate the fire safety design method, several calculation methods and user oriented computer codes have been developed in conjunction of the research projects, for example, one layer smoke movement model, two layer smoke movement model, evacuation model, calculation method for structural fire resistance, evaluation method for fire spread and so on.

The final report of this project will be published by the end of this fiscal year. It is hoped that the fire safety measures of buildings can be significantly rationalized with the use of this design method.

2. FIRE RISK EVALUATION METHOD FOR MULTI-OCCUPANCY BUILDINGS

This research project was carried out from FY 1982 through FY 1986 by Fire Safety Agency, Ministry of Home Affairs. The objective of this project is to provide fire officials with a practical and simple method to inspect and evaluate the level of fire safety of existing multi-occupancy buildings.

In this method, the level of fire safety of an existing building is assessed by the sum of the scores given to each of the primary fire protection measures of the building. Scores of a fire protection measure is determined by expert judgements or some other means according to its performance. The system of the assessment consists of the two subsystems, i.e., the evaluation method of potential fire risk and the evaluation method of evacuation performance. Both of the evaluations are made on each floor basis.

3. SOME OF THE OTHER RESEARCH ACTIVITIES

Jin and Yamada conducted the experiments to investigate the effects of heat radiation from smoke on evacuees as a continuation of their experimental studies on emotional instability of evacuees in smoke. The effect of heat radiation was assessed by the degradation of mental arithmetic ability of the subjects.

Tsujimoto proposed a method to evaluate life risk in an attempt to determine the maximum allowable life risk due to fire in buildings. He applied the method to existing hospitals and hotels and studied the relationship of the life risk and the conditions of the buildings.

Field measurements were made by BRI for the egress behavior of the audience of the pavilions of Tsukuba International Exposition, which was held in 1985. Seven theater type pavilions were selected for the measurements and the results were used for the validation of the evacuation model developed in the 5 year project of Ministry of Construction.

Field fire experiments were conducted by BRI also using the Tsukuba Expo. '85 pavilions to investigate the behavior of smoke and the effect of smoke control measures. Eight pavilions with various geometries and smoke control measures were selected for the experiments and the results were used for the validation of the two layer zone model for smoke movements.

REFERENCES

- 1) TANAKA, T. : Basic Structure of The Evacuation Safety Design Method, to be presented at this session
- 2) SEKIZAWA, A. : Fire Risk Evaluation Method for Multi-occupancy Building, to be presented at this session
- 3) JIN, T. and YAMADA, T. : The Experimental Studies on Emotional Instability in Fire Smoke (Part 5 Radiative Heat Effects on Evacuees in a Fire Smoke), Annual Meeting of Architectural Institute of Japan, 1986
- 4) TSUJIMOTO, M. : A Method of Fire Risk Analysis, to be presented at this session.
- 5) TAKAHASHI, K. and TANAKA, T. : An Evacuation Model for The Use in Fire Safety Designing of Buildings, to be presented at this session
- 6) NAKAMURA, K. : Predicting Capability of A Multiroom Fire Model, to be presented at Fire and Smoke Physics session of this meeting.

Progress Report to the 9th UJNR Panel on Fire

RISK, HAZARD AND EVACUATION IN JAPAN

T. Tanaka, Building Research Institute, Japan

NELSON: Do you expect the fire safety design method to become part of a law in Japan?

TANAKA: It is my personal understanding, and I will be able to explain it more in detail later, that the fire safety hazard law probably will be administered in parallel for some time with the construction law. It also is my understanding that the administrative agencies that have control of this to some extent understand, and are leaning towards, a revision of the law.

A METHOD OF FIRE RISK ANALYSIS
-Estimation of Life Risk in Buildings-

Makoto TSUJIMOTO

Department of Architecture
Faculty of Engineering
Nagoya University
Furo-cho, Chikusa-ku, Nagoya
464, JAPAN

ABSTRACT

As a way to determine the maximum admissible of life risk caused by building fire, a method to calculate the life risk in each floor of the building is proposed, and the distribution of life risk covering the buildings (hospitals and hotels) in Prefecture A in Japan is shown.

1. Introduction

To protect a life of occupant is the minimum requirement for the fire safety of the building. But it is generally thought to be impossible to remove all the risk of a fire from the building. So the maximum permissible of life risk must be shown in some way in order to design the fire safety of a building. Until today, however, any method of risk analysis does not enable us to estimate the life risk of an arbitrary space in a building quantitatively, and also the maximum admissible value has never been proposed. Consequently the fire safety design has been affected unreasonably by the fire regulations which always had been established in haste after the severe fires.

In this paper, after the definition of the life risk, a method to estimate the life risk in each space in a building, and the distribution of the values of the risk calculated by the method for the existing buildings, are shown.

2. Definition of Life Risk

In this paper the life risk is defined as the expected frequency that the occupants are trapped by the smoke generated by a fire. The process of calculations is shown in Fig.1 and as follows.

First the size of the set corresponding the potential risk in the space A, which is caused by the fire in the space I, is given by the frequency of fires in the space I. When F_i stands for the set, F_i is the life risk in the space A in case that there is no measure against a fire.

Second if the sprinkler system is equipped or interior finishing is restricted in the space I, F_i is reduced by multiplying the factors, S_p and/or I_n , which indicate the effect of these countermeasures.

Third the subset corresponding the case, where the evacuation time is shorter than the smoke spread time, is deducted from the set ($F_i \cdot S_p \cdot I_n$).

Fourth the subset corresponding the case, where there is at least one staircase for evacuation free from smoke is deducted also from the set. In third and fourth processes it is assumed that the smoke spreads at the fixed time (180 seconds) instantly to every space through the doors left open, and that the smoke does not spread across a closed door.

And the rest of the set is the life risk in the space A caused by the fire in the space F.

Finally the life risk of space A can be obtained by summarizing the risks caused by the fires in each space in the building. In these calculations, it is assumed that the situation to be trapped by the smoke will happen only in the spaces above the fire floor.

3. Calculation of Life Risk

The following equation is used to obtain the life risk in the space A.

$$R_a = \sum_i^n F_i \cdot S_{pi} \cdot I_{ni} \cdot P_{lai} \cdot P_{2ai}$$

R_a ; life risk in the space A

F_i ; frequency of fire in the space i

$F_i = f \cdot A_i$

f; fire rate per unit floor area

A_i ; floor area of space i

S_p ; factor indicating the effect of sprinkler system

$S_{pi} = 0.1$ sprinkler system is equipped with in the space i

$S_{pi} = 1$ " " is not equipped with " "

I_n ; factor indicating the effect of interior finishing

$I_n = 0.5$ interior finishing is restricted in the space i

$I_n = 1$ " " is not restricted " "

P_{lai} ; probability that the occupants in space A can

finish evacuation by the smoke spread time from space i

when $T_s > T_e$ then $P_{lai} = 0$

when $T_s < T_e$ then $P_{lai} = 1$

T_s ; smoke spread time

$T_s = 180$

T_e ; evacuation time from space A

$T_e = T_1 + T_2 + T_3 + T_4$

T_1 ; time from an outbreak of fire to the detection

T_2 ; time from the detection to the start of evacuation

T_3 ; evacuation time from space A into staircase

T_4 ; evacuation time in staircase

P_{2ai} ; probability that the occupants in space A can use at least one staircase free from the smoke for evacuation. It is derived from the probabilities (shown in Table 1) that the each opening between space i and staircase is open or closed.

n; the number of spaces, the fire in which causes the life risk

4. Evaluation of Life Risk

To evaluate the life risk of a building by the method stated above, it is necessary to survey the distribution of the life risk of existing buildings. So 26 hotels and 23 hospitals are selected by random sampling from the buildings, which exist in a prefecture in Japan and each floor area of which is over 500 m². And the life risks in each floor of these sampled buildings are calculated, and the distribution drawn from those values is shown in Fig.2.

By comparing the life risk of the floor intended to evaluate with this distribution chart, the degree of the risk is quantitatively known on the whole.

By the way it is very difficult to show the propriety of the assessment method of this sort. Then to inquire into this evaluation method, the life risk in each floor shown in Fig.2 is compared with the characters of the floor, which are the time of completion of the building, the number of the floors, and the total floor area below the floor to be evaluated.

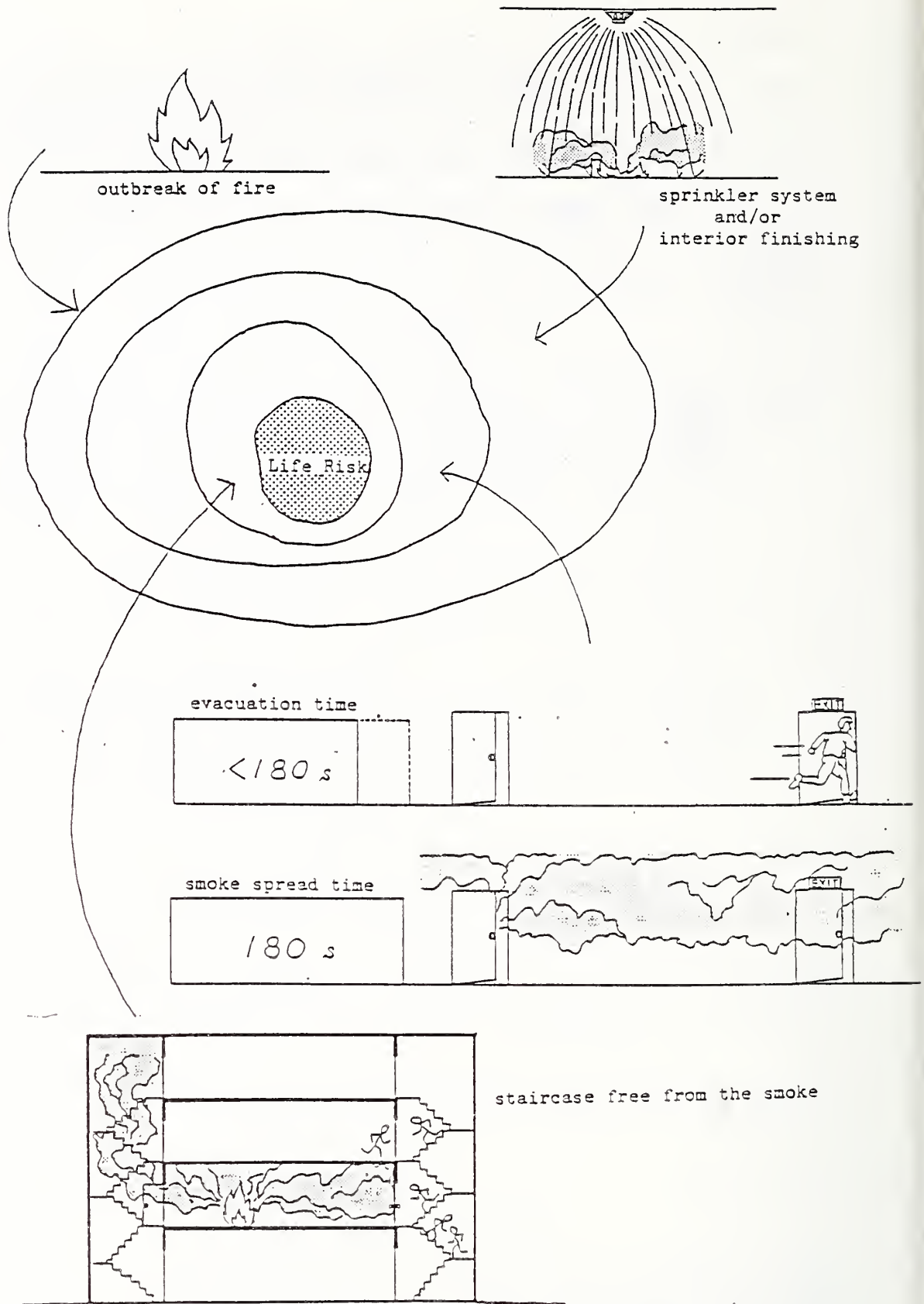


Figure 1. Schematic figure to calculate the life risk

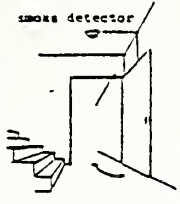
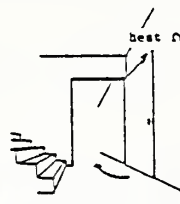
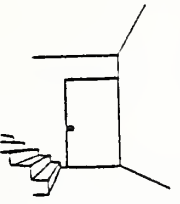
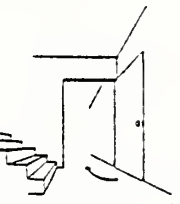
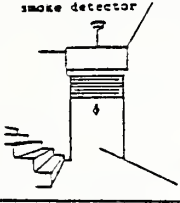
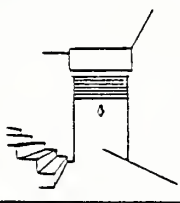
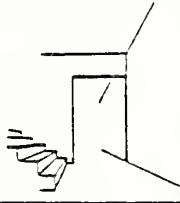
probability of a staircase door closed in case of fire			
an interlocking fire door with a smoke detector	a fire door with a fuse	a fire door closed at ordinary times	a fire door closed manually
			
0.8	0.4	0.7	0.1
an interlocking fire shutter with a smoke detector	a fire shutter closed manually	an opening	
			
0.8	0.1	0	

Table 1. An example of the probability of a door closed in case of fire

The probability of a door with an interlocking closed was derived from the result of testing the interlocking function and to the probability of a door without an interlocking closed was applied the ratio of doors kept close to all doors at the time of inquiry.

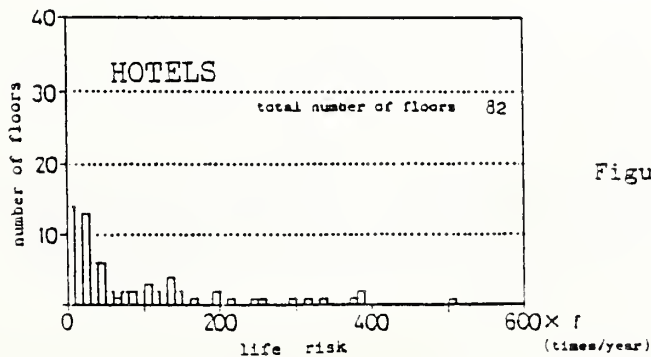
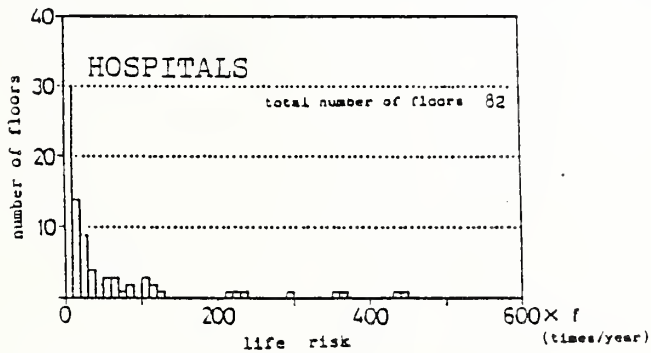
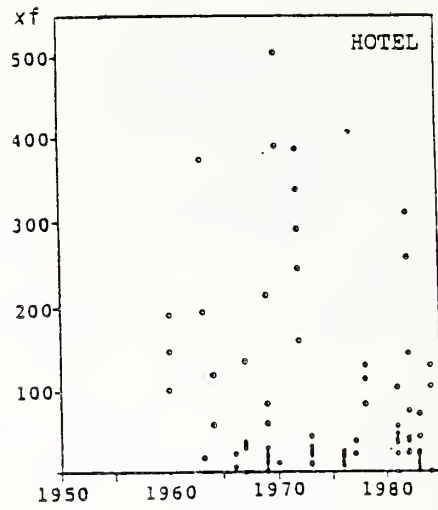
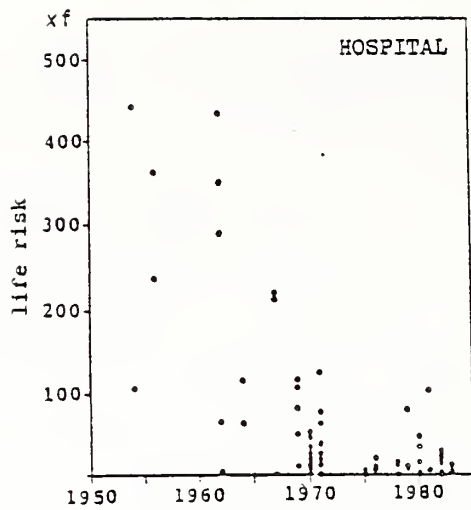
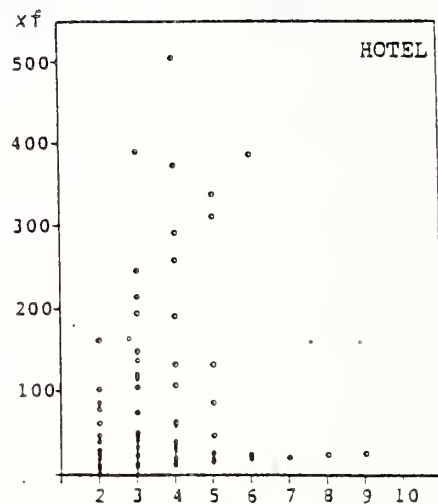
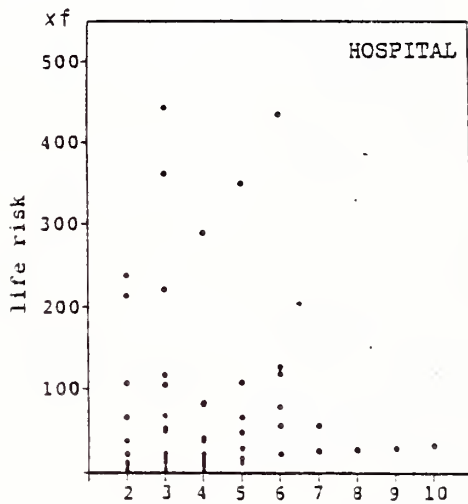


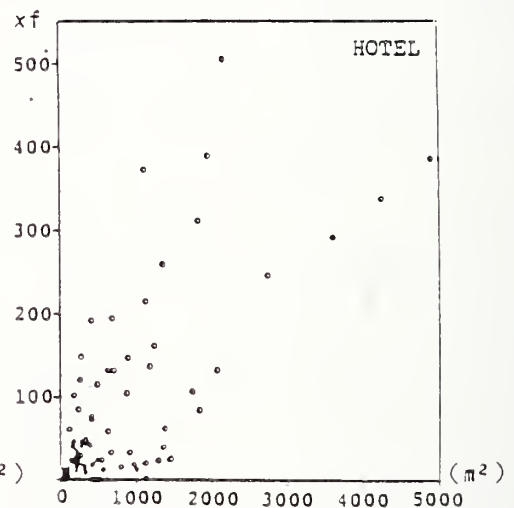
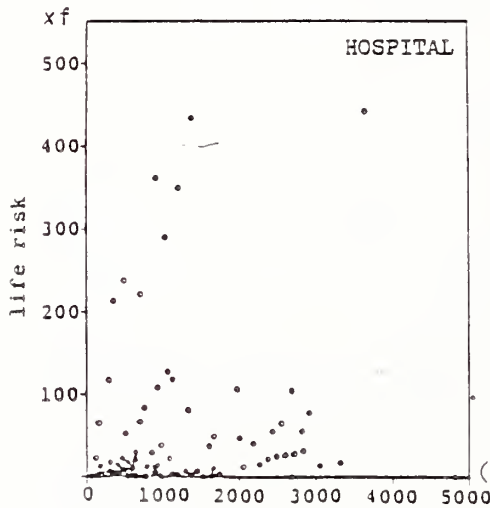
Figure 2. Distribution of life risk in a prefecture



a) relation between the life risk and the time of completion



b) relation between the life risk and the number of the floor



c) relation between the life risk and the total floor area

below the floor evaluated

Figure 3. Relation between the life risk and the characters of the floor

A METHOD OF FIRE RISK ANALYSIS

M. Tsujimoto, University of Nagoya, Japan

APOSTOLAKIS: You mentioned early in your talk that there was an acceptable level of risk somewhere. How was that acceptable level determined? By whom?

TSUJIMOTO: This distribution is properly determined, likely, in a prefecture. We decided the first 10 percent will be considered to be at risk. We decided this is the risk factor. And, furthermore, for the local agencies, it's very difficult to determine what is really the range of the fire risk.

In other words, among the officials, it's difficult to reach a consensus.

APOSTOLAKIS: Was a consensus reached?

TSUJIMOTO: As a committee we reached a consensus.

HALL: I noticed that some of the factors are dealt with as probability or probability type factors, and some take time effects and translate them into probability.

Are there any special problems involved in trying to mix these two things in one model?

TSUJIMOTO: As I explained, this is very difficult to get a rough estimate. I would like to explain the relationship between the two, and by utilizing the variable and statistical information and so on, I'd like to really deal with that.

Response Surface Approximation of a Fire Risk Analysis Computer Code

Mark Brandyberry and George Apostolakis
Mechanical, Aerospace, and Nuclear Engineering Department
University of California
Los Angeles, CA 90024, USA

ABSTRACT

Fire Risk Analysis as currently used in nuclear plants is outlined along with a discussion of uncertainties in the methods. The use of the computer code COMPBRN is discussed for use in the fire growth analysis along with the use of response surface methodology to quantify uncertainties in the code's use. Generalized response surfaces are developed for the hot gas layer temperature and depth for a room of arbitrary geometry as well as a surface for the time-to-damage in a scenario typical of those analyzed in a nuclear plant fire risk analysis.

1. INTRODUCTION

The evaluation of the risk associated with fires in nuclear power plants has attracted considerable attention in the last few years. While it was believed earlier, on the basis of crude estimates, that this risk was very small and, therefore, dominated by other risks, more detailed analysis showed that the risks from fires could be significant. The methodology is focused on the effects of fires on control and power cables and traces the impact of their failure on the plant. Furthermore, the scenarios that are identified have very low frequencies and special care must be taken to display the uncertainties. We have found that the Bayesian interpretation of probability [1 - 2] provides a convenient framework for the explicit and rigorous treatment of the uncertainties and the subjective judgments that are necessary. Since the basic methodology has been presented elsewhere [3 - 4], its details will not be presented here.

The methodology is centered around the following three tasks:

1. The identification of the "critical" locations and the assessment of the frequency of fires.
2. The estimation of fire growth times and the competing detection and suppression times.
3. The response of the plant.

A location is declared as "critical", when the occurrence of a fire there has the potential of creating an abnormal condition in the plant and damaging the engineered safety functions (ESF). Thus, tasks 1 and 3 are related. As stated earlier, only fires that affect control and power cables are considered. Figure 1 shows a situation, where the cable trays are elevated. The plant analysis has already determined that trays A and B carry cables, which if failed, would lead to undesirable consequences. The occurrence of a large fire on the floor, as shown, could fail these cables, therefore, this location merits a detailed

analysis, and is "critical". In other situations the cable trays are closer to the floor and one worries about a fire starting on one tray and propagating to the others.

In the second step the time T_G that it takes for the fire to propagate and damage the cables of the trays is estimated using the computer code COMPBRN [5 - 6]. This code uses empirical correlations for such quantities as the fire's mass burning rate and flame height to characterize the fire as a heat source. It also employs heat and mass balances to determine the extent and temperature of the layer of hot gases accumulating near the room ceiling. The heat transferred to objects within the room and the room boundaries is then calculated and the thermal response of these receivers determined. Damage is assumed to occur when the surface temperature of an object exceeds a predefined limit.

The purpose of this paper is to discuss the uncertainties associated with the use of COMPBRN and to present analytical approximations ("response surfaces") to the code's output.

2. UNCERTAINTIES

As stated earlier, the computer code COMPBRN is used to calculate the time to damage a specified component, T_G . This time we call the deterministic reference model (DRM) estimate. The question, now, is what kinds of uncertainties are associated with this number.

The uncertainties associated with modeling of physical processes can be thought of as being of two kinds: the statistical uncertainty and the state-of-knowledge uncertainty. The statistical uncertainties stem from the random nature of fire; if we perform a particular experiment a large number of times under 'identical' conditions and measure T_G , we will obtain a frequency distribution. Our physical model cannot predict the environmental fluctuations which lead to this distribution. These uncertainties are inherent in the nature of fire. Even if our knowledge of fire were to increase dramatically, we would not be able to reduce these uncertainties significantly. Such an increase in knowledge, however, would markedly reduce our state-of-knowledge uncertainties.

There are two kinds of state-of-knowledge uncertainty: the parameter uncertainty and the model uncertainty. The parameter uncertainty is due to insufficient knowledge about what the input to the code should be. The model uncertainty is due to simplifying assumptions and the fact that the models used may not accurately model the true physical process.

The DRM is a collection of approximate models which are valid under certain conditions. The model uncertainty is due not only to our uncertainty in the accuracy of each model's predictions under the conditions they were developed for, but also to our uncertainty in the synthesis of these independent models. One of our primary concerns is whether or not the synthesis contains enough component models (i.e., if all important phenomena have been modeled).

The three types of uncertainty that we have discussed, i.e., statistical, parameter and model uncertainty, must be expressed in terms of probability distributions, which will be used in the risk assessment. The development of these distributions requires, again,

substantial judgment, since conventional statistical evidence is lacking. It is judged that the variation of the estimated propagation time is dominated by state-of-knowledge uncertainties. This means that the uncertainties in the models and the parameter values are considered to overwhelm the statistical uncertainty, an assumption which is reasonable in the light of the current state of the art.

3. THE DISTRIBUTION OF T_G

As shown above, the distribution of the scenario fire growth time is a necessary output of the growth portion of the analysis. For a specific scenario to be analyzed, most of the parameters that must be used as input to COMPBRN are either fixed by the problem, e.g., its geometry, or are known to a satisfactory degree. On the other hand, significant uncertainties (at least to the extent that they must be represented by probability distributions) exist regarding the thermal and combustion properties of cable insulation and jacket material as well as other combustibles. The principal sources of uncertainty are the lack of information regarding the composition of these materials and of experimental evidence.

There are several methods for propagating the parameter uncertainties through the DRM, (Monte Carlo, Latin Hypercube Sampling, response surface methods) and each has its advantages and disadvantages [7]. The method used in most fire risk analyses so far is to form a response surface from a sampling of the DRM output and then to propagate the uncertainty distributions through the response surface by Monte Carlo simulation. This technique has the advantage of using a minimal number of computer runs while allowing the exploration of several input variables.

Techniques for setting up the computer runs and then generating the response surface(s) are generally forms of statistical experimental designs (e.g. factorial designs) and regression analysis [8]. The approach taken in this work is to use a form of a factorial design to set up the computer runs and then to form the response surface from polynomials. The parameter distributions can then be propagated through the surface(s) using Monte Carlo simulation.

4. TYPICAL SCENARIOS IN NUCLEAR POWER PLANTS

From the results of nuclear plant fire risk analyses which have already been performed, it is seen that the major source of fire risk to the plant is the vulnerability of important cables to fire damage. Also, there are only a few general scenarios which occur frequently in the various analyses. These scenarios are all combinations of an exposure fire (usually postulated to be an oil pool fire or equivalent) and one or more important cable trays in proximity to the fire. The three geometries which appear most often are shown in Figures 1-3. In these scenarios, two propagation times are usually found to be important: the time for the exposure fire to ignite the first tray, and then the time for the fire to propagate through the stack of trays to damage a second critical tray.

One of the simplest geometries, the exposure fire directly underneath a target cable tray, forms a good starting point for analysis. The objective of this analysis is to develop a simple procedure, through the use of response surface methodology and the COMPBRN computer code, to enable an analyst to calculate the propagation time T_G

without having to resort to running the computer code. Providing sufficient flexibility in the procedure to enable it to be used in differing situations (room dimensions, tray elevations) is important. In most use of response surface methods to date, the focus has been to develop a surface for a specific geometry and fire situation to be used for propagating uncertainties. The inclusion of geometrical variables complicates the procedure tremendously, as we shall see.

The analysis begins by considering the factors which will affect the scenario and are known or thought to be important. Considerable experience has been gained with the COMPBRN code at UCLA, and this has enabled the variables to be investigated to be selected on the basis of known importance to the scenario results in most cases. For the scenario in Figure 1., of major importance is the the characterization of the environment which surrounds the cable tray. In the COMPBRN code, a target which is directly in the fire plume is treated as being only subject to convective heat transfer from the plume. A heat transfer coefficient is calculated on the basis of the fire strength and the tray height. The effects of a hot gas layer (HGL), which may build up in a room, must also be considered. COMPBRN treats the HGL as a single isothermal layer with a user-input heat transfer coefficient (as in [9]). Along with the plume or the HGL, a third possible environment is when the tray is immersed in the flame itself. COMPBRN treats the flame as a temperature-averaged isothermal cylinder with the heat transfer governed by a user-input heat transfer coefficient. The code uses a simple "if-then" logic to calculate the possible tray environments and in the presence of more than one (i.e., in the plume and in the HGL), it will select the highest temperature environment.

The various temperatures and heat transfer coefficients are governed by a number of different variables. The HGL temperature is governed by the fire size and the room geometry, specifically,

- \dot{m}_o = constant pyrolysis rate (kg/ m^2 s)
- H_f = net heat of combustion (kJ/kg)
- R_f = fire radius (m)
- Z_c = ceiling height (m)
- A_c = ceiling area (m^2)
- H_D = doorway height (m)
- W_D = doorway width (m)
- k_c = ceiling thermal conductivity (W/mK)

Since T_{HGL} is a continuous function of these parameters, to provide a means for estimating T_{HGL} without using the computer code, a response surface has been developed. Since COMPBRN is very inexpensive to run, an augmented full factorial design with center and star points is utilized to provide the data for the regression analysis. The parameter ranges used are given in Table 1. Note that the response surfaces use variables which are normalized to the difference from their means as given by the normalizing equations presented in Table 1. As expected, the T_{HGL} turns out to be a complex function of its regressor variables. The least complex acceptable surface includes 19 regressor terms (see Table 2.) and reproduces the COMPBRN results within $\pm 6K$. A secondary calculation with the same computer runs shows the depth of the HGL (from the ceiling) to be well-defined by a simple linear combination of five of the regressors (Table 3.) which reproduces COMPBRN's results within ± 4 cm. It should be noted that the accuracy of

the response surfaces does not necessarily imply that COMPBRN's solutions are correct, only that there is very little extra uncertainty introduced by using the response surface.

Characterizing the plume or flame temperature at the cable tray can be simply accomplished by utilizing the same formulas that COMPBRN does. With several variables either held constant and included in the coefficients or neglected due to insignificance to the model, a simple expression for the height of the flame above the floor is [10]:

$$H_{fl} = 30.64(R_{fl})^{0.695}(\dot{m}_o)^{0.61} \quad (1)$$

Depending upon whether the flame height is below or above the cable tray height Z^* , (assumed known for an analysis) the environment temperature can be calculated from [11]:

$$Z^* > H_{fl} : T_{plume} = 298(1 + 0.00131 \frac{(\dot{m}_o H_f R_{fl}^2)^{2/3}}{Z^{5/3}}) \quad (2)$$

$$Z^* < H_{fl} : T_{flame} = ((\frac{\dot{m}_o H_f}{5.6697 \times 10^{-8}}) (\frac{R_{fl}}{(R_{fl} + 2H_{fl})}))^{1/4} \quad (3)$$

Thus, we now have reasonably simple equations to characterize the temperature of the cable tray's environment.

The other environmental factor is the convective heat transfer coefficient at the tray. For heat transfer within the flame or within the quiescent HGL, COMPBRN requires the user to input a heat transfer coefficient. In the flame, Ref. [12] suggests using a value of 20-23 W/m^2K . We usually conservatively use 23 W/m^2K . From experimental values of the gas velocities in the HGL, a value of 10 W/m^2K works well for heat transfer in the HGL. Within the buoyant fire plume above the flame, COMPBRN internally calculates a coefficient from:

$$h_{plume} = 4.97(\frac{\dot{m}_o H_f R_{fl}^2}{Z})^{1/3} \quad (4)$$

This is adapted from [13]. We now have characterized the cable tray's environment. Two other variables which control the cable damage time are the cable damage temperature, T_{DAM} , and the cable thermal conductivity k_{cbl} . Experience with the code has shown that the thermal conductivity will account for 80-90 percent of the variation in damage time with three other minor variables (cable density, specific heat, and reflectivity) controlling the rest. For our purposes, the thermal conductivity is the important variable.

Thus, we see that:

$$T_G \sim f(T_{env}, h_{env}, k_{cbl}, T_{DAM}) \quad (5)$$

Actually, it is not quite this simple and thus one of the problems with the response surface approach arises: the dependent variable should be continuous over its range of

independent variables. When using a polynomial response surface to describe the variation in a variable which has discontinuities, one must either judiciously choose the ranges of the independent variables to avoid the discontinuities, or describe all deviations from the fitted model to the user. A normal experimental design will vary each independent variable over its entire range. In our case, as an example, this causes problems if, say, the plume and HGL temperatures are fairly low and the damage temperature is high, since then the damage time will be infinite. We could leave these points out of our model and still fit our surface, but then the surface will predict erroneous values of the damage time if a user attempts to evaluate the surface at one of these discontinuous points. The discontinuities which arise when using COMPBRN and an experimental design do not occur in regular patterns (they do, however, follow the physical models) and thus are very difficult to describe to the user. Therefore, it is necessary to carefully choose the independent variable ranges so as to essentially base our analysis on : Time-to-damage given that there will be damage. Varying the damage temperature also causes difficulties in continuity since a set of parameters which cause damage in a scenario with one damage temperature may not cause damage with another (higher) damage temperature.

As a very simple example, we evaluate the time-to-damage surface for a cable tray with a damage temperature set at a typical value of 550K. Since COMPBRN uses the simple model of choosing the hottest environment to surround the cable tray, we may investigate the cable damage time with respect to the local environment temperature and heat transfer coefficient and the cable thermal conductivity without regard to the source of the hot gases.

The response surface given in Table 4 characterizes the damage time. This surface may be used for any situation in which a cable tray is immersed in an environment of hot gases without significant external radiation, whether it is a flame, plume, or HGL. The value of the heat transfer coefficient used will depend upon the specific situation. Note also that this is really a "time-to-temperature" surface since COMPBRN uses the simple criteria of an "ignition temperature". Thus, the T_{DAM} calculated could be specified by the user as time-to-ignition for scenarios to be propagated through a stack of trays above the target tray or as time-to-damage for a cable short-circuit simulation. The reader is cautioned that due to the discontinuous nature of the damage-time data (the cable temperature response may be quite erratic when the environment is less than 100K more than the damage temperature and the heat transfer coefficient is varied) the surface presented here predicts the damage time within $\pm 60sec.$ near the center of the explored region, but may become quite inaccurate with combinations of variables near the boundaries. (see Figure 4.)

5. PARAMETER SELECTION

The ranges of values which were chosen for the various variable were selected to enable an analyst to 'simulate' a fire scenario using geometries and materials which could be found in a nuclear plant. The ranges of m_o and H_f were selected to cover a wide range of flammable liquids as shown in Table 6 [14]. The range of fire radii encompasses sizes from that of a small container of fluid to a 1 meter diameter spill. Previous PRAs have postulated fire diameters of 1 foot (.305 m) to 2 feet (.61 m) in diameter. The room dimension limits and door sizes selected were judged to be representative of the smallest

room likely to be analyzed and of the largest for which hot gas layer effects are significant for the fire sizes postulated. For the time-to-damage surface, the T_{DAM} was chosen arbitrarily as a representative value. The T_{env} range was selected with the knowledge that the code will not predict damage with an environment less than about 25-50K greater than T_{DAM} , and that values of $T_{env} > 800K$ produce damage within the first time step (15 sec here) for a $T_{DAM} = 550K$ and any h_{env} in our range. The h_{env} range was calculated from the approximate maximum value of Eq. 6. and the HGL value of 10 W/mK.

7. REFERENCES

1. Kaplan, S., and Garrick, B.J., "On the Quantitative Definition of Risk," Risk Analysis, 1:11-37, 1981.
2. Apostolakis, G., "Data Analysis in Risk Assessment", Nuclear Engineering and Design, 71:375-381, 1982.
3. Apostolakis, G., Kazarians, M., and Bley, D.C., "Methodology for Assessing the Risk from Cable Fires," Nuclear Safety, 23: 391-407, 1982.
4. Kazarians, M., Siu, N.O., and Apostolakis, G., " Fire Risk Analysis for Nuclear Power Plants: Methodological Developments and Applications," Risk Analysis, 5: 33-51, 1985.
5. Siu, N.O., and Apostolakis, G., "Probabilistic Models for Cable Tray Fires," Reliability Engineering, 3: 213-227, 1982.
6. Siu, N.O., "Physical Models for Compartment Fires," Reliability Engineering, : 229-252, 1982.
7. Iman, R.L., Helton J.C., "A Comparison of Uncertainty and Sensitivity Analysis Techniques for Computer Models," Sandia National Laboratories, NUREG/CR-3904, March 1985.
8. Box, G., Hunter, W., Hunter, J., Statistics For Experimenters. John Wiley and Sons, Inc., 1978.
9. Rockett, J.A., "Fire Induced Gas Flows in an Enclosure," Combustion Science and Technology, 12(1976), 165.
10. Thomas, P.H., "The Size of Flames From Natural Fires," Tenth Symposium (Int'l) on Combustion, 844-859 (1963).
11. Zukoski, E.E., Kubota, T., "Experimental Study of Environment and Heat Transfer in a Room Fire. Mixing in Doorway Flows and Entrainment in Fire Plumes," NBS-GCR-85-487, 1985.
12. Neill, .DT., Welker, J.R., Slipecevich, C.M., "Direct Contact Heat Transfer from Buoyant Diffusion Flames," Journal of Fire and Flammability, 1, 289-301, 1970.
13. Veldman, C.C, Kubota, T., Zukoski, E.E, "An Experimental Investigation of the Heat Transfer from a Buoyant Gas Plume to a Horizontal Ceiling, Part I," NBS-GCR-77-97, June, 1975.
14. Babrauskas, V., "Estimating Large Pool Fire Burning Rates," Fire Technology, 4(19), 251-256, 1983.

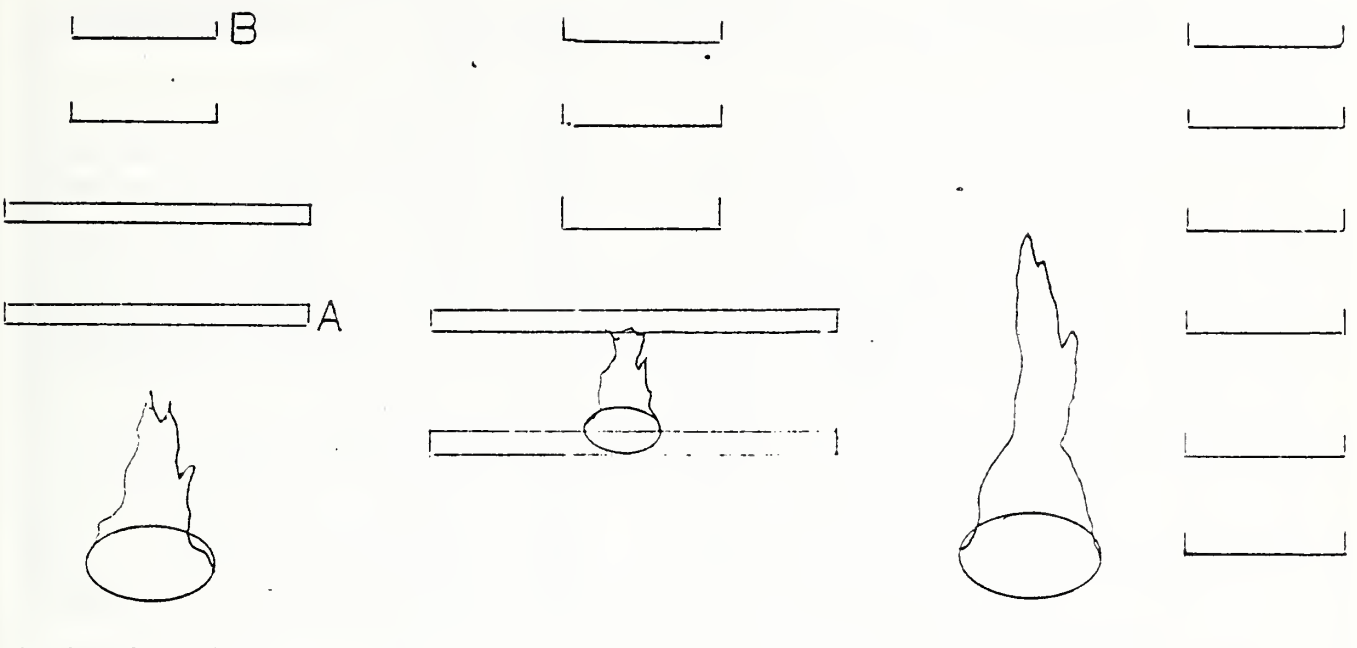


Figure 1.

Figure 2.

Figure 3.

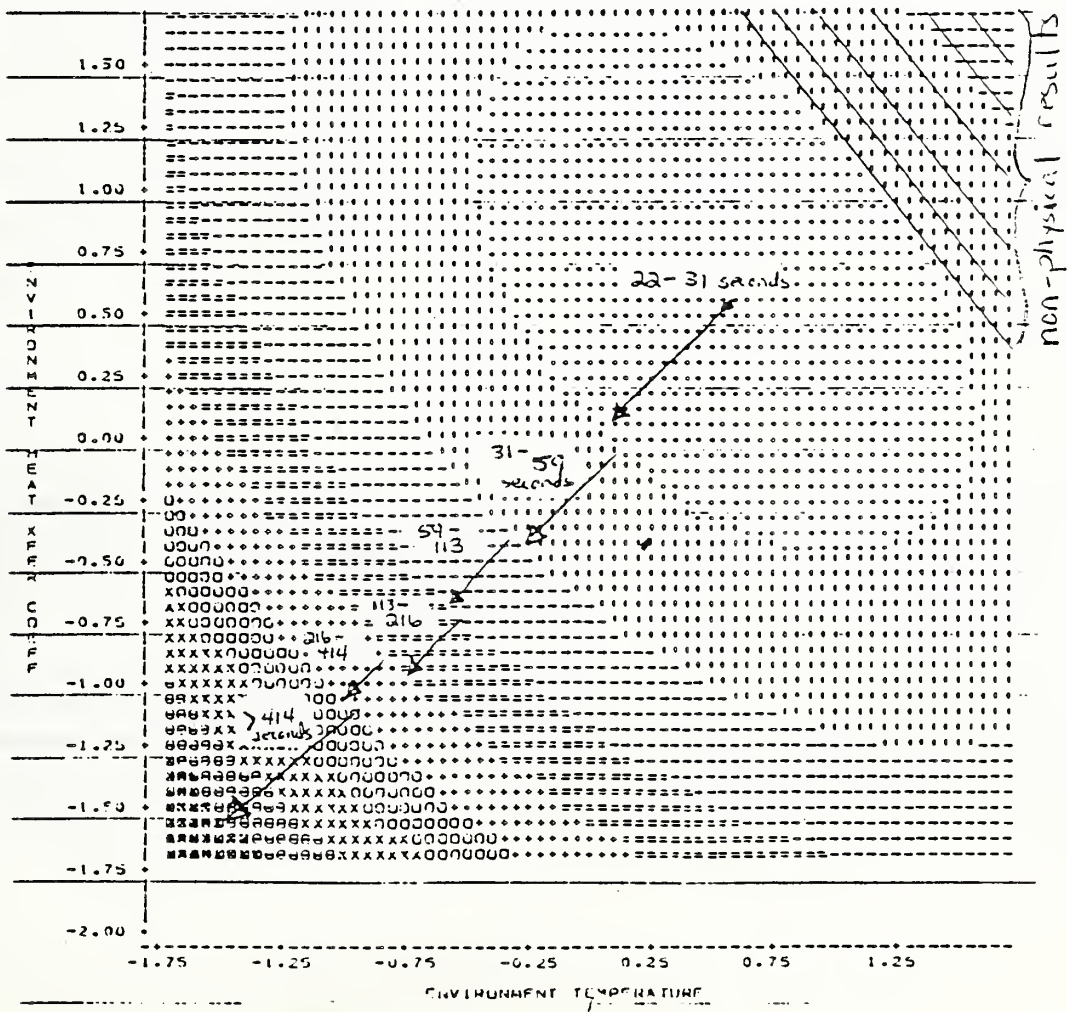


Figure 4. Contour Plot of T_G vs. T_{env} and h_{env}

PARAMETER	RANGE	NORMALIZED VARIABLE	NORMALIZING EQUATION
\dot{m}_o (kg/m ² K)	.02 - .10	X1	= $100\dot{m}_o - 6.$
H_f (MJ/kg)	20. - 47.	X2	= $.2963H_f - 9.926$
R_{fl} (m)	.09 - .50	X3	= $19.512R_{fl} - 5.756$
Z_c (m)	2.4 - 6.1	X4	= $2.162Z_c - 9.189$
A_c (m ²)	9. - 900.	X5	= $.00898A_c - 4.0808$
H_D (m)	1.8 - 3.1	X6	= $6.154H_D - 15.077$
W_D (m)	1.2 - 3.7	X7	= $3.2W_D - 7.84$
k_c (W/m ² K)	.30 - 1.3	X8	= $8k_c - 6.4$
h_{env} (W/m ² K)	10. - 300.	X9	= $.0116h_{env} - 1.7978$
T_{env} (K)	575 - 800	X10	= $.01495T_{env} - 10.2776$
k_{cbl} (W/mK)	.09 - .35	X11	= $10.8503k_{cbl} - 2.6583$

Table 1. Parameter ranges and normalized variables.

Regressor/Coefficient

X1	11.50	X1X2	1.04	X1 ²	-4.58
X2	11.27	X1X3	2.90	X3 ²	1.48
X3	30.24	X1X5	-.707	X5 ²	.730
X4	-2.42	X2X3	2.58	X8 ²	.542
X5	-2.77	X3X5	-.754	X5 ³	-.130
X6	-1.77	X3X6	-.621		
X8	-5.70	X3X8	-1.27		
Constant= 420.1					

Table 2. Response Surface for T_{HGL} (K)

Regressor/Coefficient

X1	.0149
X3	.0247
X4	.4629
X6	-.0928
X7	-.0528
Constant = 2.723	

Table 3. Response Surface for the HGL Depth (m).

Regressor/Coefficient

X9	-.4279
X10	-.3929
X11	.4599
X9X10	.3689
X9 ²	.3705
X10 ²	.4085
constant = 3.4560	

Table 4. Response Surface for $\ln(T_G)$ (Ln(sec))

Liquid	\dot{m}_o (kg/m ² K)	H_f (MJ/kg)
Heptane	.101	44.6
Gasoline	.055	43.7
Kerosene	.039	43.2
Transformer Oil, hydrocarbon	.039	46.4
Fuel Oil, heavy	.035	39.7
Methanol	.017	20.0

Table 5. Some Typical Burning Properties of Combustible Liquids.

NELSON: There are models much more sophisticated than COMPBURN, that can give more accurate answers for multiplicity of locations. Do you consider them too large of an effort in the risk analysis to attempt to use them?

APOSTOLAKIS: Well, the uncertainties are always a major issue with us, and the amount of effort that we can spend on a project like this has to be balanced against the accuracy of the result. Given the parameter and model uncertainties that I mentioned, most people would agree, at least in the nuclear safety area, that it's not worth going to more sophisticated models.

Of course, the assessment of the model uncertainty may very well require the use of these more sophisticated models.

NELSON: So we've got to prove models with models?

APOSTOLAKIS: Or experiments could help.

HALL: A quick specific question on the first exercise of looking at models. You had said that the exercise included with the code itself is quite conservative. Was that because the uncertainty range was almost all in the high side of one? For that E value? That from point 8 to 4, and if you assume one is saying that the model is bringing back the same value, so if it's wrong it's almost certainly low...

APOSTOLAKIS: That's right.

HALL: And this is the parameter for high values and then safer conditions, is that correct?

APOSTOLAKIS: That is correct.

QUINTIERE: I have a question on the response. You're seeking algebraic representations for predicting quantities of heat. In seeking these approximations you need to be sure that you identify all the attempted parameters. But many empirical correlations are being developed that would be useful in guiding this process.

The part that I don't understand is the value of using the response surfaces. Could you explain the value of using response surface in risk analysis?

APOSTOLAKIS: There are several questions that need to be answered. First, the issue of important parameters. This is, of course, always an issue because in essence you are building a new model. We are determining what parameters are important by reading the literature, knowing what turned out to be important in past applications, and asking other experts. If there are any doubts about one or two parameters, then we include them in the model and we see how the beta coefficients turn out to be.

Regarding correlations, we only use response surfaces where we do not have correlations. For example, we can get the temperature in the plume without using the code by using simple correlations. Then we do not develop a response surface; in fact, the correlation is the response surface. But for the hot gas layer, we were not able to find any correlation giving the depth or the temperature, and this is where these methods are useful.

Now, how useful are they? You have all the advantages of a simple polynomial, working with a simple polynomial. For example, you can propagate uncertainties analytically. You can see immediately by looking at the polynomial which parameters are important.

In general, it is more expensive to do a Monte Carlo simulation, but that is not the case here. And another advantage that I see is that the response surface may be used by people who are not really interested in becoming experts in fire propagation, although that may be undesirable.

AN ENGINEERING FIRE PROTECTION DESIGN ASSESSMENT SYSTEM

Harold E. Nelson
Center for Fire Research
National Bureau of Standards
Gaithersburg, MD 20899

ABSTRACT

A fire protection engineering design assessment system to provide design engineers with a tool to improve their ability to appraise the overall fire safety in a facility and evaluate the impact of fire protection measures is described. The system uses deterministic fire protection techniques and is being implemented through an interactive computer program. The inputs to the system require data on building layout, combustible contents, fire resistance, detectors, sprinklers, smoke control, occupants, and fire safety objectives or criteria. The outputs include the predicted fire generated conditions within the building as a function of time and an evaluation of the predicted performance of the facility with user specified fire safety objectives.

Introduction

This paper discusses the plan for and status of an engineering fire protection design assessment system. It also addresses the use of elements of this plan in recent analysis of a major fire incident.

Both the U.S. and Japan are actively involved in several different approaches to use recent developments in fire science and the modeling to analyze fire safety in buildings. The emerging products vary widely in scope, sophistication, and commitment demanded of the user. In general, as the degree of sophistication and adherence to first principles of fire sciences increases, the level of complexity, user commitment required, cost of the hardware involved, and CPU time increase.

The object of this engineering system is to produce a credible package of coordinated engineering tools that can produce reasonably accurate predictions, be operable on the current generation of personal computers, and respond quickly to the user's commands. Simplifying assumptions will necessarily be involved and appropriate safety factors required.

The development of the engineering approach is preceding through cooperative efforts with various U.S. Federal agencies. In each case, the objective is to support the fire protection engineering decisions that those agencies make for federally owned buildings or facilities. Two recent publications represent partial output. These are:

1. NBSIR 83-3308, "FIREFORM" - A Computerized Collection of Convenient Fire Safety Computations [1]. This report describes a menu driven collection of simple models and formulas felt to be useful in fire safety problem analysis. These and similar simple models and formulas are at the heart of the engineering system.

2. NBSIR 85-3298, "The Basic Structure of the Fire Protection Design Assessment System." [2] This report describes the basic structure and details the flow chart of the assessment system. Parts but not all of the detailed assessment system are now in operation.

The object of the project is to produce one or more systems that are compatible with building assessment and regulation, scientifically credible, and easily used by the practicing engineer. It is intended to keep the required engineering effort at a level that makes it economically feasible for most designs and building evaluations.

Background

Historically, the relationship between expenditures on fire safety and the actual impact of these expenditures has been hard to establish. Until the past decade, virtually all fire safety knowledge was empirical. Fire safety decisions were based on subjective opinions on how to prevent the recurrence of prior disasters. Materials were generally judged on the basis of large scale tests.

At the time current practice evolved, this empirical approach was sufficient. Most buildings were inherently massive and highly compartmented. Wood and paper were the prime combustibles of concern. The rate of change in building technology was slow. The accumulative history of how buildings reacted when exposed to fire was a good prediction of future expectations. It was in that atmosphere that the system of consensus codes arose. These codes covered not only fire but all other basic safety functions such as structural and plumbing requirements.

In the development of these codes credible technology was included wherever it existed. When such was not available, committee consensus judgment was used. The ultimate goal being to develop a complete system whereby a builder had sufficient information to propose a design that an authority (typically a building commissioner) could review and concur in that effort. The code approach evolved in the period between 1930 and the mid 1960s. It continues with little or no advancement to dominate fire safety decisions to this day.

The result is a rigid set of requirements. The objectives and expectations of the committees and other consensus bodies in setting the requirements are generally not recorded. Requests to these bodies for interpretations often very massively depending on the membership of the committee when the request is received. Consequently, the value and intent of any requirement is seldom apparent.

Virtually every code has an equivalency clause. The equivalency clause permits alternative approaches provided equal performance can be achieved. It is, however, difficult to demonstrate performance when the factors that need to be considered are established by consensus.

As a result, the collection of codes, standards, and criteria rather than fire safety frequently become the objective. Expertise becomes entombed in

relating fixed requirements to building materials and systems. Innovation, rational design, and cost control are constrained and frustrated.

Over the past several decades, however, a relatively small but fortunately persistent group of research scientists and engineers have made important advances in understanding and quantifying fire and the responses of buildings, peoples, and fire protection systems to fire. Their efforts have been dedicated to determining the basic principles of unwanted fires and measuring the variables involved. In recent years the scope has expanded to the development of coordinated engineering approaches to predicting the course of fire, the response of fire safety features, and the resulting impact on people, property and productive missions.

There is now an emerging fire protection engineering technology which can, in many cases, be used to evaluate the fire safety performance of a building even if it differs widely from the current perceptions of a code conforming building. This same technology can be adapted to assess the impact of a proposed or existing safety requirement as applies to a specific inventory, building, or set of circumstances. It is now possible to make a reasonable engineering analysis of fire development and impact from the moment of ignition to the final determination of the results of fire.

The design process starts with a given building condition. In fire safety design this encompasses:

- a. The building, its layout or shape, materials of construction, sub-systems (utilities, electrical, fire alarm, sprinklers, etc.);
- b. The intended use of the building, particularly in terms of the combustible materials and hazard of operation involved in the activities of the occupant;
- c. The people in the building in terms of their areas of activity and any consideration of special physical impairments (handicapped or disabilities) or other characteristics such as mission responsibilities to stay in place as long as possible at time of emergency.

As a practical design problem, some of these qualities are reasonably fixed in any building and some change from time to time. Many of these variables can affect the course or level of danger presented in a fire. To attempt to analyze every conceivable variable and all the combinations of variables is irrational.

The engineering method, that is at the heart of the engineering assessment system, follows the technique of design stress. The approach is similar to that used in structural design. In this case, the stress is thermal and environmental rather than a gravity or dynamic force load. Assessment is based on fire or occupant situations that represent the most stressful condition that the building is expected to endure. This design fire stress starts with the expected fire load conditions, either typical for the occupancy class housed or specific to a known case of concern. Other conditions such as the position of doors (i.e., open or closed) and the

location and disposition of people in the building are evaluated on the basis of:

- a. the most vulnerable situation,
- b. a selected situation of particular interest, or
- c. a series of selected design cases to determine the impact of one design case versus another.

Fire is viewed as an energy driven stress on a building and its internal environment. The building reacts to this stress by absorbing it, removing it, or undergoing change in response to the stress.

In recent years, the fire research community has made significant progress. Fire modeling and similar activities can be used to discover, quantify, and express in engineering terms the physics of fire and the manner that a building, its systems, and its occupants cope with fire stress.

The engineering assessment system is designed to bring current state-of-the-art to the practicing fire safety professional in a form that is applicable to the facilities involved and useful to and usable by fire safety professionals.

The Approach

The overall approach is shown in greater detail in NBS Report, "The Basic Structure of the Fire Protection Design Assessment System." [2] Figures 1 through 4 are flow charts from this report. These flow charts depict the structure of the engineering assessment system. The specific approach involved in the project is:

1. Assembling and as necessary advancing the current technology.

Much of the technology for the engineering approach exists. Some needs refinement. In some cases new research, data development, and technology development are needed. During the past year, CFR has exercised many of the elements in both in-house experiments and use of the engineering formulas to mathematically reconstruct the conditions that occurred in serious accidental fires.

Of critical importance to this project, a major part of the current effort is being directed towards the enhancement of the Available Safe Egress Time model (ASET.) [3] ASET is being revised to improve the manner in which heat transfer to the walls is calculated in that model, extend the model from a single room with closed doors to one that can handle a series of rooms with doors open, and provide a means for geometric changes (breaking of windows, opening or closing of doors, and similar variations) during the course of the computation. This will be the core model of the engineering assessment method.

The improved core model and a considerable number of supporting computations and formulas are being assembled into two packages. The first package will be menu driven collection of all of the pertinent formulas and an accompanying data base. This will place into the hands of the fire safety community readily

accessible tools aimed at fire protection engineers and other comparable professional. A preliminary version of this is currently in broad circulation under the title "FIREFORM." [1]

2. Merging the elements into a single coherent system.

The second objective is to assemble the core model and accessory formulas along with the appropriate data base into an interactive computerized system. The system to be usable by persons who are familiar with building construction materials and fire protection systems but not necessarily the detailed engineering formulas. The user will be provided with data input screens at his terminal. He will enter information such as the space dimensions, materials of construction or finish, and type of occupancy (office, warehouse, storage, trash room, etc.) The system will process the input and return and appraisal of the conditions to be expected in case of fire and what safety margin is likely to exist between the time needed for evacuation and the time the space reaches intolerable conditions.

The output of the system will also be able to report the formulas and variables internally used or developed by the system.

Current Uses

Currently, many of the elements of the engineering assessment system reside as individual programs on the author's computer and formulas available in various publications. These have been used many times in responding to individual fire protection engineering queries. Most recently, a number of these formulas and procedures were collected and used to make an engineering reconstruction of the fire phenomena that occurred at the Dupont Plaza Hotel and Casino fire of December 31, 1986. In the analysis of the Dupont Plaza fire, an attempt was made to accomplish the evaluation using methods that can be quickly executed on personal computers or hand-held calculators. The methods employed are, for the most part, elements destined for inclusion in the engineering appraisal system. The objective of using these simpler approaches was nearly accomplished. It was necessary, however, to resort to a more comprehensive model (emersion of the Harvard Model referred to as FIRST [4] recently developed by Mitler and Rockett) to develop a credible estimate of the development of the smoke layer in one of the rooms and the flow of fuel from one room to another. As previously noted, the development of a rapid response model to make reasonable estimates of smoke level development in vented rooms and the flow of fuel from space to space are priority needs for the development of the engineering analysis system.

A report of the analysis of the Dupont Plaza fire has been prepared by Nelson. [6]

Status and Direction

With the increasing use of the menu collection, "FIREFORM" and the exposure of the concept resulting from its use on the Dupont Plaza fire, there has been a renewed interest in the engineering system. This has resulted in additional support and the initiation of a three-year project. The object of this

project is to develop a working system, readily usable by practicing designers and fire protection engineers. The scope of this initial version will be limited to room and corridor arrangement in buildings that do not have significant, unprotected vertical openings. The system will address smoke and heat leakage from the floor of origin into stairways or shafts but will not, at this stage, address the movement through the shafts or onto other floors. The project plan calls for having an operating prototype system within one year and an implemented system in the hands of practicing engineers within three years.

References

1. Nelson, H. E.; "FIREFORM" - A Computerized Collection of Convenient Fire Safety Computations; Report NBSIR 86-3308; National Bureau of Standards; Gaithersburg, MD; 1986
2. Nelson, H. E. and Walton, W. D.; The Basic Structure of the Fire Protection Design Assessment System; Report NBSIR 85-3298; National Bureau of Standards; Gaithersburg, MD; 1986
3. Cooper, L. Y., and Stroup, D. W.; Calculating Available Safe Egress Time from Fires; Report NBSIR 82-2587; National Bureau of Standards; Gaithersburg, MD; 1982
4. Mitler, Henri E. and Rockett, John A.; Users' Guide to First, A Comprehensive Single-Room Fire Model; NBS report to be published, National Bureau of Standards, Gaithersburg, MD
5. Nelson, H. E.; An Engineering Analysis of the Early Stages of Fire Development - The Fire at the Dupont Plaza Hotel and Casino, December 31, 1986; Report in preparation.

FIRE PROTECTION DESIGN ASSESSMENT SYSTEM

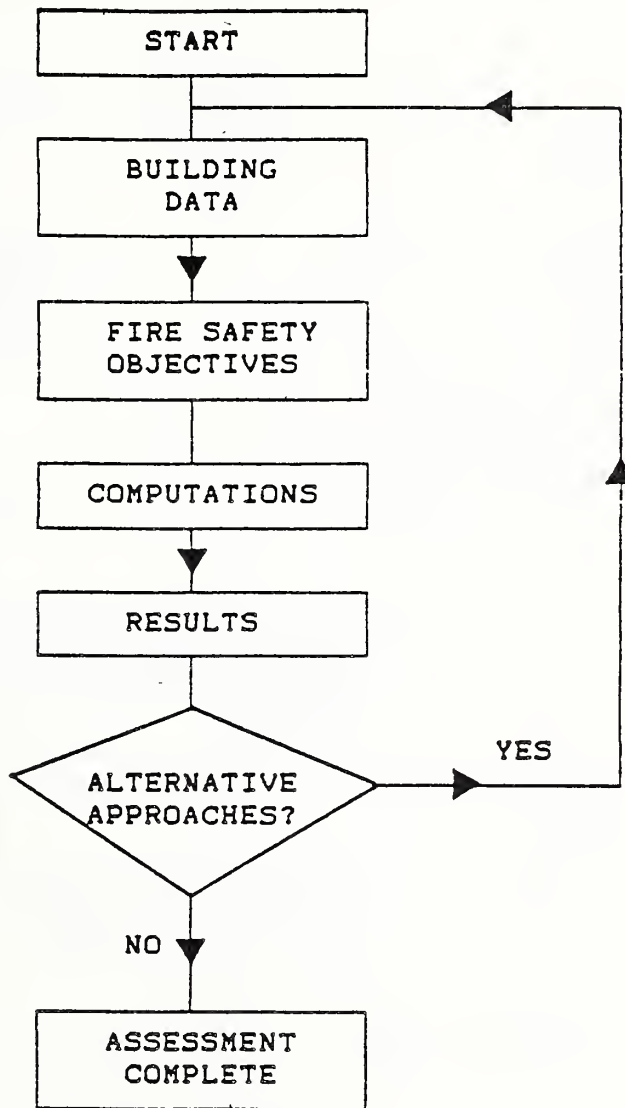


Figure 1. Fire Protection Design Assessment System General Model

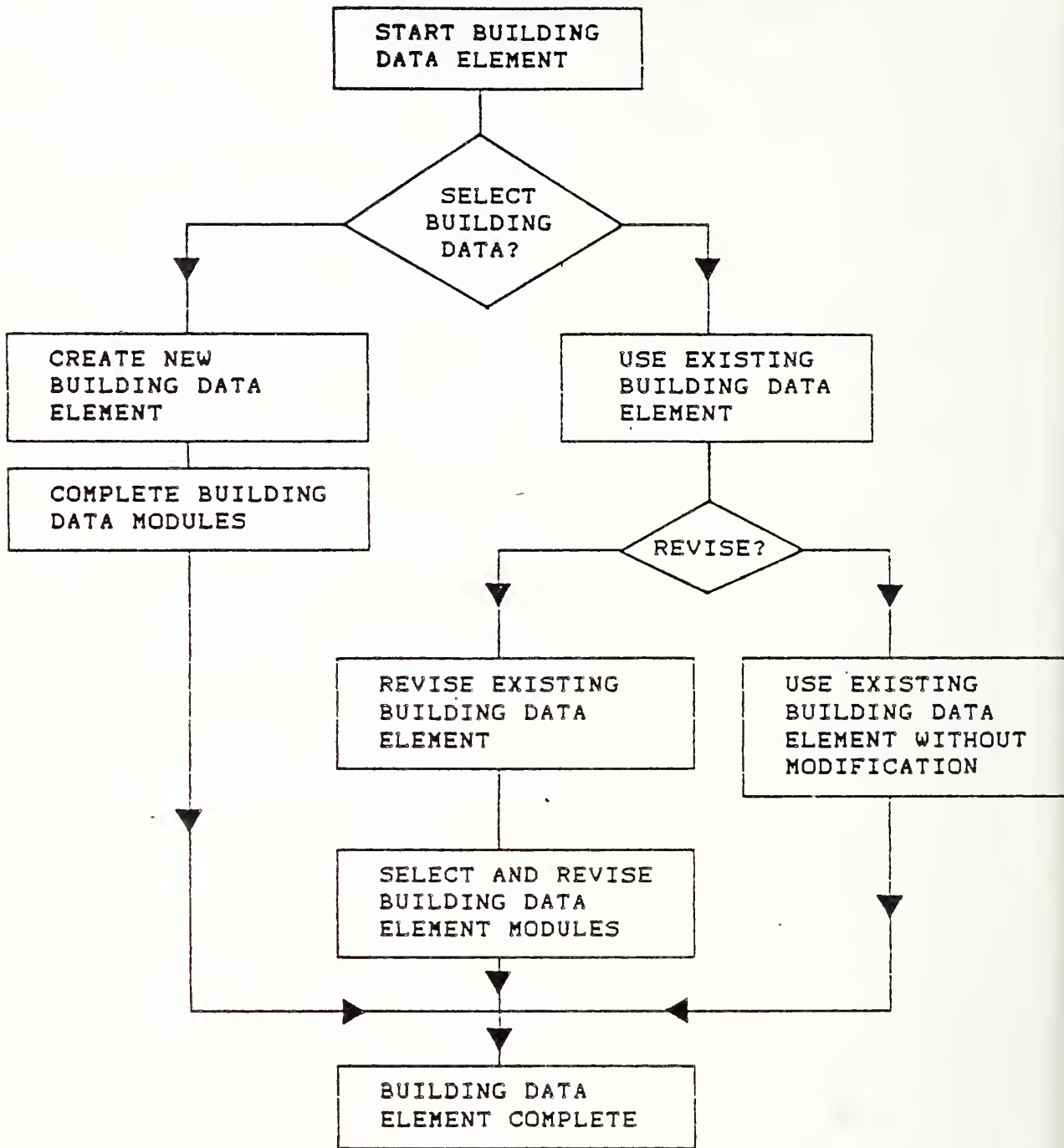


Figure 2. Building Data Element

BUILDING DATA MODULES

ARCHITECTURAL DATA

ROOM OF ORIGIN
DIMENSIONS
MATERIALS
OPENINGS
LEAKS
ADJOINING SPACE(S)
DIMENSIONS
MATERIALS
OPENINGS
LEAKS

FUEL PACKAGE DATA

FIRST IGNITED
RATE OF:
ENERGY PRODUCTION
MATERIAL DESTRUCTION
PRODUCT(S) PRODUCTION
LOCATION
EXPOSED FUEL PACKAGES
BURNING RATES
IGNITION SUSCEPTIBILITY
LOCATION
TOTAL FUEL (ROOM OF ORIGIN)
MASS AVAILABLE
PYROLYSIS RATE

STRUCTURAL FIRE RESISTANCE

COMBUSTIBLE FUEL LOAD
RATED FIRE RESISTANCE OF BUILDING ASSEMBLIES

Figure 2. (continued) Building Data Element

BUILDING DATA MODULES

DETECTION EQUIPMENT

ROOM OF ORIGIN
SMOKE
 LOCATION
HEAT
 POSITION
 RESPONSE TIME
 ACTIVATION TEMPERATURE

SPRINKLERS

ROOM OF ORIGIN
LOCATION
RESPONSE TIME INDEX
ACTIVATION TEMPERATURE

SMOKE CONTROL

VENTS
 SIZE (CAPACITY)
 LOCATION
 INITIATION METHOD
HVAC OR SMOKE CONTROL SYSTEM
 PRESSURE DIFFERENTIAL
 INITIATION METHOD

OCCUPANTS

NUMBER OF OCCUPANTS
CAPABILITIES
CONDITION (AWAKE, ASLEEP, ETC.)
MAXIMUM TRAVEL DISTANCE
DOORS
STAIRS

Figure 2. (continued) Building Data Element

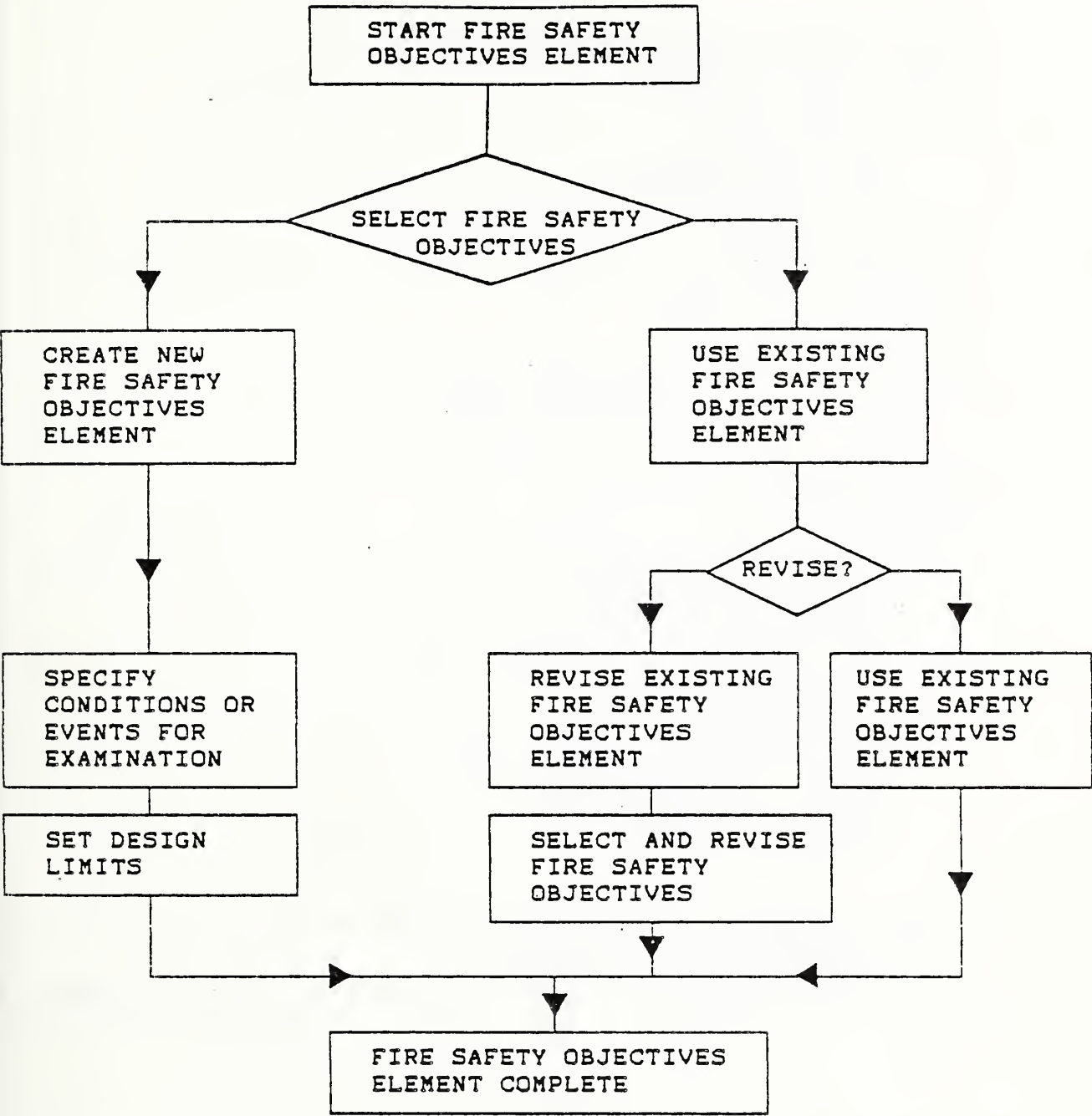


Figure 3. Fire Safety Objectives Element

CONDITIONS OR EVENTS FOR EXAMINATION

SMOKE LAYER TEMPERATURE
SMOKE LAYER LOCATION
SMOKE CONSTITUENCY
 OPTICAL DENSITY
 TOXIC CONCENTRATION
TIME TO FLASHOVER
FIRE DURATION
FIRE RESISTANCE OF A BUILDING ASSEMBLY
DETECTOR ACTIVATION
SPRINKLER ACTIVATION
SMOKE LEAKAGE
EVACUATION TIME

DESIGN LIMITS

HUMAN TOLERANCES
 HEATED GAS TEMPERATURE
 THERMAL RADIATION
 SMOKE OPTICAL DENSITY
 SMOKE TOXICITY
BUILDING ASSEMBLY TOLERANCES
 FIRE RESISTANCE
 SMOKE TRANSMISSION
CONTENTS TOLERANCES
 HEATED GAS TEMPERATURE
 THERMAL RADIATION
 CHEMICAL EXPOSURE

SAFETY MARGIN

TIME AVAILABLE FOR EGRESS
TIME TO UNTENABLE CONDITIONS/TIME REQUIRED FOR EGRESS

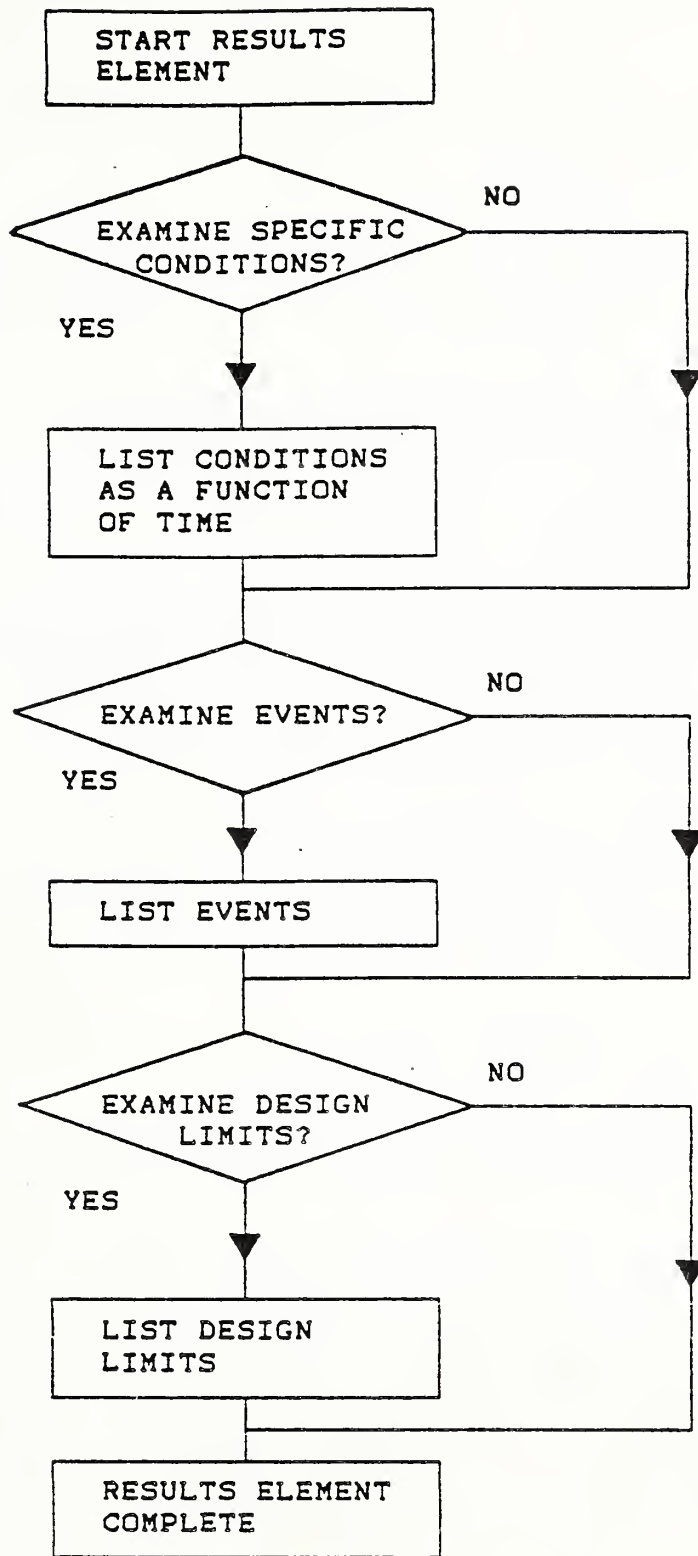


Figure 4. Results Element

AN ENGINEERING FIRE PROTECTION DESIGN ASSESSMENT SYSTEM
H. Nelson, National Bureau of Standards, USA

WATTS: You started by saying your objective was to find the least sophisticated approach that would give you an adequate result?

NELSON: That's right.

WATTS: What is your criteria for adequacy in a result?

NELSON: Technically, sufficient to make the judgment necessary with professional confidence.

APOSTOLAKIS: I wonder, since this was a real fire, whether you could get real evidence to compare the model predictions with.

NELSON: I omitted one statement. I did not do this blind; I used evidence and witnesses whenever there was question of a parameter, to attempt to choose the right parameter.

JIN: Perhaps the answer will come out in the report that you alluded to earlier, but my question is similar to the one that Dr. Apostolakis just asked. Have you shown in the report how the calculations were done? I assume that this was a real fire, and that you compared it with hypothetical correlations. Therefore, will these be shown in your report, or is it something that you might answer here in a different tone?

NELSON: I think the answer is "yes," and Dr. Jin will get one of the first reports when they arrive. If he gets a chance to look at it before the end of the week, I would value his opinion as to whether I've achieved that or not.

TANAKA: If you're going to give report number 1 to Dr. Chin, I'd like to have number 2.

NELSON: I would be very happy, I'll sign it.

TANAKA: I am at a loss to understand why 85 people or so died in the casino. Can you give some indication whether this was due to the lack of sufficient exits, or was the fire too fast for them to make the exits?

NELSON: I think three items. The early stages of the fire were not psychologically threatening and they were ignored. They had a maximum, by my calculations which may not be that accurate, of about 40 seconds to egress through a one meter wide door. There are disagreements about how many people actually got out that door, but I believe in the neighborhood of 40 to 50. Then, the smoke in the lobby was so intolerable -- this is a supposition -- this door was closed for protection purposes. At that point they attempted to break windows to evaluate. Five or six succeeded in evacuating that way, but then this window broke, and a gas flow with about 800 to 900 C flowed through

here, changing from gas to flame as it went in, I believe, about 20 seconds. The deceased were found collected in front of that door, and near the areas where the windows were broken.

So, it was speed, egress capacity and delayed action.

CUSTER: In some of your diagrams there appear to be flames up in the ceiling layer, yet you're reporting very low oxygen content?

NELSON: No, no. I skipped too quickly. The diagram I showed was 10 seconds ahead of when the oxygen went virtually to zero, so I felt it was still legitimate to show flame, through I'm not positive.

COTE: Since this was an existing fire in which there's been a fair amount of reconstruction by virtue of being able to interview people, did you have any surprises in the engineering method, in any of the pieces? Was there anything that did not work as well as you thought it would, or did not come together as well as you hoped it might?

NELSON: The largest surprise to me was that a combustible material finish that did not spread fire prior to flashover was a major contributor of fuel after flashover. I think we need to pay more attention to a property that is often referred to as heat of gasification. Also, I have learned how good Drysdale's book is.

BASIC STRUCTURE OF THE EVACUATION SAFETY DESIGN METHOD

by

Takeyoshi TANAKA

Building Research Institute
Ministry of Construction

INTRODUCTION

Traditionally, fire safety design of buildings in Japan has been accomplished through the specification standards described in The Building Standard Law, The Fire Service Law, their enforcement orders and so on. While specification standards are convenient to quickly decide the fire safety measures, their drawbacks have long been recognized. They are usually inflexible to new type of designs, new construction methods, and trivial differences from the standards. Furthermore, literal application of specification standards can sometimes bring about demands which are not optimal but even ridiculous from the viewpoint of fire safety performance.

In recognition of these problems arising from designers, building officials and others concerned, BRI started a research project called "Fire Safety Design Method of Buildings" in an attempt to provide designers with a fire safety design method alternative to the specification standards in The Building Standard Law. This paper reports the basic structure of "The Evacuation Safety Design Method" as a part of "Fire Safety Design Method of Buildings"

RELATIONSHIP BETWEEN FIRE SAFETY DESIGN METHOD AND THE BUILDING STANDARD LAW

Since the primary motivation for developing Fire Safety Design Method of Building was to establish a design method of fire safety for buildings that can be used as an alternative to the fire safety standards in The Building Standard Law and its associated orders, it was thought to be important to clarify the relationship of the two. At present, it is generally agreed that the two should coexist for the time being as a dual design system for fire safety measures, because the adequacy of Fire Safety Design Method needs to be fully examined in the world of practice. Also, it is necessary that the method have to be appreciated by many designers and building officials before its full-scale application.

The relationship between Fire safety Design Method and the fire safety standards in The Building Standard Law is illustrated by Fig.1. Since the two are supposed to function as a dual system of fire safety design, it follows that the ultimate goal have to be the same for the two. In The Building Standard Law, the principle for fire safety measures of buildings is given in Article 35, but the description was thought to be too inclusive and abstract to draw technical standards from it. So, in Fire Safety Design Method, the principle was broken down into the fundamental requirements for more concreteness as shown in Table 1.

Most of the current technical standards in The Building Standard Law directly specify materials, dimensions, construction methods etc. of various fire safety measures of buildings, which is much of the source of complaints among designers. So, in Fire Safety Design Method, attempts were made to write the technical standards in terms of performance standards as long as possible and beneficial. It should be kept in mind, however, that any technical standard is more or less of temporary nature. They cannot help but to reflect the current conditions of building construction and currently available technologies and knowledges for fire safety. So, there is a good chance that unexpected by the standards but still effective fire safety measures are invented by designers or others. Such a measure can be accepted in Fire Safety Design Method as long as it meets the fundamental requirements.

Several fire tests are the almost only technical sources to supplement the specification standards for fire safety in The Building Standard Law. On the other hand, since predictions of various aspects of fire behavior have to play a key role to run performance standards, Fire Safety Design Method is provided with relevant calculation standards and computer codes to predict fire behavior and evacuation conditions.

TECHNICAL STANDARDS FOR EVACUATION SAFETY

1. Basic Components of The Technical Standards for Evacuation Safety

On considering the basic structure of the performance based technical standards for evacuation safety of buildings, the method being used in structural design of buildings was taken as a model. In structural design, standardized loading conditions regarding dead and live loads, earthquake and wind are given and the stress which develops in each structural member is required to remain within the allowable limit of the structural material used. The loading conditions in structural design correspond to the fire conditions in Evacuation Safety Design, which consist of conditions of fire and occupants and fire scenarios. And allowable limit of stress corresponds to human tolerance against the hazards associated with fire, that is; smoke, heat, bruise and so on.

Basically, any design is can be accepted as long as it is proved that the safety standards are satisfied under the standard fire conditions. The concept of the procedure for the evacuation safety design using the performance based technical standards is illustrated in Fig. 2.

2. Items to be Checked for Evacuation Safety

The items to be checked for evacuation safety of buildings are listed in Table 2. Many of these have performance based safety standards which have to be satisfied under relevant fire scenarios.

2.1. Restriction of Use of Building Materials Excessively Hazardous to Evacuation

This restriction reflects the toxicity tests currently required to the fire proof materials by a Ministry of Construction Order. The technical standards for evacuation safety has been constructed under the premise that extremely hazardous materials are removed from buildings.

2.2. Adequacy of Evacuation Plan

In the current Building Standard Law, no description exists regarding how an evacuation plan has to be planned but the construction methods, materials, dimensions, smoke control measures etc. of stairs, corridors, exits and other building elements are directly specified without giving sufficient explanation on the objectives. However, to make an evacuation plan of a building more effective in terms of performance and cost, designers have to have clear strategies on how to evacuate the building occupants in the event of fire and evacuation routes should be designed based on the strategies. The intention of this item is to require that the designer of a building has to frame up an evacuation plan which is realistic in the light of type of occupancy, staff organization, fire detection and alarm system and other concerning conditions of the building prior to the design of the evacuation safety measures.

2.3. Security of Refuge

Final refuge of occupants in the event of fire has been traditionally considered to be public ways or some sites of equivalent nature. Since in such a place as a public way, people can get away freely whenever dangers due to fire becomes imminent, public ways and such will continue to remain as the refuges for most of the building in future as well. However, in case of buildings from which occupants cannot be evacuated in reasonable time for some reasons, such as high-rise buildings and hospitals, there may be some cases where it is more rational to secure a refuge within the building or protect some parts of the building so as to be practically used as refuges in the event of fire.

When a refuge is designed within a building or a site which is not connected with public ways, the safety from various potential dangers due to fire has to be carefully considered. The potential causes of danger for evacuees include smoke, heat, air contamination, structural collapse and so on, as are shown in Fig. 3, so safety standards need to be considered on each of them.

(1) Public ways and equivalent spaces

When a public way or such is taken as the refuge as is usual, virtually no check is required for the safety.

(2) Refuges on sites isolated from public ways

Although considered to be rare, refuges may have to be planned on building sites which has no outlet to public ways in conjunction with the evacuation routes within the building. This type of refuges need checks for the safety against certain potential dangers.

(3) Refuges within buildings

We have little experience regarding refuges within buildings, yet sometimes it is thought to be more reasonable to secure refuges within buildings rather than to forcedly try to evacuate all the occupants out of a building. When refuges are planned within buildings, however, sufficient level of safety has to be secured for every conceivable hazards due to fire, which may attack refuges through open air as well as through inside spaces.

2.4. Security of Safety of Evacuation Routes

It seems that evacuation safety means nothing but evacuation routes in The Building Standard Law. Most of its standards concerning evacuation safety primarily concern dimensions, materials, fire resistant rating and smoke control measures of the parts of building which may play a role as evacuation routes in the event of fire. When we consider technical standards for safety of evacuation based on performance, we have to analyze the potential dangers associated with evacuation. As can be seen in Fig. 4, obstruction on evacuation routes plays a key role in endangering evacuation safety as well as the direct hazards such as smoke and heat.

The evacuation routes in a building are classified into the three for clarity in design, that is, evacuation routes in the room of origin, those on the floor of origin, and those on the floors of non origin.

3. Standard Fire Conditions

The standard fire conditions summarized in Table 3 correspond to the design load standards in structural design and consist of fire conditions, occupants conditions, fire scenarios, and other conditions affecting the evacuation safety. A building which is designed according to Fire Safety Design Method needs to satisfy the safety standards for evacuation safety under these standard fire conditions. It should be kept in mind, however, that the satisfaction of the safety standards does not necessarily mean to guarantee sufficient level of safety but only secure a reasonable level of safety.

CONCLUDING REMARKS

The design method for evacuation safety incorporating performance based technical standards for evacuation safety of buildings have been drafted. They are given in terms of the safety standards and the standard fire conditions. Basically, any design can be accepted as long as the safety standards are satisfied under the standard fire conditions so that evacuation safety measures can be rationalized in terms both of safety performance itself and cost. Various prediction techniques for fire behavior and evacuation will play important roles to operate the method.

A lot of excellent findings and engineering techniques do exist in fire research area but there is little room to accommodate those in specification standards. It is important to establish a performance standards for fire safety so that those valuable results of researches can readily be transferred to the world of practice.

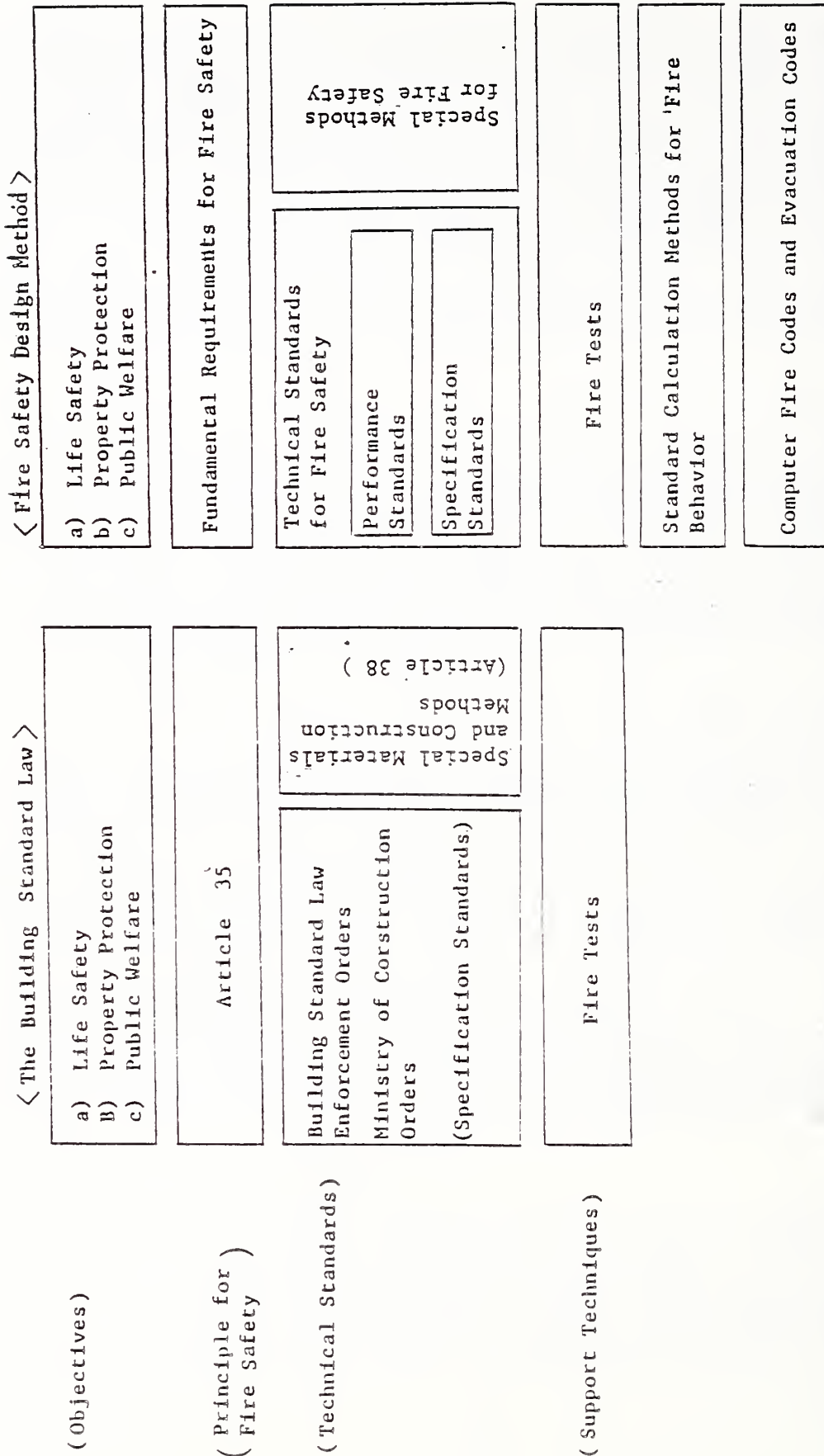


Fig. 1 Relationship Between The Building Standard Law and Fire Safety Design Method of Building

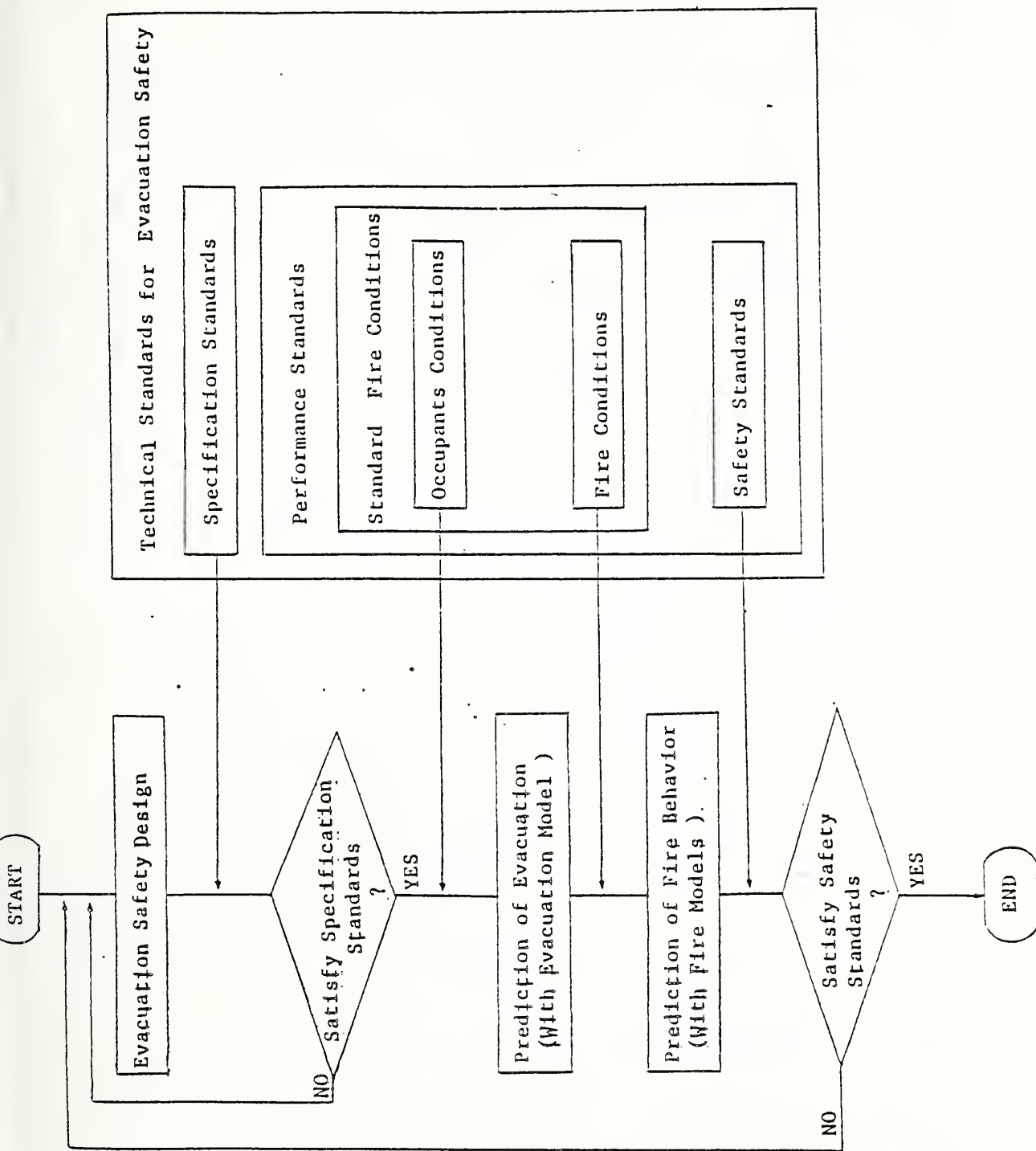


Fig. 2 Conceptual Relationship Between Evacuation Safety Design and Technical Standards for Evacuation Safety

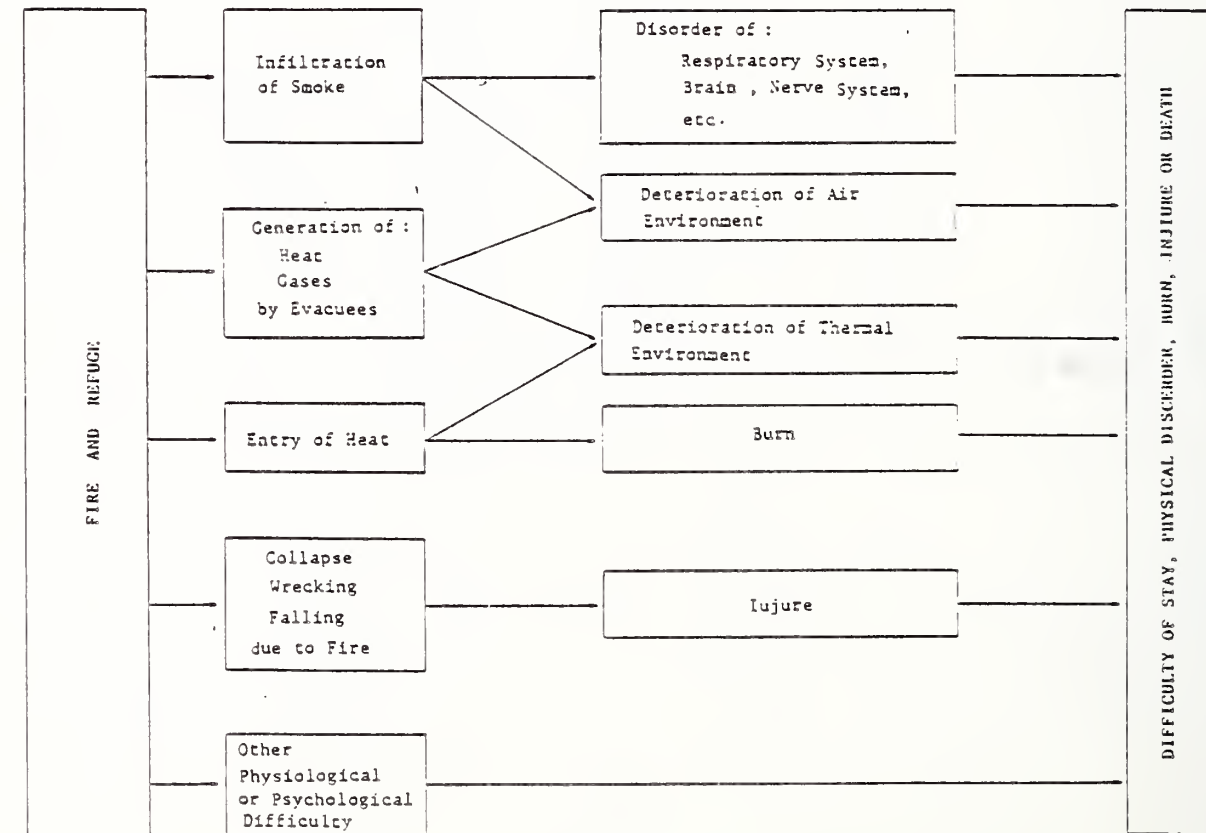


Fig. 3 Fire Hazards in Refuges

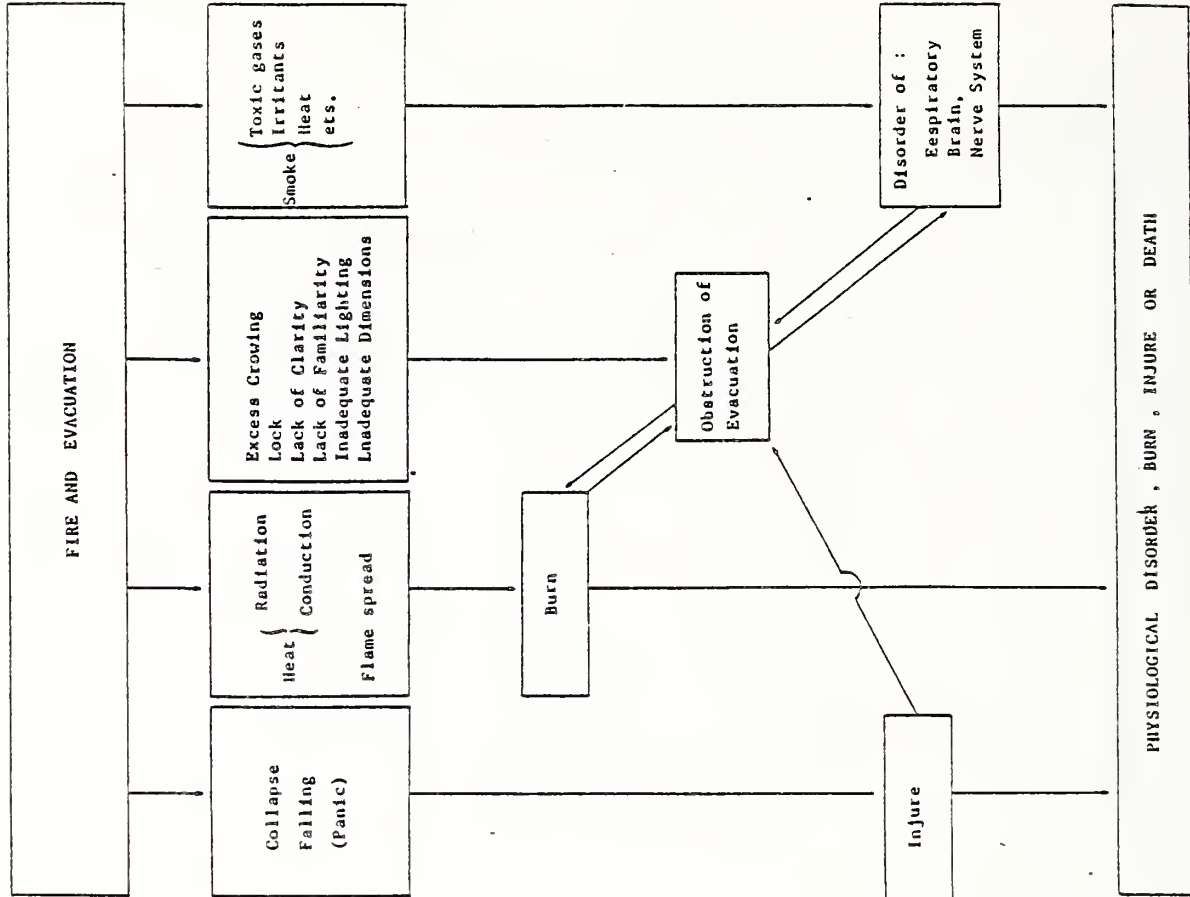


Fig. 4 Fire Hazards in Evacuation Routes

Table 1. Fundamental Requirements for Fire Safety of Buildings

I. REQUIREMENTS AS AN INDIVIDUAL BUILDING

1. Prevention of Occurrence and Rapid Propagation of Fire
2. Security of Evacuation Safety
 - 2.1. Restriction of use of building materials excessively hazardous to evacuees
 - 2.2. Adequacy of evacuation plan
 - 2.3. Security of safety of refuges
 - 2.4. Security of evacuation routes
3. Prevention of Serious Social Troubles
 - 3.1. Prevention of fire spread to others' space
 - 3.2. Prevention of collapse or damage of building which causes serious troubles of others or public
4. Security of Fire Fighting Activities
 - 4.1. Restriction of use of building materials excessively hazardous to fire fighting activities
 - 4.2. Security of activities for searching and rescuing occupants
 - 4.3. Security of activities for extinguishing fire

II. REQUIREMENTS FOR CITY FIRE PREVENTION

1. Buildings in Fire Protection Districts
 2. Buildings in Quasi-fire Protection Districts
-

Table 2. Technical standards for Evacuation Safety of Buildings

Contents of Safety to be Examined	Standards for Evacuation Safety	Symbols and Descriptions
<p>I. RESTRICTION OF USE OF BUILDING MATERIALS EXCESSIVELY HAZARDOUS TO EVACUEES</p>	<p>(by relevant toxicity test method to be developed)</p>	
<p>II. ADEQUACY OF EVACUATION PLAN</p>		
<p>III. SECURITY OF SAFETY OF REFUGES</p>	<p>(no check for safety required)</p>	
<p>1. <u>Public Ways And Equivalent Spaces</u></p>	<p>$q_{max} < 1$ (kW/m²)</p>	<p>q_{max} : maximum radiation flux to refuge (kW/m²)</p>
<p>2. <u>Refuges On Sites Isolated From Public Ways</u></p>	<p>$D > 12A^{2/5}$ (m)</p>	<p>D : horizontal distance of refuge from bldg (m)</p>
<p>2.1. Safety from Heat Radiation</p>	<p>$D > 2H$ (m)</p>	<p>A : horizontal section area of bldg (m²)</p>
<p>2.2. Safety from Smoke and Hot Gases</p>	<p>$D > 4.5 H$ (m)</p>	<p>H : horizontal distance of refuge from top of bldg (m)</p>
<p>2.3. Safety from Collapse of Building</p>	<p>$a > 2$ (m²)</p>	<p>H : vertical distance of refuge from top of bldg (m)</p>
<p>2.4. Safety from Falling Objects</p>		<p>D : horizontal distance of refuge from potential falling source (m)</p>
<p>2.5. Area of Refuges</p>		<p>H : vertical distance of refuge from potential falling source (m)</p>
<p>2.6. Prohibition of Obstruction of Fire Fighting</p>		<p>a : effective area of refuge per person (m²/person)</p>
<p>2.7. Safety from Fire Flakes and Others</p>		
<p>3. <u>Refuges Within Buildings</u></p>	<p>Any of the followings:</p>	
<p>3.1. Safety from Smoke</p>	<p>1) Refuge is out of reach of smoke from exterior openings</p>	
<p>3.1.1. Safety from smoke thru open space</p>	<p>11) Prevention of smoke infiltration by either means of the followings: a) Air tight exterior wall</p>	<p>V : volume of refuge (m³)</p>
	<p>$\frac{aA}{V} < 1.0 \times 10^{-5} \frac{1}{\Delta P}$</p>	

3.1.2. Safety from smoke thru inside space

b) Pressurization of refuge

$$60 - P < 6.0 \times 10^{-12} \left(\frac{V}{\alpha A} \right)^2$$

iii) Dilution of smoke

$$C < (1/200)C_0$$

Any of the followings:

- i) Releasing smoke to open air at a certain part of flow passage
- ii) Blockage of smoke flow by any means of the followings:
 - a) Air tight partition

$$\frac{\alpha A}{V} < 1.0 \times 10^{-6} \frac{1}{\sqrt{\Delta P}}$$

where $0 < (0 < \Delta P < \Delta P_{max})$

$$\Delta P_{max} = \begin{cases} H+30 & \text{(with top opening)} \\ H & \text{(without top opening)} \end{cases}$$

- b) Security of pressure difference at any system of partition

$$\Delta P > 1 \quad (\text{Pa})$$

- c) Prevention of smoke layer descend below openings on partition

$$s > h + 0.1(H - h) \quad (\text{m})$$

iii) Dilution of smoke

$$C < (1/200)C_0$$

3.2. Safety from Heat

3.2.1. Safety from heat thru open space

αA : area of leakage potentially exposed to smoke(m^2)
 ΔP : pressure difference(Pa)

V : volume of refuge(m^3)
 αA : area of leakage potentially exposed to smoke(m^2)
 P : relative pressure of refuge(Pa)

C : smoke concentration in refuge
 C_0 : smoke concentration in the room of origin

V : volume of refuge(m^3)
 αA : area of leakage on partition(m^2)

ΔP : pressure(Pa)

H : height of shaft(m)

ΔP : refuge side pressure relative to opposite(Pa)

s : smoke layer height of the space at fire side(m)
 h : height of opening or leakage on partition(m)
 H : average ceiling height of the space at fire side(m)

C : smoke concentration in refuge
 C_0 : smoke concentration in the room of origin

Table 2 cont'd(3)

<p>1) Safety from heat radiation</p> <p>ii) Safety from burn</p> <p>3.2.2. Safety from heat thru indoor space</p> <p>i) Safety from heat radiation</p> <p>ii) Safety from burn</p> <p>3.3. Security of Internal Environment</p> <p>1) Security of air cleanness</p> <p>ii) Security of thermal environment</p> <p>3.4. Structural Safety</p> <p>3.5. Escape Means in Emergency and after Fire</p> <p>3.6. Area of Refuge</p> <p>3.7. Freedom From Other Excessive Difficulties</p>	<p>$q_{max} < 1$ (kW/m²)</p> <p>$T_1 < 10$ (K)</p> <p>$q_{max} < 1$ (kW/m²)</p> <p>$T_1 < 10$ (K)</p> <p>$C_2 < 2$ (%)</p> <p>Either of the followings:</p> <p>i) Fire resistant structure in compliance with Bldg Stnd Law</p> <p>ii) Satisfy the standards for structural integrity</p> <p>$a > 1$ (m²/person)</p>	<p>q_{max} : maximum heat radiation flux to evacuee(kW/m²)</p> <p>T_1 : temperature rise of interior surface of refuge(K)</p> <p>q_{max} : maximum heat radiation flux to evacuee(kW/m²)</p> <p>T_1 : temperature rise of interior surface of refuge(K)</p> <p>C_2 : concentration of carbon dioxide(%)</p> <p>ΔT : temperature rise in refuge(K)</p> <p>t_s : period of stay in refuge(sec)</p> <p>a : effective area of refuge per person(m²/person)</p>
<p>IV. SECURITY OF EVACUATION ROUTES</p> <p>1. Evacuation Routes In The Room Of Origin</p> <p>1.1. Safety from Smoke</p>	<p>Either of the followings:</p> <p>1) Prevention of smoke layer descend to evacuees</p> <p>$s > 1.6 + 0.1H$ (m)</p>	<p>s : smoke layer height(m)</p> <p>H : average ceiling height of the room of origin(m)</p>

ii) Passing thru smoke

$$\int_0^{t_e} (\Delta T)^2 dt < 4.0 \times 10^3$$

$$\int_0^{t_e} (r - 2)^2 dt < 10$$

$$Q_b < 25V \quad (kJ)$$

$$P_{max} < 120 \quad (\text{person/m})$$

(specification)

(specification)

(specification)

Any of the followings:

i) Releasing smoke to open air at a certain part of flow passage

ii) Blocking of smoke flow by any means of the followings:

a) Air tight smoke partition

$$\frac{\alpha A}{V} < 4.0 \times 10^{-6} \frac{1}{\sqrt{\Delta P}}$$

where $(0 < \Delta P < \Delta P_{max})$

$$\Delta P = H$$

b) Security of pressure difference

$$\Delta P > 1 \quad (Pa)$$

c) Prevention of smoke layer descend below opening on partition

1.2. Safety from Heat

1.3. Prevention of Hazardous Burning of Interior Linings

1.4. Safety from Falling Objects

1.5. Prohibition of Excessive Crowdings

1.6. Clarity of Evacuation Routes

1.7. No Obstruction on Evacuation Routes

1.8. Adequate Dimensions of Routes

2. Evacuation Routes On The Floor Of Origin

2.1. Safety from Smoke

ΔT : temperature rise of smoke layer(K)

t : time(sec)

t_e : time trapped in smoke(sec)

r : heat radiation flux to evacuees(kW/m²)

t : time(sec)

t_e : evacuation time(sec)

Q_b : heat release during the period of evacuation due to the burning of interior₃ linings(kJ)

V : volume of the room of origin(m³)

P_{max} : maximum number of crowdings at exits per unit width(person/m)

V : volume of refuge(m³)

αA : area of leakage(m²)

ΔP : pressure(Pa)

H : height of vertical shaft(m)

ΔP : pressure of the space at the side of evacuation route relative to the opposite(Pa)

s : smoke layer height of the space at fire side(m)

	<p>s > h + 0.1(H-h) (m)</p>	<p>h : height of opening or leakage on partition(m) H : average ceiling height of the space at fire side(m)</p>
<p>111) Prevention of smoke layer descend to evacuees</p>	<p>s > 1.6 + 0.1H (m)</p>	<p>s : smoke layer height(m) H : average ceiling height of the evacuation route(m)</p>
<p>1iv) Passing thru smoke</p>	$\int_0^{t_e} (\Delta T)^2 dt < 4.0 \times 10^3$	<p>ΔT : temperature rise of smoke(K) t_e : time trapped in smoke(sec)</p>
<p>v) Dilution of smoke</p>	<p>C < (1/200)C₀</p>	<p>C : smoke concentration in a route C₀ : smoke concentration in the room of origin</p>
<p>2.2. Safety from Heat</p>	$\int_0^{t_e} (r - 2)^2 dt < 10$	<p>r : heat radiation flux to evacuees(kW/m²) t_e : evacuation time(sec) t_f : time(sec)</p>
<p>2.3. Prevention of Hazardous Burning of Interior Linings</p>	<p>Q_b < 25V (kJ)</p>	<p>V : volume of the evacuation routes(m³) Q_b : heat release during the period of evacuation due to the burning of interior linings(kJ)</p>
<p>2.4. Safety from Opening Jet from the Room of Origin</p>	<p>No check required except for very unusual structures</p>	
<p>2.5. Structural Safety</p>	<p>P_{max} < 120 (person/m)</p>	<p>P_{max} : maximum number of crowding exits or like(person/m)</p>
<p>2.6. Safety from Falling Objects</p>	<p>(specification)</p>	
<p>2.7. Prevention of Excessive Crowding</p>	<p>(specification)</p>	
<p>2.8. Clarity of Evacuation Routes</p>	<p>(specification)</p>	
<p>2.9. No Obstruction on Evacuation Routes</p>	<p>(specification)</p>	
<p>2.10. Adequate Dimensions of Routes</p>		

3. Evacuation Routes On The Floors Of Non-Origin

3.1. Safety from Smoke

3.1.1. Safety from smoke thru open space

Any of the followings:

- i) Evacuation route is out of reach of smoke from exterior openings
- ii) Prevention of smoke infiltration by either means of the followings:
 - a) Air tight exterior walls

$$\frac{\alpha A}{V} < 8.0 \times 10^{-3} \frac{1}{t_e / \Delta P} \quad (0 < \Delta P < 60)$$

b) Pressurization of route

$$60 - P < 6.0 \times 10^{-5} \left(\frac{V}{\alpha A} \right)^2 \frac{1}{t_e^2}$$

iii) Dilution of smoke

$$C < (1/200) C_o$$

iv) Passing thru smoke

$$\int_0^{t_e} (\Delta T)^2 dt < 4.0 \times 10^3$$

v) Other effective means

3.1.2. Safety from smoke thru indoor space

Any of the followings:

- i) Releasing smoke to open air at a certain part of flow passage
- ii) Blockage of smoke by any means of the followings:
 - a) Air tight partition

$$\frac{\alpha A}{V} < 8.0 \times 10^{-3} \frac{1}{t_e / \Delta P}$$

where $0 < \Delta P < \Delta P_{max}$
 $\Delta P_{max} = H$

b) Security of pressure difference

$$\Delta P > I \quad (Pa)$$

V : volume of evacuation routes(m³)
 αA : area of leakage exposed to smoke(m²)
 t_e : evacuation time(sec)

ΔP : pressure of route relative to outdoor(Pa)

C : smoke concentration in the evacuation route
 C_o : smoke concentration in the room of origin

ΔT : temperature rise of smoke contaminated part(K)
 t_e : time to pass thru smoke(sec)

V : volume of evacuation route(m³)
 αA : area of leakage on partition(m²)
 ΔP : pressure(Pa)
 t_e : evacuation time(sec)

H : height of vertical shaft(m)

ΔP : pressure of route relative to fire side(Pa)

Table 2 cont'd(7)

<p>c) Prevention of smoke layer descend below openings on partition</p> <p>$s > h + 0.1(H - h)$ (m)</p> <p>iii) Prevention of smoke descend to evacuees</p> <p>$s > 1.6 + 0.1H$ (m)</p> <p>iv) Passing thru smoke</p>	<p>s : smoke layer height of the space at fire side(m) h : height of opening or leakage on partition(m) H : average ceiling height of the space at fire side(m)</p> <p>s : smoke layer height in the route(m) H : average ceiling height of the route(m)</p>
<p>3.2. Safety from heat</p>	<p>ΔT : temperature rise of smoke contaminated space(K) t : time(sec) t_e : time to pass thru smoke(sec)</p>
<p>3.3. Structural Safety</p>	<p>r : heat radiation flux to evacuees(kW/m²) t : evacuation time(sec) t_e : time(sec)</p>
<p>3.5. Safety from Falling Objects</p>	<p>Any of the followings:</p> <p>i) Fire resistant structure in compliance with Bldg Stnd Law</p> <p>ii) Satisfy standards for structural integrity</p> <p>iii) Other effective means for structural safety</p>
<p>3.6. Clarity of Evacuation Routes</p>	<p>(specification)</p>
<p>3.7. No Obstruction on Evacuation Routes</p>	<p>(specification)</p>
<p>3.8. Adequate Dimensions of Routes</p>	<p>(specification)</p>

Table 3. Abstract of Standard fire Conditions for the Safety of Refuges and Evacuation Routes

Space of Origin	Scale of fire	Radiation source	Evacuees' condition
1. PUBLIC WAYS	N/A	N/A	N/A
2. REFUGES ISOLATED FROM PUBLIC WAYS	<p>1) Area of fire(*1) The area within which a fire can be limited by effective fire walls or fire compartments</p> <p>ii) Condition of fire(*2) Fully developed fire regardless of sprinkler systems</p>	<p>i) Fire resistant bldg. a) width(m): window width b) height(m): 2xwindow height c) radiation intensity: 100 (kW/m²)</p> <p>ii) Wooden house a) width(m): width of house viewed from the refuge b) height(m): h $h = -A^{1/2} + 4.5A^{2/5}$ where A : projected area of house(m²)</p>	<p>i) Number of evacuees The number determined by the evacuation plan</p>
3. REFUGES WITHIN BUILDINGS			<p>ii) Generation of heat & gases a) heat: 400 (kW/person) b) CO₂: 0.02 (m³/h/person)</p>
1. EVACUATION ROUTES IN THE ROOM OF ORIGIN	<p>Heat release rate and area of fire source</p> <p>i) unsprinklered spaces specified according to type of space</p> <p>ii) sprinklered spaces the smaller of: a) fire source specified by i) b) maximum fire which is unable to activate the sprinkler heads</p>		<p>i) Number of evacuees: specified according to type of spaces</p> <p>ii) evacuation ability: specified according to type of spaces and occupants</p> <p>iii) evacuation start time specified according to type of building and fire and alarming system</p>
2. EVACUATION ROUTES ON THE FLOOR OF ORIGIN	<p>All spaces which do not meet any of the followings: a) No occupant who needs to escape exist when a fire occurs in the space b) Possibility of fire occurrence is negligible c) Safer than a space on which safety standards are already satisfied</p>		
3. EVACUATION ROUTES ON THE FLOORS OF NON-ORIGIN	<p>All spaces which do not meet any of the followings: a) No occupant who needs to escape exist when a fire occurs in the space b) Possibility of fire occurrence is negligible c) Safer than a space on which safety standards are already satisfied</p>		

BASIC STRUCTURE OF THE EVACUATION SAFETY DESIGN METHOD
T. Tanaka, Building Research Institute, Japan

JIN: The report which Dr. Tanaka presented was the cumulative result of five years of research by the entire staff of the concerned people in the Construction Ministry, and for him to have condensed it into the very short time slot that was allotted to him is a tremendous feat in itself.

HALL: I have two quick questions. Were the performance standards developed using a group larger than fire scientists and other effected parties? The second question, is the large number of independent standards an important aspect in making the overall method conservative for regulation?

JIN: We in the Construction Ministry refer to this as the Overall Technology Development Program. This program, which was explained, took five years. The Construction Ministry worked in very close cooperation with both government, private, and university people. I can't recall exactly how many subgroups there were, but I believe there were more than 10 independent groups composed of people from government, private and university levels. I do not believe that we have arrived at a conservative standard.

Basically, what these standards call for is the establishment of minimum safety requirements that are built into the materials themselves. Rather than higher standards which provide the possibility of constructing better and higher buildings at the same cost, which may be possible under this system, that was not the major objective of our project. Our project was to call on the expertise of the people involved with fire standards. As is the case in the existing structural safety laws, which uses the same method in determining their standards, the same materials may be used which would result in either a good building or a bad building. This is the expertise of the constructor. All we're seeking in this regulatory situation is to provide a law which would mandate a minimum safety requirement within each material this is used.

QUINTIERE: Since this is the work of many people, is there some documentation upon which this work was established? How were the criteria established, by underlying physics or just judgment?

JIN: At the present time there is no information broken down to that extent. However, as I explained, this is the culmination of a 5-year program, and we hope to have a full report published by the year end which should contain the information you're seeking.

QUINTIERE: I must have missed it.

JIN: You did not miss it, I purposely did not refer to it. As you probably are aware, Japan, the United States and Canada are currently engaged in a joint study on toxicity, and I had hoped to have a chance to refer to that before I made any conclusive statements. Actually in terms of technical standards themselves, there are certain portions which are really not conclusive as yet.

Fire Risk Evaluation Method for Multi-occupancy Building

— A Report of Five Year Research Project —
conducted by Fire Defence Agency

by

Ai SEKIZAWA

and

Tadahisa JIN

Fire Research Institute

Fire Defence Agency

Ministry of Home Affairs

1. Introduction

This report intends to present a summary of the results of five year research project for developing a "Fire Risk Evaluation Method for Multi-occupancy Building" sponsored by Fire Defence Agency, Ministry of Home Affairs. This research work was performed by the technical committee organized by Fire Defence Agency, and ended in 1986 fiscal year.

The main purpose of this project was to provide a practical, manageable and concise method for building fire safety evaluation, which will be mainly used by fire officials in fire inspection.

Therefore, the scheme and selected factors for estimating fire risk and evacuation performance in this method are focussed on those items that address substantial fire protection measures such as sprinklers, fire alarm system, fire walls/doors, compartmentation and so forth.

Additionally, this method is actually more like a scoring system than a scientifically-based risk prediction model, and also this method is designed by using many assumptions and expert judgments. In this sense, this method will need further verification and improvement, based on a lot of case studies. But, still we consider this method to be useful as a practical tool for fire inspection and also for self-diagnosis of building fire safety by building owners.

2. Framework of the Fire Risk Evaluation Method

The framework of the Fire risk evaluation method is shown in Fig.1 on page 2. One of the significant features of our method is to evaluate each floor's fire risk independently, because each floor in a multi-occupancy building should have different potential fire risk corresponding to its variety of occupancy, occupant load/characteristics, building configuration and features of fire protection measures etc.

Also, the fire risk of a whole building can be estimated, using each floor's fire risk and an additional modification coefficient in terms of vertical fire spread risk both inside and outside of the building.

The other important feature of this method is that the evaluation system is composed of two major subsystems ; the evaluation method of potential fire risk and the evaluation method of evacuation performance, as shown in Fig.1 .

The meaning of the former one is actually the estimate of potential property damage, which we call simply potential fire risk hereafter in this report. The final estimate of each of potential fire risk and evacuation performance is expressed by using grading scores corresponding to the numerical estimation results which are derived from each evaluation method described later.

In this report, we omitted the explanation about the treatment of such factors as vertical fire spread risk, fire fighters' activity and fire prevention management which are used for modifying the final estimate, simply owing to limited space. But, we think it will not affect a readers' understanding of this outline of our fire risk evaluation method.

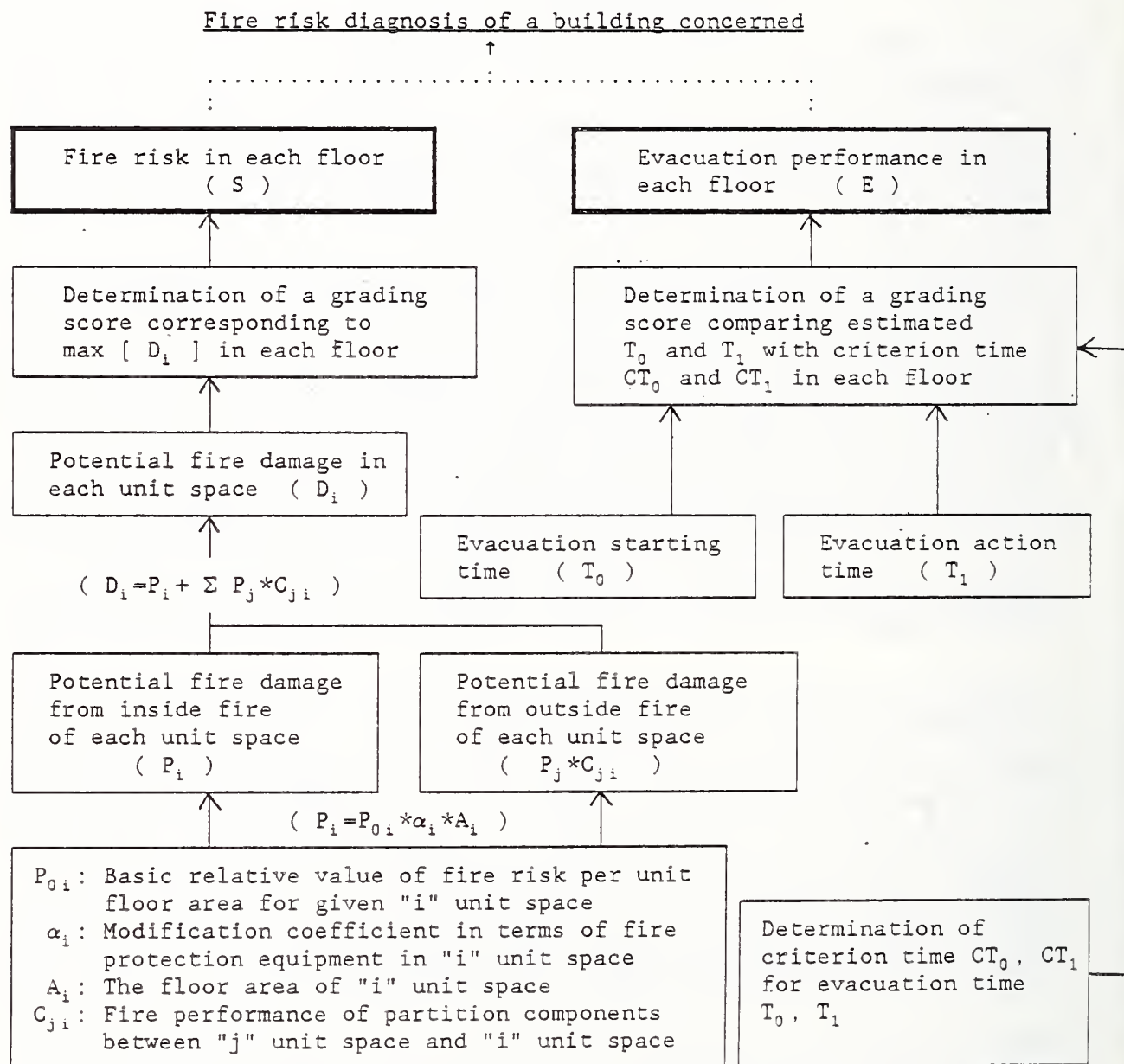


Fig. 1 Framework of "Fire Risk Evaluation Method"

3. Evaluation Method of Potential Fire Risk in Each Floor (S)

3.1 Basic idea

Potential fire risk in each floor (S) is evaluated by considering potential relative damage of fire in unit spaces, which a floor can be divided into. The basic premises in the estimation process of potential fire risk are as follows ;

- 1) Each floor in a building is considered to be an aggregation of such unit spaces as defined later. Each unit space could have different occupancy or use and also different size of floor area.
- 2) The potential fire damage in an unit space (D) is estimated by the sum of the relative damage caused by a fire inside the unit space itself and the relative damage suffering from adjoining unit spaces. So, such two factors as the potential possibility of fire outbreak / fire spread in each unit space, and the fire performance of partition components between adjoining unit spaces are the main bases for estimation of potential fire damage (D).
- 3) Potential fire risk in a floor (S) is represented by a grading score corresponding to $\max[D_i]$ in that floor.
- 4) Potential fire risk decreases in proportion to the number of compartments in the floor, if the size of floor area is held constant. Because compartmentation should work for limiting the spread of fire, and also potential fire damage in an unit space should be smaller as the size of unit space decreases.

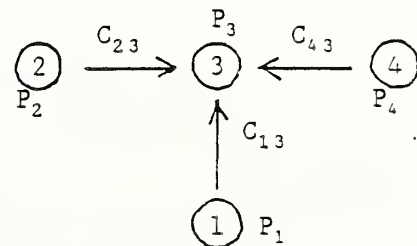
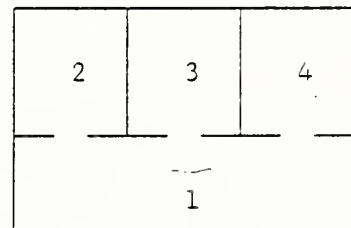
3.2 Estimation method of potential fire damage in each unit space (D)

Potential fire damage in each unit space (D_i) consists of roughly two components such as the relative damage caused by a fire inside itself and the relative damage suffering from the fire spread beyond adjoining unit spaces. In the illustration of a simple floor plan, the fire damage of #3 unit space (D_3) for example is considered to be the sum of following fire damages as ;

$$D_3 = P_3 + P_2 * C_{23} + P_1 * C_{13} + P_4 * C_{43} \dots\dots\dots [3-1]$$

where generally ;

- P_i : Relative fire damage in case that a fire occurs inside "i" unit space.
- C_{j_i} : Fire performance of partition components between "j" unit space and "i" unit space
- $P_j * C_{j_i}$: Relative fire damage of "i" unit space suffering from the fire spread beyond adjoining "j" unit space when a fire starts in "j" unit space.

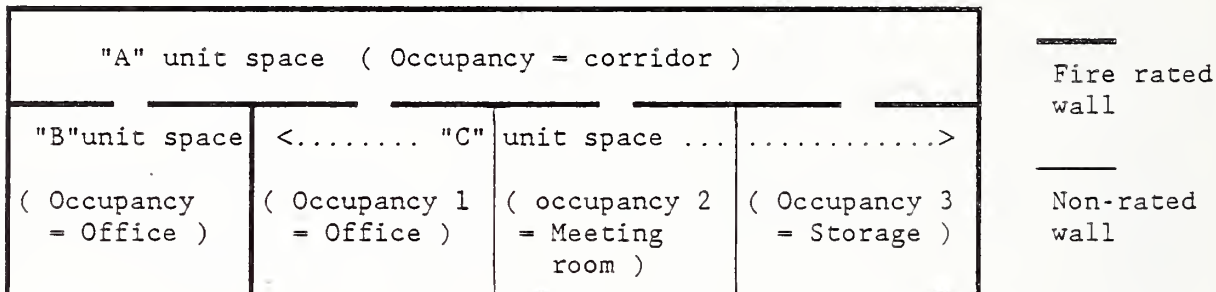


(Network)

3.3 Relative fire damage in unit space (P)

3.3.1 Definition of unit space

Unit space is basically a compartment room or space enclosed with fire rated walls and fire rated doors. Usually, each unit space has its own occupancy. However, in case that some adjoining rooms are divided with non-rated walls and openings which do not work for limiting fire spread between those rooms, we should consider a series of those rooms as a single unit space which might have several different occupancies. (See the explanatory illustration below)



3.3.2 Estimation method of relative fire damage in unit space

Relative fire damage in unit space (P_i) is estimated by using following expression [3-2].

In this expression, " P_{0ik} " is the most important basis for estimation which stands for the potential relative fire risk per unit floor area in terms of both outbreak and internal spread of fire in each occupancy space (k) of each unit space (i). This value was determined by expert judgment based on fire statistics data. (See Tab.1 on page 6)

" α_{ik} " is a modification coefficient for " P_{0ik} ", which reflects the condition of fire protection measures in each occupancy space (k) of each unit space (i). " α " works to reduce the value of " P_0 " according to the condition of fire protection equipment in case that the unit/occupancy space concerned is installed with automatic sprinklers, automatic alarm system, or wall hydrant. The value of " α " is also given by expert judgment. (See Tab.2 on page 7)

$$P_i = \sum_{k=1}^n (P_{0ik} * \alpha_{ik} * A_{ik}) \dots\dots\dots [3-2]$$

where ;

- n : The number of occupancies involved in "i" unit space
- P_{0ik} : Basic relative value of fire risk per unit floor area for given "k" occupancy in "i" unit space (/m²)
- α_{ik} : Modification coefficient in terms of fire protection equipment for "k" occupancy space in "i" unit space
- A_{ik} : The floor area of "k" occupancy space in "i" unit space (m²)

3.4 Fire performance of partition components between unit spaces (C)

Fire performance of partition components ($C_{j,i}$) stands for the relative intensity of impact by the fire spread from "j" unit space to "i" unit space; that is, the fire performance of walls and/or doors connecting unit spaces in terms of potential fire spread risk. (See Tab.3 on page 7)

In some case, " $C_{j,i}$ " is not equivalent to " $C_{i,j}$ " because there are such walls that have non-combustible finish on one side and combustible finish on the other side.

"C" does not mean the substantial fire performance of partition components, but means the relative index of it. The fire performance of partition components between a couple of particular unit spaces is represented by the maximum value (the value of the weakest part) among those "C" of walls and/or doors between these two unit spaces.

The value of "C" shown in Tab.3 was determined by expert judgment.

3.5 Determination of potential fire risk in each floor

As described before, potential fire damage in each unit space (D) is evaluated by using "P" and "C" in the expression [3-1]. Therefore, in each floor, there are the same number of "D"s as the number of unit spaces which the floor is divided into. Among those " D_i " ($i=1,2,\dots,n$), the $\max[D_i]$ is adopted for the representative estimate score [S] of potential fire risk in the floor concerned.

The grading score of "S" is given a value of "1" through "10", using the table below which shows the corresponding score for the range of "D". The lower score indicates a safer case.

Range of D_i	Corresponding grading score (S)
0 -- 30	1
31 -- 60	2
61 -- 90	3
91 -- 140	4
141 -- 190	5
191 -- 240	6
241 -- 310	7
311 -- 380	8
381 -- 450	9
451 --	10

Tab. 1 Basic relative value of fire risk by occupancy of an unit/occupancy space in multi-occupancy building (P₀)

Relative value of fire risk	Occupancy / Use of an unit space in a building
↑ 1.00	←• Industrial occupancies treating fires, and/or hazardous materials such as laboratory, boiler room etc.
0.90	←• Parking garage
0.85	←• Kitchen in restaurants
Higher 0.75	←• Stores in the presence of sizable fire load such as clothes store, book store etc.
0.70	←• Office room in the presence of sizable fire load
0.65	←• Residential unit
0.60	←• Stores well arranged and/or not in the presence of sizable fire load
Lower 0.55	←• School room, Guest seat space of theater, playhouse etc.
0.50	←• Sick room / consulting room in health care occupancy
0.40	←• Office room well arranged and/or not in the presence of sizable fire load
0.30	←• Bathroom etc.
↓ 0.10	←• Common use space such as corridors, rest room, entrance hall and elevator hall etc.

- *1 Relative fire risk values in this table were determined by expert judgment based on fire statistics. This value stands for the potential fire risk per unit floor area in terms of both outbreak and internal fire spread in an unit/occupancy space characterized by given particular occupancy/use.
- *2 Relative fire risk value in this table is denoted only for typical conditions of main occupancies. Therefore, for other occupancies or uses, the relative value needs to be determined by comparing its actual conditions with those of main occupancies shown in the table.

Tab. 2 Modification coefficient in terms of fire protection equipments installed in an unit/occupancy space (α)

Modification coefficient (α)	The condition of fire protection equipment installed in an unit/occupancy space (*1)
1.0	←• With no sprinklers
0.5	←• With sprinklers not so well maintained (*2)
0.1	←• With sprinklers well maintained
1.0	←• With neither automatic alarm nor wall hydrant
0.8	←• With automatic alarm but no wall hydrant
0.6	←• With both automatic alarm and wall hydrant

*1 As for determination of " α " in a particular unit/occupancy space, the minimum value of " α " is adopted among those categories that come under the particular condition of fire protection equipments installed in the unit/occupancy space concerned.

*2 If there is some obstruction of water discharge and/or the presence of non-covered area by sprinklers, it is considered the case as not so well maintained.

Tab. 3 Relative value of fire performance of partition components in terms of fire spread risk beyond an unit space (C)

Fire performance of partition components	C
Walls ;	
1. Fire resistant wall ranked as "A" (1 hour or more)	0.0
2. Fire resistant wall ranked as "B" (30 min. - 1 hour)	0.3
3. Fire retardant wall ranked as "A" (Non-combustible materials in both backing and finish)	0.6
4. Fire retardant wall ranked as "B" (Non-combustible materials only in finish)	0.8
Doors ;	
1. Self-closing fire door ranked as "A"	0.1
2. Automatic closing fire door ranked as "A" (smoke & heat)	0.2
3. Elevator door	0.3
4. Self-closing fire door ranked as "B"	0.5
5. Automatic closing fire door ranked as "B" (smoke & heat)	0.6
6. Non-combustible door but not deemed as fire door	0.8

* Ranking definition of "A" and "B" in this table is derived from Building Standard Law in Japan.

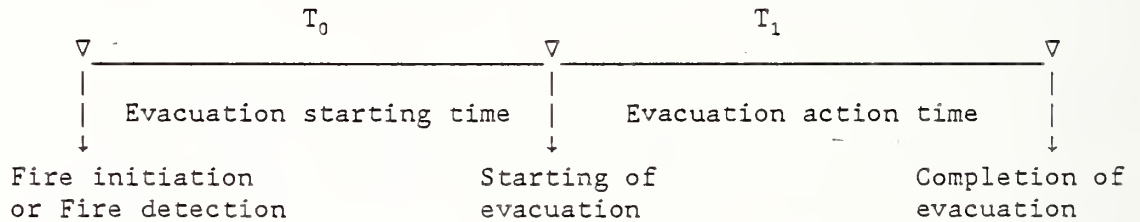
4. Evaluation Method of Evacuation Performance in Each Floor (E)

4.1 Basic idea

Evacuation performance in each floor concerned is evaluated by comparing the "time" needed for evacuation with the "criterion time" created in advance. Now, the "time" needed for evacuation can be divided into following two parts as ;

T_0 : Time needed to alert occupants and initiate their evacuation. This means the lapse of time from fire initiation or fire detection until starting evacuation of occupants. So, we call it " T_0 " or "evacuation starting time" hereafter. T_0 should be taken into account for an evacuation estimate, because in some fires a lot of fatalities are caused by delay in alerting occupants. T_0 is calculated in the slowest case and is used for the whole building concerned.

T_1 : Time needed for evacuation action itself. This means the lapse of time from starting evacuation of occupants on the floor concerned until completion by reaching a safe place. So, we call it " T_1 " or "evacuation action time" hereafter. And, T_1 is calculated in each floor..



For evaluation of evacuation performance, firstly we estimate T_0 and T_1 separately in each floor by using estimation methods mentioned later. Second, we make a grading score corresponding to evacuation performance of each floor, comparing T_0 and T_1 respectively with each criterion time which we call " CT_0 " and " CT_1 " hereafter.

The advantage of this method is that we can diagnose where the problem is in each floor, i.e., whether the problem exists in evacuation starting time or in evacuation action time. Also, we can estimate the sum of T_0 and T_1 .

4.2 Estimation method of "Evacuation starting time" (T_0)

Evacuation starting time (T_0) consists of the following four parts of the process for confirming a fire through alerting occupants about the fire as mentioned below. So, T_0 can be estimated by summing up T_{01} , T_{02} , T_{03} and T_{04} like an expression [4-1].

$$T_0 = T_{01} + T_{02} + T_{03} + T_{04} \dots\dots\dots [4-1]$$

(sec)

where ;

T_{01} : Time needed for detection of a fire incident. The length of this time depends on the condition of fire detection and alarm system in a building concerned. So, we adopted the appropriate value for T_{01} corresponding to that condition by expert judgement.

T_{02} : Time needed for confirmation of a fire. In the usual case, personnel who work at a security office in the building go to the origin of an incident and confirm it as a fire. T_{02} is estimated by calculating both the horizontal and vertical travel time from the security office room to the fire origin at the assumed furthest location.

T_{03} : Time needed to give evacuation directions to occupants from the security office. This is considered to depend on the condition of the emergency communication system like emergency telephone or speaker system in the building. The appropriate value is given for T_{03} corresponding to that condition by expert judgement.

T_{04} : Time needed for occupants to prepare for starting evacuation after they get notice of fire incident. The appropriate value is also given for T_{04} corresponding to the type of building by expert judgement, because characteristics of occupants are different by the type of building.

Each part of evacuation starting time above-mentioned is estimated as follows ;

- 1) T_{01}
 - * Fire detection and alarm system is fully equipped $T_{01} = 0$
 - * Else $T_{01} = 2\sqrt{A_0}$
- 2) T_{02}
 - * Emergency elevator is equipped $T_{02} = L_1/V_1 + (h/V_2 + 30) + 2*L_2/V_1$
 - * Else $T_{02} = L_1/V_1 + h/V_3 + 2*L_2/V_1$
- 3) T_{03}
 - * Equipped with both emergency telephone system and emergency speaker system $T_{03} = 30$
 - * Equipped with emergency speaker system only $T_{03} = 60$
 - * Equipped with emergency telephone system only $T_{03} = 90$
 - * Else $T_{03} = 120$
- 4) T_{04}
 - * If the building type is one of accommodation types like hotels, dormitories and etc. $T_{04} = 60$
 - * Else $T_{04} = 0$

Footnotes;

A_0	:	Floor area of the floor of fire origin (m^2)
L_1, L_2	:	Horizontal travel distance (m)
h	:	Height from the floor of security office to the floor of fire origin (m)
V_1	:	Horizontal rapid walk velocity (2.0 m/sec)
V_2	:	Velocity of emergency elevator (2.5 m/sec)
V_3	:	Vertical velocity of man (0.25 m/sec)

4.3 Estimation method of "Evacuation action time" (T_1)

Evacuation action time (T_1) in each floor is estimated by calculating the lapse of time needed for all occupants on the floor to reach a safe place. As for determination of a safe place, there are the following three cases according to the condition of fire stairs in the building concerned.

First, if the building has "special fire stairs"*¹ with smokeproof enclosure or outside fire stairs, the fire stairs can be deemed as a safe place. Second, if the building does not have such special fire stairs but has "simple fire stairs"*² with self-closing fire door or automatic closing fire door, a safe place is a street floor which means any floor level accessible from the street or from outside the building at ground level. Thirdly, if the building does not have any of such fire stairs as mentioned above, a safe place should be outside of a street floor. Therefore, estimation method of T_1 in each case is different according to the travel distance of evacuation as follows ;

- 1) The first case (The safe place is fire stairs on same floor)
 The most dominant part of horizontal evacuation to the fire stairs on the same floor is considered to be the time needed for all occupants to pass the exit which leads to the fire stairs. So, T_1 in each floor is calculated by using expression [4-2].

$$T_1 = N / (B * 1.5) \dots\dots\dots [4-2]$$

- 2) The second case (The safe place is a street floor)
 T_1 is estimated by the sum of the time needed for passing the exit to fire stairs described in the first case and the vertical travel time through fire stairs to reach a street floor. So, the calculation method of T_1 is expressed as follows.

$$T_1 = N / (B * 1.5) + H / V_3 \dots\dots\dots [4-3]$$

- 3) The third case (The safe place is outside of a street floor)
 In this case, horizontal travel time to reach outside of the building from fire stairs at the street floor, is added to T_1 in the second case.

$$T_1 = N / (B * 1.5) + H / V_3 + L_3 / V_4 \dots\dots\dots [4-4]$$

Footnotes;

- *1 : Fire stairs with an attached smokeproof enclosure enclosed in fire rated construction and with self-closing fire doors
- *2 : Fire stairs enclosed in fire rated construction and with self-closing or automatic closing fire door
- N : Occupant load on the floor concerned (# of persons)
- B : Total width of exits to fire stairs on the floor (m)
- 1.5 : Flow coefficient at exit (# of persons / m, sec)
- H : Height from a street floor to the floor concerned (m)
- L_3 : Horizontal travel distance from fire stairs at a street floor to outside of the building (m)
- V_4 : horizontal walk velocity (1.0 m/sec)

4.4 Estimation of evacuation performance in each floor

4.4.1 Criterion time for evacuation

Currently, there is neither a well-grounded data base nor standard methods for the determination of criterion time for evacuation.

However, in the current guide book for building fire safety design in Japan, there appear recommendations for the maximum allowable criterion time for all occupants on the floor to evacuate into fire stairs on the same floor level. This criterion time is now broadly used for building safety design in Japan, and is expressed by " $8\sqrt{A_i}$ " (A_i : floor area of "i" floor), which was given by expert judgment in an authorized committee.

But, this criterion time contains both "evacuation starting time" and "evacuation action time" in its meaning. Therefore, we decided to take the half of this criterion time length ($4\sqrt{A_i}$) for our criterion time of "evacuation action time" (CT_1), which is considered to depend on size of each floor area.

On the other hand, we should treat the criterion for "evacuation starting time" somewhat differently, because this criterion time does not seem to depend on size of each floor area, but should have a common standard time for all kinds of building. So, at present, we adopted 240 (sec) as the criterion of "evacuation starting time" (CT_0), which is supposed to be a standard value from the results of case studies.

4.4.2 Determination of grading score for evacuation performance estimate

The estimate of evacuation performance in each floor (E) is expressed by using grading score, which is "1" (the best rank) through "10" (the worst rank). This grading score is determined, based on T_0 , T_1 comparing with CT_0 , CT_1 .

In practice, we plot a point for each floor's estimate on the coordinate plane by using " T_0 value" on X axis and " T_1 value" on Y axis. And we make a grading score for each point by zoning on the coordinate plane with lines of criterion time and total time limitation of T_0 and T_1 as illustrated in Fig.2 on page 12.

By the way, in case that the sum of T_0 and T_1 is a little bit over the sum of CT_0 and CT_1 , we should think there is some problem for evacuation on the floor concerned. However, we consider this case is better than such a case that one of T_0 and T_1 is far over its criterion time, even though the sum of T_0 and T_1 does not exceed the sum of CT_0 and CT_1 . Therefore, we make a lower score as for the former case (score area "5" in Fig.2) than the latter case (score area "6" and "7" in Fig.2).

4.4.3 Modification in terms of the conditions of occupants and building

The estimate of evacuation performance (E) above-mentioned is determined, assuming usual occupants who will be capable of evacuation without assistance under the average conditions of the building configuration.

Therefore, if the characteristics of occupants and the building configuration in the floor concerned involves one or more of the following cases, the estimate should be modified by shifting up/down the grading score for each of

the corresponding cases, provided that the final modified score shall not be less than "1" and also not be more than "10".

- 1) 10%-30% of occupant load are considered to be incapable of self-movement in evacuation. (+ 1)
- 2) More than 30% of occupant load are considered to be incapable of self-movement in evacuation. (+ 2)
- 3) There is one or more obstruction(s) on a path of travel to an exit. (3 or more curvings / gap of floor level) (+ 1)
- 4) There is a dead-end hallway which is more than 20 m long. (+ 2)
- 5) There is a dead-end hallway which has an exterior balcony with a fixed ladder at the dead-end. (+ 1)
- 6) There is an exterior balcony with a fixed ladder accessible directly from main rooms. (- 1)
- 7) There is a continuous exterior balcony mostly all around the external walls. (- 2)

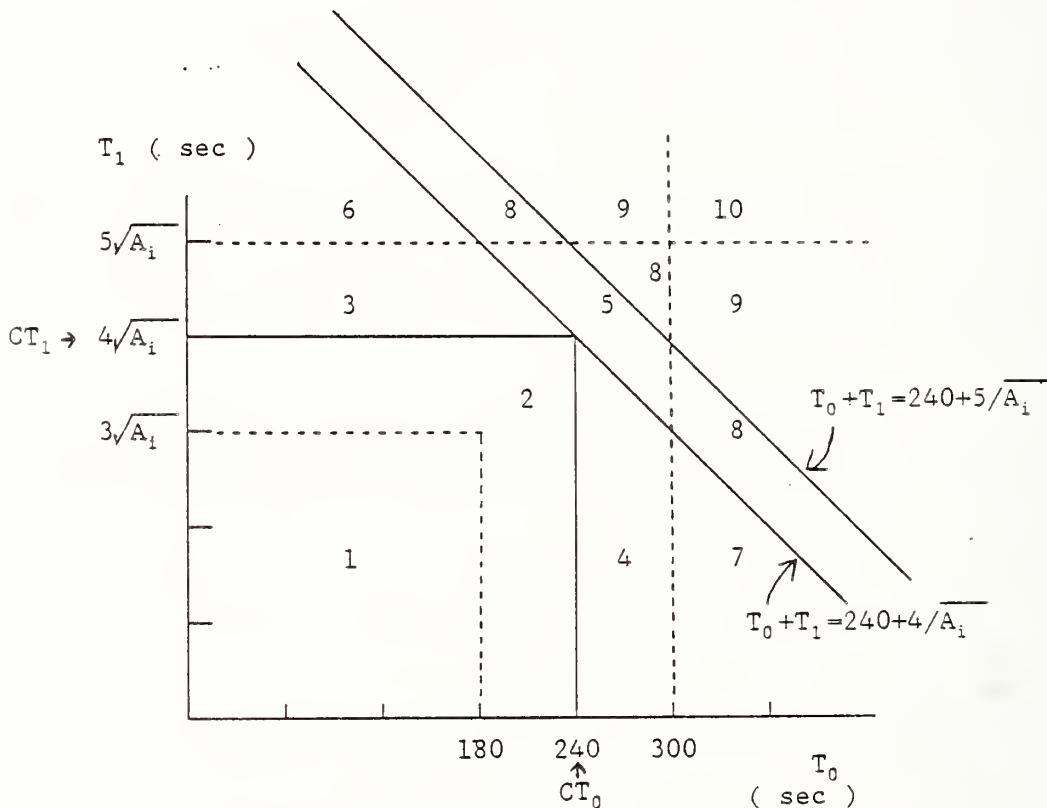


Fig. 2 Grading score of evacuation performance based on zoning by T_0 value and T_1 value

* A_i : Size of floor area of "i" floor (m^2)

FIRE RISK EVALUATION METHOD FOR MULTI-OCCUPANCY BUILDINGS

A. Sekizawa, Fire Research Institute, Japan

APOSTOLAKIS: There must be a lack of uncertainty calculated in these findings. Are you making any allowances?

SEKIZAWA: Well, I believe there are a lot of certainties in characterization. In regard to uncertainty, there are two points. One is the calculation itself does not reflect the real accuracy, and, secondly, there are many variations of the opinions. Therefore, different people may have different results. I can report to you that all 11 of the largest cities in Japan, under the direction of the Fire Agency, adopted this result. Very desirable results were expected out of this study. Also, this method is better understood today, so there is not much difference between now and then.

This method is quite different from the scientifically based prediction model, so it has a lot of uncertainty, so we need verification based on a lot of case studies in the future.

APOSTOLAKIS: But if you know the method that will make the allowance for these uncertainties, have you tried to be conservative, or have you tried to be realistic?

SEKIZAWA: What do you mean allowance?

APOSTOLAKIS: These time studies that you were estimating for the investigative damage potential seems to me not to be worthwhile. The number that comes out must be very uncertain, so whatever you do with that number later, must somehow leave no uncertainties. Are you trying to get a conservative number or what? That's what I mean by making an allowance for the uncertainty.

HALL: You mentioned that verification will be done using case studies. How will that work? What will you measure to confirm the accuracy of the method?

SEKIZAWA: It's a very hard question, but we have to build a database. Then this method will be used because we cannot verify this method directly right now.

HALL: So, would you be using some indirect plausibility checks?

SEKIZAWA: Yes.

HALL: In other words, if you can't measure the parameters directly, you simply try to work consequences out of the method that can be verified? Is that how it's worked? If you can't measure some of these key parameters directly, which now we can't then you'd be measuring at some derived consequence. Is there an example of how that might work? What kind of data might you collect?

SEKIZAWA: The database is derived from this method. The file shows, and some experts can understand the style of the buildings or if they are dangerous buildings or safer buildings by looking at the distribution, whether it is at the threshold point, or in the risky range.

HALL: Let me see if I understand you. You're saying experts can look and try to say these are safe buildings, or these are dangerous buildings? Does the method also classify them in that way?

SEKIZAWA: Yes.

AN EVACUATION MODEL FOR THE USE
IN FIRE SAFETY DESIGNING OF BUILDINGS

by

Kiyoshi TAKAHASHI

Fujita Corporation
4-6-15 Sendagaya, Shibuya-ku, Tokyo 151

and

Takeyoshi TANAKA

Building Research Institute
Ministry of Construction
Oho-machi, Tukuba-gun, Ibaraki 305

SYNOPSIS

The theories and the principal features of the computer model developed in a research project of Ministry of Construction: "Development of Fire Safety Design Method of buildings" as a tool to predict and evaluate evacuation time of people in fire are outlined. Also, the predicted results using the model are compared with the field measurements of the egress time of the audience of Tukuba Expo'85 pavilions and of the evacuation drill in a high-rise building in Tokyo.

INTRODUCTION

To date, fire safety measures of buildings in Japan have been determined almost always according to the specification standards of The Building Standard Law of Japan. However, it is necessary to replace these specification standards with performance ones as most as possible for the rationalization both in fire safety performance and cost of the measures and for more flexibility of design of architectures. In recognition of this necessity, Building Research Institute(BRI) have carried out a research project "Development of Fire Safety Design Method of Building" with the cooperation of universities, private construction companies and designers.

To introduce performance standards into a fire safety design method, many kinds of prediction methods are indispensable for evaluating various aspects of fire behaviors. And since a prediction method of fire behavior is one of the most important ones, an attempt was made to develop a computer evacuation model. This paper outlines the theories of the model and also demonstrates its predicting capability by means of the comparisons with the field measurements conducted during Tukuba Int'l Expo'85 and an evacuation drill at a high-rise building in Shinjuku, Tokyo.

EVACUATION MODEL

1. Scope of The Model

Many evacuation models have been developed by now to evaluate human behaviors in fire. And one of the directions of the developments is to try

to predict or explain human behaviors in really hazardous conditions in fire by means of introducing models concerning human reactions to fire or smoke. Those models may be interesting as a basic tool or an attempt to interpret human behaviors in fire, but it will be too ambitious to use this type of models for fire safety design purposes. The reasons are: human behavior when encountering a fire will vary from one individual to another, there is virtually no reasonable means to validate human reaction models to fire conditions at present, and it will require too much time or too many runs until the fire safety design of a building is decided because this type of models will be sensitive to fire conditions, so give different answers under different fire scenarios, including location of the room of origin, behavior of smoke movement.

On the other hand, if the scope of the application of a model is restricted to only design purposes, the model does not necessarily have to be very sophisticated. Let's take an example: suppose that the kinetic characteristics of a structural material are known only for the elastic domain, then it is possible to design a structure of a building so that the stresses of the structural elements do not exceed the limit of its elasticity thus avoiding the risk of collapse due to the uncertain knowledge in its plastic domain. Similarly, in an evacuation design, if prediction of evacuation is possible only when the level of hazard to evacuees is not too high, a building can be so designed, by means of compartmentation, smoke control and so on, that the necessary level of safety can be attained during the period of evacuation.

The present model was developed according to the consideration briefed in the above and adopts the basic premises as follows:

a) The necessary level of safety of evacuation route is maintained throughout the period of evacuation so that orderly evacuation can be carried out.

b) The evacuation plan is adequate enough to be carried out in actual fire situations as is planned.

2. Modeling of Building Spaces

Building spaces are modeled as an evacuation space system composed of six kinds of space elements i)-vi) and two imaginary spaces vii) and viii) as is shown in Fig.1. The latter two are introduced to make the concept of the calculation procedure clear.

i) room : A space with exits in which occupants exist at the onset of fire and make egress movement. A room with multiple exits is further divided into room units.

ii) path : A space on a floor with an entrance and an exit in which evacuees do not exist at first but enters from another space element and move toward the exit. A path is further divided into path units for convenience of calculation.

iii) stairs : A space which connects floors at different levels and has multiple entrances and exits. A stair functions like paths joined one after another.

iv) vestibule : A space with an entrance and an exit to a stair. A vestibule function like a path. The number of evacuees entering a vestibule is counted to judge if the evacuation on the floor has been completed.

v) hall : A space with multiple entrances and exits which are connected by multiple paths.

vi) refuge : A final destination of evacuees.

- vii) link : An imaginary space without capacity which regulates the flow of evacuees at a joint part of space elements.
- viii) crowding : An imaginary overflow space at the exit of each space element, which accommodates evacuees who cannot make immediate egress to the next space.

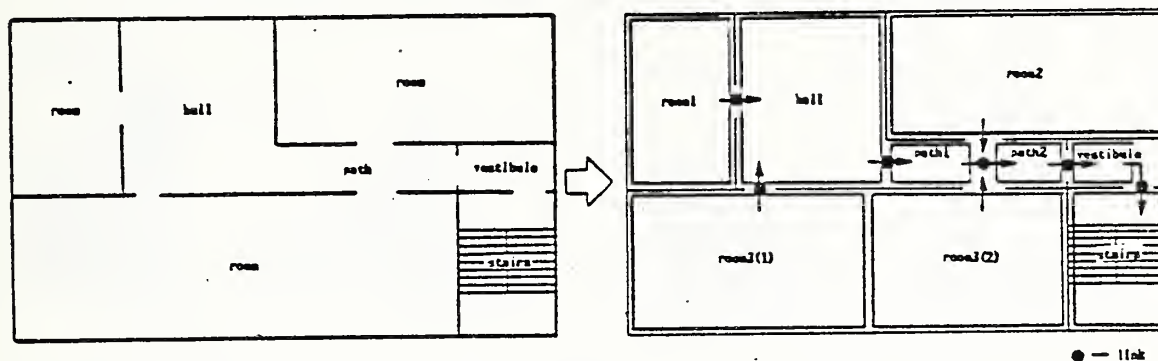


Fig.1 An Example of Modeling of Building Spaces

3. Modeling of Evacuees' Movements

1) Evacuees

It is assumed that the evacuees are homogeneous in evacuation ability and move like a fluid.

2) Initial distribution of evacuees

It is assumed that the evacuees are uniformly distributed in rooms.

3) Starting time of evacuation

In actual fires, it is not unusual that the evacuation starts significantly after the onset of fire, and this delay time can never be neglected in the total evacuation time. It is not easy to assess the starting time of evacuation because this depends on various conditions such as nature of occupants, fire detection and alarming systems, guiding method of evacuees and building spaces, but this model treats the time as input data.

4) Movements of evacuees in the space elements

1) Movement in rooms

As was stated before, when a room has multiple exits, the room is further divided into the room units each of which corresponds to an exit as is shown in Fig.2.

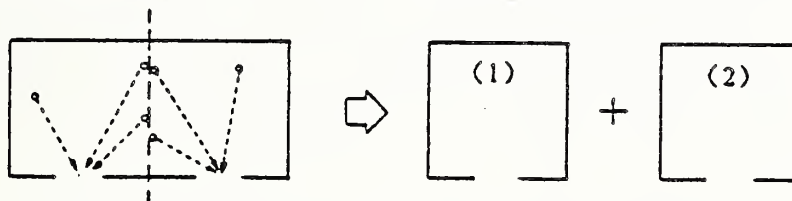


Fig.2 Division of a room into room units

The evacuees in a room unit, which are distributed uniformly at the initial point of time, starts to move toward the exit simultaneously. Two types of course of approach to an exit are considered as follows:

a-1) L-shape approach to exit

In such rooms as large offices, where many office furniture usually exist, it will be difficult for evacuees to approach to an exit directly. Hence, in such a case, it is assumed that evacuees take L-shape course to

approach to an exit.

Let's consider first the case where the exit locates at a corner of a room. It will be known that the evacuees who arrive at the exit from the start by a certain elapsed time t are those who were initially within the L-shape distance $v \cdot t$, in other words, those in the shaded area in Fig.3.

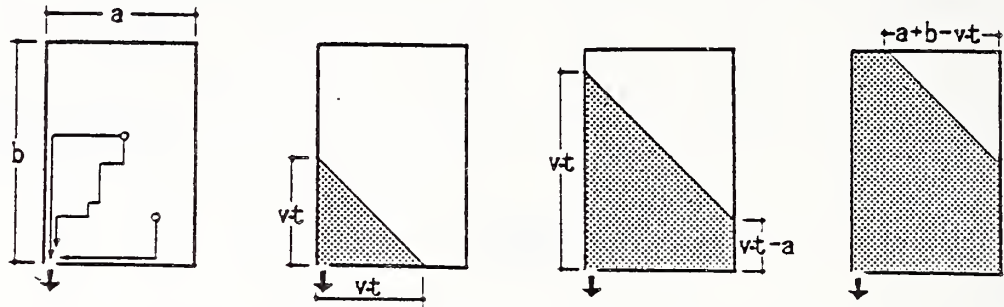


Fig.3 The Number of Evacuees Arriving at the exit Within Time t

In mathematical form, the number is given as follows:

$$P = \begin{cases} \rho \frac{(vt)^2}{2} & (0 \leq t \leq \frac{a}{v}) \\ \rho \left\{ \frac{a^2}{2} + a(vt - a) \right\} & (\frac{a}{v} < t \leq \frac{b}{v}) \\ \rho \left\{ ab - \frac{(a+b-vt)^2}{2} \right\} & (\frac{b}{v} < t \leq \frac{a+b}{v}) \end{cases} \quad (1)$$

where a : the length of shorter side of the room (m)
 b : the length of longer side of the room (m)
 t : a certain elapsed time from the start (sec)
 v : walk speed (m/sec)
 ρ : density of evacuees (person/m²)
 P : number of evacuees arriving at the exit by time t (person)

Incidentally, if ever evacuees do not take a literal L-shape course with one turn but take a course with several turns, it does not make difference in the distance to an exit as long as they do not go backward.

a-2) Centripetal approach to exits

In rooms with little obstacles for walk, such as assembly rooms without fixed seats, party rooms and gymnasiums, it will be reasonable to assume that evacuees make centripetal approach to the exit. In this case, referring to Fig.4, it can be seen that the number of evacuees arriving at an exit is given as follows:

$$P = \begin{cases} \rho \frac{\pi (vt)^2}{4} & (0 \leq t \leq \frac{a}{v}) \\ \rho \left\{ \frac{(avt) \sin \theta_1}{2} + \pi (vt)^2 \frac{(\frac{\pi}{2} - \theta_1)}{2\pi} \right\} & (\frac{a}{v} < t \leq \frac{b}{v}) \\ \rho \left\{ \frac{(avt) \sin \theta_1}{2} + \pi (vt)^2 \frac{(\frac{\pi}{2} - \theta_1 - \theta_2)}{2\pi} + \frac{(bvt) \sin \theta_2}{2} \right\} & (\frac{b}{v} < t \leq \frac{\sqrt{a^2+b^2}}{v}) \end{cases} \quad (2)$$

$$\theta_1 = \cos^{-1} \left(\frac{a}{vt} \right) \quad \theta_2 = \cos^{-1} \left(\frac{b}{vt} \right)$$

where a : the length of shorter side of the room (m)
 b : the length of longer side of the room (m)
 t : a certain elapsed time from the start (sec)
 v : walk speed (m/sec)
 ρ : density of evacuees (person/m²)
 P : number of evacuees arriving at the exit by time t (person)

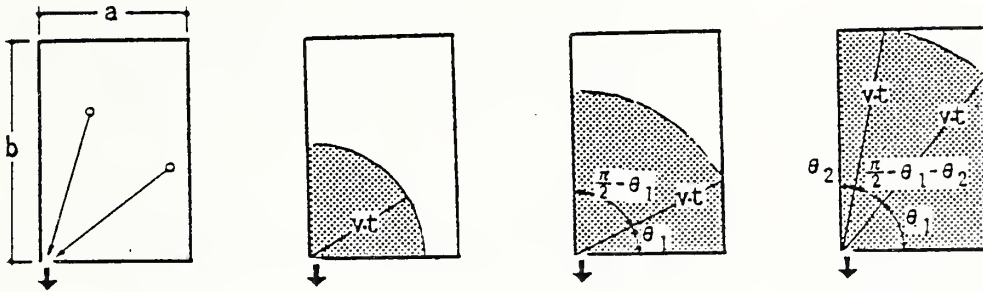


Fig.4

In general, the exit of a room unit does not necessarily locate at a corner, but as can be seen in Fig.5, a room unit can be regarded as a combination of the two parts with an exit at a corner. So, the number of the evacuees arriving at the exit can be calculated as the sum of the numbers of the evacuees of the two parts.

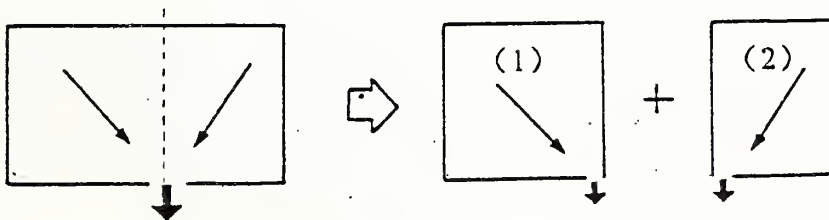


Fig.5

b) Movement between crowdings

Since evacuees try to escape from fire hazards as fast as possible, it will be reasonable to assume that in a room with multiple exits, they choose the exit through which they are likely to be able to make fastest egress from the room. As the result, the numbers of the crowdings at the exits of a room are redistributed to minimize the expected time of the dissolution of all the crowdings of the exits. Because the expected minimum time for the dissolution of all the crowdings is

$$T_{min} = \frac{\sum Cr(i)}{\sum P_{out}(i)}$$

when the egress at each exit continues at the rate of $P_{out}(i)$, the optimal redistribution of each crowding is given as

$$C'_r(i) = P_{out}(i) \cdot T_{min}$$

where $P_{out}(i)$: egress rate at exit i (person/sec)
 $Cr(i)$: number of crowding at exit i before redistribution (person)
 $C'_r(i)$: number of crowding at exit i after redistribution (person)

Note that $P_{out}(i)$ may change with time, as the condition of the space outside exit i changes.

ii) Movement in paths, stairs and vestibules

In this model, evacuees entering a space element are assumed to proceed orderly toward the exit without passing over and going backward. Since paths, stairs and vestibules are divided into the units with the length that can be cleared at the time increment, that is $v \cdot \Delta t$, it follows that the evacuees in a space unit move to the forward unit at every time step.

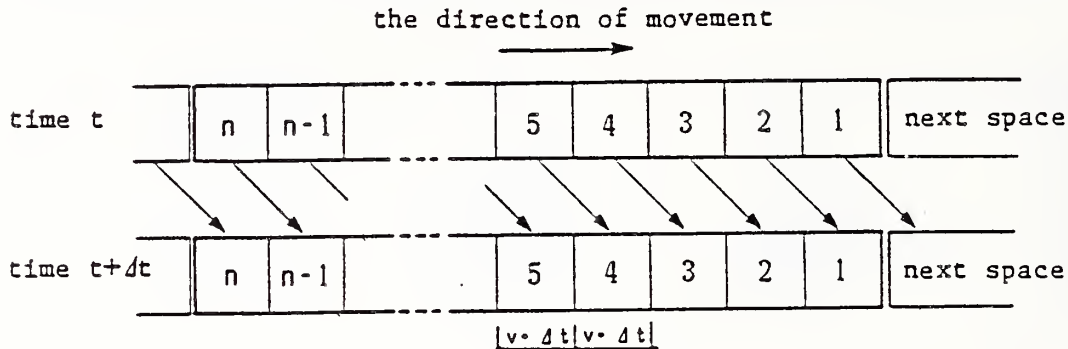


Fig.6

iii) Movement in halls

In a hall with multiple exits, the evacuees entering through an entrance are assumed to choose the exit which allows the shortest egress time from the hall taking into account the distances to the exits, the amount of crowdings and the rates of egress at the exits.

a) Exit selection in an empty hall

Let's consider first the case where the evacuees enters in an empty hall where a crowding does not exist at any exit. Let P be the number of evacuees entering through an entrance during the period of time t . If the numbers of evacuees are allotted optimally so that the egress time from the hall becomes minimum, the egress times at all the exits must become the same, that is

$$T_{\min} = t_1 + \frac{P_1}{N_1} = t_2 + \frac{P_2}{N_2} = \dots = t_i + \frac{P_i}{N_i} = \dots \quad (3)$$

where t_i : time to arrive at exit i (sec)

N_i : egress flow capacity of exit i (person/sec)

P_i : number of evacuees allotted to exit i (person)

i : exit number in order of distance

From Eqn.(3), we obtain

$$T_{\min} = \frac{\sum (N_i t_i + P_i)}{\sum N_i} = \frac{P + \sum (N_i t_i)}{\sum N_i} \quad (4)$$

So, it follows that the optimal allotment of evacuees is given as

$$P_i = N_i (T_{\min} - t_i) \quad (i = 1, 2, 3, \dots, n) \quad (5)$$

where n is the number of exit. However, this problem is not so simple, that is, the optimal solution is not necessarily given when all the exits are used. Let's take the simplest example, if all the evacuees choose the nearest exit, the egress time will be

$$T = t_1 + \frac{P}{N_1} \quad (6)$$

So, if $T < t_2$, the evacuees can go out of the hall faster when they choose only the nearest exit rather than when they choose more.

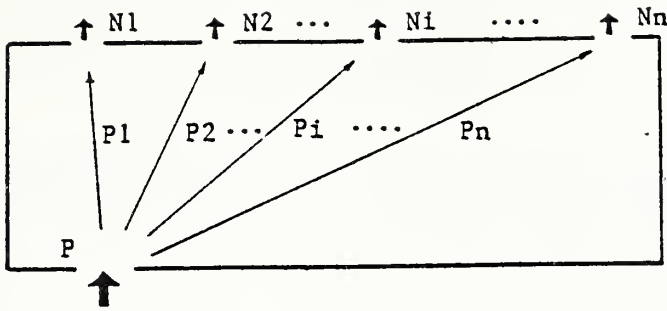


Fig.7 Exit selection in an empty hall

After all, it follows that the optimal time T_{min} and allotment P_i have to be calculated according to the procedure described in Fig.8a.

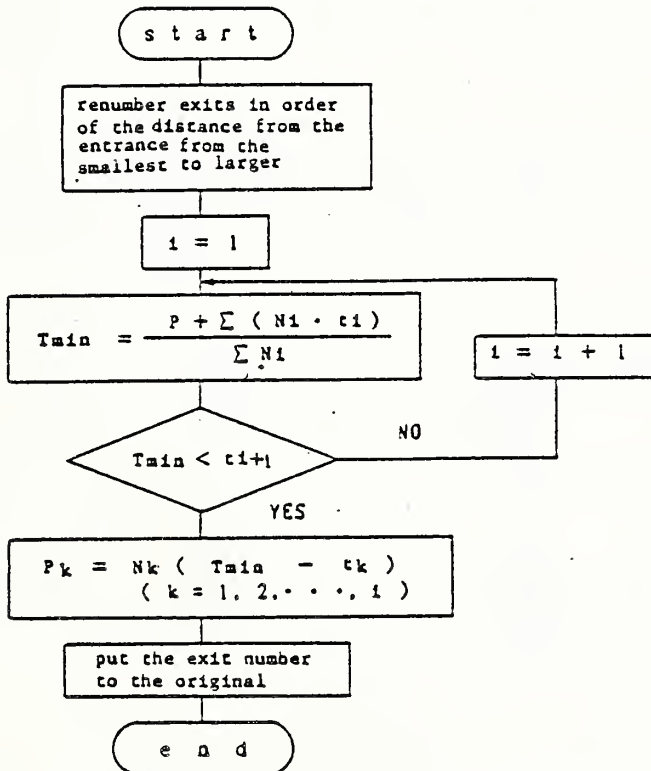


Fig.8a

b) Exit selection in crowded halls

As the time elapses, a hall will be crowded with evacuees and crowdings may be formed at exits. The evacuees entering a hall at such conditions are assumed to pick up the exit so as to minimize the egress time taking into account of the crowdings at the exits and the numbers of the evacuees approaching to the exits as well as the distances and the egress rates. In this case, since the expected egress times of the evacuees entering the hall during a time increment Δt are the same for all the exits chosen if the allotment is optimal, the following equation holds:

$$T_{min} = t_1 + \frac{C_1 + P_1}{R_1} = t_2 + \frac{C_2 + P_2}{R_2} = \dots = t_i + \frac{C_i + P_i}{R_i} = \dots \quad (7)$$

where R_i is the rate of egress at exit i at that time, and C_i is given as

$$C'_i = \begin{cases} C_i + W_i - R_i t_i & (C_i + W_i > R_i t_i) \\ 0 & (C_i + W_i \leq R_i t_i) \end{cases} \quad (8)$$

where C_i : number of the evacuees in the crowding at exit i (person)
 W_i : total number of evacuees arriving at exit i from the entrance within time t_i (person)
 R_i : rate of egress at exit i (person/sec)

From Eqn.(3), T_{min} is given as follows

$$T_{min} = \frac{P + \sum (C'_i + R_i t_i)}{\sum R_i} \quad (9)$$

and optimal allotment is given as

$$P_i = R_i \left\{ T_{min} - \left(t_i + \frac{C'_i}{R_i} \right) \right\} \quad (10)$$

However, exits have to be examined in order of the magnitude of $t_i + C_i/R_i$ from the smallest to larger as is shown in Fig.8b. Note that the procedure to yield T_{min} described in Fig.8b is general and include the case of empty halls.

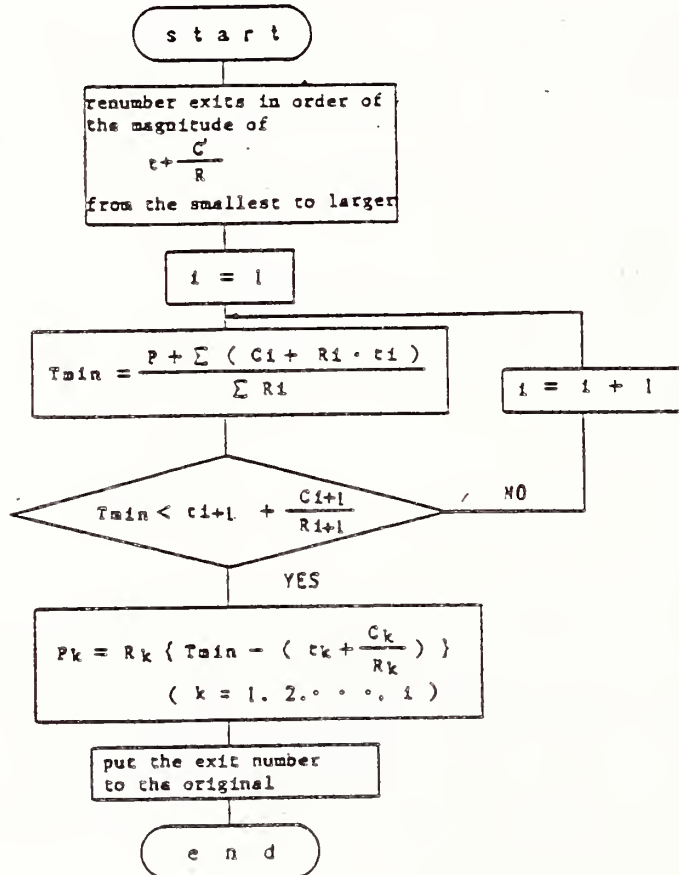


Fig.8b

c) Movement from an entrance to an exit

In this model, each entrance of a hall is connected with every exit with imaginary paths, so the evacuees entering the hall through the entrances move toward the exits just as they move in a path.

iv) Movement through a link

The movement of evacuees from a space element to another is treated by the concept of movement through a link. Since the number of evacuees which move through interface of space elements cannot be simply determined because it depends on the number of the evacuees ready to move, the available capacity of the space to move into, the widths of the openings and the number of space elements combined. Links are introduced to deal with this complex movement around the joint parts of the spaces.

a) Total number of evacuees moving through a link

Let's consider a general case where multiple space elements from which evacuees come out are combined with multiple space elements to which they move into. A link is imagined between the former and the latter as is shown in Fig.9. Suppose that during a time step Δt , movement of evacuees took

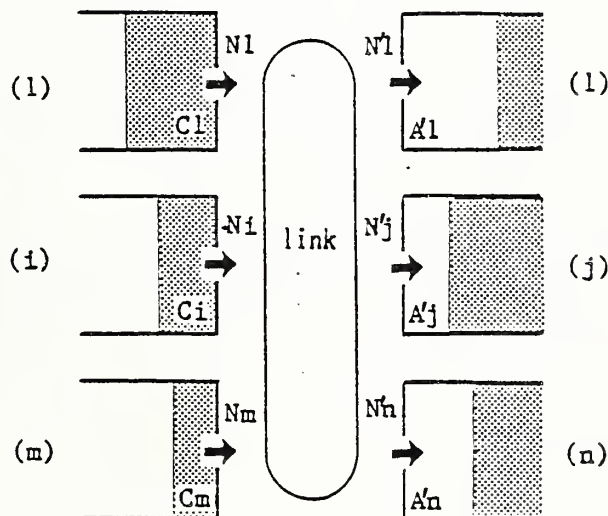


Fig.9 A link combining multiple space elements

place in each space element and evacuees have been added to the crowdings of the space elements in the upstream of the link and empty spaces have appeared in the downstream spaces. In this case, the number of evacuees which can be allowed in a downstream spaces is determined either by the available space or flow capacity of the entrance, that is

$$P'_{\max, j} = \text{MIN} (N'j \Delta t , \rho_{\max} A'j) \quad (11)$$

where $N'j$: flow capacity of entrance of space j (person/sec)
 $A'j$: space available in path j (person/sec)
 ρ_{\max} : maximum density of evacuees (person/m²)

So, the total number of evacuees allowed in the downstream spaces $\sum P'_{max,j}$ is

$$\sum P'_{max,j} = \sum \text{MIN} (N'_{j} \Delta t , \rho_{max} A'_{j}) \quad (12)$$

On the other hand, since the maximum number of evacuees which can egress from an upstream space element is determined either by the number of evacuees waiting to egress, or the egress capacity of the exit,

$$P_{max,i} = \text{MIN} (N_{i} \Delta t , C_{i}) \quad (13)$$

where C_i is the number of evacuees in the crowding of space i , and the total for all the upstream space elements $\sum P_{max,i}$ is

$$\sum P_{max,i} = \sum \text{MIN} (N_{i} \Delta t , C_{i}) \quad (14)$$

Finally, it follows that actual number of evacuees PL which move through the link is given as:

$$PL = \text{MIN} \{ \sum \text{MIN} (N_{i} \Delta t , C_{i}) , \sum \text{MIN} (N'_{j} \Delta t , \rho_{max} A'_{j}) \} \quad (15)$$

b) Allotment of evacuees to each path

Now that the total number of the evacuees moving from one side to the other, the number allotted to each space element, in other words, what portion of the total number comes out of a certain space element i in the upstream spaces and what portion goes into a certain space element j in the downstream space element, has to be determined. Suppose that they have been determined, the number of evacuees coming out from space element i : $P_{out}(i)$, and the number going into space element j : $P_{in}(j)$ are expressed as follows:

$$P_{out}(i) = \beta_i PL \quad \text{and} \quad P_{in}(j) = \beta'_j PL \quad (16)$$

where β_i and β'_j are the ratio of the evacuees allotted to upstream space element i and downstream space element j respectively. Needless to say, $\sum \beta_i = 1$ and $\sum \beta'_j = 1$. And here, β_i and β'_j are assumed to be proportional to $P_{max,i}$ and $P'_{max,j}$ respectively. Hence,

$$\beta_i = \frac{P_{max,i}}{\sum P_{max,i}} = \frac{\text{MIN} (N_{i} \Delta t , C_{i})}{\sum \text{MIN} (N_{i} \Delta t , C_{i})}$$

$$\beta'_j = \frac{P'_{max,j}}{\sum P'_{max,j}} = \frac{\text{MIN} (N'_{j} \Delta t , \rho_{max} A'_{j})}{\sum \text{MIN} (N'_{j} \Delta t , \rho_{max} A'_{j})} \quad (17)$$

COMPARISONS BETWEEN FIELD MEASUREMENTS AND PREDICTION

1. Egress of Audience from Tukuba Expo'85 Pavilions

1.1 Field measurement of the egress of the audience from Tukuba Expo'85 Pavilions

Field measurements were made for the egress behavior of the audience of seven pavilions of Tukuba International Exposition held in 1985. The plans and the sections of the seating area of the selected pavilions are shown in

Fig.10. These theaters were vacated after each films or performance for next turn.

The positions of VTR cameras for the measurements are shown also in Fig.10. Several turns of measurements were made in each theater and the results of the time of the egress completions are given in Table 1. The typical tendency of egress is shown by the example shown in Fig.11. The number of audience remaining in the theater counted from the video recordings is plotted as a function of time but the counting was only possible for the initial and the final regions of egress. For the primary region in between, it is too difficult to count the number of audience, but a simple interpolation as shown in Fig.11 is thought to be sufficient to estimate the number.

In the final region, a tailing appeared in every turn due to a part of the audience egressed leisurely and the time of egress completion was lengthen by the tailing. In a truly emergent condition, this tailing would disappear. If the tailing is cut off by extrapolating the slope at primary region as shown in Fig.11, the egress time is shortened by 10~30sec. These results are given in Table 1.

1.2 Prediction of egress time

The egress time of the audience from the theaters were predicted using the evacuation model described in the above. The two cases were considered for each theater, i.e: case(a) in which simply L-shape approach to exits is assumed in the theater space, and case(b) in which the theater is composed of space units such as rooms and paths. In the latter, the walk speeds at horizontal paths and stairs are taken as 1.0 m/s and 0.5 m/s, respectively, and in the former, 0.7 m/s was employed as the average walk speed considering that the space consists of horizontal paths and stairs. In both cases, the egress coefficients of exits on horizontal floor and on stairs, are taken as 1.5 person/(m·s) and 1.3 person/(m·s), respectively.

The results of the predictions are given in Table 1. As can be seen, the predicted egress times of case(b) are consistently longer than case(a). This means that in the prediction for case(b), crowdings are formed in some parts within seating area of the theater. In fact, crowdings were observed along the alleys in many of the theaters in the field measurement.

1.3 Comparison between the predictions and the measurements

It can be seen in Table 1 that the predicted egress times are generally shorter than the measured ones and the predictions assuming case(b) give the better agreement with the measurement except FR pavilion. So, it may be said that it is more appropriate to model a theater space as a combination of space units than to simply consider a room with L-shape approach in most of the theaters, in which crowdings are usually formed along alleys. On the other hand, in FR pavilion, since the seats were low bench type ones so that people can more freely over the seats, the calculation assuming case(a) gave a better prediction.

There are some other reasons why the measured egress times are longer than the predictions. Needless to say, the theaters are not in emergent conditions, so the people egressed more or less leisurely, in every case. In case of SH and TD pavilions, it was rainy on the day of measurements, so the people stopped outside the exits to prepare rain outfits and delayed the egress of the remaining people. In NT pavilion, people on the upper layer

went down through the same stairs besides the theater and merged with the people from the theater.

Taking these factors into consideration, the present model can be said reasonable as a prediction tool to evaluate evacuation time in fire safety design of buildings.

2. Evacuation drill in a high-rise building

2.1 Field measurement of the evacuation drill

A field measurement for egress behavior was made taking advantage of an evacuation drill carried out in a 50 story high-rise building in 1985. All the participants of the drill started the evacuation movements by the order delivered through loud-speaker simultaneously throughout the building and went down to stairs to outside the building. The outline of the building and the number of the drill participants on each floor who used the east stairwell are shown in Fig.12 and Table 2, respectively. The measurements were made on the east stairwell using the VTR cameras placed on a couple of points in the stairs and by the portable VTR cameras carried by the observers who went down the stairs with the drill participants. The evacuation took 960 sec to complete.

2.2 Prediction and comparison

The prediction were made for the east stairwell. The initial number of participants on each floor is shown in Table 2, but the number in () were estimated from the total number of the participants and the results of measurements since they were not exactly known.

As the speed of movement for the horizontal paths and for the stair, 1.2 m/s and 0.6 m/s(horizontal component of velocity) are employed respectively and as the egress coefficients through doorways, 1.5 person/(m·s) and 1.3 person/(m·s) are used for the horizontal paths and for the stairs, respectively.

The time to complete evacuation was predicted as 885 sec. The predicted time is shorter than the measured by 75 sec. This may be partly because a certain time was used for the preparation, gathering or roll calls by leaders. However, even if these factors are not taken into account 75sec of difference will be evaluated well within the allowable limit of accuracy compared with the evacuation time.

CONCLUDING REMARKS

An evacuation model has been developed to evaluate evacuation time, which is one of the important components in performance based Fire Safety Design Method of Buildings. The capability for prediction of the model were examined in comparison of the predictions with the field measurements of the egress behaviors in Expo'85 pavilions and a high-rise building. As is easily understood, a perfect prediction of people behaviors cannot be expected, however, the present evacuation model can be evaluated as reasonable as a tool to be used for design purpose.

Table 1 Results of measurements and predictions of egress completion time

NO.	CODE NAME	NUMBER OF SEATS	THEATER FLOOR AREA (m ²)	EXIT		EGRESS COMPLETION TIME (sec)				NOTE
				TOTAL WIDTH (m) (mxnumber)	DIRECTION	MEASUREMENT	(EXPECTED)	CALCULATION case (a) case (b)		
1	SU	424	540	8.8 (6.6×1, 2.2×1)	R(F), R(B)	61, 71, 75, 60, 64	50~61	52	62	
2	FR	1000	1014	5.1 (5.1×1)	L	174, 154 ^{*1}	125~155	137	275	
3	TO	508	693	6.8 (1.7×4)	B	71, 80, 77, 78, 79	60~77	50	76	
4	ST	366	315	4.0 (2.0×2)	B	94, 111, 102 ^{*1}	88~104	72	89	
5	NT	350	452	7.0 (1.4×5)	L	70 ^{*1} , 123 ^{*2} , 84, 77	60~73	34	59	
6	SH	500	563	3.6 (3.6×1)	F(R)	160, 152, 166, 157	140~150	100	107	on a rainy day
7	TD	405	401	5.4 (5.4×1)	L(F)	148, 118, 130, 121, 131	95~135	70	88	on a rainy day

F : front *1 : Tape start delayed by 2~3 sec.

B : back *2 : Opening of exit doors delayed by about 40 sec.

R : right

L : left

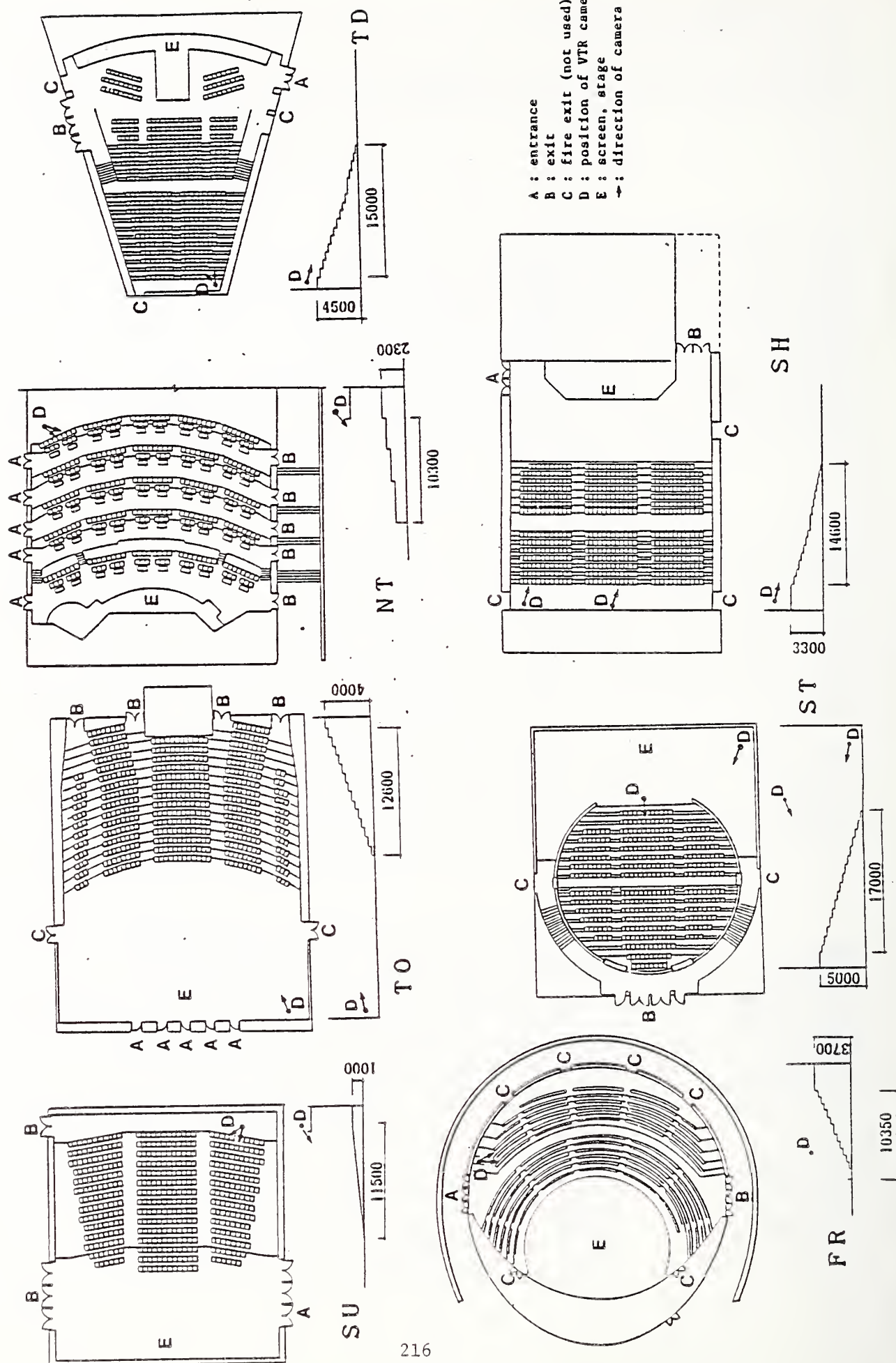


Fig. 10

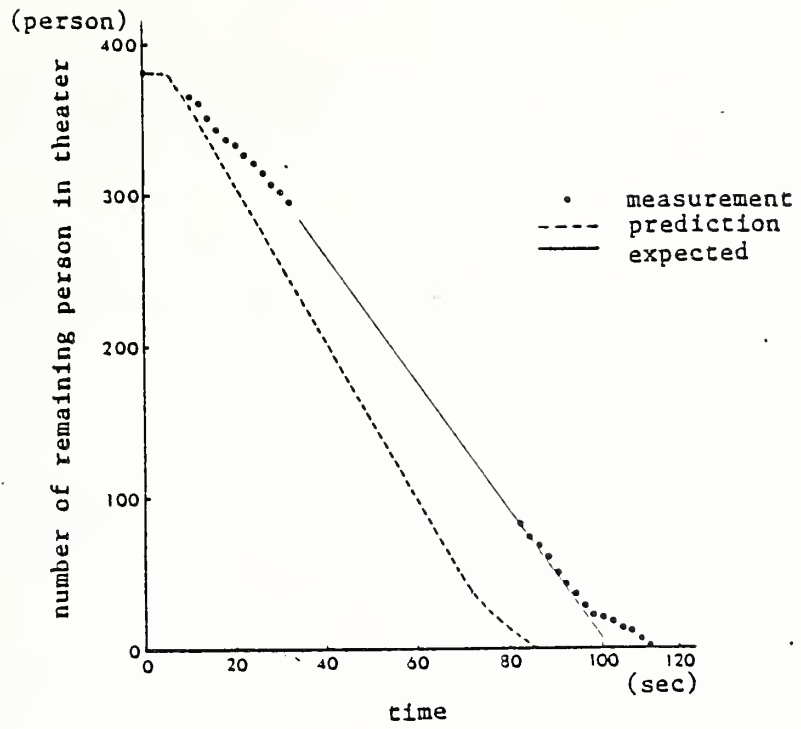


Fig.11 Typical tendency of egress from theaters

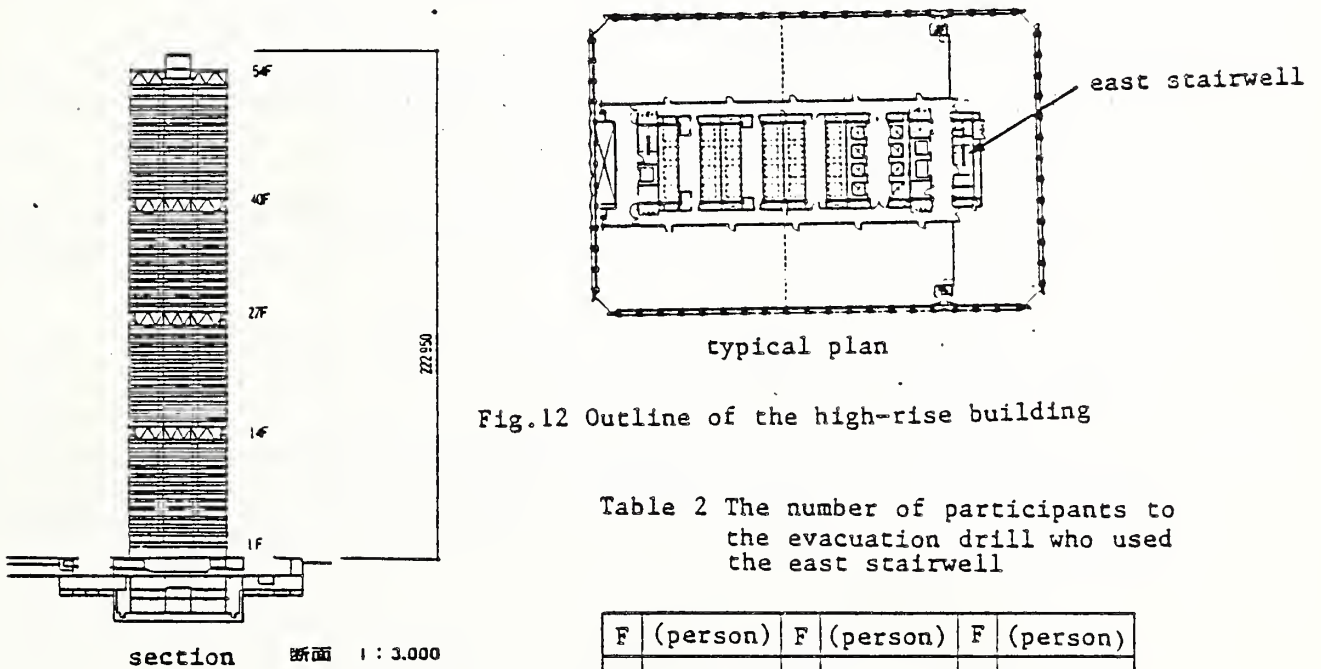


Fig.12 Outline of the high-rise building

Table 2 The number of participants to the evacuation drill who used the east stairwell

F	(person)	F	(person)	F	(person)
1	—	18	—	35	—
2	—	19	—	38	(2 1)
3	—	20	4 5	37	—
4	—	21	—	38	(2 1)
5	—	22	4 5	39	—
6	—	23	—	40	—
7	1 8	24	—	41	—
8	—	25	7 0	42	(2 1)
9	5 0	26	4 0	43	—
10	—	27	—	44	(2 1)
11	5 0	28	7 0	45	—
12	—	29	—	46	(2 1)
13	5 0	30	(2 1)	47	—
14	—	31	—	48	(2 2)
15	5 0	32	(2 1)	49	—
16	—	33	—	50	(1 5)
17	—	34	(2 1)	51	6 9 1

AN EVACUATION MODEL FOR THE USE IN FIRE SAFETY DESIGNING OF BUILDINGS
K. Takahashi, Japanese Association of Fire Science and Engineering,
Japan

NELSON: You took a lot of data with TV cameras. Are you familiar with the assumptions on flow versus density that Predeshinsky and Fruin and Pauls are using? Did your data confirm or challenge those approaches?

First, are you familiar with the work that I'm referring to?

TAKAHASHI: I'm familiar with the data from Predeshinsky.

NELSON: His theory is that the speed of the evacuees is a function of the density of the population. Did your observations confirm this, or were they not appropriate?

TAKAHASHI: I haven't really concluded anything about the evacuation speed.

NELSON: Are you familiar with the effective width theory?

TAKAHASHI: Yes, I'm very familiar with it.

NELSON: Did you observe it in your videos? Did you observe people staying away from the edges in your videos?

TAKAHASHI: I haven't really quite observed that to reach any kind of conclusion from your viewpoint; however, we focused on the time to completion. I would like to explore speed and density in the future.

HALL: Your method seems to be flexible enough to be adapted for cases where the individuals do not know the best route out, or where exits are blocked or no longer available due to the fire. Do you have plans to examine cases like this?

TAKAHASHI: We choose the best exits for this work; however, another path to the exit is along the evacuation route.

TANAKA: We have taken into consideration during the calculation process the possibility of the exit being blocked. However, we have not taken into consideration the possibility that the entrance or exit may be blocked after the fire starts.

A SUMMARY OF THE ASSUMPTIONS AND LIMITATIONS IN HAZARD I

Richard W. Bukowski P.E., Head
Hazard Analysis
Center for Fire Research
National Bureau of Standards
Gaithersburg, MD. 20899

INTRODUCTION: The first version of the Hazard Assessment Method - HAZARD I consists of a three volume report and a set of 5 1/4 in. disks containing the software necessary to conduct hazard analyses of products used in residential occupancies. All of the software provided will operate on any IBM¹ PC (XT or AT) or compatible MS-DOS computer with the following minimum hardware configuration:

- 512k MEMORY
- GRAPHICS CARD (IBM CGA OR EGA, OR HERCULES COMPATIBLE)
- HARD DISK DRIVE
- MATH CO-PROCESSOR (8087 OR 80287)
- PRINTER
- DBASEIII+ (REQUIRED ONLY FOR THE DATA BASE PROGRAM)

A block diagram of the important phenomena which must be included in a hazard analysis and their inter-dependencies is given in figure 1. The organization of the HAZARD I software package is shown in figure 2. It includes a scenario development guidance utility (PRODUCT.ONE); an interactive program for inputting data to the fire model (FINPUT); a data base program (FIREDATA) and files of thermophysical, thermochemical, and reference toxicity data; the FAST model for multi-compartment energy and mass transport; a graphics utility for plotting data (FASTPLOT); a detector/sprinkler activation model (DETECT); an evacuation model which includes human decision/behavior (EXITT); and a tenability model (TENAB) which evaluates the impact of the predicted exposure of the occupants in

¹The use of company names or trade names within this report is made only for the purpose of identifying those computer hardware or software products with which the compatibility of the programs of HAZARD I has been tested. Such use does not constitute any endorsement of those products by the National Bureau of Standards.

terms of incapacitation or lethality from temperature or toxic gases or incapacitation by second degree burns from radiant flux exposure. A step-by-step procedure for performing a hazard analysis using this software package is presented in chapter 4, and user guides for each of the programs is contained in chapter 6.

Also included in the report is the set of eight representative example cases of typical residential fires which were established by two panels of outside experts. These consist of fire scenarios, selected by a panel composed of representatives of the major fire services organizations, in each of three single-family residences which were considered to represent typical homes by a panel from the model building codes, NFPA, and the architectural community. A description of the process of developing these cases and the results obtained for each is included in chapter 5, and the complete documentation (input data file listings, program outputs and graphs of selected, predicted variables) is in Volume 2.

While the scope of this first hazard assessment method is limited to residential occupancies, the work necessary to extend it to other occupancy classes is underway. This first version is being introduced now to allow the fire protection community to become familiar with the method and its use. Feedback from users is crucial to refinement of the method and its ultimate utility.

GENERAL: HAZARD I is a first, prototype version of a methodology for making quantitative predictions of the hazard to the occupants of a building from a fire within that building. It consists of a collection of data, procedures, and computer programs which are used to simulate the important time-dependant phenomena, generally as depicted in figure 1 (although this first version does not account for all of the phenomena listed). The major functions provided include:

1. the production of energy and mass (smoke and gases) by one or more burning objects in one room, based on small- or large-scale measurements,
2. the buoyancy-driven transport of this energy and mass throughout a series of user specified rooms and connections (doors, windows, cracks, etc.),
3. the resulting temperatures, smoke densities, and gas concentrations after accounting for heat transfer to surfaces and dilution by mixing with clean air,
4. the evacuation process of a user specified set of occupants accounting for delays in notification, decision making, behavioral interactions, and inherent capabilities,
5. and the impact of the exposure of these occupants to the predicted room environments as they move through the building, in terms of the expected fatalities, and the time, location, and cause of each.

As can be seen from this list, the method involves a mix of the "hard" sciences (physics, chemistry, fluid mechanics and heat transfer) and the "soft" sciences (biology, toxicology, and human behavior). Less obvious are the areas where fundamental laws (conservation of mass, energy, and momentum) can be used, versus where empirical correlations or even "educated guesses" must be employed to bridge gaps in existing knowledge. The latter, along with compromises required by considerations of operational practicality result in the introduction of uncertainties in the results which must be quantified by experimental verification and validation. Until such is completed, the user should understand the inherent assumptions and limitations of the procedures and programs in order to make estimates of these uncertainties.

SCOPE LIMITATION: The scope of HAZARD I has been limited to one- and two-family residential structures, as a result of limitations in both technical knowledge and resources. The technical limitations involve insufficient understanding or capability to model such large-building phenomena as the distribution of heat, smoke, and gases through the HVAC system, and the complex flows in stairways. While these should have a negligible influence on hazard development in small buildings, the effects in large buildings can be great. Also, the behavioral rules first implemented in the EXITT model for small building evacuation have not yet been incorporated into the large building evacuation models.

In addition to these technical considerations, available resources required that the first data base be limited in the number of data entries supplied. The obvious solution was to concentrate on materials and products typical in residential occupancies. If one considers that the majority of US fire losses are in these areas, this does not represent a bad starting point for the first system; and the scope will be broadened in HAZARD II by improvements in the technology and expansion of the data base.

PROGRAMS AND PROCEDURES: Figure 2 presents the HAZARD I software package developed to implement the assessment of hazard as shown in figure 1. Of the nine programs shown, only five perform calculations and so have assumptions associated with them. The others (PRODUCT.ONE, FIREDATA, FINPUT, and FASTPLOT) perform utility and user interface functions only.

Of this latter group, the only point which should be made in the context of assumptions deals with the database files searched by the programs in FIREDATA. The data provided in the cone and furniture calorimeter files are measured values from individual samples tested in these devices under a specified set of conditions. While the materials are identified generically, it should be understood that such data are not necessarily representative of the behavior of that generic material. Some variation would be expected, even on a set of samples from the same lot; and no attempt was made to obtain representative samples for test. Also, data in the thermophysical properties file were taken either from manufacturer's data or from literature sources with no attempt to verify values or to determine their representativeness. Finally, the data in the toxicity file are published values from the sources indicated. Replicate tests were sometimes done, and some of the sources provide confidence intervals for these data. The material identifications are those provided in the sources and cannot be verified.

SPECIFIED FIRE: The greatest weakness of HAZARD I is in the specification of the rates of energy and mass release by the burning item(s). The procedures available to the user and their associated limitations are:

1. For the Furniture Calorimeter, a product (chair, table, bookcase, etc.) is placed under a large collection hood and ignited by a 50 kW gas burner (simulating a wastebasket) placed adjacent to the item for 120 sec. The combustion process then proceeds under assumed "free-burning" conditions, and the release rate data are measured.

Potential sources of uncertainty here include measurement errors related to the instruments and the degree to which "free-burning" conditions are not achieved (radiation from the gases under the hood or the hood itself, and restrictions in the air entrained by the object causing locally reduced oxygen concentrations affecting the combustion chemistry) in the apparatus. There are limited experimental data for upholstered furniture which suggest that prior to the onset of flashover, the influence of the compartment on the burning behavior of the item is small, where it is the only item burning and it is ignited in a similar fashion. The differences obtained from the use of different ignition sources or locations of application have not been explored.

2. Where small-scale calorimeter data are used, procedures are provided to extrapolate to the behavior of a full size item. These procedures are based on empirical correlations to data which exhibit significant scatter, thus limiting their accuracy. For example, the peak heat release rate estimated by the "triangular approximation" method for upholstered furniture averages 91% (range 46% to 103%) of the measured value for a group of chairs with non-combustible frames, but only 63% (range 46% to 83%) for other chairs with combustible frames. Also, the triangle does not include the "tail" of the curve produced primarily by the burning of the frame after the fabric and filler are consumed.

3. The data and procedures provided relate directly only to contents items under "free burning" conditions, initiated by relatively large flaming sources. Almost no data exist for release rates under smoldering combustion, nor for the high external flux and low oxygen conditions post-flashover which strongly influence the combustion chemistry. While the program MLIFUEL allows multiple items burning simultaneously to be converted to a single "equivalent" specified fire, it does not account for the energy interchange of such items. Thus, for other ignition scenarios, multiple items burning simultaneously (which exchange energy by radiation and convection), combustible interior finish, and post-flashover conditions, the procedures provided can only give estimates which are often non-conservative (the actual release rates would be greater than estimated). The only way to account for all of these complex phenomena is to conduct a full-scale room burn and input the release rates to the transport model. Alternatively, a detailed combustion model such as HARVARD V can be used as the source of the specified fire data, although it too has its own assumptions and limitations.

TRANSPORT: The distribution of energy and mass throughout the rooms included in the simulation is done in the model FAST. This is a zone (control volume) model with all of the attendant assumptions and limitations of such models. The basic assumption is that each room can be divided into two or more zones each of which is internally uniform in temperature and composition. In FAST, all rooms have two zones except the fire room, which has an additional zone for the fire plume (see figure 3 for a representative diagram). The boundary between the two layers in a room is called the interface.

Other than in very large rooms, the zone assumption does not generally represent a large source of error since, at least in the spaces close to the fire, experiments show that buoyantly-stratified layers clearly form. While in an experiment the temperature can be seen to vary within a given layer, these variations are small compared to the temperature difference between the layers.

Beyond the basic zone assumptions, the implementation of any model requires a mixture of established theory (e.g. conservation equations), empirical correlations where there are data but no theory (e.g. flow and entrainment coefficients), and approximations where there are neither (e.g. post-flashover combustion chemistry) or where their effect is considered secondary compared to the "cost" of inclusion. An example of the latter is the fact that none of the models account for the variation of the thermal properties of structural materials with temperature. While this would be fairly simple to add to the computer code, data are scarce over a broad range of temperature even for the most common materials, and the estimated error from this assumption is less than for others which should be addressed first.

With a highly complex model such as FAST, the only reasonable method of assessing the assumptions and limitations is through the verification and validation process, which is ongoing at CFR. Until the results of this process are available, the following list should provide some insight.

1. The "specified fire" input by the user is not subject to the influences of the room as discussed previously. If a large mass loss rate is entered, the model will proceed, regardless of the fact that the available oxygen will limit the portion of that mass which will burn in the room. This will result in extremely high predicted temperatures; exceeding the adiabatic flame temperature.
2. With no extant chemistry, the species yields specified will be used regardless of the oxygen concentration. It is known that the chemistry changes in low oxygen, with an attendant increase in the yields of products of incomplete combustion such as CO. Room fire test data shows that under post-flashover conditions, the production rate (yield) of CO increases (and CO₂ decreases) in the room, but much of the excess CO burns (to CO₂) in the door flame. The resulting concentrations may not differ substantially from the pre-flashover condition.

3. The entrainment coefficients are empirically-determined values. Small errors in this value will have a small effect on the fire plume or the flow in a single door plume. In a multi-compartment model such as FAST however, small errors in each door plume are multiplicative as the flow proceeds through many compartments, possibly resulting in a significant error in the furthest rooms.

4. The introduction of gases into the lower layer of each room occurs primarily due to mixing at connections and from the downward flows along walls (where contact with the wall cools the gas and reduces its buoyancy). Since for the former an appropriately-documented mixing coefficient is not known, and for the latter the associated theory is only now being developed, neither is included in FAST. Thus, the lower layer cannot receive smoke or gases and can heat only by radiation from the upper part of the room heating the lower walls and floor, which then convect to the lower layer.

5. Plumes are the only mechanism to move energy and mass into the upper layer of a room, and are formed only by the burning item(s) in the fire room and by a door jet of upper layer gases flowing through an opening. When warm, lower layer gases move through a low opening (e.g. the undercut of a door) by expansion, they are "trapped" in the lower layer of the room into which they flowed until the upper layer in the source room drops to the level of the undercut and the door jet forms. Thus, for a time the receiving room will show a lower layer temperature which exceeds the upper (a physically-impossible condition). Since the temperatures are low and no gases flow until the upper layer drops to the undercut, this should not present a problem for hazard analyses.

6. FAST is the only zone model which does not assume that room pressures remain constant. This allows FAST to track pressure fluctuations caused by transient phenomena and to work on room(s) which are not vented to the outside. Under some conditions, the door flows can become imbalanced (inflow exceeds outflow) for a significant time, causing the room pressures to rise and errors in species concentrations.

OCCUPANT BEHAVIOR AND EVACUATION: The EXITT model is a fairly-straightforward "node and arc" evacuation model to which an extensive series of behavioral rules has been added. The assumptions of interest are thus inherent in these rules, and the limitations are mostly associated with behavior not yet included. For example, the model does not have people re-entering the building, as they sometimes do. In addition, the current model is completely deterministic - a specific set of circumstances always results in a specific action. The data on which the rules were based sometimes identifies several potential actions (e.g. under this condition, 60% of the time they do A and 40% of the time they do B). This represents probabilistic branching, which will be implemented in the future.

Some of the rules are qualitative (e.g. a man's first action is to investigate) and some are quantitative (e.g. a woman between the ages of x and y walks at z meters per minute). The assumed values in quantitative rules are called parameter values, and the documentation for the model identifies each, the reason for assigning that value, and how the user can change it.

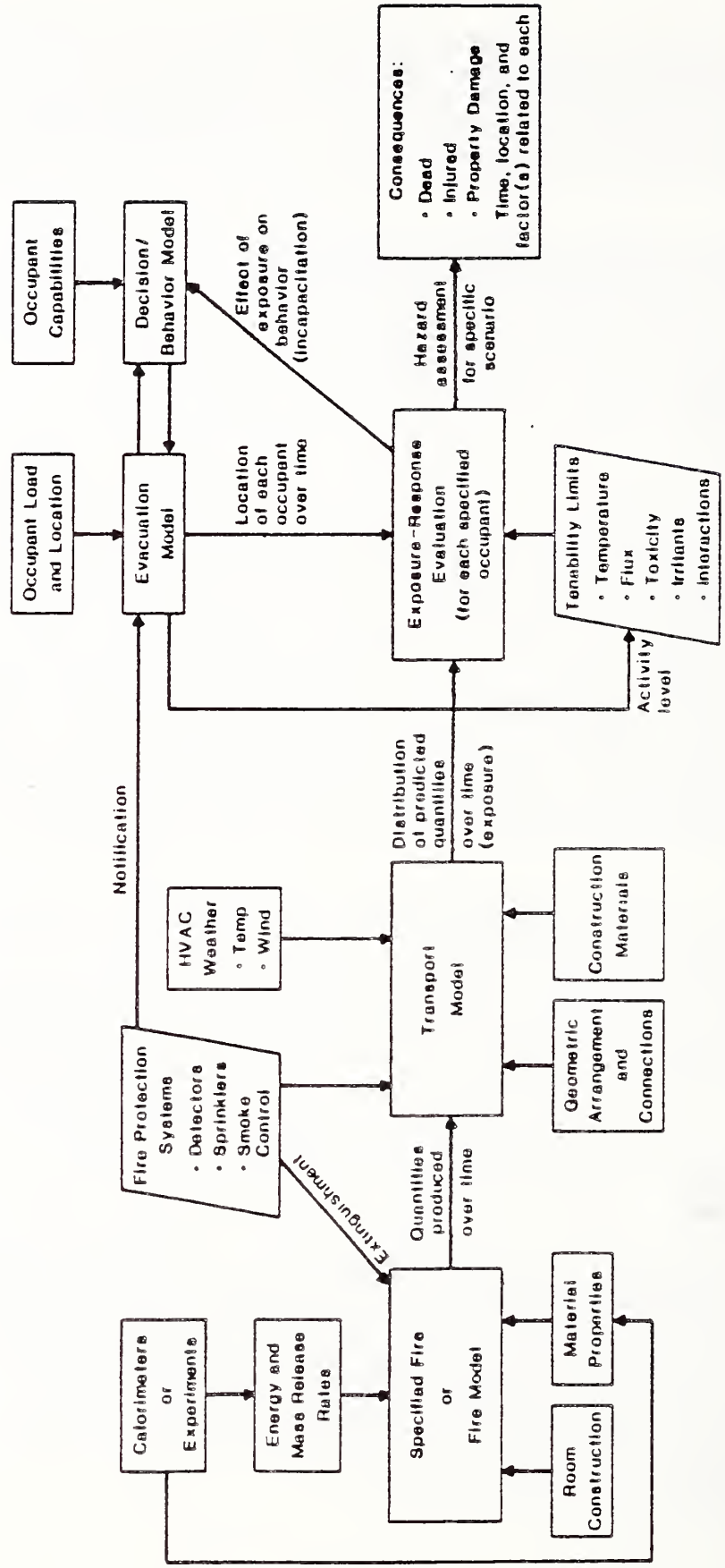
ACTIVATION OF THERMAL DEVICES: The activation of heat detectors or sprinklers is handled in the program DETACT. The report (included in an appendix to the HAZARD I report) describes the underlying theory and assumptions used. The basic assumption is one of quasi-steady ceiling layer gas flow under an unconfined ceiling (no walls). It is based on the experimental study done by Factory Mutual Research Corp. for the Fire Detection Institute and on which the NFPA 72E, Appendix C methods were developed.

TENABILITY CRITERIA: The evaluation of the impact of exposure on the occupants is done in the program TENAB. Individual determinations are done for both incapacitation and lethality from temperature and toxicity (both with a concentration-time product and a Fractional Effective Dose) along with potential incapacitation from burns due to flux exposure. No interactions are currently included (e.g. temperature exposure does not affect rate of uptake of toxic species). The basis for the threshold values used and the derivation of the equations in the FED calculation are provided in a chapter on Tenability Limits, which contains an extensive list of references. For all cases except flux exposure, the user can easily change the limit values used (and is encouraged to do so as a sensitivity test). Also, the method of presentation of the output of TENAB facilitates the observation of the sensitivity of the result to the value selected.

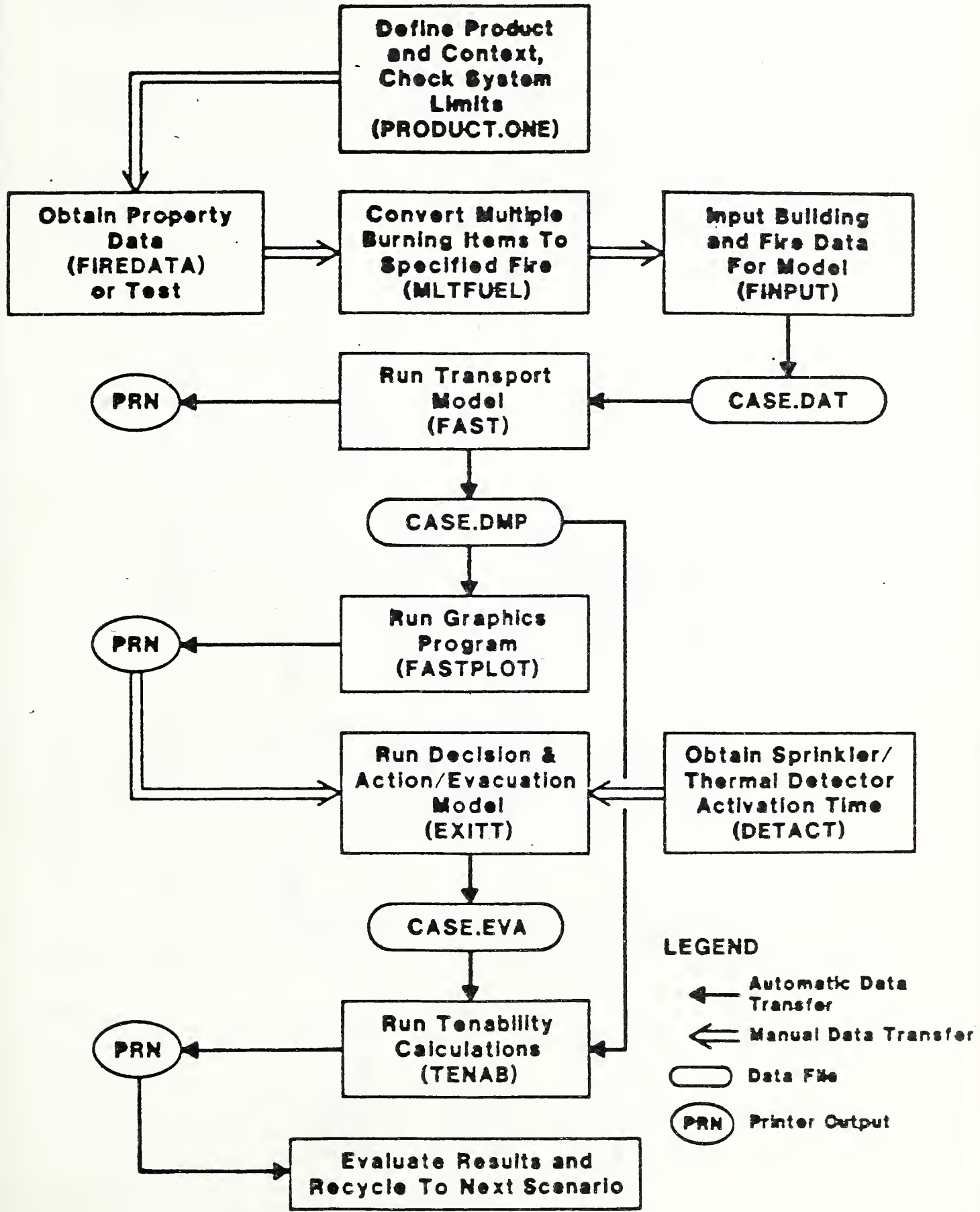
The limiting values for temperature are based on the general literature, which includes some human data. The flux criterion comes from work done with pig skin, which is generally held to be very similar to human skin (it is used for temporary grafts for burn patients). The toxicity data however, are from the body of combustion toxicology literature which is based entirely on animal exposures (primarily rodents). Thus, it must be assumed that humans will exhibit a similar physiological response to the exposure. Due to the difficulties of assessing the onset of incapacitation in an animal, the data used are primarily those where death was the end point. The values used for incapacitation are assumed to be half of the lethal level.

The Ct parameter is an attempt to include the toxic impact of the material without differentiating the constituent gases. This represents a broad assumption, and will not include the effect of diminished oxygen. The FED parameter is the first version of the N-Gas model, including the effects and interactions of the gases CO, CO₂, and HCN. Again, the effect of diminished oxygen is not included at this time. The N-Gas model is under continuing development, and additional gases will be added as the data are obtained. It is expected that oxygen and the first irritant gas (HCl) will be included in the next version.

FIGURE 1
 INTERRELATIONSHIPS OF MAJOR COMPONENTS OF A FIRE HAZARD MODEL



HAZARD I SOFTWARE



LEGEND

- ← Automatic Data Transfer
- ⇐ Manual Data Transfer
- Data File
- PRN Printer Output

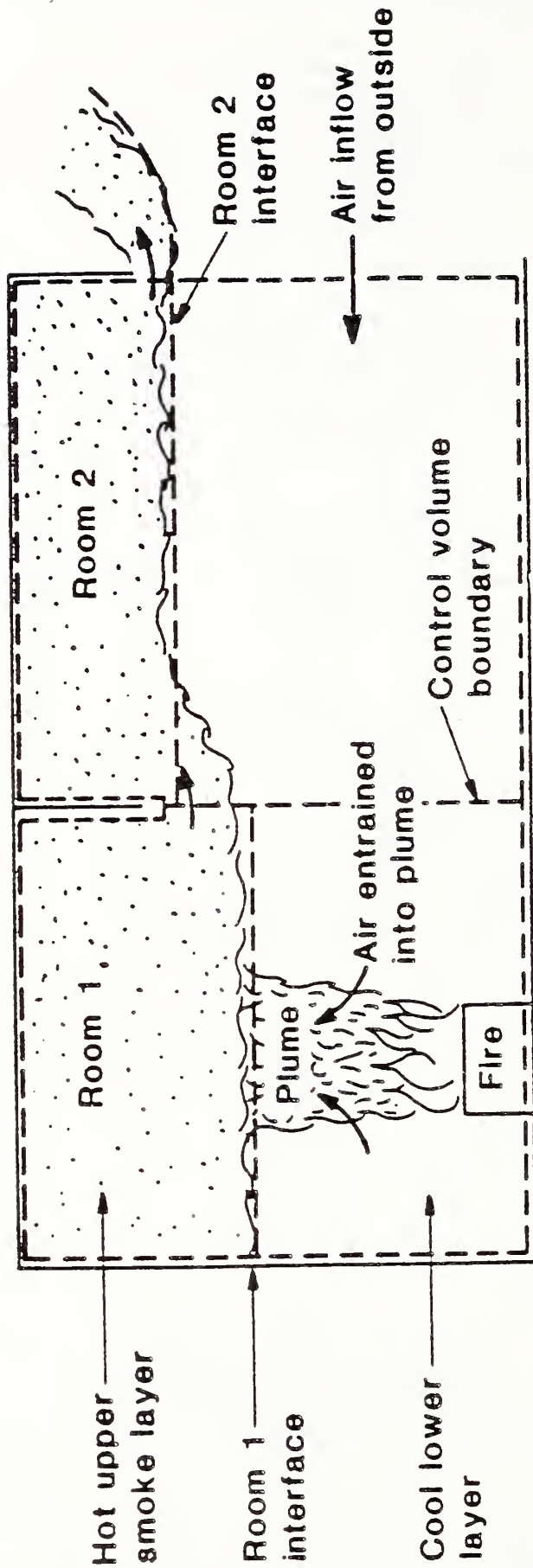


Figure 3. Schematic of upper and lower layer control volumes

A SUMMARY OF THE ASSUMPTION AND LIMITATIONS OF HAZARD ONE
R. Bukowski, given by H. Nelson, National Bureau of Standards, USA

WATTS: This model seems to have the same objective as the NFPA building fire simulation model that was written 10 years ago. How do the results of these two compare?

NELSON: I will answer your question obtusely. I believe the building fire simulation model is as good a frame for analysis as any other I have seen. However, I also feel that it didn't have scientifically sound methods for making its calculations; it was a frame awaiting methodology. As it was published, it used a regression analysis from a series of tests and/or experienced data. It was as valid as that data. Unfortunately, the data was extracted from a narrow series of residential and model home fires. Therefore, I felt it was extraordinarily limited.

If that's wrong, I invite anybody else to make their own comparison.

EMMONS: This is an excellent model which is still in its early stages, and it has obvious limitations, so we'd like to note that there are already models that could be used in place of the specified fire, and should be, I think, put in as selectable by the user, so that they may have a specified fire, or they select one that will predict the fire, and read them properly.

A final observation is somewhat more in the distant future; it is the fact that unless the improved fire growth model is included, one cannot begin to obtain real data based on rules. There are thousands of fires every year, in some of which persons die, and in a few of those we would know enough to develop buildings, the source of ignition, the growth of the fire, to be able to use the observed position about it to reduce the processes.

NELSON: And to test the human decisions too.

HALL: Your invitation on the comparison for BFSM, I think the contrast I would draw is that BFSM used a probabilistic format throughout, and it forced everything into that even if it was actually deterministic. This used a deterministic format throughout and forces everything into it even if it's probabilistic. It is as difficult to compare those as to compare Dr. Sekizawa's point score approach to this kind of modeling. The format differences are so great.

NELSON: I think that's an excellent picture.

SEKIZAWA: The question I have is, rather than determining the building itself and the hazards to the building, are there any thoughts which lean towards the content safety?

NELSON: Do you mean the impact of the contents on the safety of people?

SEKIZAWA: Yes.

NELSON: You cannot model without considering what is burning, and what is burning is contents.

SEKIZAWA: Then, in that case, who are you targeting to be the most prolific user for this model?

NELSON: I'll have to give my opinion. I believe the people who make furniture or wall linings, particularly those that make synthetic materials will wish or be forced to use this type of model to determine whether the hazard produced by their product is acceptable. Let me continue a moment. I believe that this system, HAZARD 1, will be applied to prototypical buildings to establish a baseline of hazard that is normally accepted in society, and then variables such as a new style of plastic or a new use of a material, will be entered in the system to find out the change in the overall hazard.

FIRE TOXICITY AND CHEMISTRY

PROGRESS REPORT

on
FIRE AND TOXICITY CHEMISTRY IN JAPAN

by
Hiroaki SUZUKI
Head, Smoke Control Division
Environment, Design & Fire Department
Building Research Institute
Ministry of Construction

1 Tatehara, Oho-Machi
Tsukuba-Gun, Ibaraki-Ken, 305
JAPAN

Studies of fire and toxicity chemistry have been pursued from the point of production of toxic gases from building materials, behavior of animal exposed to laboratory environment and to smoke from full scale fires in order to get lethal conditions of animal in toxic gases.

Researchers concerned with toxicity work in Japan are about 20 who belong to national research organizations, universities and laboratories under juridical foundations, etc. Some of them study independently and others cooperated each other under a project.

The project of combustion toxicity from building materials and interior goods in fires had been conducted for these 5 years since April 1982. This project has been supported by the Science and Technology Agency, Japanese Government and has covered the following subjects in corporation of research organizations and universities.

1. Establishment of combustion conditions
2. Burning tests in full-scale model rooms and in Laboratory test apparatus
3. Numerical analysis of burning procedures
4. Development of testing apparatus
5. Evaluation method of toxicity by animal exposure

The items of the results of the projects which have been conducted in these 2 years, are mentioned below.

- a) Burning behavior of building materials under fire conditions (1)
- b) Prediction methods of compartment fires in their early stages (2)
- c) Production of toxic gases in a semi full-scale compartment under forced air-control conditions (3)
- d) Application of burning conditions obtained from full-scale fire experiments to a test apparatus (4)
- e) Evaluation of toxicity of combustion products from textile (5)
- f) Toxicity test using mixed gases (6)
- g) Evaluation of combustion toxicity of building materials using a new testing apparatus (7)
- h) Toxicity effect of pure and mixed gases (8)
- i) Toxicity effects of combustion products to human bodies (9)
- j) Analysis of combustion products from fire treated wood (10)

- k) Combustion toxicity from foamed plastics (11)
- l) Incapacitation of mice exposed to combustion products generated in full-scale fire experiments (12)
- m) Evaluation of toxic gases from experimental fires in an existing building (13)

Some of these were reported in annual meetings of Architectural Institute of Japan and of Japan Association for Fire Science and Engineering as well as reported at the 5th Expert Meeting of the US-Japan-Canada Cooperative Research Group on Toxicity of Combustion Products from Building Materials and Interior Goods. The last 7 subjects are to be reported in the 9th Joint Panel Meeting UJNR Panel on Fire Research & Safety jointed with the 6th Expert Meeting of the US-Japan-Canada Cooperative Research Group on Toxicity of Combustion Products from Building Materials and Interior Goods.

Some papers which were not involved in the UJNR Joint Meeting and the Expert Meeting are summarized as follows.

K. Kishitani (14) et al exposed mice in the combustion products which generated in full-scale two storied wooden houses. Fire initiated in the living room on the first floor and spread rooms in the same floor and the upper along the staircase. Mice in a corridor on the second floor were incapacitated at 18 minutes and 43 seconds when the concentration of CO became suddenly high. The CO was 1.4% and temperature was higher than 98°C in the atmosphere. At another site, mice were incapacitated at 34 minutes and 33 seconds when CO became 0.7% and temperature became higher than 120°C.

In other case, mice were incapacitated at 39 minutes and 5 seconds when CO was 0.65% and temperature was higher than 60°C. In these full scale experiments mice seemed to be incapacitated not only caused by CO concentration but also high temperatures.

k. Kishitani et al (15) exposed mice, which were trained with electric shock and non-trained, to experimental conditions with various concentration of CO gas. In results, trained mice lost their knowledge. Heavier groups of mice in weight died in earlier time in the same concentration of CO (0.6% and 1.3%) than the lighter ones. This seemed that heavier group of mice needed more oxygen than the lighter.

M. Hirota (16) predicted the concentration of CO along with movement of smoke in the central staircase Using mathematical simulation in a 5-story-model building.

(References)

- (1) T. Tanaka, M. Yoshida and I. Nakaya: Burning Characteristics of Building Materials under Fire Conditions, (*1)
- (2) T. Yoshikawa, K. Kawagoe and T. Joh: Numerical Simulation of Early Stage of a Compartment Fire (*1)
- (3) T. Morikawa, E. Yanai: Toxic Gases Evolution from Air-Controlled Fires in A Semi-Full Scale Room (*1)
- (4) S. Yusa: Application of Burning Conditions Obtained from Full Scale Experiments to Labo-Scale Test Apparatus (*1)
- (5) M. Furuya: Evaluation of Toxicity on Combustion Gas from Fiber Materials (*1)

- (6) T. Sakurai: Toxic Gas Test by the Several Pure and the Mixed Gas (*1)
- (7) S. Yusa: Evaluations of Combustion Toxic from Various Materials by Newly Developed Apparatus (*2)
- (8) T. Sakurai: Toxic Gas Test by the Several Pure and Mixture Gases (*2)
- (9) Y. Tsuda and Y. Nishimaru: Human Effects of Poisoneous Gases Generated during Fire --- Especially, Presence of HCN and CO (*2)
- (10) T. Hirata and Sumire Kawamoto: Toxic Gases from Combustion of Wood Treated with Retardants (*2)
- (11) F. Saito and M. Yoshida: Combustion Behavior of Building Materials Using a Model Box with Air Supplied System (*2)
- (12) T. Tanaka and M. Yoshida: Incapacitation of Mice Exposed to Gases in Full-Scale Fire Tests (*2)
- (13) T. Morikawa and E. Yanai: Evaluation of Toxic Gases from Experimental Fires in an Existing Building (*2)
- (14) K. Kishitani, F. Kon, S. Sugahara, H. Sato, S. Yusa and S. Uesugi: Full-scale Fire Experiments Using Traditional Wooden Houses, Summaries of Technical Papers of Annual Meeting of Architectural Institute of Japan (1986)
- (15) K. Kishitani, M. Yun, S. Sugahara and K. Nishine: Experimental Studies on Physiological Effects by Combustion Products, Summaries of Technical Papers of Annual Meeting of Architectural Institute of Japan (1986)
- (16) M. Hirota: Application of Smoke Movement Model to Fire Safety Plan, Summaries of Technical Papers of Annual Meeting of Architectural Institute of Japan (1986)

(*1): The 5th Expert Meeting of the US-Japan-Canada Cooperative Research Group on Toxicity of Combustion Products from Building Materials and Interior Goods

(*2): The 9th Joint Panel Meeting UJNR Panel on Fire Research & Safety

Progress Report on
Fire Toxicity and Chemistry Research
in the United States

RICHARD G. GANN
Center for Fire Research
National Bureau of Standards
Gaithersburg, MD 20899

FIRE TOXICITY RESEARCH

The research directions discussed at the 8th Meeting of the U.S. Panel on Fire Research and Safety have been vigorously pursued during the past two years. These include generating the framework in which smoke toxicity measurements should be evaluated, developing the appropriate measurements to make, and reducing the dependence on animal testing for that purpose. A subsequent progress report was presented at the 5th Expert Meeting of the Tripartite Cooperative Study Group on the Toxicity of Combustion Products fourteen months ago.

Most recently, Researchers at the National Bureau of Standards have generated a large set of rat lethality data for CO, CO₂, and HCN for a range of exposure times. Staff at the Southwest Research Institute have completed studies on the toxicity of CO and HC(in air, as well as comparison with smoke from polyvinylchloride. A simplified version of the N-gas model has been incorporated in the prototype NBS fire hazard assessment method, HAZARD1, with an upgrade to be included in the next version.

A quick series of experiments coupling the Cone Calorimeter with the University of Pittsburgh animal exposure system was an engineering success. Further work is underway to determine the value of this approach to generating data for fire hazard models.

The Vinyl Institute, a division of the Society of the Plastics Industry, has completed a comprehensive study on the generation and decay of HC(in room fires. Two publications are in progress, and an integration of the results into the fire hazard models is in progress.

Forensic scientists at St. Johns University of New York, with the collaboration of NBS staff, are further refining the protocols and analytic methodology for determining HCN in blood.

NBS, with the support of the Consumer Product Safety Commission, has completed a first cut at developing the bases for comparing toxicity data from bench-scale tests with data from full-scale experiments. These preliminary results point the way for a second series of tests to be performed this summer.

The National Research Council's Committee on Fire Toxicology has issued its final report: Fire & Smoke: Understanding the Hazards. A second NRC panel, the Committee on Toxicity Hazards of Materials Used in Rail Vehicles, is dormant. A third NRC panel, Toxicity of Complex Mixtures, has incorporated results from toxicity studies of combustion atmospheres. That report is to be released soon.

While the research emphasis has been on developing input data for fire hazard assessment methods, the legislative concentration has been on stand-alone test methods. The State of New York has passed a regulation stating that all building products sold in the State must be tested for toxic potency using the University of Pittsburgh test method. Compliance is to be phased in over a four-year period. Since there may be as many as 10^6 different products to be tested, this action has started a sizable effort aimed at creating classes of products for representative testing. Since the first listing of products must be completed by December, 1987, new information on the progress in this area will be developing rapidly.

FIRE CHEMISTRY

Research in this area has been directed at understanding how polymeric materials burn and how their combustion leads to the formation of specific combustion products, e.g., soot and toxic gases.

Late in 1986, Gann, Drews and Dipert published a review chapter on polymer flammability. This discusses the fundamental concepts of materials burning, degradation and fire retardancy mechanisms, and current test methods.

Significant progress has been made in understanding the mechanisms of polymer gasification. Kashiwagi and co-workers at NBS have published several papers on the chemical degradation of and thermal profiles in burning poly(methylmethacrylate). Parker (NBS), Ohlemiller (NBS) and Atreya (Michigan State University) have studied the mechanisms of wood decomposition. Orloff and de Ris at Factory Mutual Research Corporation have studied correlations between concentrations of gaseous species produced by fires of varying size.

Studies of the effects of fire retardants (FR) on the thermal decomposition of polymers are also underway. Wilkie (Marquette University) is studying the chemistry of FR-promoted crosslinking in poly(ethyleneterephthalate). Starnes (Polytechnic University of New York) is investigating similar effects of copper compounds in poly(vinylchloride).

Soot formation is a central issue. There is a large effort in the U.S. to determine the chemistry involved in the nucleation of soot particles, the growth from C_1 molecules to species that inevitably lead to particles. Several complex chemical kinetic models have been proposed, mainly based on premixed flame data. A sizable data base on premixed flames has been obtained by Howard and co-workers at M.I.T. Recent research at NBS by Smyth and Miller has probed diffusion flames, allowing extension to the types of combustion prevalent in fires. Research at the United Technologies Research Center has investigated the effects of additives on soot yields.

Mulholland and co-workers have been studying the agglomerate structure of soot using transmission electron microscopy and computer simulation. Babrauskas and Mulholland have begun studying possible correlations between smoke yields and obscuration at bench- and full-scale.

Understanding the yields of carbon monoxide and other principal toxicants in fires is important for accurate fire hazard modeling. Tewarson at Factory Mutual Research Corporation and research staff at NBS are developing correlations for CO formation from the wealth of existing small- and large-scale data.

Canadian Overview

by

T.Z. Harmathy

Institute for Research in Construction, National Research Council of Canada
Montreal Road, Ottawa, K1A 0R6, Canada

Prepared for the 6th Canada-Japan-USA Trilateral Meeting

The staff of the Fire Research Section of the Institute for Research in Construction, National Research Council of Canada, consists of 11 professionals, 12 technical officers, 1 laboratory attendant, and 1 secretary. Of the 11 professionals 10 are research officers, and 1 is a guest worker.

The objective of the Fire Research Section is to provide research support to the effort of improving fire safety in buildings and reducing the cost of fire protection. This objective is achieved by 1) responding to the research needs of building product manufacturers, building designers, regulatory officials, and the fire services, 2) participating in the development of building codes and fire test standards, 3) building up basic information necessary for converting from the present regulation-based fire safety system to a knowledge-based system.

A significant portion of the Section's work is carried out in the National Fire Laboratory located in Almonte, Ontario, about 60 km from the NRCC campus. It is a national facility for conducting full scale studies of the characteristics of large fires, smoke control measures in tall buildings, and fire fighting techniques and equipment. The facilities are available on a contract basis to the private sector, government agencies and educational institutions for the development of new products, systems, and procedures.

The program of the Section for the 1987-88 fiscal year has not yet been approved. In its tentative form it consists of four programs:

- F3 - Fire Resistance of Building Elements and Assemblies
- F7 - Fire Performance of Materials and Products
- F8 - Hazard Assessment of Building Fires
- F9 - Fire Spread Via Exterior Walls

The four programs are subdivided into 18 projects. Two of the 18 projects are related directly to fire gas toxicity:

- F7.1 - Air quality in houses following a fire
- F7.2 - Rate of heat release and smoke

One other related project was completed in the 1986-87 fiscal year:

- F1.7 - Gaseous decomposition products of nitrogen-containing polymers

The following progress has been reported:

- F1.7 - A TGA/APCI/MS/MS system for the study of pyrolysis and combustion products was developed. Using that system, the pyrolysis of polyacrylonitrile was studied.

- F7.1 - Literature study was conducted on methods of odour control and on the composition of fumigants. Preliminary experiments were carried out. The purpose of the work is to establish criteria for the habitability of houses after fire incidents.
- F7.2 - The existing ASTM E906 heat release rate apparatus was modified to make it suitable for the test proposed by the Federal Aviation Administration (U.S.A.). Further changes in the FAA test method are expected. The test will yield information on the rate of heat release, and smoke and toxicity generated during the burning of materials used in forming the interior surfaces of aircrafts.

Several other projects of the Section overlap on the subject of smoke and toxicity: Volatile organic components in indoor air, Fully developed fires of plastics, Gas-phase combustion in fully-developed fires, and Development of facilities for a standard room-fire test.

INCAPACITATION OF MICE EXPOSED TO GASES IN FULL SCALE FIRE TESTS

by

Masashi YOSHIDA
and
Takeyoshi TANAKA

Building Research Institute
Ministry of Construction
1 Tatehara, Oho-machi, Tsukuba-gun
Ibaraki-ken 305, Japan

1. INTRODUCTION

Attempts are being made to develop the method to rationally evaluate the potentially toxic hazards of fire effluent gases due to burning of various materials in fire. The test methods to be incorporated into the evaluation methods of toxic hazards need to be laboratory scale ones in view of reproducibility, cost and labor. However, since the conditions of burning of materials can be different in many respects between small scale tests and real fires, the validity of the test and evaluation methods to be proposed need to be examined at least by some full scale fire test results. A series of experiments in which mice were exposed to the gases produced in full scale fire were conducted to contribute the data to the verification of toxicity test and evaluation methods.

2. TOXIC HAZARDS AND FIRE SCENARIOS

Once a fire breaks out, certain kinds of combustion products, which are more or less always harmful, are inevitably produced. Therefore, obviously, it is impossible to remove all the materials around us on the ground that they are potentially hazardous in the event of fire. If there is any material that needs to be rejected from the viewpoint of fire safety, it will be one which causes extremely toxic hazards. So, for clarity, we classify the hazards due to the toxicity of fire effluents into the two; (a) ordinary hazards and (b) extraordinary hazards, as follows:

- (a) ordinary hazards : the hazards caused by usual combustion products in fire, i.e. heat, oxygen depletion, carbon dioxide and, in a sense, carbon monoxide.
- (b) extraordinary hazards : the hazards caused by unusual combustion products.

As for ordinary hazards, we cannot help but suffer them, otherwise we have to sacrifice tremendous convenience we are enjoying from various kinds of organic materials. Only when the toxicity of the combustion products or the amount of the production of toxic products of a material is unusually high, we need to make the decision whether to allow or reject it considering the potential hazards in fire and the benefits in every day lives.

Another issue concerning toxic hazards due to fire effluents is the definition of the fire scenarios to be considered, i.e., on what situations of fire we should discuss the hazards of toxicity. As such scenarios, we assume that the following two are generally acceptable.

(fire condition)	(potential victims)
(i) Scenario(1) : a part of contents in the room of origin is burning.	residents in the room of origin(can be disabled, sleeping, etc.)
(ii) Scenario(2) : considerable part of the room of origin is involved in fire.	people outside the room of origin(can be evacuees, fire fighters, etc.)

In either scenario, we have to consider significantly cooled down gases, otherwise people will be killed almost in an instant by heat, but it is also important to note that the concentrations of ordinary gases in combustion product gases, e.g., oxygen and carbon dioxide, and the temperature are not independent each other in real fire since mixing with fresh air is thought to be one of the dominant mode of cooling of fire gases. One of the purpose of this series of experiments is to investigate the hazards of fire effluents under the existence of the heat of fire, which can never be disregarded in real fires.

3. EXPERIMENTS FOR SCENARIO (1)

3.1. Experimentals

3.1.1. Full scale fire test apparatus

BRI full scale fire test apparatus was used for the series of the experiments for Scenario (1). As shown in Fig.1, this apparatus has two rooms connected by a doorway. The materials were burned in the burn room. If the scenario(1) was literally interpreted the mice should have been exposed in the burn room, but they were exposed to the gases in the adjacent room because it was difficult to burn the building materials and still obtain the temperature acceptably low for the exposure in the burn room despite that the loading of material was not so large.

3.1.2. Fire source

The kinds of fuel burned in this series of experiments are as follows:

- a) Propane gas
- b) Yezo spruce (crib)
- c) Hard board (crib)
- d) Plywood (non-treated, crib))
- e) Plywood treated with 5% of DAP (crib)
- f) Plywood treated with 30% of DAP (crib)
- g) Wool carpet
- h) Nylon carpet
- i) Aclylo-Nitrile carpet

The propane gas was used as one of the fuels in an attempt to determine the reference level of toxic hazards since any unusual toxicant is not considered to exist in its combustion products, in other words, only usual products are supposed to be responsible for the hazards. On the other hand, if any unusually toxic gas is produced from the burning of a realistic material, it will cause shorter incapacitation time of mice.

3.1.3. Method of exposure

The mice are exposed to the combustion product gases at three positions of different heights as shown in Fig.1. The temperature and the concentrations of O₂, CO₂ and CO were measured at the positions of exposure. Typical examples of the measured temperature and the gas concentrations at a point are shown in Fig.3 for the cases of propane gas source and a realistic fuel. As can be seen from the example in this figure, while the temperature and gas concentration histories of propane fire exhibit almost steady state conditions at the exposure points after certain time elapsed, those for a realistic fire could hardly get such conditions.

So, monitoring the temperature of the exposure positions and deciding the appropriate time, the mice in the rotary cages as shown in Fig.2. were inserted into the three positions.

3.2. Experimental Results

3.2.1. Results of experiments

The incapacitation times of mice at each position in each experiment are shown in Table 1. The test conditions and the average temperature and gas concentrations are also given in Table 1.

3.2.2. Reference hazard level

The incapacitation times of mice exposed to the gases of propane fire are plotted versus the average temperatures of exposure in Fig. 4. As can be seen in this figure, some extent of dispersion is observed among the data, so it was thought that the incapacitation time cannot be fully explained in terms of temperature alone although most influential. So, assuming an equation similar with Harber's law but slightly modified by adding the factor on CO₂ concentration as follows:

$$(a \times (T - T_0) + b \times (C - C_0)) \times (t - t_0) = \text{Const} \quad (1)$$

where T : temperature
C : concentration
t : time

a regression technique was applied to yields the coefficients in Eqn.(1), i.e., a, b, T₀, C₀, t₀ and Const, so as to best fit the test results for propane fire. Only the CO₂ concentration data were used in obtaining the coefficients as the gas concentration data since the O₂ depletion and the CO₂ increase are so closely coupled that either gives similar results and CO concentration was negligibly low. The result of the best fit regression is shown by the solid line in Fig. 5.

3.2.3. Incapacitation time by the gases from realistic materials

The results of incapacitation times by fire effluents of realistic materials are shown in Figs. 6(a), (b), (c). It follows that a material is more hazardous than propane gas if the plots for the material lie below the reference line, but unexpectedly we could not find a material clearly more hazardous than the reference level. This may be partly because the mice were exposed to the atmosphere more or less at declining stage in the case of realistic fuels, but some other factor such as the concentrations of H₂O might have been involved in the results. If we compare the results for carpets, which are synthetic materials, with those for Yezo spruce, a natural wood, any notable difference cannot be observed. This seems to indicate that

the incapacitation of mice are determined almost by the usual causes of hazard i.e. heat, CO₂, O₂ depletion and such. The same is true with the other kinds of wood products except that the plywood treated with 30 % DAP may be somewhat more dangerous than the others.

4. EXPERIMENTS FOR SCENARIO(2)

4.1. Experimentals

4.1.1. Full scale fire test apparatus

For the series of experiments for scenario (2), the full scale fire test facility was modified as shown in Fig. 7. The opening of the burn room was narrowed to simulate ventilation controlled fires. The fire effluents flowing out through the opening was led to the flow channel set up outside the facility. The flow channel has three weirs implemented to change the temperature and the concentrations of gases along the channel by entraining fresh air at each weir.

4.1.2. Fire source

The materials burned as the fuels in this series of experiments are as follows:

- a) Propane gas
- b) Yezo spruce (crib)
- c) Plywood (non-treated, crib)
- d) Insulation board (crib)
- e) Hard board (crib)
- f) Particle board (crib)
- g) Phenol foam (crib)
- h) Isocyanurate foam(crib)

These materials were burned in the form of cribs except propane gas. Since the opening of the burn room was limited, most of the experiments were run under ventilation controlled condition.

4.1.3. Method of exposure

The mice were exposed to the gases at three positions on the flow channel at certain time after ignition, which was decided to be appropriate for the exposure judging from the temperature. As in the experiments for the scenario (1), the temperature and the concentrations of O₂, CO₂ and CO are measured at the positions of exposure and the movements of the mice were monitored by the rotation of mouse cages.

4.2. Experimental Results

4.2.1. Results of the experiments

Examples of the history of the temperature and the concentration of gases at a position of exposure are shown in Fig. 8. It can be seen in the examples that while the CO concentration for propane source is insignificant, that for a realistic material is considerably high. The results of the incapacitation time of the mice are shown in Table 2 together with the test conditions and the average temperature T and concentrations C of the gases, which were calculated as:

$$T = \frac{\int_{t_1}^{t_2} T dt}{t_2 - t_1} \quad \text{and} \quad C = \frac{\int_{t_1}^{t_2} C dt}{t_2 - t_1} \quad (2)$$

where T : temperature at the position of exposure
C : concentration of a gas at the position of exposure
t₁ : time at which exposure starts
t₂ : average time at which the mice ceased to rotate cages

4.2.1. Reference level of hazard

The incapacitation times of mice for propane fire source are plotted versus the average exposure temperatures in Fig. 9. The dispersion of the data does not appear so significant. The solid line indicates the best fit regression curve of the incapacitation time as a function of temperature alone.

4.2.2. The incapacitation time by fire effluents from realistic materials

The incapacitation times of the mice exposed to the effluents of the realistic materials are shown in Figs. 10(a), (b), (c). It can be seen that the times of incapacitation for the realistic materials are consistently shorter than those for propane fire. On the other hand, as can be seen in Fig. 10, the difference of the incapacitation times among most of the realistic materials are not remarkable although phenol foam and isocyanurate foam may be significantly more toxic than the others. In interpreting this result, it should be kept in mind that this series of experiments were mostly conducted under ventilation controlled condition and by this reason, not negligible amount of CO was yielded because of the incomplete combustion in the case of the realistic materials, while in the case of propane fire CO yield was not so significant. The effects of CO is suspected to have been important in shortening the incapacitation times for realistic materials although we have not analyzed the data in detail.

5. CONCLUDING REMARKS

Some data of the incapacitation times of mice exposed to the fire effluents of full scale fire tests were obtained. With the limitation of the apparatuses for gas analysis, the analyses of complex gases could not be made so the data may not be sufficient for constructing a method to evaluate toxic hazard of materials. However, it is felt that the hazards due to usual products of combustion can never be neglected, in particular, heat may play very important role in threatening human life in usual fire conditions. As long as this series of experiments are concerned, heat seemed to be most dominant cause of the incapacitation of the mice, although very unusual materials were not tested. More thorough studies are necessary before a solid conclusion is drawn.

Table 1 Incapacitation time and exposure condition of the mice (scenario(1))

NO	Materials	Weight (kg)	Ignition source Alcohol	Opening (cm)	Weight loss (kg)	M.P	Mouse								NO	7		AVE	*2)		AVE	-S.D
							1	2	3	4	5	6	7	8		S.D	*2)					
1	Propane Gas	10g/m		90		U	1.9	1.7	0.7				1.8	1.6	1.3	1.8	1.54	0.42	1.12			
2		12g/m		90		M	2.5	2.2					2.6	2.3	2.5	2.6	2.47	0.16	2.31			
3		6g/m		90		D	4.8	4.9	4.9						4.6	5.1	5.02	0.42	4.60			
4	Yezo spruce	4kg		90	2.5	U	5.1	4.7	5.1				4.3		4.7	5.2	4.84	0.32	4.52			
5		4.5kg		30	2.9	M	7.2	7.4	7.5				7.3		8.0	6.8	7.33	0.34	6.99			
6		4.75 kg		30	3.1	D	13.0	13.9	13.3						12.8	13.1	12.69	1.29	11.40			
7		4.7kg	0.6	30	2.9	U	16.0	13.2	15.0						14.2	13.0	14.56	1.48	13.00			
8		4.6kg	0.7	30	2.8	M	30.8	35.3	31.9						27.5	36.1	32.89	5.80	27.09			
9	Plywood	3.2kg	0.6	30	1.9	D	L	L	L						L	L*	L					
10		3.1kg	0.6	30	1.9	U	L	L	L						L	L	L					
11		3.3kg	0.6	30	1.9	D	6.9	5.3							6.0	3.1	3.50	0.32	3.18			
12	PWT-5X	2.9kg	0.6	30	1.53	M	6.4	6.5	9.1				8.6		7.8	12.5	9.05	2.38	6.67			
13		2.8kg	0.6	30	1.55	U	L	L	L						19.0	7.4	7.43	0.99	6.44			
14	PWT-30X	4.2kg		30		D	L	L	L						L	L	16.60	3.39	13.21			
						U	23.2	23.7	24.2						L	L	24.1	0.55	23.6			
						M	24.3	25.3							24.2	25.0	24.7	0.59	24.1			
						D	24.5	26.0	26.9						25.1	25.7	25.8	0.91	21.9			
						U	45.4	46.0	46.4						44.5	45.1	45.4	1.10	44.3			
						M	49.9	49.4	49.3						49.6	49.1	49.4	0.61	48.8			
						D	60.9	62.1	L						64.7	63.0	64.2	2.31	61.9			
						U	21.6	21.7	21.4						22.2	22.9	22.1	0.59	21.5			
						D	26.0	27.8	24.7						24.4	27.0	25.3	1.52	23.8			
						U	37.4	38.6	37.4						40.1	39.2	38.5	1.00	37.5			
						M	41.9	42.4	41.6						45.7	42.9	42.5	1.52	41.0			
						D	56.3	43.7	43.2						46.3	53.4	48.7	5.01	43.7			
						U	25.1	26.7	26.3						26.9	26.3	26.2	0.59	25.6			
						M	29.9	28.5							29.7	30.0	29.9	0.79	29.1			
						D	34.7	30.5	54.7						37.4	L	40.1	8.68	31.4			
						U	20.7	20.1	20.1						35.2	20.0	20.3	0.29	20.0			
						M	22.1	22.4							20.4	20.6	20.3	0.29	20.0			
						D	25.2	26.0	26.8						24.6	18.8	22.2	1.76	20.4			
						U	24.5	24.3	24.7						25.8	23.6	25.4	1.16	24.2			
						M	24.5	29.9	26.9						24.5	23.7	24.3	0.37	23.9			
						D	27.3	31.7	33.4						26.7	30.4	27.4	2.29	25.1			
						U	19.9	L	17.4						81.7	34.1	47.0	27.20	19.8			
						M	L	L	L						L	24.5	20.48	3.71	16.77			
						D	L	L	L						L	L	L					

3) L-Life

2) S.D=Standard Deviation

1) M.P=Mouse Position
 U=1.5H from the floor
 M=0.9H from the floor
 D=0.3H from the floor

Table 1-2

NO	Materials	Weight (kg)	Ignition source Alcohol	Opening (cm)	Weight Loss (kg)	M.P.	House										AVE -S.D
							1	2	3	4	5	6	7	8	AVE	S.D	
15		4.0kg	—	30	3.17	U	2.2	2.5	3.3	3.1	—	2.0	2.7	2.9	2.79	0.37	2.62
						M	4.3	3.9	—	3.9	3.7	3.7	2.1	3.3	3.56	0.71	2.85
						D	3.5	5.2	4.9	3.0	3.1	2.6	2.6	3.5	3.65	0.97	2.60
16	Hard board	3.5kg	0.6	30	2.08	U	24.8	24.2	24.7	—	25.8	25.2	25.3	24.7	25.0	0.52	24.5
						M	25.2	26.0	26.3	26.2	26.7	28.2	28.3	25.4	26.5	1.16	25.3
						D	35.6	40.0	39.7	40.9	45.3	—	43.7	42.2	41.2	3.11	38.1
17		3.6kg	0.6	30	2.18	U	47.2	47.3	46.7	—	47.1	42.6	47.3	—	46.4	1.06	44.5
						M	50.2	50.0	—	48.7	49.9	53.0	49.1	51.6	50.4	1.48	48.9
						D	57.5	55.7	54.5	55.0	57.6	54.2	56.8	55.8	55.9	1.31	54.6
18	Nylon Carpet	2.5kg	—	30	1.83	U	13.9	10.4	11.2	12.4	—	12.9	11.9	—	12.12	1.24	10.86
						M	19.0	13.4	12.2	14.0	18.4	23.1	16.7	14.9	16.44	3.63	12.77
						D	26.4	23.4	23.4	22.6	28.9	27.8	—	15.7	24.03	4.39	19.64
19		3.2kg	—	30	2.25	U	—	14.7	—	14.7	—	—	—	3.6	4.33	0.64	3.69
						M	—	18.7	—	18.4	—	—	—	17.0	8.03	0.91	7.12
						D	16.8	14.9	—	—	9.3	1.1	—	13.7	13.68	3.18	10.50
20		4.2kg	2.6	30	2.35	U	27.6	29.5	29.4	—	29.5	29.4	29.4	28.7	28.7	1.29	27.4
						M	30.7	30.3	31.0	29.5	30.5	29.1	30.5	28.2	30.0	0.99	29.1
						D	32.6	31.7	32.6	30.3	31.0	30.4	32.6	31.4	31.6	0.97	30.6
21		3.8kg	1.0	30	1.88	U	38.3	39.0	37.3	—	39.6	37.7	37.7	37.7	38.3	0.82	37.5
						M	40.5	41.7	44.8	42.5	45.8	42.9	42.6	43.8	43.1	1.69	41.4
						D	47.9	54.0	50.2	57.9	57.5	69.8	65.9	52.1	57.0	7.58	49.4
22	Aclylo-Merfle Carpet	3.2kg	1.0	30	1.68	U	20.4	21.1	21.0	—	21.7	21.0	21.0	21.0	21.0	0.38	20.6
						M	27.2	27.5	25.1	24.1	26.5	25.9	26.7	26.6	26.2	1.13	25.1
						D	30.7	31.7	36.9	31.7	36.5	37.7	32.3	32.0	33.7	2.83	30.9
23		2.6kg	0.7	30	1.47	U	16.3	23.1	23.5	—	23.5	23.5	23.6	23.5	22.4	2.71	19.7
						M	32.7	40.5	40.0	35.2	39.6	29.0	33.5	48.4	37.4	6.03	31.4
						D	69.7	1.1	1.1	57.2	—	1.1	1.1	1.1	63.5	8.81	54.7
24		2.8kg	(0.7)	30	1.17	U	67.4	81.2	74.4	—	70.9	74.5	74.5	74.5	74.3	5.12	69.2
						M	—	1.1	1.1	1.1	1.1	1.1	1.1	1.1	1.1	—	—
						D	—	1.1	1.1	1.1	1.1	1.1	1.1	1.1	1.1	—	—
25	Wool Carpet	3.6kg	(1.0)	30	1.70	U	26.6	26.7	26.1	—	27.5	26.0	26.5	26.1	26.5	0.52	26.0
						M	41.8	—	28.1	34.2	34.4	30.8	31.5	30.9	33.1	4.40	28.7
						D	48.2	58.0	49.9	63.2	58.4	43.8	54.5	54.8	53.9	6.27	47.6
26		3.4kg	0.7	30	1.28	U	21.4	22.2	21.6	—	24.0	20.4	21.7	22.3	21.9	1.10	20.8
						M	24.3	25.3	—	25.5	26.2	25.6	25.2	25.2	25.3	0.62	21.7
						D	30.4	31.0	32.3	31.0	31.5	33.6	32.8	33.8	32.1	1.27	30.8
27		3.6kg	0.8	30	1.53	U	20.7	21.1	20.8	—	21.4	20.9	21.4	20.9	21.0	0.28	20.7
						M	26.0	26.4	23.0	24.7	26.1	26.6	26.6	26.6	25.8	1.28	24.5
						D	37.9	34.7	32.0	40.5	35.9	38.1	37.6	33.3	36.3	2.81	33.5

Table 2 Incapacitation time and exposure condition of the mice (acenario(2))

Materials	Material loading (kg)	Opening W-Width H-Height (cm)	*1) E.P	Average gas concentration		Average Temp (°C)	Incapacitation time of mice											
				CO %	CO ₂ %		0 ₂ %	1	2	3	4	5	6	7	8	AVE		
Propane gas	150 g/M	30W	G1	0.09	0.79	1.35	71.5	5.5	6.5	6.9	5.6	5.6	6.0	4.3	6.3	5.9	30403	
		9511	G2	—	0.74	0.46	49.8	17.7	16.0	17.4	16.0	17.7	16.1	—	—	15.6	16.6	30502
	150 g/M	30W	G1	0.1	0.86	1.55	61.4	6.1	28.4	7.6	7.7	7.7	5.4	6.0	8.0	6.9	30502	
		9511	G2	—	0.76	0.83	42.2	L	25.6	L	—	—	14.4	17.1	L	19.4	19.4	30502
	200 g/M	30W	G1	0.13	1.07	1.95	75.2	3.0	3.5	3.2	3.7	3.7	4.1	3.1	3.3	3.4	30504	
		9511	G2	—	0.87	1.10	55.1	0.4	7.6	8.4	7.8	7.8	7.8	7.6	7.6	6.7	7.8	30504
	300 g/M	30W	G1	0.12	1.32	2.07	80.4	2.9	11.9	14.2	11.7	11.7	12.7	12.0	12.5	12.3	30505	
		9511	G2	—	1.03	1.23	60.8	6.0	6.0	5.5	3.7	3.7	3.9	3.1	3.5	3.3	30505	
	100 g/M	30W	G1	0.03	1.37	2.47	59.4	0.3	5.6	5.5	7.5	7.5	7.7	7.8	8.4	6.1	7.6	30602
		5511	G2	—	1.14	1.65	47.7	—	11.8	10.0	—	—	9.0	12.0	10.5	6.2	5.5	30602
	150 g/M	30W	G1	0.05	1.07	2.86	66.6	4.1	4.1	3.9	4.1	4.1	4.2	4.3	7.9	3.9	4.1	30702
		5511	G2	—	1.41	—	53.5	7.2	7.0	7.3	7.3	7.3	8.1	14.0	17.3	7.6	7.5	30702
200 g/M	30W	G1	0.32	1.84	3.46	65.5	4.0	4.5	3.8	4.4	4.4	4.5	5.2	4.6	4.8	4.5	30703	
	5511	G2	0.25	1.61	3.13	53.2	5.1	5.7	—	—	—	6.0	—	6.4	—	5.8	30703	
200 g/M	30W	G1	0.27	1.87	3.52	69.0	3.9	13.4	11.5	9.8	9.8	8.6	14.0	12.5	14.0	11.7	30704	
	5511	G2	0.23	1.61	2.70	55.5	6.2	5.7	6.0	4.7	4.7	4.5	4.7	4.6	7.0	6.4	30704	
Yexo spruce	23 kg	30W	G1	0.04	2.59	2.81	73.3	2.9	3.1	3.1	3.0	3.0	3.9	3.5	3.5	3.2	31001	
		9011	G2	0.03	(2.81)	2.36	60.3	5.0	6.3	4.5	—	—	5.5	5.0	5.0	4.0	5.1	31001
	24.4kg	30W	G1	0.25	3.25	3.51	74.9	—	2.4	2.7	2.9	2.9	3.1	3.2	—	3.0	2.9	31002
		9011	G2	0.19	3.36	2.89	62.0	3.9	4.1	4.0	—	—	3.7	4.1	4.3	4.9	4.1	31002
	23.4kg	30W	G1	0.04	1.84	2.15	51.9	9.0	10.0	7.6	9.8	9.8	7.3	7.4	8.0	6.8	8.2	31003
		6011	G2	0.03	1.17	0.88	41.3	—	6.6	6.2	6.5	6.5	6.6	6.3	6.4	6.4	6.4	31003
	25 kg	30W	G1	0.13	2.12	0.81	33.6	—	L	L	L	L	L	L	L	L	L	31101
		6011	G2	0.07	1.25	1.25	38.7	7.0	9.6	8.7	9.1	9.1	10.2	6.6	9.3	—	19.1	19.1
				G3	(0.06)	1.03	29.7	L	L	L	L	L	L	L	L	L	L	31101

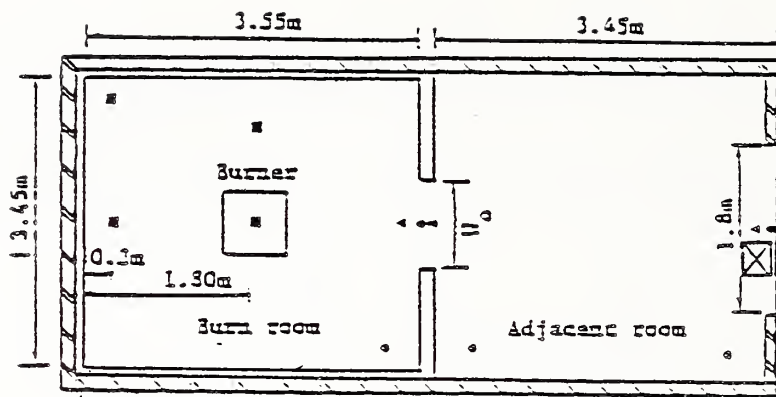
1) E.P-Exposure position

Table 2-2

Material	Material loading (kg)	Opening H-Width II-Height (cm)	E.P	Average gas concentration			Average Temp (°C)	Incapacitation time of mice								AVB		
				CO %	CO ₂ %	O ₂ %		1	2	3	4	5	6	7	8			
																	0	
Plywood	22.5kg	30W 60H	G1 G2 G3	0.07 0.06 (0.04)	1.51 (1.81) 1.05	1.70 1.46 0.91	45.2 40.8 36.1	1	25.2	12.8	12.8	11.6	13.4	12.0	21.6	17.5	11.9	
								2	22.4	28.0	—	35.5	24.4	—	24.0	—	25.9	
								3	36.1	—	—	—	—	—	—	—	—	—
	40 kg	30W 60H	G1 G2 G3	0.21 0.09 (0.04)	2.25 2.30 1.29	2.51 1.81 1.15	59.7 48.3 40.4	1	18.4	7.5	6.4	6.0	7.2	7.0	5.4	6.5	6.6	
								2	17.1	—	—	16.2	17.1	17.5	16.3	17.1	16.3	17.1
								3	40.4	—	—	—	—	—	—	—	—	—
	49 kg	30W 60H	G1 G2 G3	0.11 0.07 (0.04)	2.04 1.67 1.34	2.01 1.67 1.34	41.3 37.4 37.4	1	16.1	16.6	17.2	17.1	16.2	15.9	14.1	17.6	16.4	
								2	23.4	25.7	25.4	25.7	25.3	25.8	25.2	25.2	25.2	
								3	37.4	34.9	34.9	43.2	49.3	41.2	46.1	42.8	42.8	
	64 kg	30W 60H	G1 G2 G3	0.17 0.08 (0.05)	2.18 2.02 1.51	2.51 1.62 1.35	43.9 38.8 37.2	1	14.9	13.5	17.1	16.9	15.7	15.3	17.1	13.3	15.5	
								2	42.8	—	—	42.9	44.8	—	42.9	43.1	43.1	
								3	37.2	61.0	59.5	65.4	62.6	62.1	63.9	61.7	61.7	
69 kg	30W 60H	G1 G2 G3	0.16 0.10 (0.06)	2.04 1.82 1.50	1.96 1.49 1.41	31.6 31.4 34.8	1	28.1	27.0	27.3	28.4	47.0	46.9	22.9	26.7	26.7		
							2	39.0	46.4	—	63.9	—	—	38.9	41.6	41.6		
							3	34.8	66.4	63.1	66.9	67.0	65.1	—	—	—		
Insulation board	20 kg	30W 60H	G1 G2 G3	0.03 0.02 (0.02)	2.01 (2.28) 0.99	2.23 1.90 —	46.3 41.8 (21.8)	1	—	9.9	10.2	9.6	10.2	9.2	9.5	10.5	9.9	
								2	16.5	16.9	15.9	—	17.0	16.3	16.4	17.2	16.6	
								3	21.8	—	—	—	—	—	—	—	—	—
	40 kg	30W 60H	G1 G2 G3	— — —	2.79 — 2.32	3.39 — 2.06	57.1 46.9 44.7	1	3.8	4.9	5.8	5.6	4.7	3.8	5.0	4.2	4.7	
								2	9.4	11.4	10.1	10.4	10.6	11.1	11.2	8.8	10.4	
								3	17.9	14.4	17.2	20.0	17.5	21.4	21.4	18.3	18.5	
	20 kg	30W 60H	G1 G2 G3	0.42 0.31 (0.14)	2.63 2.36 1.32	3.15 2.15 1.40	41.0 36.0 —	1	4.9	5.4	4.7	3.4	4.2	4.3	4.9	4.0	4.5	
								2	6.4	6.7	8.2	—	7.7	7.2	6.1	4.9	6.7	
								3	—	12.1	—	—	11.2	—	—	—	—	—
40 kg	30W 60H	G1 G2 G3	0.12 0.14 (0.14)	2.65 2.73 2.19	3.03 2.36 1.92	55.9 46.0 42.5	1	5.1	6.2	6.4	6.2	6.0	6.0	6.2	—	6.0		
							2	12.4	12.4	12.0	12.3	12.9	12.5	12.2	12.4	12.4		
							3	15.5	16.2	15.0	21.4	19.0	23.0	17.0	20.1	18.4		
40 kg	30W 60H	G1 G2 G3	0.55 0.38 (0.29)	3.80 3.70 2.93	4.54 3.42 2.09	79.0 58.0 52.6	1	—	2.3	2.4	2.5	—	2.2	—	2.3	2.3		
							2	4.2	4.1	3.5	3.4	4.0	4.1	3.7	3.0	3.8		
							3	5.7	6.1	6.4	5.9	7.0	6.3	7.9	6.5	6.5		
Hard board	20 kg	30W 60H	G1 G2 G3	0.02 0.02 0.01	2.04 1.77 1.30	2.18 1.38 0.98	42.5 31.0 29.6	1	16.8	17.0	19.0	22.1	21.0	17.7	—	18.8		
								2	—	—	—	—	—	—	—	—	—	
								3	—	—	—	—	—	—	—	—	—	
	40 kg	30W 60H	G1 G2 G3	— — —	2.36 — (—)	2.60 — —	48.7 — —	1	8.6	8.6	8.5	7.6	9.6	8.1	7.9	9.7	8.6	
								2	21.5	21.5	21.9	21.1	21.5	21.5	21.5	18.8	21.2	
								3	29.4	31.0	33.3	34.0	31.1	31.5	36.4	31.5	32.7	
40 kg	30W 60H	G1 G2 G3	— — —	2.65 — (—)	2.81 — —	56.1 46.4 —	1	4.7	—	6.4	6.4	6.0	5.4	6.3	6.7	6.0		
							2	11.1	11.9	11.9	13.2	12.3	11.3	12.2	12.0	12.0		
							3	19.5	—	20.2	22.5	21.3	20.7	23.7	21.0	18.5		

Table 2-3

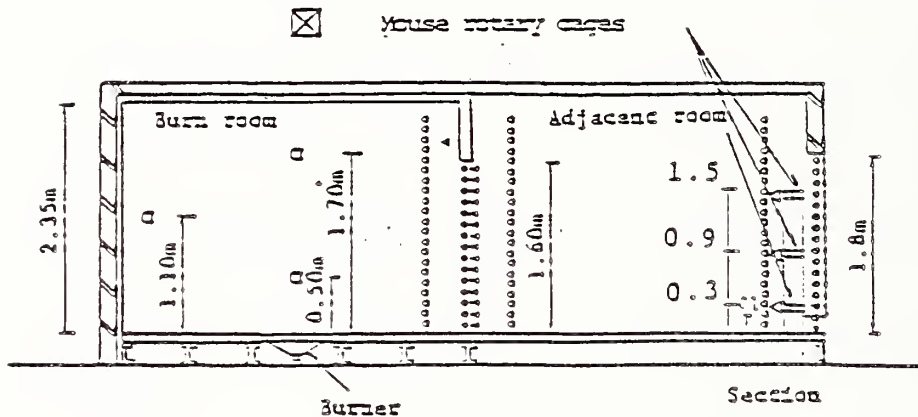
Materials	Material Loading (kg)	Opening W-Width H-Height (cm)	E.P	Average Gas concentration			Average Temp (°C)	Incapscitation time of mice								AVE
				CO %	CO ₂ %	O ₂ %		1	2	3	4	5	6	7	8	
Particle board	60 kg	30W 60H	61	0.05	2.17	2.57	55.0	6.3	6.1	6.3	6.0	7.1	7.1	6.5		
			62	0.06	2.55	2.18	46.0	9.9	10.0	9.9	11.2	9.8	10.4	10.1		
			63	—	2.00	2.14	55.3	14.1	15.6	13.2	14.6	15.9	16.2	15.0		
	60 kg	30W 60H	61	0.06	2.11	2.43	45.6	11.7	11.6	11.5	12.8	11.5	12.0	11.9		
			62	0.06	2.34	1.97	40.2	20.1	20.8	—	20.3	20.9	20.7	17.4		
			63	(0.09)	1.56	1.68	39.7	30.7	27.4	32.0	30.4	32.9	35.7	31.2		
Phenol foam	20 kg	30W 60H	61	0.01	1.31	1.43	37.8	1.1	1.1	43.7	1.1	43.6	45.0	43.9		
			62	0.03	1.38	1.06	29.8	1.1	1.1	1.1	1.1	1.1	1.1	1.1		
			63	0.02	0.95	0.02	25.7	1.1	1.1	30.6	1.1	1.1	1.1	1.1		
	40 kg	30W 60H	61	0.05	1.45	1.61	40.1	30.0	26.9	—	32.1	28.2	29.9	29.6		
			62	0.04	1.05	1.30	36.7	53.4	54.2	—	52.2	50.0	49.3	51.6		
			63	0.03	0.98	1.05	34.0	1.1	1.1	1.1	1.1	1.1	1.1	1.1		
	60 kg	30W 60H	61	0.10	1.83	1.98	40.9	16.2	17.3	16.2	18.4	16.2	18.0	17.1		
			62	0.07	1.17	1.66	30.4	33.3	35.6	—	32.6	37.2	34.6	34.7		
			63	0.06	1.24	1.35	37.5	55.5	51.1	54.6	51.8	—	—	50.9		
Isocyanurate foam	10 kg	30W 60H	61	0.21	2.27	3.18	46.2	6.7	6.0	5.7	6.9	4.2	4.8	6.1		
			62	0.12	2.19	2.01	42.0	1.1	37.2	—	18.7	20.5	1.1	17.4		
			63	0.08	0.80	1.28	34.0	1.1	1.1	1.1	1.1	1.1	1.1	1.1		
	20 kg	30W 60H	61	0.36	2.45	3.01	39.6	5.7	8.0	7.9	8.3	6.9	8.1	7.6		
			62	0.18	1.97	2.23	40.1	24.1	26.6	—	—	24.1	—	23.2		
			63	0.10	1.03	1.22	—	1.1	1.1	1.1	1.1	1.1	1.1	1.1		
	20 kg	30W 60H	61	0.52	2.75	3.91	45.7	5.2	4.3	4.8	3.8	—	—	4.1		
			62	0.23	2.73	2.61	42.9	18.0	15.1	15.6	—	19.4	10.9	19.0		
			63	0.14	1.16	1.35	35.4	1.1	1.1	1.1	1.1	1.1	1.1	1.1		
Isocyanurate foam	10 kg	30W 60H	61	—	—	—	63.0	—	6.3	—	5.0	6.7	5.4	5.6		
			62	—	—	—	38.0	12.4	—	—	14.8	1.1	1.1	1.1		
			63	—	—	—	26.0	1.1	1.1	1.1	1.1	1.1	1.1	1.1		
	10 kg	30W 60H	61	0.20	2.00	2.53	42.1	5.6	—	5.6	4.6	—	5.6	5.2		
			62	0.11	1.44	1.22	33.8	1.1	1.1	1.1	1.1	1.1	1.1	1.1		
			63	0.10	0.78	0.93	29.1	1.1	1.1	1.1	1.1	1.1	1.1	1.1		
7.5 kg	30W 60H	61	0.15	1.55	1.97	34.5	6.8	6.9	—	8.2	7.4	7.8	7.5			
		62	0.11	1.35	1.17	29.8	1.1	1.1	1.1	1.1	1.1	1.1	1.1			
63	0.10	0.79	0.97	26.1	1.1	1.1	1.1	1.1	1.1	1.1	1.1	1.1				



Symbols

- Suction thermocouple
- Bare thermocouple
- ▷ Gas sampling
- Heat flux meter on the walls
- Heat flux meter on the ceiling
- ▷ Bidirectional pressure probe

Plan



Burner

Section

Fig.1 Experimental setup for scenario(1) experiments

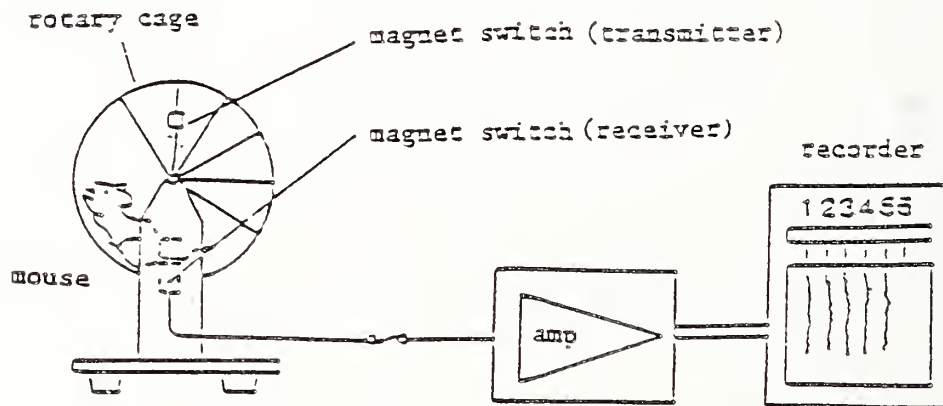
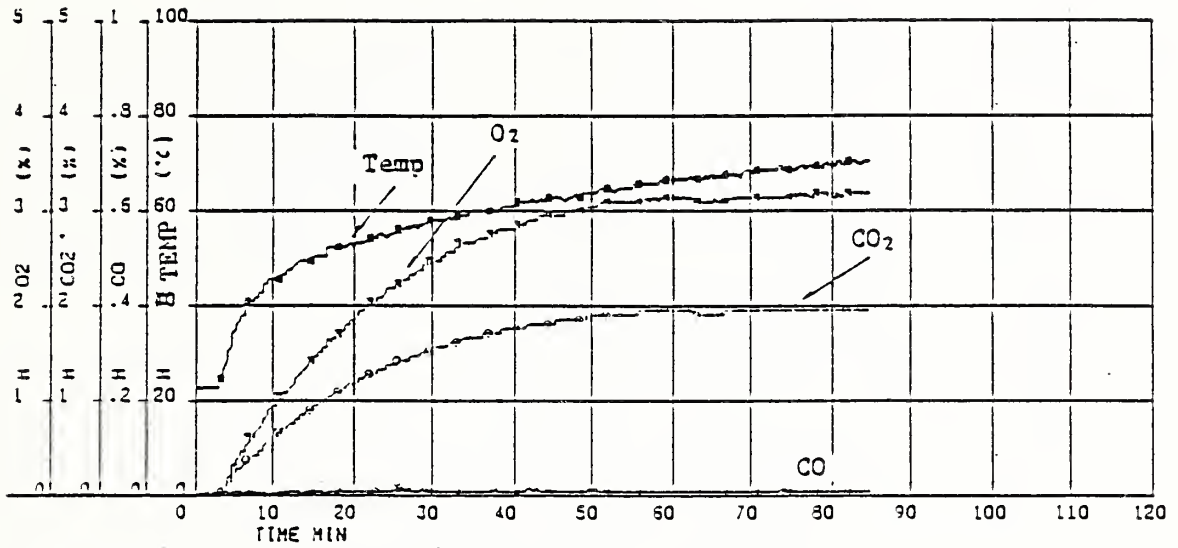
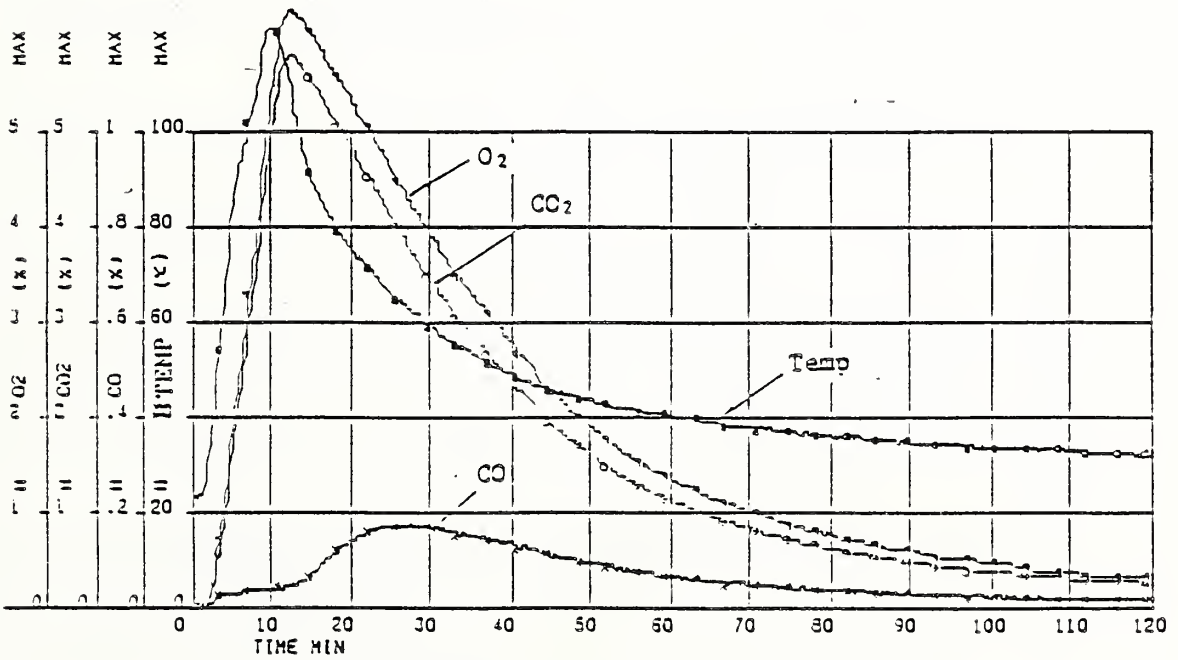


Fig. 2 Mouse Rotary Cage



a) Propane gas



b) Yezo spruce

Fig. 3 Example of the temperature and gas concentration histories

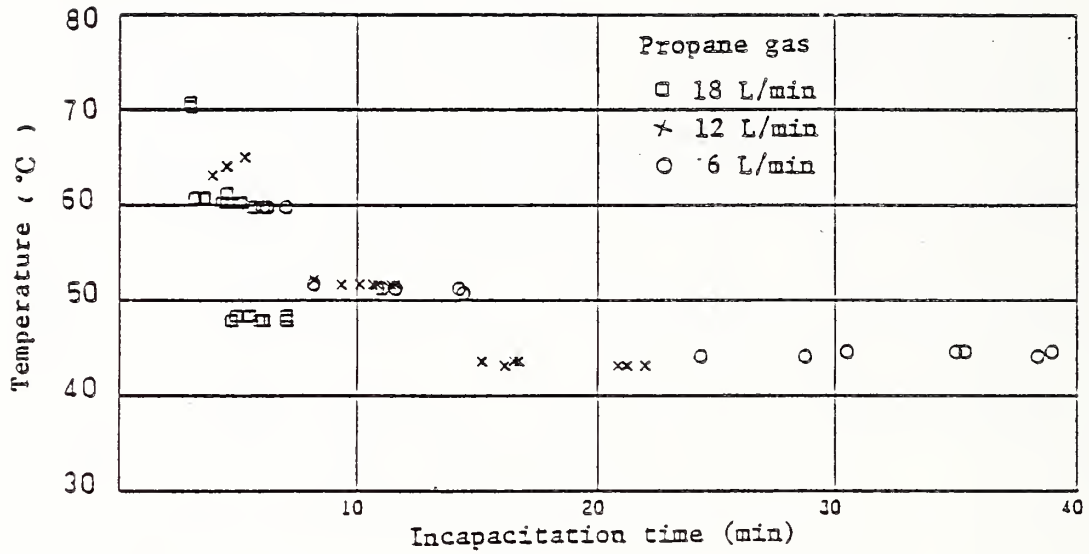


Fig.4 Incapacitation time V.S. temperature for propane gas (scenario(1))

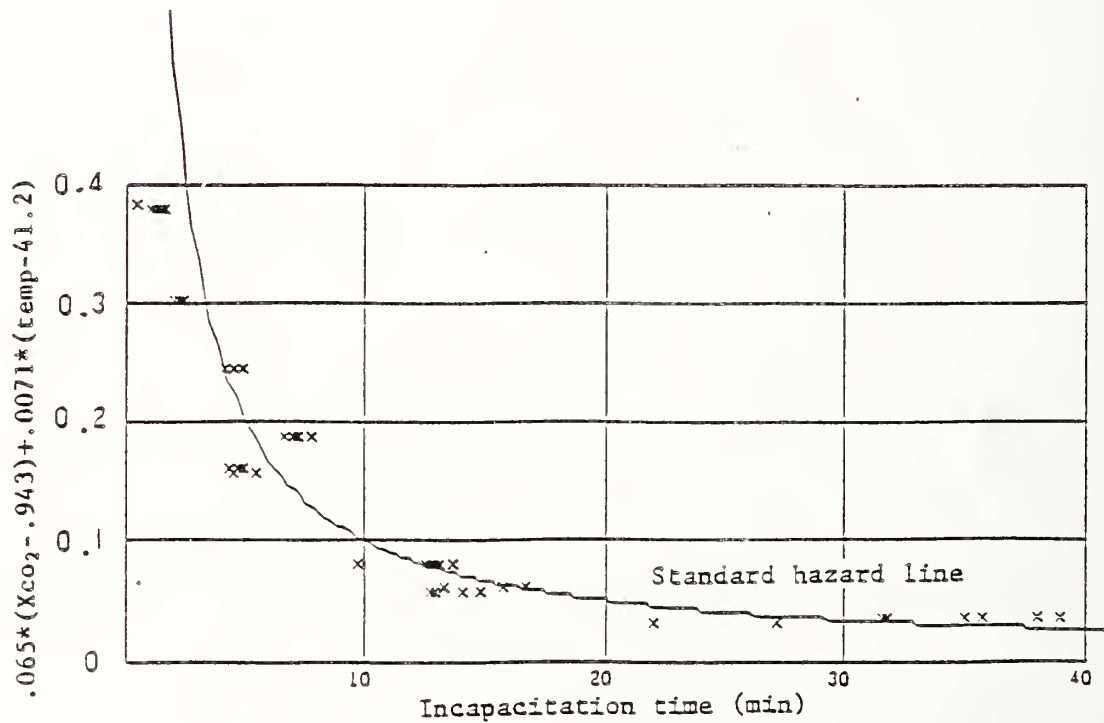
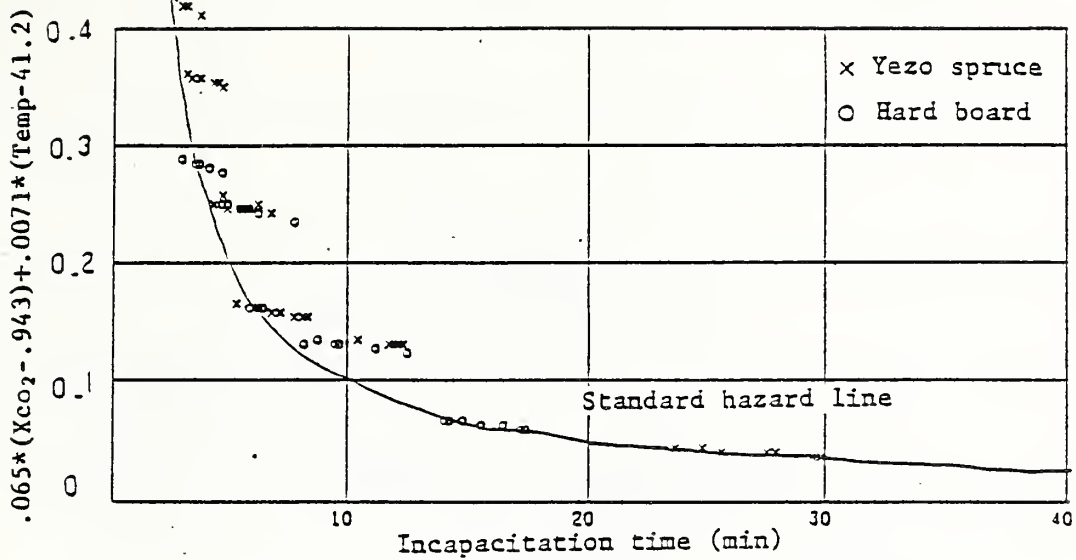
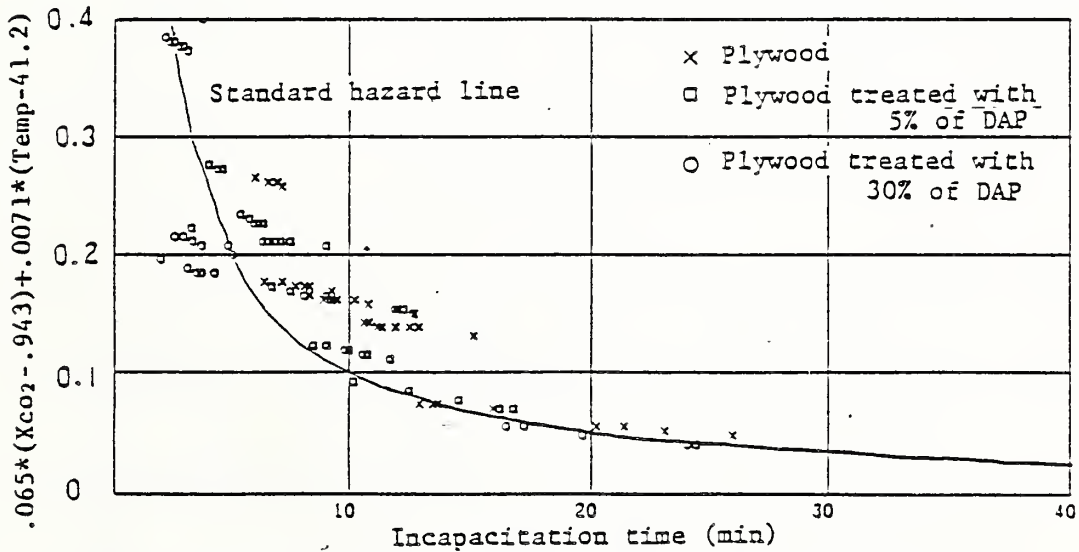


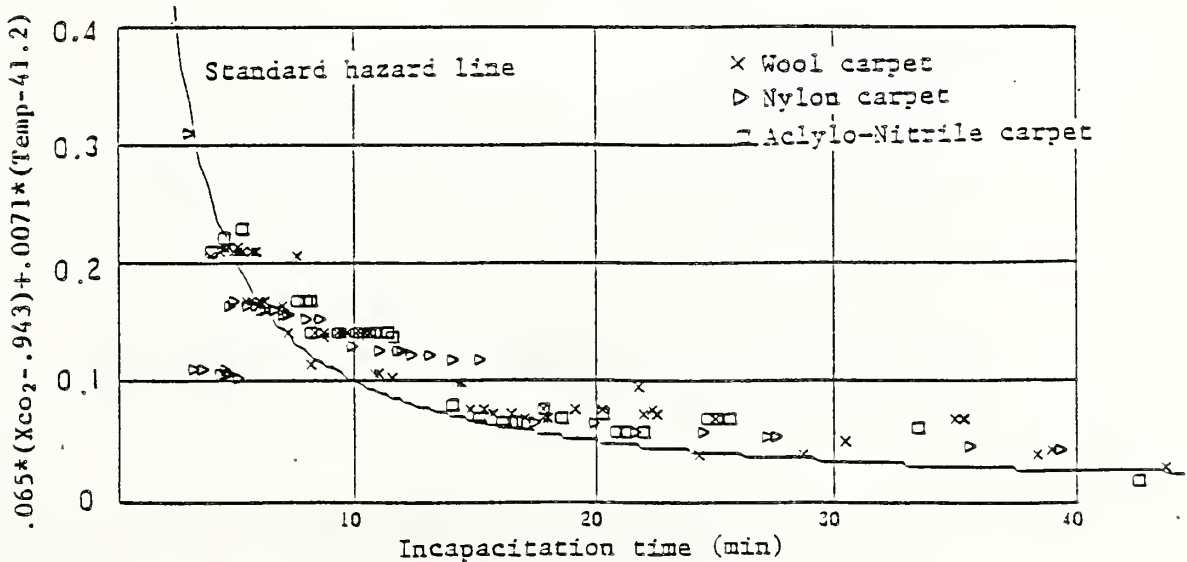
Fig.5 Best fit regression of the incapacitation time for propane gas



a) Yezo spruce and Hard board



b) Plywood, PWT-5% and PWT-30%



c) Wool carpet, Nylon carpet and Aclylo-Nitrile carpet

fig.6 Incapacitation times for realistic materials

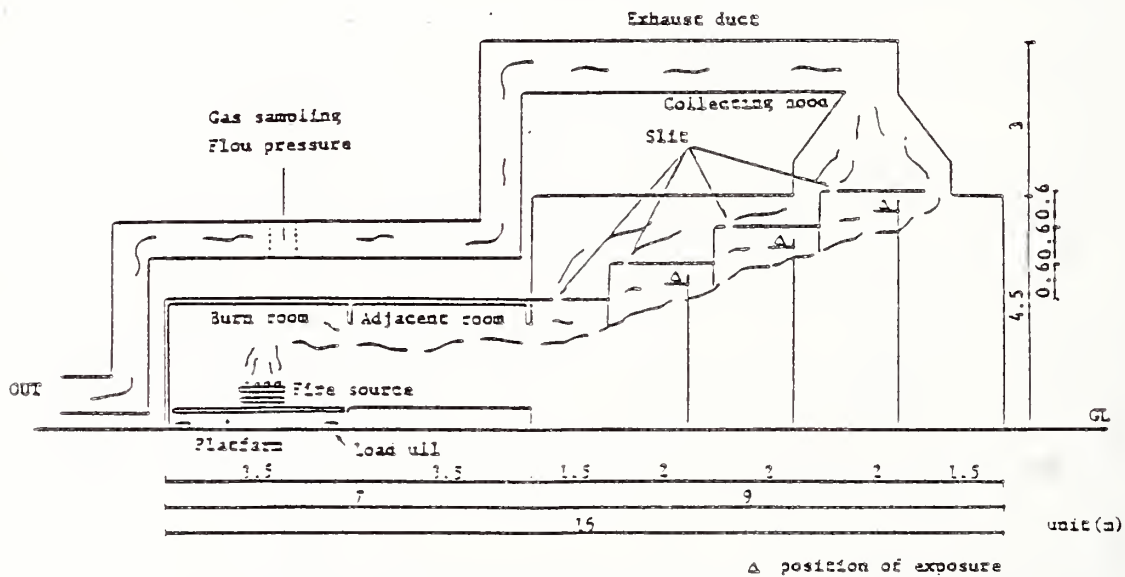
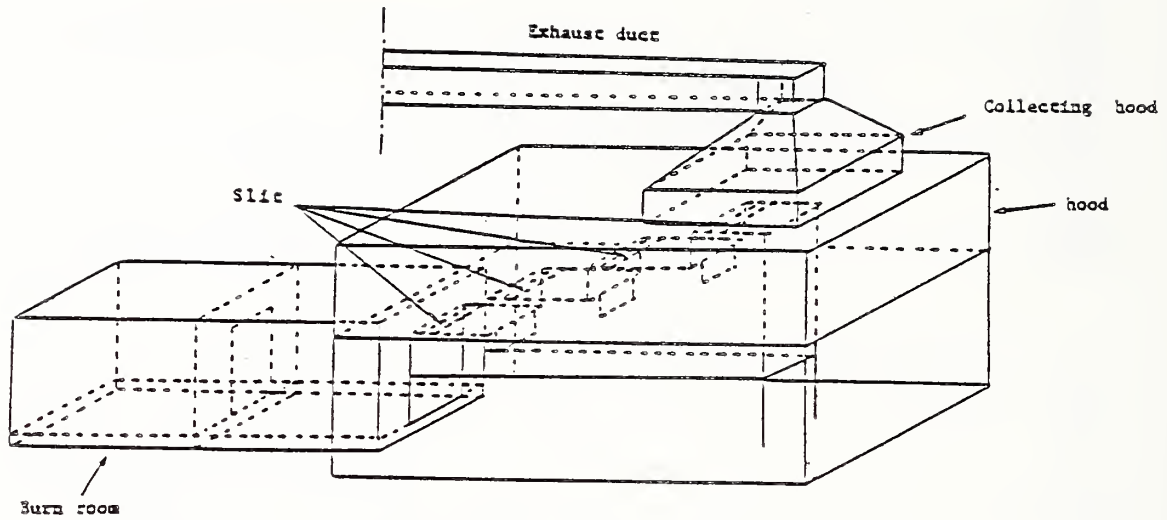
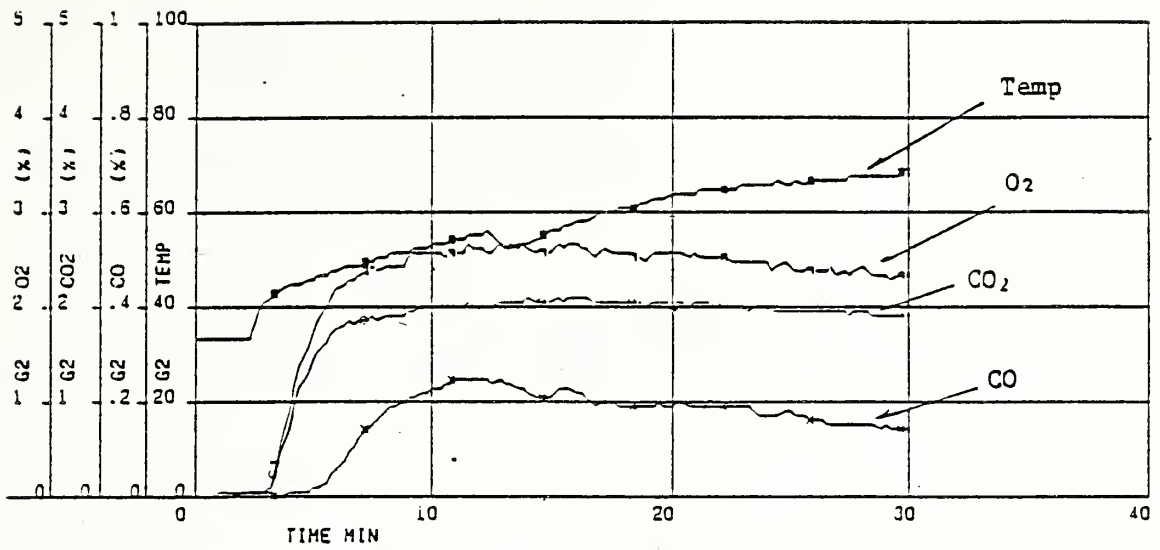
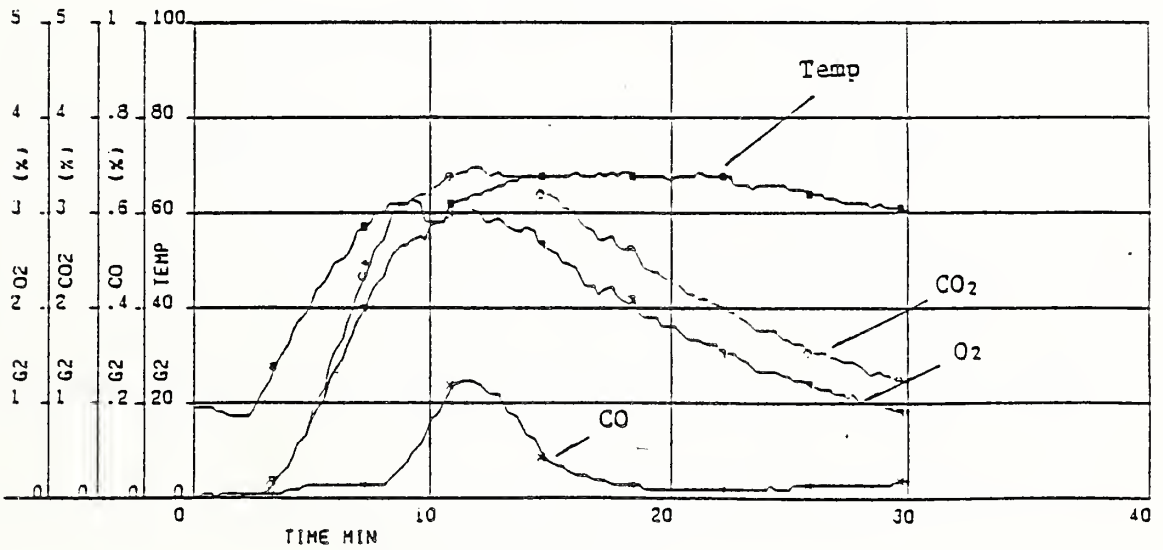


Fig.7 Experimental setup for scenario (2) experiments



a) Propane gas



b) Yezo spruce

Fig.8 Example of the temperature and gas concentration histories

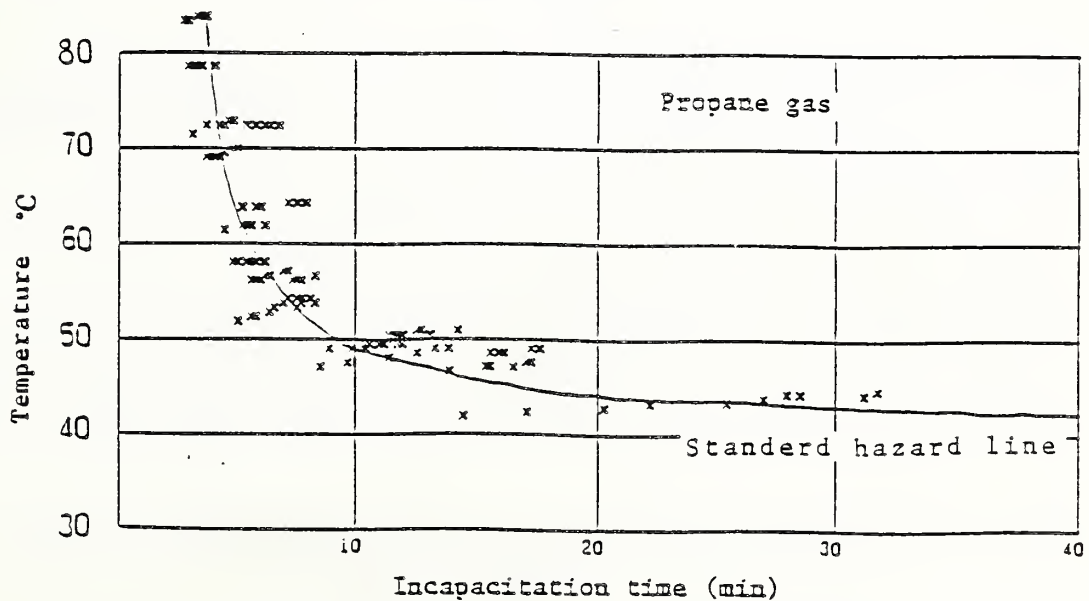
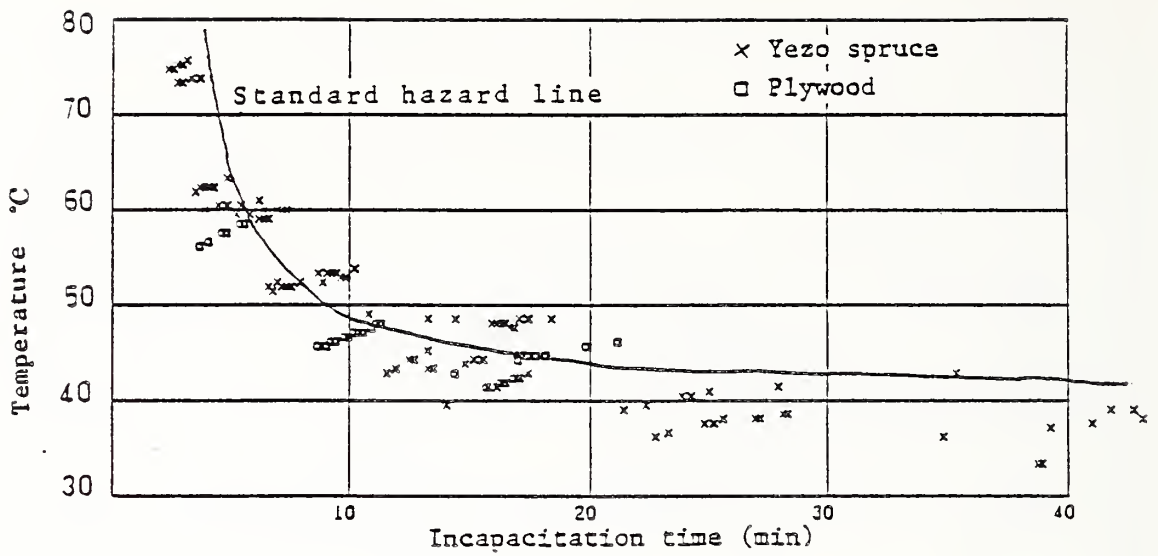
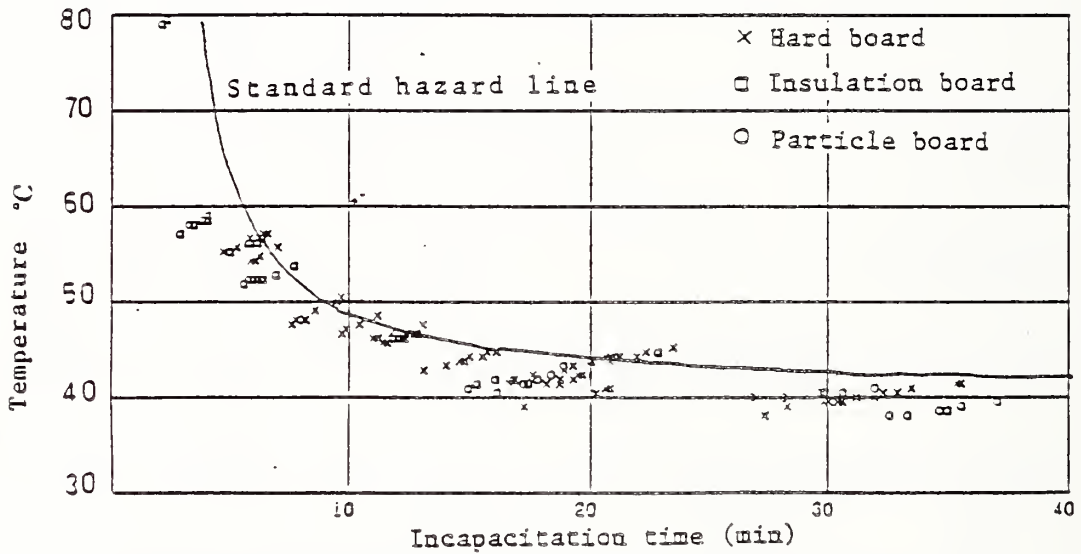


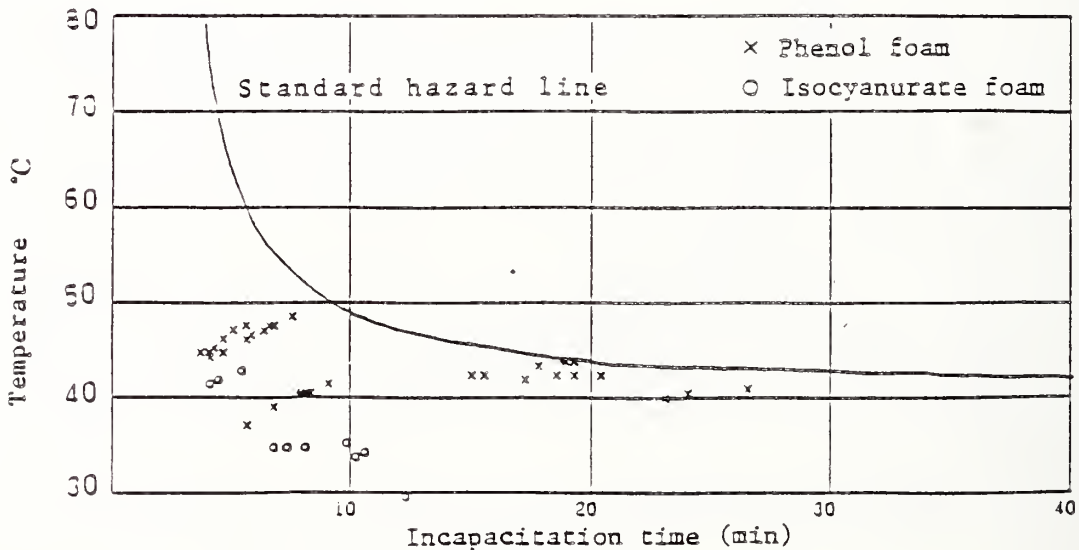
Fig.9 Incapacitation time V.S. temperature for propane gas (scenario(2))



a) Yezo spruce and Plywood



b) Hard board, Insulation board and Particle board



c) Phenol foam and Isocyanurate foam

Fig.10 Incapacitation time of mice for realistic materials
256

DETERMINATION OF THE KINETIC PARAMETERS AND THE
HEAT OF COMBUSTION OF THE VOLATILES FOR WOOD

William J. Parker¹
Center for Fire Research
National Bureau of Standards, USA

ABSTRACT

An apparatus for measuring the heat of combustion of the volatiles and the kinetic parameters for the mass loss rate of the various chemical components of wood as a function of their degree of char is described. The results of some of the measurements on cellulose made with this apparatus are presented.

1. INTRODUCTION

The research described in this paper is part of a project in the Center for Fire Research (CFR) at the National Bureau of Standards (NBS) to provide a heat release rate model for wood that can be used as a sub-model for the flame spread and room fire growth models. A heat release rate model has been described by Parker (1) which takes char shrinkage and multiple chemical components into account along with the change in the thermophysical properties with temperature and mass retention fraction. The mass retention fraction is defined as the mass at any given time divided by the original mass and is designated in this paper by the symbol, Z . The crucial factor in validating the model is to have reliable input data on the thermophysical and thermochemical properties of the wood and its chemical components. These components include cellulose, lignin, mannan, xylan and galactan. This paper describes the method used for the determination of the heat of combustion of the volatiles and the kinetic parameters which describe the rate of mass loss during pyrolysis. The heat of combustion of the volatiles released during the pyrolysis of char forming materials is less than the heat of combustion of the same material as measured with an oxygen bomb calorimeter and can vary during the course of the pyrolysis.

Ordinarily, the kinetic parameters (i.e., the effective activation energy and pre-exponential factor) are measured by thermogravimetric analysis (TGA). However, the heating rates in TGA are typically less than 20 degrees per minute. Consequently, a considerable fraction of the material has pyrolyzed by the time it reaches the temperature range of rapid pyrolysis that would be typical in the interior of a burning piece of wood. Thus, the calculated activation energy is characteristic of a lower temperature reaction, perhaps more typical of smoldering. While 100 °C/min heating rates are available in the TGA apparatus they result in unacceptably large temperature gradients in the specimen. Measurements are needed in the temperature range at which most of the pyrolysis occurs during flaming wood combustion. This temperature range will depend on the component. It will

¹ Part of this work was performed during the author's tenure as a visiting scientist at the Forest Products Laboratory during the summer of 1985.

be relatively high for lignin, low for hemicellulose, and in between for cellulose (2). Generally, however, most of the pyrolysis occurs at temperatures between 300°C and 400°C even though the pyrolysis process is initiated below 300°C and the char continues to degrade even at temperatures above 600°C.

The heat of combustion of the volatiles might be deduced from measurements in an oxygen bomb calorimeter on virgin material and on chars of the same material at a series of mass retention fractions. However, the net heat of combustion is required for modeling, while the oxygen bomb calorimeter measures the gross heat of combustion. The quantity of liquid water formed must be known at each mass retention fraction in order to make the correction. Also the determination requires many specimens, each of which must have a mass of a gram or more of the charred material. This means that several grams of the original material are needed. The separation of pure unaltered components of wood is very tedious and so the quantities available, except for cellulose, are limited.

Susott (3) measured the heat of combustion of the volatiles from forest fuels using a combination of TGA and evolved gas analysis (EGA). The EGA uses a catalytic converter to completely oxidize the volatile pyrolysis products to carbon dioxide and water. The amount of oxygen consumed in this process is measured and used to calculate the potential heat release rate. This rate is divided by the mass loss rate, determined by TGA, to yield the heat of combustion of the volatiles. This technique has the advantage of requiring a very small specimen size, on the order of 5 mg. However, it does have the disadvantage of depending on two specimens having the same identical mass loss rate history in two different instruments. Furthermore, the rate of temperature rise of the specimen is limited to around 20 °C per minute, which limits the applicability to the lower temperature reactions.

2. EXPERIMENTAL

Because of the above difficulties, the PYROCAT (combination pyrolyzer and catalytic converter) was developed to measure the kinetic parameters and the heat of combustion of the volatiles for this project. In its present state this method is applicable to materials containing only carbon, hydrogen and oxygen. By heating the specimen rapidly to the temperature region where the measurements are being made, steep temperature gradients in the specimen are confined to the early period where less than 10% of the mass is lost. The specimen is pyrolyzed in a stream of nitrogen and the volatiles are swept into a catalytic converter where they are converted to carbon dioxide and water as in Susott's method (3). In the PYROCAT, however, the converted gases are passed through carbon dioxide and water vapor analyzers as well as the oxygen analyzer. From the concentrations, X_{O_2} , X_{CO_2} and X_{H_2O} , of oxygen, carbon dioxide and water vapor measured in the analyzers and the mass flow rate, m_{N_2} , of nitrogen flowing into the system, the molar flows of carbon, hydrogen and oxygen from the specimen can be calculated from the formulas (4):

$$m_C = 3m_{N_2} X_{CO_2} / (1 - X_{O_2} - X_{CO_2}) / 7 \quad (1)$$

$$m_H = m_{N_2} X_{H_2O} / (1 - X_{H_2O}) / (1 - X_{O_2} - X_{CO_2}) / 14 \quad (2)$$

$$m_O = 4m_{N_2} [(X_{H_2O} / (1 - X_{H_2O})) / (1 - X_{O_2} - X_{CO_2}) + 2(X_{O_2} + X_{CO_2}) / (1 - X_{O_2} - X_{CO_2}) - 2X_{O_2}^0 / (1 - X_{O_2}^0)] / 7 \quad (3)$$

where $X_{O_2}^0$ is the measured oxygen concentration prior to the run. The calculation does not depend on nor provide any information on how these elements are combined in the hundreds of different chemical species making up the volatile pyrolysis products. However, the total mass flow from the specimen is equal to the sum of the masses of these three elements. Furthermore, the external oxygen supply rate required for complete combustion of these volatiles is given by

$$m_{O_2} = (8m_C / 3 + 8m_H - m_O) \quad (4)$$

Huggett (5) found that, to within an engineering approximation of $\pm 5\%$, the heat released per unit mass of oxygen consumed is 13.1 MJ/kg for a large variety of polymeric solids. The potential rate of heat release can be calculated by multiplying the oxygen mass requirement evaluated in equation 4 by this constant. The heat of combustion is simply the ratio of the rate of heat release to the rate of mass loss. Thus both the heat of combustion of the volatiles and the mass loss rate for the calculation of the kinetic parameters can be determined on a single specimen. Data from several specimens pyrolyzed in different temperature ranges need to be accumulated to determine the kinetic parameters.

The PYROCAT was first used in a project at the Forest Products Laboratory during the summer of 1985 to obtain the heat of combustion of the volatiles and the kinetic parameters for the components of Douglas fir. Figure 1 shows a schematic of the apparatus. A 2.5 cm diameter quartz tube passes through two 30 cm long tube furnaces. A flow of 26 mg/sec of preheated nitrogen comes in from the right. It passes over the specimen which is located in an aluminum pan on top of a chrome plated copper block heat sink. The cellulose specimens were in the form of 0.75 mm (30 mil) thick sheets with masses between 275 and 325 mg. The other materials were in the form of powders with masses between 50 and 300 mg. Oxygen flows in from the left through a 12.5 mm diameter quartz tube mixing with the nitrogen and the pyrolysis products. The short ceramic rod located in the outer quartz tube in the zone where the two tube furnaces are in contact serves to increase the velocity of the nitrogen at that location. This was intended to block the diffusion of oxygen into the region of the specimen. No confirming measurements of the oxygen concentration in this region were made. However, there was no visual indication of char oxidation in any of the specimens tested. The nickel-chromium heating wire was added to raise the temperature of the pyrolysis products and to induce some cracking so that there would be no condensation on the quartz tube in this region. The wire was found to be sufficiently heated by the furnace that it was not necessary to apply electrical power to it. There was never any evidence of condensation. As the mixture passes out through the platinum gauze catalyst at 900°C the

pyrolysis products are converted to carbon dioxide and water. The nitrogen and oxygen flows into the system were measured with rotameters. The oxygen flow was adjusted to provide a 35% oxygen concentration in the catalytic converter in the absence of pyrolysis. This initial concentration was high enough to insure that the concentration never dropped below 21%. This insured that the conversion was complete as indicated by the absence of a measurable concentration of carbon monoxide. After passing through a heated filter to eliminate the possibility of particulates reaching the analyzers, the exhaust stream divides. One part goes through an infrared water vapor analyzer and the rest through a cold trap and desiccant before going through the oxygen and carbon dioxide analyzers. There are rotameters in the exhaust of each of the analyzers to insure that the flows are in the range specified by the manufacturers. This is around 10 ml/sec. The CO meter is present simply to indicate if there is detectable CO in the exhaust.

Prior to the test several flow rates of methane were added to the nitrogen and converted to carbon dioxide and water vapor in the catalytic converter in order to calibrate the analyzers. In addition, the carbon dioxide analyzer and the oxygen analyzer were checked with bottled calibration gas. There is a solenoid valve, not shown in figure 1, which cuts off the flow of oxygen into the tube when the end is open for specimen insertion. Otherwise oxygen would flow out over the specimen. Nitrogen flowing out of the end of the tube during specimen insertion prevents the diffusion of atmospheric oxygen into the system. Chromel-alumel thermocouples, 0.25 mm (10 mil) in diameter, are attached to the copper block and to the specimen. In the case of powdered specimens the junction is buried in the powder while for cellulose it is threaded through the sheet. Since there is a positive pressure in the line, any leakage in the system beyond the quartz tube where the combustion gases are well mixed would not affect the concentrations measured in the analyzers.

The uniformity of the specimen exposure over its lateral extent was estimated by cutting up a cellulose specimen into nine equal parts and measuring the total mass loss of each piece with a balance after a mass loss of approximately 30% was obtained. There was a 25% difference in mass loss per unit area across the length of the specimen which could not be eliminated. Considering that the rate of mass loss of cellulose essentially doubles every 10 degrees this represents a temperature difference of about 3 degrees.

The output voltages from the analyzers and thermocouples were recorded at 5 second intervals on a floppy disk. Capacitors were placed across the inputs to the computer in order to reduce the noise. The data were analyzed later using an electronic spread sheet.

3. RESULTS FOR CELLULOSE

Figure 2 is a plot of the millimoles per second of carbon, hydrogen and oxygen flowing out of the specimen as a function of time for one of the cellulose runs. The specimen temperature increased from 350 to 370°C over the course of the run. The upswing of the hydrogen at the beginning was due to the release of water. Most of this water peak was lost because of a

transient in the oxygen concentration caused by cutting off the supply during specimen insertion. Although the shapes of the curves depend on the temperature history of the specimen they do demonstrate that the carbon, hydrogen and oxygen content of the volatiles can be followed during the run. Figure 3 shows the fractional mass loss rate as a function of the mass retention fraction (Z) for a cellulose specimen. The fractional mass loss rate is the sum of the mass flow rates hydrogen, carbon and oxygen from the specimen divided by its original mass. The right hand edge of the plot where Z=1 corresponds to the virgin cellulose. The mass loss rate rose to a maximum as the pyrolysis proceeded because the specimen temperature continued to rise as seen in the figure 4. In principle the specimen temperature does not need to be constant. It is only necessary that it gets into the proper range before the specimen has lost more than a small portion (say 10 percent) of its original mass. However, a correction has to be made for the temperature change that occurs over the gas transit time from the thermocouple to the analyzers. The greater the change the greater the potential error in the correction. The gas transit time was 15 seconds. No correction was applied for flow dispersion.

The fractional mass loss rate and the temperature at mass retention fractions of 0.9, 0.8, ..., 0.3 were picked off the fractional mass loss rate and temperature curves for each of seven runs on cellulose, each in different temperature ranges. These were used to produce a set of Arrhenius plots, one for each mass retention fraction, like the one in figure 5 for Z=0.6. From these plots the effective activation energy and pre-exponential factor were determined as a function of the mass retention fraction. The average value of the effective activation energy over the mass retention fraction range of 0.9 to 0.3 was determined to be 45 kcal/mole with a range of ± 3 kcal/mole. Using this average value of the effective activation energy, the pre-exponential factor in units of fractional mass loss per second could be expressed by

$$A = 2.5 \times 10^{13} (Z-0.06) \quad (5)$$

Figure 6 shows the average heat of combustion of the volatiles as a function of the mass retention fraction over all of the runs on cellulose. The vertical bars indicate the range of the data and the points represent the averages. The average of all runs over the complete pyrolysis period is 13.8 MJ/kg.

4. DISCUSSION

The PYROCAT appears to be a promising tool for determining the instantaneous carbon, hydrogen and oxygen content of the volatiles during pyrolysis. This information was used here to determine the instantaneous heat of combustion of the volatiles and the mass loss rate needed for the calculation of the kinetic parameters. The accuracy of the results is limited by (1) perturbations in the oxygen concentration at the beginning of the test due to specimen insertion, (2) a small temperature variation across the specimen, (3) changes in specimen temperature with time, (4) small changes

in the flow rates of nitrogen and oxygen into the system during the test and (4) system noise.

The mass loss rates for cellulose could be described quite well by an Arrhenius equation. However, because of the complexity of the reactions involved it would be difficult to assign any physical significance to an activation energy. Hence the term, "effective activation energy," is used here simply as a parameter to calculate the mass loss rate. There are a wide range of activation energies reported in the literature for cellulose in nitrogen with a number of investigators reporting values around 54 kcal/mole (6) primarily using TGA. Although it varied some with the mass retention fraction an average value of 45.1 kcal/mole was obtained on this project. This is in reasonable agreement with the 42 kcal/mole reported by Lipska and Wodley (7) between 276 C and 360 C using isothermal pyrolysis.

The net heat of combustion of cellulose as reported by Huggett (5) is 16.1 MJ/kg. The average net heat of combustion of its volatiles measured on this project was 13.8 MJ/kg. The lower value was due to dilution by the water released in the char forming process. This dilution was greatest during the beginning of the pyrolysis period where the heat of combustion of the volatiles was only projected to be about 9 MJ/kg. Shafizadeh (8) found a gross heat of combustion of 15.2 MJ/kg for the volatiles from cellulose based on the difference in the heat of combustion of cellulose and its char using the oxygen bomb as described earlier in this paper. Assuming that his measured char yield of 14.9% was pure carbon, a correction was made here for the heat of vaporization of the water. On this basis the net heat of combustion of the volatiles was calculated to be 13.7 MJ/kg which is in agreement with the average value of 13.8 MJ/kg found in this project.

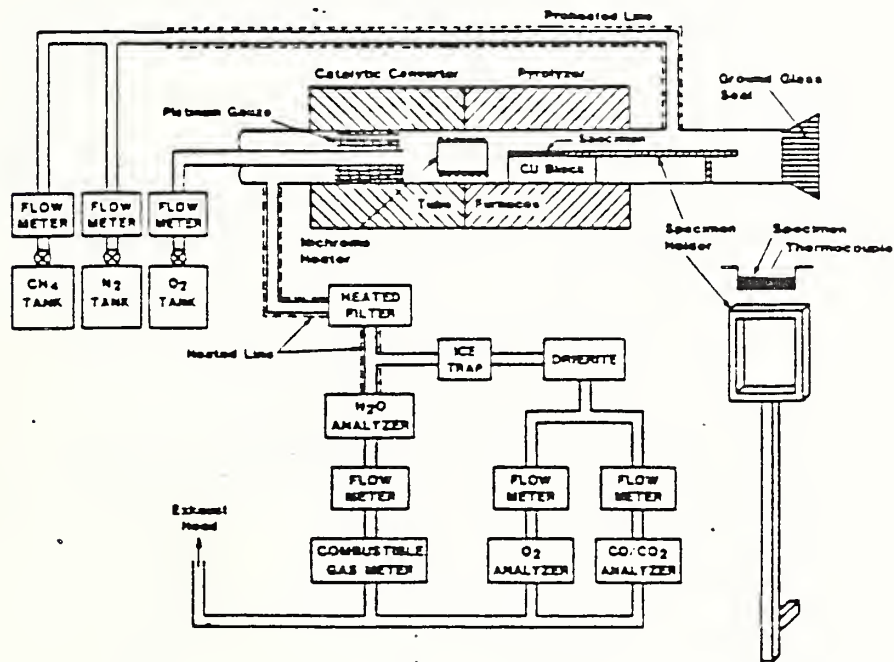
4. ACKNOWLEDGMENT

I am grateful to the Forest Products Laboratory for providing me with the opportunity to carry out the experimental part of this research as a visiting scientist in their laboratory.

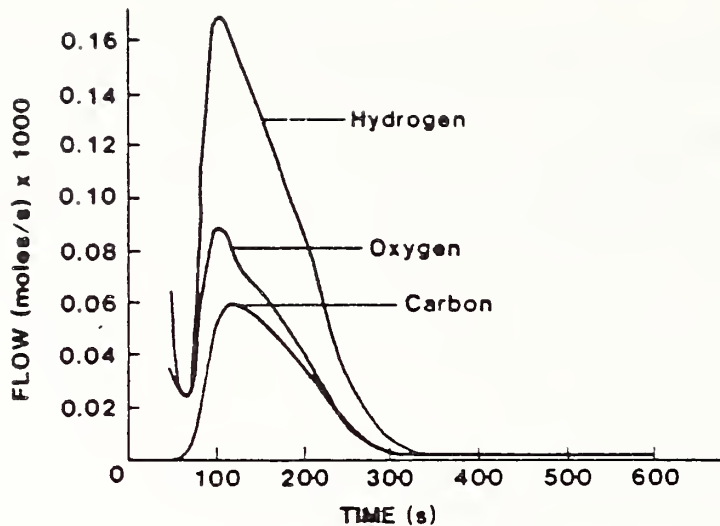
5. REFERENCES

1. Parker, W.J., "Prediction of the Heat Release Rate of Wood," Fire Safety Science-Proceedings of the First International Symposium, pp 207-216, (1985)
2. Beall, F.C. and Eickner, H.W., "Thermal Degradation of Wood Components: a review of the literature," U.S.D.A Forest Service Research Paper FPL 130 (May 1970).
3. Susott, R.A., "Characterization of the Thermal Properties of Forest Fuels by Combustible Gas Analysis," Forest Sci. Vol.28, No. 2, pp. 404-420 (1982)
4. Parker, W.J., "Development of a Model for the Heat Release Rate of Wood- A Status Report," NBSIR 85-3163, Nat. Bur. Stand. (U.S.), May 1985.

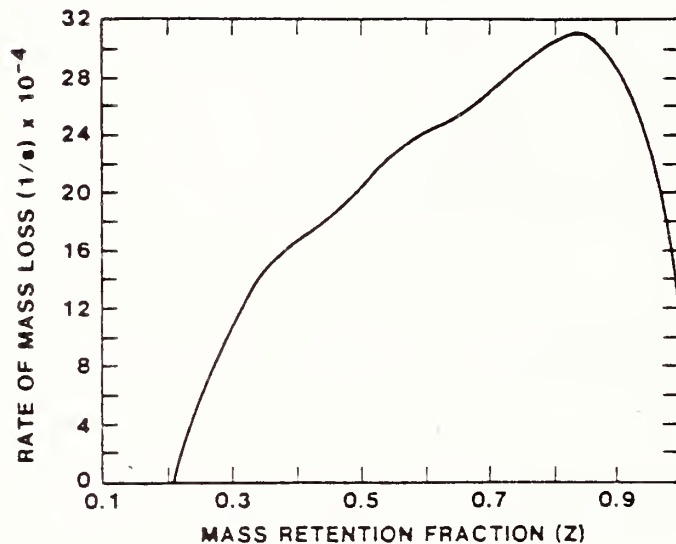
5. Huggett, C., "Estimation of the Rate of Heat Release by Oxygen Consumption Measurements," Fire and Materials, Vol.4, pp. 61-65 (1980).
6. Roberts, A.F., "A Review of Kinetics Data for the pyrolysis of Wood and Related Substances," Combustion and Flame, 14, pp. 261-272 (1970)
7. Lipska A.E. and Wodley, F.A., J. App. Polymer Sci., 13 pp. 851-865 (1969).
8. Shafizadeh, F., "Combustion, Combustibility, and Heat Release Rate of Forest Fuels," AIChE SYMPOSIUM SERIES No. 177, Vol. 74, pp. 765-82 (1978).



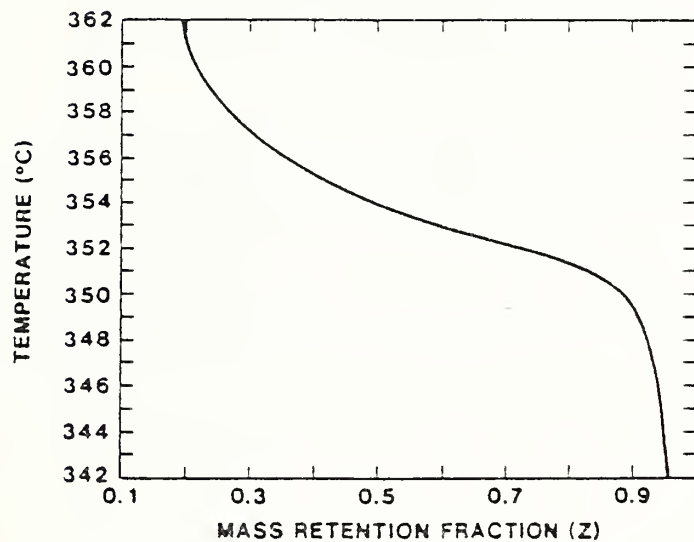
1. Schematic of PYROCAT (Pyrolyzer and Catalytic Converter)



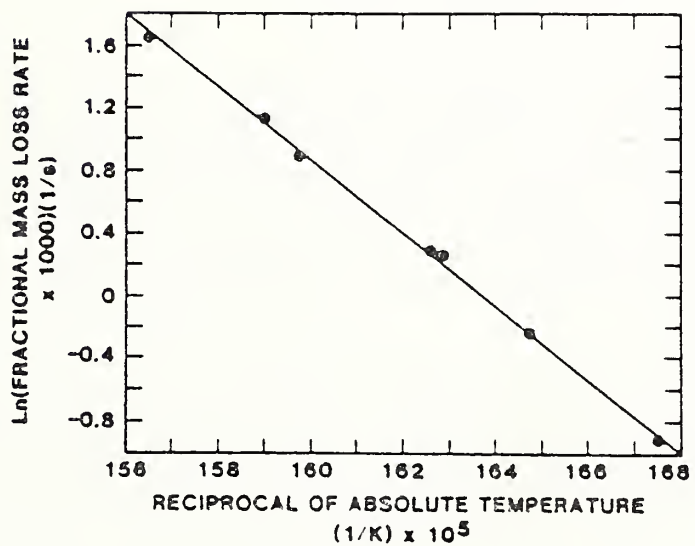
2. Molar Flow Rates of Carbon, Hydrogen and Oxygen from Cellulose Specimen in the 350°C to 370°C Temperature Range



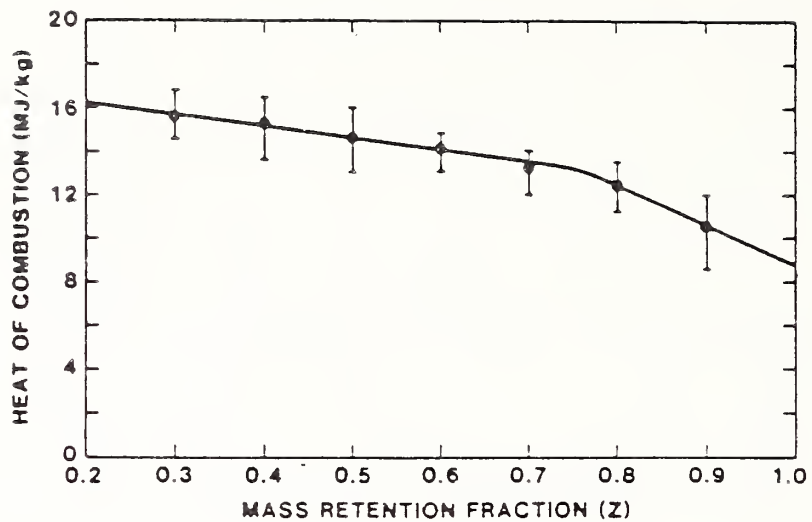
3. Fractional Mass Loss Rate of Cellulose Specimen



4. Temperature of Cellulose Specimen



5. Arrhenius Plot for Cellulose at a Mass Retention Fraction of 0.6



6. Heat of Combustion of Volatiles from Cellulose

CORRELATION FOR THE GENERATION OF CARBON MONOXIDE
IN SMALL- AND LARGE-SCALE FIRES

Archibald Tewarson
Factory Mutual Research Corporation
Norwood, MA 02062 USA

Ninth Meeting of the United States/Japan Panel
on Fire Research and Safety, May 1987

ABSTRACT

Generation of carbon monoxide in small- and large-scale fires, under variable ventilation conditions, is discussed. The ratio of the mass generation rate of CO to mass generation rate of material vapors, defined as the yield of CO, was found to have a weak dependency on fire scale, but a strong dependency on the chemical structure of the materials and additives and fire ventilation; it was highest for the highly halogenated materials and decreased as the chemical structure changed from aromatic to aliphatic.

The yield of CO was found to increase with decrease in fire ventilation, reaching values as high as 0.30 or about 20% of the maximum possible theoretical yield of CO.

From the application of the National Bureau of Standards' N-gas model for fire toxicity, it was found that hazardous conditions could be created if mass air-to-material vapor ratio was about 1.4 to 2.0 times the mass air-to-fuel stoichiometric ratio for diffusion flames of propane, propylene and wood cribs, assuming CO and CO₂ to be the only products of concern. However, if the fire products were diluted by about fifteen to twenty times their volume by air, hazardous conditions were found to be absent even when fires were highly under-ventilated and the yield of CO was very high.

1. INTRODUCTION

Accurate data on the causes of deaths associated with fires are difficult to obtain. However, it is generally accepted that 70 to 80% of fire deaths result from smoke inhalation [1]. Smoke is a mixture of various gaseous, liquid and solid compounds such as CO, CO₂, depleted O₂, HCl, HCN, saturated and unsaturated hydrocarbons, alcohols, aldehydes, etc. Some of the compounds present in smoke, individually or in combination, are considered to be responsible for not only immediate or delayed deaths, but also for impeding escape and causing injuries.

CO, one of the major toxicants present in smoke, binds the red blood cells and forms carboxyhemoglobin (COHb), which interferes with oxygen transport in the body. COHb concentrations of 50 to 60% are generally accepted as fatal [1]. Human physiological response to CO has been investigated by several researchers, some of their results are summarized in Figure 1, taken from Reference 2. CO is the cause or a contributing cause in 80% of fire deaths based on the data collected in Maryland [1]. The effects of CO exposure to rats and mice have also been investigated [1,3,4]. For example, CO concentrations of 2667 and 8636 ppm for 15 minutes of exposure are found to cause incapacitation and death in 50% of exposed rats, respectively [3]. Factors that are considered

to be important for CO hazard in fires are [1-4]: 1) concentration of CO; 2) exposure time; 3) health of the people expected to be exposed; and 4) concentrations and generic nature of other compounds generated in the fire, which may affect the CO response of exposed people.

This paper presents an analysis of the generation of CO in fires to show correlations between small- and large-scale fires.

2. GENERATION OF CO

CO is generated in flaming and nonflaming fires and is associated with incompleteness of combustion. CO concentration in fires is governed by several factors: 1) nature of chemical bonds and additives in materials; 2) fire ventilation, which includes mixing and flow of fire products and air; and 3) fire size.

The mass generation rate of CO is directly proportional to the mass generation rate of material vapors, where the proportionality constant is defined as the yield of CO. Thus at any time t , the yield of CO can be expressed as:

$$Y_{CO}(t) = \dot{G}_{CO}''(t) / \dot{G}_f''(t), \quad (1)$$

and the overall average yield of CO as:

$$Y_{CO} = \int_0^t \dot{G}_{CO}''(t) dt / \int_0^t \dot{G}_f''(t) dt, \quad (2)$$

$$\text{or, } Y_{CO} = W_{CO} / W_f, \quad (3)$$

where Y_{CO} is the yield of CO (g/g); \dot{G}_{CO}'' is the mass generation rate of CO per unit surface area of the material ($\text{g}/\text{m}^2\text{s}$); \dot{G}_f'' is the mass generation rate of material vapors per unit surface area of the material ($\text{g}/\text{m}^2\text{s}$); W_{CO} is the total mass of CO generated in the fire (g); and W_f is the total mass of material vapors generated in the fire (g).

In fires, CO is generated as a result of the conversion of the carbon atoms (and oxygen atoms if present in the structure). The maximum possible theoretical yield of CO can be calculated from the elemental composition of the material,

$$k_{CO} = n (MW)_{CO} / (MW)_f, \quad (4)$$

where k_{CO} is the maximum possible theoretical yield of CO (g/g); n is the number of carbon atoms in the structure of the material; $(MW)_{CO}$ is the molecular weight of CO, which is equal to 28 g/mole; and $(MW)_f$ is the molecular weight of the material calculated from its elemental composition (g/mole). The generation efficiency of CO thus can be expressed as:

$$f_{CO} = Y_{CO} / k_{CO}, \quad (5)$$

where f_{CO} is the generation efficiency of CO.

2.1 EFFECT OF NATURE OF CHEMICAL BONDS ON THE GENERATION OF CO

Materials consist of combinations of atoms, such as carbon, hydrogen, oxygen, nitrogen, sulfur, halogen, etc. The generation of CO depends on the nature of chemical bonds between these atoms as shown in Figures 2 and 3. In the Figures, Y_{CO} is plotted against the molecular weight of saturated and unsaturated hydrocarbons. Aliphatic hydrocarbons with single, double and triple bonds are defined as alkanes, alkenes and alkynes, such as ethane, ethylene, and acetylene, respectively. Benzene is an aromatic hydrocarbon. Hydrocarbons with chemical structures consisting of both aliphatic and aromatic units are defined as arenes such as styrene and toluene.

Data in Figure 2 show that Y_{CO} increases with increase in the degree of unsaturation in the carbon-carbon bonds and presence of aromatic rings in the structure. For example, Y_{CO} increases from normal heptane (C_7H_{16}), heptene (C_7H_{14}), and heptyne (C_7H_{12}) to toluene (C_7H_8). Data in Figure 3 show that Y_{CO} also increases when hydrogen atoms are substituted with larger groups such as a methyl radical, CH_3 (substituted alkanes) and when structures are cyclic with loss of hydrogen atoms (cyclic alkanes or alkenes). For example, Y_{CO} increases from normal pentane (C_5H_{12}), methyl butane (C_5H_{12}) to cyclopentane (C_5H_{10}). The data in Figures 2 and 3 show that the molecular weight also affects Y_{CO} .

Table 1
Yield of CO for Well-Ventilated and
Under-Ventilated Fires of Materials

Material	Well-Ventilated Fires ^a	Under-Ventilated Fires ^b
Methane (gas)	NR	0.175
Propane (gas)	0.005	0.229
Propylene (gas)	0.020	0.200
Hexane (liquid)	0.011	0.195
Toluene (liquid)	0.066	0.107
Methanol (liquid)	0.001	0.236
Ethanol (liquid)	0.002	0.219
Isopropanol (liquid)	0.002	0.168
Acetone (liquid)	0.003	0.304
Pine (solid)	0.004	0.138
Polymethylmethacrylate (granular)	0.010	0.189
Silicone (solid)	0.021	NR
Polyethylene foams	0.023	NR
Polyethylene (granular)	0.024	0.180
Polypropylene (granular)	0.024	NR
Nylon (granular)	0.038	NR
Flexible polyurethane foams	0.010 to 0.042	NR
Rigid polyurethane foams	0.025 to 0.051	NR
Polystyrene foams	0.060	NR
Polystyrene (granular)	0.060	NR
Polyvinyl chloride (granular)	0.063	NR
Fluoropolymers (granular)	0.120	NR

a: Data taken from Reference 6.

b: Data taken from Reference 7.

NR: Not reported.

The effect of chemical structure on the generation of CO is also noted in materials other than hydrocarbons. The data are listed in Table 1 for well-ventilated flaming fires. The data in Table 1 show that Y_{CO} increases from aliphatic to aromatic to halogenated structures.

2.2 EFFECT OF FIRE VENTILATION ON THE GENERATION OF CO

The fire ventilation can be defined in terms of mass air-to-fuel-stoichiometric fraction (ϕ),

$$\phi = \delta \dot{M}_a / G_f'' A k_a, \quad (6)$$

where δ is the fraction of entrained air which reacts with material vapors; \dot{M}_a is the mass flow rate of air (g/s); A is the surface area of material (m^2); and k_a is the mass air-to-fuel stoichiometric ratio. In the calculations, δ is usually considered as unity. When $\phi < 1.0$, fires are defined as under-ventilated, and when $\phi > 1.0$, fires are defined as well-ventilated.

Data for Y_{CO} for under-ventilated fires ($\phi < 0.83$), are included in Table 1, which are significantly higher than the data for well-ventilated fires. Depending on the material, Y_{CO} values can be as high as 0.30 for under-ventilated fires. High Y_{CO} values have also been found in other studies on propane diffusion flames [8]. In a small-scale flow-through furnace heated to 800°C, very high Y_{CO} values have been measured for highly under-ventilated conditions, as can be noted in Table 2 [9].

Table 2
Maximum Yield of CO Under Highly
Under-Ventilated Combustion^a

Material	Y_{CO} (g/g)	k_{CO} (g/g)	f_{CO}
Methanol	0.88	0.88	1.00
Ethanol	0.80	1.22	0.66
Acetone	0.91	1.45	0.63
n-Hexane	1.01	1.95	0.52
Benzene	1.24	2.15	0.58
Benzene-Methanol (1:1)	1.05	NA	NA

a: Data taken from Reference 9. Fuel flow rate = 0.005 g/s;
Dimensions of the tube furnace are not given in the paper.
NA: Not applicable.

Data for Y_{CO} , calculated from the ratio of the mass generation rate of CO to mass generation rate of material vapors, are available for small- to large-scale fires, which are plotted in Figure 4 against air-to-fuel stoichiometric fraction. The data in Figure 4 show that as ϕ decreases, Y_{CO} increases, and for $\phi \leq 2.0$, Y_{CO} increases very rapidly. For propane and propylene diffusion flames, the maximum value of Y_{CO} is about 0.27, occurring at a ϕ value of about 0.80, which is similar to Beyler's data included in Table 1 for $\phi < 0.83$ [7]. For small- to large- size wood crib fires, and larger-scale wood-lined tunnel fires, the maximum value of Y_{CO} is about 0.24, occurring at a ϕ value of about 0.50. The Y_{CO} profiles for wood cribs burning in our apparatus and various sizes of enclosures and in larger-scale wood-lined tunnel fires are very similar.

The data in Figure 4 also show that for similar ϕ values, there is a good correlation between Y_{CO} data for fires of small- and large-size cribs and wood lined on the walls of a larger-scale tunnel.

2.3 EFFECT OF FIRE SCALE ON THE GENERATION OF CO

From Eq. (1),

$$\dot{G}_{CO}'' = Y_{CO} \dot{G}_f'' \quad (7)$$

and

$$\dot{G}_f'' = \dot{q}_n''/L, \quad (8)$$

where \dot{q}_n'' is the net heat flux received by material, equal to the sum of external heat flux and flame heat minus the surface reradiation loss (kW/m^2); and L is the heat of gasification of the material (kJ/g).

If fire products and air are well mixed and \dot{V}_T is the total volumetric flow rate of fire product-air mixture, then the concentration of CO can be expressed as:

$$C_{CO} = \dot{G}_{CO}'' A/\dot{V}_T, \quad (9)$$

where C_{CO} is the concentration of CO (g/m^3).

From Eqs. (7) and (9),

$$C_{CO} = Y_{CO} \dot{G}_f'' A/\dot{V}_T \quad (10)$$

Eq. (10) suggests that the concentration of CO in various fire scales would be governed by Y_{CO} and by $\dot{G}_f'' A/\dot{V}_T$ (which can be defined as the effective concentration of material vapors).

Data presented in Figure 4 suggest that Y_{CO} has a weak dependency on the fire scale for wood crib and wood-lined tunnel fires. Data presented in Table 3 also suggest that the yields of CO as well as CO_2 and HCN have weak dependencies on the fire scale. Data presented in previous sections, however, show that Y_{CO} is strongly dependent on fire ventilation; thus the concentration of CO is expected to depend more strongly on fire ventilation, flow and mixing of fire products and air rather than on the fire scale.

With increase in fire scale the following will increase: 1) \dot{q}_n'' , and from Eq. (8), \dot{G}_f'' ; 2) A ; and \dot{V}_T . From Eq. (10), increase in \dot{G}_f'' and A will result in an increase in CO concentration, whereas an increase in \dot{V}_T will result in a decrease in CO concentration. The net affect of the increase of fire scale on the concentration of CO thus is not as obvious as it appears to be.

2.4 CO FIRE TOXICITY

For the assessment of smoke toxicity without using animals, National Bureau of Standards has proposed a N-gas model [11]. The N-gas model assumes that toxicity of fire smoke is determined mainly by a small number of gases; these may act additively, synergistically, or antagonistically [11]. The model suggests that all the animals exposed to fire products are expected to die when

$$\sum_{j=1}^m C_j / (LC_{50})_j \geq 1.0,$$

where C_j is the concentration of the compound j (ppm); m is the number of chemical compounds generated in the fire, and $(LC_{50})_j$ is the concentration of compound j producing death in 50% of the animals for a defined exposure period (ppm). The suggested relationship has been found to be valid for mixtures of CO and HCN with concentrations in the range of 25, 50 and 75% of their respective LC_{50} values [11].

Table 3
Average Yields of CO_2 , CO, and HCN
for Well-Ventilated Turbulent Flaming Fires of Materials^a

Material	Surface Area (m ²)	Y _j (g/g)		
		CO ₂	CO	HCN
Methanol	4.68	1.29	< 0.001	NA
	2.32	1.30	< 0.001	NA
	0.008	1.32	< 0.001	NA
Rigid Polyurethane Foam	7	1.50	0.027	0.010
	0.008	1.51	0.036	0.012
Polymethylmethacrylate	2.37	2.11	0.008	NA
	0.073	2.10	0.010	NA
	0.008	2.15	0.011	NA
High Temperature Hydrocarbon Fluids	2.37	ND	ND	ND
	0.008	2.64	0.019	NA
Heptane	0.920	2.83	0.0150	NA
	0.059	2.92	0.0090	NA
	0.410	2.82	0.0081	NA
	0.008	2.84	0.0091	NA
Corrugated Paper Boxes with Shredded Paper (19% by Weight) on Wood Pallets (38% by Weight)	53	1.25	0.0085	NA
	0.060	1.12	0.0082	NA
Corrugated Paper Box with Shredded Paper (25% by Weight)	0.060	1.25	0.019	NA
Corrugated Paper Box with Shredded Paper (62% by Weight)	0.062	1.33	0.005	NA
Pine Wood Crib	0.007	1.31	0.004	NA
Douglas Fir	0.007	1.27	0.004	NA
Red Oak	0.007	1.29	0.002	NA
Cellulose Powder	0.007	1.29	0.002	NA

a: Data taken from References 6.

ND: Not determined.

NA: Not applicable.

In this paper, we have used the N-gas model for simplified application to CO and CO_2 mixtures for diffusion flames of propane and propylene and wood cribs. From Eq. (10), expressing C_{CO} in ppm,

$$C_{CO} \text{ (ppm)} = (Y_{CO} / \rho_{CO}) (\dot{G}_f / V_T) \times 10^6 \quad (11)$$

and for CO₂,

$$C_{CO_2} \text{ (ppm)} = (Y_{CO_2} / \rho_{CO_2}) (\dot{G}_f / \dot{V}_T) \times 10^6 \quad (12)$$

Recently Levin et al [12] have developed a relationship for the toxicological synergism between CO and CO₂ for hazardous environment

$$m C_{CO} / (C_{CO_2} - b) \geq 1.0 \quad (13)$$

where m is the slope and b is the intercept of the curve showing toxicological synergistic relationship between the concentration of CO₂ and CO. For C_{CO₂} < 50,000 ppm, m = -28 and b = 117,000 ppm and for C_{CO₂} > 50,000 ppm, m = 150 and b = -313,000 ppm [12].

From Eqs (11), (12) and (13), condition for hazardous environment can be expressed as follows

$$\frac{m (Y_{CO} / \rho_{CO}) (\dot{G}_f / \dot{V}_T) \times 10^6}{(Y_{CO_2} / \rho_{CO_2}) (\dot{G}_f / \dot{V}_T) \times 10^6 - b} \geq 1.0 \quad (14)$$

Using $\rho_{CO} = 1165 \text{ g/m}^3$ and $\rho_{CO_2} = 1842 \text{ g/m}^3$ at 293°K and expressing left hand side of Eq. (14) as toxicity parameter, T_x, the following relationships can be derived:

1) For C_{CO₂} ≤ 50,000 ppm

$$T_x = \frac{-0.2054 Y_{CO}}{0.0046 Y_{CO_2} - (\dot{V}_T / \dot{G}_f)} \quad (15)$$

2) For C_{CO₂} > 50,000 ppm

$$T_x = \frac{0.4114 Y_{CO}}{0.0017 Y_{CO_2} + (\dot{V}_T / \dot{G}_f)} \quad (16)$$

Figure 5 shows a plot of the toxicity parameter plotted against air-to-fuel stoichiometric fraction for propane, propylene and wood crib, where data for CO and CO₂ were measured in our apparatus [6]. The data in Figure 5 show that if fire products are not diluted, hazardous conditions, where T_x ≥ 1.0, are achieved for φ ≤ 1.8 for propane and propylene and φ ≤ 0.8 for pine wood cribs. If fire products are diluted, hazardous conditions change such as shown in Figure 6 for propane and pine wood cribs. The data show that hazardous conditions are not present in the fires of wood cribs and propane when fire products are diluted by air by about ten and fifteen times their volume, respectively, even if the yield of CO may be very high and fires may be highly underventilated.

2.5 CONCLUSION

From the analysis of the data presented in this paper, the following can be concluded: 1) the yield of CO is weakly dependent on the fire scale for turbulent fires; 2) the yield of CO is strongly dependent on the chemical structure of the materials; it increases as the structure changes from aliphatic to aromatic to highly halogenated; 3) the yield of CO is strongly dependent on the fire ventilation; it increases with decrease in ventilation. Values as high as 0.30 have been found for the yield of CO in highly under-ventilated fires; 4) combination of the data from National Bureau of Standards' fire toxicity study on CO and CO₂ and our flammability study suggest that if CO and CO₂ were the only gases of concern, the hazardous environments may not be present if fire products are diluted by about ten and fifteen times their volume by air for wood cribs and propane, respectively, even if fires are highly under-ventilated and Y_{CO} values may be very high. It is interesting to note that fire products from other materials can also be diluted to eliminate hazardous conditions, but the extent of dilution may depend on the generic nature of the material. It may be possible to rank materials on the basis of extent of dilution required to eliminate hazardous conditions.

ACKNOWLEDGEMENT

Financial Support for the study by the National Bureau of Standards, Center for Fire Research under Grant No. 60NANB4D-0043 is deeply appreciated.

NOMENCLATURE

A	Surface area of the material (m ²)	τ	Time (s)
C _{CO}	Concentration of CO (g/m ³ or ppm)	.	.
f _{CO}	Generation efficiency of CO (-)	V _T	Total volumetric flow rate of fire product-air mixture (m ³ /s)
G _f ["]	Mass generation rate of material vapors per unit surface area of the material (g/m ² s)	W _{CO}	Total mass of CO generated (g)
G _{CO} ["]	Mass generation rate of CO per unit surface area of the material (g/m ² s)	W _f	Total mass of material vapors generated (g)
k _a	Mass air-to-fuel stoichiometric rate (g/g)	Y _{CO}	Yield of CO (g/g)
k _{CO}	Maximum possible theoretical yield of CO (g/g)	<u>Greek Symbols</u>	
L	Heat of gasification of material (kJ/g)	δ	Fraction of entrained air which reacts with material vapors
MW	Molecular weight (g/mole)	ρ _j	Density of compound j (g/m ³)
n	Number of carbon atoms (-)	<u>Subscripts</u>	
q̇ ["]	Heat flux per unit surface area of the material (kW/m ²)	f	Material vapors
T _x	Toxicity parameter (-)	n	Net
		<u>Superscripts</u>	
		.	Per unit of time (1/s)
		"	Per unit surface area (1/m ²)

REFERENCES

1. Fire and Smoke: Understanding the Hazards. Committee on Fire Toxicology. Board on Environmental Studies and Toxicology Commission on Life Sciences, National Research Council, National Academy Press, Washington, DC 1986.
2. Tewarson, A., "The Effects of Fire-Exposed Electrical Wiring Systems on Escape Potential from Buildings. Part I - A Literature Review of Pyrolysis/Combustion Products and Toxicity - Poly (Vinyl Chloride)," Factory Mutual Research Corporation, Norwood, MA, Technical Report 22491, RC75-T-47, December (1975).
3. Hartzell, G.E., Priest, D.N., and Switzer, W.G., "Modeling of Toxicological Effects of Fire Gases: II. Mathematical Modeling of Intoxication of Rats by Carbon Monoxide and Hydrogen Cyanide," J. Fire Sciences 3, 115 (1985).
4. Kaplan, H.L., Grand, A.F., and Hartzell, G.E., "A Critical Review of the State-of-the-Art of Combustion Toxicology," Southwest Research Institute, San Antonio, TX, Final Report SWRI Project No. 01-6862, June 1982.
5. Tewarson, A., "Prediction of Fire Properties of Materials, Part I. Aliphatic and Aromatic Hydrocarbons and Related Polymers," National Bureau of Standards, Gaithersburg, MD, Technical Report NBS-GCR-86-521, December 1986.
6. Tewarson, A., "Prediction of Fire Properties of Materials," National Bureau of Standards, Gaithersburg, MD, Technical Report (to be issued).
7. Beyler, C.L., "Major Species Production by Solid Fuels in a Two-Layer Compartment Fire Environment," Fire Safety Science, Proceedings of the First International Symposium, Hemisphere Publishing Corporation, New York, NY, p. 431, 1986.
8. Lomax, S., and Simmons, R.F., "The Formation of Carbon Monoxide from Diffusion Flames," Fire Safety Science, Proceedings of the First International Symposium, Hemisphere Publishing Corporation, New York, NY, p. 441, 1986.
9. Morikawa, T., "Effect of Supply Rate and Concentration of Oxygen and Fuel Location on CO Evolution in Combustion," J. Fire Sciences 1, 364, 1983.
10. Tewarson, A., "Fully Developed Enclosure Fires of Wood Cribs," Twentieth Symposium (International) on Combustion, The Combustion Institute, Pittsburgh, PA, p. 155, 1984.
11. Babrauskas, V., Levin, C., and Gann, R.G., "A New approach to Fire Toxicity Data for Hazard Evaluation," ASTM Standardization News, September 1986.
12. Levin, B.C., Paabo, M., Gurman, J.L., Harris, S.E., and Braun, E., "Evidence of Toxicological Synergism Between Carbon Monoxide and Carbon Dioxide," Toxicology (to be published).

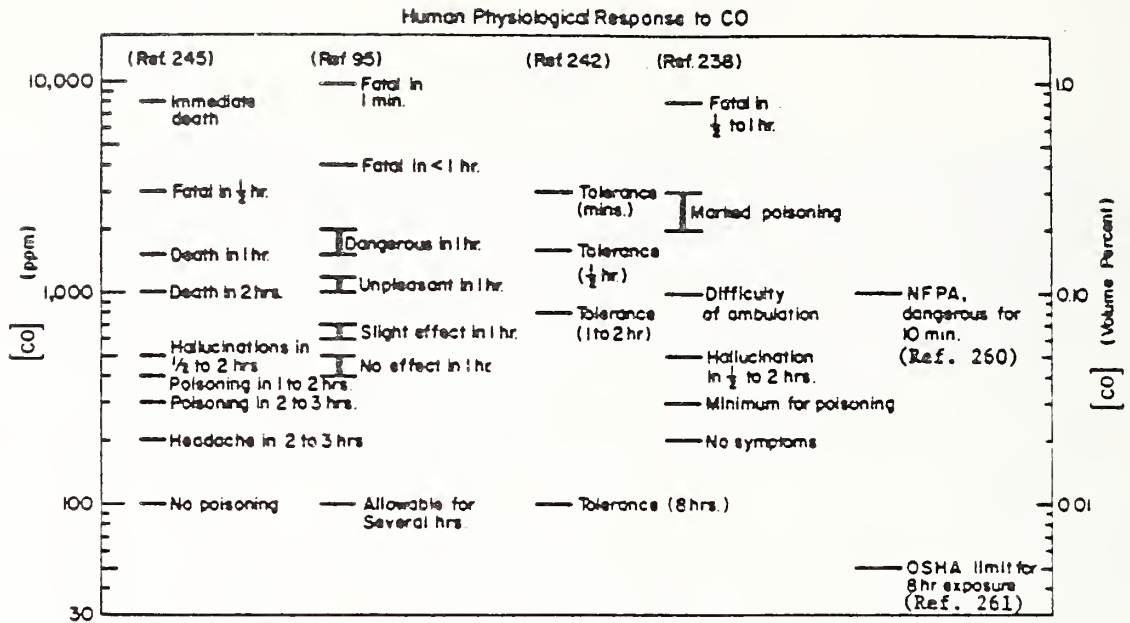


Figure 1. Summary of Results of Some Selected Studies on Human Physiological Response to CO, Taken from Reference 2. Reference Numbers Identified in the Figure Appear in Reference 2.

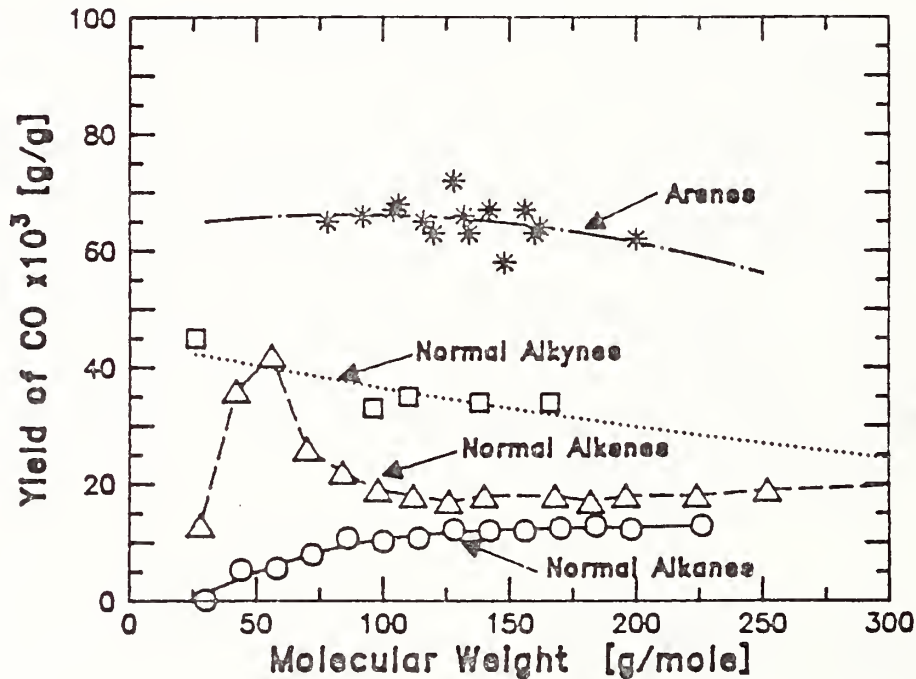


Figure 2. Yield of CO as a Function of Molecular Weight for Well-Ventilated Fires of Normal Alkanes, Alkenes and Alkynes and Arenes. Data Taken from Reference 5.

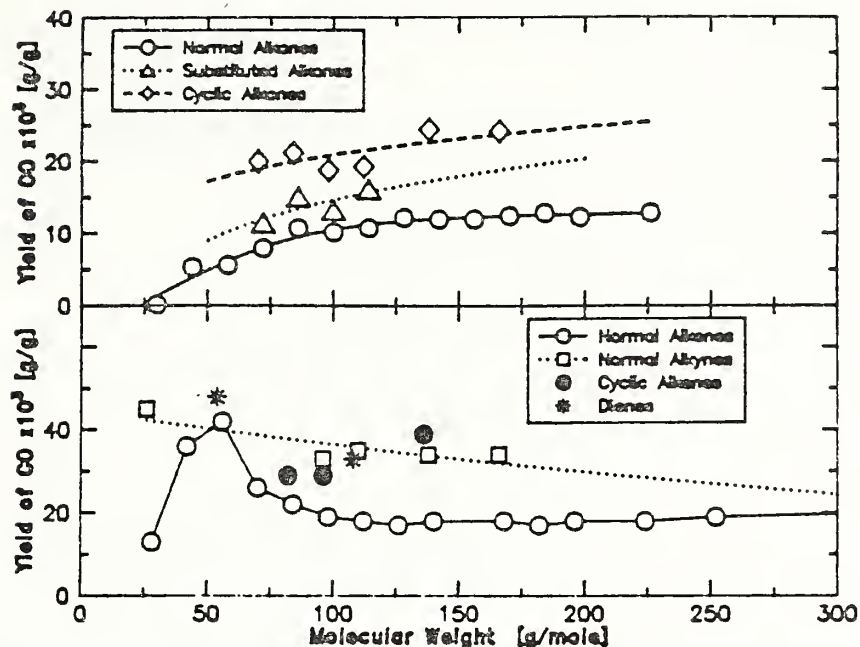


Figure 3. Yield of CO as a Function of the Molecular Weight for Well-Ventilated Fires of Normal, Substituted and Cyclic Alkanes, Alkenes, Dienes and Alkynes. Data Taken from Reference 5.

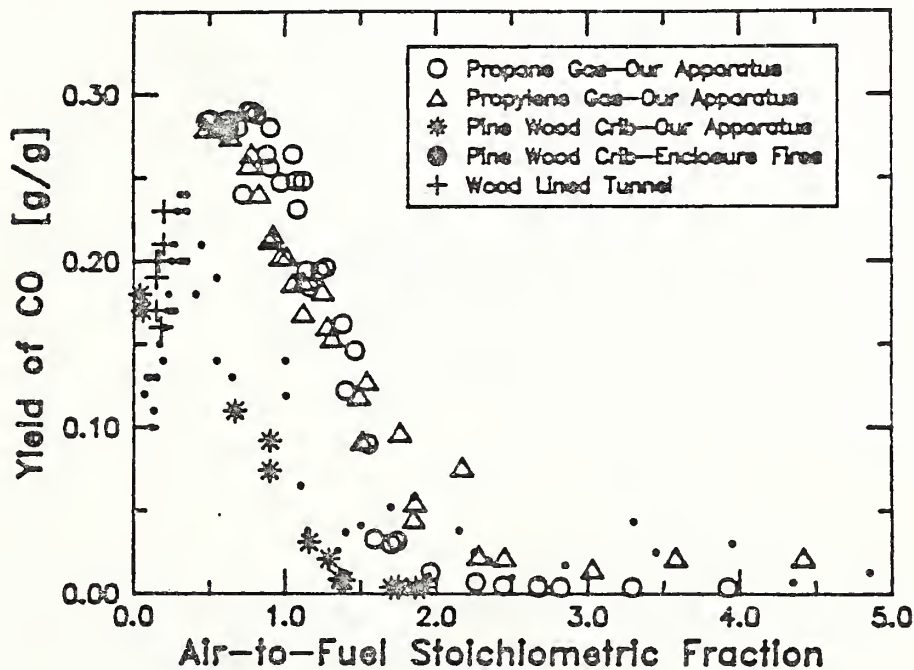


Figure 4. Yield of CO as a Function of Air-to-Fuel Stoichiometric Fraction. Data Taken from References 6 and 10.

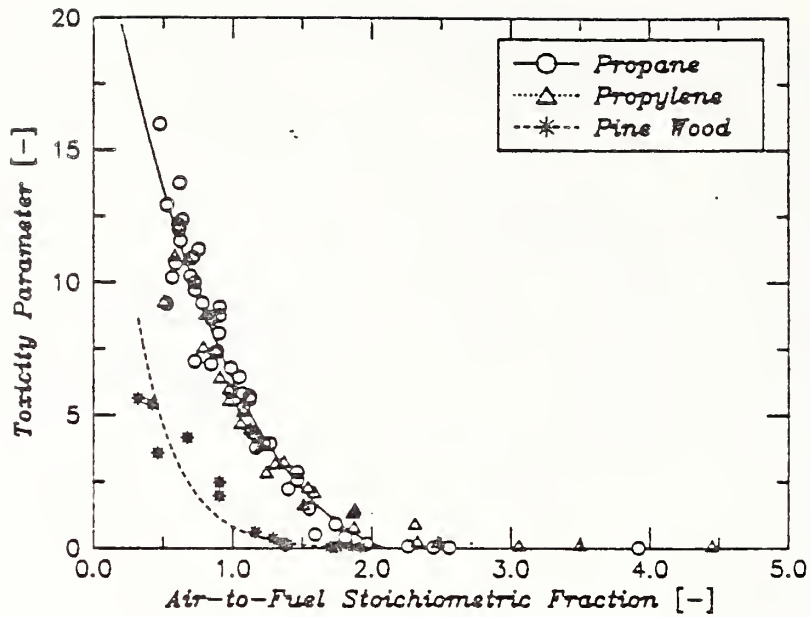


Figure 5. Toxicological Effects Due to CO and CO₂ Generated in Diffusion Flames. No Downstream Dilution of Fire Products.

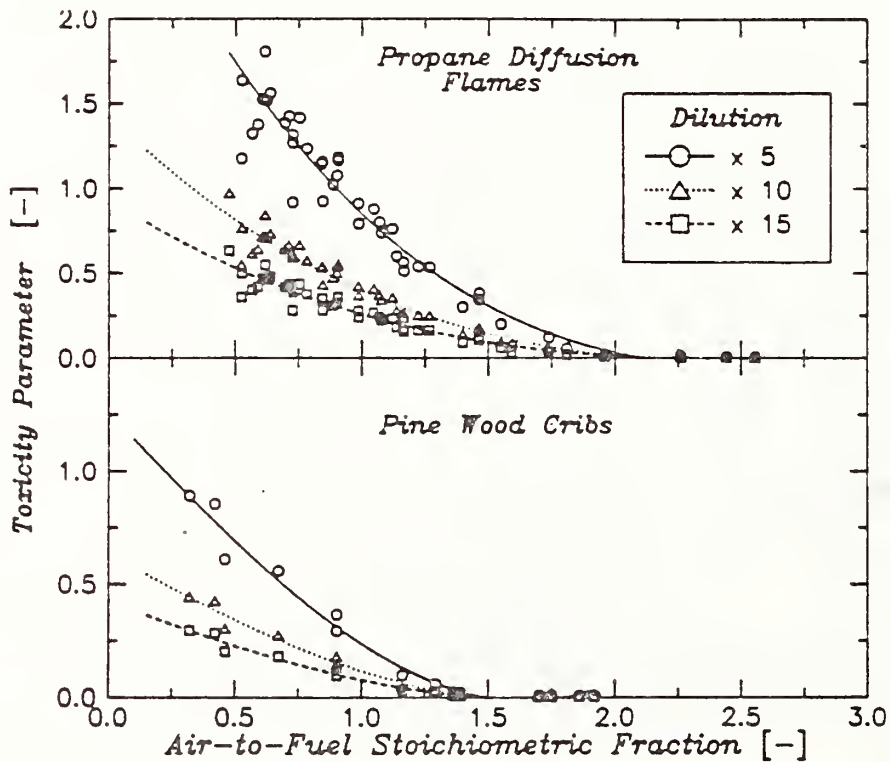


Figure 6. Toxicological Effects Due to CO and CO₂ Generated in Diffusion Flames. Varying Downstream Dilution of Fire Products.

RISK, HAZARD, AND EVACUATION (CONT.)

EXITT - A Simulation Model of Occupant
Decisions and Actions in Residential Fires

Bernard M. Levin
Center for Fire Research
National Bureau of Standards
Gaithersburg, Maryland 20899, USA

ABSTRACT

EXITT is a discrete event simulation of occupant decisions and actions in a simulated fire. Before the simulation starts, the characteristics of a residence, a fire in that residence, and the occupants of the residence are entered into the computer. Based on a large set of decision rules, the occupants "make" decisions which are a function of the smoke conditions in the building, the characteristics and status of the occupants (including their capabilities), and the available travel routes. The occupants investigate the fire, alert and assist others, and evacuate the building. The simulation ends when all the occupants are either out of the building or are trapped by the smoke.

1. INTRODUCTION

The EXITT model simulates occupant decisions and actions in fire emergencies in small residential buildings. In assigning decisions to an occupant, the computer considers such factors as: age of occupant; sex; whether occupant is asleep; smoke conditions; whether smoke detector is sounding and how loud it sounds; whether occupant needs help in moving; and location, capabilities, condition and status of the occupants. This version of the model does not consider the heat or toxic components of the smoke. The permitted actions include: investigate the fire; alert others; awake others; rescue others; and evacuate/escape. Actions not permitted in the current version include: telephoning fire department from within the building; fighting the fire; and re-entering the building to make a second rescue.

This paper describes the EXITT model, with emphasis on the rules used in determining the simulated decisions and actions of the occupants. The simulation is currently being developed as a series of progressively more sophisticated models. This paper describes an early interactive version of the model.

A more extensive description of the model, including a users's guide is in preparation and should be published during the summer of 1987 [Levin, 1987]. Upon its publication, the computer program will be available from the author and from the Center for Fire Research.

Imbedded in the decisions rules are parameters that can be easily changed.

Developing improved values for these parameters is a major part of the future development of the model.

This simulation program is designed to run on the IBM-PC computer (and similar microcomputers using the MS-DOS operating system) using the BASICA programming language.¹

The user controls the model through the keyboard by answering simple questions that appear on the screen. (A "batch" version of the model, that does not require or permit user interaction during the running of the model, is also available in the FORTRAN programming language: the decision rules in this paper apply also to the batch version.) The decisions of the occupants are reported on the screen and on the printer. The movements of the occupants are displayed graphically on the screen, reported on the printer, and stored in a data file. The user can suppress outputs on the printer and on the screen.

All the decision rules programmed in the computer model are designed to make the decisions as similar as possible to those that building occupants would make. The decision rules are based on: 1. a limited number of controlled experiments; 2. case studies of occupant actions in residential fires; and 3. the judgment of the author. Whenever the rules are based directly on data in the literature or specific case studies, reference is made to such data. Otherwise, the rules are based on the author's judgment.

The fires, buildings and occupants that are modelled can come from two sources: 1. three buildings--each with two or more fires and two or more sets of occupants--are stored in the computer programs and associated data files; and 2. the user can substitute a new building, fire and/or set of occupants by answering a large number of simple questions appearing on the screen.

2. INPUT VARIABLES AND PARAMETERS

Building. The building is represented within the computer by nodes that represent rooms, exits and secondary locations within rooms; and by links or distances between adjacent nodes. The major data used to define a building are: the number of rooms, nodes and exits; the height of each room; the room location of each node; nature of each exit (door or window); and the distances between adjacent nodes. Windows that cannot or would not be used in a fire are not entered into the computer as exits, e.g., those with a window air conditioner installed.

Smoke. The program is designed to use the output of the FAST model--or any other similar model--for distributing smoke throughout the building over time [Jones, 1984]. EXITT assumes a two layer smoke model. However, it is

¹The use of company names or trade names within this paper is made only for the purpose of identifying those computer hardware or software products with which the compatibility of the programs of EXITT has been tested. Such use does not constitute any endorsement of those products by the National Bureau of Standards.

assumed that a small proportion of the smoke in the upper layer gets into the lower layer so that there is an odor of smoke in the lower layer. Exitt accepts as input the smoke density in the upper layer and the depth or height of the two layers in each room at the beginning of each time period, e.g., every five seconds.

The measure of optical density for which the model is being calibrated is the one used by Jin in his studies of human behavior in smoke.

$$OD = \ln (L_0/L)$$

where L_0 is the initial light intensity which reduced to a value of 1 over a path of one meter. This measure is consistent with the well recognized fact that when people perceive a physical stimulus, the perceived intensity tends to vary directly with the log of the physical intensity of the stimulus.

One important factor in making action choices in a residential fire is the properties of the smoke in the occupant's room. A measure of the psychological impact of smoke is determined as follows:

$$S = 2 * OD * D / H \quad \text{where,}$$

S is the psychological impact of the smoke.

OD is the optical density of the smoke in the upper layer,

D is the depth of the upper layer, and

H is the height of the room.

This expression is based on the assumption that the impact varies directly with the optical density (i.e., the log of the amount of smoke in the upper layer) and with the depth of the upper layer relative to the height of the room. The formula is an arbitrary representation of this assumption.

Some of the decision rules and definitions that involve S include:

Occupants will not move to a node where $S > 0.5$ unless the depth of the lower layer ($H-D$) is at least 1.2 meters, i.e., unless the occupant can crawl under the smoke.

Occupants will not move to a room where $S > 0.4$ unless the depth of the lower layer is at least 1.2 meters.

Occupants will increase their travel speed by 30% after encountering a room where $S > 0.1$.

Occupants will terminate an investigation if they are in a room where $S > 0.05$. They will terminate their investigation before entering a room where $S > 0.1$.

Once an occupant is in a room where $S > 0.1$, he will respond more quickly: the changes are described below as consequences of believing the fire to be serious.

When $S > 0.4$ there are prohibitions and penalties: these are described below as consequences of encountering "bad smoke."

Each of the above mentioned thresholds is an input parameter and can be easily changed as we continually improve the calibration of the model, i.e.,

modify the model to better correspond to behavior in real fire emergencies. Although the values selected are consistent with a conservative interpretation of Jin's data [1976], these values will be reconsidered as part of the further development of the model.

Noise and Alarm. The background noise level in a room affects the ability of an occupant to hear the alarm, both in real fires and in the model. The background noise is preset at 35 decibels. The user can easily override this value, on a room by room basis, by entering a larger value when defining the fire scenario.

Another input, related to a specific fire scenario, is the loudness of each smoke detector in each room, including the room in which it is located--it is a function of distances and of which doors are open. The impact of the alarm is a function of the difference between the volume of the alarm and the background noise.

Characteristics of the Occupants. The user has an opportunity to either define or modify the characteristics of the occupants through the keyboard. The characteristics are: age, sex, normal travel speed, whether or not the occupant needs help in evacuation, whether or not the person is awake, room location, and, if the occupant is asleep, a measure of how difficult it is for the occupant to awaken.

There are a number of additional parameters imbedded in the decision rules which are described below. These include: the age below which a child is considered as a baby unable to initiate any action; and the times required to perform various actions, such as waking a sleeping adult occupant when the fire does not appear to be serious. Some of these additional parameters are described in Section 5, Delays, Pauses and Action Times.

3. DECISION RULES

Introduction. There are two types of occupants: those who are fully capable when awake and those who need assistance in moving. The decision rules apply only to those who are capable when awake. Those who need assistance moving make no decisions and their movements are determined by their "rescuer".

At the beginning of the simulation, all occupants are unaware of the fire and the potential danger. Actions and decisions are assigned, in part, based on the smoke conditions in each room at the beginning of the appropriate time period.

The following paragraphs describe the sequential steps the computer follows in determining the decisions and actions of one occupant for one time period. The computer goes through these steps for each capable occupant for the first time period and then repeats the process for each subsequent time period, in turn, until all the occupants are either out of the building or trapped by the fire. (For each step, the computer considers all occupants before proceeding to the next step.)

Aware of Fire. The first step in determining the actions of an occupant is to determine if and when an occupant is sufficiently aware of the fire cues (i.e., smoke, sound of alarm and visible flame) to undertake an action. If the occupant became aware of the fire cues in a previous time period, he will remain aware of the fire cues for this and all subsequent time periods. An occupant becomes aware of the fire when the fire cues are sufficiently strong. Obviously, stronger cues are needed to awaken and alert a sleeping occupant than to alert an awake occupant. The fire cues are: the sound of the smoke detector; the odor of smoke; and, for awake occupants, visible smoke and visible flame. If the weighted sum of the intensities of the cues reach a prescribed threshold, the occupant will be flagged as being aware of the fire cues. (If the fire cues are of borderline intensity, the occupant will become awake and aware after an assigned delay.) If the fire cues are not sufficiently strong for the occupant to become aware of the fire during the current time period, the consideration of this occupant for the time period is completed.

The following basic equation, for determining if and when an occupant will start to respond to the fire cues, was suggested by the empirical results of Nober et al. [1981]. While Nober studied only the response of the smoke detector alarm, his results were generalized for the odor of smoke, and the sight of smoke.

$$T = 70 - 4(C-20) \quad \text{and}$$

$$C = (A-N)+X1+X2+X3+X4 \quad \text{where,}$$

T is the delay time, in seconds, before the occupant will start his first action;

C is the sum of the sensory impacts on the occupant;

A is the sound intensity of the smoke detector as heard by the occupant;

N is the background noise;

X1 is impact of an awake occupant seeing flame. It is set sufficiently high to assure a rapid response whenever an awake occupant is in the same room as a visible flame and set equal to zero if the occupant is asleep;

X2 is impact of an occupant smelling smoke--it is a function of the smoke density and smoke depth and applies to both sleeping and awake occupants. It varies directly with S, the psychological impact of smoke when the smoke remains above 1.2 meters. However, its value dramatically increases when the upper smoke level gets down to the height of a person in a bed;

X3 is impact of an awake occupant seeing smoke--it is a function of the product of the smoke density and smoke depth in the upper layer and also varies directly with S; and

X4=0 if the (typical) occupant is asleep and X4=15 if the occupant is awake. This reflects the fact that more stimuli are require to awake than to alert an occupant. The value of 15 is based on the data in Nober [Nober et al, 1981]. Occupants who have difficulty waking could be assigned negative values of X4.

Subject to the restrictions:

A-N cannot be less than zero. If N>A let A-N = 0;

If $C < 20$ then $T = \text{infinity}$ (i.e., 99999 in the computer). This restriction is based on Nober's data where occupants usually either responded within 70 seconds or remained asleep for the remainder of the test period.

$X1$ and $X3$ equal zero if the occupant is asleep.

The model as described above assumes that the response is a function of the sum of the impacts of different sensory cues. This assumes that the relevant aspects of the perceptual processing of olfactory, visual and auditory cues are similar. There does seem to be a surprisingly consistent perceptual rule (Fechner's Law) that the intensity of a perception varies directly with the log of the physical stimulus. (While this rule has broad applicability, it is not universal and only approximate [Boring, 1950].) Since our measure of the psychological impact of all the cues are based on the log of a physical measure, the impacts to the three types of cues can be assumed to be roughly comparable. The decision to sum the impacts of the three cues is based on the assumption that simple behavioral rules are better than complicated ones when there is no technical reason to select a complicated one. Furthermore, simple summing is consistent with the results of Fletcher and Munson who found that a tone heard binaurally seems twice as loud as the same tone heard monaurally [Licklider, 1951].

The physical measure of each fire cue is measured in different units and they must be converted to a single measure of sensory impact. The cue most easy to quantify, and the one for which we have the most data, is the sound of the smoke alarm which is measured in decibels. It was decided to use "equivalent decibels" as the single measure of sensory impact. The impacts of the other sensory cues are "converted" to equivalent decibels, i.e., the values of $X2$ and $X3$ are transformed to the number of decibels that would approximate an equivalent impact in alerting occupants. (When the flame is visible to an awake occupant, the value of $X1$ is set sufficiently high to ensure a rapid response.) The transformation factors are input parameters: their values will be the subject of future research and analysis.

While occupants respond more quickly to strong fire cues, there is a minimum duration of time required to awaken or become aware of the fire cues, select an action, and perform preparatory actions. These minimum times range from 1 to 10 seconds depending on whether the occupant is asleep and the amount of smoke.

For each occupant, a time to start his actions is computed independently at each time period until the occupant starts his first action: that is, a different time to start his actions will be computed each time period. He will start his action at the earliest time among those computed.

Assigning Actions to Occupants Who Are Aware of Fire. If an occupant has been assigned an action in a previous time period, he will be given an opportunity to complete that action before any consideration is made regarding additional actions.

Investigation Top Priority. The normal first action is to investigate the fire cues to determine the nature of the hazard. However, there are a number of exceptions, i.e., situations that would make investigation either

a lower priority or an unreasonable choice. [Levin, 1985] If the computer determines that none of these exceptions applies, the computer assigns the room with the most smoke as the GOAL, labels the occupant as investigating, and assigns him the task of going to the room with the most smoke.

One special situation that would cause investigation to be a low priority arises when an adult female occupant is in the same building as a baby--in a case study provided by Keating and Loftus a mother rescued her baby before determining if it was necessary. [Keating and Loftus, 1984]

Investigation is not permitted: if the occupant has already completed an investigation; if the occupant has been in a room with moderate or bad smoke; or if the occupant has been awakened or alerted by an occupant for whom investigation is not permitted.

If the exceptions do apply, the computer considers the following alternative actions in the order given below.

Help Occupant in Same Room. The computer determines if there is another occupant in the same room who needs help. If that occupant is fully capable but asleep, he will be awakened. If he needs assistance moving, he will get that assistance. (If more than one occupant qualifies for help, the sleeping occupant is given priority.)

Help Occupant in Different Room. If there is one or more persons in a different room(s) who needs to be alerted, rescued or awakened, the computer will make two assignments: tentatively assign the fully capable occupant a person to alert, rescue or awaken; and assign the capable occupant the action of going to the room of that person. (Once he arrives at that room, a new action will be assigned based on fire situation at that time and the capabilities of the persons in the room. Exception: if he is going to the room of an awake and capable person who needs to be alerted, he will automatically alert that occupant.) The priority order of these tentative assignments for helping persons in different rooms is: alert capable adult; rescue other occupant; wake other occupant; and alert child.

Investigate. If investigation is still a permitted choice, the occupant is assigned the task of investigating. The computer assigns the room with the most smoke as the GOAL, labels the occupant as investigating, and assigns him the task of going to the room with the most smoke.

Egress. If none of the above alternative assignments apply, the occupant is assigned the action of evacuating.

Every capable occupant is considered for helping an occupant in the same room before any occupant is considered for helping an occupant in a different room.

In this version of the model, an occupant over the age of ten functions as an adult, that is, they follow the priority list presented above for adults.

A child who is 8,9, or 10 will rescue any occupant in the same room and will go to another room to awaken or alert another occupant but will not go to another room for the purpose of rescuing an occupant. Children 7 and younger do not assist others out of the building but will wake or alert other occupants who are older. A child is considered to be a baby if his age is equal to or less than the parameter BABY: babies do not initiate any actions. The tentative value of BABY is 3.

The general rationale for the above priority order is to determine if there is a need for positive action, to assist those known to require help, and then to assist those who might require help. (When it is unknown if a sleeping occupant has awakened, he can be considered as someone who might require help.) If two people are known to require help, provide help to the one needing more limited help, that is, a sleeping but otherwise capable occupant. The rule that supercedes all others is to help someone in the same room before helping an occupant in different room.

4. TRAVEL WITHIN THE BUILDING

Occupants move within the building from node to node. The path assigned is determined by finding the shortest path to an exit based on a shortest path algorithm which contains an option for assigning penalties for going through bad smoke and for leaving through windows.

The route to be taken to a designated room, the best exit, or another designated node is determined by a shortest path algorithm. Normally when the occupant is investigating or going to assist another occupant, a straightforward shortest distance is determined.

If the occupant wishes to egress or evacuate the building, or if the occupant had encountered too much smoke when going to assist another occupant, then the path with the lowest number of demerits is selected. Each meter of travel is assigned one demerit, leaving by a window is assigned 100 demerits, and going to a node through bad smoke is assigned 200 demerits. If the smoke at a node is intolerable, that node cannot be part of a route. If smoke is blocking all routes to the designated node, the occupant will decide to escape. If the occupant is escaping, the route out of the building with the least demerits is selected. If all escape routes are also blocked, he will be considered trapped. (See section on Smoke in Section 2 for decision rules regarding moving or not moving through bad smoke.)

As an occupant attempts to move, whenever he encounters an intolerable amount of smoke based on the criteria in Section 2, he will stop moving and the computer will redetermine his best route to his destination, i.e., the route with the fewest demerits. If the shortest path algorithm fails to find an acceptable path, the computer will look for the best route out of the building. If all exit routes are blocked by smoke, the occupant is considered trapped.

5. DELAYS, PAUSES AND ACTION TIMES

Introduction. The time consuming activities of an occupant can be classified into three categories.

Movement from one node to another. He travels the shortest path at the speed defined below.

Delays and pauses. These activities include time to awaken, time to make decisions, and time to prepare for action.

Assisting actions, i.e., waking another occupant and preparing another occupant for egress.

Speed. The travel speed of each occupant is set at:

1.3 meters per second for normal conditions;

1.69 m/s (30% faster than normal) if an occupant should consider the fire to be serious (e.g., he has been in a room with heavy smoke);

0.65 m/s (50% of normal) if the occupant is assisting another occupant, or 0.845 m/s if the occupant also considers the fire to be serious;

0.78 m/s (60% of normal) if the smoke is bad (i.e., $S > 0.4$) and if the depth of the lower layer is less than 1.5 meters, i.e. if the occupant has to "crawl" under the smoke. (0.52 m/s if the occupant is also assisting another occupant.)

The normal travel speed and all the modification factors are parameters that can be set by the user. While these values will be reconsidered as part of further model development, they are similar to those reported by Jin [1976].

Whenever an occupant moves, his actions are printed on the screen and on the printer, recorded in a data file, and graphically represented on the screen. (Printing on the screen or on the printer can be suppressed.)

Delay Times. The delay time, the decision time, and the time to perform assisting actions (hereafter, collectively called Delay Times) depend on the occupant characteristics, the fire characteristics and the impact of the fire cues on the occupant. The length of these Delay Times are determined by a set of decision rules as described below. These Delay Times can be changed rather easily and all assigned values should be considered as tentative.

Minimum Response Time. The normal (i.e., smoke is not bad) minimum response (delay) time is 6 seconds for awake occupants: this includes decision and preparation time. The normal minimum response time for sleeping occupants is 10 seconds: this also includes decision and response times. These values are based on the work of Nober [Nober et al, 1981]. The status of sleeping occupants is changed to awake status whenever the remaining response time is 6 seconds or less.

TPAUSE. An occupant is assigned normally a delay time of TPAUSE seconds whenever: he completes his investigation or terminates his movement along a route because of intolerable smoke; or changes his mind about helping

another occupant. This delay includes the time required to choose a new action. TPAUSE is tentatively set equal to 3 seconds.

Decrease in Preparation Time Due to Heavy Smoke. When an occupant is subjected to normal fire stimuli, a ten second response Delay Time is assigned to a sleeping occupant and six seconds to an awake occupant. (Note the response time will be greater if the fire stimuli are not sufficiently strong for an immediate response.) However, if the occupant believes the fire to be serious, the maximum Delay Time for the occupant becomes four seconds and if the smoke in the room is bad, the maximum Delay Time becomes 1 second.

Hesitation Due to Not Being Alone. Research by Latane and Darley [Latane and Darley, 1968] has shown that when the fire cues are noticed but not immediately compelling, adults will hesitate in their responses if other capable adults are in the same room. A simple explanation is that there is a failure to respond due to a feeling of shared responsibility. The computer program accounts for this by delaying responses by one time period for each time period where: there is no one that needs to be rescued, alerted, or roused; there is a second capable occupant in the room; the smoke detectors are not sounding; and the sum of the psychological impacts of the fire cues is less than 30, i.e., if $C < 30$ then $T = 99999$, where C and T are defined in Section 2. (The threshold for this hesitancy is 30 rather than 20 to reflect that more stimuli or cues than the "minimum for response" are required to prevent the "hesitation due to not being alone.")

Time Required to Alert, Wake or Prepare for Evacuation. Whenever one occupant assists another, time for providing or receiving the service must be assigned. The following times are assigned:

If Occupant J is alerting a fully capable and awake adult, he moves to the node of the other occupant. Once he arrives at that node, Occupant J starts his next action with no delay or decision time charged. The occupant being alerted is assigned a Delay Time of five seconds or 2.5 seconds depending on whether the alerting occupant believes the fire to be serious.

There are two types of assistance that an occupant may be flagged as needing: waking; and help moving. If an occupant is asleep and does not need help moving, the delay is five seconds for the occupant doing the waking. For the occupant who is being awakened the delay is ten seconds - 5 seconds for waking plus 5 seconds decision and preparation time. However, if the assisting occupant believes the fire to be serious, then his time devoted to waking would be only 2.5 seconds and the total Delay Time for the previously sleeping occupant would be 5 seconds.

If an occupant needs help moving, the Delay Time (at the time the assisting occupant arrives at the location of the other occupant) is usually 10 seconds if the disabled occupant is awake and 12 seconds if he is asleep. However, if the disabled occupant is a baby, the Delay Time, in seconds, is the baby's age plus 4. (It does not take long to pick up a baby and wrap him or her in a blanket.) In addition, if the capable occupant believes the fire to be serious, the previously determined Delay

Time is halved. For example, if the fire is believed to be serious, the Delay Time for helping a 2 year old baby would be 3 seconds $((2+4)/2)$.

5. SMOKE DETECTORS

The building may have up to three smoke detectors. These smoke detectors are independent and are not interconnected in any way. It is necessary to provide the locations of the smoke detectors and how loud each detector would sound in each room of the building. A smoke detector will sound if the smoke density of the upper layer smoke is at least .015, and the depth of the upper layer is .15 meters or greater.

An option in the program is to consider the smoke detectors as broken. It is, therefore, easy to determine the effect of smoke detectors by running the program twice with the same fire and occupants, once with smoke detectors working and once with them broken.

6. CURRENT LIMITATIONS AND FUTURE DEVELOPMENT

The model as described in this paper is a preliminary version of a model under development. The development, improvement and expansion of the model is a continuing activity. The user should be aware of the limitations of the current model which will be distributed in the summer of 1987. These limitations include:

1. The model is deterministic. Only typical behavior is modelled; aberrant behavior is not permitted.
2. Improved calibration is required to upgrade its validity. Calibration means changing parameter values in the model based on: a. analyses of data in the technical literature; b. judgments of a panel of experts; c. analyses of in depth interviews of survivors of residential fires; and, d. attempts to simulate behavior in real fire emergencies for which we have information. An intensive effort to improve the calibration of the model, is scheduled for the next year.
- 3 Some typical actions are not included, e.g, fighting the fire.
4. Occupants respond to smoke conditions but not to heat conditions.

The current development program is designed to overcome and eliminate these limitations. The program can be made probabilistic, and heat will be added as a factor in decision making and route selection.

The model permits the user at the keyboard to override a very limited set of the occupant decisions assigned by the computer. Within the next few months, the user will be given the opportunity to override most, if not all, of these assigned decisions. This will permit the model to be used in studying the effect on safety of alternative decisions by the occupants.

REFERENCES

Boring, E.G., A History of Experimental Psychology, Appleton-Century-Crofts, Inc. New York, 1950, p.289.

Jin, T., Visibility through Fire Smoke (Part 5 Allowable Smoke Density for Escape from Fire, Report of Fire Research Institute of Japan, No.42, September 1976.

Jones, W.W., A Model for the Transport of Fire, Smoke and Toxic Gases (FAST), NBSIR 84-2934, National Bureau of Standards, Gaithersburg, MD, 1984.

Keating, J.P. and Loftus, E.F., Post Fire Interviews: Development and Field Validation of the Behavioral Sequence Interview Technique, National Bureau of Standards, Report Number GCR-84-477, Gaithersburg, Md., 1984. Interview records provided by the authors in private communication.

Levin, B.M., Design as a Function of Responses to Fire Cues, General Proceedings of Conference Research and Design 85: Architectural Application of Design and Technology Research held at Los Angeles, California, March 14-18, 1985, American Institute of Architects Foundation, Washington, D.C., 1985, pp.289-294.

Levin, B.M., EXITT--A Simulation Model of Occupant Decisions and Actions in Residential Fires: Users Guide and Program Description, NBSIR 87-3591, National Bureau of Standards, Gaithersburg, MD, 1987.

Latane, B., and Darley, J.M., Group Inhibition of Bystander Intervention in Emergencies, Journal of Personality Psychology, Vol.10, No.3, Nov. 1968, pp.215-221.

Licklider, J.C.R., Basic Correlates of the Auditory Stimulus, in S.S. Stevens, Handbook of Experimental Psychology, John Wiley & Sons, Inc, New York, 1951, p.1031.

Nober, E.H., et al, Waking Effectiveness of Household Smoke and Fire Detection Devices, Fire Journal, Vol.75, No.4, July 1981, pp.86-91,130.

EXITT - A SIMULATION MODEL OF OCCUPANT DECISIONS AND ACTIONS IN RESIDENTIAL FIRES

B.M. Levin, National Bureau of Standards, USA

HALL: As was mentioned earlier in the week, this is not only an important model in its's own right, but this is an important aspect of HAZARD 1.

JIN: I have two questions. You said that any person, not necessarily an expert on fire, could be a user of this model. Could you be more specific on that? Could just an ordinary individual use it? My question is when you said ordinary people, can you define whether it would apply, for example, mostly to designers of new buildings? Would they find this useful in determining whether to build a building a certain way because of certain circumstances of people, or would it be for existing buildings where people who are concerned with fire safety could use it as a means of analyzing the safety level of the building? Is it mostly intended for the ordinary public, as a public education system method concerning fire evacuation, or would it be for the use of firemen to educate the public in evacuating their own homes?

These are all possibilities, but where is the focus of your building this model?

LEVIN: First, it's a simple enough model so that it can be used by the general public. My son took it upon himself to write instructions so that a person who knows nothing about a computer can use it, even to the point that once you put a disc in the machine you must close the computer door.

In terms of the professional use of the model, I do not visualize it being used very much by people who are interested in design. It is being used now in the HAZARD model that Bud Nelson described in Mr. Bukowski's paper, but I think of it being used a lot in public education. However, I think it may be more useful for helping the people design the programs for the public. For example, when I first joined the Center for Fire Research, I was told that it was safe to sleep only with the doors to the bedrooms closed. However, most Americans will not sleep with their bedroom door closed if they have an infant child in another room. I think my model can be used to analyze this situation in a more professional manner than has been done.

I think the model has another use in addition to your list, in helping us determine where we should put our efforts in learning more about human behavior and fire. The gaps in our knowledge become very apparent when working with a model.

JIN: In this particular model you talk primarily about the action of the people. What I would like to point out is that the action of people is variable. People tend to do things differently under similar circumstances. Professor Keating's data must have shown through an accumulation of the tremendous volume of data, an average action of a person. This is not to say that everybody that he interviewed acted the same way under the given circumstances. In actuality, given the same situation, perhaps a group of people A would act 60 percent one way, B group would act 20 percent another way, and C group would act 10 percent, and so on. I have long studied this problem of human behavior under this type of stress, and I believe that

statistical input also is very necessary. As Mr. Nelson said yesterday, statistical input is very valuable. Perhaps you may input this into your modeling in the future.

LEVIN: Of course. I do plan to put in the probabilities as you suggested, recognizing that it is a difficult thing to do in terms of developing what the probabilities should be. On the other hand, I found something very interesting in analyzing Professor Keating's raw data. I've looked at the data of Dr. Woods from England, from Professor Bryan here in the United States, from Keating, and they always point out that the first action, a percentage of the time it's investigation, but then they list a lot of other actions that occur as a first action.

Professor Keating's raw data gave me an opportunity to look at this phenomena in more depth. His raw data are in-depth interviews where he asked people not only what they did, but what they tried to accomplish. From this data, I was able to infer how much people knew about the fire when they first became aware that there was something wrong.

When I looked at the first response of people who knew something was wrong, but did not know the specifics of the fire, I found they almost invariably, over 90 percent of the time, investigated. One of the exceptions was a mother who went to rescue her baby, not knowing whether there was a need to rescue her or not. In my model, mothers rescue their infant babies before they investigate. In Professor Keating's data all those who woke up in a room with flames, of course, did not investigate, but if we were analyzing the data the way the data had previously been analyzed, they would just have been classified as somebody who did not investigate.

You're, of course, right that we must worry about probabilities, but I feel less uncomfortable due to my analysis of Professor Keating's data.

EMOTIONAL INSTABILITY IN FIRE SMOKE

(Experiment of human behavior in smoke filled corridor)

Tadahisa JIN, Tokiyoshi YAMADA

Fire Research Institute
Fire Defense Agency
Ministry of Home Affairs
3-14-1 Nakahara, Mitaka-shi, Tokyo 181

ABSTRACT

An experimental study was conducted to estimate smoke and heat effects on an emotional instability under smoke condition. Mental arithmetic and walking speed are used as index of the instability and moreover a feeling on smoke and heat was investigated by a questionnaire. From the experiment, high adaptability of humane to smoke condition was recognized in thinner smoke, and the heat of smoke affects a thinking ability down over about 2,000 (kcal/m²h) was found.

1. BACKGROUND

A smoke obstruction against safety evacuation has been pointed out through many fires in the past. A density of CO gas and lack of O₂ in fire smoke are physiological limited factors to decide life or death. However physical and psychological effects of thinner smoke, a decrease of visibility through smoke and/or smoke irritation for instance, tend to give evacuees panics and indirectly lead to death.

Many experimental studies on such smoke effects have been conducted in our laboratory with the smoke of normal temperature. In these experiments, hot smoke effect on human were not considered, so an additional experiment was conducted to estimate a complex effect of heat and smoke with electric heat radiator instead of hot smoke.

About 30 subjects were exposed to a smoke environment and in each experiment, the physiological and psychological effect of smoke and heat radiation was investigated by mental arithmetics and a questionnaire.

2. METHOD AND CONDITION OF EXPERIMENT

31 subjects participated in this experiment. The experiment was conducted in the smoke filled corridor. Each subject was imposed to walk forward in this corridor answering the arithmetic questions, simple additional and subtractive calculations, as show in Fig. 1.

2.1. EXPERIMENTAL CONDITION OF THE CORRIDOR

The experiment was conducted in the straight corridor of about 11 m depth, 2.5 m height, 1.2 m width. On its floor, five mats, in which an on-off switch was equipped, were set to know the stand position of subjects in a smoke environment. At each of these five points, subjects stopped to answer arithmetic questions as mentioned later.

The corridor was filled with white smoke generated by smoldering Japanese cedar crib chips in electric furnace before starting each experiment. At the beginning of the experiment, a smoke density expressed by the extinction coefficient was adjusted to 1.2 (1/m) and weakened slowly to the 0.1 (1/m) during 30 minutes. In this 30 minutes duration, two or three subjects individually entered into the corridor by turns under some kinds of smoke density levels.

A temperature inside the corridor was about 20 °C. At the inner position of A and B, the heat was radiated to subjects with electric radiator (at A -->12 Kw, B -->3 Kw) set at a ceiling.

A maximum heat flux density was 2,030 (Kcal/m²h) at A-point and 1,370 (Kcal/m²h) at B-point of the 1.5 m height from the floor level. Mean Radiant Temperature measured with glove thermometer levels about 82 °C at A-point and 75 °C at B-point.

Inside the corridor was illuminated by fluorescent lamps at some points, and illumination levels in the range of 30 to 100 (lx) on the floor.

2.2 MENTAL ARITHMETIC

A mental arithmetic method was adopted to estimate a degree of emotional instability under smoke condition in this experiment. A rate of correct answer to simple arithmetic questions was expected to decrease as increasing the human emotional instability in certain degree. So this rate was selected as an index of emotional instability. The arithmetic questions were informed to each subject by a loud speaker to hear at everywhere in the corridor.

The mental arithmetic questions were transcribed with an endless tape and 10 questions were continuously given at each of five answer positions (A to E). The three kinds of question interval speed, 1.5 (sec/question) for male and 2.0 to 2.5 (sec/question) for female were selected to correct the individual difference.

This set of 10 questions was repeatedly given at intervals of 10 sec. Subject was imposed to answer at each five point and to move forward at next deeper position for this 10 sec. interval and again stop to answer the questions at new point. The answers were voice recorded with a handy type tape recorder and was rated the answers later.

These data are normalized by the correct rate of 90 questions under normal condition, (no smoke and heat radiation), for there are self differences of calculation ability.

2.3 SUBJECTS

31 adults aged 20 to 51 (male 14, female 17) participated in this experiment. These females were mainly house wives and males were personnels of F.R.I.

Before the experiment, no detail informations of the corridor were not given and the corridor state without smoke was not displayed. Only fundamental instructions of experiment and notices for safety experiment were given, i.e., a corridor filled with smoke is strait and has an end, subjects are allowed to return back whenever they want to break.

The subjects were protected from irritating smoke with 16 times piled towel on their mouth and nose. About 90 % of soot are removed by this towel as investigated in the past.[1]

3. RESULT AND CONSIDERATION

The Fig. 3 shows how the correct rate of answer to arithmetic questions changes as the subjects go forward in the corridor. The rate at A-point decreases at less than 10 % of those of other position even in case of no smoke. It may indicate the effect of heat radiation to emotional instability, however when the heat radiation is small, such as B-point no decrease is not found.

The walking speed between each answer position is measured in each experiment with mat switches as reference data represents the emotional instability. The followings are further considerations of this walking speed and the correct rates from the view point of the emotional instability.

3.1. INTERRUPTION OF EXPERIMENT

At the beginning of each experiment, a smoke density was not necessarily of the same level. The average values were in the rage of $C_s = 0.92 \pm 0.21$ (1/m). At first time experiment trial, 17 subjects (male 6, female 11) could reach the deepest A-point, and other 14 subjects (male 8, female 6) returned back before reaching to the A-point.

Fig. 3 shows a relation between attainable distance and the normalized correct answer rate to arithmetic questions of the latter 14 subjects. Seven subjects abandoned to walk forward in corridor at the nearest point of E (2.8 m from entrance) and the correct rate drops to about seven percent of normal correct rate. The six subjects of these seven subjects broke at the second trial under condition of $C_s = 0.66$ (1/m) and moreover two of them did at the third trial ($C_s = 0.62$).

At the first trial in thick smoke, three subjects returned back at D-point (5.3 m distance from entrance), other three at C-point (6.9 m), one at B-point (8.6 m), and the each correct answer rate was about 35 %, 55 % and 75 %. The correct rate decreases as the subjects returned back earlier, so this result indicated the emotional instability is larger when the subjects returned back earlier.

3.2. CORRECT ANSWER RATE AND EMOTIONAL INSTABILITY

Some subjects could reach the end of corridor in the first trial under thicker smoke. Fig. 3 shows the relation between the attainable distance and the correct answer rate. This average rate of 17 subjects levels at the lowest just after entering the corridor (at E-point) and it tends to rise up at deeper position. However, in the inquiries conducted after experiment, the subjects indicated that they felt more unrest as going forward.

These results indicate that the low correct answer rate does not necessarily explain the instability for this type of subjects. The cause of discrepant results seems to be led by an observatory fact, subjects assimilate the smoke condition.

From the view point of physiological aspect, an abrupt encounter against irritating smoke attacks subjects' eyes and/or throats, and disturb to open their eyes. This physiological discomfort lets the correct rates fall down, however the discomfort was lighten with the lapse of time.

The assimilation factor compensates the correct rate physiologically but can not recover the emotional instability as the same degree in psychological aspects. So the rate rises up as seen in Fig. 3.

3.3. HEAT FLUX EFFECT ON CORRECT ANSWER RATE

In Fig. 3, included the mental arithmetic results under no smoke condition with dot line. The data at A-point drop 10 % lower than those of after points. This decrease is considered to be caused by the heat radiation from an electric heater set at the ceiling.

The same drops at A-point was also apparently recognized under smoke condition presented with normal line. Nevertheless, no drops are not found at B-point.

The maximum heat flux intensity was 2,030 (Kcal/m² h) at 1.5 m height from floor of A-point and 1,370 (Kcal/m² h) at B-point. So the limit value of heat flux effect on a thinking ability is within the range of between 2,030 and 1,370 (Kcal/m² h).

3.4. SMOKE DENSITY EFFECT ON CORRECT ANSWER RATE

Fig. 4 shows how the smoke density affects the correct answer rate. It indicates that the correct rate decreases as increasing the smoke density almost linearly. This relation has an agreement with the other experimental results conducted in the past.[2]

The assimilation effect is recognized in this figure clearly. The dot line shows the second trial results of the same subjects. The correct rates get about 30 % better than those of the first trial. It concluded that the assimilation depend on the number of experiment trial and the exposed time duration in smoke condition.

3.5. WALKING SPEED IN FIRE SMOKE

The walking speed between each point was measured in this experiment. Fig. 5 shows the results. The walking speed goes down in proportion to the distance from the entrance. The variance between male and female data are not distinct in absolute walking speed, however the declining rate of female in the deeper point is higher.

The smoke density effect on the walking speed was shown in Fig. 6. It was almost the same result of the correct answer rate, that is, the walking speed goes down as increasing smoke density. The drop rate of walking speed is lower than the other former experimental result.[3] This may be caused by experimental conditions and methods' difference, especially the use of towel to protect fire smoke are important. About 90 % of soot in smoke is filtered out with this towel and it lessens the smoke irritation effect of smoke.

4. INQUIRY RESULT

Some questions were given to each subject after experiments. One of them is question on discomfortable factor of smoke: "What are the discomfortable factors of smoke? Select three factors concerned with fire smoke from following items in order!" The Table 1 shows the result.

Some differences were found between male and female. For the male, the physiological factors are mainly selected. The irritation to eyes and/or throats is the first or second selected item, "The obstruction of inhalation" is selected as second or third discomfortable factor. As compared with the above male's answer, females tend to feel discomfort due to psychological factor.

As the first cause of discomfort, the obstruction of visibility is selected as well as the irritation and inhalation problem. And as the second factor, this obstruction of visibility is also cited. This experimental result indicates that the emotional instability in thick fire smoke is not necessarily caused by the same factor for male and female. Under thin smoke condition, without distinction of sex, the smoke irritation and heat flux are selected as first or second factor.

The table 2 shows the inquiry result of the feeling on radiation heat flux. At the B-point, the power of electric heater (about 3 Kw) is so small to effect on subjects discomfort. The answer was mainly "just felt heat a little", the other point (point-A with 12 Kw heater), 44 % subjects answered "hot but not intolerable" under smoke condition, however this rate increase to 50 % under no smoke condition. Moreover the 7 % subjects answered "intolerably hot" under smoke condition, and the 29 % under no smoke condition.

The intensity of heat flux on subjects is almost the same between under smoke of $C_s = 1.0(1/m)$ and no smoke condition in this experiment. So the existence of smoke itself may psychologically affect the feeling on heat flux.

5. CONCLUSION REMARKS

From this experiment in the corridor, the following remarks are obtained.

1. The emotional instability caused by physiological factor, such as smoke irritation, is more important than that by psychological unrest under high irritant smoke.
2. The degree of suffering from fire smoke decreases as time goes by. The assimilation to smoke condition is recognized in thin smoke, so condition of the moment, when evacuee first encounter against fire smoke, is very important. However, the long time stay in the smoke occurs human unrests.
3. The walking speed in fire smoke decreases as increasing smoke density and walking distance from entrance in the corridor.
4. For this experiment, the discomfort of subjects against the fire smoke was caused mainly by the irritation of physiological factor for male, on the other hand the psychological effect, the decrease of visibility for instance, is important factor for female.
5. The thinking ability is affected by the heat flux of over 2,000 (kcal/m²h) in fire smoke.

The emotional instability in fire smoke is composed of psychological and physiological aspects. The degree of contribution of each factor is not clear up in this experiment. Further investigations in this task are expected in future.

References

- 1) T.JIN: KASAI, Japanese Assoc. of Fire Sci. & Eng. Vol.32, No.5, p.26, (1981)
- 2) T.JIN: Bull. of Japanese Assoc. of Fire Sci. & Eng. Vol.32, No.2, p.1, (1982)
- 3) T.JIN: J. Fire & Flammability : 9, p.135, (April 1978)

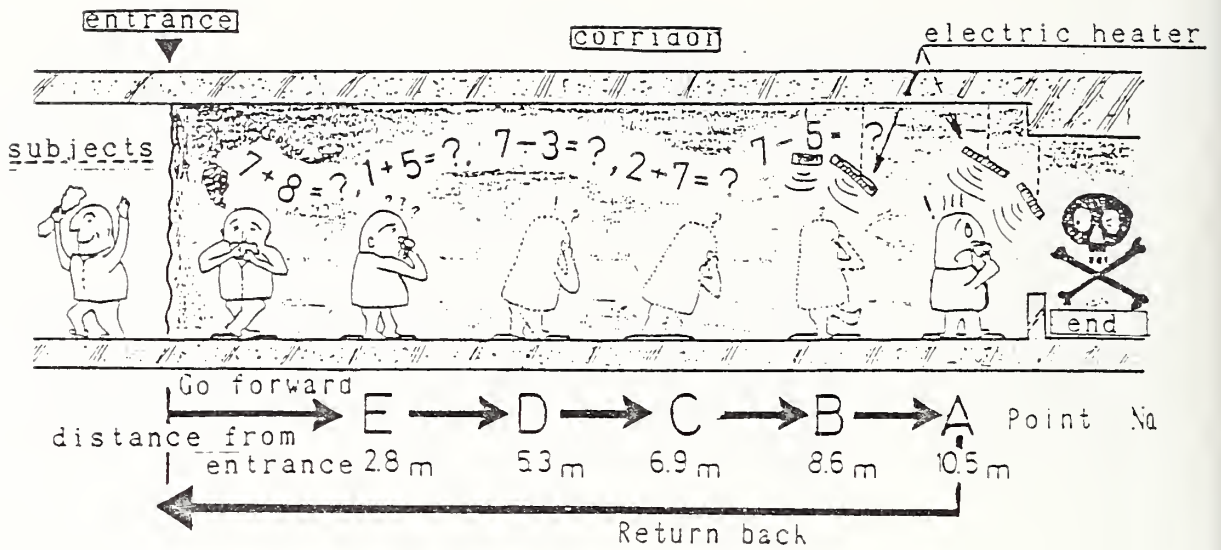


Fig. 1 ; The outline of experiment.

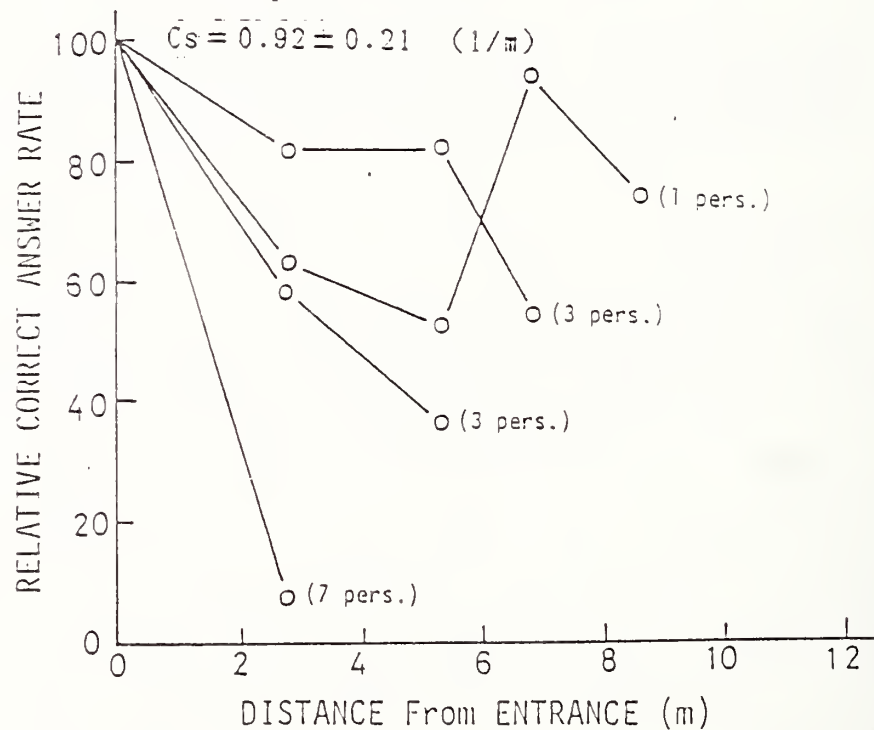


Fig. 2 ; The relation between the distance from entrance and the correct answer rate.
(For the 14 subjects (8 males, 6 females) returned back with interruption)

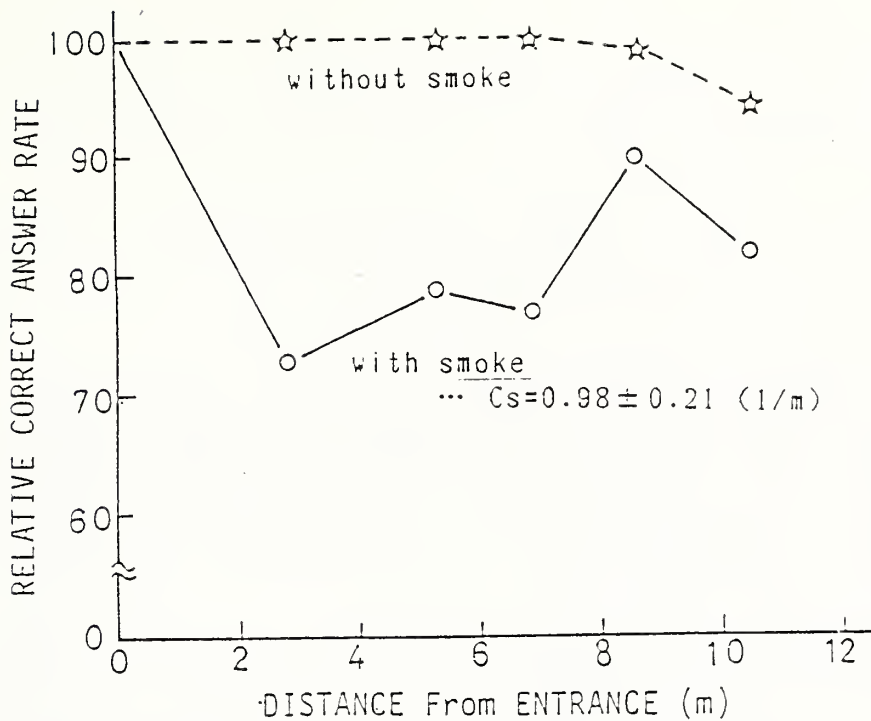


Fig. 3 ; The relation between the distance from entrance and the correct answer rate.
 (For the 17 subjects (6 males, 11 females) reached at the end of corridor in first trial)

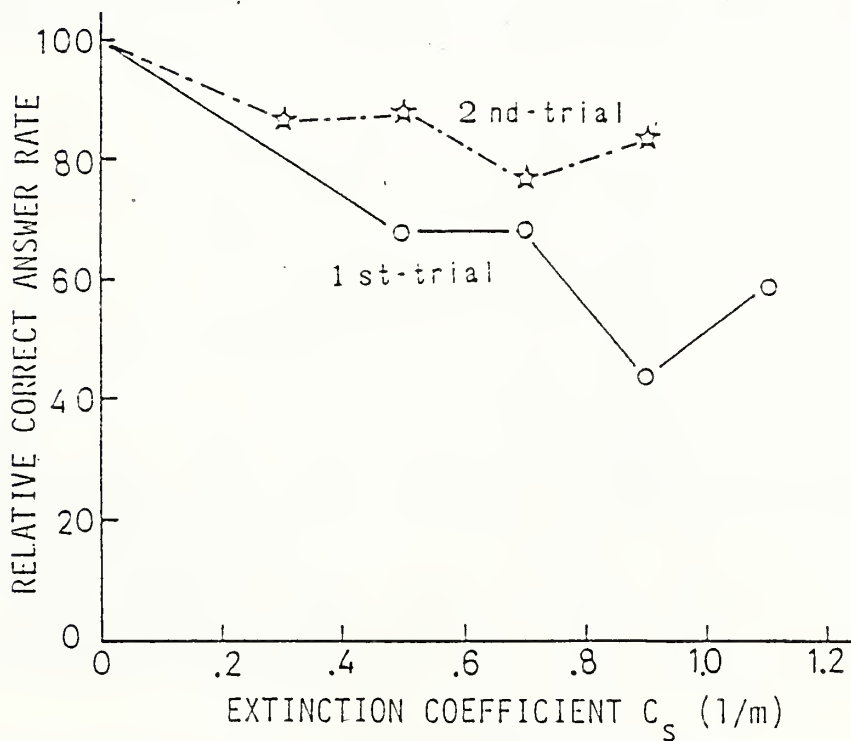


Fig. 4 ; The relation between the smoke extinction coefficient and the correct answer rate.
 (At the E-point and in the first and second trial)

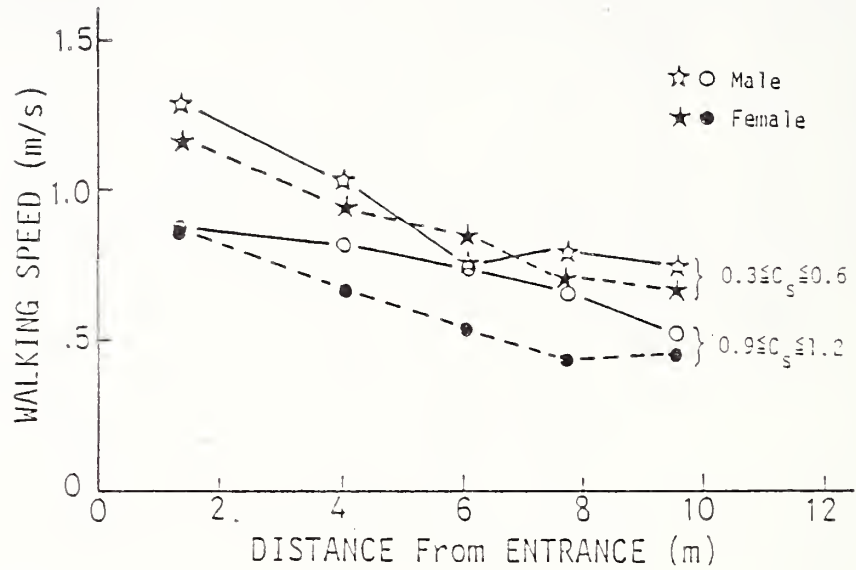


Fig. 5 ; The relation between the distance from entrance and the walking speed.

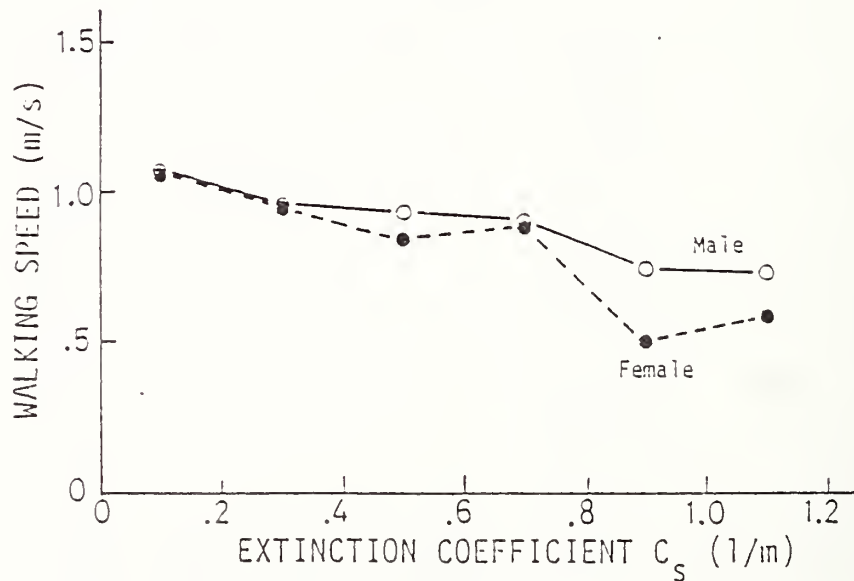


Fig. 6 ; The relation between the smoke extinction coefficient and the walking speed.

Table 1; The discomfortable factor of the fire smoke

Q. " Select three factors concerned with fire smoke
from following items in order !"

	selection items	male (%)			female (%)		
		1 st	2 nd	3 rd	1 st	2 nd	3 rd
THICK SMOKE	a foul smell	1(7%)	2(14%)	3(21%)	1(6%)	0(0%)	1(7%)
	b smoke irritation	8(57%)	4(29%)	1(7%)	7(41%)	6(35%)	2(13%)
	c obstruction of inhalaion	5(36%)	4(29%)	5(36%)	4(24%)	3(18%)	6(40%)
	d obstruction of visibility	0(0%)	3(21%)	3(21%)	5(29%)	6(35%)	5(33%)
	e heat	0(0%)	1(7%)	0(0%)	0(0%)	1(6%)	0(0%)
	f feeling of isolation	0(0%)	0(0%)	1(7%)	0(0%)	1(6%)	1(7%)
	g others	0(0%)	0(0%)	1(7%)	0(0%)	0(0%)	0(0%)
THIN SMOKE	a foul smell	2(14%)	2(17%)	3(30%)	2(13%)	7(50%)	2(15%)
	b smoke irritation	6(43%)	0(0%)	2(20%)	3(19%)	4(29%)	2(15%)
	c obstruction of inhalaion	3(21%)	3(25%)	4(40%)	2(13%)	1(7%)	3(23%)
	d obstruction of visibility	0(0%)	1(8%)	0(0%)	0(0%)	0(0%)	1(8%)
	e heat	3(21%)	5(42%)	1(10%)	8(50%)	0(0%)	2(15%)
	f feeling of isolation	0(0%)	0(0%)	0(0%)	1(6%)	2(14%)	2(15%)
	g others	0(0%)	1(8%)	0(0%)	0(0%)	0(0%)	1(8%)

Table 2; The feeling for the heat radiation under smoke and no smoke conditions

Q. " How do you feel for the heat flux on you at the deepest point-A ? "

(for all subjects)

selected items	with smoke	with out smoke
1. intolerably hot	2 (7%)	8 (29%)
2. hot but not intolerable	13 (44%)	14 (50%)
3. comfortably warm	7 (23%)	4 (14%)
4. just feel heat a little	4 (13%)	2 (7%)
5. no feeling	4 (13%)	0 (0%)

EMOTIONAL INSTABILITY IN FIRE AND SMOKE -- EXPERIMENT OF HUMAN BEHAVIOR IN SMOKE FILLED CORRIDOR

T. Jin and T. Yamada, Fire Research Institute, Japan

EMMONS: In your last chart there were a number of people who felt that the heat was intolerable, and there were 13 who had no feeling. That seems odd that some found it intolerable and some didn't feel anything?

JIN: Ordinarily in the general public, I believe, there couldn't be such a situation, but this particular group may have had some individuals who were impervious to heat. I'd like to ask Mr. Sekizawa to give an answer on that as perhaps he studied it more.

SEKIZAWA: I'm one of those who did not particularly feel any effects of the heat, so I can vouch for that. My attention was focused on being able to withstand the smoke rather than feeling the heat. I did notice the heat, but I didn't find it intolerable...it was just hot.

HOTTEL: I'm concerned about whether the sample of the subjects were typical because of thinking about three characteristics of subjects that might make them act differently. One, speed of addition under normal conditions, which might be high in engineers if you have an abnormal proportion of them there, giving a weighted answer. Another is a natural tendency to emotional instability as against the characteristic of getting a job done that you're supposed to do. Those are very different characteristics, and which of those drove a person is hard to visualize. Was it emotional instability, or that characteristic of "I want to do a job well."

In your first set of tests, for example, how different people got hot would be related to those things. It seems to me that these characteristics would cause one to worry about whether a sample high in engineers was typical of humanity.

JIN: Before answering that I would just like to indicate that in using these test individuals, we used each one only once. And, of course, since we used housewives for the females we used them only once. I indicated employees of the Institute; however, other than Sekizawa, who was involved in the test, the test individuals were do-called part-time employees, student employees, who are not particularly involved in smoke activities. Even then, I was very concerned that there was a non-representational cross section among the males, and I was prepared to throw out all the data relevant to the male responses, but the responses were very close to the females, so I used them.

LARGE FIRES AND NUCLEAR WINTER

George F. Carrier

Harvard University
Division of Applied Sciences
Cambridge, MA 02138

1. INTRODUCTION

In their attempts to estimate the effects of a major nuclear exchange on the subsequent dynamic and thermodynamic state of the atmosphere most (maybe all?) of the investigators believe that the smoke from large urban fires might be the most substantial contributor to the evolution of the state of that atmosphere. Accordingly, many of the questions that must be answered deal with issues related to large fires. In this brief discussion before an audience drawn from the "fire community" I think it will be useful to distinguish three aspects of the composite phenomenology. The first, chronologically, is that which deals with a characterization of the hypothesized weapons usage scenario and must provide as its output a characterization of the conditions that would prevail shortly after the exchange has occurred. I will use the general and imprecise phrase, "a characterization of", several times because, as nearly as I can tell, no-one has compiled carefully and credibly a list of all of the specifications that play significant roles in the analysis of the phenomena that could occur. In this particular instance I do have in mind the need for a characterization of the redistribution of structural combustibles (largely wood and synthetic materials?) and the redistribution of non-combustible material (structural concrete, stone, plaster, reinforcing and any other sources of rubble) the degree of exposure of highly volatile fuels (e.g. devastated filling stations, broken gas lines, the contents of commercial warehouses where solvents, polymers, etc. are stored), and perhaps many others. I admit immediately that I do not know, for example, the kind of detail needed in the characterization of the rubble distribution but I will return to that topic shortly.

I do suggest that the foregoing subdivision of the composite problem is not an issue to be submitted to the fire community.

The second subdivision of the estimation process is that which addresses the phenomenology that starts with the foregoing "redistribution inputs" and has as its output a quantitative description of the characterizing features of the deposition of smoke in the atmosphere at, perhaps, a day or so after the exchange.* This subdivision is the business of the fire community and I will return to it.

The third, highly intricate, aspect of the phenomenology requires the unravelling of the evolution of the state of the atmosphere that would

*This rather fuzzy timing statement avoids lots of alternative conflict durations that stem from alternate options related to the timing of weapons deliveries. There may be many options (and classes of such options) that can be studied if and when they seem to deserve attention.

accompany the interaction of solar radiation, the smoke laden atmosphere ("initially" in the state at the end of subdivision #2), and the land masses and ocean of the planet. This also is not the business of the fire community and I will return now to aspect #2.*

2. LARGE FIRES

It seems highly plausible and it is widely believed that the mechanical devastation caused by the use of a multi-kilo-ton weapon on a target in an urban or near-urban location would be accompanied by the exposure of so much highly volatile "fuel" that fires, very heterogeneously distributed over an area of a few to several km², would be initiated and sustained. The distribution in space and time of pyrolyzate production, of flame location, of smoldering reaction, of air access, and of oxygen depletion, would also be very heterogeneous. It follows that, depending on the evolution of the distributions so listed, such macroscopic quantities as total heat release per unit time, air entrainment rate as a function of altitude and time (which also depends on the ambient dynamic state of the atmosphere) fraction of "fuel" consumed, total rate of smoke generation, character of the smoke generated (e.g. fraction formed in flaming combustion vs. fraction formed in smoldering) and many others are not entities for which there is a well documented body of knowledge and understanding. To the contrary, in fact, there has been, even for the much smaller fires that have received scientific scrutiny, almost no attention whatever to the dependence of burning rate on any of the parameters characterizing fuel type, fuel distribution geometry, fuel wetness, and external or self-induced wind field. Without a quantification of the foregoing dependencies, one cannot hope to estimate in a credible way the distribution of smoke deposition altitudes. Furthermore, without analogous correlations of (1) the amount of smoke generated and (2) the variation of optical properties of that smoke with combustion type (again e.g. smoldering vs. flaming) with the foregoing parameters, one cannot tighten up the estimates of the amounts and properties of the smoke that is distributed over those altitudes. And, of course, the frustration that stems from the absence of the information to which we have just alluded is amplified greatly by the knowledge that a very broad variety of rubble types and of possible rubble distributions must inevitably imply that the number of experiments and the number of mechanisms whose effects must be incorporated into the predictive models seem to be ever increasing functions of the time during which we have been examining this problem.

3. STATUS OF THE FIRE PROBLEM

Several investigators have modelled the dynamics of large fire plumes. I know of three approaches:

(1) Extension of the classical Morton, Taylor, Turner plume theory. All of these adopt a postulated fuel consumption rate based largely on anecdotal reports of the duration of large historical fires (e.g. the Hamburg fire of World War II). Ordinarily, the analysis is based on time independent conservation laws.

*All readers will realize, of course, that many other questions such as, "what is the effect of all this on the biota (especially agricultural biota) and the human population in various parts of the planet?" may be of serious concern to all of us.

(2) Large hydro-code calculations. These also postulate the fuel consumption history but, in this case, the consumption rate varies with time and the fire evolves with time. I have not seen many attempts to validate the hydrocode results by comparing known results in other parameter ranges with code results.

(3) Initial attempts to devise models that distinguish the effects of heterogeneity. These are at an early stage of development but without this approach it is doubtful that models will be developed within which one can treat the fuel consumption rate as an output of the analysis rather than a postulated input.

In none of the foregoing families of estimation procedures has there been any consideration of the "sheltering of fuel" by non-combustible rubble. Two aspects of that sheltering require attention. One would speak to its role in altering the low level velocity field and its implications for the availability of oxygen; the other would influence the rate at which heat transfer to, and hence pyrolyzation of, the fuel would be altered by the field of obstacles. Both of these may have important implications for the net fuel consumption rate, for the amount of smoke produced and possibly for the properties of that smoke. The role of rubble deserves attention.

When a plume emerges from an intense fire in a very humid lower atmosphere it can rise to altitudes at which, despite the entrainment aloft of drier air, some of the moisture condenses. Observations suggest that, in many such plumes, the water droplets accumulate large amounts of smoke (I know of no quantification associated with these events) and the rain that sometimes ensues carries significant amounts of particulate matter to the ground. Other observations suggest that, in many such fires, capping clouds of condensed moisture form above the darker plume but rain does not ensue. In these cases it is unclear as to whether the presence of the condensate has any significant effect on the morphology of the smoke.

If one is to acquire a predictive capability regarding the amounts of smoke and the optical properties of the smoke that might be deposited in the upper troposphere as a result of nuclear weapon usage one must find a far better quantification of the processes that occur in the upper reaches of the plume than has yet been attempted. It seems clear that the degree of supersaturation achieved by the plume gases is an important parameter in the determination of the droplet formation and growth; and the local dynamics is important in the determination of the degree of supersaturation. Since the amount of smoke that survives the early scavenging and the optical properties of that smoke are crucially important in the hypothesized alteration of the atmospheric state, it is clear that any ability to quantify those alterations has as a prerequisite a quantified characterization of the dynamics and cloud physics of the upper part of the plume.

4. NATURAL VARIABILITY

At this time, in addition to very large uncertainties in the possible weapons usage and to those in the atmospheric response models there are, as described in the foregoing, very large uncertainties in the amounts, properties, and distributions of smoke that would ensue from a given weapons usage. At this time, there is in place no ongoing

organized experimental program with goals that would provide a body of knowledge from which one could hope to build an understanding which would allow him to scale the behavior of the necessarily smaller experimental fires to those of interest in the Nuclear Winter context. Unless one addresses the questions discussed in the earlier sections of this paper, one will not have, at this time or at any other time, any credible means of reducing the current enormous uncertainty regarding the potential severity of the Nuclear Winter phenomenology.

There is, of course, no guarantee that a large and successful research effort directed to these and other questions could reduce those uncertainties. It is very possible that the sensitivity of the burning rate--and therefore the plume height--and therefore the moisture dependent scavenging processes--and therefore the surviving optical blockage--to the atmospheric stability and humidity (they are coupled, of course), to the distribution of rubble, to the variability of the fuels contained in urban areas, and to the variability of other parameters (e.g. weapons usage scenario) would leave us with a possible range of smoke depositions that is as broad as that that characterizes our present state (lack) of knowledge.

I favor an effort to improve our understanding of large fires and their atmospheric depositions but (to repeat myself) it is not clear that such an effort will remove the current uncertainties concerning the atmospheric modifications at issue.

Bibliography

- Albini, F.A. 1984 Wildland fires. *American Scientist* 72, 590-597.
- Bohren, C.F., and Huffman, D.R. 1983 Absorption and Scattering of Light by Small Particles. New York, N.Y.: John Wiley.
- Bohren, C.F., and Brown, G.M. 1981 Once in a blue moon. *Weatherwise* 34(3), 129-130.
- Briggs, G.A. 1984. Plume rise and buoyancy effects. Atmospheric Science and Power Production, pp. 327-366. Oak Ridge, TN: U.S. Department of Energy, Technical Information Center.
- Brünswig, H. 1982. Feuerstrum über Hamburg. Stuttgart: Motorbuch Verlag.
- Carrier, G.F., Fendell, F.E., and Feldman, P.S. 1985 Firestorms. *Journal of Heat Transfer* 107, 19-27.
- Carrier, G.F., Fendell, F.E., and Feldman, P.S. 1984. Big fires. *Combustion Science and Technology* 39, 135-162.
- Colbeck, I., and Harrison, R.M. 1986 The atmospheric effects of nuclear war--a review. *Atmospheric Environment* 20, 1673-1681.
- Committee for the Compilation of Materials on Damage Caused by Atomic Bombs in Hiroshima and Nagasaki 1981. Hiroshima and Nagasaki--The Physical, Medical, and Social Effects of the Atomic Bombings. New York, N.Y.: Basic Books.
- Crutzen, P.J. 1984 Darkness after a nuclear war. *Ambio* 13, 52-54.
- Crutzen, P.J., Galbally, I.E., and Bruhl, C. 1984. Atmospheric effects from post-nuclear fires. *Climatic Change* 2, 323-364.
- Crutzen, P.J., and Birks, J.W. 1982 The atmosphere after a nuclear war: twilight at noon. *Ambio* 11, 114-125.
- Dotto, L. 1986 Planet Earth in Jeopardy: Environmental Consequences of Nuclear War. New York, N.Y.: John Wiley.
- Levi, B.G., and Rothman, T. 1985 Nuclear winter: a matter of degrees. *Physics Today* 38(9), 58-65.
- Luke, R.H., and McArthur, A.G. 1978 Bushfires in Australia. Canberra, Australia: Australian Government Publishing Service.
- Lyons, J.W. 1985 Fire. New York, N.Y.: Scientific American Books.
- Malone, R.C., Auer, L.H., Glatzmaier, G.A., and Wood, M.C. 1986. Nuclear winter: three-dimensional simulations including interactive transport, scavenging, and solar heating of smoke. *Journal of Geophysical Research* 91D, 1039-1053.

- Manins, P.C. 1985 Cloud heights and stratospheric injections resulting from a thermonuclear war. Atmospheric Environment 19, 1245-1255.
- Morton, B.R. 1957 Buoyant plumes in a moist atmosphere. Journal of Fluid Mechanics 2, 127-144.
- Mullholland, G.W., ed. 1987 Report on DNA/NBS Sponsored Workshop on Smoke Emission and Properties, November 13-14, 1986. Gaithersburg, MD: National Bureau of Standards, Center for Fire Research.
- National Academy of Sciences, Committee on the Atmospheric Effects of Nuclear Explosions 1985 The Effects on the Atmosphere of a Nuclear Exchange. Washington, D.C.: National Academy Press.
- Pittock, A.B., Ackerman, T.P., Crutzen, P.J., MacCracken, M.C., Shapiro, C.S. and Turco, R.P. 1986 Environmental Consequences of Nuclear War. Volume 1: Physical and Atmospheric Effects. New York, N.Y.: John Wiley (SCOPE 28).
- Pyne, S.J. 1984 Introduction to Wildland Fire--Fire Management in the United States. New York, N.Y.: John Wiley.
- Pyne, S.J. 1982 Fire in America -- a Cultural History of Wildland and Rural Fire. Princeton, N.J.: Princeton University,
- Radke, L.F. 1983 Preliminary measurement of the size distribution of cloud interstitial aerosol. Precipitation Scavenging, pp. 71-78, New York, N.Y.: Elsevier.
- Radke, L.F., Stith, J.L., Hegg, D.A., and Hobbs, P.V. 1978 Airborne studies of particles and gases from forest fires. Journal of the Air Pollution Control Association 28, 30-34.
- Rodhe, H. 1987 Book reviews, "Environmental Consequences of Nuclear War" and "Planet Earth in Jeopardy: Environmental Consequences of Nuclear War." Bulletin of the American Meteorological Society 68(2), 143-144.
- Rogers, R.R. 1979 A Short Course in Cloud Physics, 2nd ed. New York, N.Y.: Pergamon.
- Schneider, S.H. 1987 Climate modeling. Scientific American 256(5), 72-80.
- Slinn, W.G.N. 1984 Precipitation scavenging. Atmospheric Science and Power Prediction, pp. 466-532. Oak Ridge, TN: U.S. Department of Energy, Technical Information Center.
- Turco, R.P., Toon, O.B., Ackerman, T., Pollock, J.B., and Sagan, C. 1983 Nuclear winter: global consequences of multiple nuclear explosions. Science 222, 1283-1292.
- Twomey, S. 1977 Atmospheric Aerosols. New York, N.Y.: Elsevier.

LARGE FIRES AND NUCLEAR WINTER

G. Carrier, Harvard University, USA

ZUKOSKI: I understand that you're interested in getting this stuff up to 30,000 feet. It seems to me that even the old Turner Taylor Model is going to likely fail us, because in a place like Los Angeles, the size of the fire could be 30,000 feet.

CARRIER: I agree that one can expect sort of marginal results at best from that kind of model, but what I was talking about were extensions of the model, in which, for example, the point source is long gone, and in which the actual state of the atmosphere, its degree of stratification, is taken into account. There even have been some investigations in which we try to take account of the ambient circulation, but it only can be expected to give us gross estimates of the height of the column, and cannot begin to give us the kind of detail we need in connection with the condensation removal questions in particular.

I should add that the model has been very useful on some occasions in showing how inappropriate some other kinds of calculations are by virtue of the total unacceptability of the results when viewed against the Turner Taylor Model as a comparison base.

EMMONS: First, relative to the general circulation problem, is it possible that one could study some other planet to find a model that would be valid? I think, for example, Venus always would be covered with a cloud. Would that provide a possibility for developing a model appropriate in this more general situation?

CARRIER: There have been some attempts to use the Martian dust cloud phenomena as a validation base for the modified GCM's, I suppose with some success. However, our knowledge of what goes on, on a scale that would allow us to talk about precipitation patterns on the earth, would be very important to those who wish to indulge in agriculture after such an event. It doesn't permit that small of scale of phenomena to be resolved, so it's of limited validity.

Venus, of course, has such a different rotation rate, and such enormous stability that I think any suggestions that might provide useful information of that sort have been put aside rather quickly. There are natural phenomena which provide severe tests in one way or another of GCM's, and people are actively searching for cases in point that might help with the validation or refutation of the things that are not being found in this context.

EMMONS: My second question is a very detailed one. The presence of a water cloud above the smoke cloud implies separation of the smoke cloud from the gases. Has gravity slipped from that?

CARRIER: The optical interaction of sunlight with the moisture cloud is such, I think, that it gives an altered appearance to the region where there are water droplets. I was not suggesting, and indeed it's known not to be true, that there are no smoke particles in that region. There are, but one does not have a clear picture, or even a consistent picture, from observation to

observation as to how much there is, and how much of it is in or on the droplets as opposed to separate from the droplets. I didn't mean to suggest separation, and I'm quite sure there can't be one.

OPEN TECHNICAL SESSION

FMRC Sprinkler Research

CHENG YAO
Manager, Research Division
Factory Mutual Research Corporation
Norwood, Massachusetts 02062
U.S.A.

Ninth Meeting of the United States/Japan Panel
on Fire Research and Safety, May 1987

1. INTRODUCTION

Traditionally automatic sprinkler systems have been designed to control the fire spread and to wet and cool the building structure, thereby preventing collapse and complete wreckage. Sprinkler protection requirements of different storage occupancies in terms of water density and area of water demands were developed primarily from large-scale fire test programs which used a defensive strategy or conservative concept of "fire control." This concept permits lower densities and assumes large numbers of sprinklers operating (in the range of 20 to 30). Fires in today's high-piled storage occupancies have challenged the control concept, pushing the sprinklers of current design to the limit of their effectiveness. A new approach to provide a cost-effective solution to the high challenge storage fire protection was urgently needed.

Factory Mutual has supported a substantial sprinkler technology research program to study the principles of sprinkler fire protection. Knowledge developed has been used as a basis to reexamine the sprinkler protection concept and to develop new and effective sprinklers for the occupancies which cannot be protected with standard (spray) sprinklers. This work led to the development of the large-drop sprinkler (1971-1980) to control high-challenge storage fires, fast-response residential sprinklers (1976-1979) to maintain a survivable environment in residential areas, and the early suppression fast response (ESFR) sprinkler system (1984-1986) to suppress severe storage hazard fires that are beyond the protection capability of even large-drop sprinklers without supplementation with expensive in-rack sprinklers.

It is the intention of this paper to present an overview of our sprinkler technology program and to give examples of some recent and future advances in the application of this technology.

2. SPRINKLER TECHNOLOGY RESEARCH

The objectives of the sprinkler technology research program are:

- 1) to quantify the thermal responsiveness of automatic sprinklers, which can be used to determine the fire challenge at the time of sprinkler operation;
- 2) to quantify the fire challenge in terms of its combustibility and extinguishability, which can be used to predict the density of water required to be delivered at the top of the burning storage array for early fire suppression;

- 3) to quantify the sprinkler discharge characteristics, which can be used to predict the density of water actually penetrating the fire plume and delivered onto the top of the burning array;
- 4) to develop a phenomenological model of a sprinklered fire in a storage warehouse including mathematical simulation of various components of a comprehensive sprinkler performance model, which can be used to predict performance of sprinkler systems against different types of fire challenges.

2.1 SPRINKLER RESPONSE PREDICTION

For a given fire situation, sprinkler response time is determined by the thermal responsiveness of the sprinkler and the gas temperature and velocity at the sprinkler location. Assuming the heat responsive element of a sprinkler is heated purely by forced convection until actuation, the thermal responsiveness of the sprinkler heat sensing element can be quantified by a Response Time Index (RTI). RTI can be measured in Factory Mutual's plunge test tunnel. Ten different brands of sprinklers responded with fairly constant RTI over the velocity (1.5 to 5.2 m/s) and temperature ranges examined⁽¹⁾. RTI and sprinkler temperature rating had been demonstrated to be sufficient to predict response of conventional (slow-response) sprinklers in full-scale rack storage fire tests⁽²⁾.

The introduction of low RTI fast-response sprinklers for the protection of slow growing fires in residential situations has demonstrated⁽³⁾ that the heat loss by conduction from the heat sensing element to the sprinkler fitting can become a significant factor in the determination of the sprinkler response time. An attempt was then made to incorporate conductive heat loss in the thermal response model⁽⁴⁾.

Adding a conductive heat loss term, the heat balance on the heat sensing element becomes:

$$mc (dT_e/dt) = hA (T_g - T_e) - C'(T_e - T_o) \quad (1)$$

where m = mass of element,
 c = specific heat of element,
 h = convective heat transfer coefficient,
 A = surface area of element,
 C' = conductance of sprinkler,
 T_e = temperature of element,
 T_g = gas temperature,
 T_o = ambient temperature,
 t = time.

Substituting

$$RTI = u^{1/2} (mc/hA),$$

$$C = C' (RTI/mc).$$

The solution of Eq (1) for a plunge test can be written:

$$\frac{RTI}{1+C/u^{1/2}} = \frac{-t_r u^{1/2}}{\ln [1-\Delta T_{ea} (1+C/u^{1/2})/\Delta T_g]} \quad (2)$$

where ΔT_{ea} is the actuation temperature of the heat responsive element above ambient.

The conduction parameter, C, can be measured in the plunge test tunnel using a "prolonged exposure technique"⁽⁴⁾. The C value measured among 11 sprinkler models range from 0.5 to 1.56 m^{1/2} s^{1/2}. Figure 1 shows the temperature rise ΔT_e as a function of time, calculated for C=0 (no conductive heat loss) and for C=1 (a realistic value). The element with C=1 actuates much later than that for C=0. A series of room fire tests has been conducted using both pool fires and crib fires. Actual sprinkler response times correlate well with predictions based on the model using the measured gas temperature and velocity values and laboratory values of RTI and C⁽⁴⁾. It is also demonstrated that conduction correction is not necessary to predict response time for fast-response sprinklers in industrial applications such as ESFR sprinkler systems.

2.2 QUANTIFICATION OF FIRE CHALLENGE AT SPRINKLER RESPONSE

The principal challenge a storage fire presents to a sprinkler system at the time of sprinkler response is the combustibility of the ignition stacks of storage commodities. This combustibility may be expressed in terms of convective heat release rate at the time of sprinkler actuation, the associated upward thrust of the fire plume and the ceiling flow characteristics of the fire products. Empirical correlations of ceiling flow velocity and temperature have been established in terms of convective heat release rate and ceiling clearance for cases where a quasi-steady approximation of the ceiling flow is valid⁽⁵⁾. In order to predict the low RTI sprinkler response accurately, generalized correlations of the gas temperature and velocity in the initial transient ceiling flow has to be established.

A series of storage fire tests has been conducted under the Fire Products Collector (FPC), a large calorimeter which collects all fire products and determines the fire's heat release rate. The thrust of the plume, derived from the measured initial transient plume temperature and velocity profiles, has been correlated with the fire growth history. The same tests will be repeated under a 30-ft (9 m) high ceiling to develop generalized correlations for initial transient ceiling flow and the fire growth history (heat release rate history) and ceiling clearance.

A computer program for predicting the ESFR sprinkler response will be developed using the correlations for transient ceiling flows developed in this work. The accuracy of the computer prediction of ESFR sprinkler response and the fire plume thrust force will be compared with the measured values in the fire tests.

2.3 QUANTIFICATION OF STORAGE FIRE SUPPRESSION - RDD

Over the last decade, attempts have been made to quantify the fire suppression requirement for different stored commodities at the time of sprinkler actuation while the fire is still confined within the ignition stacks of storage array. This fire suppression parameter is denoted as the required delivered density of the storage array or RDD. The RDD is the water density which must

be delivered to the top surface of a burning storage array in order to achieve early suppression.

A large-scale fire suppression test apparatus, as shown in Figure 2, was developed. It consists of a special water applicator that is capable of spreading a fairly uniform distribution of water directly over the top surface of the fuel, thus simulating water that has penetrated the fire plume. This apparatus is positioned below the FPC. The water applicator is actuated at a specific heat release rate (as measured by the FPC), which corresponds to that of an ESFR sprinkler actuating in a 30-ft (9 m) high building (see Section 2.2).

Figure 3 shows the results of three RDD tests of identical rack storage of plastic commodity in a 8-ft x 8-ft x 20-ft high (2.4-m x 2.4-m x 6.1-m) configuration. Water was applied at the same heat release rate. The fire was suppressed at a delivered density of 0.47 gpm/ft² (19.2 mm/min); at 0.42 gpm/ft² (17.2 mm/min) fire redeveloped, and at 0.50 gpm/ft² (20.4 mm/min) a faster suppression was achieved.

Numerous combinations of storage commodity and configuration and ignition condition were examined. The storage commodities tested were:

- 1) Polystyrene jars in compartmented cartons;
- 2) Metal lined double triwall cartons;
- 3) Aerosol products of different hazard levels;
- 4) Roll paper of different forms, including polyethylene film coated and chemically treated.

2.4 COMMODITY HAZARD EVALUATION FOR FIRE CONTROL

Sprinkler protection requirements of storage occupancies for fire control systems were developed from large-scale fire tests using different standardized test commodities. The qualitative test procedure presently used to evaluate or classify the hazard of a storage commodity relies to a large degree on subjective judgement of trained observers. The objectives of this new project is to develop an improved commodity evaluation test procedure based on the combustibility and controllability of the storage commodity as quantified by the FPC. The test procedure is similar to the RDD test, except that the water applied is not intended to suppress the fire, but merely keep the fire from becoming out of control.

Based on both freeburn and fire control test results, five parameters were selected for indexing the fire hazard of storage commodities. They are fire growth rate, maximum convective and radiative heat release rates, convective energy release and maximum automatic sprinkler link temperature response. All the fire control parameters were determined as functions of water delivered density. Classification criteria based on these parameters will be established upon the successful validation with the full-scale fire test results.

2.5 QUANTIFICATION OF SPRINKLER PERFORMANCE - ADD

Under a no-fire condition, the water distribution over a specific area of concern (for example, the top cross-section area of the ignition stacks) is a function of sprinkler design, sprinkler location, number of operating sprink-

lers and discharge pressure. In the presence of a fire, however, the density actually delivered at the top of the ignition stacks, the Actual Delivered Density (ADD), is influenced by the updraft of the fire plume. The upward draft in the plume presents a barrier to the penetration of drops; only a fraction of the discharge density can be delivered at the base of the fire plume.

As shown in Figure 4, the ADD apparatus consists of four simulated storage commodities and a heptane-spray fire source. In each of the simulated commodities, there are four water collection pans. Under each pan there is an automated water metering system. There are 20 water collection pans, 16 at the top and 4 at the base of the flue spaces separating the simulated commodities. This apparatus is placed under a large suspended ceiling which is movable to provide different clearances between the test array and sprinklers.

In addition to ADD tests at specific test conditions, a statistical technique is being used to design, collect, analyze and map the ADD performance of the sprinkler over a broad range of operational variables. Figure 5 shows a performance map for one of the prototype ESFR sprinklers.

2.6 COMPUTER MODELING OF SPRINKLER SPRAY AND FIRE PLUME INTERACTION

The drops may be generally expected to penetrate if the terminal drop velocity is greater than the gas velocities in the fire plume, or the drop size (d) is larger than a critical maximum drop size (d_c) that can just be stopped by the centerline plume flow. This type of penetration is referred to as gravitational penetration. A second type of penetration, momentum penetration, occurs if the total thrust of the water spray (M_s) overpowers the upward thrust of the plume (M_p).

Numerical computation to model sprinkler spray interaction⁽⁶⁾ with a fire plume gas has been run on the computer for a wide range of sprinkler discharge conditions and fire intensities to predict spray penetration ratio, Pen.

$$\text{Pen} = \text{ADD}/D_a$$

where D_a is the rate at which water is applied to a unit area without fire.

Analysis of these solutions has led to the identification of a parameter controlling the penetration of droplets to the base of the fire plume. Penetration ratios calculated are shown in Figure 6 as a function of a thrust ratio, M_s/M_p , a drop-size ratio, d/d_c , and a velocity ratio, U_{inj}/U_{po} , evaluated at the elevation of the spray source. Here U_{inj} is the droplet effective injection velocity and U_{po} is the plume centerline velocity. These controlling parameters involves both characteristics of the momentum and gravitational penetration mechanisms. When the combined controlling parameters are greater than a critical value, more than 80% of the water discharge arrives at the plume base.

The water flux, drop size distribution and thrust force of the ESFR sprinkler will be measured. These data will be used as an input to the model to check the ability of this model to predict spray-plume interaction in terms of ADD.

2.7 1/12 SCALE SPRINKLER SYSTEM MODELING

In addition to the simple density/area rule, sprinkler performance is effected by at least six principal variables: ceiling clearance; sprinkler temperature rating; sprinkler responsiveness (RTI); water pressure; sprinkler type and orifice size; and burning and extinguishment characteristics of the combustible. Large numbers of parametric tests have been conducted to investigate the interrelations between the sprinkler variables in a reduced-scale model (1/12, 5 of full scale). According to the principle of Froude number modeling⁽⁷⁾, the fire heat release rate is scaled to $L^{5/2}$, where L is a representative length dimension. Drop diameter and the initial drop velocity and the diameter of the heat sensing element are all scaled to $L^{1/2}$. A model building 1.44-m high was constructed to represent a full-scale building 18-m high.

The first series of modeling tests were designed to simulate full-scale fire tests, using the standard 1/2 in. (13 mm) sprinklers to control the fire in the rack storage of ordinary combustibles in cardboard cartons. A total of 164 fire tests was performed with various combinations of clearance, temperature rating, RTI and water pressure. Where comparisons were possible, model results generally agreed with full-scale test experience.

Another series of modeling tests to simulate full-scale early suppression fire tests using the ESFR sprinkler system is underway.

2.8 PHENOMENOLOGICAL MODELING OF SPRINKLERED WAREHOUSE FIRES

Work is about to begin on the development of a phenomenological sprinkler performance model intended to simulate a high-challenge sprinklered warehouse fire. The model will be used in situations for which there are no specific full-scale test data, but the relevant commodity combustibility and extinguishability data described in Sections 2.3 and 2.4, and the sprinkler characterizations described in Sections 2.1 and 2.5 are available. Phenomena to be incorporated in the fire simulations include: 1) freeburn fire growth in terms of heat release rate and flame spread; 2) plume and ceiling layer flows as described in Section 2.2; 3) sprinkler actuation times and spray discharge characteristics; 4) spray-plume interactions in terms of the parameters described in Section 2.6; and 5) delivered water suppression capability as characterized by data/correlations described in Sections 2.3 and 2.4 including effects on fire heat release rates (and possibly flame spread) so as to allow calculations to proceed until the fire is suppressed and/or flame spread ceases. The model will be initially formulated as a deterministic calculation, but uncertainties in simulating these phenomena will be quantified and eventually incorporated into a probabilistic formulation that can be exercised along with probabilistic descriptions of the fire scenario (ignition location, storage configuration details, etc.).

3. THE DEVELOPMENT OF THE ESFR SPRINKLER SYSTEM

ESFR stands for Early Suppression Fast Response. The objective of the ESFR program was to develop an ESFR sprinkler system which will provide "early suppression" performance on high challenge storage fires represented by up to 25-ft (7.6 m) high rack storage of standard plastic commodity in a 30-ft (9.1 m) high building. Such a severe fire challenge is beyond the protection

capability of standard and even the large-drop sprinklers without supplementary and expensive in-rack sprinklers.

The basic ESFR concept is that if a sufficient quantity of water can be delivered onto the burning storage commodities at the early stage of development to suppress the fire quickly before a severe challenge situation is reached, fewer number of sprinklers will operate and less fire and water damage will result.

In principle, early suppression performance is determined by three factors which can be independently measured: 1) Response Time Index (RTI); 2) Actual Delivered Density (ADD); 3) Required Delivered Density (RDD). The RTI and the time-dependant nature of ADD and RDD determines the early suppression performance of the ESFR sprinkler system. The premise of the ESFR system is to ensure ADD in excess of RDD, regardless of the ignition location.

After two years of extensive research and development, a prototype, designated as CPF sprinkler, was chosen as representative of the ESFR sprinkler⁽⁸⁾. It is of pendant design and has a K factor of $14 \text{ gpm/psi}^{1/2}$ ($20.1 \text{ dm}^3/\text{min/kPa}^{1/2}$), 0.7 in. (17.8 mm) orifice diameter. The sprinkler link used is rated at 165°F (74°C) with a RTI of $50 \text{ ft}^{1/2} \text{ s}^{1/2}$ ($28 \text{ m}^{1/2} \text{ s}^{1/2}$).

The most important performance requirement of the ESFR system is to provide ADD in excess of RDD under a worst-case scenario of up to 25-ft (7.6 m) high rack storage of standard plastic commodity in a 30-ft (9.1 m) high building, regardless of the ignition location. Figure 7 shows the ADD value of the ESFR prototype sprinkler at different clearances between the sprinkler and the top of the storage for two different sprinkler-fire source configurations; i.e., one and four sprinklers centered above the fire source. In comparison with the RDD values measured for different storage heights, the prototype ESFR meets performance requirements for different ignition (fire source) locations. It also shows that with one sprinkler discharging centered over the fire source, high clearance is critical; with four sprinklers, low clearance is critical.

Eleven large-scale fire tests⁽⁹⁾ of double- and multiple-row rack storage fire tests were conducted. Results of these fire tests not only confirm that the prototype ESFR sprinkler would perform well in critical conditions described above, they also demonstrate that even under the worst failure mode condition tested, ignition between two sprinklers with one of them plugged, the fire was still controlled with 11 sprinklers.

Factory Mutual has just released a draft installation standard for public review. The ESFR sprinkler system protects palletized, solid-piled and open frame single-row, double-row, multiple-row and portable rack storage of most common materials up to 25-ft (7.6 m) high, in buildings up to 30-ft (9.1 m) high. Specific commodities protectable by ESFR sprinklers include Class I through IV commodities, cartoned unexpanded plastics, and cartoned foamed-in-place polyurethane packaging material. Also, any lesser hazard commodities, lower storage heights, or lower ceiling heights are all protected with the same water demand: 12 sprinklers at a minimum of 50 psi (345 kPa).

4. THE DEVELOPMENT OF THE RESIDENTIAL SPRINKLER SYSTEM

The quick-response concept in sprinkler technology as applied to residential occupancies has been brought to fruition by FM through the support of the United States Fire Administration (USFA)/Federal Emergency Management Agency (FEMA). From 1976 to 1982, research results demonstrated the need of fast-response (low RTI) sprinklers with different discharge patterns for providing adequate life-safety and property protection in residential fires. Based on the information gained^(10,11), new-generation, quick-response (low RTI) residential sprinklers have been developed by the U.S. Sprinkler Industry. In 1980, a new version of the NFPA-13D Standard on Installation of Residential Sprinkler Systems was adopted by the National Fire Protection Association (NFPA). In 1983, research results indicated that there is a need of sidewall sprinkler installation rules with regard to system water demand and sprinkler location⁽¹²⁾.

Currently, USFA/FEMA is sponsoring a two-phase research program at FMRC to investigate the Effect of Beams and Ceiling Slopes on Residential Sprinkler Performance, and to evaluate the Performance of Quick-Response Sprinklers in Office and Hotel Occupancies.

REFERENCES

- 1) Heskestad, G. and Smith, H.F., "Investigation of a New Sprinkler Sensitivity Approval Test: The Plunge Test," FMRC 22485, Factory Mutual Research Corporation, Norwood, Massachusetts, December 1976.
- 2) Kung, H.C., Spaulding, R.D. and You, H.Z., "Response to Sprinkler Links to Rack Storage Fires" FMRC J.I. OG2E7.RA, November 1984.
- 3) Pepi, J.S., "Relationship Between Thermal Response and Fire Suppression Characteristics of Automatic Sprinkler in a West-Pipe System" Presentation at Fire Detection and Suppression Symposium, SFPE, March 9-11, 1987.
- 4) Heskestad, G. and Bill, R.G., "Quantification of Thermal Responsiveness of Automatic Sprinklers - RTI, ETC." Presentation at Fire Detection and Suppression Symposium, SFPE, Maritime Institute of Technology, Linthicum Heights, Maryland, March 9-11, 1987.
- 5) You, H.Z. and Kung, H.C., "Strong Buoyant Plumes of Growing Rack Storage Fires," Twentieth Symposium on Combustion, The Combustion Institute, 1984.
- 6) Alpert, R.L. and Friedman, R., "Computer Modeling of Sprinkler Spray Interaction with a Fire Plume" Presentation to the Scientific Section of the International Meeting at Avila, Spain, October 7-9, 1986.
- 7) Heskestad, G., "Parametric Study of Sprinkler Fire in Reduced-Scale Model" FMRC J.I. OGOE5.RU, June 1986.
- 8) Fire Detection and Suppression Symposium, SFPE, Maritime Institute of Technology, Linthicum Heights, Maryland, March 9-11, 1987.
- 9) Chicarello, P.J., Troup, J.M.A., Dean, R.K., "Large-Scale Fire Tests Evaluation of Early Suppression Fast Response (ESFR) Automatic Sprinklers," Prepared for National Fire Protection Research Foundation, and Factory Mutual Research Corporation, FMRC OM2R5.RR and OMOJ7.RR, May 1986.
- 10) Kung, H.C., Spaulding, R.D. and Hill, E.E., "Sprinkler Performance in Residential Fire Tests," Technical Report FMRC Serial No. 22574, Factory Mutual Research Corporation, Norwood, MA, July 1980.

- 11) Kung, H.C., Spaulding, R.D., Hill, E.E., and Symonds, A.P., "Field Evaluation of Residential Prototype Sprinkler, Los Angeles Fire Test Program," Technical Report, FMRC J.I. OEOR3.R(1), Factory Mutual Research Corporation, Norwood, MA, February 1982.
- 12) Kung, H.C., Spaulding, R.D., and Hill, E.E., "Residential Fire Tests with Sidewall Sprinklers," Technical Report, FMRC J.I. OJ1N0.RA, Factory Mutual Research Corporation, Norwood, MA, December 1985.

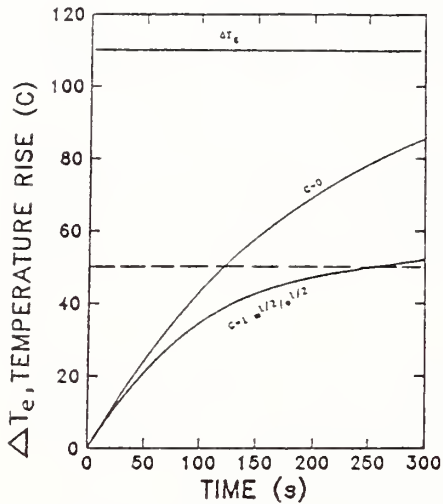


Fig. 1 Temperature rise of a hypothetical, $RTI = 200 \text{ (m/s)}^{1/2}$ sprinkler in environment of constant temperature ($\Delta T_g = 110^\circ\text{C}$) and velocity (1 m/s) for two different values of the conduction parameter

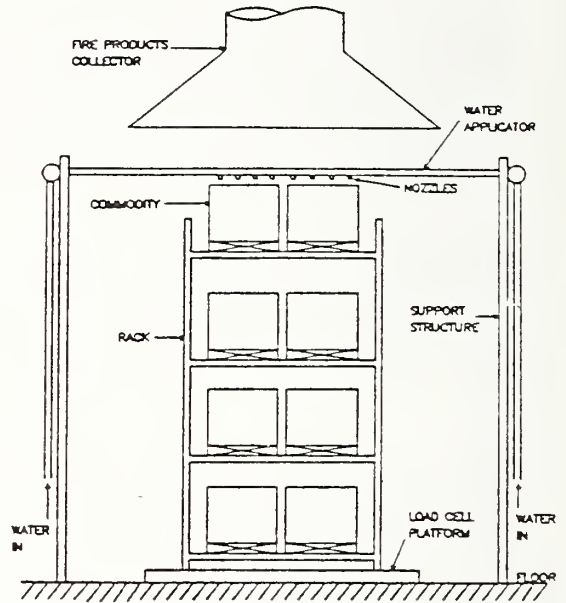


Fig. 2 Test setup for the determination of heat release rate and required delivered density of storage commodities within the ignition stack of storage arrangement

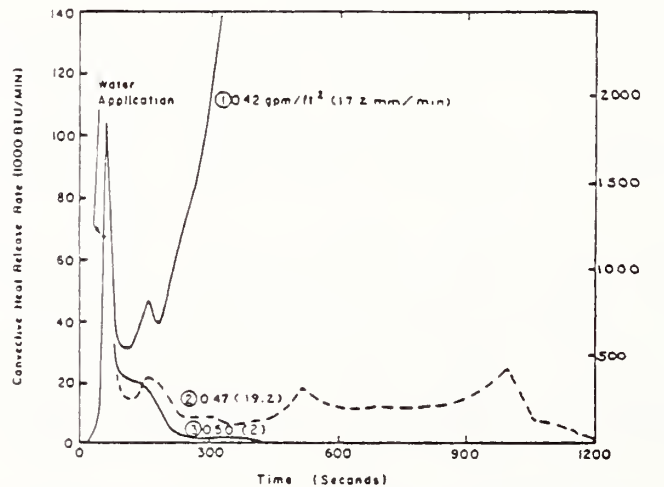
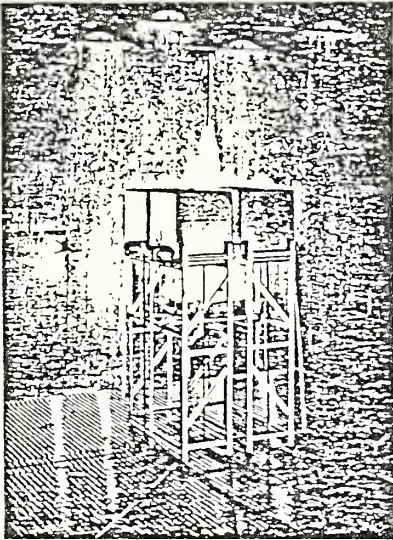


Fig. 3 Results of three RDD tests of 20-ft (6.1 m) high rack storage of plastic commodities



ig.4 ADD test apparatus for measuring the ADD performances of candidate ESFR sprinklers

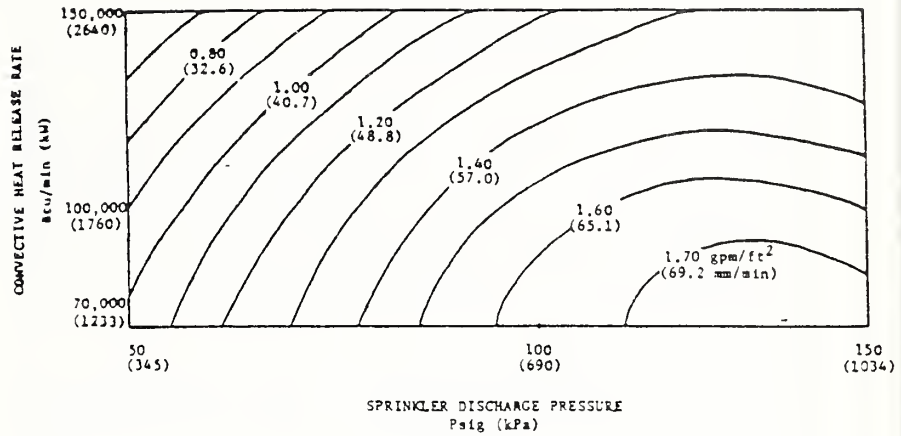
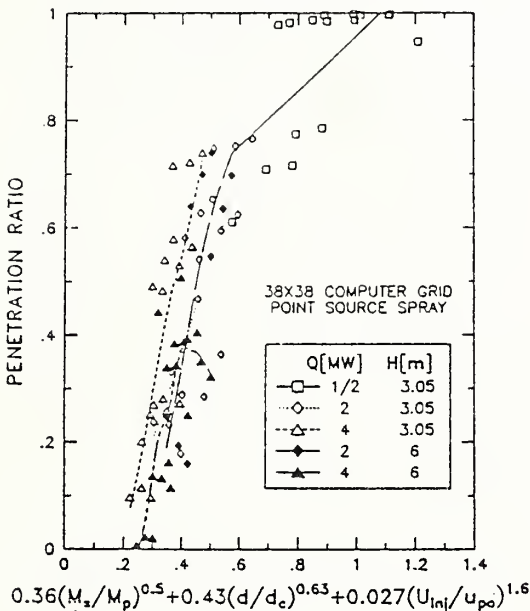


Fig. 5 ADD performance map for prototype ESFR sprinklers with the fire source centered between two discharging sprinklers, 10 ft (3 m) clearance, 10 ft (3 m) spacing between sprinklers



ig.6 Optimized correlation for heat release and ceiling height effects (one sprinkler operated directly over the fire source)

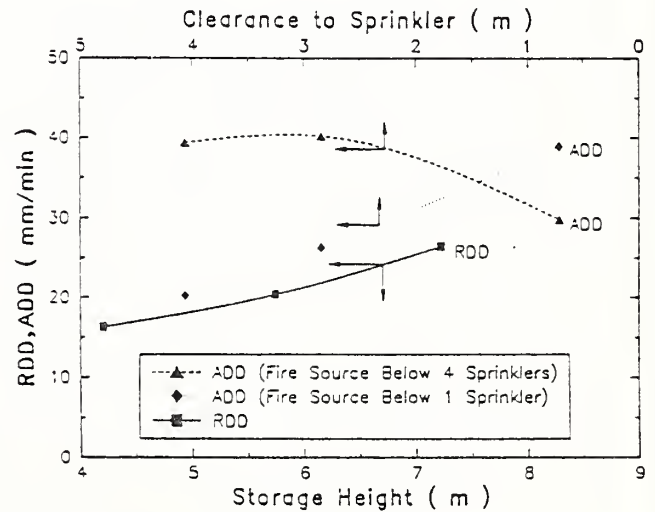


Fig.7 Comparison of ADD value measured at different clearances with RDD values measured for rack storage of plastic commodity at different storage height (CPF sprinkler, 3 m x 3 m spacing, 345 kPa, 1034 kW convective heat release rate)

FMRC SPRINKLER RESEARCH

C. Yao, Factory Mutual Research Corporation, USA

HASEMI: Did you consider the radiation effect?

YAO: At the moment, we ignore the radiation effect. In this on-going program, we're going to use a 9-meter high ceiling and will be looking carefully into the radiation effect on sprinkler response. In a month or two, we will have a report addressing the radiation effect and sprinkler response in an industrial fire situation.

If it becomes important, we may have to modify the model to include radiation, but that would not effect the RTI measurement or conductive term measurement. We just measure them separately.

ZUKOSKI: You had some measurements of transient plume motion?

YAO: Yes.

QUINTIERE: I noticed on the slide for the B ceiling that it appeared to be a combustibile ceiling. If that is the case, what is the effect of a combustibile ceiling?

YAO: The slide I showed was borrowed from a large drop sprinkler program that we ran ten years ago. The ceiling was involved about three or four minutes after ignition. Also, as soon as you suppress a fire, even a fire like that, it disappears within ten seconds. Without a fire plume to feed it, the ceiling flow doesn't propagate itself without a fire pushing it. In the model, we use a non-combustibile ceiling. We assume, at this moment, we're talking about a sprinkler operating within thirty or forty seconds; I don't think the ceiling has a chance to get involved. It may char a little, but if it suppresses the fire as fast as we want, we don't have to worry about it. But, when we validate the model in Rhode Island, we will use a combustibile ceiling to validate the results.

Progress in Modeling Sprinkler Performance

DAVID D. EVANS, WILLIAM D. WALTON AND
BERNARD MCCAFFREY
Center for Fire Research
National Bureau of Standards
Gaithersburg, MD 20899, USA

ABSTRACT

The Center for Fire Research has begun the construction of a fire suppression submodel to be included in one of the current zone fire models. Initial studies will concentrate on the extinction of liquid pool fires by water sprays, but may be generalized to other fuels within the same submodel framework. Studies related to the overall performance of sprinkler systems that are detailed in this report are: Sprinkler response time predictions within enclosures, sprinkler spray characteristics, droplet evaporation time predictions, and wood crib fire suppression.

1. INTRODUCTION

Water spray sprinkler systems are a common and effective means of providing automatic fire protection for facilities. For decades, these systems have been put in place in industrial facilities to provide for prevention of spread and possible extinction of accidental fires. During the past decade, considerable research has been performed to extend the use of sprinklers to ordinary residential living spaces in which new technology systems may provide both property and life safety protection in the event of accidental fires.

Even though there is considerable qualitative information about the various physical and combustion phenomena associated with fire suppression using water sprays, there is relatively little quantitative information available from measurements in studies of room fire extinguishment. In the common cases of a bedroom or living room fires, which have been studied for over a decade to quantify fire growth processes, there exists plenty of debate as to the relative importance of several mechanisms that operate simultaneously during the suppression of a furniture fire. In each case, the possible physical and chemical mechanisms involved may be enumerated. In most cases, quantitative studies under idealized research conditions can be found in the literature to quantify the individual physical and energetic mechanisms contributing to the fire suppression action of the water spray in a compartment fire. The energetics associated with the extinction of fires by a) cooling of a solid liquid fuel below some critical temperature, b) dilution of a miscible liquid fuel, c) separation of the fuel vapors from a means of oxidation, d) reducing the critical level of radiation flux from the flame and surroundings back to the fuel, e) dilution of the oxidizer concentration by steam are well known. Additionally, there are data available, albeit less than is desirable, which

propose to give critical water spray fluxes needed to extinguish selected fuel packages.

Except for the recent work of Pietrzak et al [1], there has not been any efforts to produce a single predictive model for analysis of extinguishment of accidental fires in enclosures using water sprays. The Center for Fire (CFR) at the National Bureau of Standards (NBS) has underway a research program to construct modules of an extinction model which may be implemented into one of the available fire growth room fire codes, such as FIRST [2] or FAST [3]. Although the technical content of the suppression subroutines may change as more information is obtained through the next decade of research necessary to perfect the modeling, the framework should remain unchanged. For example, the position of the automatic sprinkler within the enclosure, the initial trajectory and drop sizes in the spray, and the volume flow rate of water will always be required as input to the model. As the spray may interact directly with the burning surface, or be blocked by obstructions, the addition of a suppression module to the current room fire models will require more input into the model about the fuel and room geometry than is currently used in routine execution of the existing codes. The initial framework for the suppression submodel and required changes to the existing room fire models is being assembled this year. During the next year, predictive methods for liquid pool fire extinction within ventilated enclosures will be formulated and partially validated. As part of the support for the fire suppression submodel limited studies were completed in 1986 to quantify individual physical phenomena involved with the prediction of sprinkler performance and the collection of full scale test data. The results of these studies conducted as part of the in-house CFR research program, the extensive cooperative research studies with U.S. and foreign government agencies, and the CFR university grants program are summarized below.

2. SPRINKLER RESPONSE TIME

Of primary importance to the modeling of sprinkler system performance is the prediction of the time of activation of the sprinkler which determines at what time during the growth of the fire suppression by water spray will begin. Two activities were completed. First, the formulation and coding of the compartment fire sprinkler activation model that considers the effects of an accumulated warm gas layer in the upper portion of the room was completed and added to the popular ASET code [4]. As part of this overall analysis, studies of two-layer plume flow characteristics were completed at laboratory scale by Evans and Morehart [5]. Figure 1 shows an example case of the agreement between predicted and measured plume flow temperatures above and below the warm-cool layer interface in an enclosure. This analysis forms the basic analysis that allows the substantial research work and experimental information available for tests using very large or unconfined ceilings to be used in the modeling of sprinkler activation in small rooms typical of residential living spaces.

Second, the extensive analytical information for thermally activated devices installed below large unobstructed ceilings was organized into both tabular form and a user friendly computer codes by Evans and Stroup [6,7]. These works provide practicing fire protection engineers with a needed tool for

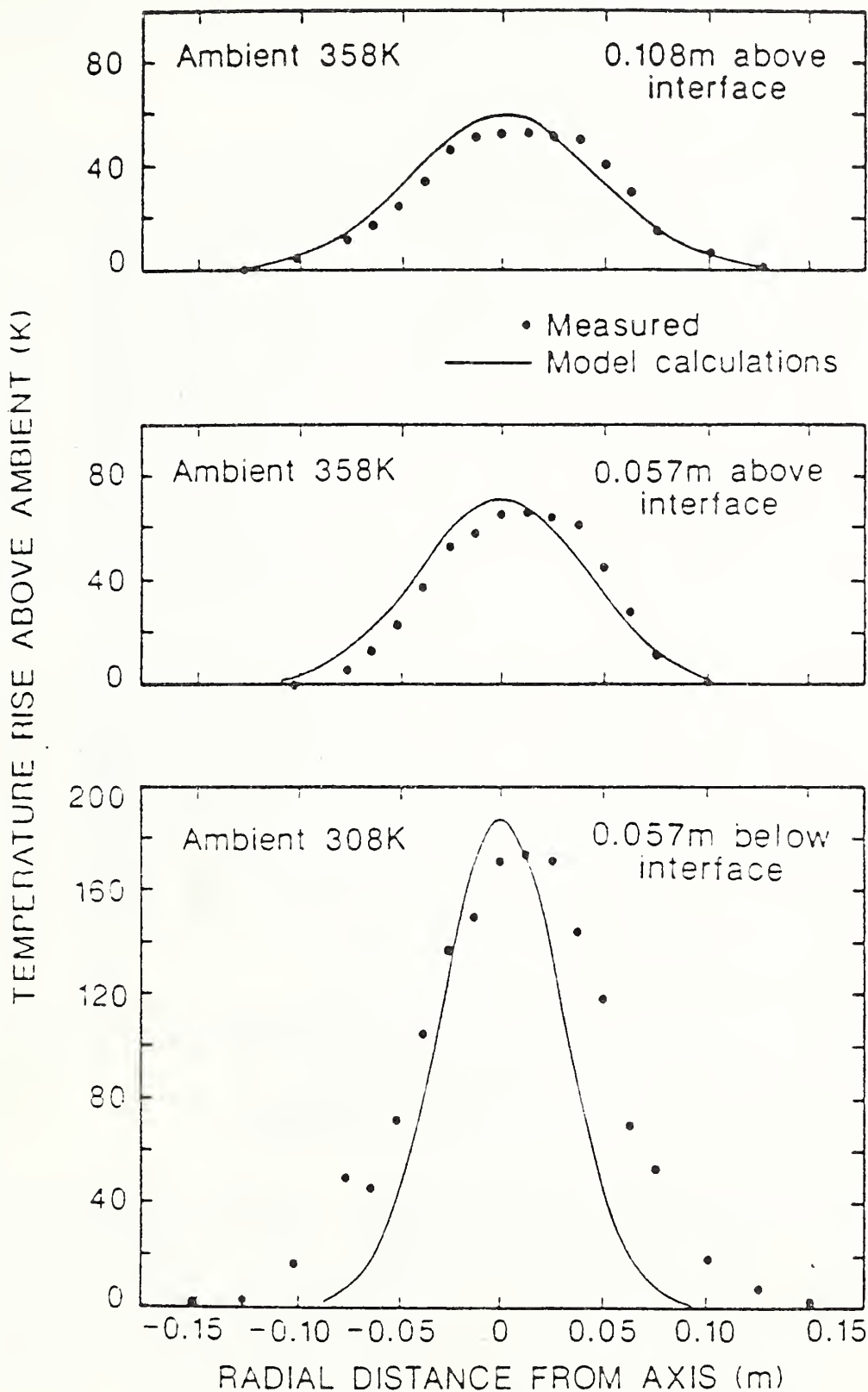


Fig. 1. Measured and predicted temperatures for burner located 0.77 m below the ceiling.

analysis of expected sprinkler system response time that can easily be used as a guide for selection of appropriate equipment and installation spacing.

3. SPRINKLER SPRAYS

Sprinkler spray drop size and trajectories are important input information to the fire suppression subroutines under development at CFR. Wendt and Prah1 at Case Western Reserve University in Cleveland Ohio have reported on studies of spray trajectories produced from idealized and actual sprinklers [8]. One objective of their study was to understand the dynamics of the water sheet break-up that determines initial dropsizes and trajectories at the sprinkler. Another was to formulate a model for the spray-gas interactions that was capable of predicting water spray flux distributions in the absence of fire. Figure 2 shows a comparison of the calculated and measured radial distribution of water spray flux per unit area at floor level from their tests of idealized sprinklers. Using radial spray distributions that are easily measured, and the available physical models, adequate information for initial drop size distributions and trajectories may be calculated that potentially avoid the difficult and tedious task of physical drop size measurement for the purpose of suppression modeling. Further studies are required in which both spray distribution and drop size (unavailable to these investigators) information is used to validate the model.

Extensive drop size distribution measurements are being collected in cooperative studies funded in part by the Swedish Fire Research Board which have brought together extinguishment specialists in CFR, the British Fire Research Station, and the Polytechnic of the South Bank, London to examine the interactions of sprinkler sprays with hot gas layers. To provide initial spray drop size and trajectory information from actual sprinkler hardware, the spray characteristics are being measured at CFR. Figure 3 shows a histogram of the spray droplet distribution and droplet velocity distribution from a pendent sprinkler at a sample location near the discharge from the deflector. Average velocity of droplets in the spray is indicated to be 5.65 m/s an angle of -86.2° to the plane of the deflector. This is one of over a hundred positions measured in this single spray.

Detailed initial trajectory, drop size and radial spray flux distributions from sprinklers will be used to further evaluate the predictive capabilities developed by Wendt and Prah1 in future studies.

4. DROPLET EVAPORATION

The Center for Fire Research through cooperative studies with the University of Maryland is quantifying the heat transfer processes involved in the evaporation of water droplets on hot surfaces. Investigators diMarzo and Evans hope to eventually construct a thermal model for solid fuel extinction based on the detailed understanding of both single and multiple droplet evaporation processes. Initial studies have been performed on the simplified problem of single droplet evaporation from a heated non-porous aluminum surface. Later studies will examine the effects of porosity, material thermal conductivity, and external heat flux.

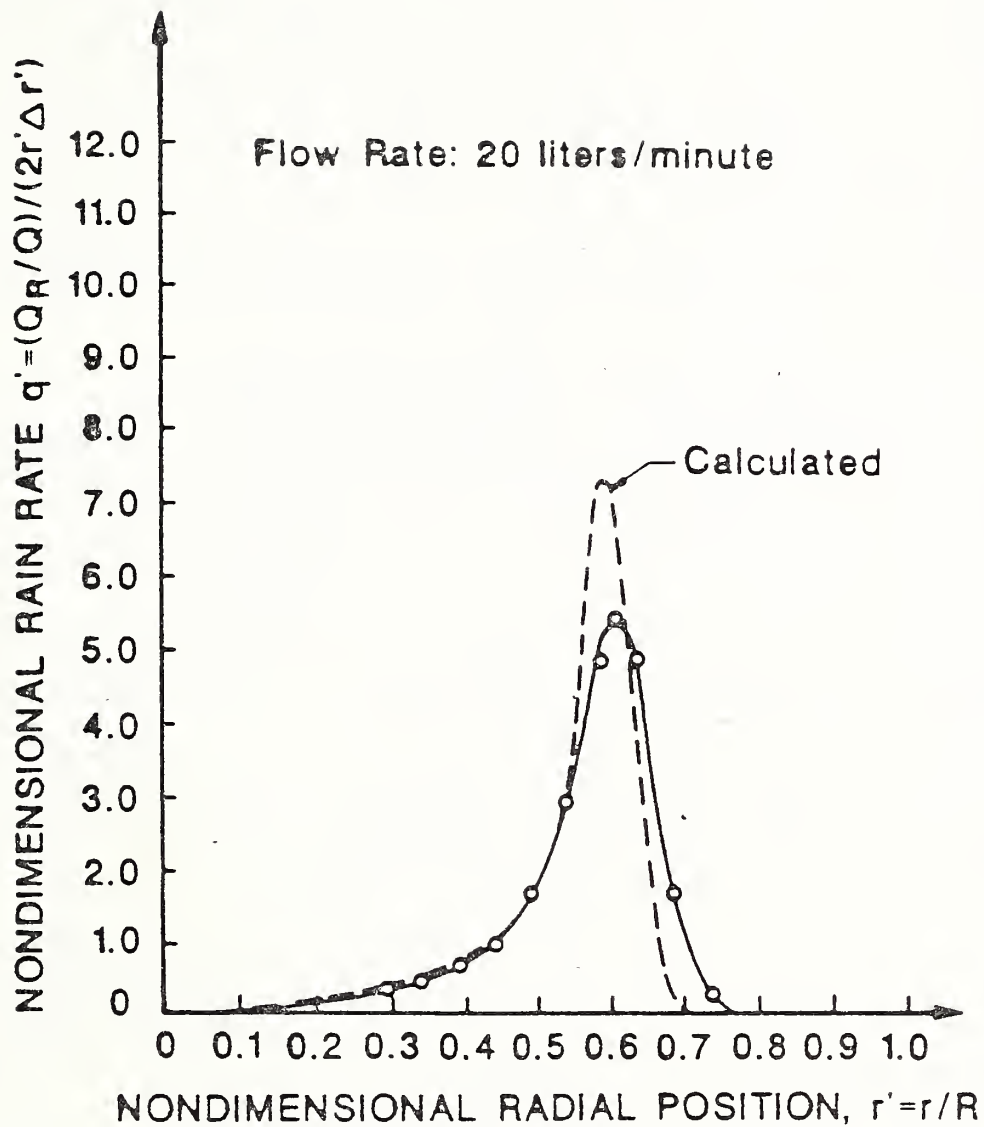


Figure 2 Calculated and measured radial distributions of water spray flux per unit area for an idealized sprinkler.

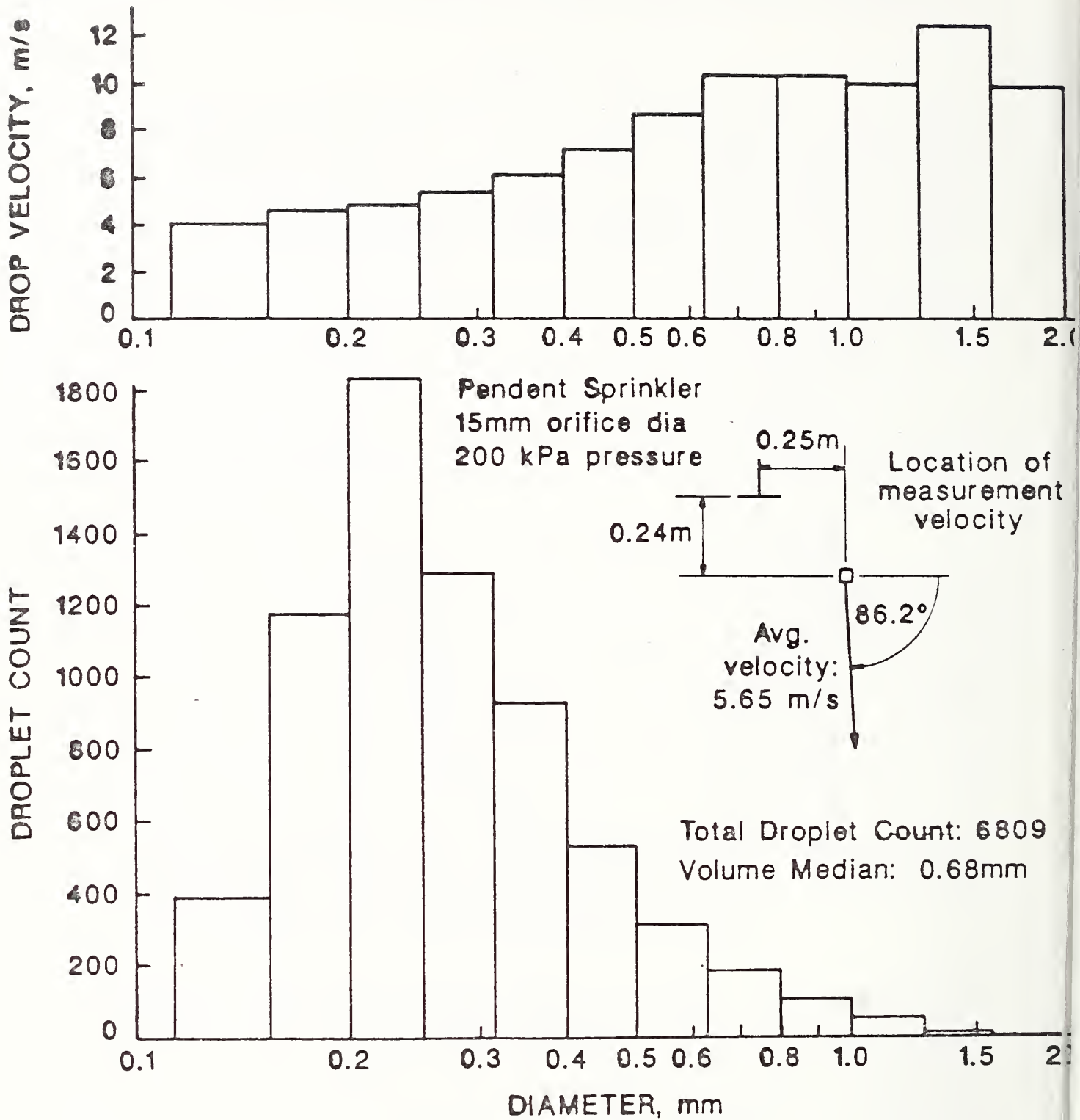


Figure 3 Droplet size distribution and velocity distribution in the spray from a pendent sprinkler

Initial studies [9] examined the case of high thermal conductivity solids for which the surface temperature of the solid under the evaporating droplet is nearly constant. Setting this constant temperature equal to the available analytic solution for the contact temperature between semi-infinite bodies of differing thermal properties essentially decouples the analysis of the solid substrate and droplet evaporation processes. This permits a rather simple overall analysis of the evaporation process that yield predictions of evaporation time which are compared with measured values in Figure 4 for three different initial drop diameters. Figure 5 shows the comparison of calculated and measured time dependent variations of droplet volume for a 30 microliter droplet evaporating on an aluminum surface initially at 98°C.

Further studies underway quantify the evaporation process for low thermal conductivity solids, and multiple droplet exposures characteristic of sprays effects during fire suppression.

5. LARGE SCALE TESTING

Water spray extinguishment phenomena associated with both actual furniture fires and research fuel loads such as cribs have been examined by Walton at CFR. This research has two objectives, one is to provide practical information on the performance of actual sprinkler system. The other is to examine the range of water sprays and activation time that are effective in controlling fires in easily characterized fuels for aiding the development of sprinkler suppression models.

In an applications based study for the U.S. General Services Administration and the U.S. Fire Administration it was shown that new technology residential fast response sprinklers could be effective protection for office space fires that presently require the use of greater flow rate standard sprinklers [10].

A series of tests underway at this time is designed to examine the effect of water spray flux on the extinguishment of various fuel packages. Initial tests have focused on fires in wood cribs constructed of fir with a total weight of approximately 21 kg. The cribs consist of 8 layers with 6 sticks per layer where each stick is 38 by 44 by 609 mm. A sprinkler head is located 1.75 m above and 2.02 m away from the crib. Water spray flux to the area of the crib is measured in a separate test.

Water is applied to the crib when the maximum and nearly steady burning rate of the crib has been obtained. Rate of heat release measurements of the crib fire are taken using oxygen consumption calorimetry. Figure 6 shows the heat release rate for three tests where time has been shifted so the sprinkler operation occurs at the same time (approximately 450 s) for each of the tests. The spray flux per unit area for test 511 was 0.058 mm/s, for test 514 was 0.054 mm/s and for test 516 was 0.041 mm/s. Although these tests cannot be compared directly because of the different ignition sequences, it appears the initial reduction in heat release rate due to the application of the three different spray fluxes of water was nearly the same for all tests. Further work will be performed in an effort to understand this phenomena as it may be an important finding that could simplify modeling of the suppression process.

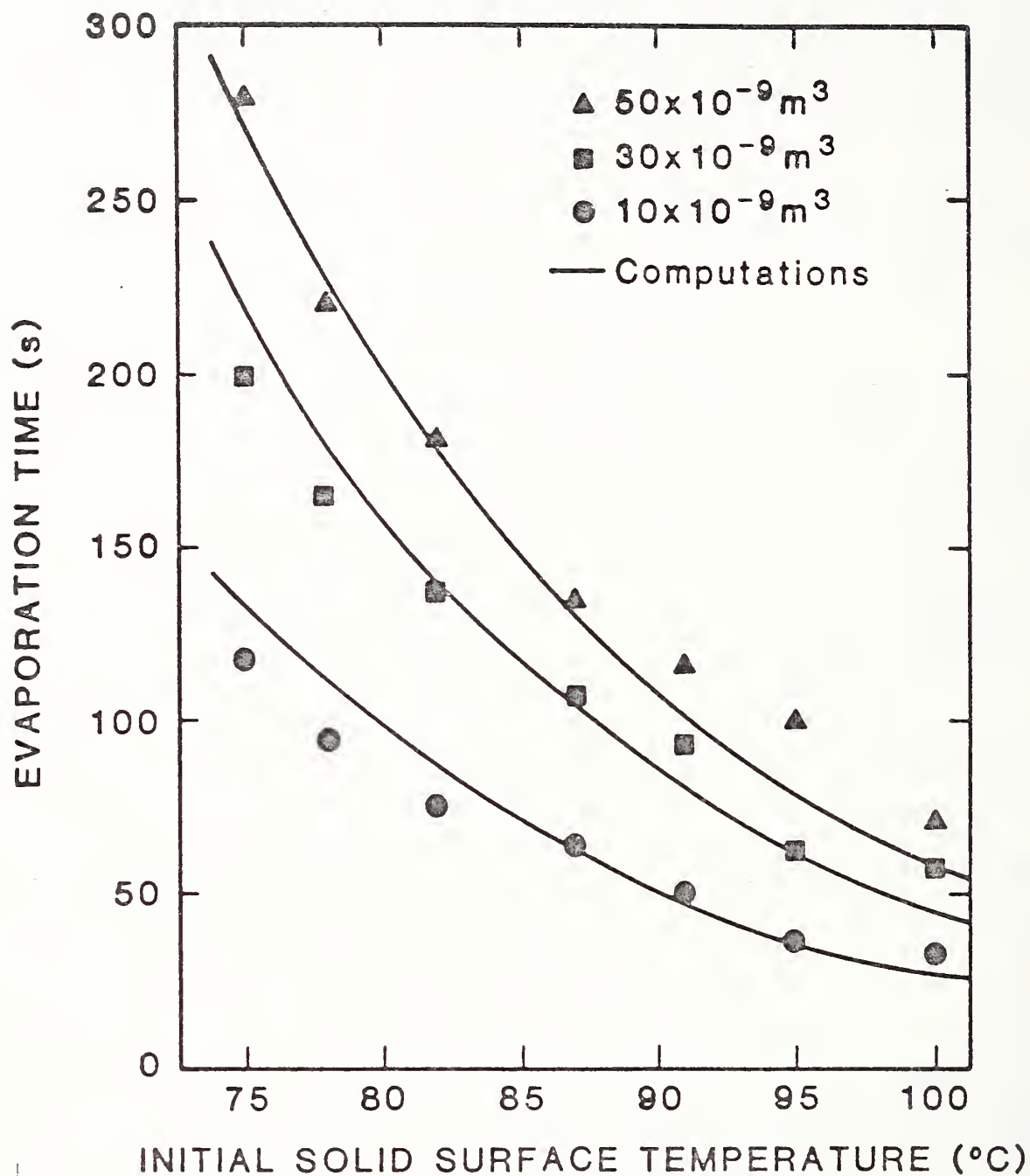


Figure 4 Predicted and measured droplet evaporation times for three droplet diameters

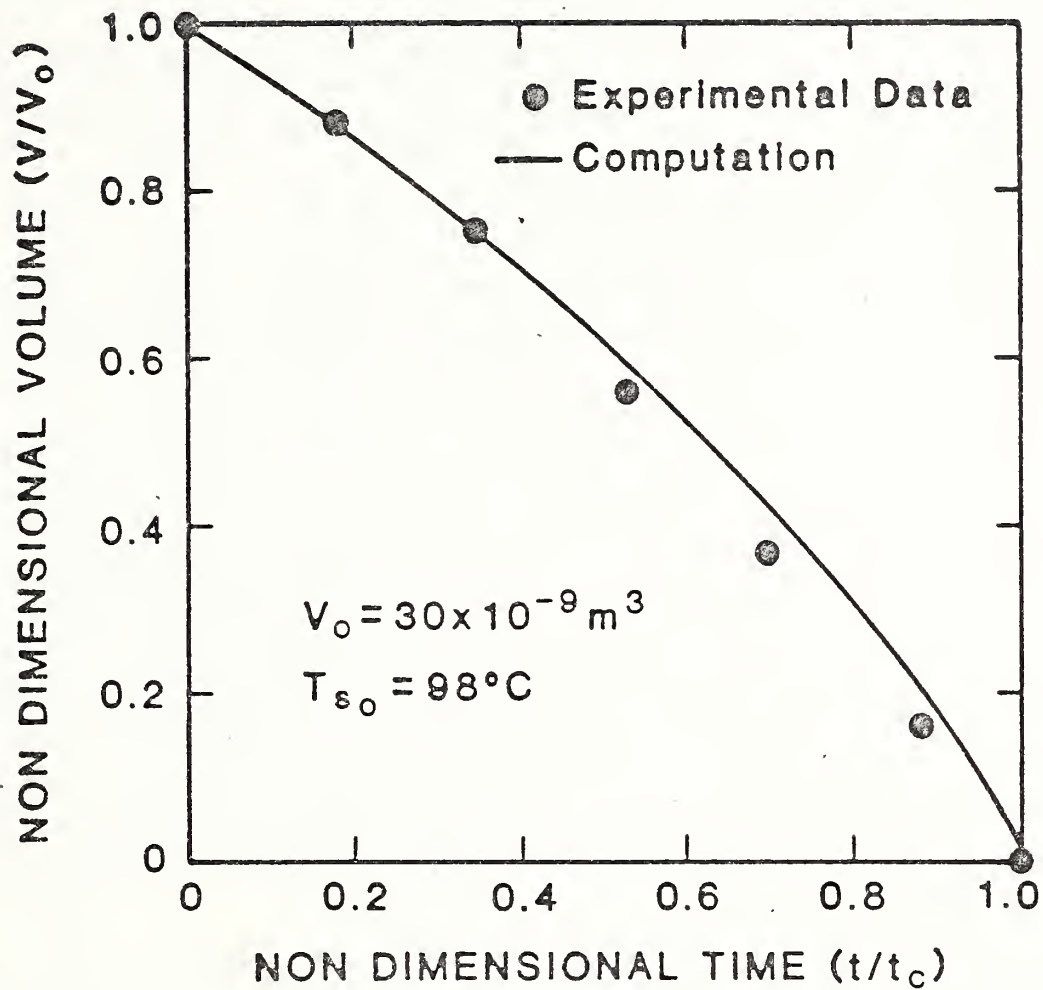
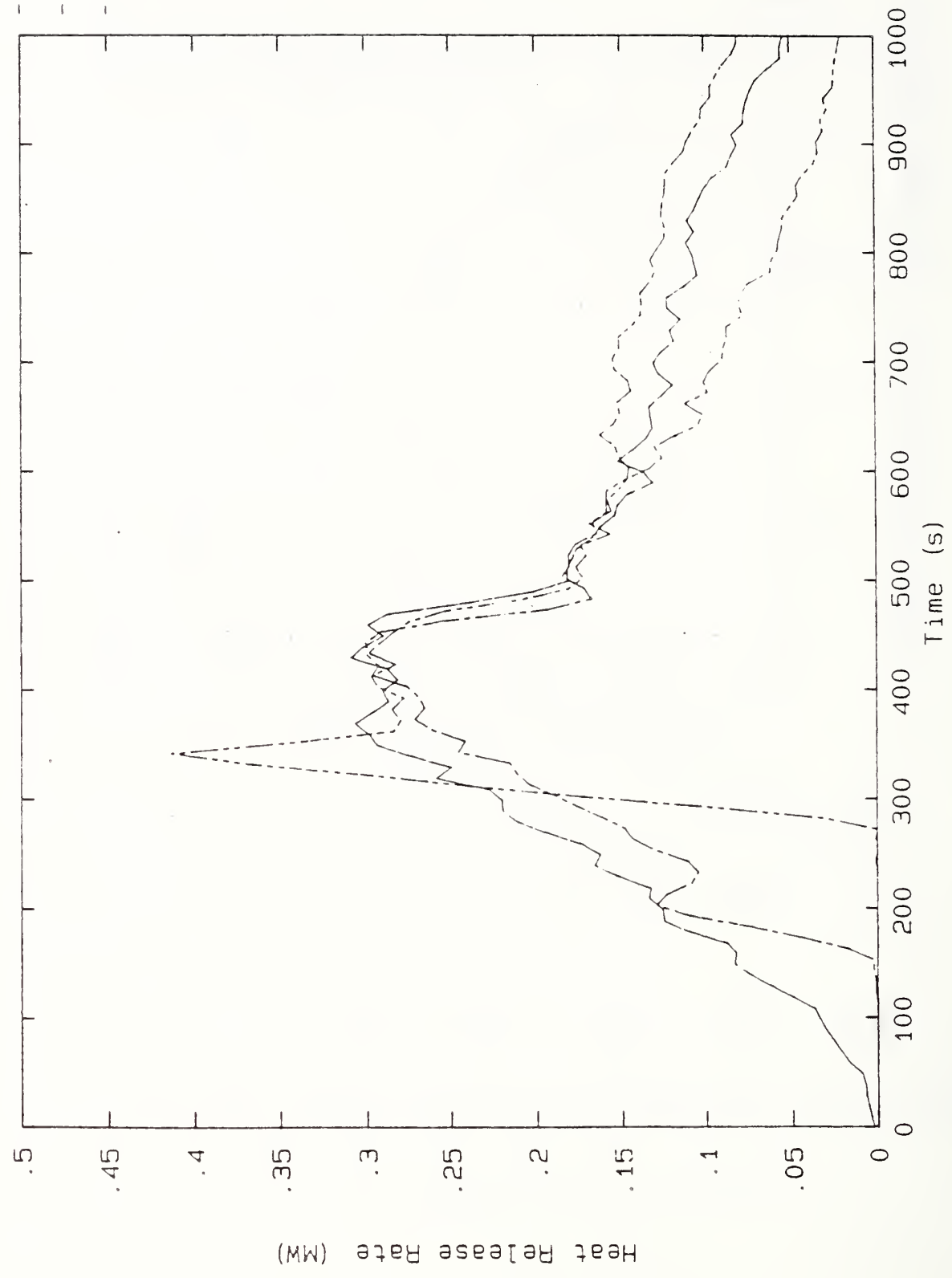


Figure 5 Calculated and measured time dependent variation of droplet volume for a 30 microliter droplet

— 511
- - - 514
- · - 516



HEAT RELEASE RATE

Figure 6 Heat release rate history for three crib fires before and after sprinkler response.

6. FUTURE WORK

Studies will continue to quantify the effects of sprinkler discharges on fire growth. The thrust of new programs will be on the detailed studies of the effects of low water volume discharges on fire spread rates. Work will continue on the formulation of the suppression submodel to be accommodated in one of the zone fire models under development at CFR.

7. REFERENCES

- [1] Pietrzak, L.M., Johanson, G.A., and Ball, J.A., A Physically Based Fire Suppression Computer Simulation for Post-Flashover Compartment Fires, Vol. III, Simulation Formulation, Software Documentation and Experimental Requirements, Mission Research Corporation Report MRS-R-846, 735 State Street, P.O. Drawer 719, Santa Barbara, CA 93102, March 1986.
- [2] Mitler, H.E. and Rockett, J.A., User's Guide to FIRST, A Comprehensive Single-Room Fire Model, in preparation as an NBSIR.
- [3] Walton, W.D., Baer, S.R., Jones, W.W., User's Guide for FAST, NBSIR 85-3284, U.S. Dept. of Commerce, National Bureau of Standards, Gaithersburg, MD 20899, December 1985.
- [4] Walton, W.D., ASET-B, A Room Fire Program for Personal Computers, NBSIR 85-3144-1, U.S. Dept. of Commerce, National Bureau of Standards, Gaithersburg, MD 20899, December 1985.
- [5] Evans, D. and Morehart, J., Investigation of the Effects of a Stratified Two Layer Environment on Fire Plume Temperatures, Proceedings of the 1987 ASME-JSME Thermal Engineering Joint Conference, Honolulu, Hawaii, March 22-27, 1987, Volume I, pp. 381-386, 1987.
- [6] Stroup, D., Evans, D., and Martin, P., Evaluating Thermal Fire Detection Systems, NBS Special Publication 712 (English Units) and 713 (SI Units), U.S. Dept. of Commerce, National Bureau of Standards, Gaithersburg, MD 20899, April 1986.
- [7] Evans, D.D. and Stroup, D.W., Methods to Calculate the Response Time of Heat and Smoke Detectors Installed Below Large Unobstructed Ceilings. Fire Technology, Volume 22, 1, p. 54-65, February 1986.
- [8] Wendt, B., and Prah1, J.M., Discharge Distribution Performance for an Axisymmetric Model of a Fire Sprinkler Head, NBS-GCR-86-517, U.S. Dept. of Commerce, National Bureau of Standards, Gaithersburg, MD 20899, October 1986.
- [9] DiMarzo, M., Evans, D.D. and Trehan, A.K., The Cooling Effect of a Single Evaporating Droplet on a Hot Semi-infinite Metal Body, Proceedings of the 1987 ASME-JSME Thermal Engineering Joint Conference, Honolulu, Hawaii, March 22-27, 1987, Volume 1, pp. 409-416, 1987.
- [10] Walton, W.D. and Budnick, E.K., Office Occupancy Sprinkler Tests, in preparation as a NBSIR.

COMBUSTION BEHAVIOUR OF BUILDING MATERIALS USING
A MODEL BOX WITH AIR SUPPLIED SYSTEM

Fumiharu SAITO

Testing Lab of Center for Better Living
2 Tatehara Oho-cho, Thukuba-gun,
Ibaraki Pref, Japan

Masashi YOSHIDA

Building Research Institute, Ministrg of Construction
1 Tatehare Oho-cho, Tsukuba-gun,
Ibaraki Pref, Japan.

PREFACE

Fire behavior of compartments depends on the relation between the building conditions such as geometrical configuration of the compartments and size of openings including doors and windows, and the material conditions such as interlining materials, furniture etc.(hereafter, referred to as materials). existing in the compartments.

Recently, research on mathematical modeling of fire behavior of compartments has been developed remarkably, and it becomes possible to estimate it accurately.

However, it is still difficult to estimate burning behavior on the stage of flashover which is a characteristic phenomenon of changing of burning behavior during a steady state of compartment fire, because the combustion mechanism of various materials at that stage is quite complicated.

Many combustibility test methods have been developed in order to estimate the fire risk of materials. In most cases, plate shape specimens of materials have been tested in an open space with sufficient air supply for burning. Since these tests have not been conducted in any limited ventilating conditions such like those at real compartment fire, it is difficult to utilize these test results for estimating fire behavior of compartments.

For the purpose of such estimation, it is essential to evaluate, quantitatively, the burning behavior of materials in the condition in which major factors of compartment fire are took into consideration as parameters.

While many kind of factors which might govern compartment fire have been pointed out. it is possible to extract major factors from them by focusing the target which we want to clarify in a fire scenario.

The aim of this study is to explain the burning behavior of materials in compartment fire.

Burning of materials in a compartment fire is a oxidizing reaction in the limited space; therefore, the fire behavior is controlled by the relationship between the rate of release of combustibles from the materials and rate of air supply to the compartment. The rate of release of combustibles is in proportion to exposed area of the materials, On the other hand, rate of air supply depends on the temperature on the compartment and shape of openings of it.

Temperature in a compartment under fire, fundamentally, depends on calorific value and rate of pyrolysis of the materials involved. However, it should be noticed that those two values which we consider are the special values in the condition of compartment fire, and are not the values which are described in a table of constants of materials. Furthermore, the rate of pyrolysis is accelerated by feedback of heat within the compartment.

From the above point of view, a combustibility test apparatus with a forced ventilation system has been developed, and several materials have been tested with the variation of exposed area of the material and rate of air supply.

The aim of the study is to clarify the burning characteristics of materials with relation to rate of air supply; and in addition, toxicity of smoke generation from the burning has been evaluated by recording the behaviour of mice using a rotary cage installed the a adjusting switch which were exposed to the smoke.

1. Combustion mechanism of materials in compartment fire.

When burning behavior of materials in compartment fire is to be quantified experimentally, it is necessary to design a test apparatus and to develop a test method suitable for the purpose of quantification.

Once compartment fire occurs and develops, the burning behavior changes, in general, from a stage of fuel rich combustion to a stage of ventilation control fire where the rate of pyrolysis of materials is balanced with rate of air supply. It may be usually considered that compartment fire immediately turns into a developed stage of fire from flashover. However, on condition of materials involved and shape of openings, there is another stage of fire in which the compartment is filled with smoke and only smoke but no flame spouts from the openings. It may be called as smoky fire. And in proportion as the area of openings decrease, the duration of the smoky fire lengthens. By investigations into many cases of recent building fire, it has been recognized that the smoke release period is very long because the openings of building are rather small. it is also well recognized that rate of release of smoke and CO gas in fire greatly affects the

safety of lives of residents in the building. Therefore, this release rate is one of the most important characteristics of materials in case of consideration into the stage of smoky fire.

Combustion of materials can be classify, in general, into smoldering and flaming. Since the smoldering is considered as a burning behavior which occurs at the lower limit of combustion on the surface of burning materials, application of the theory of smoldering to solve the combustion mechanism of smoky fire brings a lot of problems with it. Namely, the factors controlling the oxidizing reaction in a closed space filled with pyrolytic decomposition products and with limited air supply differs from the factors controlling the oxidizing reaction in a open space with sufficient air supply and lower limit of combustion of pyrolytic decomposition products.

The oxidizing reaction of combustibles in a compartment can be defined as the primary oxidizing reaction, and that of combustibles released out from the compartment into surrounding air can be defined as the second oxidizing reaction. In this second oxidizing reaction, the aspect of the reaction varies widely depending on the phase of mixing of the combustibles with surrounding air. In other words, it should be noticed that, even if the concentration of combustibles released out from the compartment of fire is thick enough, there is a difference on degree of oxidizing reaction between the case that the combustibles are released into an open space with sufficient air and the case that they are released into a limited space such as a corridor in the building.

In general, ratio of oxidizing reaction of combustible materials in a compartment against that at the outside of the compartment varies depending on Ratio of Air Supply (ratio of rate of air supply against the area of exposed surface of the material involved in the compartment) That is; When the RAS (ratio of air supply) is small, the compartment is filled with lots of smoke because of shortage of air. In this case, if the temperature of the smoke is relatively low, only the smoke but no flame runs out from the openings; but if the temperature of the smoke is rather high, flaming occurs at the outside of the openings. When the ratio of air supply is large, combustion occurs much more in the compartment than at the outside of the compartment. When a fire load of heat, smoke etc. resulting from a compartment fire is to be quantified from the point of view of the risk of upward fire spread in buildings, oxidizing reaction of pyrolytic decomposition products spreading in an open space should be investigated. On the other hand, when the fire load which flows and spreads in a building is to be quantified, oxidizing reaction in a limited space imagined as a corridor etc. should be investigated. Therefore, it is necessary to design a fire scenario suitable for the purpose of each study.

Figure-1,2 shows an example of results of fire tests in a model inner dimension of which is 0.84m wide, 1.68m deep and 0.84m high with a opening adjacent to unlimited open space. Even if the

rate of decomposition of the interlining material in the compartment model is almost constant, rate of discharge of smoke and CO gas through the opening varies depending on the oxidizing condition of the smoke and gas at the outside of the compartment. When oxidation of the smoke and gas does not occur, rate of discharge of smoke and CO gas becomes large. However, when the oxidation occurs, the rate of heat release becomes large, but rate of discharge of CO gas extremely decreases. In addition, in case that the compartment has a large opening or depth of it is short, the degree of oxidizing reaction in the compartment is relatively large, because of increase of air supply or well mixing of the pyrolytic products with air.(model C)

It is presumed that ratio of degree of oxidizing reaction inside and outside of a compartment depends on the pyrolytic decomposition mechanism of materials involved in the compartment, the arrangement of the materials, configuration of the compartment and the openings etc. Accordingly, there remains a lot of problems to be solved in order to estimate the ratio of oxidizing reaction theoretically.

From the above mentioned point of view, limitation has been made to consider the oxidizing reaction in a compartment(primary oxidizing reaction) as a first step to elucidate the combustion reaction of materials on compartment fire, and accordingly, some apparatus have been conducted for the purpose of understanding the combustion characteristics of materials with the parameter of rate of air supply. This may cause both an evaluation, from safety side, of toxicity of smoke spreading in a building, and an estimation of fire load to division construction with regard to the heat release.

2 Experiments

2. Specimen

The tested materials are shown in Table-1. Three dimensional specimen was constructed with three side of walls and a ceiling, and was set on the back side of the combustion chamber. There were two types of specimens the exposed area of which was 0.154m^2 and 0.207m^2 .

2.2 Test Apparatus and Test Method

The test apparatus consists of a heat source, a combustion chamber, an air supplying system, a mice exposure chamber and a gas analyzing system as shown in Figure-2.

Ceramic burners of 10cm by 10cm were used as the heat source and were set in front of the wall surface of the specimen with spacing of 1.0cm. The mixture of 3.0 l/min. of propane gas and 14.0 l/min. of air (primary air) was supplied to the heat

source. The rate of heat release of the heat source was 5.1KJ/sec. Another amount of air supply to the combustion chamber(secondary air) was decided taking into account the full scale test data executed by the Building Research Institute, Ministry of Construction, Japan.

3 Test Results

From the measured values of gas flow rate and gas concentration through the chimney of the apparatus, rate of heat release(RHR), total heat release, rate of CO release(RCO) and the amount of generation of CO were calculated by the oxygen consumption technique. Heat release per a unit mass loss(KQ) and generation of CO gas per a unit mass loss(KCO) were calculated by the weight difference of the specimen between that before test and that after test. and by the total heat release and the total CO gas release.

In order to evaluate the toxicity of generated smoke and gas, the generated gas was taken into the mice exposure chamber at a rate of 100 l/min.(this value was lead from the number of change of air of 50 times/hour). And incapacitation time of the exposed mice was measured by means of recording the movement of rotary cages of the mice.

4. Discussion

1) Test with air supplied system

i) It has been recognized from the test results that RHR(rate of heat release)and RCO(rate of CO release) both from materials were in proportion to the exposed surface area of the materials.(Fig 3,4) It has been also recognized that there was a close relationship among the heat release, the characteristics of CO gas release and ASR(rate of air supply per unit area of exposed surface of the material). In other words, it has been observed that RHR is in proportion to ASR, and that RCO is in inverse proportion to ASR. A similar tendency has been observed in an effective heat release of materials(the amount of heat release per unit pyrolytic decomposition amount) and the amount of CO gas release, respectively.(Fig 5)

ii) In the process of the oxidizing reaction of pyrolytic decomposition products on the compartment, it is considered that the pyrolytic decomposition mechanism of wooden materials is relatively simpler than that of plastic materials which may generate many kind of intermediate products. This idea seems to be supported by the test results which shows the fact that the characteristics of heat release and CO gas release of wooden materials has close relationship with ASR, but that the characteristics of plastic materials has no clear relationship with ASR.(Fig 5.2 , 5.3)

The following experimental equation has been obtained with regard to the characteristics of heat release and CO gas release of wooden materials:

Experimental Formula (Air Supplied System)

$$\begin{aligned} \text{RHR/m (KJ/s.m)} & : 2.0 \phi \\ \text{ROO/m (g/s.m)} & : 2.0-0.014 \phi \\ \text{KQ(KJ/g)} & : 0.4 \phi \\ \text{KCO(g/g)} & : 0.35-0.004 \phi \end{aligned}$$

$$\phi : \text{Air Supply Ratio} = \frac{\text{Rate of Air Supply(l/s)}}{\text{Surface area(m}^2\text{)}}$$

There is a limitation on application of the equation, because KQ can not exceed the amount of heat release in complete combustion while KQ increases in proportion to the rate of air supply.

iii) KQ is in proportion to KCO, and it's proportional coefficient depends on the material.

2) Comparison between the air supply system and natural air infiltration

Air supply into the compartment in real fire is made by the buoyancy of heated gas and air in the compartment. And mixing of air with the pyrolytic decomposition products in the compartment is done depending on the flow of heated gas in it. On the other hand, with a forced air supply system, the pyrolytic decomposition products is mixed with air better than in condition of natural air infiltration, and oxidizing reaction is done more effectively. Thus, it is necessary to understand the relationship between effectiveness of forced air supply system and that of natural air infiltration in order to apply the test results taken under the condition of forced air supply to evaluation of compartment fire.

J. Rockett and K. Steckler have proposed an equation to estimate the rate of air flow into a compartment using temperature of hot layer and opening factor under the steady state burning condition taking into account the real compartment fire. And it is also possible to estimate the rate of air flow into the compartment using measured information of RHR.

Accordingly, rate of air flow into two types of model box of 0.84m x 1.68m x 0.84 and 0.84 x 0.84m x 0.84m, which have openings adjacent to open space, was measured by bi-directional pitot tubes during fire tests. Figure-6 shows the relationship between the measured air flow and the air flow estimated by temperature, opening factor and RHR.

In case that burning also occurs at the outside of the compartment in addition to inner combustion, air flow tends to be over-estimated by the portion of RHR made at the outside of it.

It is impossible to evaluate the combustion reaction of compartment fire at the inside of the compartment independent from that at the outside. However, in case that the combustion reaction made at the outside of compartment is very little, it is still possible to estimate rate of air flow into it by RHR. Moreover, according to the observation on the air flow at the openings during the fire test, it seems the most realistic approach that to estimate the rate of air flow into the compartment by RHR, and the estimation has been used for discussion of the test results.

1) Rate of pyrolytic decomposition

Pyrolytic decomposition is promoted by the feedback heat made in the compartment because the heat release in it is in proportion to ASR. (Fig 8)

2) Characteristics of heat release

Figure-10 shows the relationship between ASR and KQ. that is; KQ increases in proportion to increase of ASR, and reaches to the level of 80% of theoretical complete combustion when ASR exceeds 40. The line on the Figure shows the calculated results by the experimental formula of the case of forced air supply. It is considered that effective mixing of pyrolytic decomposition products with air and over-estimation of rate of air flow cause increases of the value of heat release (KQ) in case of forced air supply in comparison with that in case of natural air infiltration at the same ASR condition.

(3) CO gas release

When opening area is small, oxidizing reaction is made only in the compartment because temperature of the smoke is low even if the condition of mixture of gas and air which runs out from the opening reaches in the flammable condition. However, when the opening area is large, oxidizing reaction with flaming occurs at both inside and outside of the compartment, because temperature and concentration of smoke satisfies the energetic and component condition for combustion. Rate of CO gas release in the latter case is smaller than that in the former case.

When the opening area is small and flaming is not observed at the outside of the compartment, there is a good agreement between the measured characteristics of CO release and that calculated by the experimental formula of the case of forced air supply.

(4) Ratio of KQ and KCO

It has been recognized that there is a close relationship between the heat release and CO gas release on the combustion of materials, and that value of KQ/KCO is in proportion to ASR.

CONCLUSION

In the early stage of compartment fire, smoky fire, which is an oxidizing reaction in the fuel rich condition, exists, because the temperature rise is low and the amount of air supply to the compartment is small. And it is known that the continuation of a fire causes the collapse of glass of windows and openings, and that due to increase of opening area, the rate of air supply increases and the fire becomes vigorous. The smoky fire in the early stage of fire is one of the serious problems for the safety of residents in buildings which should be solved as soon as possible. Therefore, this experimental study was conducted for the purpose of evaluating combustion of materials in the early stage of fire. It has been recognized that the evaluation of the burning characteristics of materials utilizing the method of the forced air supply is useful in some conditions; that is, the case of small opening. However, there still remains many problems in understanding all of the burning behavior of materials as a function of ASR.

(end)

Table 1 Test Materials

Abbreviation	Material	Thickness(mm)	Oxygen Index
PW	Plywood	4.0	-
IB	Fiber Insulation Board	9.0	21.0
PVC	PVC Foam	25.0	29.0
ISF	Polyisocyanurate Foam	25.0	23.0
PF(R-1)	Phenolic Foam (Resole Type)	25.0	38.0
PF(N)	Phenolic Foam (Novolac Type)	25.0	26.5

Table 2-1 Size of Specimen

type	a (cm)	b (cm)	c (cm)	exposed surface area (cm ²)
A	30.0	25.0	11.0	0.154
D	21.5	25.0	21.5	0.207

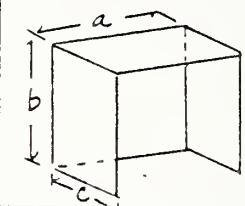


Table 2-2 Specification of Test Apparatus

inner dimension	0.25×0.50×0.25 (m)		
volume of chamber	0.0312 (m ³)		
linings	wall:3	ceiling:1	
exposed surface area	0.154	0.207 (m ²)	
rate of air supply	230	345	460 (l/min)
propane	3 l/min (5.1 KJ/s)		
pre-mix air	14. l/min		
test duration	10 min		

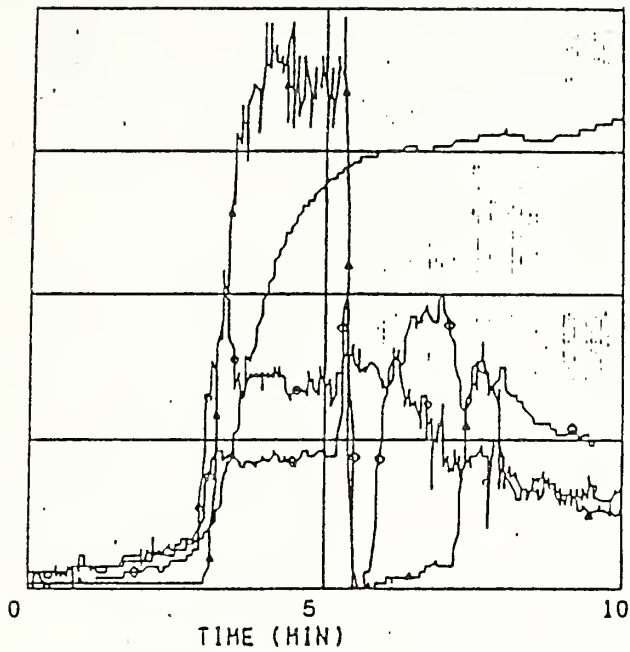
Table 2-3 Air-Supply-Ratio.

	exposed surface area (m ²)	rate of air supply (l/min)	air supply ratio (l/s·m ²)
Type	0.154	460	49.8
A		345	37.3
		230	24.9
Type	0.207	460	37.0
D		345	27.8
		230	18.5

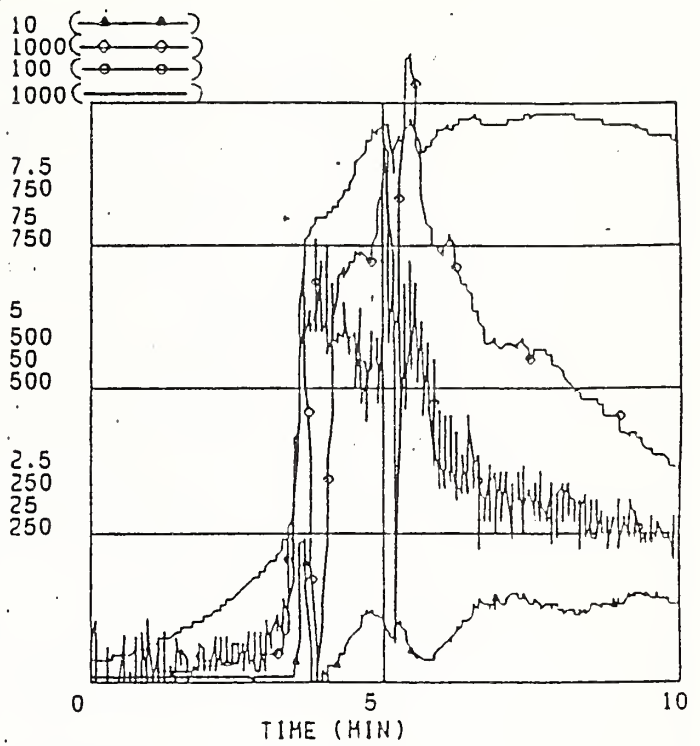
Table 3 Experimental Formula (Air Supplied System)

RIIR/m ² (KJ/s·m ²)	:	2.0φ
ROO/m ² (g/s·m ²)	:	2.0-0.014φ
KQ(KJ/g)	:	0.4φ
KCO(g/g)	:	0.35-0.004φ

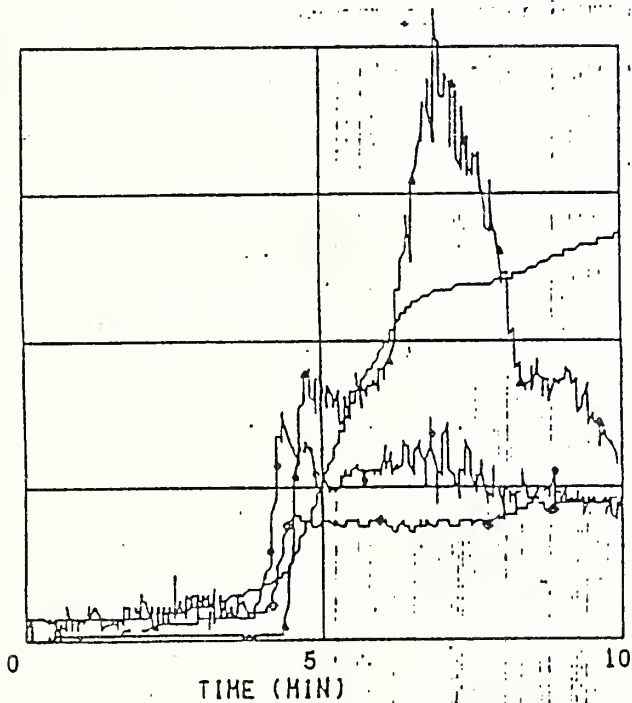
φ: Air Supply Ratio = Rate of Airsupply(l/s)/Surface area(m²)



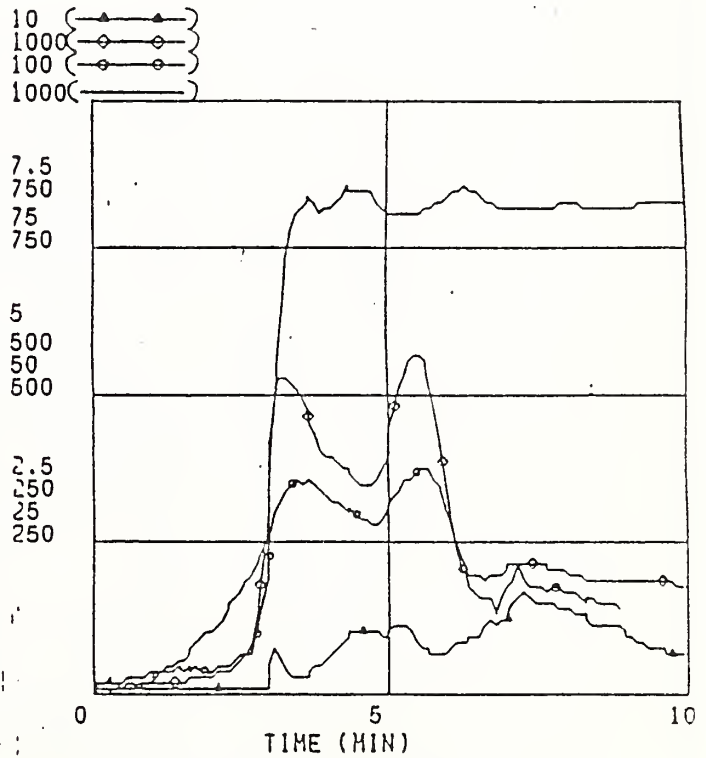
SAMPLE 1B92Aa-85*9*18



SAMPLE 1B9-Ab-85*9*19

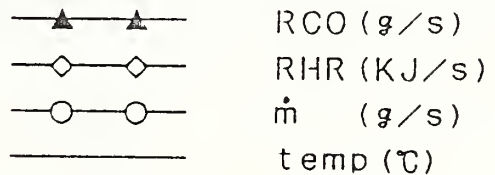


SAMPLE 1B9-ACa-85*9*18



SAMPLE 1B9-C-a-870226-1-temp15

Fig 1-1 Summary of Test Results (Model Box)



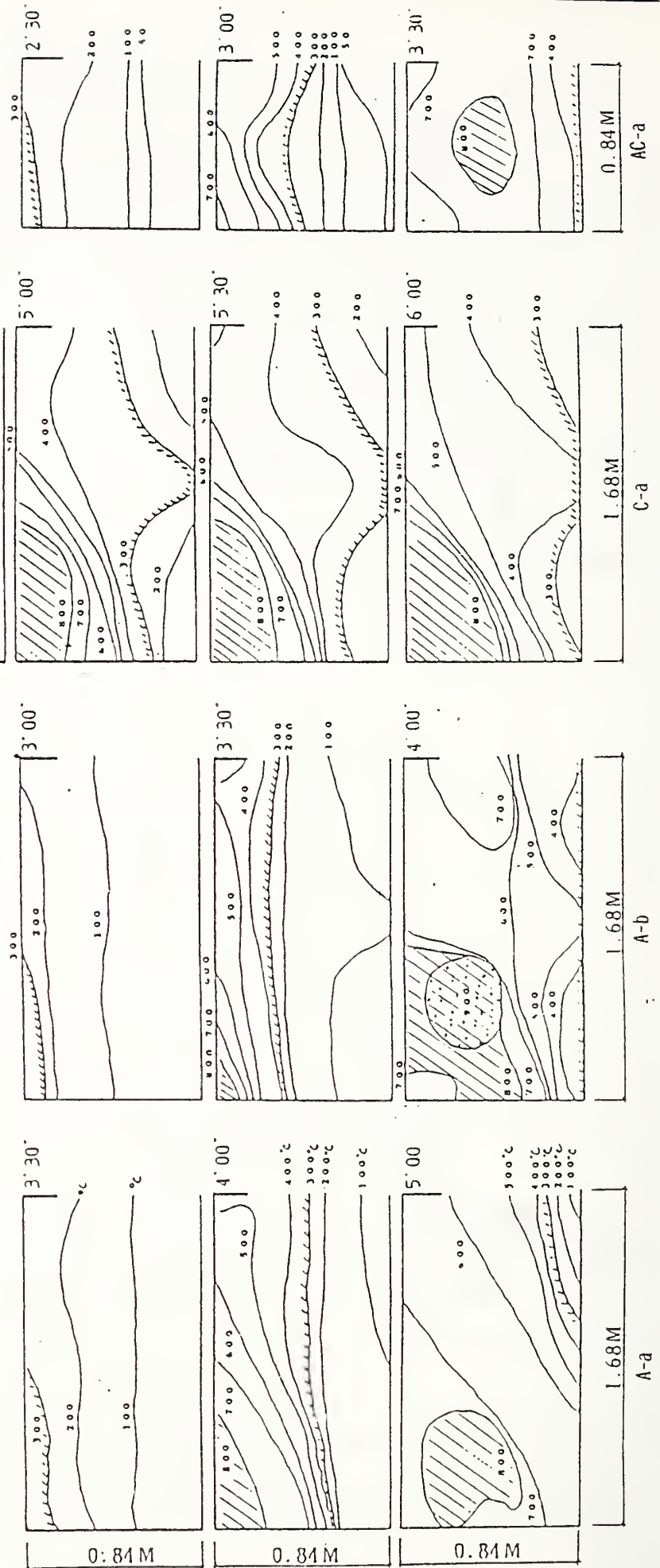
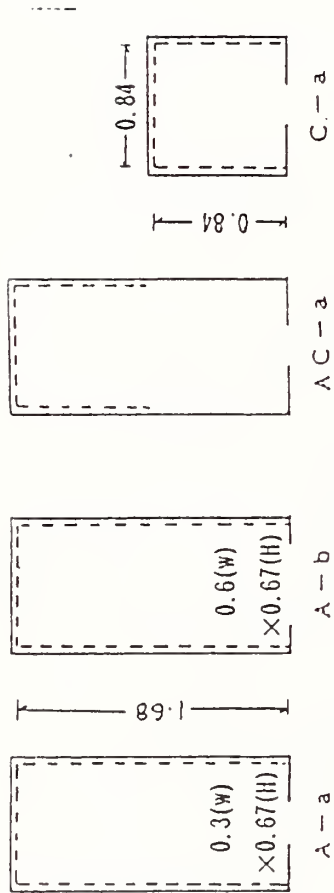


Fig 1-2 Temperature Distribution (Model Box)

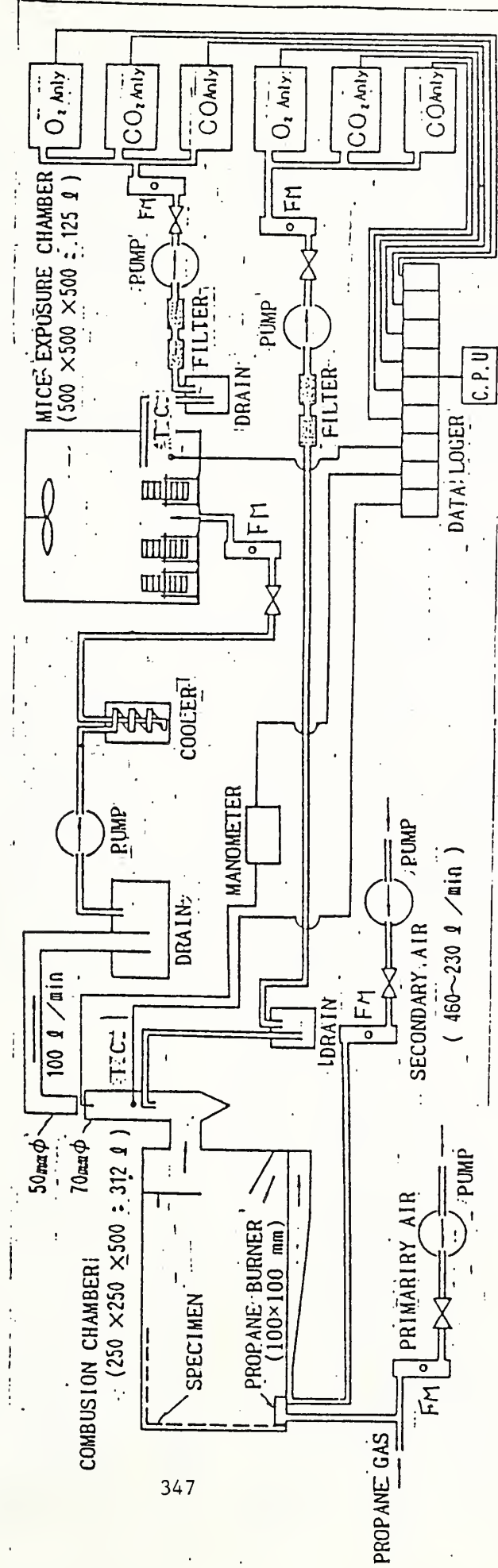


FIG. 2 AIR SUPPLY SYSTEM TEST APPARATUS

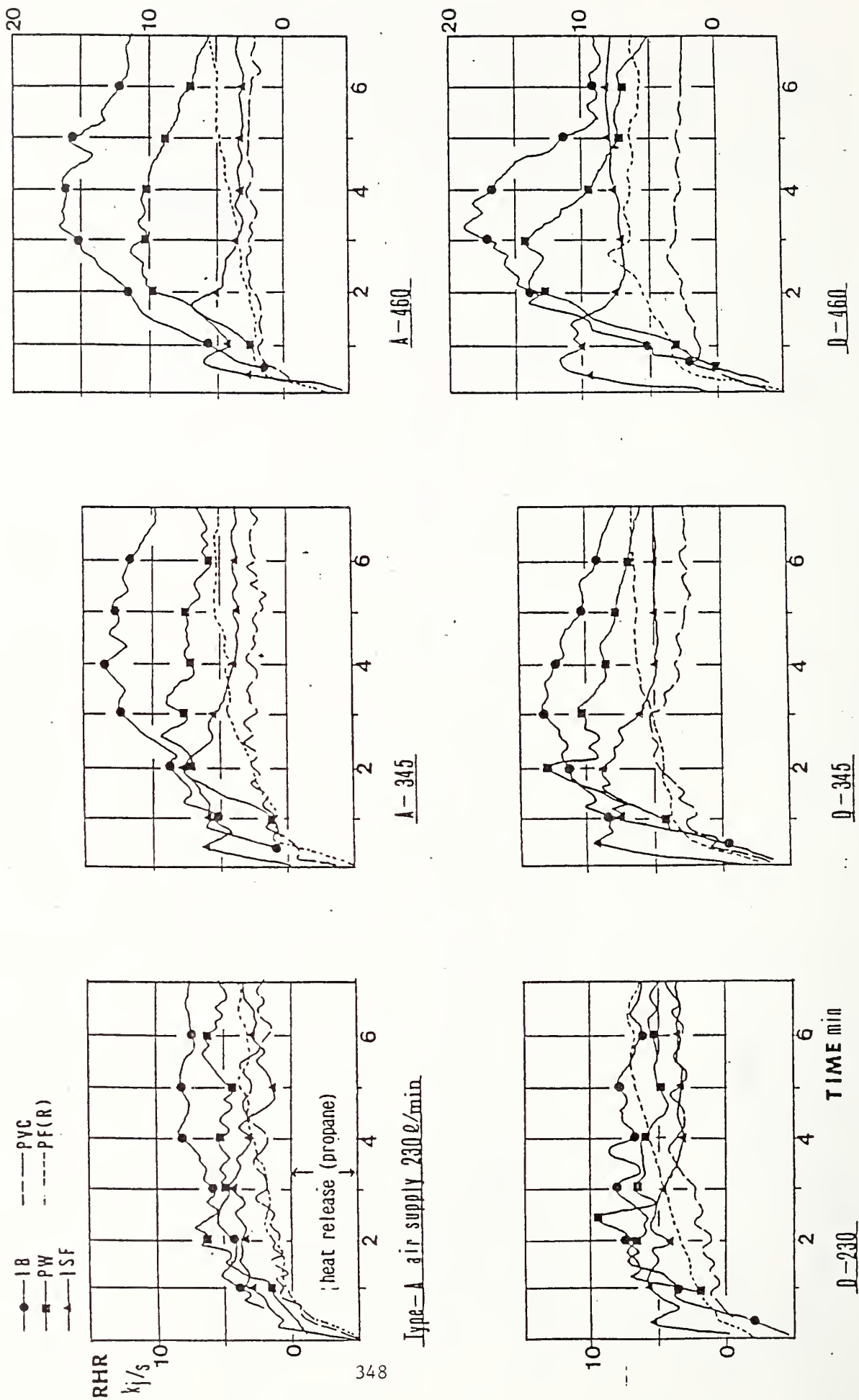
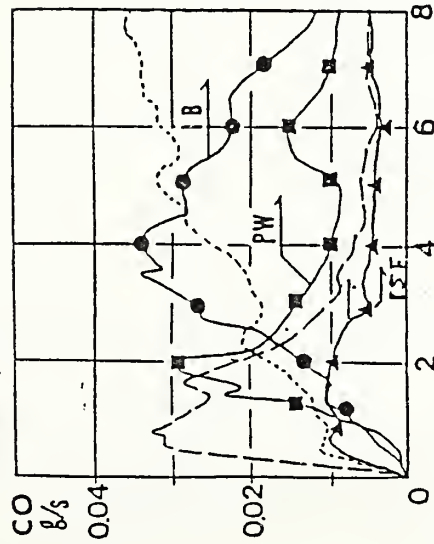


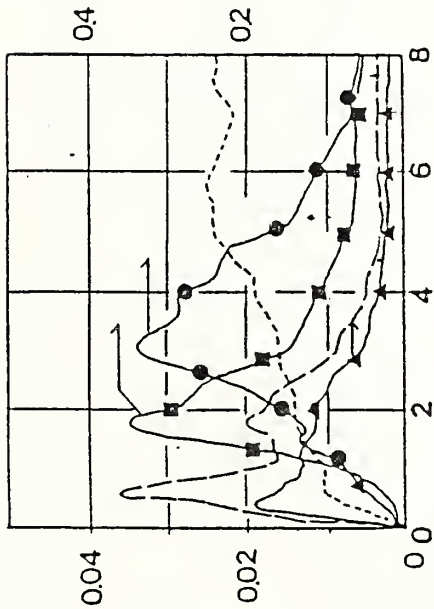
Fig 3 Rate of Heat Release with Air Supplied System

● B
 — PW
 — SF
 — PVC
 — PF(R)

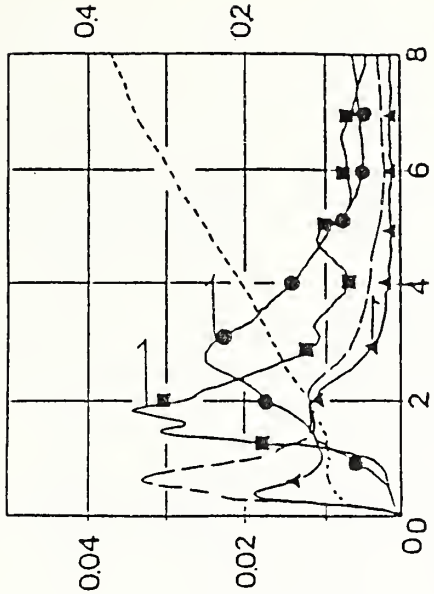


Type-A air supply 230 l/min

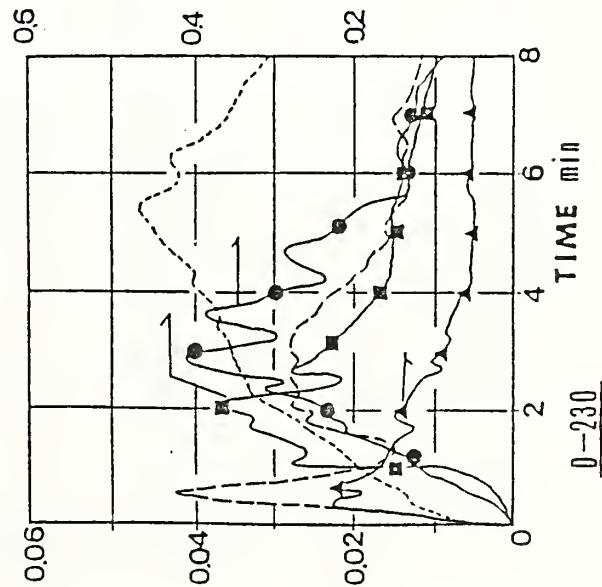
349



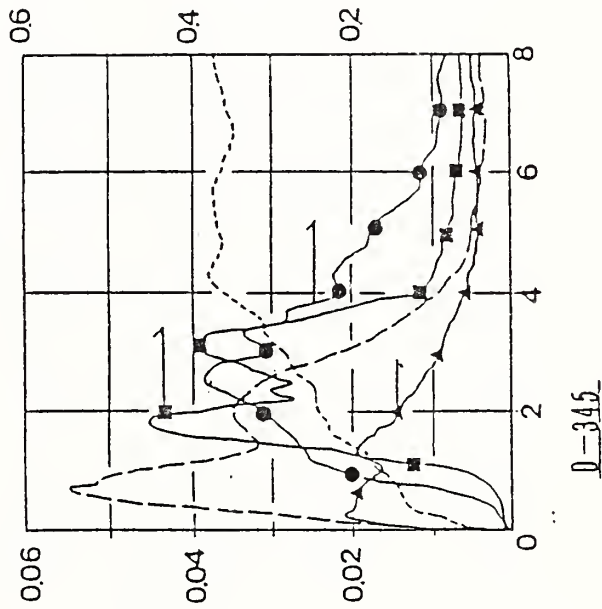
A-345



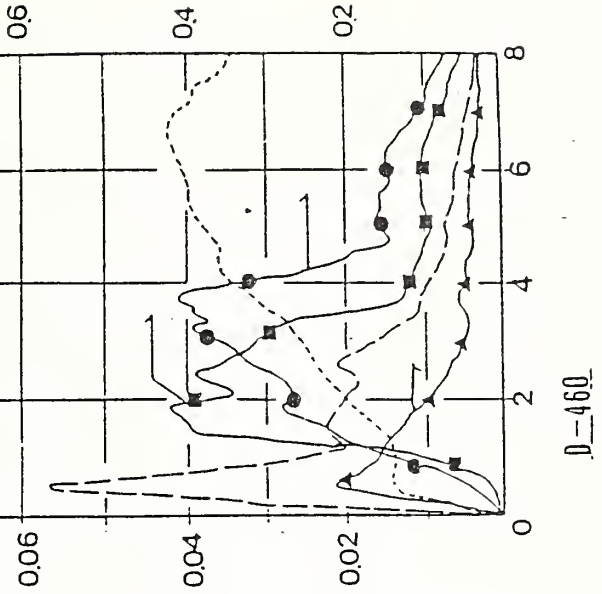
A-460



D-230



D-345



D-460

Fig 4 Rate of CO Gas Generation with Air Supplied System

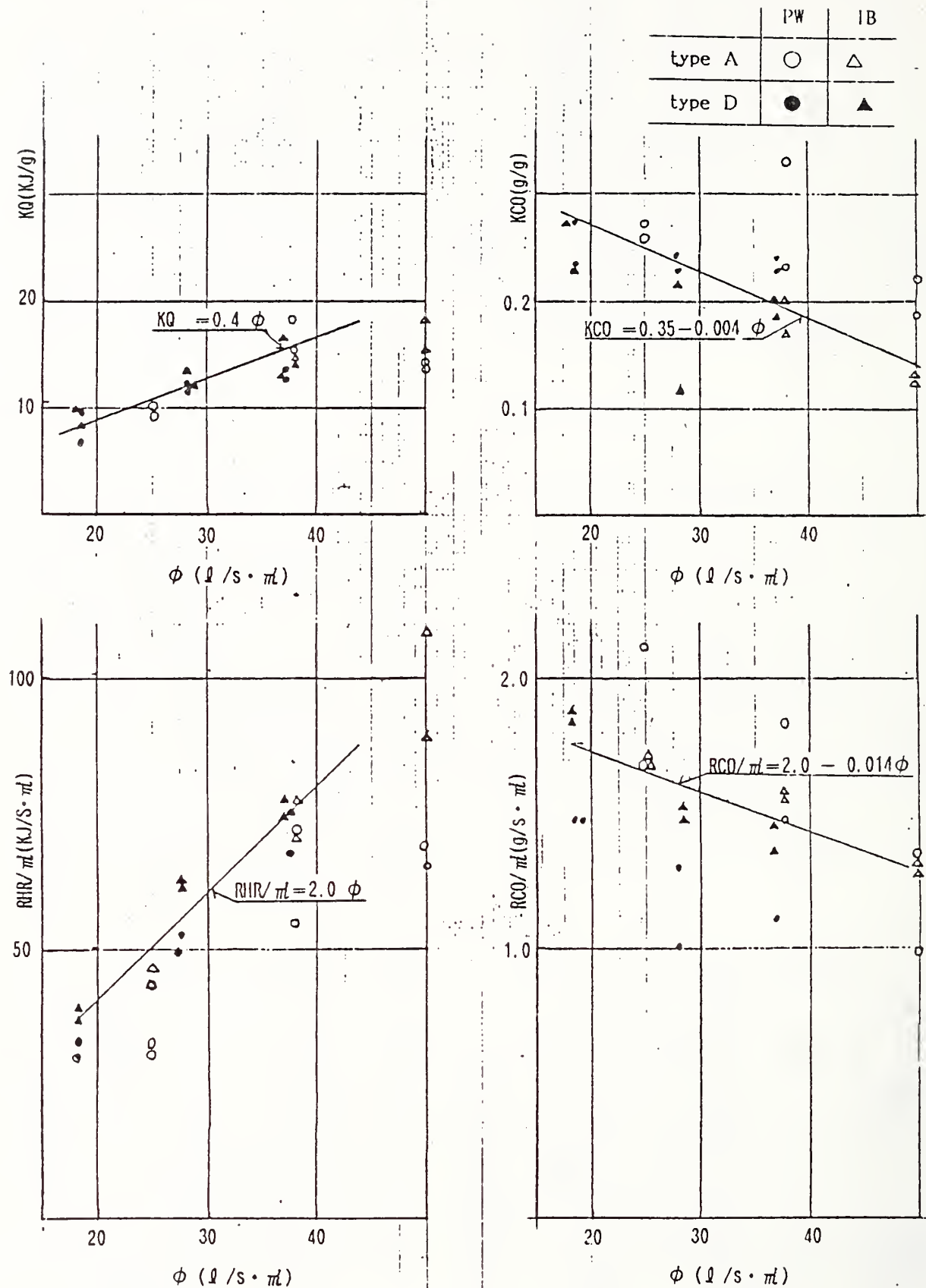


Fig 5 Relation Between the RIIR, RCO, KQ, KCO vs ASR (ϕ)

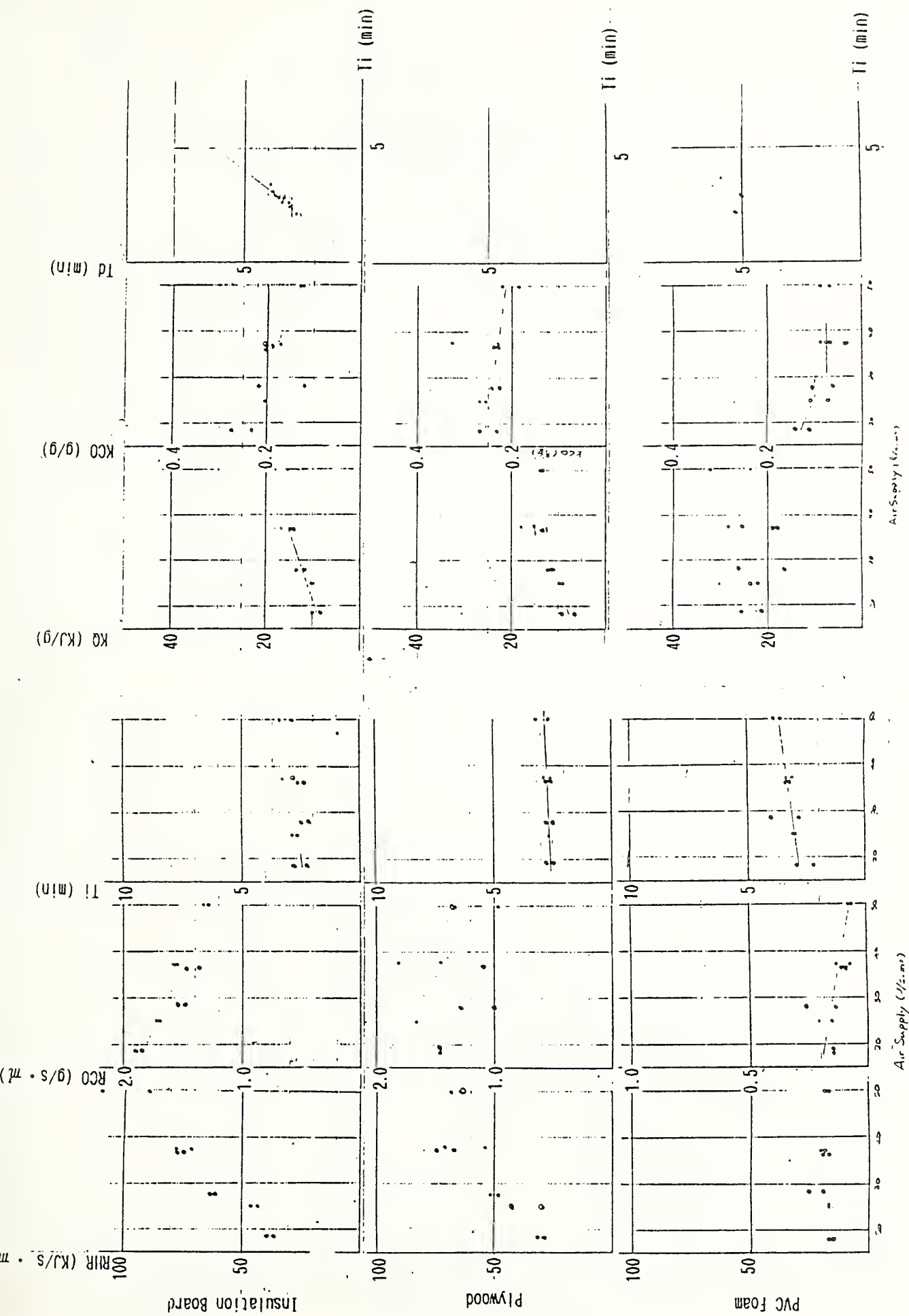


Fig 5-2 Rearranging the Test Result of Various Materials with Air Supplied System(1) Ti : Time to Death

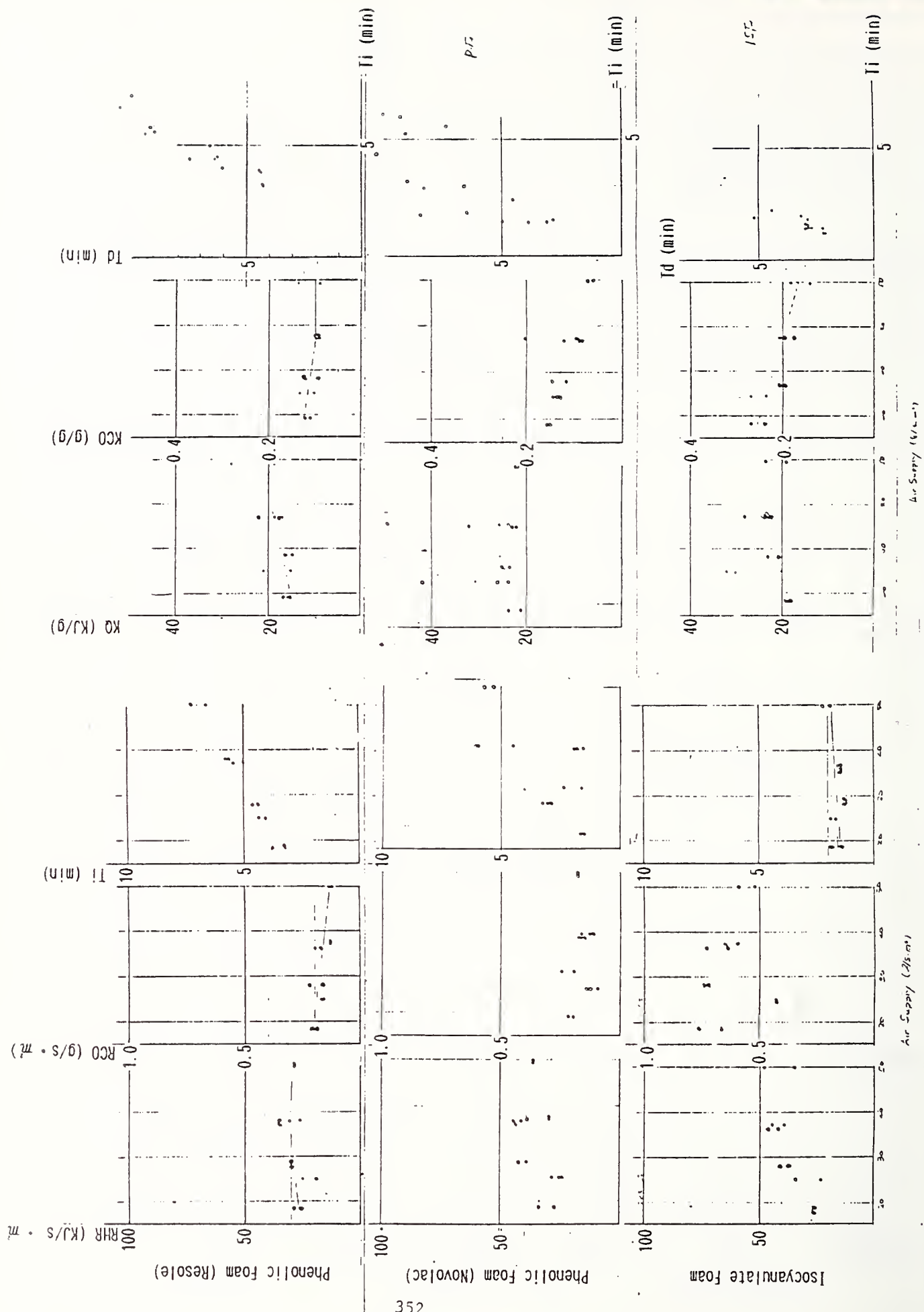


Fig.5.3 Rearranging the Test Result of Various Materials with Air Supplied System Td : Time to Death

$$\text{Calculated Value (m}^3/\text{s)} = \left[\frac{2}{3} \cdot \alpha \sqrt{2g \cdot \rho_0 (\rho_0 - \rho)} \cdot A \sqrt{H} \right] \times \rho_2$$

$$\text{Calculated Value (m}^3/\text{s)} = [\text{RHR}/(2700\text{K}/\text{kg})] \times \rho_2$$

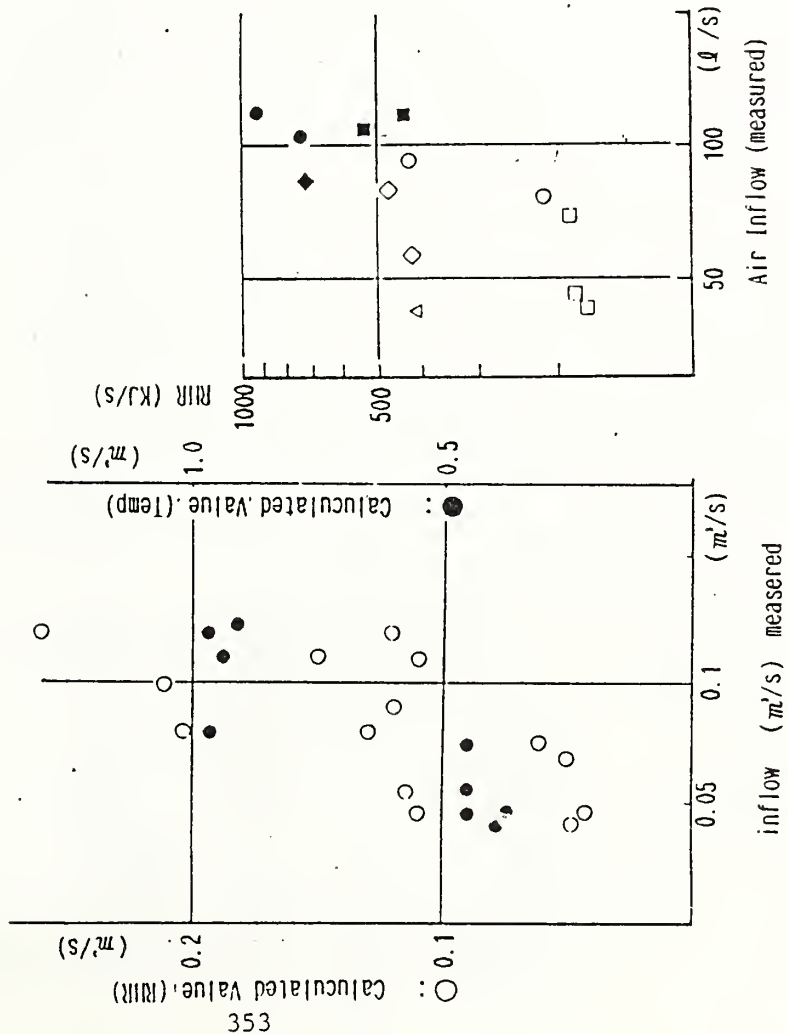


Fig 6 Air Inflow from Opening to Model Box (IB)

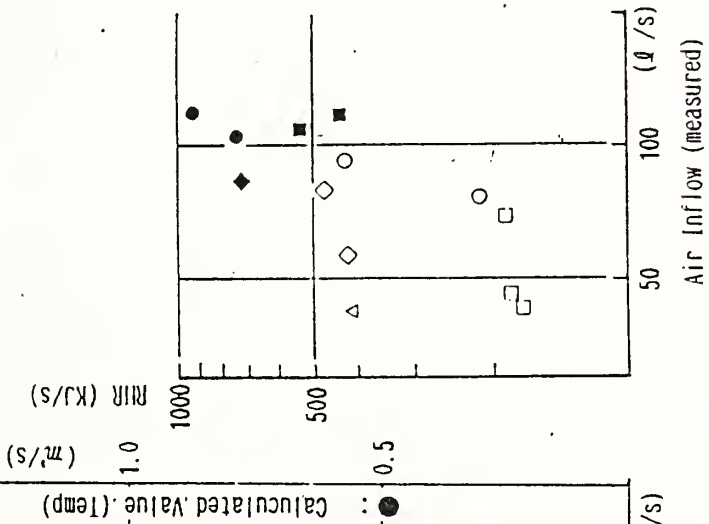


Fig 7 RHR vs Air Inflow (IB)

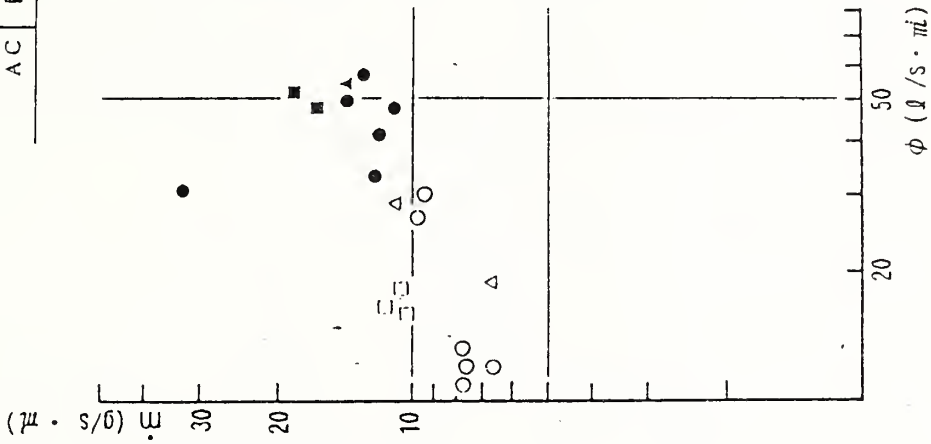


Fig 8 Mass Loss Rate vs A.S.R. (IB)

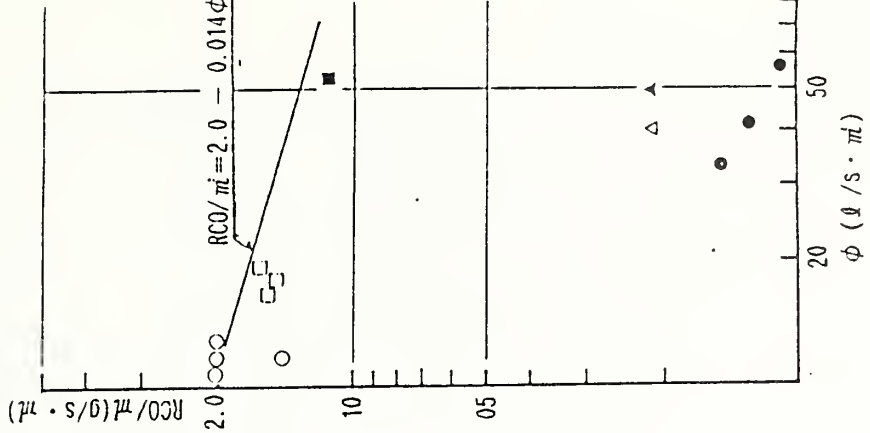


Fig 9 Rate of CO gas Generation vs A.S.R. (IB)

opening		a		b	
model	A	○	●	○	●
	B	◇	◆	◇	◆
	C	△	▲	△	▲
	AC	□	■	□	■

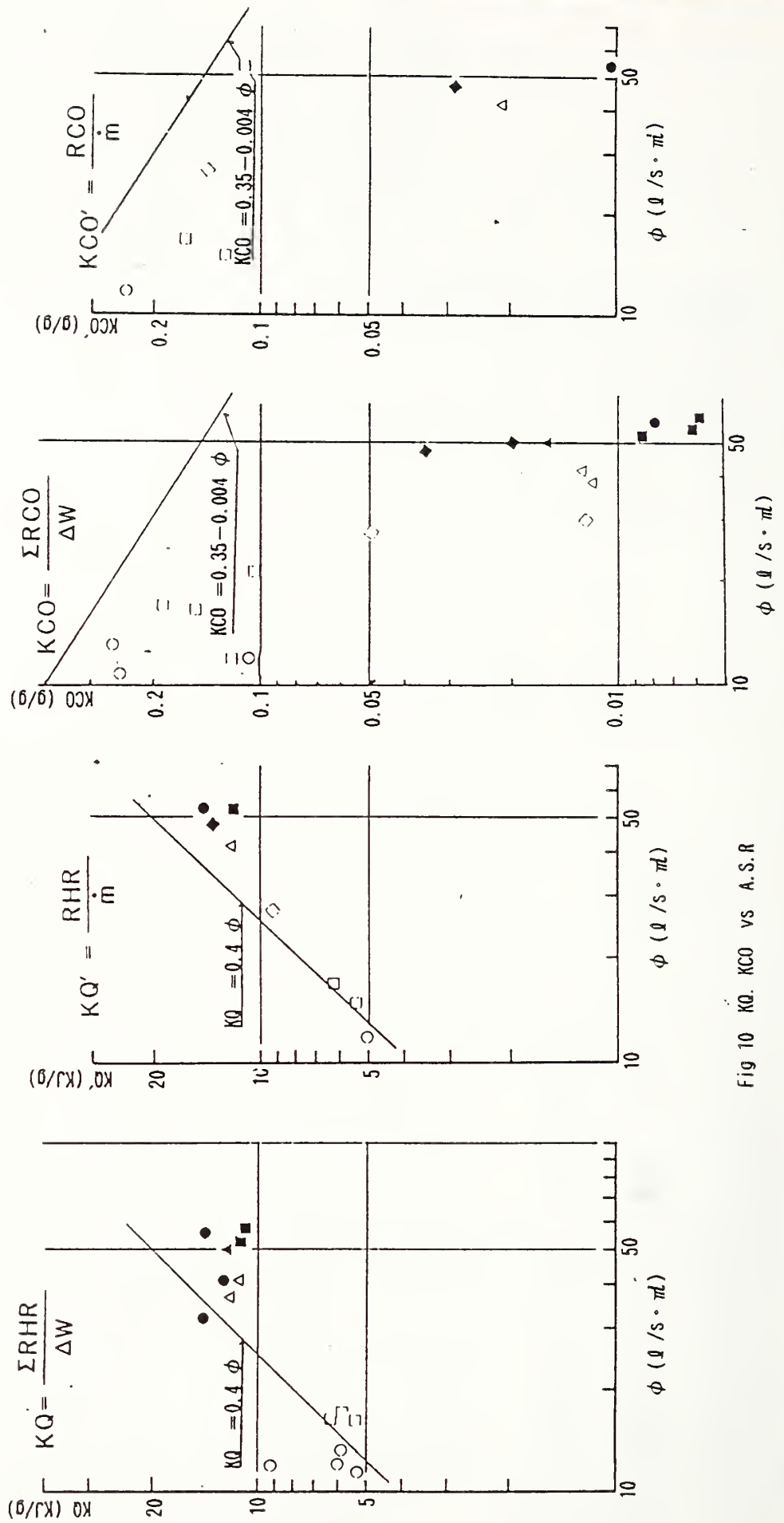
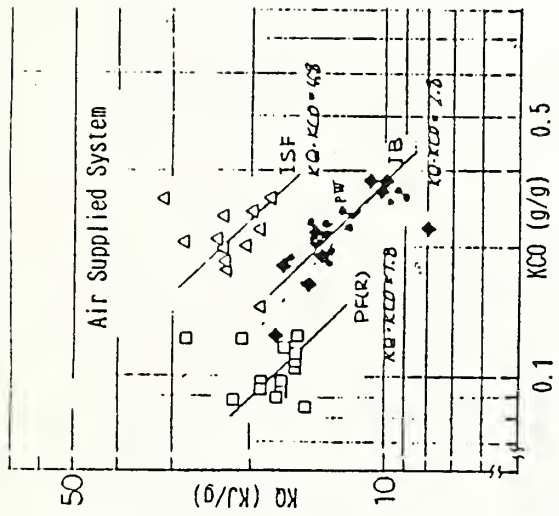


Fig 10 KQ, KCO vs A.S.R



opening	a	b
model A	O	●
B	◇	◆
C	△	▲
AC	□	■

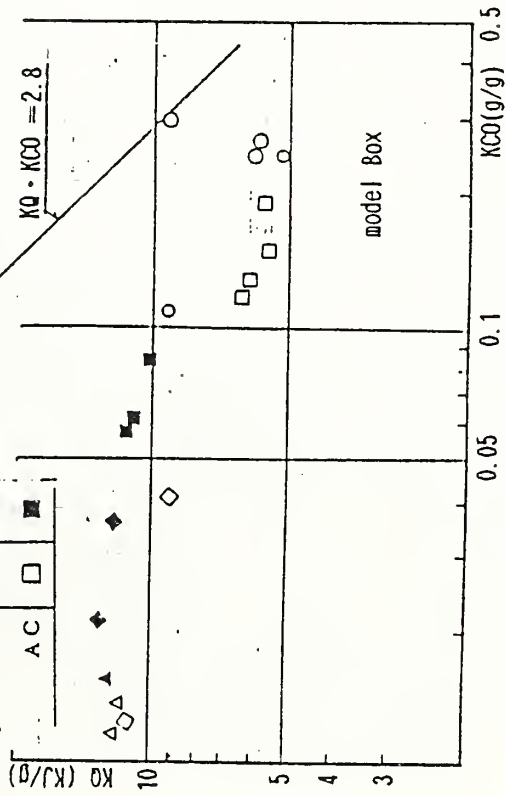


Fig 11 KQ vs KCO (IB)

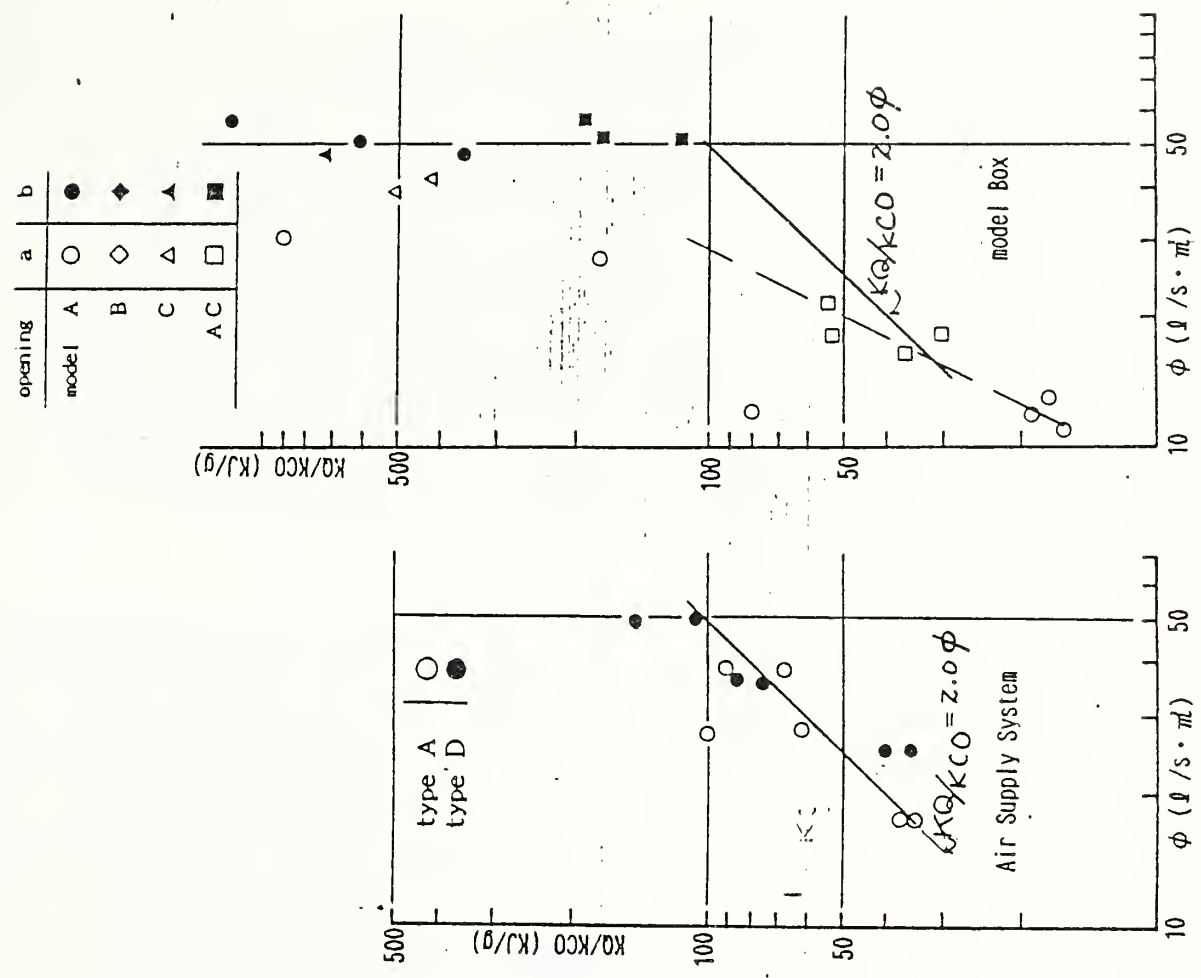
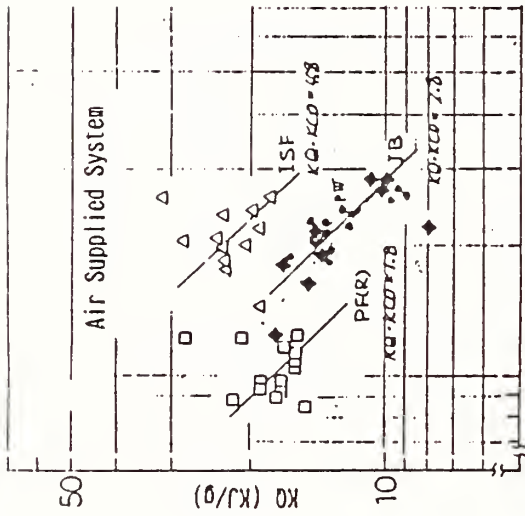


Fig 12 KQ/KCO vs Air Supply Ratio (IB)



opening		a	b
model	A	○	●
	B	◇	◆
	C	△	▲
	AC	□	■

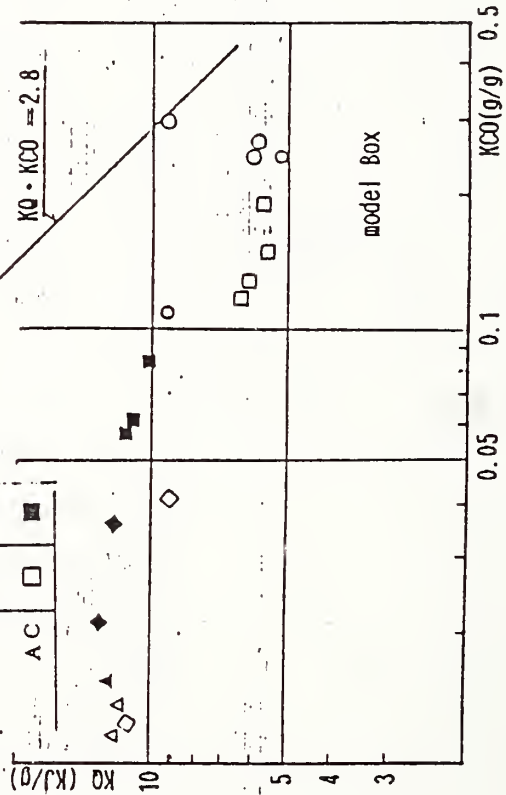


Fig 11 KQ vs KCO (TB)

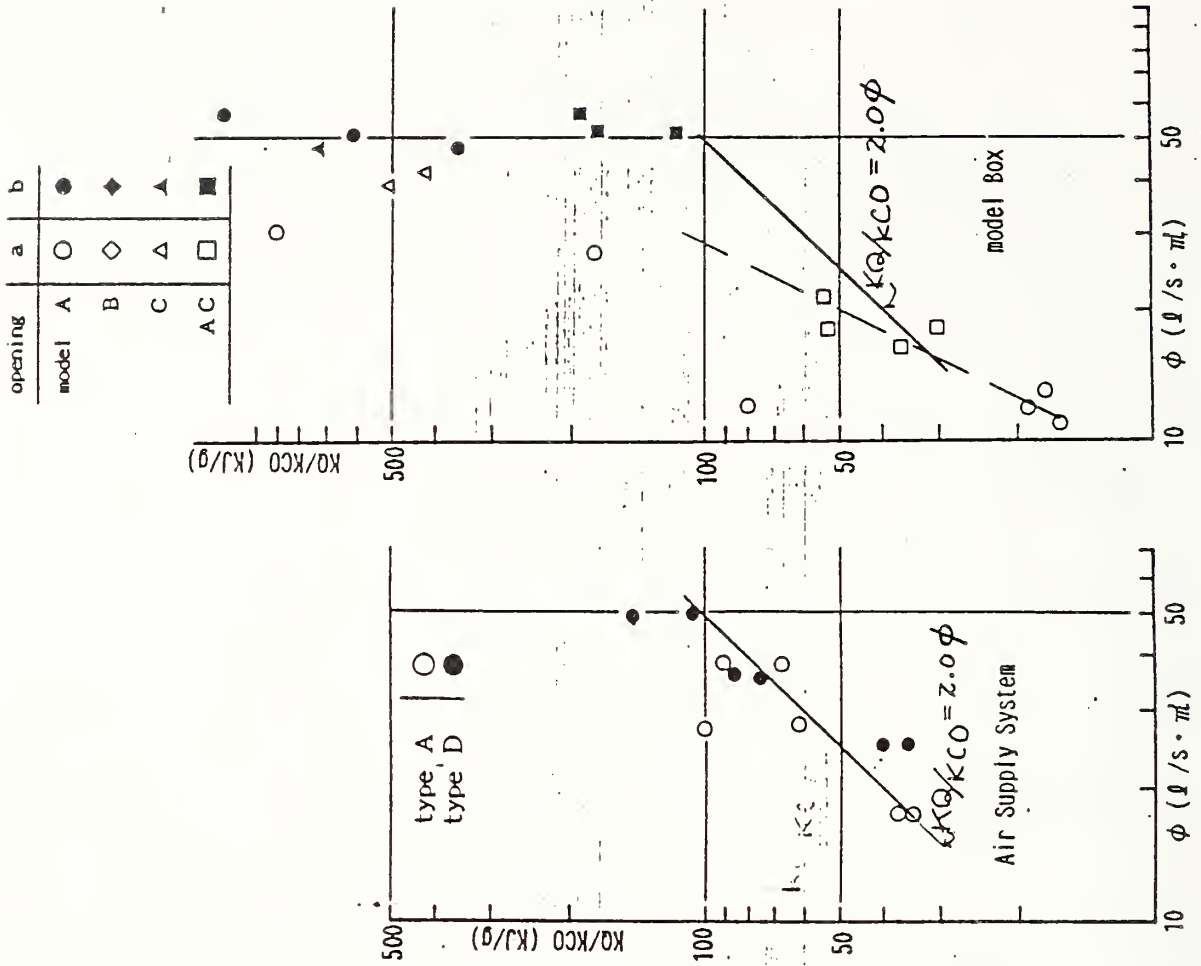


Fig 12 KQ/KCO vs Air Supply Ratio (TB)

FIRE INDUCED FLOW IN A CLEAN ROOM WITH
DOWNWARD VERTICAL LAMINAR FLOW

BY

Osami SUGAWA*. Yasushi OKA**, and Hirofumi HOTTA***

- *) Center for Fire Science and Technology, Science University of Tokyo, 2641 Yamasaki, Noda, Chiba 278
- ***) Department of Architecture, Faculty of Science and Technology, Science University of Tokyo
- ***) R&D Division, Nohmi Bosai Kogyo Co.,Ltd. 3-53-7 Honmachi, Shibuya-ku 151 Tokyo

ABSTRACT

A clean room was used for this experiment which had downward vertical flow of about 22-cm/sec. A line fire source was set near to the center. Heat flux of the fire source was about 6KW. Temperature, downward and upward velocities were measured. The equilibrium zones where dynamic pressure given by upward flow balanced against the one given by downward flow were pursued experimentally. Flow visualization was also conducted to measure the location of eddies. The fire induced flow was treated as a viscous incompressible, 2-dimensional flow. Navier-Stokes equations were applied to the flow with the Boussinesq approximation. Assumptions of adiabatic condition and non-slip flow condition at boundary were adopted. Implicit finite difference scheme method was employed for the numerical calculation. Distributions of temperature, velocity, and locations of the equilibrium zones were almost coincided with the calculated ones.

1. Introduction

The interaction and behavior between fire produced flow and ventilation flow in air conditioned or clean rooms are matters of some concern in the area of fire safety and fire detection. Generally, the buoyant flow from an early stage of a fire is very weak compared with the forced ventilation air flow. The early stages of a fire produced air flow would generally be diluted with and included within the forced ventilation flow. Consequently the detection of a fire is drastically delayed. To ensure adequate fire safety, it is important to detect a fire as early as possible. The buoyant flow from a very early stage of fire is very weak to get to the sensor mounted on the ceiling. The Japanese fire code requires all fire detectors to be placed on the ceiling of rooms. However if we consider the effects of the flow in clean room, it is likely that such detectors would be inadequate for the efficient detection of the early stages of a fire. As the first step of the study on an interaction between ventilation flow and fire induced flow, we began with the 2-dimensional counter flows of upward and

downward flow in a clean room. Laminar downward flow is given in the clean room, therefore, if we employ the line fire source, the flows in the clean room could be treated as a two dimensional flow.

2. Experimental

2-1. Room: Figure 1 shows the vertical cross section of the experimental clean room with a downward vertical flow. Clean air supplies into the room through HEPA (High Efficiency Particulate Air) filters set in the ceiling, and returns to the ducts located both sides of the room. Table 1 shows the specifications of the experimental clean room.

Table 1 Specification of the Clean Room

Size	: 6.4 m(W) x 9 m(L) x 3.2 m(H)
Ventilation	: Downward Vertical Laminar Flow...Supply system : 200 times/h
Down flow	: 0.30 m/sec (nominal value)
velocity	: 0.22 m/sec (observed value in this time)
HEPA filters	: 570 mm x 1170 mm x 42 sets, separator type

Chemical benches were set on both sides of the room. These were different sizes and shapes. There was no symmetrical interior arrangement in the room.

2-2. Fire Source:

The line fire source of 1 cm(W) x 85 cm (L) was employed to get a two-dimensional fire induced flow. Methanol was used as a fuel which was supplied from a fuel server at a constant rate of 0.37-0.4

ml/sec. An important consideration regarding the choice of the fire source is its characteristic form of two-dimensional upward flow and also its stationary heat release rate. The line fire source was positioned just off center, of the room approximately 297 cm apart from the right side wall. The height of the source was about 78 cm above the free access floor. Combustion of the fuel had been kept constant for about 1 hour before the run started.

2-3. Measurement: In order to measure the temperature in the clean room, thirty-three 0.32 mm diameter alumel-chromel thermocouples with 10 cm spacing between them were placed on a about 3 m movable wire. The set of the thermocouple line was moved horizontally and vertically to cover the all regions of

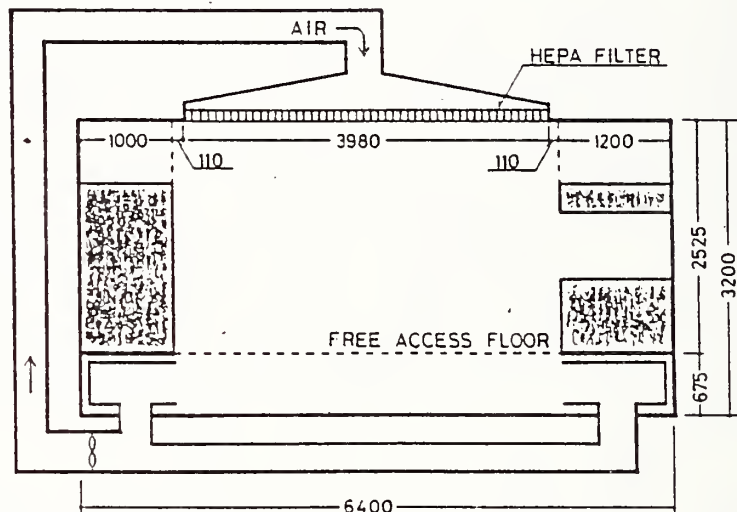


Figure 1 The cross section of the clean room for experiment. unit:mm

the air flow. Figure 2 shows the positions in the room where temperatures were measured. Another three thermocouples were set on the HEPA filter and on both sides of walls. A bidirectional tube was used to measure the dynamic pressure for downward and upward flow. The tube was moved systematically for vertically and/or horizontally, as shown in Figure 3, to find out the locations where the dynamic pressure measured zero indicating a balance between upward and downward flows. A smoke-wire system was utilized to visualize the positions where the velocity indicated almost zero, as well as indicate the size and positions of eddies and flow patterns.

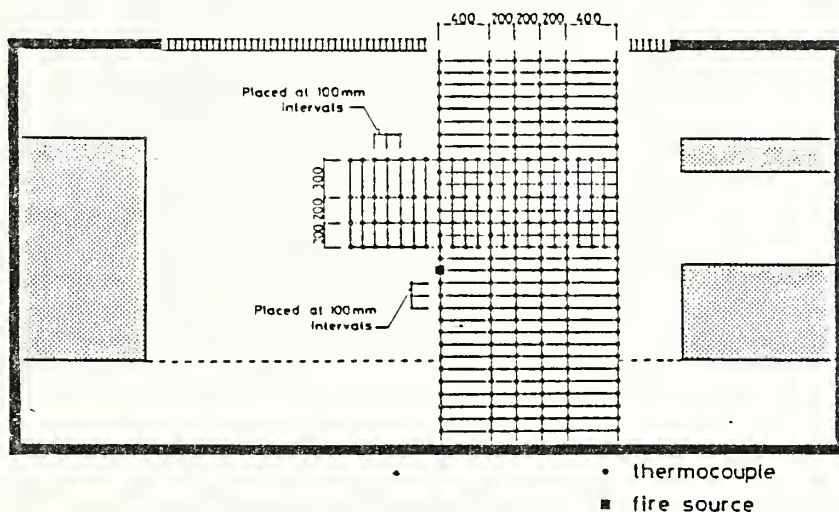


Figure 2
The positions where temperatures were measured by K type thermocouples.

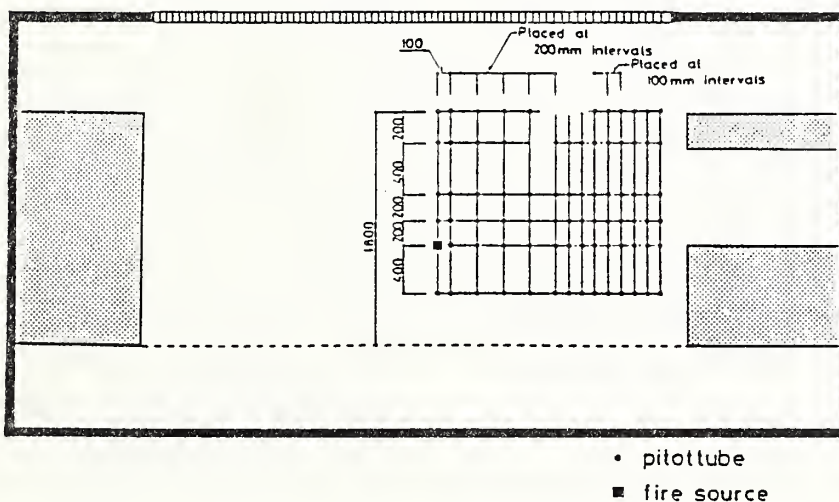


Figure 3
The positions where velocities were measured.

2-4. Simulation Model

A field model was employed to describe the flow characteristics in the clean room. The following assumptions were made:

- 1) The fire induced flow and downward flow were treated as viscous incompressible fluid.
- 2) The driving force for convection was governed by density differences as calculated from temperature differences.

- 3) Buoyant force as calculated from temperature difference was included into Navier-Stokes equation.
- 4) Adiabatic condition for wall and floor was employed.
- 5) Two-dimensional flow was induced in the clean room even the the fire source and fire induced flow were given.
- 6) Free access floor gave no effect to the air flow.
- 7) Effective thermal diffusibility and eddy viscosity were kept constant.
- 8) Fire source was given at constant heat release rate of 6KW.

The calculation was started under the initial conditions of a constant downward air flow formed in advance to the start of the model fire.

In this study two dimensional rectangular coordinates (x,y) were employed with the cell size of 10 cm x 10 cm. Calculations were based on a differential field model under the preceding assumptions. The purpose of the present study is not to develop a technique or method for numerical calculations, but is a computer experiment which is able to verify the full scale experiment carried out in a clean room. The basic concept to construct the numerical equations can be found in reference 1,2 although they deal with the fire induced flow in free boundary. Physical parameter values used in the calculation are demonstrated in Table 2.

Table 2

i)	Equation of Heat Flow	:	Incompressible viscous fluid
	Finite difference method:	:	Implicit
ii)	Boundary Condition		
	Temperature of Heat Source	:	450 °C
	Temperature Atmosphere	:	20 °C
	Down flow Velocity	:	0.2 m/sec
iii)	Physical Properties		
	Effective Thermometric Diffusibility	:	2.2×10^{-4} m /sec
	Effective Eddy Viscosity	:	4.515×10^{-2} m /sec
iv)	Finite Difference scheme		
	Time Interval	:	0.1 sec
	Mesh Interval X-direction	:	0.1 m
	Mesh Interval Y-direction	:	0.1 m
v)	Solving Simultaneous Method		
	Maximum Iterate Counts	:	250 times
	Criterion of Convergence	:	1.0×10^{-5}
	Solving Method	:	Successive Over Relaxation
	Type of Data	:	Double Precision

3. Results

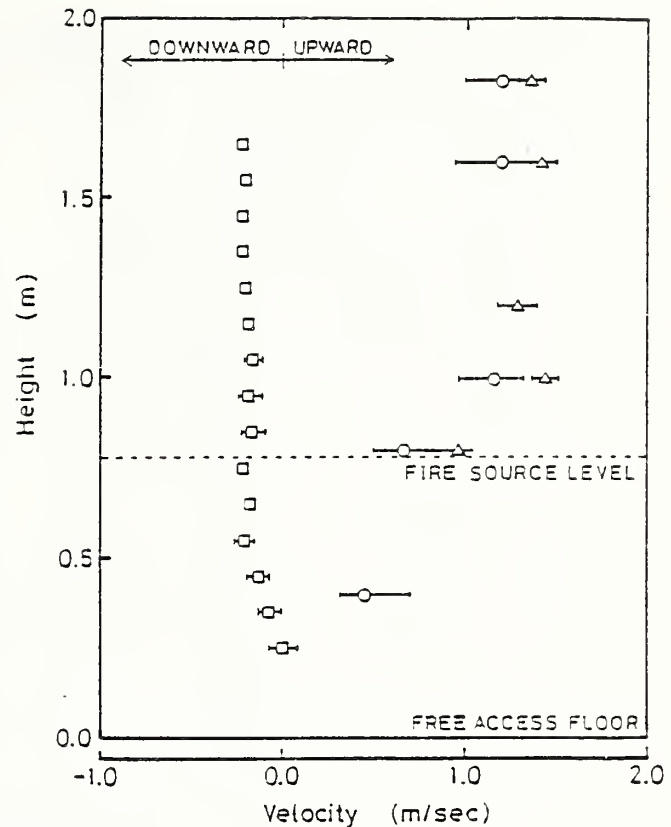
3-1. Experimental results

a) heat Flux

The heat flux was calculated based on the consumption rate of the fuel and its heat of combustion at 25 C to gaseous CO₂ and H₂O. The estimated heat flux was about 6KW. The free board of the aluminum vessel was about 2-3 mm and which was kept constant during the experiment.

b) velocity

Velocities of the down flow were measured firstly without the line fire source. They were plotted in Figure 4 with the mark of \square . Down flow velocities indicated 0.2 - 0.22 m/sec independent of height in region of 0.55 - 1.65 m above the free access floor. The vertical velocities of the down flow began to reduce as they approaches to the height of 0.4 m above the free access floor. Visualization of the down flow was determined with the smoke-wire and generated smoke. The direction of the down flow shifted clearly from a vertical to a horizontal direction in the region of 0.4m - 0.5m above the free access floor. This phenomena was caused by the pulling of the down flow by the return air intake for through the ducts which were set on the concrete floor. These ducts were located along both walls and were 0.6 m below the free access floor. The center line upward flow without down flow indicated about 1.3 - 1.4 m/sec independent of height in the measuring region except just above the fire source. The velocities without down flow are demonstrated in Figure 4 with the mark of Δ . Figure 4 also shows center line upward velocities with down flow by the mark of \circ . The behavior of the upward velocities with and without down flow were very similar with each other. However, the difference in the velocities between both upward flows was about 0.2m/sec. and which was attributed to the pushing caused by the down flow.



- \square without fire source and with down flow
- Δ with fire source and without down flow
- \circ with fire source and with down flow

Figure 4 Variation of upward velocity along the center line.

c) temperature

Typical results on temperature distribution in the vertical direction are shown in Figure 5. The center-line temperature distribution is not included in this figure. As hot air went up toward the ceiling, it spread out beneath the ceiling as it was pushed down by down flow. The location, therefore, where the maximum excess temperature appeared dropped slightly with increasing of the horizontal distance from the center line. In the case of without down flow, the maximum excess temperatures in the vertical distribution at various points were observed just under the ceiling.

d) dynamic pressure equilibrium

A bidirectional tube was moved systematically in a vertical and/or horizontal direction. Dynamic pressure as well as temperature at the tube point were examined. Probe and thermocouple were maintained at each position, 10 cm spacing between each, for 2 - 3 min. Differences in pressure were recorded on an analog pen recorder and showed slight deviations from the mean value. In the marginal zone where both upward and down flow were present, the equilibrium zone in the dynamic pressure were provided where dynamic pressure given by upward flow balanced against the one given by downward flows. The equilibrium zone are shown in Figure 6.

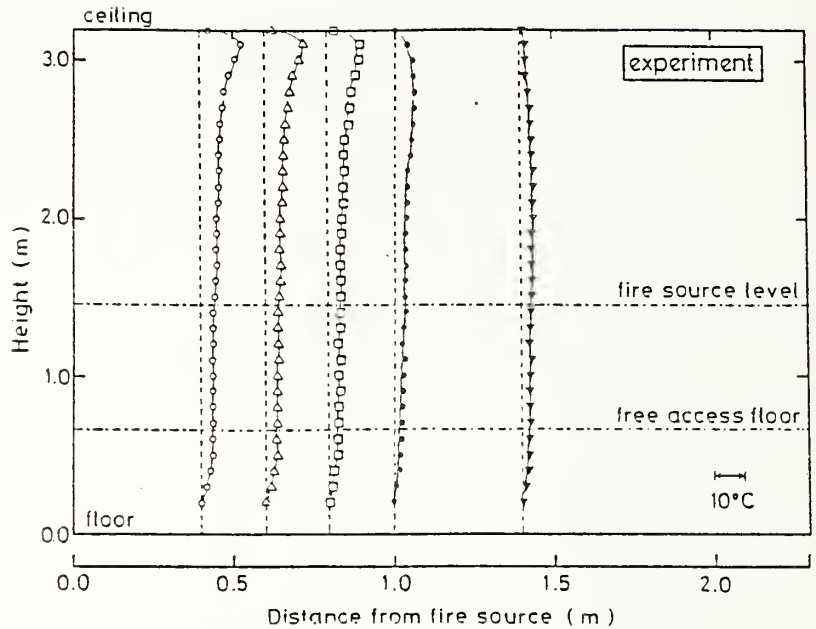


Figure 5 Vertical distribution of temperature in the clean room with down flow.

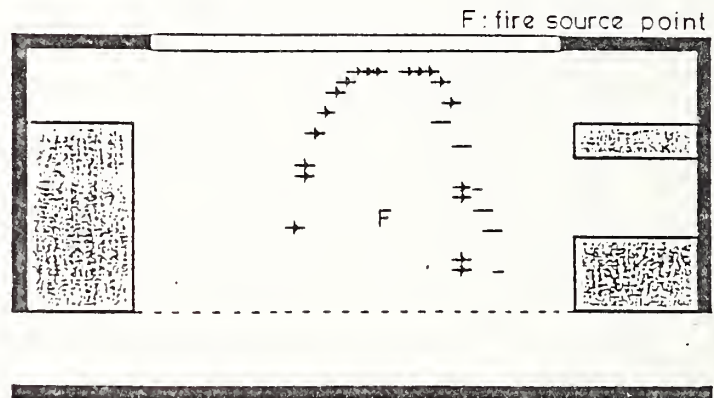


Figure 6 Equilibrium zones where dynamic pressure balanced against the one given by downward flow. - : experiment, o : calculated

3-2. Computed Results

Calculation were performed for the same configurations as the clean room where the experiments carried out. Down flow from the ceiling was taken into account in the calculation. The heat source position was chosen at just off-center center corresponding to the experimental position of the fire source.

a) heat source

Temperature of the heat source for the calculation was chosen from results of experimental measurement. Calculated heat flux increased with time from $t=0$ to 10 sec, and reached the stationary state after 10 sec showing about 6KW.

b) velocity

Figure 7 shows the calculated and experimental center line upward velocities. Calculated upward velocities was about 0.85 m/sec in the computational section just above the fire source.

The closest measuring position corresponding to the calculated velocities was about 2 cm above the fire source, and indicated 0.5 - 0.8 m/sec. Calculated velocities increase with an increase in height within the region 0 - 0.3 m above the fire source. In the region of 0.3 - 0.9 m above the fire source, they appeared to be maintained almost constant of about 1.1 - 1.2 m/sec. In the upper region, however, over 1 m above the fire source calculated velocities decreased with height.

In the lower regions beneath the fire source, upward velocity decreased towards the free access floor. At 0.4 m below the fire source, calculated velocities were about 0.3 m/sec and measured ones were 0.3 - 0.7 m/sec. The results of calculated velocities seem correspond well with the measured one.

c) temperature

Figure 8 shows the vertical temperature distributions of calculated temperatures. These temperatures are slightly higher than the measured ones. Highest excess temperature measured at a distance of 0.4m from the center line was observed at around 10cm under the ceiling. Compare with this, calculated ones, highest temperatures occurred 30 - 40 cm under the ceiling at 0.4, 0.6, and 0.8m from the center. The hot layer under the ceiling obtained from calculation is deeper than the measured ones. The vertical profiles of both sets of temperatures, however, are very similar with each other. We adopted adiabatic condition, therefore, no heat loss was taken into account in the calculation. The discrepancy in temperature between calculation and measurement elucidates that the heat loss must be taken into account to get well concordant results with the experiment.

d) dynamic pressure

The equilibrium zone in dynamic pressure given by the balance between upward and downward flows were estimated depending on the calculated velocities and densities. The flow density was given as a function of temperature. We employed the equilibrium zone where the ratio between the upward and downward dynamic pressure indicate 0.9 - 1.1. Estimated equilibrium zone are plotted in Figure 6. There coincide with locations of measured ones.

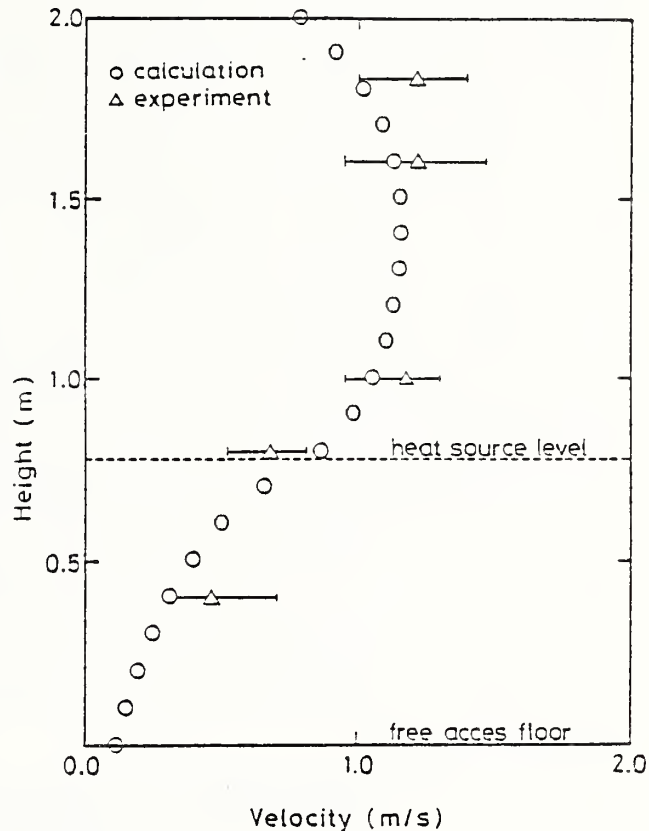


Figure 7 Variation of the center line velocities of experimental data and calculated ones.

4. Discussion

Figure 9 shows average temperatures and velocities along the center line from the fire source with and without down flow.

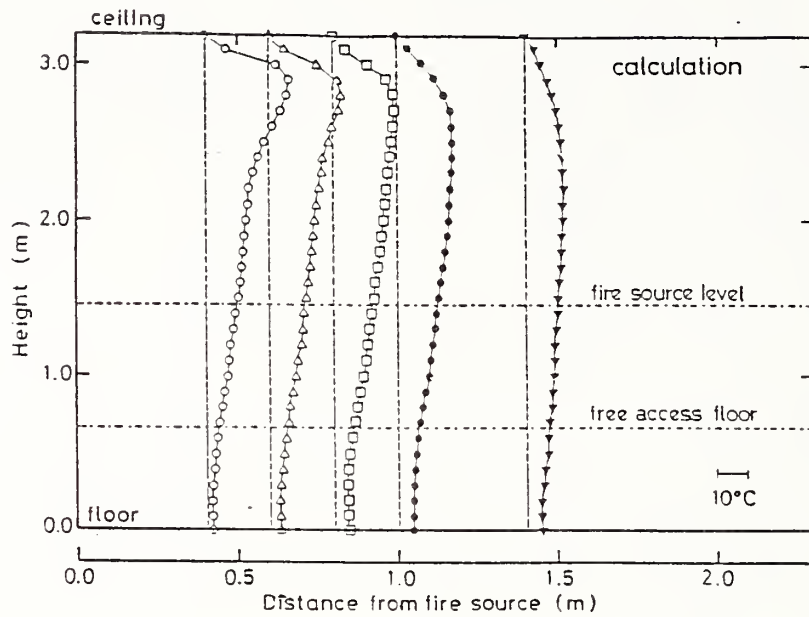


Figure 8 Vertical distribution of calculated temperatures in the clean room.

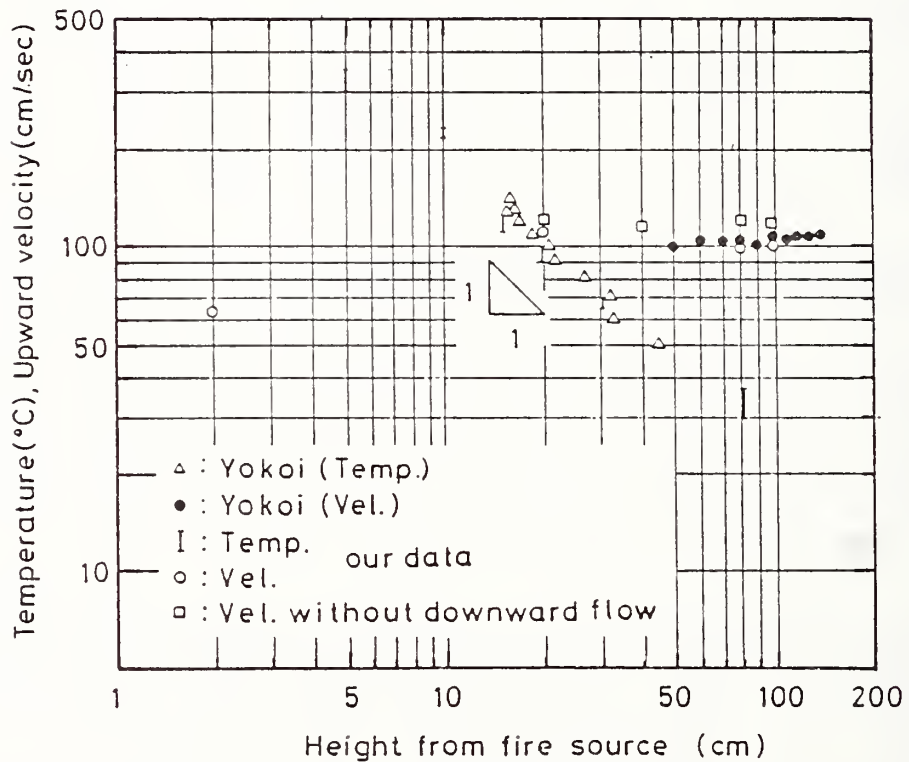


Figure 9 Variations of temperatures and velocities along the center line of the upward flow with and without down flow. Yokoi's data are also plotted.

The result clearly describes that excess temperature decreased with increase of height in the measuring region of 0.05m to 0.8m above the fire source. Average velocity was approximately constant along the center line in the region of 0.2m - 1.0m. However, within the near field to the fire source, it seems to increase with height. We also plotted Yokoi's results, reference 3 - 5, in Figure 10 who carried out the experiments without any ventilated flows. Yokoi utilized a line fire source of about 1 m length and 1 cm width using MeOH as a fuel. The size and shape of the fire source he used is almost same as ours. The behavior of temperature and velocity along the center line are compared with Yokoi's data. It was found that our data were in fair agreement with Yokoi's. Therefore, the upward flow we made can be taken as a line fire source. Despite the effect of the downward flow, our data clearly demonstrated that the temperature and velocity distribution of the upward flow from the fire source was conserved along the center line. The downward flow only began to effect the upward flow with increasing distance from the fire source. In the far region from the center line, the horizontal distribution of upward velocity and temperature spread out widely, and their width are wider than those obtained by Yokoi. Convection in the clean room was clearly visualized by the smoke-wire method. Figure 10 shows the calculated stream lines calculated. Even in the ventilated enclosure with down flow, convection seems a governing flow. Entrainment to the upward flow, therefore, is thought to be a driving force of the upward flow in the far region from the center line of the plume.

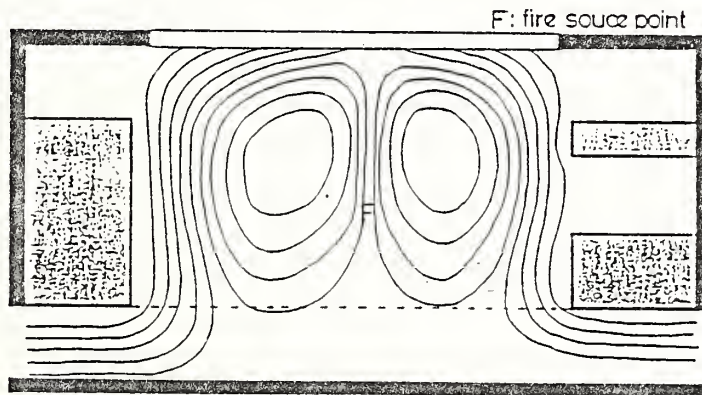


Figure 10 Calculated stream lines. "F" is a position of fire source.

An experimental study on the flow behavior with ventilated flow in a clean room has just started. We have still discrepancies between measured values of temperature and velocity and calculated ones. It is necessary to obtain physical parameters, such as diffusion coefficient and thermal diffusibility in the counter flows, to enable the calculated values to be closer approximations to the measured conditions.

5. References

- 1) Hasemi Y. "Numerical Calculation of the Natural Convection in Fire Compartment". BRI Research Paper No. 69, Feb. 1977

- 2) Morita M., Nishimoto T., Handa T., and Hayashi K.,
"Feasibility of Numerical Computational Methods of Heat Flow
in Fire Compartment." Proceedings 8th UNJR Meeting, Tsukuba,
1985
- 3) Yokoi S., "Upward Current from an Infinite Line Fire Source"
(in Japanese), Bull. of the Fire Prevention Society of Japan
Vol. 10, No. 1 (1961)
- 4) Yokoi S., "Kasai" Vol. 3, No. 1 (1953)
- 5) Yokoi S., "Study of the Prevention of Fire-Spread Caused by
Hot Upward Flow", BRI Research Paper No. 34, Jun. 1960

FIRE TOXICITY AND CHEMISTRY (CONT.)

TOXICOLOGICAL EFFECTS OF DIFFERENT TIME EXPOSURES
TO THE FIRE GASES: CARBON MONOXIDE OR HYDROGEN CYANIDE
OR TO CARBON MONOXIDE COMBINED WITH HYDROGEN CYANIDE OR CARBON DIOXIDE

Barbara C. Levin, Joshua L. Gurman¹, Maya Paabo, Laura Baier², and Trudi Holt²
National Bureau of Standards, Gaithersburg, MD 20899

ABSTRACT

The toxicity of single and multiple fire gases is being studied to determine whether the toxic effects of a material's combustion products can be explained by the toxicological interactions (as indicated by lethality) of the primary fire gases or if minor, more obscure gases need to be considered. LC₅₀ values for Fischer 344 rats have been calculated for carbon monoxide (CO) and hydrogen cyanide (HCN) (as individual gases in air) for 1, 2, 5, 10, 20, 30, and 60 minute exposures plus relevant post-exposure periods using the NBS Toxicity Test Method apparatus. The concentration-time products for the various HCN exposures plus 24 hour post-exposure times are constant, but the concentration-time products for CO decreased for the 1, 2, and 5 minute exposures and then increased for the longer times. In exposures ranging from 5 to 60 minutes, the toxic effects of CO plus HCN were additive and, except for the 5 minute exposures, the presence of 5% carbon dioxide (CO₂) decreased the LC₅₀ values of CO. These results will be used in the computer model currently under development in the Center for Fire Research to predict the hazard that people will experience under various fire scenarios.

1. INTRODUCTION

Experimental research is being conducted at the National Bureau of Standards to characterize the toxicological effects of the individual and combined primary gases produced in fires. The three main purposes of these studies are: (1) to accumulate baseline data to determine the extent to which the lethality of a material's combustion products can be explained by the major gases produced in fires; (2) to develop a bioanalytical test procedure, which minimizes the use of animals, to predict the approximate LC₅₀ values of polymeric materials and to screen for extremely potent or unusually toxic thermal degradation products; and (3) to provide input data for computer fire hazard models designed to predict the human tenability of fire gas atmospheres.

In prior research [1,2]³ in the Center for Fire Research at the National Bureau of Standards, LC₅₀ values for Fischer 344 rats were calculated for the individual gases, carbon monoxide (CO), hydrogen cyanide (HCN), or decreased oxygen (O₂), for 30 minute exposures plus relevant post-exposure periods using the NBS Toxicity Test Method apparatus. Thirty minute combination experiments

¹American Iron and Steel Institute, Washington, DC

²University of Pittsburgh School of Public Health, Pittsburgh, PA

³Numbers in brackets refer to the literature references listed at end.

with CO and HCN indicated that they act in an additive manner. Synergistic effects were found when the animals were exposed to certain combinations of CO and carbon dioxide (CO₂). A comparison of the concentrations of the major combustion products generated from a number of polymeric materials at their LC₅₀ (30 minute exposure plus 14 day post-exposure) values with the combined pure gas results indicated that, in most cases, the observed toxicity could be explained by the toxicological interactions of the examined primary fire gases - CO, CO₂, and HCN. These results have provided necessary information for the computer model currently being developed in the Center for Fire Research to predict the hazard that people may experience under various fire scenarios.

The research to be described here was sponsored by the Society of the Plastics Industry, Inc., the International Isocyanate Institute, the U.S. Army Medical Research Institute of Chemical Defense, and the National Bureau of Standards. These experiments were designed to extend the 30 minute results to other exposure times. LC₅₀ values were determined for CO and HCN (as individual gases in air) for 1, 2, 5, 10, 20, and 60 minute exposures plus relevant post-exposure periods using the NBS Toxicity Test Method apparatus. The additivity of the toxic effects of CO and HCN observed during 30 minute exposures and the effect of 5% CO₂ on the LC₅₀ values of CO were examined for the other time periods.

2. METHODS

2.1 Materials: The gases (CO, CO₂, HCN, and N₂) utilized in this study were commercially supplied in various concentrations in air or nitrogen. Since certain distributors add SO₂ to their HCN tanks as stabilizers, one of the HCN gas cylinders was analyzed by both infrared analysis and BaSO₄ titration. The results of these tests, which were confirmed by our distributor, indicated that less than 1 ppm SO₂ was present in our HCN cylinders.

2.2 Animals: Fischer 344 male rats, weighing 200-300 grams, were obtained from the Harlan Sprague-Dawley Company⁴ (Walkersville, MD), Hilltop Lab Animals (Scottsdale, PA) or from Taconic Farms (Germantown, NY). They were allowed to acclimate to our laboratory conditions for at least 10 days prior to experimentation. Animal care and maintenance were performed in accordance with the procedures outlined in the National Institutes of Health's "Guide for the Care and Use of Laboratory Animals." Each rat was housed individually in suspended stainless steel cages and provided with food (Ralston Purina Rat Chow 5012) and water ad libitum. Twelve hours of fluorescent lighting per day were provided using an automatic timer.

2.3 Animal Exposure System: The acute inhalation toxicity of the primary fire gases alone and in combination was assessed using the chemical analysis system

⁴Certain commercial equipment, instruments, materials or companies are identified in this paper in order to specify the experimental procedure adequately. In no case does such identification imply recommendation or endorsement by the National Bureau of Standards, nor does it imply that the equipment or material identified is necessarily the best available for the purpose.

and, with the exception of the one minute HCN experiments, the 200 liter animal exposure chamber that was designed for the NBS Toxicity Test Method[3]. The animal exposure system is a closed design in which all the gases are kept in the 200 liter rectangular chamber for the duration of the experiment. In the one minute HCN experiments, a 4.5 liter flow-through exposure system was used in place of the 200 liter chamber. This change was deemed necessary to reduce the amount of HCN gas used in the one minute experiments and to perform the experiments under negative pressure to prevent an inadvertent HCN exposure of the personnel.

2.4 Gas Analysis: Carbon monoxide and CO₂ were measured continuously by non-dispersive infrared analyzers. Oxygen concentrations were measured continuously with a paramagnetic analyzer. The CO, CO₂, and O₂ data were recorded by an on-line computer every 15 seconds. All gases that were removed for chemical analysis (with the exception of HCN) were returned to the chamber. Syringe samples (100 μl) of the chamber atmosphere were analyzed for HCN approximately every three minutes with a gas chromatograph equipped with a thermionic detector [4]. All given gas concentrations are the average exposure values which were calculated by integrating the area under the instrument response curve and dividing by the exposure time. The variability in these square-wave exposures increased as the exposure time increased. For example, the average percent change from the average one minute CO values was 0.4%; whereas that for the 60 minute CO values was 8.5%. For HCN, the average percent change from the 5 minute values was 1.3%; while that from the 60 minute values was 15.1%.

2.5 Blood Analyses: Animals designated for blood analysis were cannulated. This procedure involved anesthetizing the animals with pentobarbital sodium (0.09 g/kg) and surgically inserting a cannula into the animal's femoral artery. Sixteen to 24 hours later, blood samples (0.5 ml or 0.8 ml, if blood cyanide was also measured) were taken during and following the exposures from unanesthetized cannulated rats with syringes flushed with heparin. The carboxyhemoglobin (COHb) and pH were measured with a Co-Oximeter 282 (Instrumentation Laboratory Inc., Lexington, MA) and a Corning 168 pH Blood Gas System, respectively. Hydrogen cyanide in the blood was determined by a head space technique using a gas chromatograph equipped with a nitrogen/phosphorus detector.

2.6 Test Procedure: The various gases were added to the chamber until the desired concentrations (monitored by the analytical instrumentation) were reached. A fan in the chamber assured adequate mixing of the gases prior to exposure of the animals. Six rats were exposed in each experiment except the one minute HCN experiments, in which 5 rats were exposed per test. Animals were placed in restrainers which were then inserted into the portholes located along the front of the exposure chamber such that only the heads of the animals were exposed. To achieve square-wave exposures, these portholes were fitted with rubber stoppers during the time that the gas concentrations were reaching equilibrium. Insertion of the restrained animals caused the rubber stoppers to fall into the chamber and simultaneously exposed the animals to the chamber atmosphere. Exposures were for set exposure times of 1, 2, 5, 10, 20, 30, and 60 minutes. Blood was taken from the cannulated animals at zero time, at various times throughout the exposure and just before the end of the

exposure (one or two animals were cannulated in each experiment). The toxicological endpoint was death. The percentage of animals dying at each gas concentration was plotted to produce a concentration-response curve from which LC_{50} values were calculated for each exposure time and for the exposure plus post-exposure period. The LC_{50} in these cases is defined as the concentration of test gas in the chamber (ppm or %, where 1% = 10000 ppm) which caused 50% of the animals to die during the exposure only or during the exposure plus the post-exposure observation period. The LC_{50} values and their 95% confidence limits were calculated by the statistical method of Litchfield and Wilcoxon [5]. All animals (including the controls) were weighed daily from the day of arrival until the end of the 14 day post-exposure observation period except for the cannulated ones which were sacrificed following exposure. In some cases where the animals were still losing weight at the end of the 14 day post-exposure observation period, they were kept until they either recovered (as indicated by three days of successive weight gain) or died.

2.7 Experimental Design for Individual and Combined Gas Studies: The LC_{50} values and their 95% confidence limits were determined for the individual gases - CO and HCN for 1, 2, 5, 10, 20, 30 and 60 minutes. Although 30 minute data have been published previously [2], some of these values were reexamined. In the case of the combined CO and HCN experiments, the additivity of the toxic effects of the two gases was examined by exposing the animals to combinations of approximately 50% of the LC_{50} values of each gas for each time period. In the case of the combined CO and CO_2 experiments, the concentration of CO_2 was kept constant at roughly 5%, while the concentration of CO was varied to determine the effect on the LC_{50} for each exposure period.

2.8 Kinetic Blood Uptake Studies: Some experiments were designed to determine the effect of the presence of other gases on the rate of formation and final equilibrium level of COHb, blood cyanide and arterial pH. In these experiments, all six rats were cannulated and exposed to pre-set concentrations of the gases. Blood (0.5 ml) was sampled at approximately one minute intervals sequentially from different rats such that an excessive amount of blood was not taken from any one rat.

3. RESULTS

3.1 Carbon Monoxide: Two sets of LC_{50} values and 95% confidence limits for CO in air were calculated for each of the different exposure times ranging from one minute to 60 minutes. These LC_{50} values were obtained with animals supplied by the Harlan Sprague-Dawley Company (pre-1986 30 minute values), Hilltop Lab Animal Company (all other pre-1986 values) or from Taconic Farms (1986 and later values) and are shown in Table 1. The two sets of values are plotted in Figure 1 along with the plot of the CO concentration-time products, which are calculated by multiplying the LC_{50} values by their respective exposure times. The COHb equilibrium levels and the rate of formation of COHb depends upon the test concentration to which the animals are exposed (Fig. 2).

3.2 Hydrogen Cyanide: The LC_{50} values and their 95% confidence limits for HCN in air for the exposure times ranging from one to thirty minutes plus a 24 hour post-exposure observation period are shown in Figure 3 and Table 2. The

Table 1. LC₅₀ Values^a for Carbon Monoxide Exposures for Various Times

Exposure time (min)	CO ^b (ppm)	CO ^c (ppm)
1	-	107000 (102000-112000)
2	36000 (34000-38000)	42500 (42000-43000)
5	12600 (12400-12800)	14000 ^d (12000-16000)
10	7600 (7300-7900)	9800 (9200-10500)
20	5600 (5400-5800)	7400 (7100-7700)
30	4600 (4400-4800)	6600 (6100-7300)
60	3400 (3100-3600)	4900 (4600-5200)

a. Calculated using deaths within exposure plus 24 hours

b. Data prior to 1986

c. 1986 data

d. Calculated via the Litchfield and Wilcoxon procedure for significantly heterogeneous data [5].

60 minute LC₅₀ value does not have 95% confidence limits because it was not statistically calculated, but rather was estimated from the results of six experiments. In these exposures (78, 84, 89, 90, 100, and 100 ppm), 25% of the animals died at the three lower concentrations, and 100% of the animals died at the three higher concentrations. Since the concentration-response curve was so steep, it was deemed unnecessary to try to obtain further data points between the 25% deaths and the 100% deaths.

Table 2. Acute Inhalation Exposures to HCN

Exposure time (min)	Lethality LC ₅₀ ^a (ppm)	Incapacitation EC ₅₀ ^b (ppm)
1	3000 (2500-3600) ^c	1700 (1200-2400)
2	1600 (1400-1800)	1100 (800-1300)
5	570 (460-710)	390 (310-490)
10	290 (250-340)	170 (150-190)
20	170 (160-180)	ND
30	110 (95-130)	ND
60	90	ND

a. LC₅₀ based on deaths occurring within exposure plus 24 hours post-exposure.

b. EC₅₀ based on lack of righting reflex of animals immediately following exposure.

c. 95% confidence limits.

ND. Not determined.

The values which had been determined prior to 1986 were checked and had not changed. Also shown in Table 2 are the concentrations of HCN which caused incapacitation (as indicated by the lack of the righting reflex) in 50% of the animals following exposures of 1 to 10 minutes. Time-weighted average blood cyanide levels from representative exposures are shown in Figure 4.

3.3 Carbon Monoxide and Hydrogen Cyanide: Prior thirty minute experiments on the lethal effects of combinations of CO and HCN in air indicated that these two gases act in an additive manner such that if:

$$\frac{[\text{CO}]}{\text{LC}_{50}\text{CO}_{(30 \text{ min})}} + \frac{[\text{HCN}]}{\text{LC}_{50}\text{HCN}_{(30 \text{ min})}} \approx 1 \pm 15\% \quad (1)$$

some of the exposed animals will die (the values in brackets are the test concentrations of the gases) (Table 3). If the left hand side of the above equation is greater or less than this value, all the animals will die or live, respectively. When this equation is equal to 1, 50% of the test animals would be expected to die. However, as the concentration-response curves of CO and HCN as individual gases are very steep, the deaths of 1 to 5 animals during these 30 minute experiments were considered indicative that the concentrations of the combined gases were close to the LC₅₀ values. The estimated ± 15% variability is based on the observation that the number of deaths within the range of approximately 0.98 and 1.10 varied from 1 to 5 and the scarcity of information for the range between 0.86 and 0.98 (Table 3).

Table 3. Carbon Monoxide and Hydrogen Cyanide - 30 Minute Exposures

Exp. No.	Fraction of LC ₅₀			No. died Six animals	COHb (%)
	CO	HCN	CO + HCN		
1	1.00	0	1.00	3	84*
2	1.00	0	1.00	5	83
3	0.75	0.27	1.02	4	79*
4	0.75	0.38	1.13	6	67*
5	0.52	0.58	1.10	3	-
6	0.50	0.53	1.03	5	67*
7	0.49	0.49	0.98	5	71*
8	0.38	0.48	0.86	0	-
9	0.28	0.78	1.06	3	45*
10	0.27	0.79	1.06	3	43*
11	0	0.98	0.98	2	-
12	0	1.00	1.00	1	-
13	0	1.08	1.08	4	-

LC₅₀ of CO = 4600 ppm

LC₅₀ of HCN = 160 ppm

* Animal died during exposure.

LC₅₀ values used in these calculations were based on deaths within the 30 min exposures only.

When approximately 50% of the LC₅₀ values of each of the different time exposures (10, 20 and 60 minutes) of CO and HCN were combined, the number of animals that died out of the six exposed was between 2 and 4 (Table 4). In the 5 minute experiments, the HCN concentrations were kept constant between 47 - 53% of the 5 minute LC₅₀ value and the CO was varied to determine the effect of HCN on the CO LC₅₀ value. This new CO (with HCN) LC₅₀ value was 7600 ppm, which, if doubled, would fall within the 95% confidence limits (12000 - 16000 ppm) of the CO without HCN LC₅₀ five minute value of 14000 ppm.

Table 4. Additivity of Carbon Monoxide and Hydrogen Cyanide Toxicity

Exposure time (min)	Percent of LC ₅₀ ^a			No. animals died/tested
	CO	HCN	Total	
10	52	47	99	3/6
	52	47	99	2/6
20	51	60	111	4/6
	50	57	107	4/6
60	51	56	107	2/6
	53	56	109	4/6

a. 1986 data

Table 3 also shows that as [CO] decreases and [HCN] increases; the animals die at lower concentrations of CO and, consequently, COHb levels lower than if the CO were given alone. A standard curve developed in our laboratory of equilibrium levels of COHb generated at various atmospheric CO concentrations showed that the COHb values obtained in the combined CO and HCN experiments are systematically lower than those expected at equilibrium from comparable CO exposures (data not shown). The degree of reduction of COHb depends on the HCN concentration. Polymeric materials showed similar results, in that animals exposed to the thermal decomposition products from polymeric materials which produce relatively high HCN concentrations have lower levels of COHb than those predicted by the atmospheric concentrations of CO.

This lower-than-expected level of COHb in the presence of both HCN and CO was examined to determine if the HCN was affecting the initial rate of uptake and formation of COHb or the final equilibrium levels. Figure 5 shows that at the concentrations tested (1470 ppm of CO alone or 1450 ppm CO plus 100 ppm HCN), the initial rate of formation of COHb was the same in the presence and absence of HCN. The final COHb equilibrium, however, was lower when the animals were exposed to both gases.

3.4 Carbon Monoxide and Carbon Dioxide: In 30 minute experiments, sublethal

concentrations of CO₂ (1 to 17.3%⁵) in combination with sublethal levels of CO (2500 to 4000 ppm) caused deaths of some of the rats both during exposures and the following 24 hours (Fig. 6) [1]. The solid line in Figure 6 was drawn to separate the experiments in which some animals died from those with no deaths. Based on this line, the most toxic combination of these two gases appears to be approximately 5% CO₂ and 2500 ppm CO. Above and below 5% CO₂ (1 to 17.3%), more CO (but still concentrations below the 95% confidence limits of the CO LC₅₀ value) was necessary to produce the deaths.

The LC₅₀ values of CO for the time exposures of 5, 10, 20 and 60 minutes were determined in the presence and absence of approximately 5% CO₂ and, with the exception of the 5 minute case, the LC₅₀ values were statistically significantly lower (based on the 95% confidence limits) in the presence of 5% CO₂ than in its absence (Table 5). In the 5 minute exposures, the CO LC₅₀ value in the presence of 5% CO₂ was lower than in the absence of CO₂, but the 95% confidence limits overlapped.

Table 5. LC₅₀ Values for CO Alone and CO Plus CO₂

Exposure time (min)	CO ^a (ppm)	CO + 5% CO ₂ ^a (ppm)
5	14000 (12000-16000)	11700 (10800-12700)
10	9800 (9200-10500)	7800 (7500-8200)
20	7400 (7100-7700)	5600 (5500-5800)
30	6600 (6100-7300)	3900 (3400-4500)
60	4900 (4600-5200)	3100 (2800-3400)

a. 1986 data

4. DISCUSSION

The atmosphere produced by a fire is a dynamic, rapidly changing combination of toxic gases, particulates, reduced oxygen and high temperatures. Each component of this combination is capable of producing conditions which are incompatible with life or will act to prevent safe egress from a burning building. As statistics have shown that the majority of fire fatalities result from smoke inhalation and not from burns [29], the importance of the identification of the responsible combustion products produced from materials under different fire conditions becomes apparent. Of equal importance is information on the toxic concentrations of these gases for various exposure times.

The toxicologist is faced with the problems of determining the toxicity of the individual combustion products and their combinations and how these toxic effects are affected by changing exposure times. Many studies have been

⁵Even though 17.3% CO₂ was not tested by itself, it is considered non-lethal because 17.7% CO₂ in the presence of 3200 ppm of CO did not produce any deaths (Fig. 6).

performed on the toxicity of single common fire gases, e.g., see review by Kimmerle [6] plus papers on CO [1,2,6,7,8,9,10,11,12]; CO₂ [1,2,9, 12]; HCN [2,6,8,10,11,13]; and O₂ [2,7,10,11,12]. Some studies have examined the toxicological interactions of various combinations of these fire gases or the additional effects of decreased oxygen atmospheres, e.g., CO and HCN [2,6,10,13,14,15,16,17,18,19,20,21,22,23] CO and CO₂ [1,12,24,25,26,27, 28]; CO₂ and O₂ [2,12]; CO and O₂ [7,10,12]; HCN and O₂ [10]; CO, CO₂, and O₂ [2,10,12,27]; and CO, CO₂, HCN, and O₂ [10].

Prior research at NBS has examined an initial set of primary fire gases - CO, CO₂, HCN, and low O₂ - as both individual gases and in various combinations. Our toxicological results on 30 minute exposures of rats to these single gases showed good agreement with values found in the literature (Table 6). In our determination of the LC₅₀ values for CO for the different exposure times, we found that the values shifted when the animal supplier changed even though both sets were designated Fischer 344 male rats. Therefore, it is important in any set of experiments to determine the LC₅₀ values for the specific animals being used and to check periodically the values to ensure that they have not changed.

Table 6. Thirty Minute Lethal Exposures to Individual Gases

<u>Gas</u>	<u>Animal Species</u>	<u>LC₅₀</u>	<u>Post Exposure Time</u>	<u>Reference</u>
CO (ppm)	rats	5000-6000 ^a	0	9
	rats	5500	NI	6
	rats	4600 ^b	0 ^f	2
	rats	5000 ^c	0 ^f	2
	rats	5000 ^d	0	20
	rats	5275 ^e	24 hrs ^g	19
	rats	6600 ^b	0 ^f	this paper
	mice	3570	NI	31
	mice	3500	10 min	11
HCN (ppm)	rats	142	NI	6
	rats	200	NI	6
	rats	160 ^b	0	2
	rats	110 ^b	24 hrs	2
	rats	157 ^e	0	23
	rats	116 ^e	24 hrs ^g	19
	mice	166	10 min	11

- a. estimated from data provided
- b. square-wave exposure
- c. gradual exposure
- d. amount needed to kill in 30 min
- e. calculated from CT product
- f. animals kept 14 days, but all deaths occurred during the 30 min exposure
- g. animals kept 24 hours, but no changes were observed after one hour.
- NI. not indicated.

Haber's rule states that the toxic concentration multiplied by the exposure time is equal to a constant. If this rule held true for all cases, one could examine one exposure time and extrapolate to all other times. There are very few cases in which Haber's rule has been shown to hold true, and the reason is that living organisms have the ability to metabolize and excrete most drugs and toxicants before they accumulate to fatal levels. An interesting finding from the current study, however, is that the concentration-time product for the HCN LC₅₀s is a constant if the 24 hour post-exposure deaths are included in the LC₅₀ calculation. On the other hand, as expected, the CO LC₅₀ concentration-time product increases for the exposure periods ranging from 5 minutes to 60 minutes. An unforeseen result was the initial decrease in the CO concentration-time products for the 1, 2, and 5 minute exposure times. This probably means that the animals need more than 5 minutes to eliminate these high levels of CO.

We had found previously that the toxicities of CO and HCN were additive if calculated as ratios of their 30 minute lethal concentrations. Our research reported here shows that the additivity observed during the 30 minute experiments is also seen in experiments in which the exposure times are 5, 10, 20, and 60 minutes. Although different experimental designs were used by Hartzell et al. [18], Kishitani and Nakamura [10], Lynch [19], Smith et al. [22], Pitt et al. [21], and Yamamoto and Kuwahara [23], these investigators also concluded that the toxicological effects of CO and HCN were additive. Kimmerle [6] and Moss et al. [20], on the other hand, claimed that CO and HCN showed synergistic effects. They hypothesized that the synergism they observed in their experiments could arise from an HCN-induced increase in respiration rate which would cause a more rapid uptake of carbon monoxide. Results reported by Matijak-Schaper and Alarie [11], however, show that HCN causes a significant decrease in the respiration rate of mice. This decrease became apparent three minutes after the start of an exposure to 100 ppm of HCN. As little as 20 ppm of HCN caused a 20% decrease in the respiratory rate and 63 ppm caused a 50% decrease. These investigators also showed that CO produced a respiratory rate depression, although the onset was later than that seen with HCN. Therefore, the two gases together are unlikely to increase the CO uptake rate. Our examination of this issue showed that as the CO concentration decreases and the HCN concentration increases, the COHb level decreases (Table 3). This decrease is actually lower than the COHb equilibrium level expected from the comparable CO concentration. Our investigation of the kinetic uptake of CO and the formation of COHb in the presence and absence of HCN showed that the initial rate of formation of COHb is the same; however, the final COHb equilibrium level is reduced when HCN is present (Fig. 5). In other words, the animals are not receiving more CO in the presence of HCN, but less. This depressive effect of HCN on CO uptake may help explain why some people dying in fires have low COHb levels (<50%) [14,15,16,17,29].

Higgins et al. [13], however, did not observe any statistically significant changes in the 5 minute LC₅₀ value of HCN when rats were also exposed to enough CO (2100 ppm) to generate 25% COHb. Their 5 minute HCN LC₅₀ value (503 ppm with 95% confidence limits of 403 to 626 ppm) agrees well with our five minute LC₅₀ value of 570 ppm with 95% confidence limits of 460 to 710 ppm. When they exposed rats to 2100 ppm of CO plus HCN, the LC₅₀ value of HCN

became 467 ppm with 95% confidence limits of 395 to 553 ppm. Calculating equation (1) using exposure concentrations of HCN and CO of 503 and 2100 ppm, respectively and 5 minute LC_{50} values of HCN and CO of 503 ppm and 14000 ppm, respectively results in a value of 1.15, which is within the experimental error of the calculation.

There is little human data that one can compare with the animal results. One such set of data comes from Anderson and his coworkers [14,15,16,17] and their studies of fire deaths in the Glasgow area and the United Kingdom. They found that 78% of the fire deaths had blood cyanide levels greater than normal. Although they considered HCN a contributory factor, they did not find any evidence of the additivity of the toxicities of CO and HCN. Their conclusions are based on the assumption that 50% COHb is the lethal concentration and since high levels of blood cyanide were usually found in conjunction with high levels of CO, they concluded that these deaths (>50% COHb) were due to CO. If, however, as found in our animal studies, 50% COHb is not sufficient to cause death, then reevaluation of their data may show the additive effects of CO and HCN.

A detailed study has been made on the interaction of CO and CO_2 [1]. Pryor et al. [12] found that 40% (400,000 ppm) CO_2 was necessary before one rat died in a 30 minute exposure, an indication that CO_2 is relatively non-toxic. However, except for the 5 minute exposures, our experiments indicated that the presence of 5% CO_2 decreased the CO LC_{50} values for the exposure times tested. This synergistic interaction appears to be due to two mechanisms: 1. CO_2 , at low concentrations, acts as a respiratory stimulant, which increases the rate of uptake of CO (Fig. 7); and 2. CO and CO_2 together produce an increased and prolonged respiratory and metabolic acidosis (Fig. 8). Acidosis is a disturbance of the acid-base balance of the body and, in this case, results from an increase in acidic chemicals (e.g., carbonic acid from the reaction of CO_2 with H_2O and lactic acid as a result of anaerobic metabolism). Depression of the central nervous system is the major effect of acidosis. pH values below 7.0 will cause disorientation and coma. If such severe acidosis is not treated, death will occur [30].

5. SUMMARY

1. Carbon monoxide LC_{50} values (the concentration of CO necessary to kill 50% of the Fischer 344 rats during the exposure) were determined for exposure times ranging from 1 to 60 minutes and found to be 107000 ppm for 1 minute, 42500 ppm for 2 minutes, 14000 ppm for 5 minutes, 9800 ppm for 10 minutes, 7400 ppm for 20 minutes, 6600 ppm for 30 minutes, and 4900 ppm for 60 minutes. These values were higher than values determined previously with rats from a different supplier.

2. Hydrogen cyanide LC_{50} values (calculated based on deaths during the exposure plus a 24 hours post-exposure observation time) were 3000 ppm for 1 minute, 1600 ppm for 2 minutes, 570 ppm for 5 minutes, 290 ppm for 10 minutes, 170 ppm for 20 minutes, 110 ppm for 30 minutes, and 90 ppm for 60 minutes.

3. The CO concentration-time products decreased as the time increased from 1 to 5 minutes and increased from 5 to 60 minutes; whereas, the HCN concentration-time products were constant throughout all the tested times.
4. The toxicity (as indicated by deaths of the rats) of the combined CO and HCN gas exposures were additive for the tested times ranging from 5 to 60 minutes.
5. The combined CO and CO₂ gas exposures indicated that 5% CO₂ decreased the LC₅₀ values (i.e., increased the toxicity) of the CO for the tested times ranging from 10 to 60 minutes. The decrease in the 5 minute LC₅₀ exposures were not statistically significant.

6. REFERENCES

1. Levin, B. C., Paabo, M., Gurman, J. L., Harris, S.E., and Braun, E. (1987). Toxicological interaction between carbon monoxide and carbon dioxide. Toxicology (In Press).
2. Levin, B.C., Paabo, M., Gurman, J.L., and Harris, S.E. (1987). Effects of exposure to single or multiple combinations of the predominant toxic gases and low oxygen atmospheres produced in fires. Fundam. Appl. Toxicol. (In Press).
3. Levin, B. C., Fowell, A. J., Birky, M. M., Paabo, M., Stolte, A., and Malek, D. (1982). Further development of a test method for the assessment of the acute inhalation toxicity of combustion products. NBSIR 82-2532, National Bureau of Standards, Gaithersburg, MD.
4. Paabo, M., Birky, M.M., and Womble, S.E. (1979). Analysis of hydrogen cyanide in fire environments. J. Comb. Tox. 6, 99-108.
5. Litchfield, J. T., and Wilcoxon, F. (1949). A simplified method of evaluating dose-effect experiments. J. Pharmacol. & Exp. Therapeut. 96, 99-113.
6. Kimmerle, M. G. (1974). Aspects and methodology for the evaluation of toxicological parameters during fire exposure. J. Fire & Flamm./ Comb. Tox. 1, 4-51.
7. Cagliostro, D. E. and Islas, A. (1982). The effects of reduced oxygen and of carbon monoxide on performance in a mouse pole-jump apparatus. J. Comb. Tox. 9, 187-193.
8. Hartzell, G. E., Priest, D. N., and Switzer, W. G. (1985). Modeling of toxicological effects of fire gases: II. Mathematical modeling of intoxication of rats by carbon monoxide and hydrogen cyanide. J. Fire Sci. 3, 115-128.

9. Herpol, C., Minne, R., and Van Outryve E. (1976). Biological evaluation of the toxicity of gases produced under fire conditions by synthetic materials. Part 1: Methods and preliminary experiments concerning the reaction of animals to simple mixtures of air and carbon dioxide or carbon monoxide. *Comb. Sci. Technol.* **12**, 217-228.
10. Kishitani, K., and Nakamura, K. (1979). Research on evaluation of toxicities of combustion gases generated during fires. In "Fire Research and Safety" (Ed. by M.A. Sherald), National Bureau of Standards Special Publication 540; Proceedings of the Third Joint Panel Conference of the U.S.- Japan Cooperative Program in Natural Resources held at the National Bureau of Standards, Gaithersburg, MD (March, 1978)
11. Matijak-Schaper, M. and Alarie, Y. (1982). Toxicity of carbon monoxide, hydrogen cyanide and low oxygen. *J. Comb. Tox.* **9**, 21-61.
12. Pryor, A. J., Fear, F. A., and Wheeler, R. J., 1974: Mass Life Fire Hazard: Experimental Study of the Life Hazard of Combustion Products in Structural Fires. *J. Fire & Flam./Comb. Tox.*, **1**, 191-235.
13. Higgins, E. A., Fiorca, V., Thomas, A. A., and Davis, H. V. (1972). Acute toxicity of brief exposures to HF, HCl, NO₂, and HCN with and without CO. *Fire Tech.* **8**, 120-130.
14. Anderson, R. A., Thomson, I., and Harland, W. A. (1979). The importance of cyanide and organic nitriles in fire fatalities. *Fire & Matls.* **3**, 91-99.
15. Anderson, R. A., Watson, A. A., and Harland, W. A. (1981a). Fire deaths in the Glasgow area: I. General considerations and pathology. *Med. Sci. Law.* **21**, 175-183.
16. Anderson, R. A., Watson, A. A., and Harland, W. A. (1981b). Fire deaths in the Glasgow area: II. The role of carbon monoxide. *Med. Sci. Law* **21**, 288-294.
17. Anderson, R. A., Willetts, K. N., Cheng, K. N., and Harland, W. A. (1983). Fire deaths in the United Kingdom 1976 - 82. *Fire & Matls.* **7**, 67-72.
18. Hartzell, G. E., Switzer, W. G., and Priest, D. N. (1985). Modeling of toxicological effects of fire gases: V. Mathematical modeling of intoxication of rats by combined carbon monoxide and hydrogen cyanide atmospheres. *J. Fire Sci.* **3**, 330-342.
19. Lynch, R. D. (1975). On the non-existence of synergism between inhaled hydrogen cyanide and carbon monoxide. Fire Research Note No. 1035, Fire Research Station, Borehamwood, Hertfordshire, WD6 2BL, England.
20. Moss, R. H., Jackson, C. F., and Seiberlich, J. (1951). Toxicity of Carbon monoxide and hydrogen cyanide gas mixtures. *Arch. Indust. Hyg. Occup. Med.* **4**, 53-64.

21. Pitt, B. R., Radford, E. P., Gurtner, G. H., and Traystman, R. J. (1979). Interaction of carbon monoxide and cyanide on cerebral circulation and metabolism. *Arch. Environ. Hlth.* **34**, 354-359.
22. Smith, P. W., Crane, C. R., Sanders, D. C., Abbott, J. K., and Endecott, B. (1976). Effects of exposure to carbon monoxide and hydrogen cyanide. In the Proceedings of an International Symposium on The Physiological and Toxicological Aspects of Combustion Products held at The University of Utah, March, 1974. Published by the National Academy of Sciences, Washington, DC, pp. 75-88.
23. Yamamoto, K., and Kuwahara, C. (1981). A study on the combined action of CO and HCN in terms of concentration-time products. *Z. Rechtsmed.* **86**, 287-294.
24. Crane, C. R., Sanders, D. C., Endecott, B. R., Abbott, J. K., and Smith, P. W. (1977). Inhalation toxicology: I. Design of a small animal test system. II. Determination of the relative toxic hazards of 75 aircraft cabin materials. Report No. FAA-AM-77-9, Dept. of Transportation, Federal Aviation Administration, Washington, DC.
25. Edginton, J. A. G., and Lynch, R. D. (1975). The acute inhalation toxicity of CO from burning wood. Fire Research Note No. 1040. Fire Research Station, Salisbury, Wiltshire, U. K.
26. Gaume, J. G., Bartek, P., and Rostami, H. J. (1971). Experimental results on time of useful function (TUF) after exposure to mixtures of serious contaminants. *Aerospace Med.* p. 987-990.
27. Rodkey, F. L. and Collison, H. A. (1979). Effects of oxygen and carbon dioxide on carbon monoxide toxicity. *J. Comb. Tox.* **6**, 208-212.
28. Nelson, G. L., Hixon, E. J., and Denine, E. P. (1978). Combustion product toxicity studies of engineering plastics. *J. Comb. Tox.* **5**, 222-238.
29. Birky, M. M., Halpin, B. M., Caplan, Y. H., Fisher, R. S., McAllister, J. M., and Dixon, A. M. (1979). Fire fatality study. *Fire & Matls.* **3**, 211-217.
30. Guyton, A.C. (1976). Textbook of Medical Physiology. Fifth Edition, W.B. Saunders Co., Philadelphia, London, and Toronto.
31. Hilado, C.J. and Cumming, H.J. (1977). Effect of carbon monoxide in Swiss Albino Mice. *J. Comb. Tox.* **4**, 216-230.

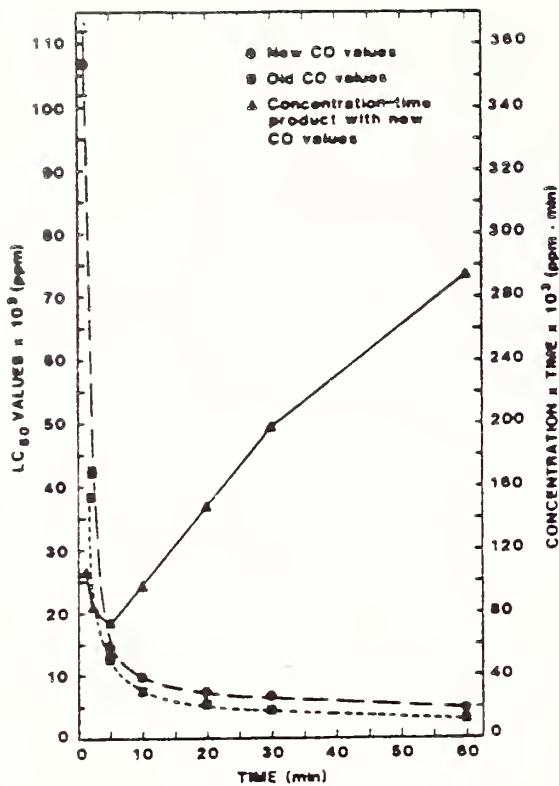


Figure 1. LC_{50} values and concentration-time products for CO for various exposure times.

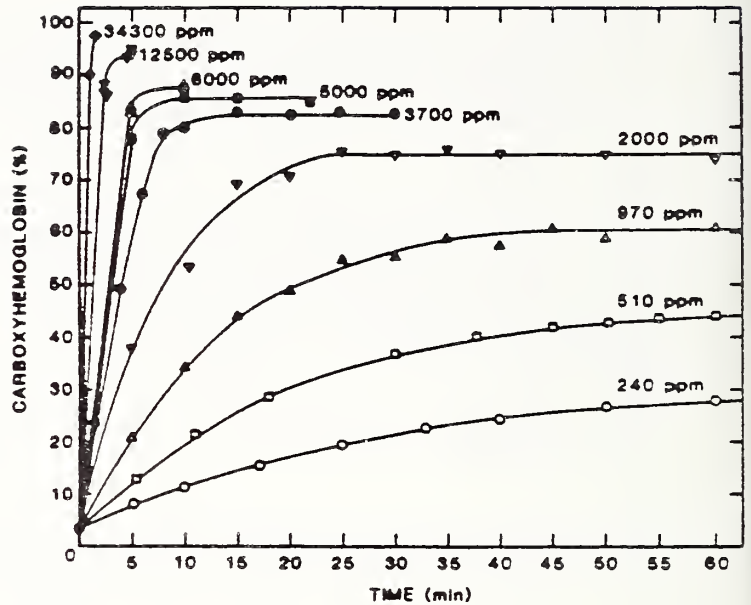


Figure 2. Rate of formation of COHb from exposures to various atmospheric concentrations of CO (ppm = CO concentration).

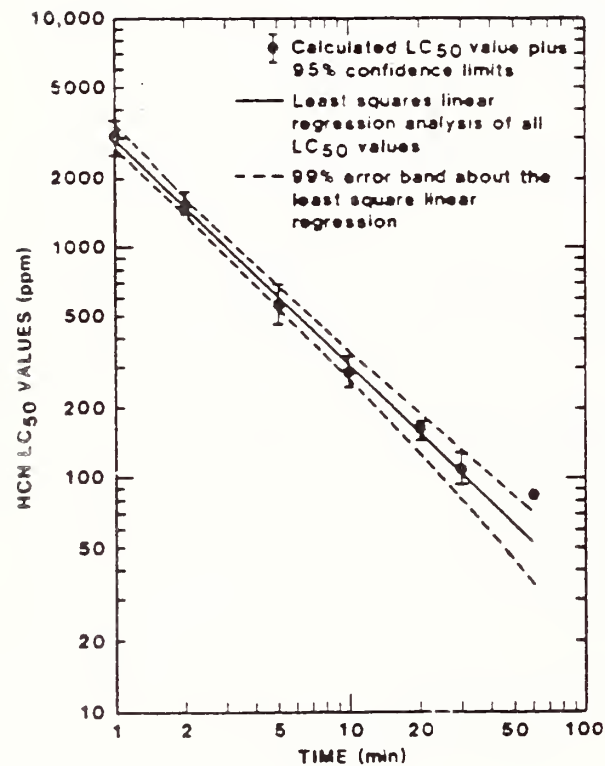


Figure 3. HCN LC_{50} values for different exposure times plus a 24 hour post-exposure period

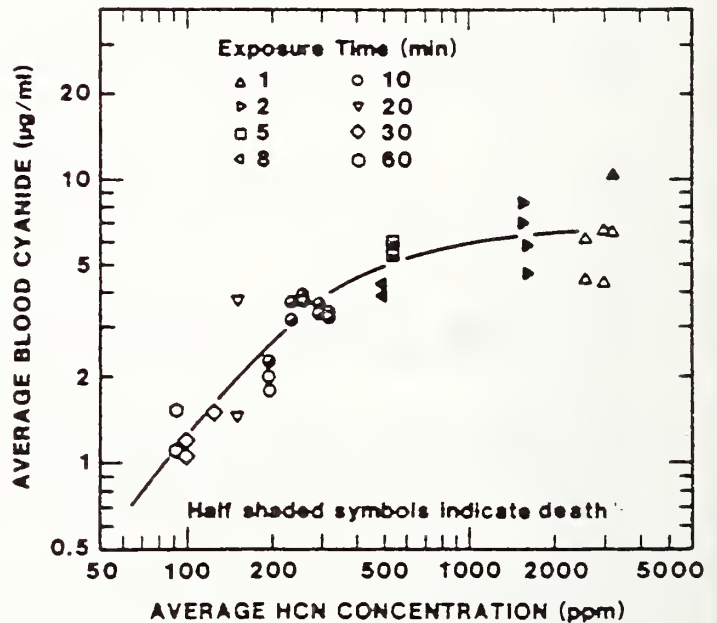


Figure 4. Time-weighted average blood cyanide levels in animals exposed to LC_{50} values of HCN for various exposure times.

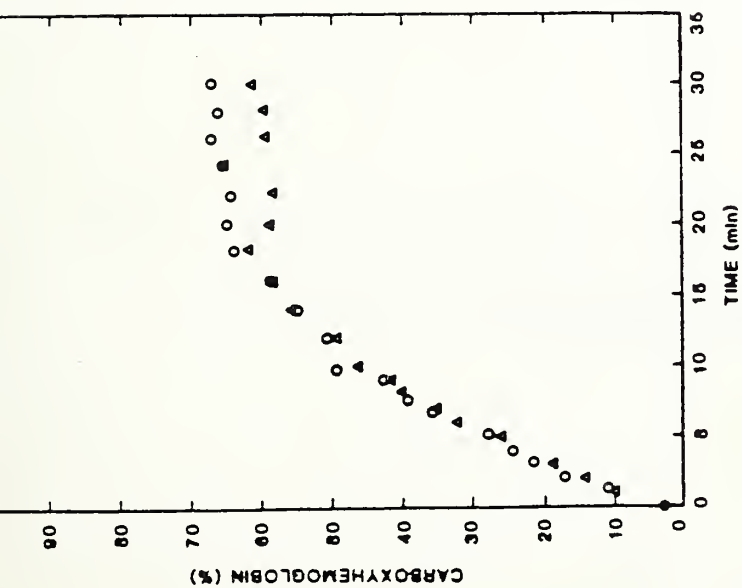


Figure 5. Formation and equilibrium levels of COHb in rats exposed to 1470 ppm of CO alone (O) or 1430 ppm of CO plus 100 ppm HCN (Δ).

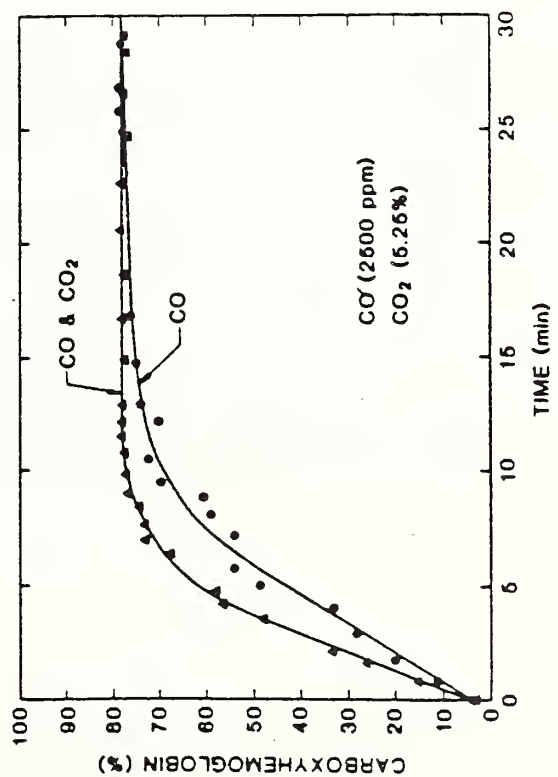


Figure 7. COHb formation during exposure to 2500 ppm CO alone (O) or with 5.25% CO₂ (Δ).

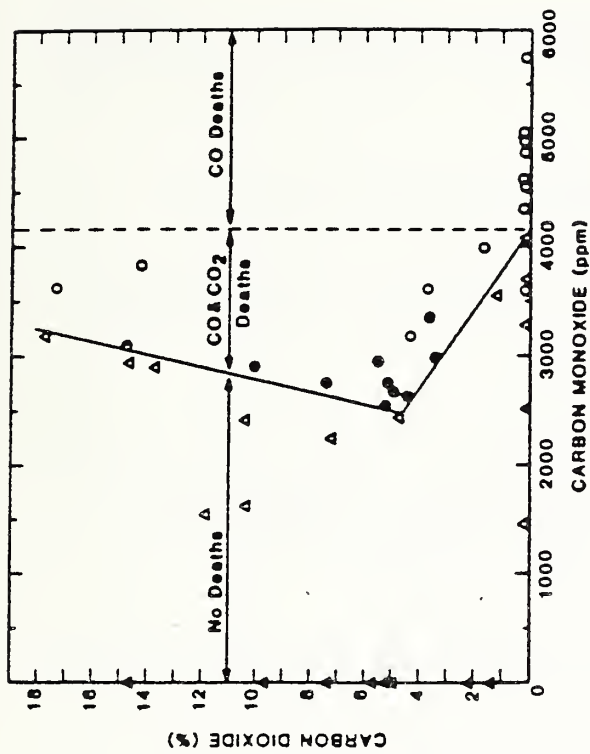


Figure 6. Deaths resulting from CO or CO₂ alone and from combined exposures to CO plus CO₂. No deaths (Δ); Deaths within-exposure (O); Deaths within- and post-exposure (\bullet). The solid line separates the experiments in which no deaths occurred from those in which one or more animals died.

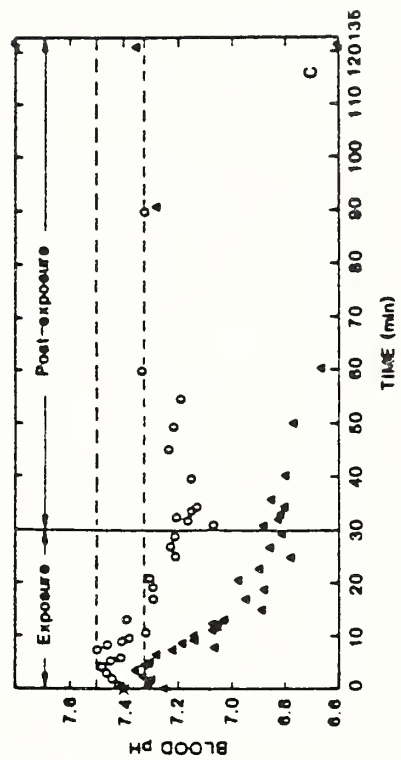


Figure 8. Changes in arterial blood pH during end following exposures to 2500 ppm CO alone (O) or with 5.25% CO₂ (\bullet). Mean and standard deviation of the controls (n=56) is indicated by the X and dashed lines.

TOXICOLOGICAL EFFECTS OF DIFFERENT TIME EXPOSURES TO FIRE GASES; CO OR HCN OR
CO COMBINED WITH HCN OR CO₂

B.C. Levin, National Bureau of Standards, USA

VOICE: This may be somewhat related to the next topic, but what's the concentration level of combination of CO and CO₂?

LEVIN: They can vary. Based on the curve seen in Fig. 6, you can see the variation. For example, if the CO were 3500 ppm and the CO₂ was 4 percent, you should have deaths.

TSUCHIYA: What is the oxygen concentration?

LEVIN: In all of these pure gas cases, we have kept our oxygen concentration at about normal, ambient level. Sometimes in our material decomposition, because it is a closed system and the animals use some oxygen and the combustion uses some oxygen, it may drop to about 18 percent in some cases.

VOICE: Could you clarify that? When you add five percent CO₂, what is the actual molar percentage of oxygen in that test? When you add just CO₂, let's say?

LEVIN: Well, what we're doing here is using cylinders of CO₂ in oxygen, so that we're changing the nitrogen concentration in the system.

VOICE: You're substituting CO₂ for nitrogen. Thank you.

TSUCHIYA: I also appreciate this study. I found that these show synergism of CO and CO₂. This is the only case so far statistically confirmed with fire gases. I appreciate this result. Second point, I'd like to see your slide on CT product (Fig. 1).

LEVIN: This one?

TSUCHIYA: Yes, that's correct. You mentioned that in the case of CO, that it does deviate from Haber's rule?

LEVIN: Right.

TSUCHIYA: Is this finding correct?

LEVIN: That's correct.

TSUCHIYA: And the second point, about HCN, you mentioned that CT is constant.

LEVIN: It appears to be when the LC₅₀ values include the deaths that occur within the first 24 hours following the exposures.

TSUCHIYA: But rather, I think, this is again normal phenomena. I studied many sets of animal data presented by other people, and I found for Haber's Rule it may be written: $ACT = 1$. A is a proportionality constant, C is the concentration, T is the time, okay?

So we know that actually when experimental data deviate from this rule at both ends, the high concentration or very low concentration, and we modified Haber's Rule into this form, then we found experimental data can be better represented and we found values of C_0 and T_0 in many cases, with many different gases. But proof of these, biologists like you, need to give physical meaning to these constants.

This case (HCN) is a special case of difference, a special case where T_0 is 0. I see the data that way, because I studied other sets of animal data, and those data fit well in this type of an equation. It is normal for the case of C_0 and other gases, that C_0 and T_0 are positive values, but in the case of hydrogen cyanide, T_0 is quite often zero, so this is one of those cases.

LEVIN: Thank you very much.

TEWARSON: On that slide, the primary equation that you wrote, it says mCO divided by CO_2 minus b, where b is the intercept. Now if I look at it here, is that intercept the LC_{50} of CO_2 ?

LEVIN: No. m is the slope and b is the intercept of these two lines, and those numbers change depending on whether CO_2 is above or below 5 percent. I have that in a paper I'll send to you. The reference is Levin et al., Fundamental and Applied Toxicology, Vol. 9, pp. 236-250, 1987.

TOXIC GAS TEST BY THE SEVERAL PURE AND MIXTURE GASES

Toshirou Sakurai

Research Institute of Marine Engineering
5-12, Fujimicho 1-chome, Higashimurayama city
Tokyo 189 Japan

Abstract

The relationship between incapacitation time and apnoea time of mice and gas concentration in case of single toxic gas condition and mixed gas condition with 6 types of toxic gases (CO, CO₂, HCl, HCN, NH₃, NO₂) and N₂ gas was investigated for the purpose of establishing an estimating method for toxicity of combustion gases generated from interior materials of building fire.

1. Test gases and mice

Six type gases were used; those were CO, CO₂, HCl, HCN, NH₃ and NO₂. Those gases except HCN were obtained as pressurized or liquified highly pure gases. HCN gas was generated from KCN.

At first, the tests were carried out with several concentration of the single gas. After those tests, the toxicity of some combinations of the toxic gases was examined. Low levels of concentration of each gas in the mixture were chosen so that by the concentration at the single gas condition, incapacitation time of mice came to 10 minutes or 20 minutes. However, the concentration of CO₂ was set at 2, 5 and 8%. Also, the relationship between incapacitation time of mice and ambient temperature was investigated.

The mice used in the study were female of ICR type of Jcl mice; the weight was within 18(gf) to 22(gf).

2. Test method and test apparatus,

Toxic gases are mixed in the gas controller, and the mixture is led to mice exposing chamber of the combustion gas toxicity test apparatus (The Notification No. 1231 of the Ministry of Construction). Eight mice are put in rotating cage individually and exposed to the toxic gases in the exposing chamber. Incapacitation time of each mouse is recorded. Apnoea time of each mouse is judged by eye. And concentration of each mouse is measured by gas analyzers.

The concentration of each toxic gas is adjusted roughly by controlling the intake flow rate and intake duration of gas. The toxic gases are mixed with the carrier gas of air of flow rate 10 (l/min) in a mixing chamber before lead to the exposing chamber so as not to expose mice directly with the thick toxic gases. In case of tests used mixture including CO₂ and N₂; CO₂ and N₂ are used as the carrier gas. And for in case of test single CO₂, O₂ concentration was kept on about 21(%) by supplying O₂ into the test chamber so as to eliminate the effect of hypoxia.

Concentration of CO, CO₂, HCl, NO₂, NH₃ and O₂ are measured during each test by continuous gas concentration analyzers; the maximum concentration (or minimum concentration of O₂) are recorded as the representative gas concentration of the test. The concentration of HCN is measured by the gas detecting tubes after one minute starting of intaking the gas and for three minutes.

Each rotating cage of mouse generates a electrical signal for half a rotation of the cage. Incapacitation time of the mouse is calculated from the record of the signals. The time after that a mouse dose not move for more than five minutes is defined as the incapacitation time of the mouse, because great diviation of incapacitation time of mice occasionally observed when the time after that a mouse dose not

move completely is defined as the incapacitation time.

Ambient temperature in the exposing chamber is controlled within $30 \pm 2(^{\circ}\text{C})$ and $40 \pm 2(^{\circ}\text{C})$ except the case of tests for relationship between ambient temperature and incapacitation time of mice.

3. Test results

Test results of single gas, the relationship between gas concentration and incapacitation time of mice and the relationship between incapacitation time and apnoea time are given an example in Figure - 1 to Figure - 8 .

Experimental curves of the relationship shown in those figures are described as equation (1). Table - 1 shows the coefficients 'a' and 'b' in the equation for each type of gas and the gas concentration on the experimental curve at the incapacitation time of mice of 5, 10, 20 and 30 minutes.

$$C \text{ (or } T) = a / t + b \dots\dots\dots (1)$$

- Where, C : concentration of gas (% or ppm)
- T : temperature ($^{\circ}\text{C}$)
- t : incapacitation time of mice (minutes)
- a, b : coefficient depending on the type of gas

By the equation (1), gas concentration relating to five minutes of incapacitation time of mice was calculated for each type of toxic gas. And measured gas concentration was yield to a non-dimensional gas concentration index (Ig) by the following equation:

$$I_g = (C_m - b) / (C_5 - b) \dots\dots (2)$$

- Where, C_m : measured gas concentration
- C_5 : gas concentration corresponding to five minutes of incapacitation of mice on the experimental curve

The relationship between incapacitation time of mice and gas concentration index derived equation (2) are given an example in Figure - 9 to Figure - 10. The curves in those figures are ideal curves; $I_g = 5 / t$.

Results of the tests with mixture gases, the relationship between incapacitation time of mice and algebraical sum of gas concentration index of the component toxic gases and the relationship between incapacitation time of mice and apnoea time of mice are given an example in Figure-11 to Figure-24. However, concentration of CO_2 and O_2 were not yield to gas concentration index because the concentration was low.

4. Consideration

Results of tests with single gas condition, except CO_2 , the test results are in accord with the ideal relationship of $I_g = 5 / t$; and those shows that the product of gas concentration index and incapacitation time of mice is constant. Table-1 show outline of consideration of the relationship between gas concentration and incapacitation time and the relationship between incapacitation time and apnoea time.

Results of tests with mixture gas condition, Table-2 to Table-6 show outline of consideration of the relationship between gas concentration and incapacitation time and the relationship between incapacitation time and apnoea time.

Table 1

Name of gas	Expos. temp. (°C)	Coefficient of gas		Gas concentration on the experimental curve				Unit of C or T	Consideration for the difference between incapacitation time and apnoea time
		a	b	5 (min)	10 (min)	20 (min)	30 (min)		
CO	30	2.34	0.016	0.484	0.250	0.133	0.094	%	The difference was big; incapacitation time was longer than apnoea time.
CO ₂	30	9.97	20.0	22.0	21.0	20.5	20.3	%	It is the same in the case of single condition of CO.
HCl	30	10.3	0.904	2.97	1.94	1.42	1.25	%	The difference was little, especially it was very little in case of thick.
HCN	30	491	25.3	123.5	74.4	50.0	41.7	ppm	It was the same in the case of single condition of CO.
NH ₃	30	3.15	0.378	1.01	0.639	0.536	0.483	%	It was the same in the case of single condition of HCl.
NO ₂	30	1.14	0.029	0.257	0.143	0.086	0.067	%	It was the same in the case of single condition of HCl.
N ₂ (O ₂)	30	-16.6	9.77	6.4	8.2	8.9	9.2	%	The difference was little in case of thin concentration.
Exposed temp.		71.2	41.1	55.4	48.2	44.7	43.5	°C	The difference was very little.

Experimental curve : $C \text{ (or } T) = a / t + b$

Where C : concentration of gas T : temperature

t : incapacitation time of mice (min)

a, b : coefficient depending on the type of gas or temperature

Table 2

Combination of gases	CO		CO ₂ %	O ₂ %	Temp. °C	RH %	Consideration	
	10 min *	20 min *					Relationship between gas concentration index and incapacitation time	Difference between incapacitation time and apnoea time
CO + N ₂	X	X	0	10	30	—	Mixture with thin concentration of O ₂ , incapacitation time was shorter than thick.	The difference was big in case of thick concentration of O ₂ (15%), that was little in case of thin (10%).
	X	X	0	10	30	—		
	X	X	0	15	30	—		
	X	X	0	15	30	—		
CO + CO ₂	X	X	2	20	30	—	Mixture with thick concentration of CO ₂ , incapacitation time was longer than thin.	The difference become big in proportion to concentration of CO ₂ increase.
	X	X	2	20	30	—		
	X	X	5	20	30	—		
	X	X	5	20	30	—		
	X	X	8	19	30	—		
	X	X	8	19	30	—		
CO+CO ₂ +N ₂	X	X	2	10	30	—	Mixture with thick concentration of CO ₂ , incapacitation time was longer than thin. Mixture with thick concentration of O ₂ , incapacitation time was longer than thin.	The difference become big in proportion to concentration of CO ₂ increase.
	X	X	2	15	30	—		
	X	X	8	10	30	—		
	X	X	8	15	30	—		
CO+CO ₂ +N ₂	X	X	2	18	30	—	Mixture with thick concentration of CO ₂ , incapacitation time was longer than thin. The difference was very little between the temperature 30 °C and 40 °C.	The difference become little in proportion to concentration of CO ₂ increase. In case of temperature 40°C, compared with temperature 30 °C, the difference was very little especially in case of thick concentration of CO.
	X	X	2	18	30	—		
	X	X	5	15	30	—		
	X	X	5	15	30	—		
	X	X	8	12	30	—		
	X	X	8	12	30	—		
	X	X	5	15	40	—		
	X	X	5	15	40	—		

* : This is show that the gas concentration corresponding to 10 minutes and 20 minutes of incapacitation time of mice on the experimental curve.

Table 3

Combination of gases	CO		HCl		CO ₂ %	O ₂ %	Temp. °C	RH %	Consideration	
	10 min *	20 min *	10 min *	20 min *					Relationship between gas concentration index and incapacitation time.	Consideration
CO + HCl	X		X		0	20	30	—	Relationship between gas concentration index and incapacitation time.	Difference between incapacitation time and apnoea time.
	X	X	X	X	0	20	30	—	Incapacitation time was longer than the case of single CO or HCl.	The difference was little.
		X	X	X	0	20	30	—		
		X	X	X	0	20	30	—		
CO+HCl+CO ₂	X	X	X	X	2	20	30	—	Mixture with thick concentration of CO ₂ , incapacitation time was shorter than thin.	The difference become little in proportion to concentration of CO ₂ increase.
	X	X	X	X	2	20	30	—		
	X	X	X	X	5	20	30	—		
	X	X	X	X	5	20	30	—		
	X	X	X	X	5	20	30	—		
	X	X	X	X	5	20	30	—		
	X	X	X	X	8	19	30	—		
	X	X	X	X	8	19	30	—		
CO+HCl +CO ₂ +N ₂	X		X		2	18	30	—	Compared with in case of CO+HCl+CO ₂ , mixture with thin concentration of O ₂ , incapacitation time was shorter than thick.	It was the same in the case of CO+HCl+CO ₂ .
	X	X	X	X	2	18	30	—		
		X	X	X	2	18	30	—		
	X	X	X	X	2	18	30	—		
	X	X	X	X	5	15	30	—		
	X	X	X	X	5	15	30	—		
	X	X	X	X	5	15	30	—		
	X	X	X	X	5	15	30	—		
	X	X	X	X	5	15	40	—	Compared with the case of 30°C, in case of 40°C, incapacitation time was shorter than the case of 30 °C.	Compared with the case of 30°C, in case of 40°C, the difference was shorter than the case of 30 °C.
	X	X	X	X	5	15	40	—		
CO+HCl +CO ₂ +N ₂	X	X	0.8 %	0.8 %	5	15	30	—	Mixture with thin concentration of CO, incapacitation time was shorter than the case of CO + CO ₂ + N ₂ .	It was the same the case of single HCl.
	X	X	0.8 %	0.8 %	5	15	30	—		

Table 5

Combination of gases	CO		HCN		CO ₂ %	O ₂ %	Temp. °C	Rh %	Consideration	
	10 min *	20 min *	10 min *	20 min *					Relationship between gas concentration index and incapacitation time	Difference between incapacitation time and apnoea time
CO+HCN +CO ₂ +N ₂	X	X	X	X	5	15	40	60	Incapacitation time was short compared with the case of exposed temperature 30°C.	The difference become little compared with the case of exposed temperature 30°C.
					5	15	40	60	Incapacitation time was short compared with in the case of exposed Rh 60 %.	It was the same in the case of exposed Rh 60%.
CO+HCN +CO ₂ +N ₂	X	X	25 ppm	25 ppm	2	18	30	—	It was the same in the case of CO+CO ₂ +N ₂ .	It was the same in the case of CO+CO ₂ +N ₂ .
					2	18	30	—		

Table 6

Combination of gases	CO		NH ₃		CO ₂ %	O ₂ %	Temp. °C	Rh %	Consideration	
	10 min *	20 min *	10 min *	20 min *					Relationship between gas concentration index and incapacitation time	Difference between incapacitation time and apnoea time
CO + NH ₃	X	X	X	X	0	20	30	—	It was the same in the case of single CO and NH ₃ .	It was the same in the case of single NH ₃ .
	X	X	X	X	0	20	30	—		
			X	X	0	20	30	—		
			X	X	0	20	30	—		
CO+NH ₃ +CO ₂	X	X	X	X	5	20	30	—	Incapacitation time was slightly short compared with in the case of CO+NH ₃ .	The difference was slightly little compared with in the case of CO+NH ₃ .
	X	X	X	X	5	20	30	—		
			X	X	5	20	30	—		
			X	X	5	20	30	—		

Table 4

Combination of gases	CO		HCN		CO ₂ %	O ₂ %	Temp. °C	Rh %	Consideration	
	10 min *	20 min *	10 min *	20 min *					Relationship between gas concentration index and incapacitation time	Difference between incapacitation time and apnoea time
CO + HCN	X		X		0	20	30	—	In case of mixture with thick CO, incapacitation time was shorter than that of single condition of CO or HCN of same concentration.	The difference was big that of single condition of CO or HCN of same concentration.
	X	X	X	X	0	20	30	—		
		X	X	X	0	20	30	—		
		X	X	X	0	20	30	—		
CO+HCN+CO ₂	X	X	X	X	2	20	30	—	Mixture with thick concentration of CO ₂ , incapacitation time was shorter than thin.	The difference become little in proportion to concentration of CO ₂ increase.
	X	X	X	X	2	20	30	—		
	X	X	X	X	5	20	30	—		
	X	X	X	X	5	20	30	—		
	X	X	X	X	5	20	30	—		
	X	X	X	X	8	19	30	—		
CO+HCN+CO ₂ +N ₂	X	X	X	X	2	18	30	—	It was the same in the case of CO+HCN+CO ₂ .	It was the same in the case of CO+HCN+CO ₂ .
	X	X	X	X	2	18	30	—		
	X	X	X	X	2	18	30	—		
	X	X	X	X	5	15	30	—		
	X	X	X	X	5	15	30	—		
	X	X	X	X	5	15	30	—		
CO+HCN+CO ₂ +N ₂	X	X	X	X	5	15	30	80	In case of high humidity, the incapacitation time was shorter than the low humidity.	In case of high humidity, the difference was less than the low humidity.
		X	X	X	5	15	30	80		

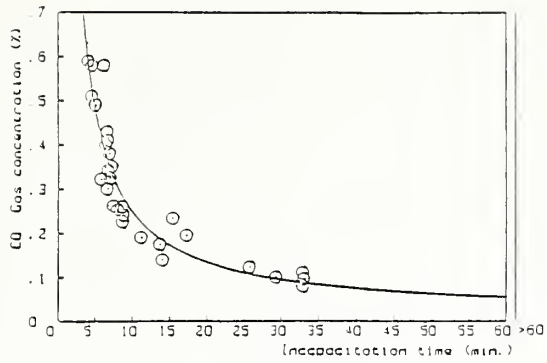


Fig. 1 CO gas concentration vs. incapacitation time, temp.: 30°C

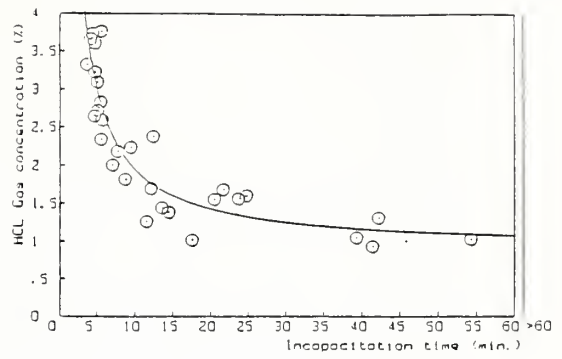


Fig. 2 HCl gas concentration vs. incapacitation time, temp.: 30°C

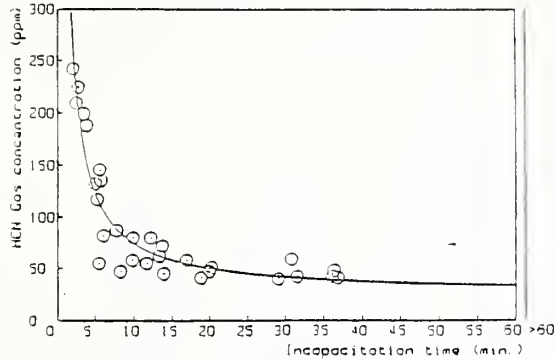


Fig. 3 HCN gas concentration vs. incapacitation time, temp.: 30°C

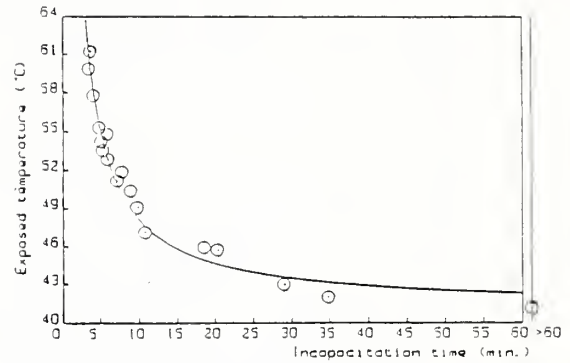


Fig. 4 Exposed temperature vs. incapacitation time

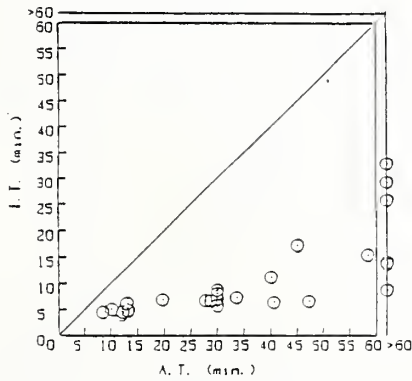


Fig. 5 Incapacitation time vs. apnoea time in case of CO gas, temp.: 30°C

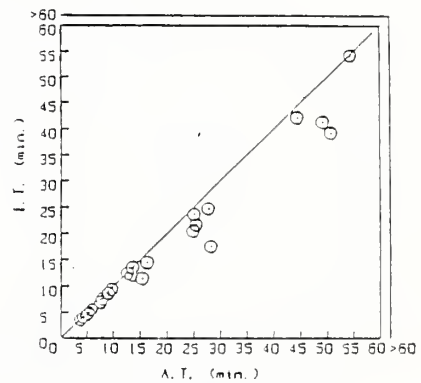


Fig. 6 Incapacitation time vs. apnoea time in case of HCl gas, temp.: 30°C

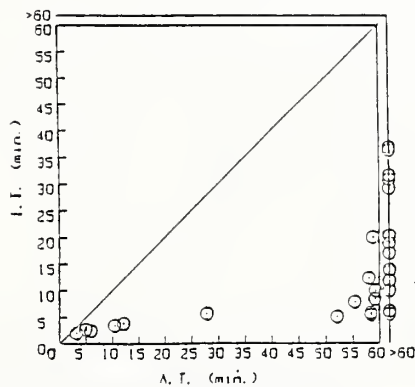


Fig. 7 Incapacitation time vs. apnoea time in case of HCN gas, temp.: 30°C

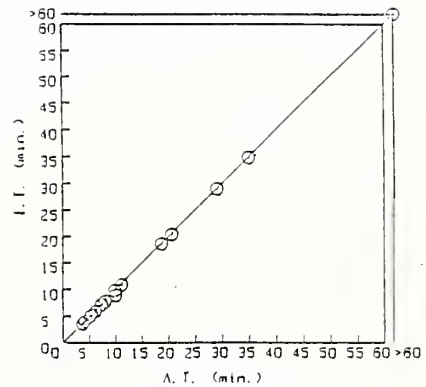


Fig. 8 Incapacitation time vs. apnoea time in case of temperature

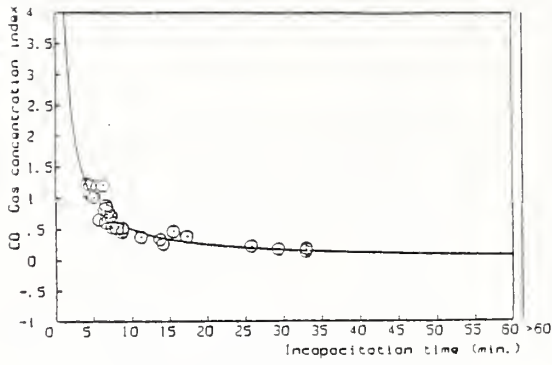


Fig. 9 CO gas concentration index vs. incapacitation time, temp.:30°C

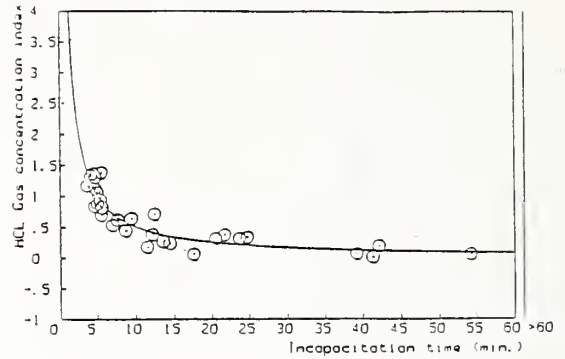


Fig. 10 HCL gas concentration index vs. incapacitation time, temp.:30°C

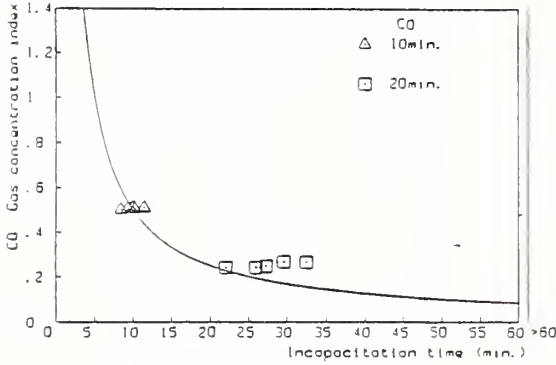


Fig. 11 CO gas concentration index vs. incapacitation time in case of CO,CO₂,H₂,O₂,SO₂, temp.:30°C

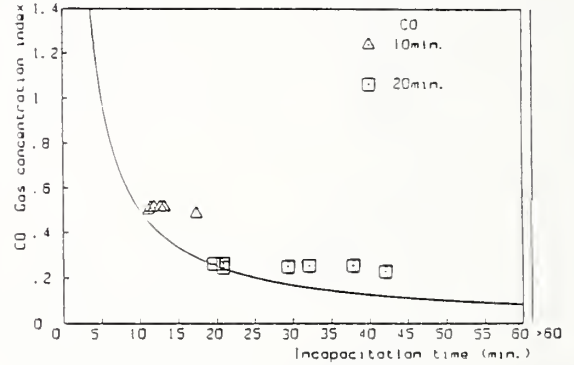


Fig. 12 CO gas concentration index vs. incapacitation time in case of CO,CO₂,H₂,O₂,SO₂, temp.:30°C

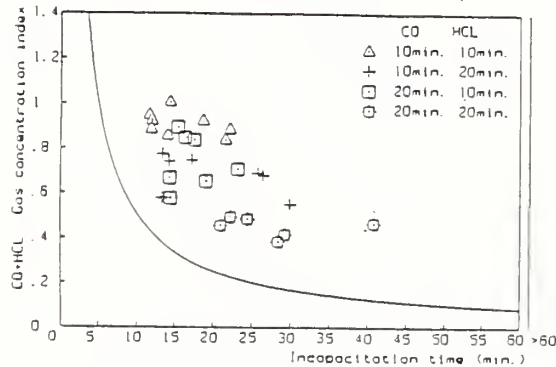


Fig. 13 CO+HCL gas concentration index vs. incapacitation time in case of CO+HCL, temp.:30°C

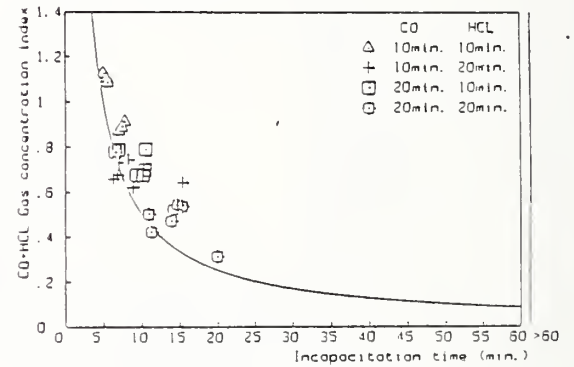


Fig. 14 CO+HCL gas concentration index vs. incapacitation time in case of CO+HCL,CO₂,H₂,O₂,SO₂, temp.:30°C

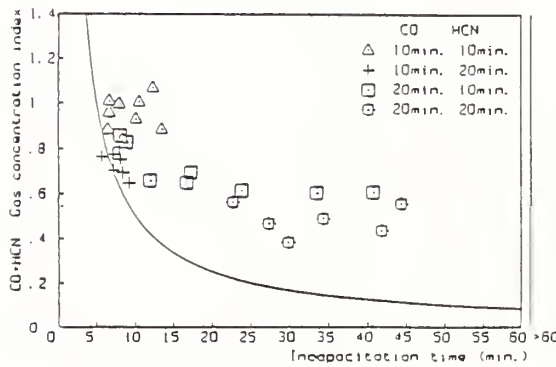


Fig. 15 CO+HCN gas concentration index vs. incapacitation time in case of CO+HCN, temp.:30°C

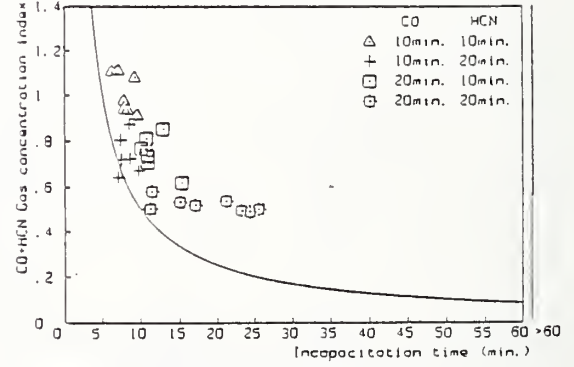


Fig. 16 CO+HCN gas concentration index vs. incapacitation time in case of CO+HCN,CO₂,H₂,O₂,SO₂, temp.:30°C

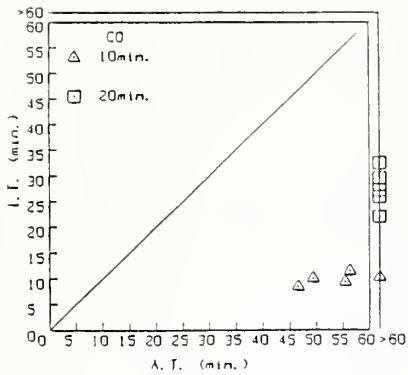


Fig. 17 Incapacitation time vs. apnoea time in case of CO , CO_2 , H_2 , O_2 , SO_2 , O_3 , CS_2

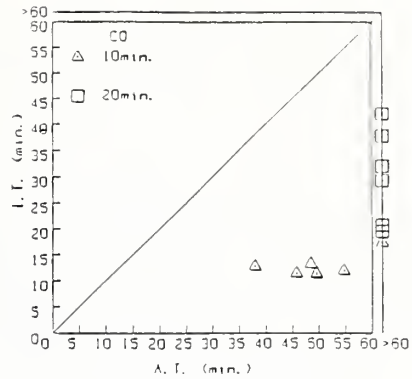


Fig. 18 Incapacitation time vs. apnoea time in case of CO , CO_2 , H_2 , O_2 , SO_2 , O_3 , CS_2

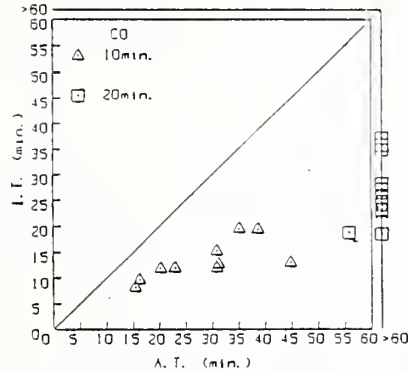


Fig. 19 Incapacitation time vs. apnoea time in case of CO , CO_2 , H_2 , O_2 , SO_2 , O_3 , CS_2

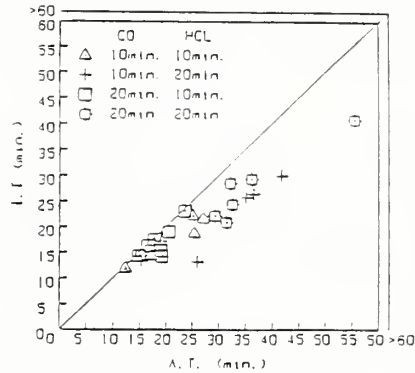


Fig. 20 Incapacitation time vs. apnoea time in case of CO/HCL , $Temp.: 30^\circ C$

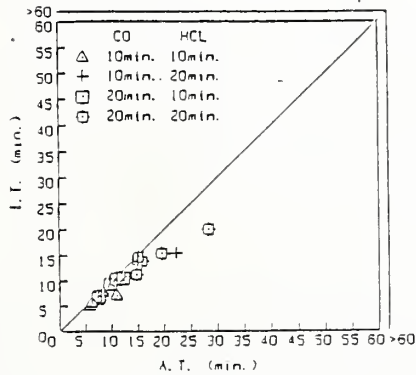


Fig. 21 Incapacitation time vs. apnoea time in case of CO/HCL , CO_2 , H_2 , O_2 , SO_2 , O_3 , CS_2 , $Temp.: 30^\circ C$

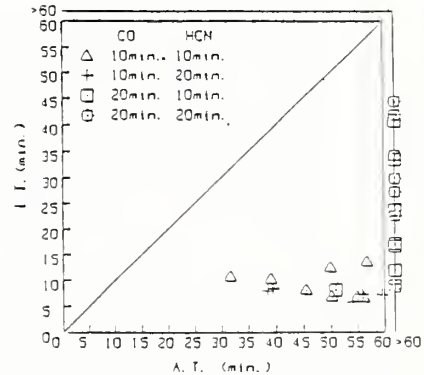


Fig. 22 Incapacitation time vs. apnoea time in case of CO/HCN , $Temp.: 30^\circ C$

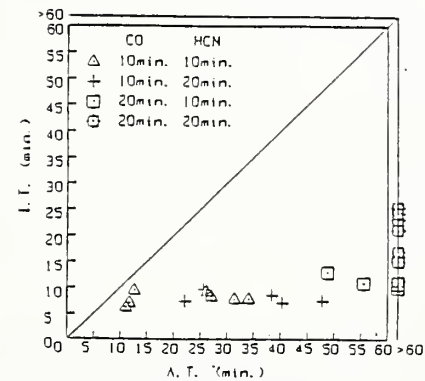


Fig. 23 Incapacitation time vs. apnoea time in case of CO/HCN , CO_2 , H_2 , O_2 , SO_2 , O_3 , CS_2 , $Temp.: 30^\circ C$

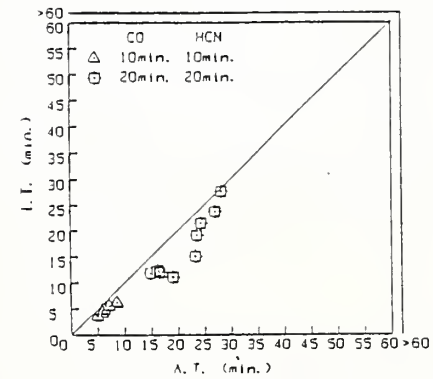


Fig. 24 Incapacitation time vs. apnoea time in case of CO/HCN , CO_2 , H_2 , O_2 , SO_2 , O_3 , CS_2 , $Temp.: 40^\circ C$, $Rh.: 60\%$

TOXIC GAS TEST BY THE SEVERAL PURE AND MIXED GASES

T. Sakurai, Japanese Association of Fire Science and Engineering, Japan

LEVIN: During your talk, you mentioned that your results on CO and CO₂ differ from my results. I believe the reason for this difference is from differences in the experimental procedures. I am not looking at lethal levels of CO, adding CO₂ and looking for decreases in the time of death because at those high concentrations of CO, the additional CO₂ may not make a big difference. I am looking at lower levels of CO, adding the CO₂, and finding that deaths occur. Sometimes these deaths occur 24 hours later, so the time to death within the exposure are not as important as the occurrence of death. The insult that the CO₂ adds may take time for the body to recognize or for the effect to take place. So, in your case, you're looking at the incapacitation level and looking for changes in the time. I think this may be the difference.

SAKURAI: In our case too, we do not experiment with CO₂ toxicity as such. As I explained at the beginning, when CO₂ concentration is increased, in 30 minutes, you have to have more than 20 percent; otherwise, incapacitation wouldn't occur, but the maximum was only 8 percent. We are interested only in effect of CO₂, that is the main objective of our experiments.

And, another thing, we are looking at the animals' incapacitations within 30 minutes or one hour, a rather short time. Your case is like 24 hours, so it is possible to get some different results because of the difference of time.

TSUDA: You have mentioned the additivity of CO₂. In the case of the patient sent to the hospital because of the CO poisoning, they would have such a test. In that case, not only O₂, we add the CO₂ also, mixed CO₂, in order to encourage the breathing of the patient, and then take out CO from the patient, so that the patient will be away from the toxicity of CO.

What do you think of this kind of phenomena?

LEVIN: I'd like to say that the CO₂ does stimulate respiration. If you're in the presence of CO, it will stimulate the uptake of the CO. If you are in the presence of oxygen, it will increase the rate of oxygen uptake into the body. Under these latter conditions, CO is reduced in the body (it's breathing it out). However, CO₂ also increases the acidosis of blood, and this may add a complication.

Strategy of Fire Suppression by Using Fire Retardants.

Toshisuke Hirano
University of Tokyo
7-3-1 Hongo, Bunkyo-ku, Tokyo 173.
and
Ichiroh Nakaya
Building Research Institute
1 Tatehara, Oho-cho, Tsukuba-gun,
Ibaraki 305, Japan.

ABSTRACT

The demand for the building materials treated with fire retardant chemicals is increasing. To assure healthy and safe human life, these materials should not pollute the air in the building even when they are involved in fires. The chemicals used for fire retardation are desirable to be inexpensive and easy to make treatment in addition to having no adverse effects on the physical properties of the materials. Unfortunately, none of the currently available chemicals meets all of these requirements. To develop the ideal chemical, a cooperative study by many researchers or specialists of various research fields, such as combustion science, chemical engineering, mechanical engineering, chemistry, toxicology and economy, is necessary. The development of the ideal chemical is the current world-wide concern. For the great success in this work, we proposed the initiation of an international cooperative study on this topic.

1. The role of fire retardants in fire suppression.

In many countries, some fire protections are required for materials used in a building. If all of them were incombustible, there would be no building fire but the number of furnishings and furnitures would be deadly limited and our lives would become restricted, unhealthy and wearisome. As we can't do without combustible materials, this is not a realistic method to overcome fire hazards.

There are two ways to improve the quality of materials against fires. One way is to combine a combustible material and an incombustible one. The other way is to treat a material with fire retardant(s). In the former way, the material is usually concealed behind the incombustible material. Furthermore, the total amount of combustibles, which may be important for the evaluation of fire hazards under fully developed fire conditions, is not decreased. So the latter way seems to be preferable in real situations.

The facility added to the materials by the treatment with fire retardants, is increase in the ignition delay time, slowing down of the flame spread speed or decrease in the pyrolysis or heat release rate. Usually these facilities don't work individually but together in a complex way. Such as, flame spread speed will be slowed down when ignition delay time become long or heat release rate are decreased.

2. Current fire retardants

In Japan, the number of chemicals permitted to use for fire retardations were about 250 in 1980(1). They are used as additive fire retardants, reactive fire retardants or surface coatings.

The additive fire retardants are generally used for cellulosic materials

or thermoplastic resins with few exceptions(2). The chemicals used as the additive fire retardants are injected by putting pressure or penetrated into cellulosic materials, or added to the polymer during processing plastic resins.

These chemicals belong to the halogenated compounds, the organo-phosphorus compounds, the halogenated organo-phosphorus compounds and/or the inorganic compounds(Table 1). The advantages of these fire retardants are easiness in processing and this lowers the manufacture cost. At the same time, however, the chemicals may be easy to migrate and to ooze from the materials.

Table 1. Typical chemicals used as additive fire retardants.

Types	Typical Chemicals
Halogenated Compounds	Polychloroparaffin Chloro-polyethylen Perchloro-pentacyclodecane Tetra-bromoethane Hexabromo-cyclodecane
Organophosphorous Compounds	Trimethyl-phosphate Triethyl-phosphate Tributyl-phosphate Trioctyl-phosphate Tributoxyethyl-phosphate Octyl-diphenylphosphate Triphenyl-phosphate
Halogenated Organophosphorous Compounds	Tris-chloroethyl-phosphate Tris-2-chloropropyl-phosphate Tris-2,3-dichloropropyl-phosphate Tris-2,3-bromopropyl-phosphate Tris-bromochloropropyl-phosphate 2,3-dibromopropyl-phosphate 2,3-chloropropyl-phosphate
Inorganic Compounds	Antimony Oxide Boron Compounds Aluminium Compounds Molybdenum Compounds

The reactive fire retardants are reactive monomers or crosslinking agents and are primarily used in unsaturated polyesters, epoxy resins and polyurethane foams(2). The chemicals used as the reactive fire retardants are chemically reacted with the polymer structure at some processing stage.

These chemicals belong to the acid compounds and/or the phospheric polyol compounds(Table 2). The main advantage of these chemicals is the permanence of the fire retardance imparted. In most cases chemically reacting the fire retardant into the polymer essentially eliminates long-term migration of the fire retardant. But these materials may be more expensive in the long run because of reacting the materials with the polymer. In some case the processing techniques are very difficult(2).

Table 2. Typical chemicals used as reactive fire retardants.

Types	Typical Chemicals
Acids Compounds	Tetrachlorophthalic anhydride Tetrabromophthalic anhydride Chlorendic acid Chlorendic anhydride Diallyl chlorendate
Polyols	Polyols which contain Halogen groups Phosphorous groups Halogen and phosphorous groups

The use of surface coatings has been mainly concentrated to increase the fire retardance of wooden products or textiles by painting. The surface coatings can be non-intumescent or intumescent. The non-intumescent coatings have a long history and are more widely used than the intumescent in addition that they are more economical. On the other hand, intumescent coatings are undoubtedly more effective in providing a high degree of protection on the underlying material(3). In any way, this type of fire retardant is easy to process but sometimes lacks the permanence of the fire retardance.

The chemicals used in the non-intumescent coatings belong to halogenated alkyd, fire retarded polyurethanes, epoxy resins with a reasonable degree of fire retardance, meramine-formaldehyde resins or phenol-formaldehyde resins. On the other hand, those used in the intumescent coatings belong to carbonific compounds, catalysts which promote decomposition of the carbonific compounds, spumific compounds or resin binders(3).

3. Suitable fire retardants

Most of the fire retardants belong to the halogenated compounds or the halogenated organocompounds. It is well known that the amount of smoke evolved during the burning of halogenated polymers are significantly greater than those derived from the corresponding non-halogenated polymers. Furthermore, halogenic acids, which are known to be highly toxic, are emitted as the final product.

These flame retardants which act chemically in the gas phase are of course generally react readily with active flame propagating species such as a hydroxyl radical. Then these active species are no longer available for the oxidative reaction of the gaseous fuel products. As cracking of the carbon-rich compounds tends to occur through the oxidation process, the lack of the active species cause eventually the formation of large amount of the carbon-rich solids which constitute smoke or carbon monoxide, which is also highly toxic, by incomplete combustion. The evolution of the smoke or toxic gas species is undesirable because it impedes egress and fire brigade activities which enlarge damages to be caused by fires. Thus the additives introduced to reduce the flammability of materials may increase the fire hazard at the same time.

The other flame retardant chemicals belong to inorganic or organo-

phosphorus compounds. These chemicals take effects mainly in solid phase and are usually encourage the formation of a char layer and/or water. The char layer is well known to act as the good thermal barrier. And water will increase the total latent heat of the material's pyrolysis. As the emission of the carbon-rich volatiles are suppressed, they are seldom to promote the formation of toxic gas species or smoke during the combustion of materials. But the cost to get satisfactory fire retardance using this kind of chemicals is more expensive than using the halogenated compounds.

The ideal chemicals used as additive fire retardant should be inexpensive, colorless, easily incorporated into the polymer composition, stable to heat and light, efficient in its fire retardant properties, nonmigrating, and have no adverse effects on the physical properties of the polymer. The toxicology of the chemicals and the gases produced by combustion are also of great concern(2). The same items should be required to the chemicals used as the reactive fire retardant or the surface coating. Unfortunately, most currently available chemicals seldom meet all these requirements.

4. The expected study subjects

Fire retardant chemicals take effect in gas phase and/or solid phase. In gas phase they quench active species or slow down the oxidative reaction speed. In solid phase, they suppress the production of combustible volatiles.

It is known that the hydroxyl radical plays great role in oxidative reactions of hydrogen and carbon. To quench the hydroxyl radicals, halogen atoms are usually used. These halogen atoms finally become halogenic acids. These acids are highly toxic. Furthermore, a great amount of smoke is produced as described previously.

On the contrary, the amount of smoke generation should become small if the concentration of the hydroxy radical is increased. This might be verified by the empirical knowledge that the generation of smoke is dramatically decreased when water spray is introduced into the flame region and that metal oxide with some crystal water act as smoke suppresser.

To control combustion reactions simply by dilution, the amount of inert gas required may be very large. If the adequate amount of inert gas can be introduced, this lowers the gas temperature and slow down the reaction speed of oxidation of combustible compounds because it help removing of active species by promoting their recombination reactions, which may increase the amount of smoke.

If carbons can be fixed into the solid phase and no carbon rich volatiles are not produced, the amounts of smoke generation and heat release should be reduced. Phosphorus compounds are known to promote the dehydration reaction in solid phase and to form a char layer at a fuel surface. Though there seems to be no report about the smoke suppression by phosphorus compounds, the amount of heat release is known to decrease by the treatment with the phosphorus compounds. This might be because these compounds also work in gas phase as the trap of active species(4).

Covering fuel surface by thermal barrier like a char layer or some coatings are effective to keep the fuel pyrolysis at low rate. The char layer is known to have poor thermal conductivity and high pyrolysis temperature. Phosphorus compounds are usually used for this purpose. This reaction is said to be dehydration but the details of its mechanism has not been fully revealed yet because it proceeds in the solid phase.

Intumescent or non-intumescent coatings are also used as the thermal

barrier. Sometimes, the spumific agents are added into the coatings or fire retardants to form thick thermal insulating layer over the fuel surface. The spumific mechanism has fairly well revealed. As the coated chemicals exist on the fuel surface, they are easy to migrated and to lose the fire retardance.

As described previously, the ideal fire retardant chemicals should be inexpensive, colorless, easy to process, stable to heat and light, harmless even when the materials treated by them were burned, but the chemical, that meets all of these requirements, has not been produced yet. To resolve all of the problems remained, the new ideal fire retardant chemicals or retarded materials should be developed using the knowledge obtained through studies in various research fields (Figure 1).

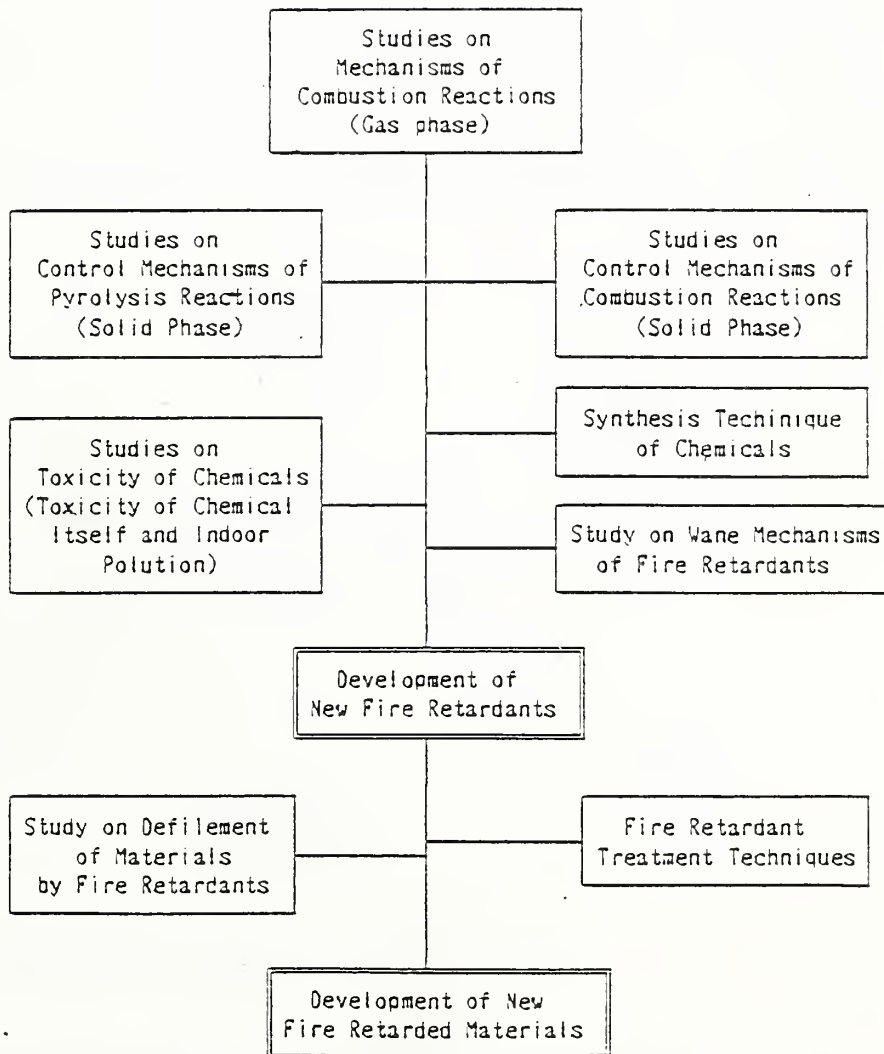


Figure 1. A Diagram to Develope New Fire Retarded Materisls.

5. Currently required research activities

In last July, a new group has founded in Japan to study the controlling mechanisms of combustion reactions. This group is composed of the specialists of various research fields and they belong to various organizations. For example, there are chemists, mechanical engineers, chemical engineers and combustion scientists who belong to universities, governmental institutes or private companies. In this group, discussion to understand controlling mechanisms of combustion reactions has mainly been done. Through the discussion, all of the members understood what is known or unknown.

The controlling mechanisms of combustion reactions by currently used chemicals have almost revealed but further studies to find the other possible mechanisms are still needed for the development of the ideal combustion control technique. To promote this study, the fundamental study by combustion scientists with the supports of chemical and mechanical engineers may be important. Furthermore, the discussions in the aspects of chemistry, toxicology and economy are indispensable because newly developed materials treated by the new chemical should be easy to produce, safe and cheap.

So the development of new types of fire retardants and extinguishers is desirable to be commenced by combustion scientists, chemical engineers, mechanical engineers, chemists, toxicologists and economists (Figure 2).

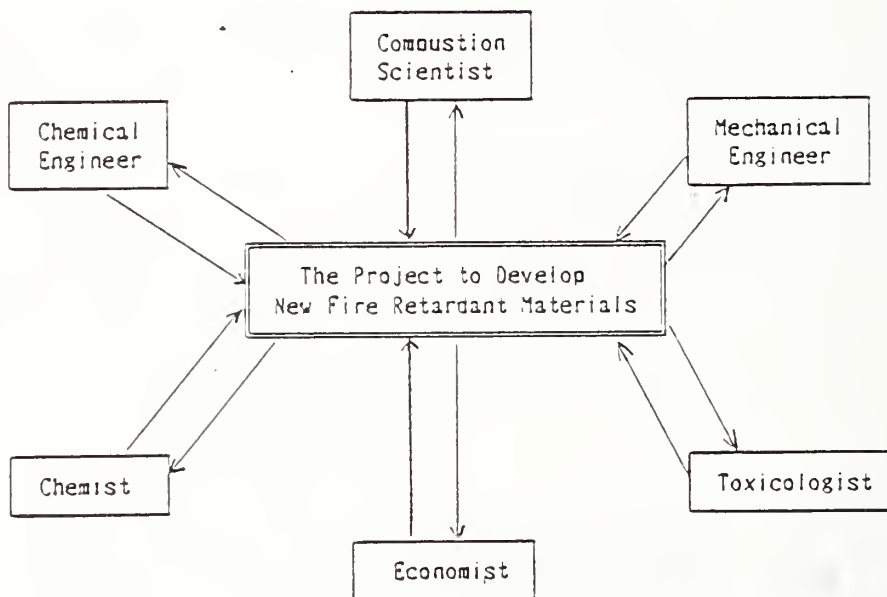


Figure 2. Tentative Plan for The Project Study.

As the development of new type of fire retardant chemicals or retardation techniques is world-wide concern, it will be wonderful if this project study can be promoted internationally. We proposed the initiation of a cooperative study to Dr.Gann(NBS), Dr.Harmathy(NRCC), Dr.Woolley(FRS) and

have a panel discussion on the theme of "Now and Future Aspects on Combustion Control in Fire" in the Second International Symposium on Fire Safety Science to be held in Tokyo on June 13-17, 1988.

Now we would like to propose the initiation of an international cooperative study to all of attendants at this conference again.

References.

1. Japan Fire Retardant Association: Sen'i To Bouen, San Print (1978).
2. A.H.Landrock: Handbook of Plastics Flammability and Combustion Toxicology, Noyes Publication (1983).
3. C.F.Cullis and M.M.Hirschler: The Combustion of Organic Polymers, Oxford University Press (1981).
4. H.B.Palmer and D.J.Seery: Combust. Flame 4, 213 (1960).

STRATEGY OF FIRE SUPPRESSION BY USING FIRE RETARDANTS

I. Nakaya and T. Hirano, University of Tokyo, Japan

TEWARSON: In the United States, there is a great interest to produce non-originated low smoke additives. In my individual research, I find that for most incorporation that is introduced, mostly into the final product, it does not only reduce smoke corrosive compounds, but also has reduced the level of emission. I would like to hear what is being done in Japan.

HIRANO: We are in the process of putting all this information, state and city posts together, so upon the completing of this report, we will provide you with a copy in the new form. When you receive the report, I would appreciate your comments.

As far as the flame suppression deterrent is concerned, they also have any number of activities in Japan. As far as practical applications are concerned, traditionally the Japanese have imported the kind of fire suppression deterrent technique from the United States, not vice versa.

I will try to expand upon the initial stage. Dr. Nakaya came up with the idea that he continue with the initial stage. As far as the basic research activities are concerned, there are a number of basic research activities in different countries all over the world, and on different topics. In this instance, we appreciate the fact that there is information and many documents available on various subjects.

Of course, each country is interested in developing excellent fire retardants. We too are interested in developing excellent fire retardants. In order to support this activity, we need basic research.

One more unsettled problem remains. This is due to the fact that our policy is not clear. As far as my personal policy is concerned, it's clear in my mind. However, the collective policy, various people with different disciplines, must come up with an integrated policy. We have not yet come up with an integrated policy and that's the reason why this is still fuzzy.

In addition to that, we also would appreciate Dr. Gann's participation on the thermal decomposition issue. As far as the cable fire is concerned, Dr. Tewarson can contribute to our organization. At the present, we have started to study fiber optics.

STUDIES ON THE TOXICITY OF SMOKE CONTAINING HYDROGEN CHLORIDE

G. E. Hartzell, A. F. Grand and W. G. Switzer
Department of Fire Technology
Southwest Research Institute
6220 Culebra Road
San Antonio, Texas 78238

ABSTRACT

Studies of rodent lethality due to exposure to HCl, as well as to mixtures of HCl and CO, have shown different apparent toxicological effects at low and at high concentrations of HCl. At low concentrations of HCl, sensory irritation causes a decrease in respiratory minute volume, with somewhat slower loading of CO and a delay in incapacitation. This effect is observable only at low concentrations of CO. At much higher HCl concentrations, pulmonary irritant effects are observed leading to postexposure lethality. An empirical analysis of the data for mixtures of HCl and CO suggests that exposure doses leading to lethality may be additive.

The lethal toxic potency (LC_{50}) of PVC smoke may be largely, but not entirely, accounted for by the HCl produced. However, PVC smoke exhibits a greater incidence of early postexposure deaths. The early deaths, which may be partially attributable to a combined effect of CO and HCl, may also be linked to the pattern of respiratory penetration by the smoke. There is evidence that components other than HCl are present which cause PVC smoke to be more irritating than HCl alone.

INTRODUCTION

Hydrogen chloride (HCl) is a relatively common component of fire effluents about which there has been much speculation and controversy. The studies reported here represent a continuation of our efforts to clarify the role of HCl in combustion toxicology.

In order to place new work in perspective, findings from selected previous studies will also be discussed. An attempt will also be made to develop the practical application of this knowledge to exposure of human subjects.

EXPERIMENTAL METHODS AND MATERIALS

EXPOSURE OF ANIMALS

Apparatus

The exposure apparatus used in these studies, illustrated in Figure 1, is similar in size and shape to that commonly used in the NBS smoke toxicity test [1]. However, it was modified to create a "flow-through" system. The air flow through the exposure chamber ranged from about 30 L/min up to about

200 L/min. This wide range of air flows was due to modification of the exhaust system during the course of the program in order to provide greater flexibility and control in generating and maintaining specific gas atmospheres. The higher flow rates permitted more rapid equilibration of the test atmospheres and more stability in the atmosphere once established.

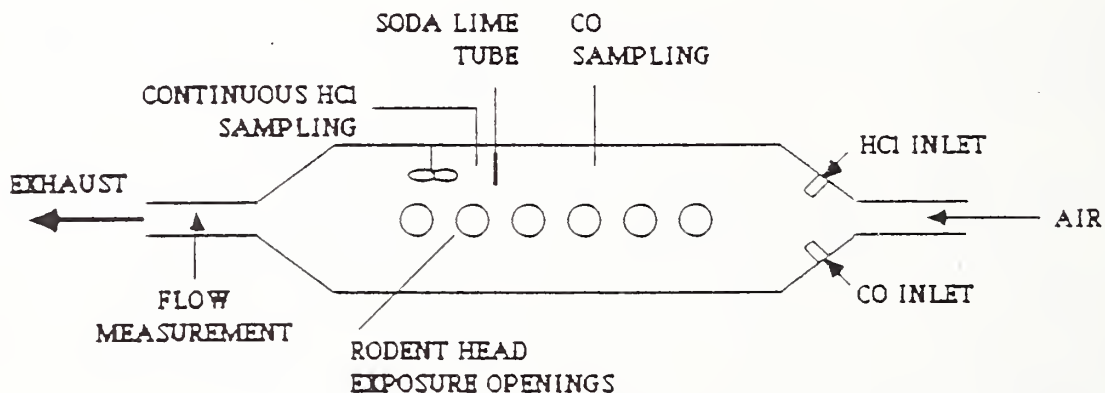


Figure 1. Flow-through exposure apparatus

The animal restraints and isolation system, used to protect the animals from the test atmosphere until equilibrium was established, was the same as that used in a previous study [2]. Incapacitation was determined using conventional leg-flexion shock avoidance apparatus [3].

Exposure Protocol

Each animal exposure test involved the exposure of six, young adult, male Sprague-Dawley rats positioned in tubular restrainers to provide for head-only exposure. Following insertion of the tubed animals into position through the wall of the chamber, the animal isolation system was closed and breathing air provided during the establishment of the desired test atmosphere. Thirty-minute exposures were initiated upon opening of the isolation system and termination of supplemental breathing air to the animals. End points recorded were incapacitation and lethality. Surviving animals were observed until either postexposure death or 14 days. Animals surviving 14 days were subsequently sacrificed.

Values for LC_{50} 's and 95-percent confidence limits were calculated from the data using a standard probit program.

For experiments during which it was desired to follow the time course of blood pH or COHb saturation, blood samples were withdrawn sequentially from several rats implanted with femoral artery cannulas. No cannulated rats were used in the calculation of LC_{50} values.

GENERATION OF TEST ATMOSPHERES

Pure Gas Atmospheres

"Pure gas" atmospheres were generated by the metering of the appropriate gases from cylinder sources into the exposure chamber, with continuous analytical monitoring of concentrations. Supplemental O_2 was provided as necessary to maintain the O_2 concentration at $20.5 \pm 1.0\%$.

Sources were:

Carbon Monoxide (99.9%): Scientific Gas Products
Hydrogen Chloride (99.5%): Scientific Gas Products

Polyvinyl Chloride (PVC) Fire Effluent Atmospheres

A continuous combustion apparatus, developed at SwRI, was used for the studies reported. Shown in Figure 2, it consists of a quartz tube 1 m long and 7.6 cm in diameter, with two radiant heating devices positioned exterior to the tube. One of several stainless steel combustion boats (ranging from 50 to 110 cm in length), containing a weighed quantity of PVC, was pulled at a constant rate of travel inside the tube past the radiant heater. The heat flux, sample weight and rate of travel of the combustion boat were predetermined to achieve the desired concentration of HCl in the fire effluent.

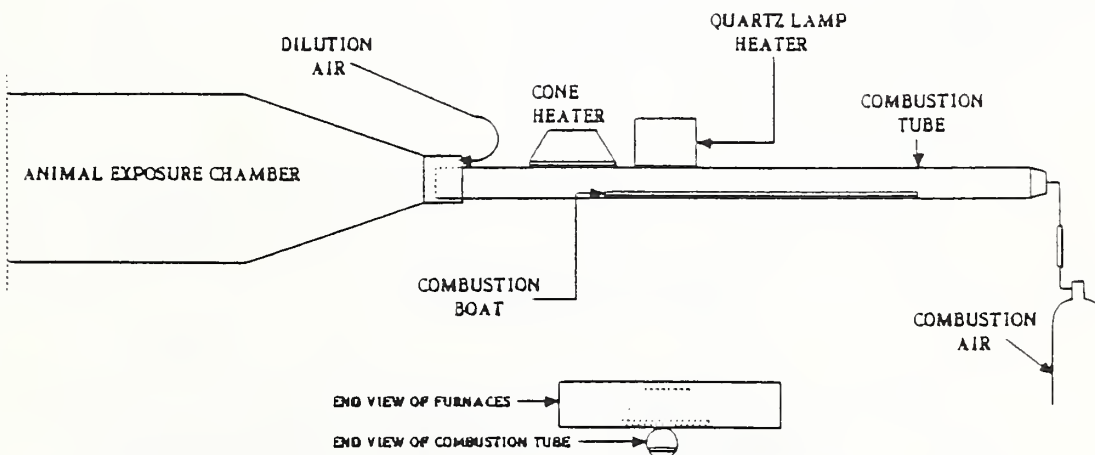


Figure 2. Continuous combustion apparatus

A constant flow of dry air (20 L/min) was metered into the combustion tube, with additional room air (from 30 L/min to approximately 200 L/min) being drawn into the system by an exhaust blower. The total flow of air through the apparatus was measured either by an orifice meter in the exhaust line or by calculation based on dilution of a carefully metered pure gas prior to the combustion experiments.

Different radiant heat furnaces were used for flaming and for nonflaming conditions. Nonflaming combustion was conducted at 3 W/cm^2 , using a cone heater (the same as used in the NBS cone calorimeter). However, the cone heater was unable to produce the higher fluxes (6 W/cm^2) necessary for flaming PVC experiments. Therefore, a tungsten-quartz lamp heating device was used for the flaming mode. A small coil of resistance wire, connected to a variac and mounted inside the combustion tube, was the ignition source used to sustain flaming combustion.

Shown in Figure 3 is the relationship found between the HCl concentration produced and the quantity of PVC burned, expressed as $\text{mg}\cdot\text{L}^{-1}$. The latter values were estimated from the mass of PVC charged, sample travel and air flow rates.

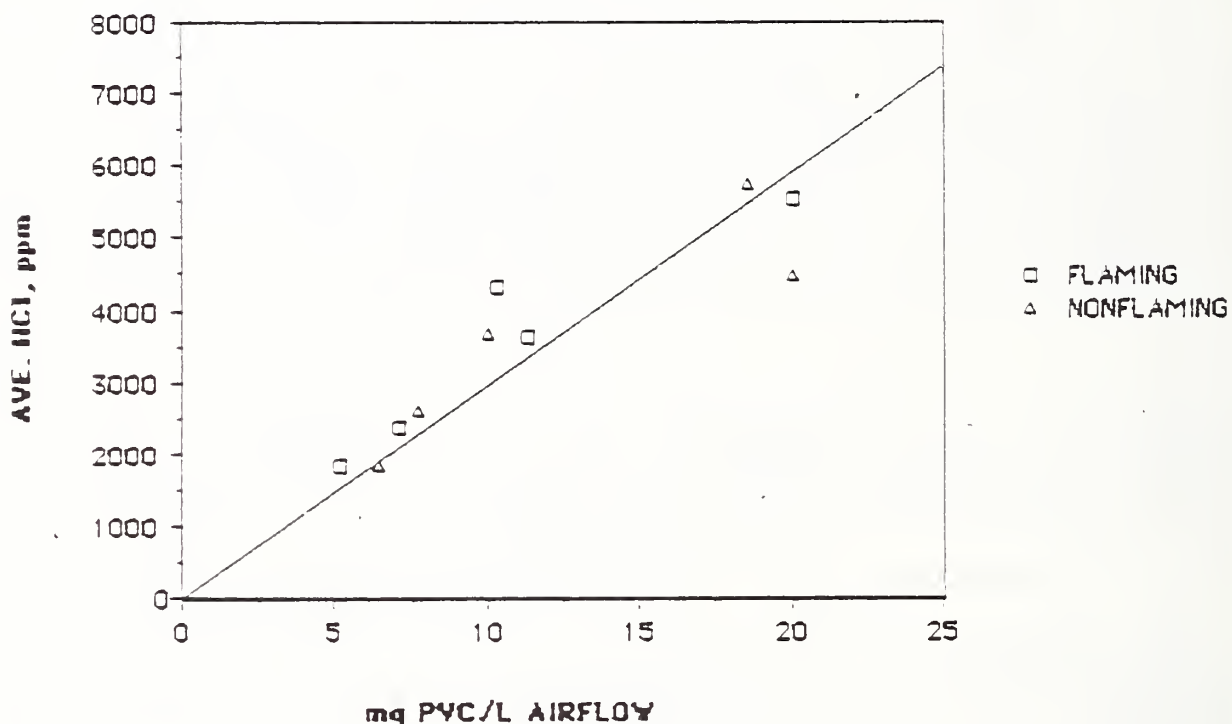


Figure 3. Plot of HCl concentration produced as a function of mass of PVC charged per liter of airflow

The polyvinyl chloride (PVC) used was natural, unplasticized material in pellet form supplied by the B. F. Goodrich Chemical Company. It contained two parts lubricant and two parts stabilizer per hundred parts resin.

ANALYSIS OF TEST ATMOSPHERES

Asphyxiant Toxicants

Analyses of exposure atmospheres for CO , CO_2 and O_2 were continuously conducted using a closed loop sampling system and the following instruments:

Carbon Monoxide:	Beckman 865
Carbon Dioxide:	Beckman 865
Oxygen:	Beckman OM-11

Hydrogen Chloride

The method used for continuous monitoring of hydrogen chloride (HCl) gas, both in a "pure gas" atmosphere and in smoke, was based on that reported in a French standard test method [4], with instrumentation and procedures modified in our laboratories. Complete verification of this method, including measurement of interferences, has not been done. Therefore, for most experiments, "back-up" analyses of HCl were also performed by soda-lime tube (SLT) sampling followed by aqueous extraction and titration [5].

A schematic drawing of the continuous HCl method is illustrated in Figure 4. A sample of an atmosphere containing HCl is drawn continuously by a pump into a gas-solution impinger containing 0.1 N HNO₃ aqueous solution. A silver/silver chloride electrode (or electrode pair) and a pipette for introduction of silver nitrate (AgNO₃) titrant are positioned in the cell. The basic principle is to maintain a predetermined electrical potential (emf) in the test solution by automatically metering in AgNO₃ to react with chloride ion. The rate of addition of titrant is directly proportional to the concentration of HCl in the sample gas stream.

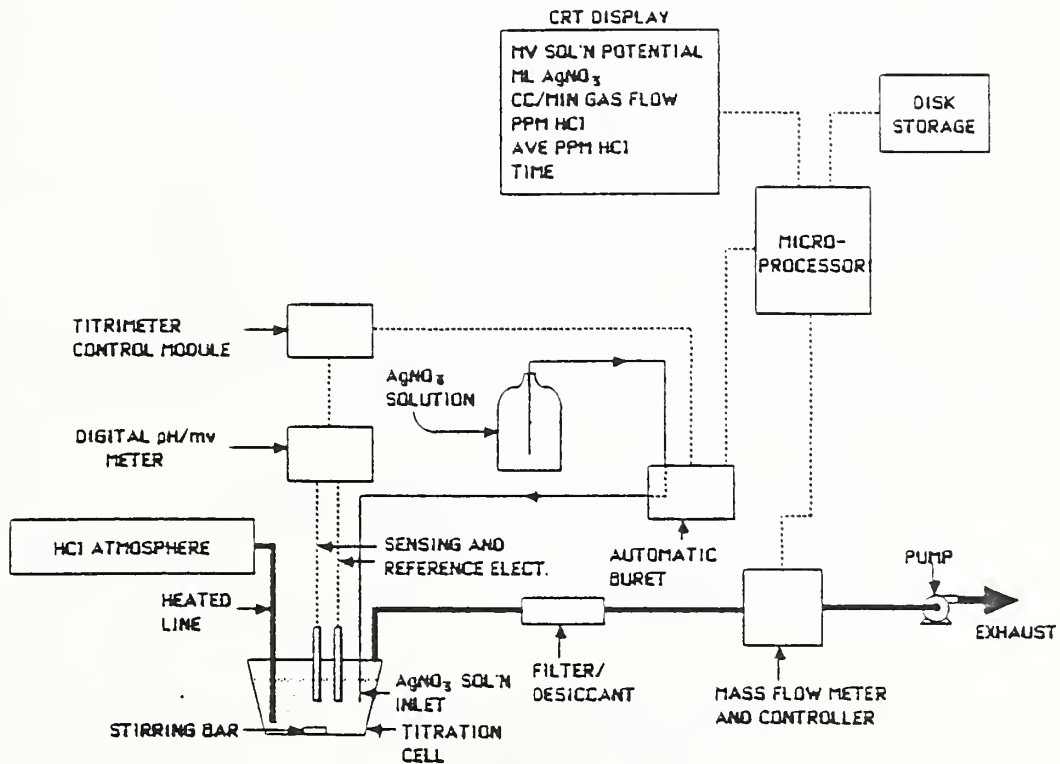


Figure 4. Continuous analysis of HCl

In operation, any increase in HCl is detected as a change in the emf of the solution. This value (mv) is monitored by a digital pH/mv meter connected

to a "stat titrator" control module, which controls the dispensing of silver nitrate titrant solution through an automatic buret. When the emf of the solution deviates from the set point due to addition of chloride, the buret dispenses AgNO_3 in order to return the emf to the set point. This process continues as needed to maintain the solution at the set point, which is near the equivalence point of a silver-chloride titration.

The higher the concentration of HCl in the test atmosphere (or the higher the gas flow rate), the faster the silver nitrate is run into the titration cell. The output of the automatic burette (mL of titrant) is linked directly to an Apple IIe microcomputer for computation of HCl concentration. A mass flowmeter is used to monitor (and control) the gas flow, its output also going to the computer. Calculations are performed every 10 seconds in order to time-average the quantity of AgNO_3 being used. Due to fluctuations in the quantity of HCl introduced into the impinger during any given 10-second increment, an additional time average is performed over three successive readings. This final averaging "smoothes out" the curve of HCl vs time. The increment of time for each calculation and the interval for determining the "average" HCl are both under the control of the operator. The following data are displayed on the computer monitor every 10 seconds (or any other increment selected):

- 1) emf of the solution (mV);
- 2) total volume of AgNO_3 consumed (mL);
- 3) sample gas flow rate (cc/min);
- 4) concentration of HCl (ppm);
- 5) "average" HCl concentration (ppm) over the selected time interval; and
- 6) current run time (minutes and seconds).

Immediately following each experimental run, a plot of HCl concentration vs time may be constructed from the stored data.

RESULTS

A total of eight LC_{50} (30-minute exposure plus 14-day observation) values were determined. Data obtained are summarized in Tables 1 and 2.

TABLE 1. CARBON MONOXIDE LC_{50} VALUES*
(30-MINUTE EXPOSURE + 14 DAYS)

Atmosphere	LC_{50} (ppm)
CO	6400
CO (600 ppm HCl)	5700
CO (1000 ppm HCl)	5300
CO (1000 ppm HCl/PVC smoke)	7100

*Values are rounded to the nearest 100 ppm

TABLE 2. HYDROGEN CHLORIDE LC₅₀ VALUES*
(30-MINUTE EXPOSURE + 14 DAYS)

Atmosphere	LC ₅₀ (ppm)
HCl	3800
HCl/PVC (Nonflaming)	2900
HCl/PVC (Flaming)	2100
HCl (3000 ppm CO)	2100

*Values are rounded to the nearest 100 ppm

DISCUSSION

Although hydrogen chloride can exert toxicological effects in a variety of complex ways, two are relevant to this study: 1) as a sensory irritant and 2) as a pulmonary irritant. At low concentrations, it is primarily a sensory irritant resulting in depression of a rodent's respiratory rate and respiratory minute volume (RMV). The effect, which is concentration-related rather than dose-related, is often quantified as that concentration causing a 50-percent decrease in respiratory rate (RD₅₀). The RD₅₀ for the Sprague-Dawley rat is about 600 ppm [2].

Sensory irritation is an effect of the inhalation of HCl which, although generally not leading to lethality, does have a perturbing effect on the inhalation and resulting toxicity of CO. Earlier work (time-to-effect studies) reported that in the presence of HCl, respiratory rate and minute volume depression increase somewhat the observed times to the toxicological effects of CO, particularly if the CO concentration is relatively low, i.e., less than about 4000 ppm [2]. Above approximately 4000 ppm CO, the presence of the irritant has increasingly less influence on times to physiological effects due to the very rapid loading of CO. Concentrations of HCl above about 1000 ppm have little additional effect over that observed with 1000 ppm since increasingly less additional depression of RMV occurs above that concentration. The overall effect of the presence of HCl on intoxication of rats by CO is relatively minor and is mostly observed in a "window" of perhaps 400 to 1000 ppm HCl and with CO concentrations up to about 4000 ppm.

It must be emphasized that the effects of a sensory irritant on CO toxicity may be limited to rodents. The significance and applicability to human exposure remain to be determined from primate studies. There is evidence that, with primates, exposure to a sensory irritant results in decreased arterial blood pO₂ values which may increase its sensitivity to CO [6].

A comparison of the sensory irritant effect of smoke produced from the burning of PVC with that of simple gaseous HCl is of particular interest. An equivalent concentration of HCl contained in PVC smoke (nonflaming decomposition) increased observed times-to-incapacitation over most of the concentrations of CO studied, not just at the lower concentrations, thus giving indication of sensory irritation somewhat greater than that produced by HCl, alone. Furthermore, the 30-minute LC₅₀ of CO in the presence of 1000 ppm HCl contained in PVC smoke (nonflaming) (7100 ppm with 95-percent confidence of 4300 to 6500 ppm) was greater than that for CO in the presence of simple HCl

(5300 ppm with 95-percent confidence of 6300 to 8000 ppm). This "lower toxicity" of CO in the presence of smoke produced from the nonflaming decomposition of PVC is another indication that irritants more potent than HCl may be present which act to depress further the RMV and slow the loading of CO. (The greater irritancy of PVC smoke than would be expected from the HCl content has previously been reported based on experimental measurements [7]). It must be emphasized that these effects are reported for exposure of rodent; primates, including humans, have not been studied.

Hydrogen chloride, when present at high concentrations, is thought to penetrate into the lower respiratory tract and exerts its lethal toxic effect as a pulmonary irritant [3]. Pulmonary edema and subsequent death often follow exposure to HCl at high concentrations. Postexposure lethality results from exposure doses much lower than those required for either incapacitation or within-exposure lethality [8].

Concentration-response relationships for postexposure lethality of rats exposed to HCl have been studied over a range of exposure times from 5 minutes to 60 minutes [9]. Exposure doses (LC_{50} 's) ranged from about 80,000 ppm-min to about 170,000 ppm-min, respectively. Higher exposure doses can be tolerated if the HCl concentration is relatively low. Conversely, progressively higher concentrations of HCl result in tolerance to decreasing exposure doses. The 30-minute LC_{50} (postexposure lethality) for HCl was determined to be about 3700 ppm within a static system [9] and about 3800 ppm for a flow-through system. Considering the 95-percent confidence limits for postexposure lethality due to pulmonary irritants, the difference between these two values is not significant.

Very limited experience with baboons has indicated that 150,000 ppm-min (5- to 15-minute exposures) is probably on the threshold of postexposure lethality [9]. Although there has been no experience with human exposures under controlled conditions, somewhat conservative estimates based on the nonhuman primate experience would indicate that perhaps 100,000 ppm-min would likely result in very severe complications and even death.

The 30-minute (plus 14-day observation) LC_{50} of HCl as contained in smoke from the nonflaming decomposition of PVC (little or no CO present) was found to be 2900 ppm (95-percent confidence of 2200 to 3700 ppm). Although somewhat lower than the value of 3800 ppm (95-percent confidence of 3100 to 4800 ppm) for HCl, itself, it would be most reasonable to conclude that the postexposure lethal toxicity (LC_{50}) of nonflaming PVC smoke can largely be accounted for by the HCl content. Further support for this statement can be obtained from the data plotted in Figure 3, in which an HCl concentration of 2900 ppm corresponds to a PVC concentration (mass charged) of about $10 \text{ mg}\cdot\text{L}^{-1}$. Although this value is somewhat lower than that reported from the NBS cup furnace test [1], a greater observed toxicity of PVC smoke would be expected from the combustion method used in this study due to the absence of any HCl generation delay time and also the absence of HCl decay.

The mechanism of action of HCl is so very different physiologically from that of CO, that it would be anticipated that these two toxicants should be considered separately in predicting hazardous exposure conditions through the use of the Fractional Effective Dose model [10]. Fractional doses would not be expected to be additive, as in the case of CO and HCN. However, the LC_{50}

data on mixtures of CO and HCl tempt one to consider additivity on an empirical basis. In Table 3 are shown data for some limited mixtures of CO and HCl in which the summation of fractional lethal doses approximates unity for 50-percent lethality with 30-minute exposures. In Table 4 is shown a comparable treatment of data using PVC as the source of HCl. It would appear that the increased lethal toxicity of HCl as contained in smoke from the flaming combustion of PVC may be attributed only in part to the contribution of CO produced. The full explanation may be quite complex, however, since the gas/aerosol/particulate nature of real smoke may result in a different pattern of respiratory penetration. For example, particulate deposition in the upper respiratory tract may obstruct breathing of rodents and further stress an already compromised oxygen transport system.

TABLE 3
SUMMATION OF FRACTIONAL EFFECTIVE (LETHAL) DOSES FOR 30-MINUTE EXPOSURE
OF RATS TO MIXTURES OF CO AND HCl

CO		HCl		Σ FED (Lethality)
ppm	Fractional Lethal Dose	ppm	Fractional Lethal Dose	
6400	1.0	—	—	1.0
5700	0.89	600	0.16	1.05
5300	0.83	1000	0.26	1.09
3000	0.49	2100	0.55	1.04
—	—	3800	1.0	1.0

TABLE 4
SUMMATION OF FRACTIONAL EFFECTIVE (LETHAL) DOSES FOR 30-MINUTE EXPOSURE
OF RATS TO MIXTURES OF CO AND HCl AS PRODUCED FROM PVC

CO		HCl		Σ FED (Lethality)
ppm	Fractional Lethal Dose	ppm	Fractional Lethal Dose	
ca. 700	ca. 0.11	2100 (flaming)	0.55	ca. 0.66
7100	1.11	1000 (nonflaming)	0.26	1.37
—	—	2900 (nonflaming)	0.76	0.76

As discussed earlier, smoke from the nonflaming decomposition of PVC would appear to be more irritating than expected from the HCl content. Thus, in the case of CO being the major toxicant, the summation of FED's was found to be considerably greater than unity when HCl from nonflaming PVC smoke was present at the sensory irritation level. Although smoke from the nonflaming combustion of PVC would appear, based on summation of HCl FED's, to be more toxic (as a pulmonary irritant) than expected, the significance of the difference is questionable.

Particularly striking, both in the case of the flaming combustion of PVC (with which up to 1680 ppm CO was produced) and in the case of HCl in the presence of 3000 ppm CO supplied from a cylinder source, was the incidence of postexposure deaths the same day as the exposure, usually within an hour.

This is rare, except at high concentrations, for HCl, alone. Data showing the incidence of these early postexposure deaths are shown in Table 5.

TABLE 5
COMPOSITE LETHALITY OF RATS EXPOSED TO ATMOSPHERES
CONTAINING HYOROGEN CHLORIDE*

Atmosphere	Animals Exposed	Number of Deaths			LC ₅₀ HCl in ppm	
		Exposure	Day 0	Days 1-4		Days 5-14
HCl	60	0	0	21	9	3800
PVC Smoke-Nonflaming	36	0	0	10	8	2900
PVC Smoke-Flaming	30	1	4	5	19	2100
HCl + 3000 ppm CO	30	1	2	8	17	2100

* At nominal approximate HCl concentrations of 1800, 2600, 3500, 4300, 5500 and 6500 ppm.

Attempts to elucidate the effect of CO on the postexposure lethality of HCl were inconclusive, but did suggest somewhat impaired ability of rats to return to homeostasis following exposure. Exposure of rats to a mixture of 5300 ppm HCl and 3000 ppm CO was characterized by a relatively rapid initial drop in blood pH and slower than normal postexposure unloading of COHb. Even with these data (compared with those for CO alone), it is difficult to speculate as to the cause of the incidence of same day postexposure lethality. The observations reported with rodents may pose some significance in the case of immediate postexposure complications following human exposures to mixtures of CO and HCl (e.g., prolonged hypoxemic conditions after rescue or escape).

In summary, it would seem that the lethal toxicity of combinations of CO and HCl can be predicted from an FED model. However, only limited success was obtained when applied to real smoke from PVC. This may be due to complications in respiratory penetration patterns involved with the complex gas/aerosol/particulate mixtures found in smoke.

ACKNOWLEDGEMENT

This work was supported under U. S. National Bureau of Standards Grant No. 60NANB6D0635. Development of the analytical and combustion methodology described was supported by the Vinyl Institute of The Society of the Plastics Industry, Incorporated.

REFERENCES

1. Levin, B. C., A. J. Fowell, M. M. Birky, M. Paabo, A. Stolte and D. Malek, "Further Development of a Test Method for the Assessment of the Acute Inhalation Toxicity of Combustion Products," NBSIR 82-2532, National Bureau of Standards, Gaithersburg, Maryland (1982).
2. Hartzell, G. E., H. W. Stacy, W. G. Switzer, D. N. Priest and S. C. Packham, "Modeling of Toxicological Effects of Fire Gases: IV. Intoxication of Rats by Carbon Monoxide in the Presence of an Irritant," J. Fire Sciences, Vol. 3, pp. 263-279 (July/August 1985).

3. Klimisch, H. J., J. E. Doe, G. E. Hartzell, S. C. Packham, J. Pauluhn and D. A. Purser, "Bioassay Procedures for Fire Effluents: Basic Principles, Criteria and Methodology," J. Fire Sciences (In Press).
4. French Standard (AFNOR) FD X 70101 December 1982, "Analysis of Combustion and Pyrolysis Gases - Smoke Chamber Method."
5. Grand, A. F., H. L. Kaplan, J. J. Beitel, W. G. Switzer and G. E. Hartzell, "An Evaluation of Toxic Hazards from Full-Scale Furnished Room Fire Studies," Fire Safety: Science and Engineering, ASTM STP 882, T. Z. Harmathy, Ed., American Society for Testing and Materials, Philadelphia, Pennsylvania, pp. 330-353 (1985).
6. Kaplan, H. L., A. Anzueto, W. G. Switzer and R. K. Hinderer, "Effects of Hydrogen Chloride on Respiratory Response and Pulmonary Function of the Baboon," J. Toxicology and Environmental Health, submitted for publication (March 1987).
7. Barrow, C. S., Y. Alarie and M. F. Stock, "Sensory Irritation and Incapacitation Evoked by Thermal Decomposition Products of Polymers and Comparisons with Known Sensory Irritants," Arch. Env. Health, Vol. 33, p. 79 (1978).
8. Kaplan, H. L., A. F. Grand, W. G. Switzer, D. S. Mitchell, W. R. Rogers and G. E. Hartzell, "Effects of Combustion Gases on Escape Performance of the Baboon and the Rat," J. Fire Sciences, Vol. 3, pp. 228-244 (July/August 1985).
9. Hartzell, G. E., S. C. Packham, A. F. Grand and W. G. Switzer, "Modeling of Toxicological Effects of Fire Gases: III. Quantification of Post-Exposure Lethality of Rats from Exposure to HCl Atmospheres," J. Fire Sciences, Vol. 3, pp. 195-207 (May/June 1985).
10. Hartzell, G. E., D. N. Priest and W. G. Switzer, "Modeling of Toxicological Effects of Fire Gases: II. Mathematical Modeling of Intoxication of Rats by Carbon Monoxide and Hydrogen Cyanide," J. Fire Sciences, Vol. 3, pp. 115-128 (March/April 1985).

STUDIES ON THE TOXICITY OF SMOKE CONTAINING HYDROGEN CHLORIDE
G. Hartzell, A. Grand, and W. Switzer, Southwest Research Institute, USA

TEWARSON: Would you discuss the impact of the low HCl concentrations?

HARTZELL: Low concentrations of HCl, such as a few hundred parts per million, are extremely irritating, and may very well cause a person to not want to escape. Physiologically, he could escape a much higher concentration. And the concentrations required to kill are very high. In terms of toxicity, hydrogen chloride is really not all that toxic. On a scale of irritants, hydrogen chloride is not very irritating. There are worse irritants. We know very little about behavioral effects, not physical but behavioral effects, of people exposed to these very strong irritants.

TSUCHIYA: Can you describe the this difference with PVC flaming smoke and PVC non-flaming smoke?

HARTZELL: The non-flaming is not particularly visible, very light smoke, whereas the flaming is quite noticeable. To some extent, we're able to get the same results of HCl and CO, as we obtained from flaming PVC. However, flaming PVC also had soot particles and water, so there are other complications.

GANN: You mentioned a factor of 30 between the mortality data and some escape data. Is this hundred versus 30?

HARTZELL: At the last Tripartite Committee meeting, results from Dr. Alarie's lab on running speed and potential for escape, remembering that the LC₅₀'s were widespread, something like several thousand parts per million, they measured the onset of slowing of burning of a couple hundred parts per million, and significantly determined well below 1,000. Dr. Alarie announced that the difference between the two would be a factor of 7.

TOXIC GASES FROM COMBUSTION OF WOOD TREATED WITH RETARDANTS

Toshimi HIRATA and Sumire KAWAMOTO

Forestry & Forest Products Res. Inst.
P. O. Box 16, Tsukuba Norin Kenkyu Dancni-Nai,
Ibaraki, 305 Japan

ABSTRACT

Combustion toxicity of wood has been attributed to CO. That for wood treated with retardants, however, could not satisfactorily be explained exclusively by the CO evolution. Therefore, toxicants other than CO were researched. First, evolutions of NO_x and SO₂ were determined from retardant treated wood during JIS A 1321 tests by means of IR spectroanalyzers. Secondly HCN evolution from the wood heated in an imaging furnace was measured by ion chromatography with an electrochemical detector. The HCN results are discussed in terms of the dependences on air flow rate and temperature. The data are useful for the reasonable explanation of the combustion toxicity of the retardant treated wood.

1. INTRODUCTION

Combustion toxicity of wood treated with several retardants has been reported(1), which is determined in incapacitation and death of mice according to the Ministry of Construction Noticefication 1231. The reported data have been rearranged and reviewed with respect to the incapacitation time against the CO concentration in the mouse-exposed chamber and the survived mouse percentage against the retardant contents. The results obviously show that the combustion toxicity cannot be explained exclusively by the CO evolution, though it has been accepted to be attributed to the CO production.

In the rearrangement a relation between the CO concentration and incapacitation time was approximated by a regression function

$$Y = 6.43 X^{-0.46} \quad (1)$$

where Y is the incapacitation time and X the maximum CO concentration, as shown in Fig. 1. It is noticeable that two samples treated with guanidine sulfamate and ammonium sulfamate yielded a lot of plots downward deviated from the regression line, and that on the contrary, boron compound treated samples gave many plots deviated upward. On the other hand, the plots about the death of mice indicate interesting tendencies that the survived mice increased with the content of boron compounds, but that with ammonium phosphate and ammonium sulfamate they decreased after the increases to the maxima, as shown in Fig. 2. Furthermore, for the guanidine sulfamate treated samples, the survived mouse percentage at four chemical content levels are 0 except 4.2 % at a 15 % chemical content level. Since the CO evolution decreased with the increase in the chemical content, these observations suggest that combustion toxicity for retardant treated wood depends not only on CO but also other toxic gases. Therefore, the present study has been carried out to search such toxicants.

2. EXPERIMENTAL

2-1. Samples

Wood used for the JIS A 1321 Surface Flammability Test is 22 x 22 x 1

cm red lauan (*Shorea*, *rubroshorea* section) of the air-dried specific gravity 0.43 to 0.51. The surface of specimens which was finished by a planer is approximately parallel to the fiber direction. By means of a full-cell process they were impregnated with diammonium hydrogen phosphate, ammonium bromide, guanidine sulfamate, ammonium sulfamate, boric acid, sodium tetraborate decahydrate, sodium chloride, or sodium borate plus boric acid. All of the chemicals were CP grade. Before and after the impregnation the specimens were conditioned at constant temperature 22° C and relative humidity 65 %. Therefore, the chemical contents in the specimens could be determined from the weight differences. Before the tests they were dried at 40° C for 72 h and then cured with silica gel for 24 h in order to preclude effects of water in the wood on the combustion.

Another sample for isothermal heating is pulverized Japanese cedar (*Chriptomeria japonica*) wood which passed through a 16 mesh but not through a 40 mesh screen. The sample was immersed in diammonium hydrogen phosphate, ammonium dihydrogen phosphate, guanidine sulfamate, or ammonium sulfamate solution in the different concentrations. The sample recovered from the solution was freeze-dried and the chemical contents were calculated from the weight increase. The water-extracted amount from the wood was found to be negligible. Before the heating the samples were dried longer than 48 h at a temperature 60° C.

Resin samples of urea-formaldehyde and melamine-formaldehyde, tested partly, were prepared in the laboratory. The former resin was synthesized from 1 mole of urea and 1.8 mole of formaldehyde in catalysts, hexamethylenetetramine and sodium hydroxide by being hardened with a hardener ammonium chloride at a temperature 105° C. The latter was prepared from pure oligomer soak MA-50 (from Honen Food Oil Inc.) by heating at 120° C for 2 h. Both the samples were pulverized so as to pass a 200 mesh screen. Before the heating they were also dried at 60° C.

2-2. Heating and gas analysis

For measurement of NO_x and SO_2 the 22 x 22 x 1 cm specimens were heated in a surface flammability test apparatus in accordance with JIS A 1321-1975. A part of combustion gas in a flow rate 3 L/min was introduced from the smoke chamber into Fuji Electric Infrared Gas Analyzers Model ZAL and ZBYB to analyze SO_2 and NO_x , respectively.

On the other hand, the pulverized wood about 1000 mg or resin about 30 mg was heated by an imaging furnace in a thermal balance Sinku Riko TG 1500RH-J-S at a temperature 600°, 800°, or 1000° C in an air flow rate 30, 100, 300, or 600 mL/min. The sample temperature reached a desired value from the room temperature within 1 min. Pyrolysis gas was introduced into a series of two spiral traps through a pass heated at 300° C, as shown in Fig. 3. The traps were chilled by dry ice-methanol in Dewar flasks but the first one was heated at the gas inlet portion by the mantle heater of 300° C. Therefore, it condensed products in a wide temperature range. The products in the traps were resolved in 0.1 N sodium hydroxide solution and analyzed for CN^- by Yokogawa-Hokusan Ion Chromatoanalyzer Model IC-100 with an electrochemical detector Model ED-11.

3. RESULTS AND DISCUSSION

3-1. Evolutions of NO_x and SO_2

Concentration of NO_x in the smoke chamber increased with the heating time, as shown by examples in Fig. 4. The gas accumulated in the smoke chamber reached the maximum concentration in a time range near 10 min. It is noted that the concentration started to increase earlier with specimens treated with nitrogen containing retardants.

The maximum NO_x concentration in 10 min increased with the contents of guanidine sulfamate, ammonium phosphate, and ammonium sulfamate, but was reduced with boron compounds and sodium chloride, as shown in Fig. 5. That for ammonium bromide seems to increase with the small certain content but to be retained constant at this increased value in spite of the content increase more than the certain point around 10 kg/m^3 . Similar relations were found for the maximum NO_x concentration normalized for the weight loss of specimens, namely, the maximum NO_x concentration per unit weight loss. NO_x is accepted to be originated from both of fuel and air, and called fuel NO_x and thermal NO_x , respectively. The increase in NO_x from the specimens treated with the nitrogen containing retardants is obviously attributable to the fuel NO_x production, as shown in Fig. 6, where the NO_x per unit weight loss is shown to increase with the nitrogen content of the treated specimens. It may be said on the basis of a regression line in the figure that guanidine sulfamate and ammonium sulfamate produced more NO_x than ammonium bromide and ammonium phosphate at an equivalent nitrogen content. It should be noted that the latter two retardants contain nitrogen in ammonium groups while guanidine sulfamate has it in amino and imino groups, and that ammonium sulfamate at a middle place of the NO_x production has both ammonium and amino groups. Therefore, amino and imino groups might produce more NO_x than an ammonium group.

The decrease in NO_x with the treatments by the chemicals other than the above retardants is inferred to be caused by the reduction in thermal NO_x , since NO_x increased with $\text{td}\theta$, as shown in Fig. 7. The $\text{td}\theta$ is assumed to be an indicator for heat release, which decreased with the retardant treatment. By the way, NO_x from the untreated wood is attributable to not only thermal one but also to fuel NO_x , because wood usually contains nitrogen less than 1 % of the weight(2-7).

Also SO_2 was generated from the combustion and accumulated in the smoke chamber, as shown in Fig. 8. The generation is especially high from the specimens treated with sulfur containing retardants. The maximum SO_2 concentration per unit weight loss of specimens increased with the ammonium sulfamate and guanidine sulfamate contents, and slightly with ammonium bromide, as shown in Fig. 9. However, those for ammonium phosphate and boron compounds decreased with the contents, and that for sodium chloride is constant independently of the content. Since the sulfur content of ammonium sulfamate (28.1 % in the weight) is higher than that of guanidine sulfamate (20.5 %), the higher SO_2 concentration was yielded from the ammonium sulfamate treated wood than from the guanidine sulfamate treated one. The SO_2 production per unit weight loss seems almost equally to increase with the sulfur content between the guanidine sulfamate and ammonium sulfamate treated samples, though the latter samples gave a linear regression line with a slightly steeper slope and more scattered plots, as shown in Fig. 10. Since wood usually contains sulfur less than 0.1 % of the weight(5,8), the untreated specimens seem to produce low SO_2 concentrations. Sulfur as well as nitrogen is believed to present in proteins in wood. It is considered that the proteins is first pyrolyzed and then SO_2 is formed. The pyrolysis and the SO_2 formation would be affected by the retardants.

3-2. Evolution of HCN

All HCN production values were converted into the molar concentration in the sodium hydroxide solution per one gram of burnt samples.

The HCN productions from the wood samples increased with the retardant contents, as shown in Fig. 11 where results from the heating at 800°C are given. It is shown that the HCN production is the highest from the guanidine

sulfamate treated wood and the lowest from the ammonium phosphate treated samples. No difference is discernible between the samples treated with diammonium hydrogen phosphate and ammonium dihydrogen phosphate. The HCN increase with the retardant content is linear in a low air supply rate as 30 mL/min, but in higher air flow rates the increase rate decreasingly changed with the content and was inclined to be leveled off. The HCN production was reduced with the heating temperature lowered to 600° C. Also at this temperature in 30 mL/min of air flow rates the production increased linearly with the retardant contents, as shown in Fig. 12. From the linear plots the HCN production per unit mass of retardants was determined and listed together with that at 800° C in Table 1. The table clearly shows the decrease in the HCN production with the reduced temperature.

The effects of air are more definitely seen in Fig. 13. Here the differences of the HCN production among the retardant contents are shown to be noticeably large in the lowest air flow rate but gradually to decrease with the increase in the air flow. The HCN production in the highest air flow 600 mL/min, especially from the ammonium phosphate treated wood is almost equal irrespectively of the different content of the retardant.

The nitrogen contents in the weight of retardants are 35.9 % for guanidine sulfamate, 24.6 % for ammonium sulfamate, 21.2 % for diammonium hydrogen phosphate, and 12.2 % for ammonium dihydrogen phosphate, respectively. Therefore, the HCN production appeared to depend on the nitrogen content. From plots of the HCN production against the nitrogen content in Fig. 14, however, it is seen that again guanidine sulfamate produced the highest HCN and ammonium phosphate gave the lowest HCN production in an equivalent nitrogen content. This suggests that HCN production is different depending on conformation of nitrogen compounds and that amino and imino groups yield more HCN than an ammonium group. Furthermore, it should be noted that guanidine sulfamate owned C-N bonds by itself.

The HCN productions from urea and melamine resins decreased with the increase in the air supply 30 to 100 mL/min, and slightly decreased or was retained constant in spite of the air supply more than 100 mL/min, as shown in Fig. 15. The temperature dependences of the HCN production in 30, 300, and 600 mL/min of the air flows are given in Fig. 16, where the temperature dependence is shown to decrease with the air flow rate.

The monomers of the two resins, urea and melamine have two and three amino groups bonded to carbon, respectively, as shown in Fig. 17. Furthermore, melamine combines three nitrogens in its heterocycle. Then both of the monomers own two nitrogens for every carbon. From the elemental analysis, the urea and melamine resins are estimated to contain nitrogen in an approximately equal quantity, namely about 31 and 28 % of the weight, respectively. Nevertheless, the latter resin usually gave HCN more than two times of that from the former.

The urea resin suddenly starts to lose the weight in a high rate at about 230° C in both air and helium atmospheres of the thermogravimetry (TG) (9). On the other hand, it is found that the melamine resin decomposes slowly at first and rapidly loses the weight at about 360° C in air and 405° C in helium flow of the TG(10). The rapid weight loss probably reveals the heterocyclic ring cleavage. It is interesting that the thermally stable resin produced more HCN than the unstable resin. It might occur in the pyrolyses that the less stable resin caused a lot of scission of C-N bonds to form more oxidized products, while the melamine resin retained more C-N bonds for a longer time and formed more HCN. In addition it has to be taken into consideration that the heterocycles of the melamine resin, which imparted the high thermal stability, have three C-N bonds for every carbon,

and that the urea resin has for the most part two C-N covalent bonds for every carbon except side groups such as methylol, methylene, and so forth. These factors may be the cause of the different HCN productions between the two resins.

If the whole of nitrogen in the samples is converted into HCN, though the reaction mechanism in fact may be different depending on the nitrogen compounds, one gram of the retardants or the resins should produce HCN ranging from 8700 ppm in mole for ammonium dihydrogen phosphate to 25600 ppm for guanidine sulfamate. At the present study, however, the HCN production is far low, namely, which ranges from 0.07 % of the above potential value for diammonium hydrogen phosphate to 0.91 % for the melamine resin. Guanidine sulfamate yielded the highest percentage 0.21 % of the treated wood samples, which compares one half of the highest value of ones for the urea resin.

4. CONCLUSIONS

- 1) Evolution of NO_x from combustion of wood increased with nitrogen containing retardants and decreased with other retardants due to reduction in thermal NO_x . Amino and imino groups in the retardants produced more NO_x than an ammonium group.
- 2) Wood treated with sulfur containing retardants yielded more SO_2 than other retardants.
- 3) HCN production from wood treated with nitrogen containing retardants increased with the contents, and decreased with the increase in the air flow rate and the decrease in temperature 800° to 600° C. Amino and imino groups in the retardants produced more HCN than an ammonium group.
- 4) Urea resin produced less HCN than melamine resin, probably because the urea resin was easier to be decomposed and oxidized at the C-N bonds than the melamine resin.
- 5) It can more satisfactorily explain results previously reported of combustion toxicity(1) that toxic gases other than CO, especially HCN were observed from combustion of wood treated with guanidine sulfamate, ammonium sulfamate, and ammonium phosphate.

Acknowledgement

The authors wish to express their thanks to Dr. S. Yusa, Building Res. Inst., for the advice and cooperation in the HCN measurements, and to Mr. Y. Fukui, Forestry & Forest Products Res. Inst., for the NO_x and SO_2 measurement.

References

- 1) Uesugi, S., Fukui, Y., and Abe, H.: J. Japan Wood Res. Soc., 27, 428 (1981).
- 2) Nikitin, N. I.: "The Chemistry of Cellulose and Wood", Israel Program for Scientific Translation, Jerusalem, p. 34(1962).
- 3) Furukawa, T.: J. Japan Forestry Soc., 45, 99(1963)
- 4) Kato, Y., Doi, K., and Furukawa, T.: J. Japan Forestry Soc., 45, 191(1963)
- 5) Tilman, D. A.: "Wood as an Energy Resources", Academic Press, N. Y., p. 71, 73, and 84(1978)
- 6) Bethl, J. S. and others: Rept. Office Technol. Assessment Congress U. S., OTA-C-78-339, p. 246(1979)
- 7) Karchesky, J. and Koch, P.: U. S. Forest Service General Technical Rept., SO-24(1979) .
- 8) Sakurai, K.: Bull. Forestry Forest Prods. Res. Inst., No. 335, 141(1986)
- 9) Hirata, T., Oguro, A., and Inoue, A.: Wood Preservation, 12, 279(1986)

10) Hirata, T.: Not published.

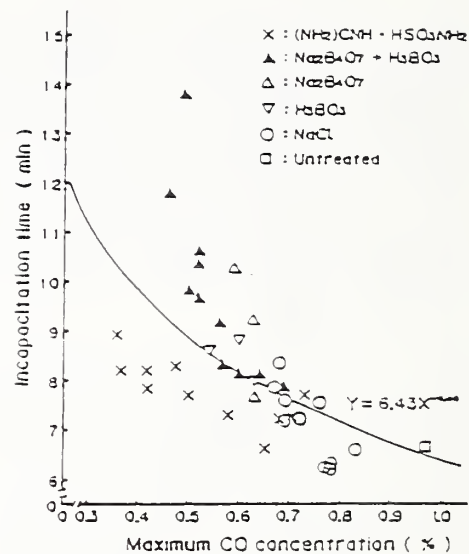
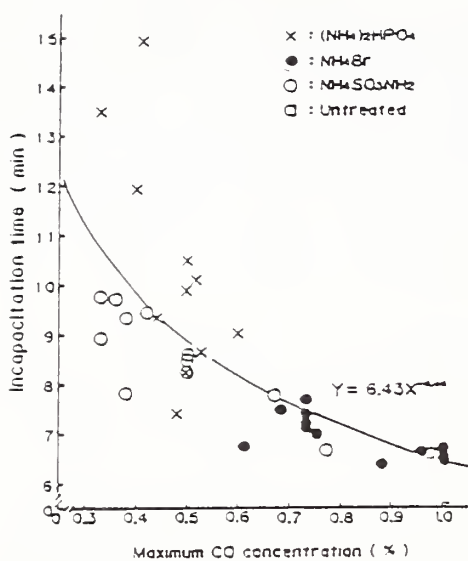


Fig. 1 Changes in incapacitation time with CO concentration

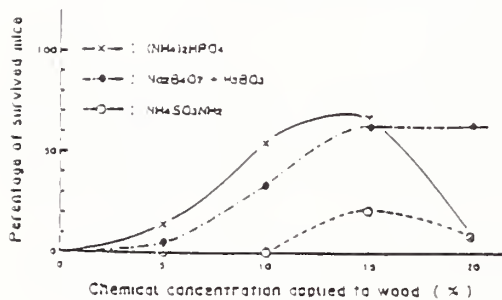
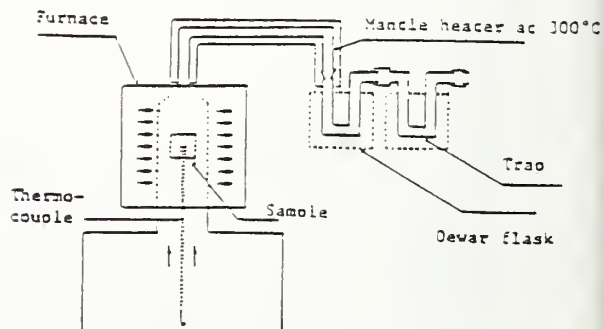


Fig. 3 Heating apparatus and HCN traps

Fig. 2 Changes in percentage of survived mice with retardant concentration applied to wood specimens



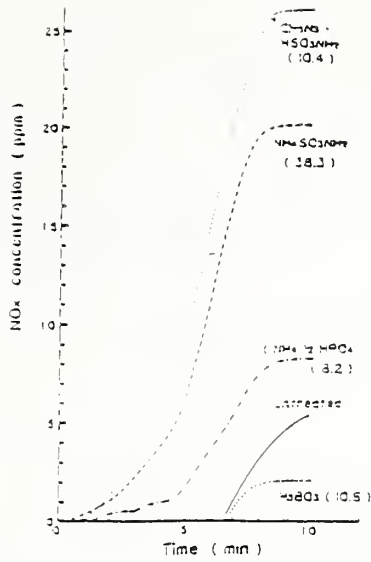


Fig. 4 NO_x increase with heating time

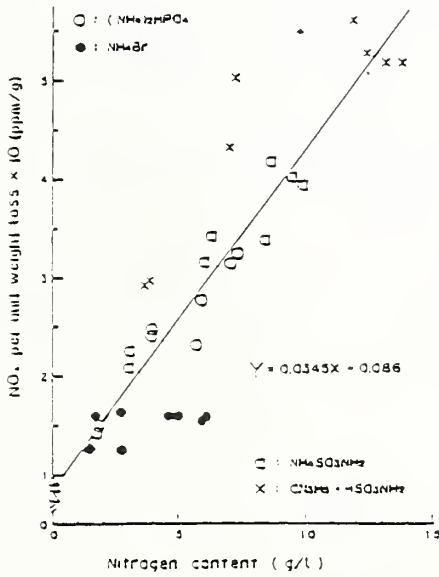


Fig. 6 NO_x increase with nitrogen content

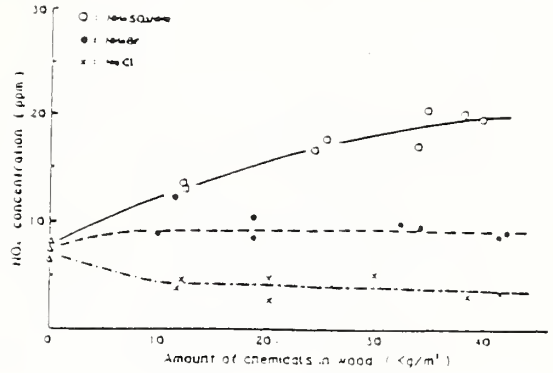


Fig. 5 - 1

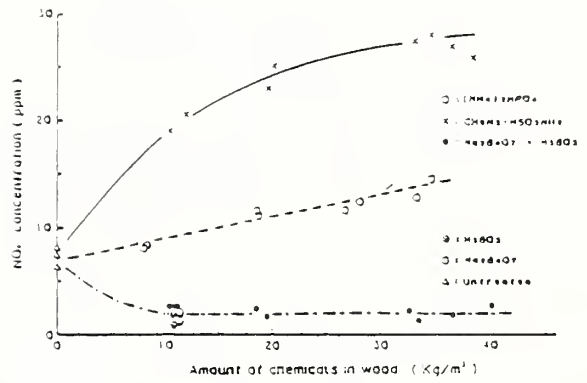


Fig. 5 NO_x evolutions

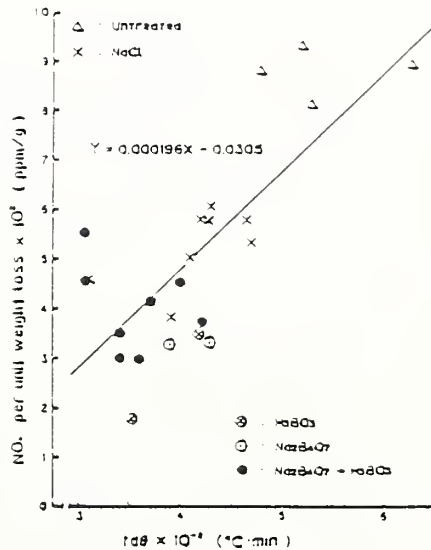


Fig. 7 NO_x increase with tΔθ

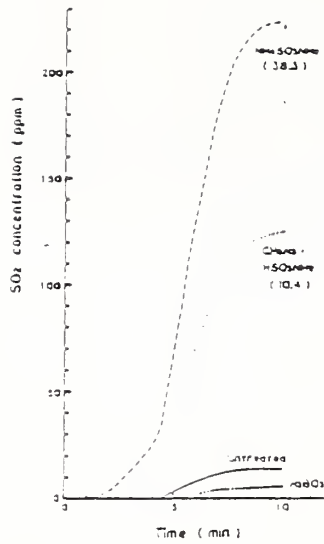


Fig. 8 SO₂ increase with heating time

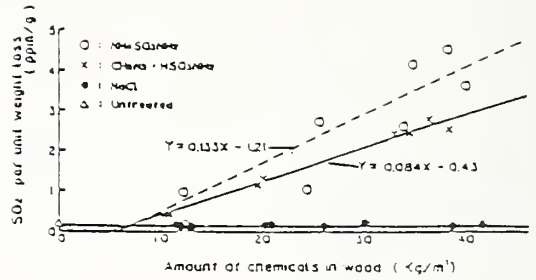


Fig. 9 - 1

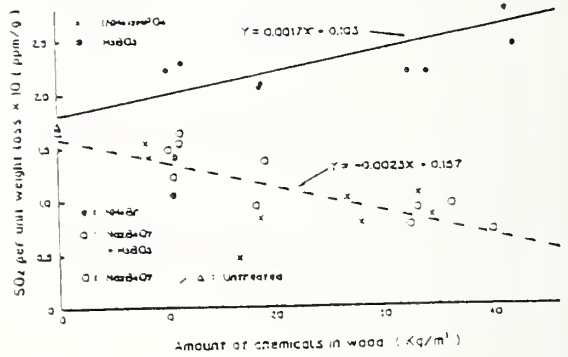


Fig. 9 Changes in SO₂ productions with retardant contents

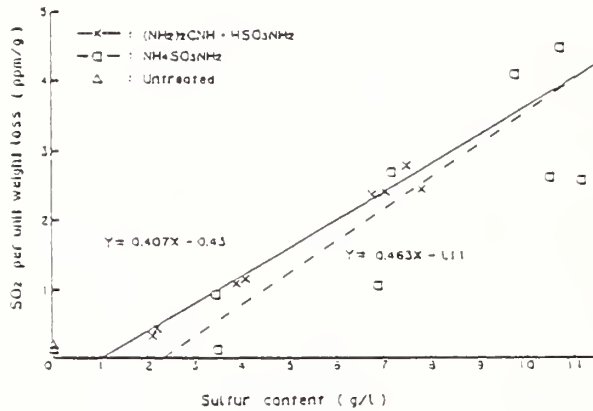


Fig. 10 SO₂ increase with sulfur contents

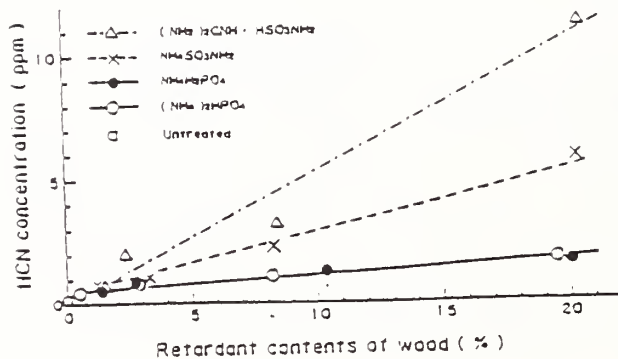


Fig. 11 - 1 Air flow rate: 30 mL/min

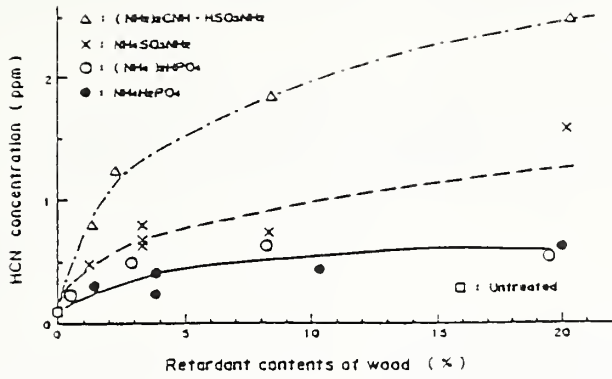


Fig. 11 - 2 Air flow rate:
300 mL/min

HCN increase with
retardant contents at
temperature 800° C

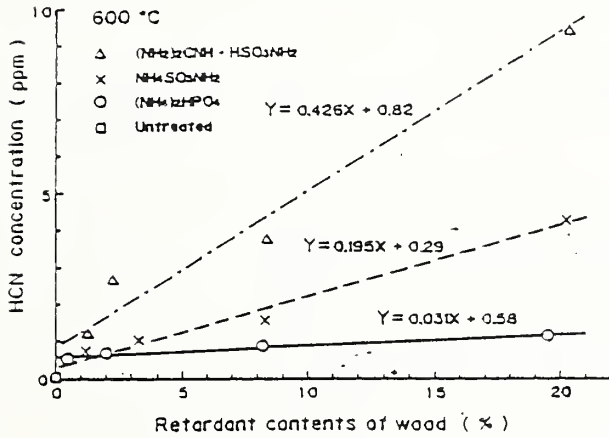


Fig. 12 HCN increase with
retardant contents at
temperature 600° C

Table 1 HCN production per one gram of retardants or nitrogen(ppm)

Retardants	800° C Retardant	Nitrogen	600° C Retardant	Nitrogen
NH ₄ H ₂ PO ₄ and (NH ₄) ₂ HPO ₄	6.4	34.6	3.1	14.6
NH ₄ SO ₃ NH ₂	27.4	112.0	19.5	79.3
CN ₃ H ₅ .HSO ₃ NH ₂	52.6	146.5	42.6	118.7

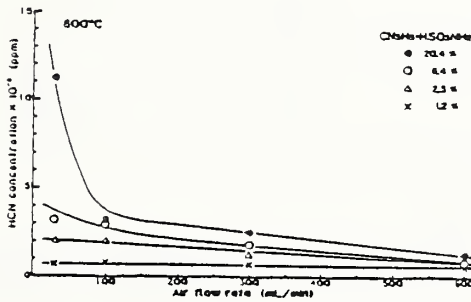


Fig. 13 - 1

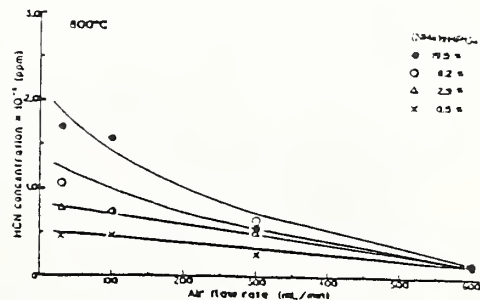


Fig. 13 - 2

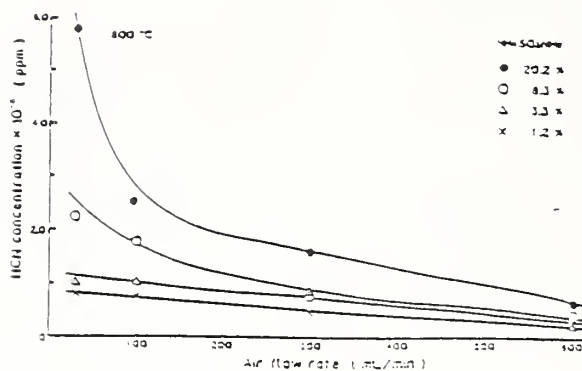


Fig. 13 Changes in HCN production with air flow rate

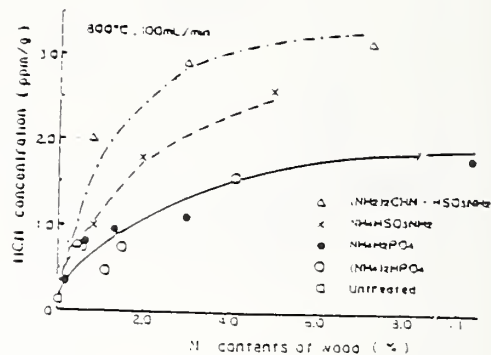


Fig. 14 Changes in HCN production with nitrogen contents

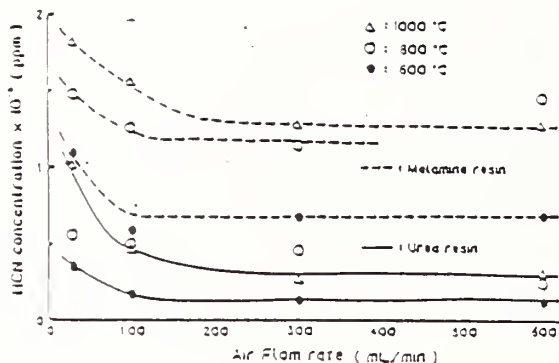


Fig. 15 HCN production from urea and melamine resins

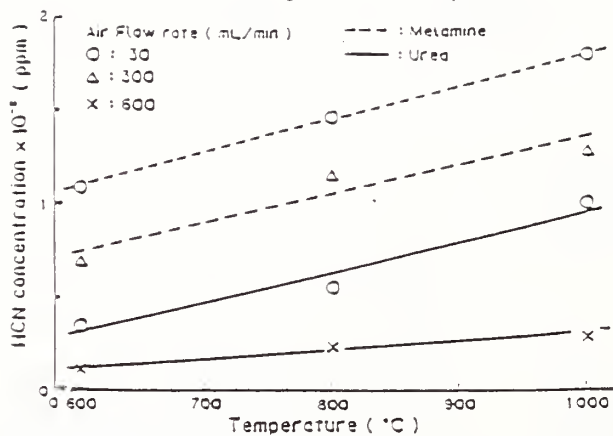


Fig. 16 Temperature dependences of HCN production from urea and melamine resins

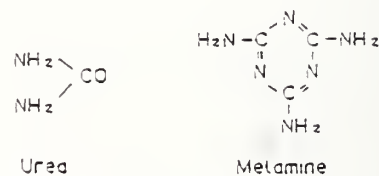


Fig. 17 Chemical formulae of urea and melamine

TOXIC GASES FROM COMBUSTION OF WOOD TREATED WITH RETARDANTS
T. Hirata, Forestry and Forest Products Research Institute, Japan

GANN: If these same experiments were done in large scale, and the compartment were allowed to proceed to flashover, is there a reasonable possibility that all the nitrogen that is released would be converted to NO_x ?

HIRATA: I don't think so.

BENCH- AND FULL-SCALE TOXICITY TESTS OF FRP FURNITURE

by Andrew Kim and Yoshio Tsuchiya
IRC, NRC, Ottawa, Canada, K1A 0R6

prepared for presentation before 6th Canada-Japan-USA
Trilateral Cooperative Study on Fire Gas Toxicity
to be held at Factory Mutual Research Corporation, May 1987

Introduction

Dormitory-type buildings, such as university residences or penal institutions, are compartmentalized to minimize fire spread from one room to another. A severe fire, however, will still spread smoke and toxic gases to other parts of the building, posing danger to the residents. The severity of the fire and the production and spread of the smoke and toxic gases depends on the contents of the room, interior lining materials, and ventilation. In many dormitories the rooms contain simple furnishings, often made from fire-retardant materials.

Bench-scale tests and full-scale tests were conducted at the Fire Research Section, Institute for Research in Construction, National Research Council of Canada (NRCC) to study the toxicity of fire gases produced by three types of fibreglass reinforced plastic (FRP) furnishings. The first part of the tests consisted of pyrolyzing a milligram quantity of the specimens and, using a gas chromatograph/mass spectrometer with a pyrolysis unit (Pyrolysis/GC/MS), the pyrolysis products were identified and semi-quantified. Then a gram quantity of the specimen was burned in a horizontal quartz tube, the combustion products were collected by scrubbing with water, and the water soluble components of the combustible gases were analyzed by ion chromatography (IC).

In the second part of the investigations, full-scale room burn tests were carried out using the room-burn facility at the National Fire Laboratory, NRCC. Prior to the burns, preliminary tests were conducted to determine the type and severity of a fire involving combustible materials normally found in a dormitory room. That fire was then simulated using a gas burner with a nominal 300 mm x 300 mm porous top surface (propane sand burner) [1]. Finally, the FRP furnishings made from the three different types of fire-retardant material were burned in the test room, using the simulated fire as ignition source.

Materials

Furniture made from three types of FRP (with different types and amounts of fire retardants) were tested. They were identified by their colours as orange, white and blue furniture.

Bench-Scale Tests

Pyrolysis/GC/MS

A milligram quantity of the specimen was pyrolyzed using a Chemical

Data System Inc. Model #100 Pyroprobe* at a nominal temperature of 1000°C. The products were directly injected into a Hewlett Packard Model 5996 GC/MS. A methyl-silicone bonded phase capillary column, 50 m × 0.2 mm i.d., was used for the GC separation. The oven temperature was programmed to increase from -50°C to 250°C at a rate of 4°C/min. The components of the GC effluent were identified by MS, using a spectra library and a search program, both of which were supplied by the manufacturer of the instrument.

IC Analysis of Combustion Products

In a 1 m long, 17 mm i.d. quartz tube, a 270 mm long section of which was heated in a tube furnace, a 0.5 g specimen was burnt on a ceramic boat in an air current. The temperature of the oven was controlled at 800°C. The combustion gases were scrubbed with water; the dissolved components were analyzed by IC.

All chemicals used in IC analysis were of reagent grade and used as received from the commercial sources. The IC separation was carried out on a 4.6 mm i.d 25 cm long PRP-X100 column (Hamilton Co.). The packing material was poly(styrene-divinylbenzene). The carrier was a 4 millimolar p-hydroxybenzoic acid aqueous solution, controlled at pH 8.6 with NaOH. It was delivered to the column at the rate of 2 mL/min by a Spectra Physics SP8700 pump. The samples were introduced through a Rheodyne 7010 valve and a 7001 Auto Injector fitted with a 200 µL loop. The detection was performed with a Vydac 6000CD conductivity detector. The concentrations of CN⁻ were checked with cyanide specific electrode separately.

Results

Approximately 60 organic compounds were generated from the pyrolysis of FRP samples. Most of the compounds were common for all three samples. The pyrolysis products of orange and blue furniture were especially similar. The most significant products were styrene for all three, methyl methacrylate for orange and blue furniture, and benzofurandione for white furniture. The quantities of these compounds were roughly a few percent by weight of original materials.

Hydrogen chloride was the main toxic gas detected by IC. A trace quantity of hydrogen bromide was also detected. Quantitative results are shown in Table 1. Based on the measured quantities of HCl in the pyrolysis products, it was estimated that both the orange and blue furniture contained about the same amount of fire retardant, whereas the white furniture contained only 20% of the amount in the other two.

Full-Scale Tests

Test Room

The test room was built according to the ASTM "Proposed Method for ROOM FIRE TEST OF WALL AND CEILING MATERIALS AND ASSEMBLIES" [1]. The interior

*Some commercial equipment is identified in this paper to adequately describe the experimental procedure. Such identification does not imply recommendation or endorsement by the National Research Council, nor does it imply that the equipment identified is the best for the purpose.

floor dimensions were 2.44 m × 3.66 m, and the ceiling height was 2.44 m. The test room was a concrete-block structure with a concrete floor. The interior surfaces were covered with calcium-silicate boards having a density of 736 kg/m³ and a nominal thickness of 12 mm.

The room had one 0.76 m × 2.03 m doorway in the centre of one of the 2.44 m × 2.44 m walls. A plywood door (covered with ceramic fibre insulation on the inside surface) was installed in the doorway. The central 0.8 m × 1.0 m portion of the door was covered with polycarbonate glazing to allow the viewing of the interior when the door was closed. A gap of approximately 30 mm was left between the bottom of the door and the sill.

A schematic drawing of the experimental set-up is shown in Fig. 1. At the top of the doorway, immediately adjacent to the exterior wall, a hood was installed to collect the combustion products leaving the room. The hood measured 2.4 m × 2.4 m, with a depth of 1.1 m. It was connected through a 0.92 m cubic plenum to a 0.4 m diameter horizontal exhaust duct with a circular aperture of 0.3 m at the entrance. The downstream end of the exhaust duct contained a fan with a capacity of 2.4 m³/s. The length of the horizontal exhaust duct was approximately 6 m.

Instrumentation

A thermocouple and a bi-directional flow-probe were installed in the centre of the exhaust duct, approximately 3.6 m from the centre of the hood, and a laser smoke meter was placed in the duct approximately 0.3 m downstream from the thermocouple location.

Two gas-sampling ports were provided, one at the side of the room, approximately 1.2 m above the floor, the other in the exhaust duct, approximately 4.3 m downstream from the centre of the hood. The CO and CO₂ concentrations were measured using non-dispersive infrared analyzers, and O₂ concentrations, a paramagnetic oxygen analyzer. Additional gas samples were taken in evacuated flasks from the room and the exhaust duct for IC analysis.

Description of Tests

The tests were carried out in two phases. The first phase consisted of three preparatory tests (Tests #1, #2, and #3). They were aimed at studying the burning characteristics of combustible solids typically found in a dormitory room, so that these "typical" fires could then be simulated by a propane sand burner. The simulated fire would then be used as the ignition fire in the second phase tests.

The combustible materials in the tests consisted of 2 mattresses, 4 towels, 4 bed sheets, 2 pillow cases, 2 bedspreads, 2 blankets, 2 pillows, 2 pairs of jeans, 2 jean jackets, 8 books, 1 newspaper, 12 magazines, 1 pad of writing paper, 1 roll of toilet paper, 2 T-shirts, 1 package of matches, 2 parkas, 1 plastic model and 1 can of Lysol. The can of Lysol was sprayed on all combustible materials prior to ignition to create intentionally a severe fire.

In Test #1, the combustible materials were purposely arranged to yield as severe a fire as possible (for example, all books, magazines, and papers were torn and crumpled, and the sheets and towels were torn and spread out).

In Test #2, these materials were piled in the test room without giving consideration to the arrangement. Test #3 was devised to simulate Tests #1 and #2 using a propane sand burner (300 mm x 300 mm size) with no solid combustibles in the room.

The second phase testing consisted of three full-scale fire tests (A, B, and C) with three types of FRP furniture. The furniture consisted of a bed, a clothes locker, a desk, and a stool, arranged in the test room to resemble the furniture arrangement of a typical dormitory room (Figs. 2 and 3). These were the only combustibles in the room. The propane sand burner (providing the ignition fire) was placed at the junction between the bed and the clothes locker to give the furniture maximum fire exposure. The tests were started by spark ignition of the sand burner. The propane flow rate to the burner was controlled to correspond to the heat release rate and duration of the fire created by burning combustibles in the preparatory tests.

It was hypothesized that in a real fire situation, e.g., one created intentionally by an occupant in a prison, the door would be kept closed at the beginning, and it would take approximately 3 min for people outside of the room to notice the fire and open the door. Accordingly, for the initial 3 min of each test, the door was closed, and the temperature and the concentrations of CO, CO₂, and O₂ in the room were measured. At 3 min, the door was opened and left open for the remainder of the test.

Gas temperatures, velocities, and concentrations of CO, CO₂, and O₂, and optical density in the exhaust duct were continuously measured, following the opening of the door. Gas samples were also collected in evacuated flasks, using the sampling port on the side of the room, at 1 min, and 2 min 30 sec. A few more gas samples were collected after that time from the exhaust duct at irregular intervals.

Results

Figure 4 shows the concentration of oxygen in the room vs time for Test #2. The oxygen concentration decreased sharply during the initial 3 min of the test. When the door was opened at 3 min, there was a sudden influx of fresh air into the room, while hot, smoky fire gases exited through the upper half of the doorway. The oxygen concentration in the room suddenly increased and the combustibles reignited. The subsequent fire growth was very rapid.

Figure 5 shows the concentration of CO in the room vs time for Test #2. The maximum concentration occurred while the door was closed. The peak value, 0.7%, was dangerously high, considering that the danger level is 0.4% for short-term exposure to CO [2].

Test #3 was a simulation test of Tests #1 and #2, using a propane sand burner. After several tries, the propane flow rates were determined to approximate the room temperature and the release rate in Tests #1 and #2. The variation of the propane flow rate used in Test #3 is shown in Table 2.

The rate of heat release for the tests with the three types of FRP furniture is shown in Fig. 7. The information was derived using the "Oxygen depletion method" [1]. The heat-release rate in Test A (orange furniture) was small compared to that in Tests B and C. In Test A it was close to that

of the ignition fire (Test #3), indicating that the orange furniture did not contribute much to the severity of the fire. In contrast, the white furniture ignited quickly and, once ignited, contributed significantly to the room fire.

All three types of furniture produced heavy smoke with some toxic gases. Figure 8 shows for Tests A, B, and C, the variation of the optical density of the fire gases measured with a laser smoke meter across the 0.4 m diameter exhaust duct. The gas flow rate was approximately 0.7 m³/s and included some entrained fresh air.

The results of the toxicity test for the fire gases in Tests A, B, and C are shown in Table 3. The primary toxic components were HCl and HBr. Gas samples taken at 1 min and 2.5 min represent gas concentrations in the test room with the door closed. The remaining concentrations relate to the samples collected in the exhaust duct. The latter values were converted into rate of generation of these gases in the room, using information on the gas flow rate in the exhaust duct.

The concentrations of HCl given in Table 3 were not very high compared to the danger level, which in a 30-60 min exposure is 1500-2000 ppm [2]. HBr has a threshold limit value (TLV) of 3 ppm [2], but no data are available on the concentration of HBr causing acute toxicity. Even though there is not necessarily a direct relationship between the TLV and the danger level, knowing that the danger levels for HBr and HCl are in the same range, one can estimate that the probable danger level of HBr, based on the TLV for HBr and HCl (5 ppm), is approximately 1000 ppm in a 30-60 min exposure.

The white furniture, which contained benzofurandione and styrene, produced gases of particularly high concentration in HBr for the first minute during Test B. A possible explanation for the finding is that the furniture was burning fiercely at that time and, with the door closed, all the fire gases accumulated in the room. In this test the locker ignited within 30 sec of the test, resulting in rapid fire development in the room. The intense fire lasted for approximately 30 sec, after which the flames started to decrease. No flame was visible at 1 min 10 sec, probably because of the lack of oxygen in the room. Among the three types of furniture, only the white furniture contained Br.

Comparing the HCl and HBr concentrations in Test B, it was noted that the concentration of HBr in the first two measurements (taken from the room at 1 min and 2.5 min) was much higher than that of HCl. However, the HBr concentration in the remaining three measurements (taken from the exhaust duct at 4 min, 6 min, and 10 min) was approximately the same or even lower than that of HCl. A probable explanation is that HBr has a higher boiling point than HCl, and thus has a higher tendency to condense on surfaces. Therefore, the HBr concentration in the exhaust duct is expected to be lower than in the test room. The true HBr generation rate in the room might have been substantially larger than the rate calculated from HBr concentration measurements in the exhaust duct.

While the door was closed, concentrations of CO and CO₂ in the room were dangerously high in all tests. The maximum concentration of CO was between 0.4% and 1.0%, higher than the 0.4% danger level for short-term exposure of CO. The average concentration of CO₂ was between 5% and 7%,

slightly lower than the 10% danger limit for short-term exposure [2].

Even with a sufficiently large ignition fire, the orange furniture did not burn well, owing probably to the fire retardant contained in the material. However, the blue furniture with the same amount of fire retardant burned reasonably well. This observation can be attributed to the difference in geometry of the two lockers, which were made by two different manufacturers. The orange locker was wide and shallow and had four shelves, whereas the white and blue lockers had only one shelf at the top and were narrower and deeper. In Tests B and C, the flame impinged directly on the bottom of the locker's top shelf and on its inside back surface. With the orange locker (Test A), the flames impinged only superficially on the front surface of the locker.

Summary

Full-scale room burn tests were carried out to study the toxicity of the fire gases produced by three different types of FRP furniture, referred to as orange, white, and blue. Combustibles typically found in a dormitory room were used to produce an ignition fire, which was sufficiently large to nearly cause flashover in the room.

According to the hypothetical scenario (door closed for the first 3 min), the occupant would have been in danger because of high CO and CO₂ and very low O₂ concentrations in the room during the first 3 min, even without any FRP furniture present.

References

1. "Proposed Method for ROOM FIRE TEST OF WALL AND CEILING MATERIALS AND ASSEMBLIES", pp. 1618-1638, 1982 Annual Book of ASTM Standards, Part 18.
2. Sumi, K. and Tsuchiya, Y., "Assessment of Relative Toxicity of Materials Toxicity Index", paper presented at the International Symposium on Toxicity and Physiology of Combustion Products, University of Utah, March 22-26, 1976, NRCC 15367.

TABLE 1. Determination of HCl and HBr
in % by weight of original samples

Sample	HCl (%)	HBr (%)
Orange	2.76	trace
Blue	2.93	undetectable
White	0.58	0.1

TABLE 2. Propane Flow Rate

Time (min)	Propane flow rate (L/min)
0 - 1.5	375
1.5 - 3.0	0
3.0 - 3.5	300
3.5 - 4.0	375
4.0 - 5.0	350
5.0 - 6.0	320
6.0 - 7.0	275
7.0 - 8.0	250
8.0 - 10.0	225
10.0 - 12.0	175
12.0 - 16.0	125
16.0 - 24.0	105
24.0 - 30.0	85

TABLE 3. Results of Analysis using Ion Chromatography

(A) TEST A (orange furniture)

Time (min)	HCl concentration (ppm)	HCl generation rate in the room (g/min)
1.0	175.8	-
2.5	0.0	-
4.0	16.5	1.22
6.0	135.8	9.33
10.0	164.3	11.65
15.0	88.9	7.62
25.0	34.4	3.14

(B) TEST B (white furniture)

Time (min)	HCl conc. (ppm)	HCl generation rate in the room (g/min)	HBr conc. (ppm)	HBr generation rate in the room (g/min)
1.0	14.7	-	1132.1	-
2.5	1.4	-	79.3	-
4.0	23.8	1.64	29.8	4.55
6.0	98.9	6.10	29.2	4.00
10.0	14.8	0.83	10.2	1.27

(C) TEST C (blue furniture)

Time (min)	HCl concentration (ppm)	HCl generation rate in the room (g/min)
1.0	360.9	-
2.5	17.6	-
4.0	436.9	31.48
6.0	1184.4	75.87
10.0	874.7	50.78
15.0	114.5	9.59

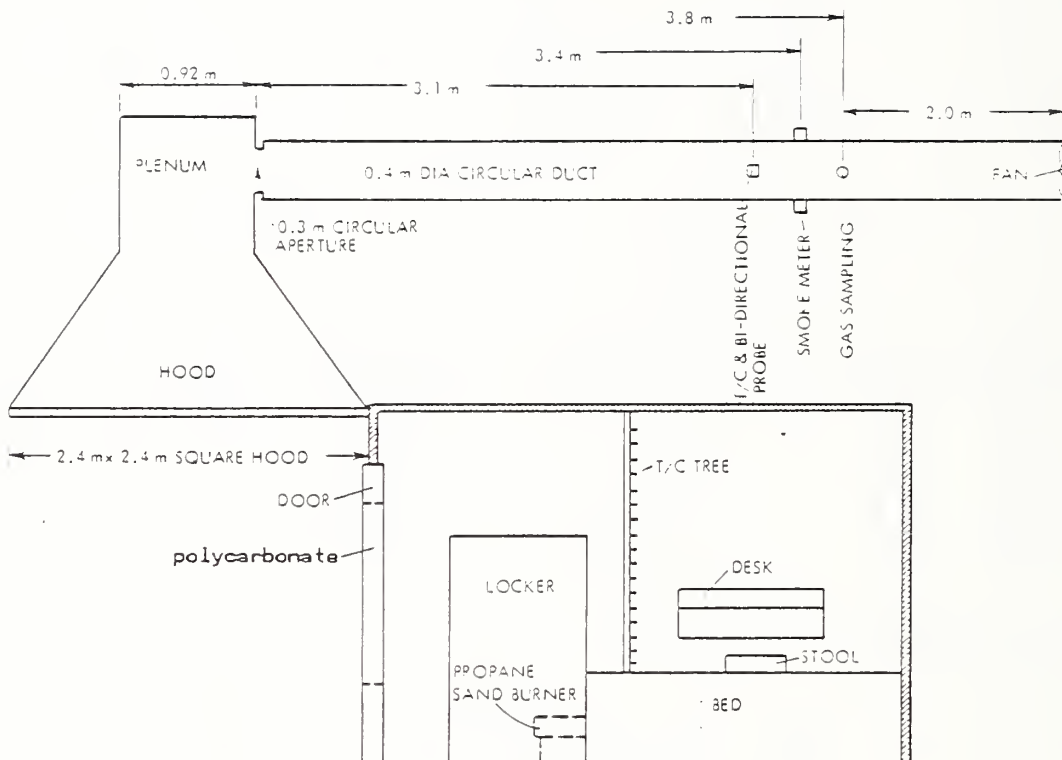


FIGURE 1
 SCHEMATIC DIAGRAM OF TEST ROOM

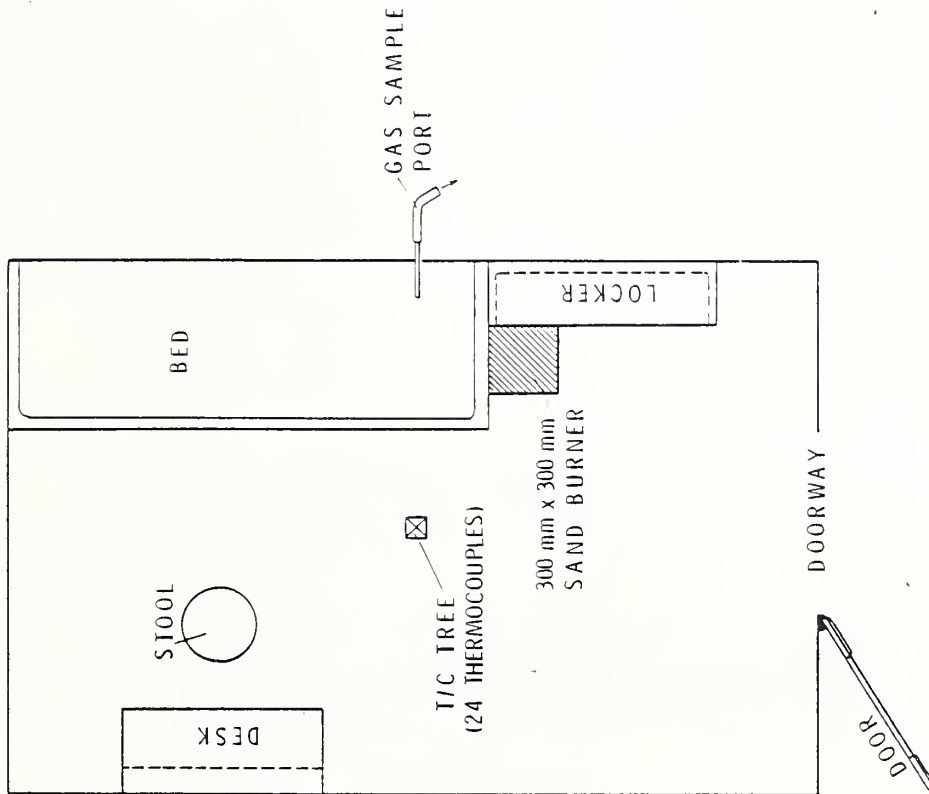


FIGURE 2
EXPERIMENTAL SET-UP FOR TEST A
(ORANGE FURNITURE)

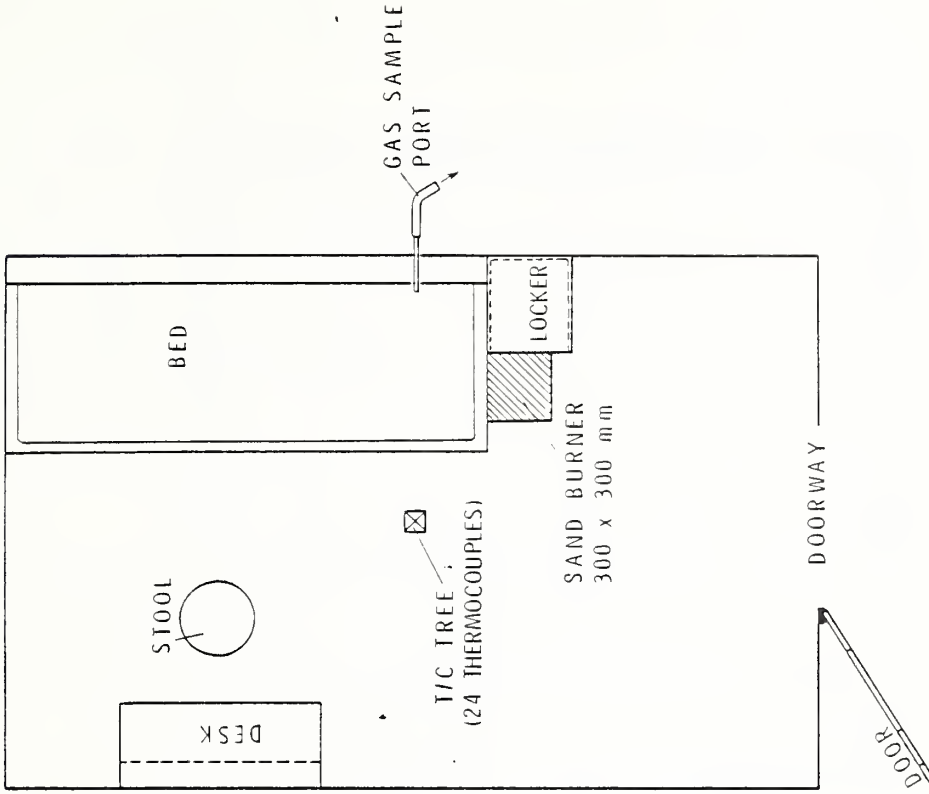


FIGURE 3
EXPERIMENTAL SET-UP FOR TEST B AND C
(WHITE AND BLUE FURNITURE)

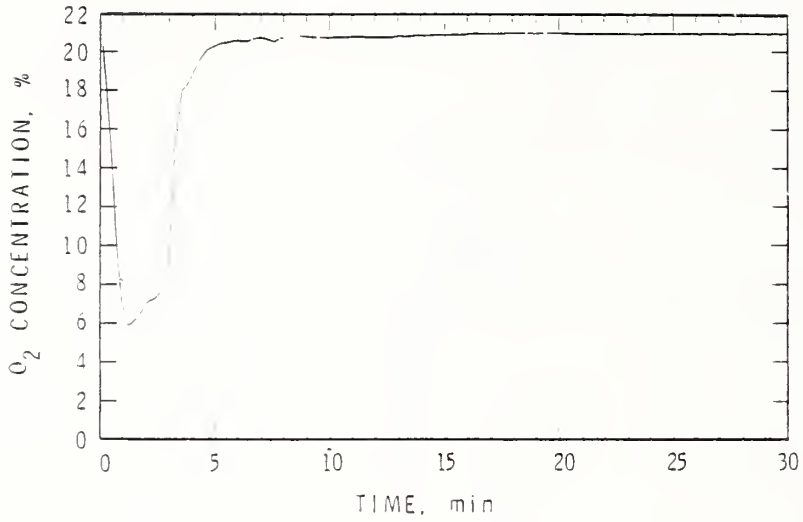


FIGURE 4
 CONCENTRATION OF OXYGEN IN THE ROOM
 vs TIME IN TEST No 2

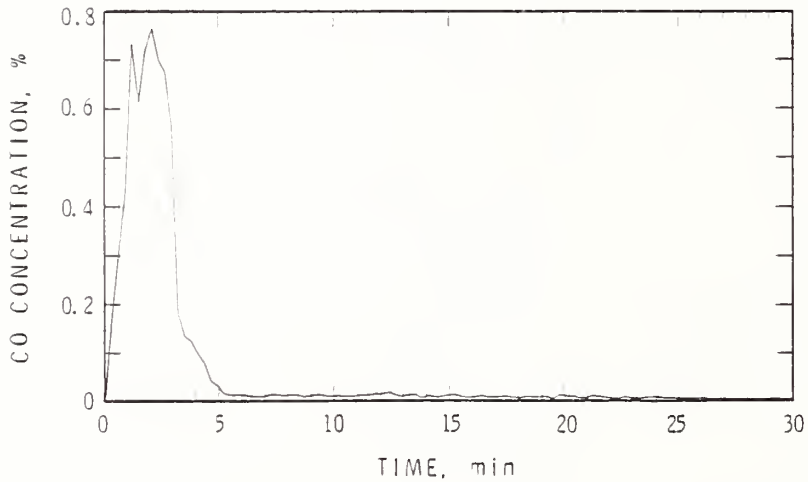


FIGURE 5
 CONCENTRATION OF CO IN THE ROOM vs
 TIME IN TEST No 2

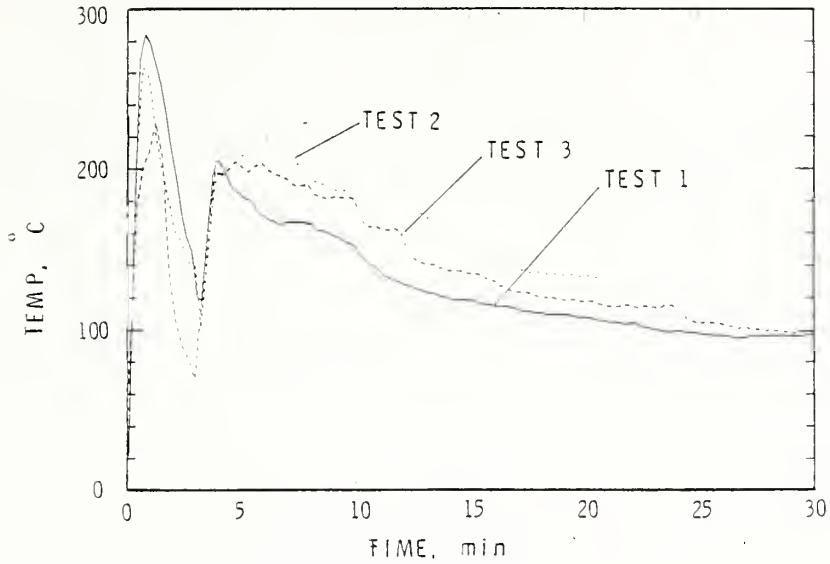


FIGURE 6
 AVERAGE ROOM TEMPERATURE vs TIME IN THE
 PREPARATORY TESTS

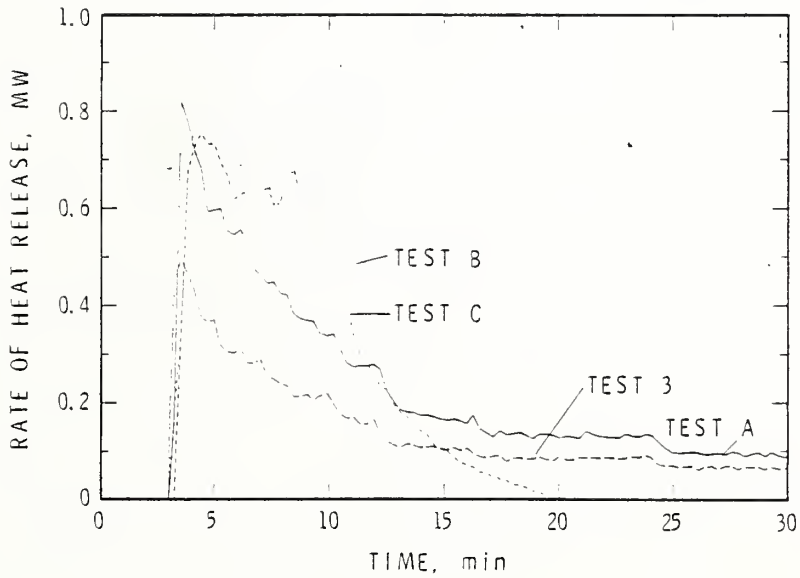


FIGURE 7
 RATE OF HEAT RELEASE vs TIME FOR THREE TESTS
 WITH FRP FURNITURE AND FOR THE REFERENCE
 TEST (TEST No 3)

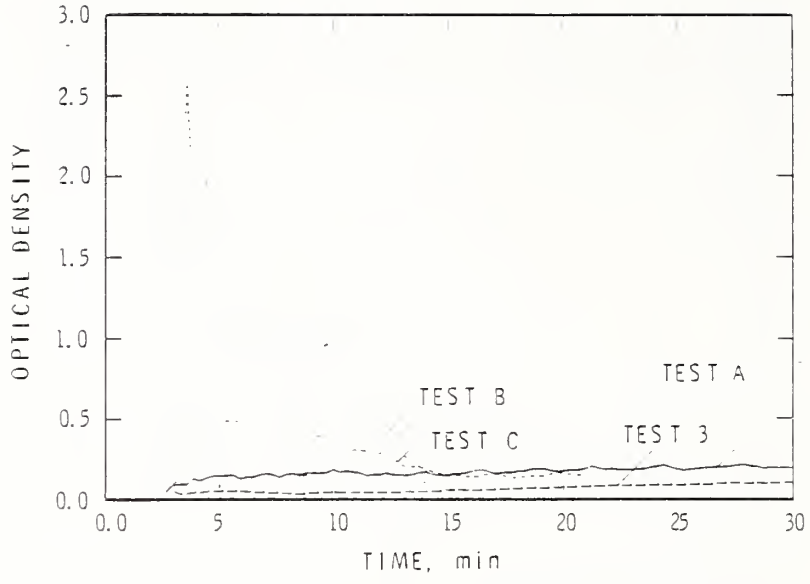


FIGURE 3 •
OPTICAL DENSITY vs TIME FOR THE THREE TESTS
WITH FRP FURNITURE AND FOR THE REFERENCE
TEST (TEST No 3)

BENCH AND FULL SCALE TOXICITY TESTS OF FRP FURNITURE
A. Kim and Y. Tsuchiya, National Research Council of Canada

TEWARSON: You were measuring temperature, and on the basis of that, you set the propane flow. After that, you were measuring rate of heat release, and that, I suppose, was in the duct. Is that rate of heat release reaction, chemical heat release rate, or convective heat release rate?

KIM: Convective heat release.

TEWARSON: Okay, so that is a convective heat release. Therefore, if one is using gas temperatures in the room, is it in any way proportional to convective heat release rate?

KIM: No, temperature use is after that.

TEWARSON: HCN stays in the air in the room, is that in the room or in the duct?

KIM: In the duct.

TEWARSON: But your Table 3 says HCN generation rate in the room.

KIM: HCN rate is determined at the duct. PPM means determined at the room, 1.2 meters from the floor.

TEWARSON: And also the temperature in the Figure 7 is the temperature in the duct?

KIM: I don't think so, the temperature is in the room.

TEWARSON: I was confused as to whether it was only in the room.

KIM: The temperature in the duct is much lower than in the room.

TEWARSON: Is there an actual simulation using the room? How many thermocouples were used?

KIM: One to three thermocouples were used.

TEWARSON: At one place?

KIM: At one place.

TEWARSON: These were measured in the duct?

KIM: Yes, everything mixed at the duct.

GANN: The rates of heat release that you show, are there enough to flashover the room?

KIM: Yes, but in this case, my calculations are scenario-based.

GANN: Did the room flash over? The reason I ask this, if this sample is totally burned, and if the room is very hot, I would expect near quantitative yields of HCl. In a very crude visual integration of the numbers table, it doesn't seem to give that.

KIM: It seemed valid.

GANN: CO levels were very low?

KIM: We have a complete record.

MORIKAWA: This is a full-scale test. The temperature seems not to be going up much, and the CO density was low when we were testing. Maybe you should have had more things so that you would have had the conditions of flashover.

KIM: Of course I mentioned that. However, we have only one set for each material.

EVOLUTION OF TOXIC GASES FROM EXPERIMENTAL FIRES IN AN EXISTING BUILDING

T. Morikawa and E. Yanai
Fire Research Institute, Ministry of Home Affairs,
14-1, Nakahara 3 Chome, Mitaka, Tokyo 181

T. Nishina
Shizuoka Prefectural Institute of Public Health
and Environmental Science,
4-27-2 Kitaandō, Shizuoka 420

ABSTRACT

Two compartment fire experiments were conducted in a two story ferro-concrete building to investigate evolution of toxic gases and toxicity of atmospheres in the burn room and its surrounding area. One was the combustion of natural polymer contents, and the other was for synthetic polymer-containing contents. Major toxicants evolved such as CO, HCN, HCl, SO₂, NO_x, acrolein, formaldehyde were determined and toxic effects were evaluated by means of toxicity index, $Z(C_i/C_{fi})$. Mice and rabbits were used as test animals and exposed to fire effluent gases in the burn room and exposure boxes. For rabbits, blood analysis and other biological examinations were carried out to find out the cause of the death or incapacitation.

INTRODUCTION

Recently there has been a growing number of fires which have caused death by toxic gases poisoning.

Synthetic materials have often been blamed for great evolution of toxic gases, although as much toxic gases could be evolved from natural materials such as wood and wool. Toxic gases evolution depends not only on the material burning but also on such factors as fire atmospheric temperature, oxygen concentration, and perhaps room size.

For the present study, fire experiments were conducted in a dormitory that was to be dismantled, to investigate the evolution of fire toxic gases in a home environment using chemical and biological analyses.

EXPERIMENTAL

Fire experiments

The building offered for fire experiments was a two story ferro-concrete building which had been a nurses dormitory. The plan view of the first floor is shown in Fig. 1, and that of the second floor was almost the same. Two rooms, the third and seventh rooms on the first floor were used as burn rooms. They are the same in shape and space, and have a floor space of 16m² and the ceiling height of 250cm each. The fixed combustibles of each room are 350kg (22kg/m²) in weight including built-in closets and cabinets, tatami (straw mat), window frames and pillows. But the combustibles below the tatami-covered floor were excluded, because they are not usually involved in fire.

Furniture, carpets, curtains, apparel and other house contents were carried into each room. Such mobile combustibles were 450kg for each room. The list of the mobile combustibles is presented in Tab. 1. The fixed and mobile combustibles in Room 3 were all natural polymers such as wood, wool, cotton, and leather; while those in Room 7 were 27% synthetic and 73% natural polymers by weight.

The layout of the combustibles for room 3 is shown in Fig. 2, and that for room 7 is nearly the same. A sketch of the burn room, corridors

and a stairway hall is shown in Fig. 3. All the doors and windows except a window in the landing of the stairway hall were closed. The opening of the window in the landing was 73cm x 100cm (height). The first floor corridor was blocked with fire resistive boards at the far end of the stairway hall, so that smoke and gases could not go into the corridor beyond the boards.

A cotton cushion (50cm x 50cm, 200g) which was smoldering over the entire surface was used as a fire source; It was inserted between another cushion and a blanket on the floor with a bedding layer over all.

Measurements and analyses

Temperature and optical smoke density were measured at various points in the burn room, the corridor, and the stairway hall, using C.A. thermocouples of 0.32mm dia. for temperature measurement and smoke meters with a tungsten lamp as a light source and SE cell as a detector for smoke measurement.

Fire effluent gases were sampled into 200ml syringes and 5% teflon bags at two points; one just below the ceiling in the center of the burn room and the other at the landing of the stairway hall, as shown in Fig. 3. Gas samples were taken at appropriate time intervals during the fire experiment. Sampled gases were subjected to gas chromatography, ion chromatography and colorimetric analyses.

Animal exposure tests were conducted using mice (dd strain, female 20g) and rabbits (Japanese white, female, 2kg) as test animals. Four mice were placed in the center of the burn room, two just below the ceiling and two on the floor, and 3 mice were placed just below the ceiling of the second floor of the stairway hall. Another 3 mice were placed in each of 2 animal exposure boxes, into which fire effluent gases were introduced. One box received gas from a point just below the ceiling in the burn room and second from the second floor stairway hall. The fire effluent gases were cooled by ice water before being introduced into the animal exposure boxes. Each mouse was contained in a free rotary wheel.

The box has a room for 3 rabbits accommodation in addition to an animal exposure room where also 3 mice were accommodated. The head of each rabbit was inserted into the animal exposure room.

Time to incapacitation, or, time to wheel rotation stop was measured for all the mice. A behavioral observation was made for mice and rabbits in animal exposure boxes. Rabbits were subjected to electrocardiographic analysis, body temperature measurement and urine tests during the exposure. Blood analysis and patholo-histological examinations were conducted for rabbits after they stopped breathing.

RESULTS AND DISCUSSION

Behavior of fires

Temperature in the burn room with time for Exp. 1 and Exp. 2 are shown in Fig. 4. The maximum temperature was recorded at nearly 1000°C for both experiments. Optical smoke density failed to be measured a little after flaming because of fire heat. During the smoldering stage, the maximum optical smoke density in the burn room was recorded at 6m^{-1} for Exp. 1 and 0.2m^{-1} for Exp. 2.

In Exp. 1, after a 39 min.-long period of smoldering, flaming occurred, then soon ceased after spreading to a cardboard box containing paper waste. At 49 min., when one of the windows (140cm high and 270cm wide) facing outside was opened to 15cm wide, flaming occurred again, and developed to some extent. At 81 min., when the window was closed, flames disappeared again apparently because of suffocation. At 86 min., when the window was opened again to one fourth of the width, flaming came back, and developed

to flashover at 108 min. Then smoke and flames came out of the window. After 120 min. the fire was in its decay stage.

In Exp. 2, after smoldering continued for 30 min., flaming occurred and developed nearly to flashover. However, it ceased suddenly when fire almost spread to the ceiling, probably because of oxygen deficiency. At 50 min., when one of the windows was opened by 15cm, flaming occurred again, and the fire developed to flashover at 60 min. with very thick yellow brown smoke coming out of the window. Fire became more violent after 72 min. when the window was opened by one fourth of the width. A few minutes later, some of the window panes were broken by fire heat, and fire developed even more violently. Then fire entered into the decay stage.

Evolution of toxic gases

For Exp. 1 toxic gas concentrations in the burn room with time are shown in Fig. 5. During the smoldering combustion, almost no change was seen in concentration of all the gases determined. Around 40 min. after ignition when flaming occurred, O_2 concentration dropped to 18% and CO_2 concentration rose to 3%, CO concentration also rose to 0.3%. However, other toxicants such as HCN were not recognizably detected. Substantative changes in concentration of gases did not occur until flashover at 108 min.. After flashover most toxic gas concentrations rapidly increased, reached their peaks, and then decreased. The concentrations at 110 min. were: CO 5%, CO_2 16%, HCN 530ppm and acrolein 16ppm. The concentration of O_2 was 2.8%.

Toxic gas concentrations in the stairway hall were not determined until flaming occurred, because closed windows and a door on the corridor side of the burn room were kept intact before that.

After the flashover, most toxic gas concentrations increased rapidly, though much less than in the burn room, as shown in Fig. 6.

For Exp. 2, toxic gas concentrations in the burn room with time are shown in Fig. 7. As was the case with Exp. 1, most toxic gas concentrations increased just after the occurrence of flaming, then decreased after cessation of the flaming, and again increased drastically to the maximum after flashover. The concentrations just after the flashover were: CO 6.5%, CO_2 13%, HCN 2500ppm, HCl 800ppm and acrolein 150ppm, and were much higher than those in Exp. 1. The concentration of O_2 was 3%. Toxic gas concentrations in the stairway hall after the occurrence of flaming are shown in Fig. 8. Most toxic gas concentrations hit their peaks around at 80 min.. The maximum concentrations were: CO 2%, CO_2 7%, HCN 400ppm and acrolein 10ppm. The minimum concentration of O_2 was 13%. The maximum concentration of HCl, which occurred around at 60 min., was 187ppm.

The oxygen concentration as a function of the CO_2/CO ratio in the burn room is shown in Fig. 9 for both Exp. 1 and Exp. 2. It is noted that in the fully developed stage of fire, the CO_2/CO ratio is lower in Exp. 2 than in Exp. 1, although the oxygen level was almost the same in both experiments. This indicates that the relative ventilation was lower in the former experiment because of the former's large burning rate.

Biological analysis

1) Behavior of animals

Times to incapacitation of mice in free rotary wheels after ignition are presented in Tab. 2 for both Exp. 1 and Exp. 2. Incapacitation did not occur in any case of the mice during the smoldering combustion which lasted until 39 min. in Exp. 1 and 32 min. in Exp. 2. In the burn room, incapacitation occurred shortly after the start of flaming, and in the stairway hall it had to wait until flashover occurred. The mice in the animal exposure boxes placed outside the building took a little longer

time to incapacitation, probably because fire effluent gases were cooled before introduced into the boxes.

The results of the observation of rabbits are presented in Tab. 3. As all the rabbits were exposed to fire gases which were cooled, their body temperature did not rise during the experiment. Sniveling was observed during the smoldering stage of fire in which CO was almost negligibly low in concentration. Sniveling must have been caused by irritant gases at instrumentally undetectable concentration, especially acrolein which could irritate even at below 1 ppm in concentration. Paralysis of limb appeared as well as chain strokes 1-5 min. before breathing stop occurred. Another noted behavior was occasional closing of eyes during the exposure.

2) Blood analyses

Levels of CO-Hb and cyanide in the blood of rabbits just after their breathing stop almost equivalent to incapacitation are shown in Fig. 10. Cyanide levels are higher for Exp. 2 than for Exp. 1, while CO-Hb levels are almost the same for both experiments. The lethal equivalence curve is based on CO-Hb lethal level of 50% and cyanide level of 3ug/ml.

In these experiments, CO seemed to be a larger contributor to incapacitation than HCN. Erythrocyte and leucocyte counts, and hematocrit values in the blood of rabbits are presented in Tab. 4. Both erythrocyte and leucocyte counts decreased a little, but hematocrite values decreased as much as 22.4% on the average.

3) Other analyses

Electrocardiographic analysis, urine tests, histological examinations were conducted for rabbits.

It was found in electrocardiographic analysis that there were a reverse of T wave and a large fluctuations of beat rates. In the urine tests, blood and protein were detected in urine, which indicates that kidney trouble was caused by the gases inhaled during the exposure. The organs on which pathlo-histological examinations were conducted were heart, kidney, lung and spleen. Abnormalities were recognized in some of the organs including cardiac muscle necrosis, probably due to oxygen deficiency.

Toxicity evaluation

Interactions of toxic effects of different gases have not yet been established. Total toxicity index (C_i/C_{fi} , where C_i is the concentration of gas component i , and C_{fi} is its lethal concentration) was used in the present study in evaluating the toxicity of fire effluent gases, since toxic effects of every toxicant are treated equally in this method. Lethal concentrations for 5-10 minutes exposure are 5000ppm for CO, 350ppm for HCN, 500ppm for HCl and SO₂, and 30 ppm for acrolein [1]. The lethal concentration of formaldehyde was estimated to be 180ppm, because acrolein is reported to be 6 times stronger than formaldehyde in toxicity to rats [2].

The total toxicity index in the burn room with time is shown in Fig. 11 for Exp. 1 and Exp. 2.

In both experiments, the total toxicity index was far below 1 in the burn room during the smoldering combustion stage when no animals collapsed. At the flashover, the total toxicity index increased rapidly, reached its maximum in a few minutes, and then soon began to decline. Generally after flashover, the total toxicity index was higher in Exp. 2 than Exp. 1. The maximum total toxicity index was 13 for Exp. 1 compared with 26 for Exp. 2.

The toxicity index of CO was compared with the sum of toxicity indexes of other toxicants, as shown in Fig. 12. It can be seen from this that the former is apparently larger than the latter.

In the stairway hall, the total toxicity index increased rapidly after flashover, and the maximum value was 3.6 for Exp. 1 and 5.9 for Exp. 2 which endorsed the incapacitation caused to the animals in the exposure boxes.

REFERENCES

- 1 Terrill, J. B. et al. Science, 200, pp. 1343-1347 (1978)
- 2 Alexeeff, G. V., J. Fire Sciences, 2, pp.362-379 (1984)

Tab. 1 List of mobile combustibles

Exp. 1		Exp. 2	
Chests of drawers	120 kg	Chests of drawers	63 kg
Desk	18	Desk	41
Chair	2	Chair	4
Book case	10	Book case	28
Foot warmer	4	Foot warmer	11
Shoes case	7	Shoes case	20
Carpet (wool)	20	Television set	27
Curtains (cotton)	4	Telephone	2
Beddings (cotton)	88.2	Carpet (PAN)	5
Pillows (cotton)	3	Curtains (PAN, Polyester)	11.1
Blankets (wool)	8.4	Beddings (PAN, PA, polyester)	28.4
Clothes (cotton, silk, and wool)	27.8	Mattress (flexible urethane foam)	8.4
Rubber	3	Pillows (synthetic)	2.2
Shoes	3	Blankets (PAN)	7.4
Leather	8.1	Clothes (PAN, PA, polyester)	18.8
Cardboard boxes	11	PVC sheets	2
News papers	10	Artificial leather	2.9
Books	100	News papers	10
Wood sticks	11	Books	100
Wall papers	4	Wood sticks	11
Plywood	27.8	Plywood	27.8
		Rigid urethane foam	7
		PVC wall papers	4
Total	443 kg	Total	488 kg
		(Synthetic 27.8%)	

Tab. 2 Time to incapacitation of mice

Location	Tested mice	Time to incapacitation (min)	
		Exp. 1	Exp. 2
Burn room (Ceiling)	No. 1	40	Failure
	2	38	38
Burn room (Floor)	1	60	38
	2	50	38
Stairway hall	1	109	64
	2	109	68
	3	109	68
Exposure box (Burn room)	1	49	34
	2	49	34
	3	48	34
Exposure box (stairway hall)	1	111	62
	2	111	62
	3	112	62

Tab. 3 Results of observation of rabbits in exposure boxes

Tested rabbits	Weight	Body temp. (°C)		Observed time after ignition (min)		
		Before exposure	After exposure	Paralysis	Sniveling	Breathing stop
Exp. 1						
For burn room						
No. 1	2.0	38.80	38.80	108	23	110
2	2.1	38.88	38.70	108	23	110
3	2.1	38.90	38.90	108	23	110
For stairway hall						
No. 1	2.1	38.80	38.10	112	-	113
2	1.8	40.10	41.00	113	-	113
3	2.3	38.80	38.80	112	-	114
Exp. 2						
For burn room						
No. 1	2.3	38.40	38.23	33	21	33
2	2.1	38.73	38.73	34	21	33
3	2.1	38.80	38.00	33	20	34
For stairway hall						
No. 1	1.9	38.30	38.00	66	30	71
2	2.2	38.80	38.80	66	30	69
3	2.2	38.70	38.80	66	49	67

+: time was not clear

Tab. 4 Erythrocyte and leucocyte counts and hematocrit values of rabbits in exposure boxes

Tested rabbits	Erythrocyte counts $\times 10^6/\text{mm}^3$		Leucocyte counts $\times 10^3/\text{mm}^3$		Hematocrit values %	
	Before exposure	After exposure	Before exposure	After exposure	Before exposure	After exposure
Exp. 1						
For burn room						
No. 1	331	357	6,800	6,800	42.0	37.0
2	441	372	10,800	6,800	34.1	27.0
3	403	333	8,400	4,700	33.0	24.0
For stairway hall						
No. 1	493	433	9,300	6,000	40.0	30.0
2	433	411	4,000	6,700	37.0	29.0
3	333	302	2,700	4,300	33.0	31.0
Exp. 2						
For burn room						
No. 1	302	486	6,300	1,300	41.0	33.0
2	413	433	6,300	2,300	40.0	31.0
3	322	467	6,300	6,300	41.0	34.0
For stairway hall						
No. 1	311	330	4,300	6,000	41.0	33.0
2	470	429	9,100	4,000	41.0	28.0
3	468	LA	9,000	LA	34.0	LA

LA: Laboratory accident

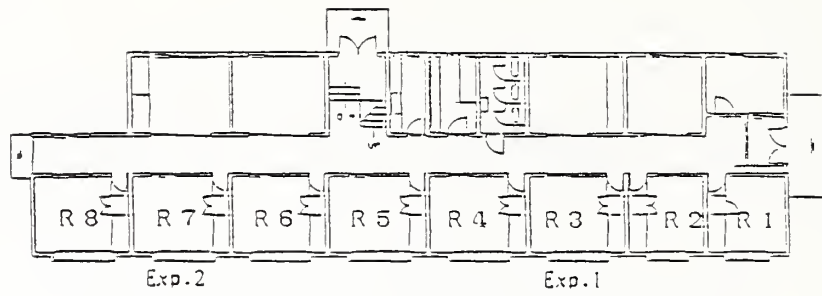
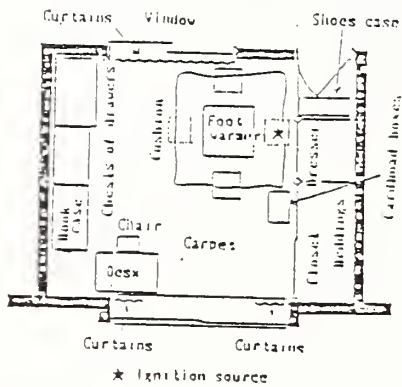


Fig. 1 A plan view of the first floor of the building offered for fire experiments



Exp. 1

Fig. 2 Layout of the room contents for Exp. 1

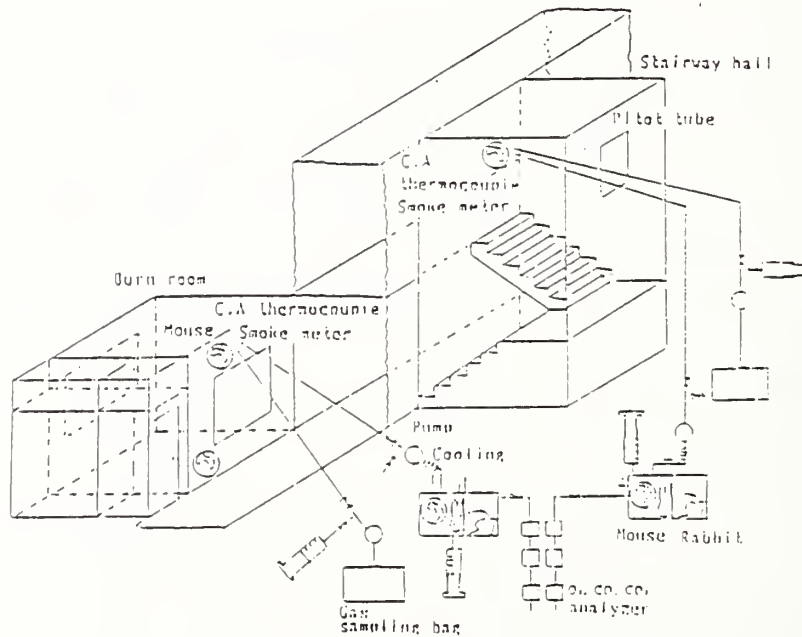


Fig. 3 A sketch of experimental set-up

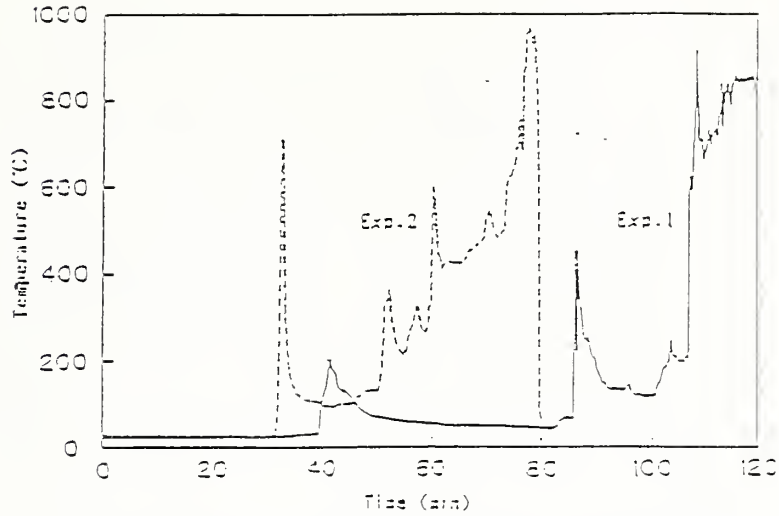


Fig.4 Variations of temperature with time just below the ceiling in the center of the burn room

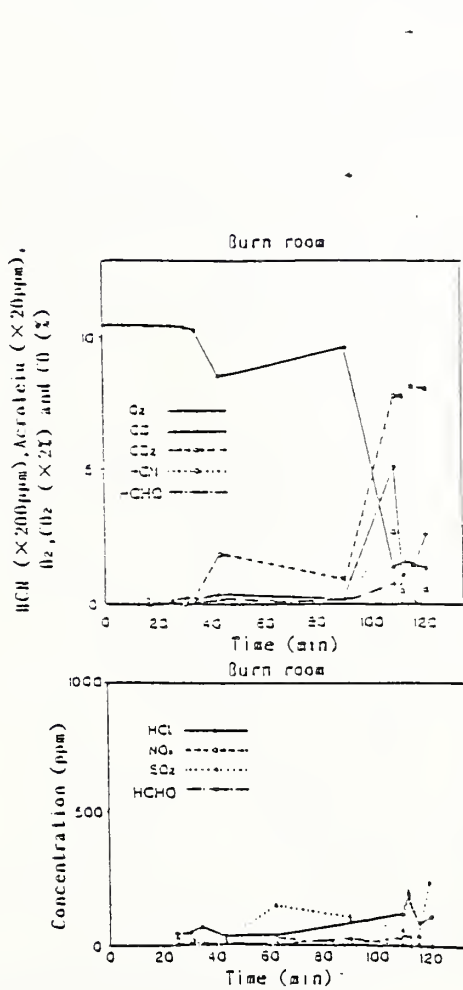


Fig.5 Variations of concentrations of gases with time in burn room for Exp.1

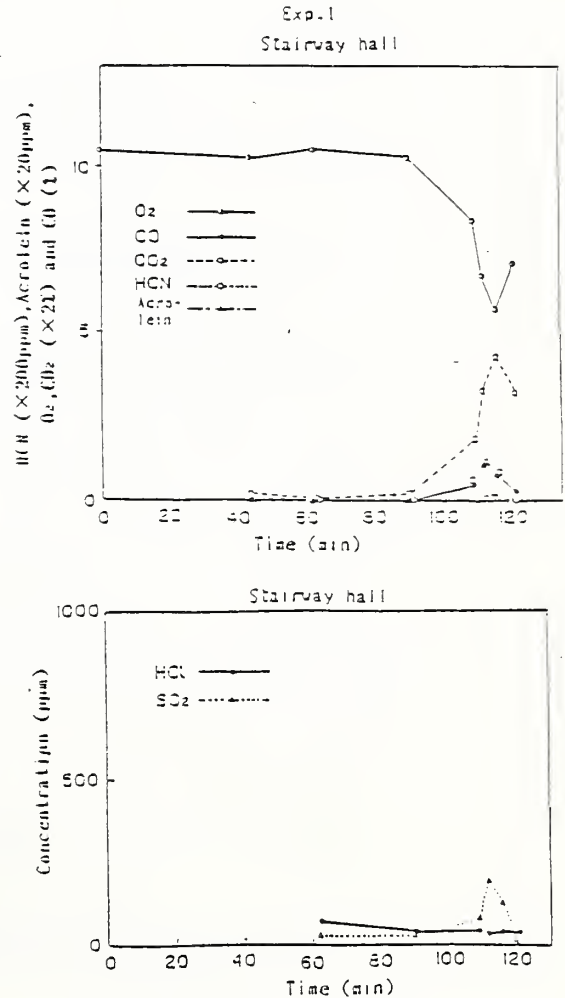


Fig.6 Variations of concentrations of gases with time in stairway hall for Exp.1

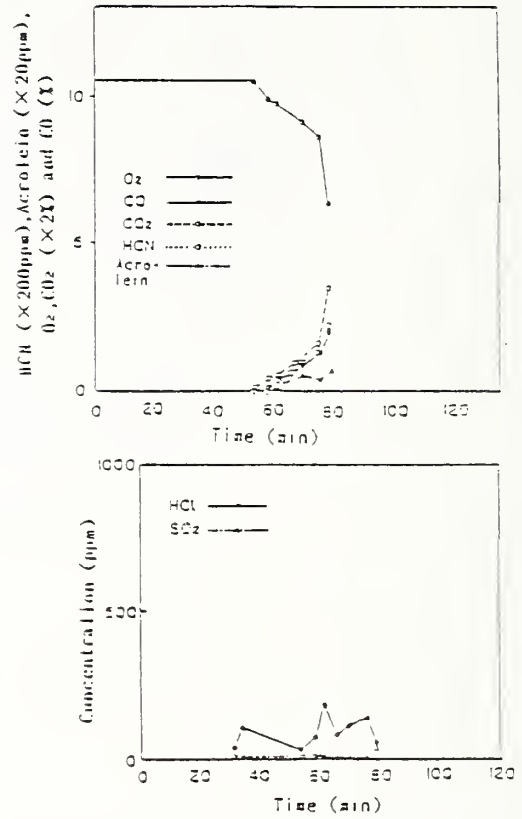
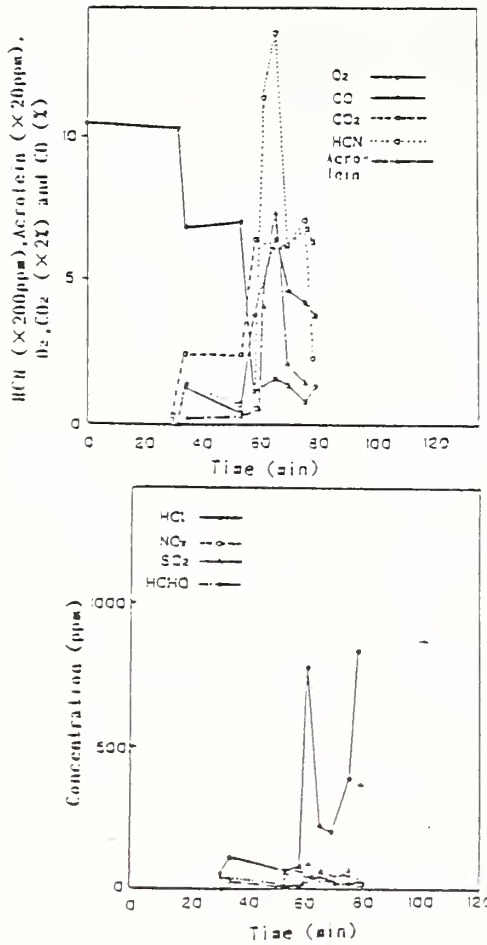


Fig. 7 Variations of concentrations of gases with time in burn room for Exp.2

Fig. 8 Variations of concentrations of gases with time in stairway hall for Exp.2

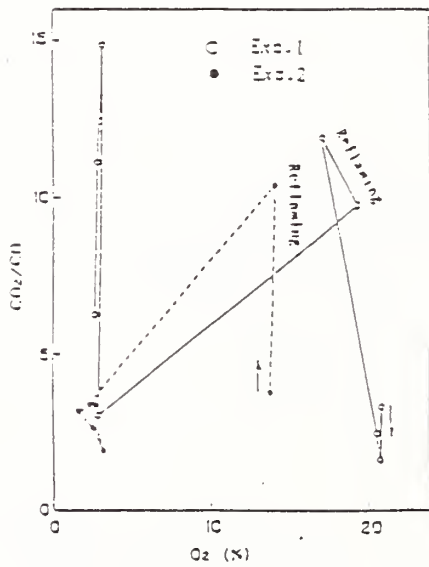


Fig. 9 CO₂/CO ratio vs. O₂ concentration

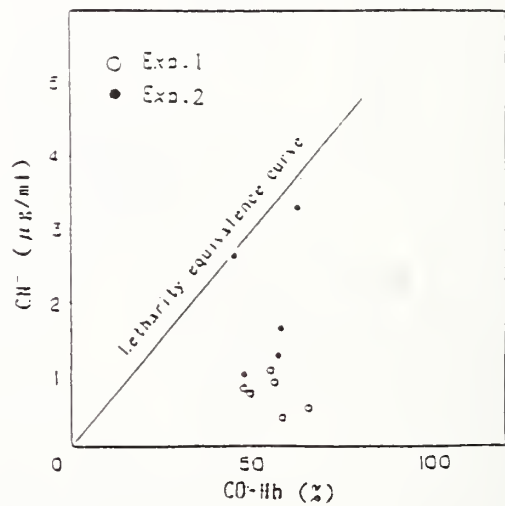


Fig. 10 CO-Hb vs. cyanide concentrations in blood of rabbits just after breathing stop

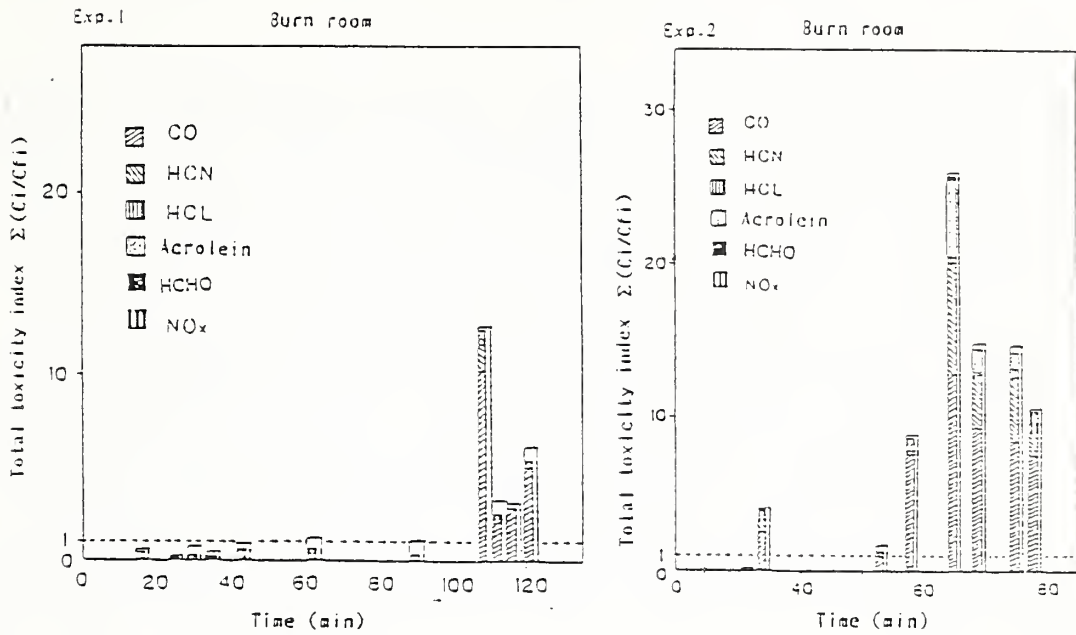


Fig.11 Variations of total toxicity index with time in burn room for Exp.1 and Exp.2

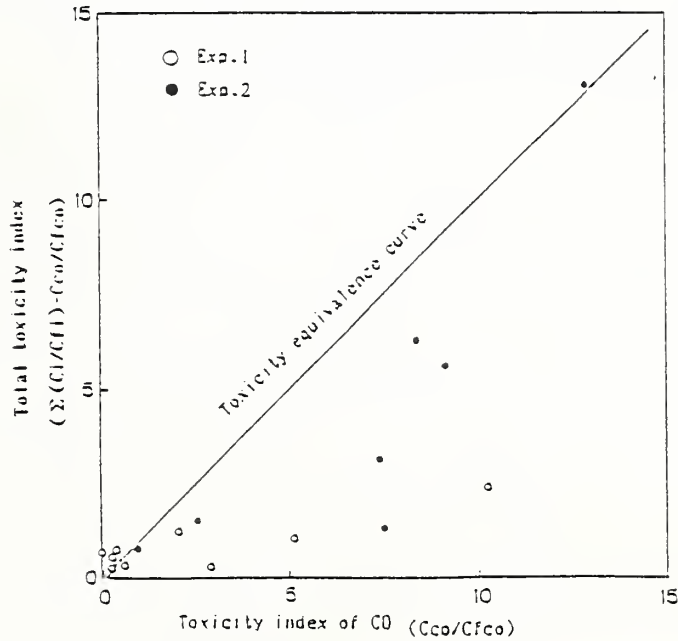


Fig.12 Toxicity index of CO vs. sum of toxicity index of gases excluding CO

EVOLUTION OF TOXIC GASES FROM EXPERIMENTAL FIRES IN AN EXISTING BUILDING
T. Morikawa, E. Yanai, and T. Nishina, Fire Research Institute, Japan

HARTZELL: In reading over the text of the behavior of fires, it seems to me that the way in which the fires were manipulated was different in the two cases because of difficulty in keeping the fire going. In fire number two, for example, the fire apparently burst into flame which would have gone out had the window not been open to cause the flame to continue. Somehow, it seems to me that because of the difference in the way these two fires were handled, it's difficult to compare not only the times of the events, but also what happened because they were not treated identically.

MORIKAWA: As far as the condition of the equipment is concerned, there were common denominators between the two. One, the smoldering was the same; also, the window was shut before and also opened. That kind of manipulation was the same. However, the time was different and then the flashover manipulation was the same. So, we feel that we obtained satisfactory data out of this experiment by focussing on the flashover phenomena and the smoldering.

HARTZELL: On the animal data, regarding heartbeat, for example, and other things, how many of the animals were involved in that data? One animal or many animals?

MORIKAWA: As far as the electrocardiogram was concerned, we measured only one animal per experiment. However, we used three animals in the cage.

LEVIN: When did you gather the blood data?

MORIKAWA: Right after the breathing stopped, we immediately took the animal out and then examined the red cells and the white cells. Therefore, breathing had stopped, but the heart was still beating.

HUMAN EFFECTS OF POISONOUS GASES GENERATED DURING FIRE
- ESPECIALLY, PRESENCE OF HCN AND CO

Yukio TSUDA and Yoichi NISHIMARU

Department of Legal Medicine, Yokohama City University
School of Medicine
3-9 Fukuura, Kanazawa-ku, Yokohama 236, Japan

ABSTRACT

In Japan it is well documented that there are about 2000 fire fatalities for a year.

Their cause of death had competed with a burn for high temperature, asphyxiation for oxygen-starvation and carbon monoxide poisoning. But there has been a significant increase in the number of fire victims recently, not only due to burns but also because of poisonous gases produced from fires.

Structural problems buildings as well as construction materials and living commodities contribute to the production of such gases. It is known that the burning of various materials lead to oxygen depletion and release of CO₂, CO, HCN, HCl, NH₃ and other gases.

Many reports and references have already been made regarding O₂, CO₂, CO. But the emphasis shall be on which is of the greatest interest to the author. Therefore, the author discusses human effects of poisonous gases generated during fire- especially, presence of HCN and CO.

INTRODUCTION

In Japan, it is well documented that there are about 2000 fire fatalities for a year (Table 1).

There categories are death due to burning, death by carbon monoxide poisoning and asphyxia, death by contusion and fracture, human torch suicide and others.

Detailed autopsy studies of 67 fire fatalities in Department of Legal Medicine, Yokohama City University School of Medicine for four years from 1982 to 1985.

A medicolegal analysis was made of 67 cases in which COHb and CN⁻ in blood levels were determined.

According to the study for the author many fire fatalities are due to CO and HCN.

Findings from Fatality Study

Table 1 shows a number of fire fatalities for eight years from 1978 to 1985 in Japan, Kanagawa Prefecture and Yokohama City.

Fig.1 is shown a number of fire fatalities who were autopsied in Department of Legal Medicine, Yokohama City University School of Medicine.

According to the author's study approximately 30%-40% of the fire fatalities are due to human torch suicide.

Burns have been classified into four degrees:
First degree - reddening of the skin (erythema)
Second degree - blistering of the skin (blister)
Third degree - loss of epidermis (crust)
Fourth degree - charring of subcutaneous tissue (carbon-azation)

Burns degree of self-ignition (human torch suicide) are third degree and fourth degree but their carbon monoxide level in blood is normal or low level, and poorly diagnosed include soot in the trachea in addition to burn of respiratory tract and they are not pugilistic attitude. Blood color is red.

On the other hand, the cases of the fire fatalities are shown the first degree, the second degree, the third degree and fourth degree. Many fatalities are found dead in houses after a fire. Note the soot present in the trachea, and the edema of the larynx. There were 30%-80% saturation of the blood with carbon monoxide. Blood color is crimson. Its presence in blood together with soot in the air passages which are usually acutely engorged, constitutes proof that the victim was alive at the time of fire and, usually, that the death was due to the fire. In this manner it is possible to explain deaths which occur in a fire when no burns or other signs of violence are found on the body and there is no evidence of natural disease.

In these circumstances it is usual to find that the blood of adult victims, especially the elderly, is about half-saturated with carbon monoxide; the results range from case to case between 30 and 80 per cent. Although other factors, for example shock, may play a part, this degree of saturation in an elderly person is of itself capable of causing death.

However, the number of the lower degree fatalities and burns caused after death have increased recently; they are hard and yellowish in color.

Blood color is not crimson often and a thin, friable, chocolate colored, sickleshaped hematoma is not present in the epidural space in the anterior and middle cranial fossae inferiorly.

According to the authors' study, they are due to poisonous gases generated during fire.

Those gases are CO_2 , CO, HCN, HCl, NH_3 and other gases.

Therefore, the authors have examined these poisonous gas-factors in blood of the fire fatalities, especially CO and CN^- .

RESULTS OF BLOOD EXAMINATION

Inhalation of fumes had caused death from carbon monoxide and anoxia.

According to the authors' study, they are due to some poisonous gases generated during fire - CO_2 , CO, HCN, HCl, NH_3 and other gases.

The authors have examined these poisonous gas factors in blood of the fire fatalities, especially CO and CN^- .

i) Concentration of COHb (Fig. 2)

Under 10% : 22 cases, the level of 10% : 6 cases

the level of 20% : 7 cases, the level of 30% : 6 cases,

- the level of 40% : 3 cases, the level of 50% : 3 cases,
 the level of 60% : 2 cases, the level of 70% : 3 cases,
 the level of 80% : 9 cases, the level of 90% : 1 cases.
- ii) Concentration of CN^- in blood (Fig. 3)
 Under 1 ppm : 3 cases, Under 10 ppm : 9 cases,
 the level of 10 ppm : 3 cases, the level of 20 ppm : 6 cases
 the level of 30 ppm : 5 cases, the level of 40 ppm : 5 cases
 the level of 50 ppm : 12 cases, the level of 60 ppm : 4 cases
 the level of 70 ppm : 2 cases, the level of 80 ppm : 2 cases
 the level of 90 ppm : 2 cases, above 100 ppm : 14 cases.
- iii) pH of blood (Fig. 4)
 Under 6.29 : 4 cases, 6.30-6.39 : 4 cases,
 6.40-6.49 : 11 cases, 6.50-6.59 : 10 cases,
 6.60-6.69 : 7 cases, 6.70-6.79 : 8 cases,
 6.80-6.89 : 8 cases, 6.90-6.99 : 5 cases,
 7.00-7.09 : 4 cases, 7.10-7.19 : 2 cases,
 7.20-7.29 : 2 cases, 7.30-7.39 : 1 cases,
 7.40-7.49 : 1 cases.
- Except 2 cases, 65 cases were acidosis.
- iv) Mutual relation of concentration COHb and CN^- (Fig. 5)
 The cases which are the concentration of high level of CN^-
 and the concentration of low level of COHb have increased
 recently.
- v) %O₂Hb (Normal value : 85-98%)
 Under 10% : 34 cases, the level of 10% : 16 cases,
 the level of 20% : 11 cases, the level of 30% : 3 cases,
 the level of 60% : 1 case, the level of 90% : 2 cases.
 The low level of %O₂Hb results from anoxia.

SUMMURY

In old day, the cause of death had competed with a burn for high temperature, anoxia for oxygen-starvation and carbon monoxide poisoning.

But there has been a significant increase in the number of fire fatalities recently, not only due to burns but also because of poisonous gases produced from fires.

These facts were demonstrated by findings from inspection and autopsy of fatalities, and by results of blood examination of fatalities. The concentration of COHb in blood of fire fatalities is low level and they have contained CN^- in blood.

HCN gas is absorbed through the mucose the tr^achea and lungs by inhalation . When cyanide is absorbed and enters the blood stream, functions of the originate ferment are suppressed in internal organs and tissue cells; and the oxygen in blood is prevented from being consumed. CN absorbed in the blood stream in other words, immediately unites with ferments such as cytochrome-oxydase, which are widely dispersed in cells and interferes with their functions.

As a condition of recovering victims who were helped from a fire, how much of the damages done by CN, which is more poisonous than CO is reversible?

This is a question that draws much interest and needs further investigation in the future.

	Yokohama City	Kanagawa Pref.	Japan
1978	27	81	1854
1979	54	118	2070
1980	39	110	1947
1981	42	132	1971
1982	30	86	1849
1983	33	91	1825
1984	21	79	2085
1985	35	78	1747

Table 1 : Fire Fatalities

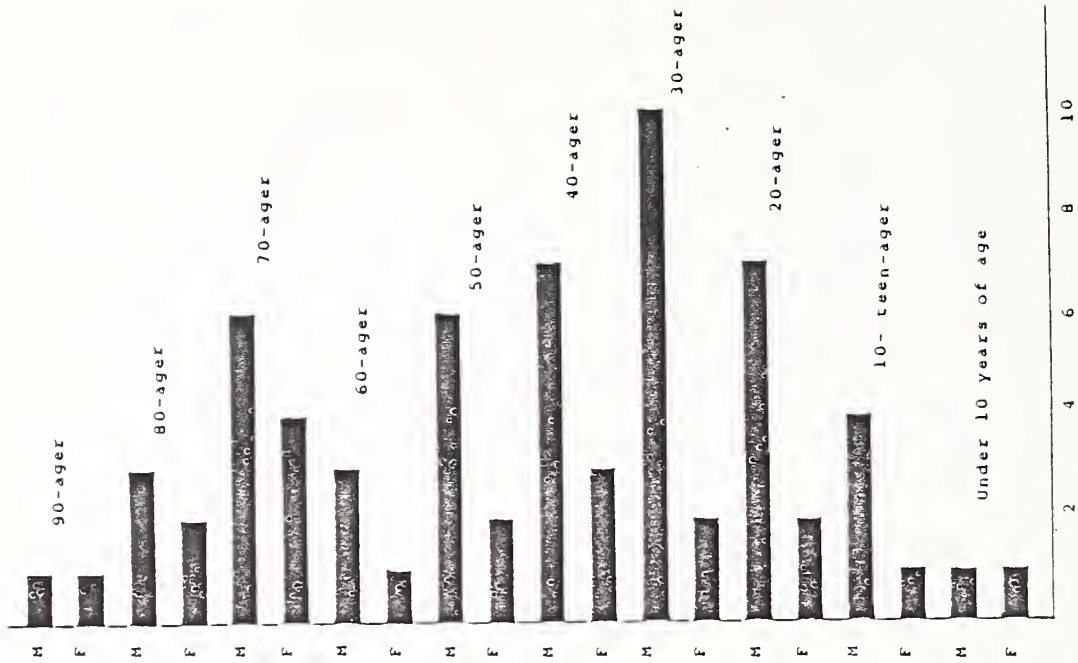


Fig. 1

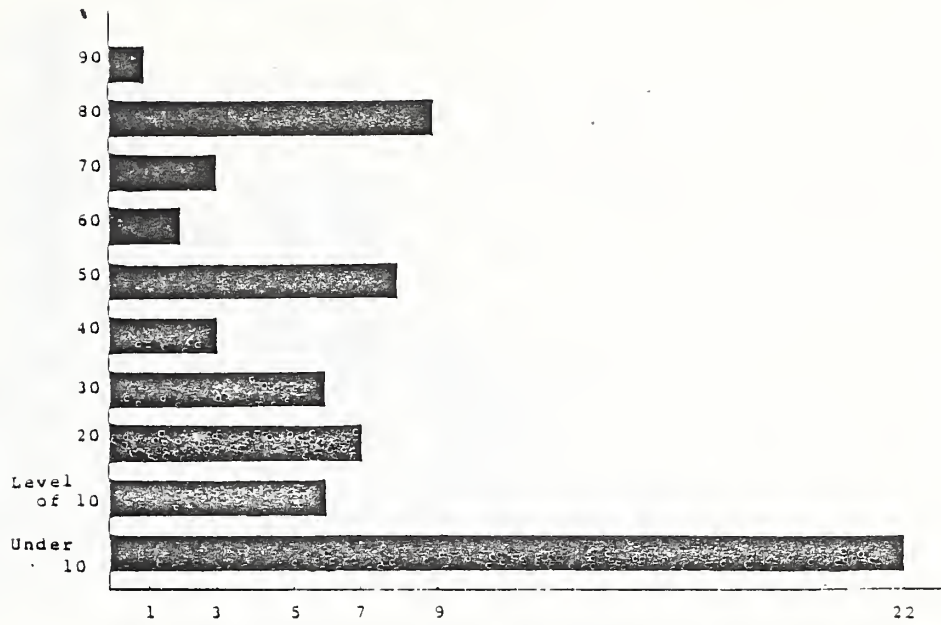


Fig. 2

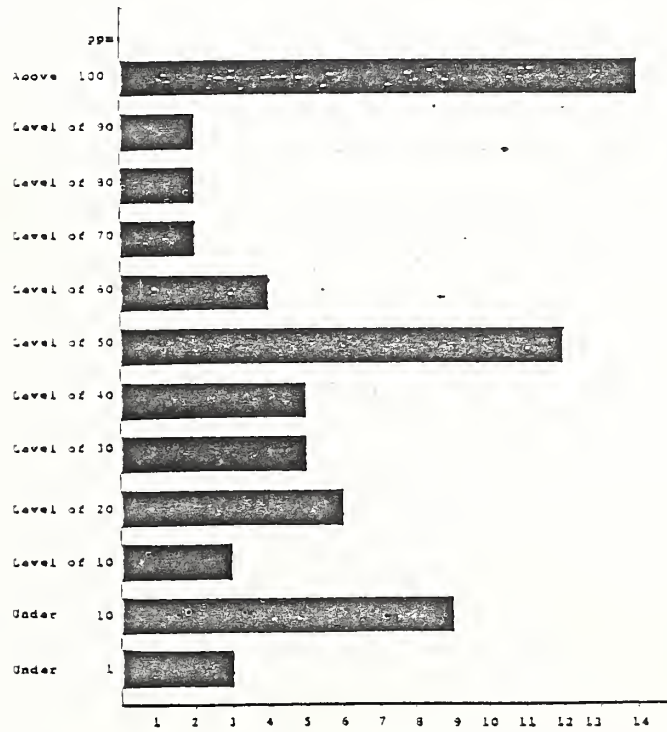


Fig. 3

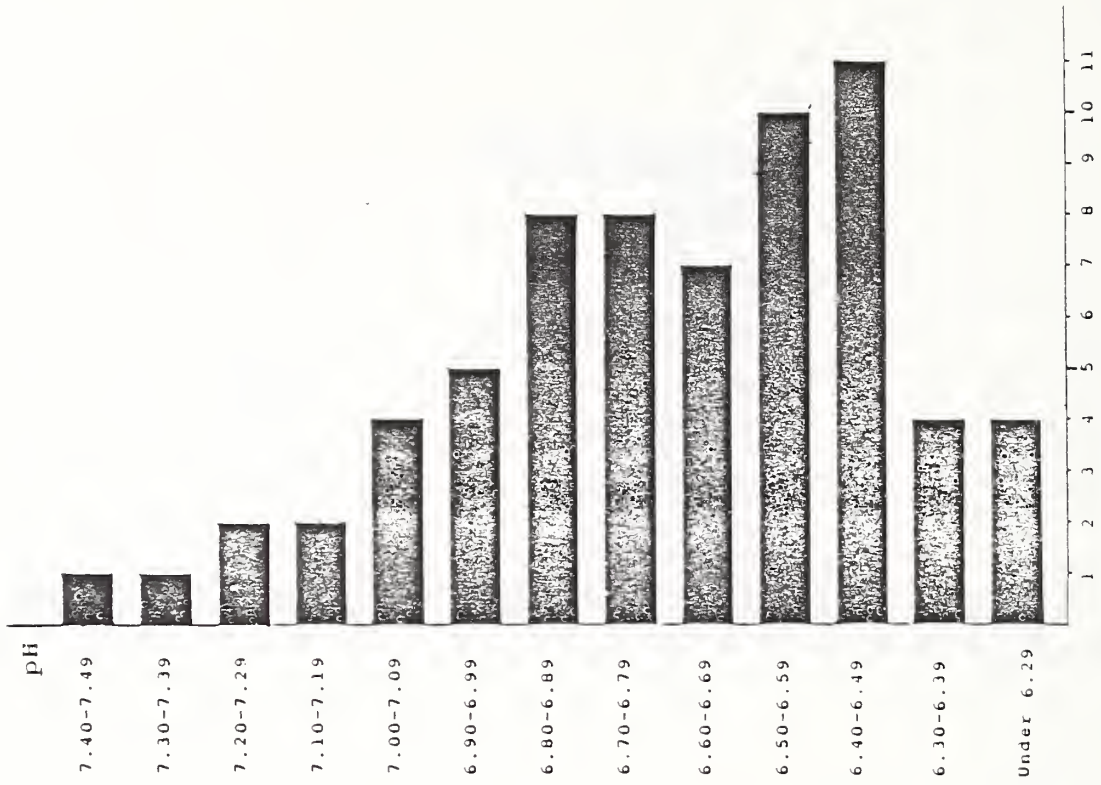


Fig. 4

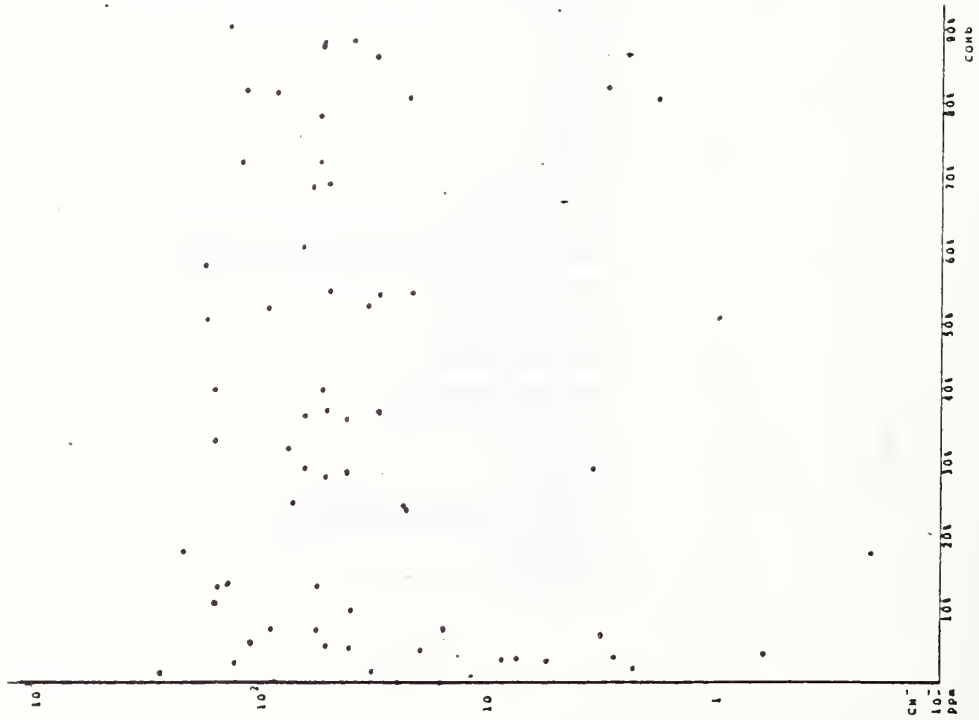


Fig. 5

A Proposed Method for the Simultaneous Analysis of
HCN and NO_x in Fire Gases
by

R. D. Curtis* and Yoshio Tsuchiya
IRC, NRC, Ottawa, Canada, K1A 0R6

Prepared for presentation before
6th Canada-Japan-USA Trilateral Cooperative Study on Fire Gas Toxicity
to be held at Factory Mutual Research Corporation, May 1987

Abstract

In fires involving the burning of nitrogen-containing construction materials and building contents (e.g., carpets made of nylon or polyacrylonitrile), various toxic inorganic gases are generated. These gases can be trapped and absorbed in aqueous or alkaline media and the anions resulting from their dissociation may be studied by Ion Chromatography (IC). In particular, an ion chromatographic method based on the method of DuVal, Fritz and Gjerde (1) was studied for the simultaneous analysis of HCN and NO_x. The method proved to be satisfactory for the simultaneous quantification of cyanide, nitrate, and nitrite ions. A linear range for CN⁻ analysis was established from 0.5 ppm to 20 ppm in solution.

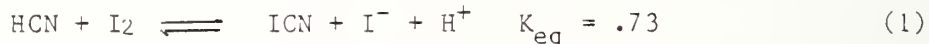
*presently a graduate student at Dalhousie University, N.S.

INTRODUCTION

During building fires, various quantities of inorganic and organic gases are produced. Samples of these gases can be trapped and then scrubbed with an alkaline solution. Dissolved gases in the solution dissociate, at least partially, to their respective anions. The resulting anion mixture is then prepared for analysis and subjected to an IC separation. The main advantage of the IC method is its ability to separate and quantify a variety of anions whose predecessors are commonly found in fire gases (e.g., HCN, HCl, HBr, HI, NO_x).

Due to their relatively high toxicity, the analysis of HCN and NO_x is important. Many methods have been developed for the analysis of cyanide ion. A commonly used method is the absorption of HCN gas in strongly alkaline media and then determination of free cyanide using the specific ion electrode. Various IC methods also exist (2, 3), however, there has been no effective method for the simultaneous analysis of HCN and other fire gases such as NO_x. The problem has been that cyanide chromatographs very poorly at low pH (less than 8) and interferes with other common anions at higher pH (8 to 12). Tsuchiya (4) has reported a simultaneous method using both a conductivity detector and an amperometric detector for monitoring the IC effluents. The high sensitivity of the amperometric detector to cyanide (5) has made its application advantageous. However, the pH used was 4.5 which is generally considered unacceptable for the analysis of cyanide. At this pH the cyanide is present mostly as HCN molecules with little cyanide ions. The chromatographic separation of cyanide is poor at low pH. In fact it passes through the column with little or no retention and elutes at or near the solvent front. Thus the method is susceptible to interference from other nonretained species which are easily oxidized at the electrode surface. In particular, sulfide (another weak acid present as an HS⁻/S⁼/H₂S mixture) may present severe interferences.

The proposed method involves the conversion of hydrogen cyanide to cyanogen iodide and hydroiodic acid using an ethanolic iodine solution. The reaction which has been known for years (6) is shown below (Eq. 1).



The reaction, as described by Beran and Bruckenstein (7), is pH dependent and quantitative over the pH range 2 to 7. Thus the alkaline solution containing free cyanide must be adjusted to pH using a noninterfering buffer just prior to the reaction with iodine. As well, for the reaction to be quantitative, an excess of iodine must be added. This excess iodine must be removed prior to the IC analysis. Assuming a quantitative reaction, the amount of free iodide generated should be proportional to the original amount of cyanide in the sample. Thus cyanide is determined indirectly by chromatographically separating and quantifying iodide ion.

EXPERIMENTAL

Chemicals

All chemicals were of reagent grade and used as supplied from the commercial source. Water for all aqueous solutions was prepared using a

Corning Mega-Pure System* which was composed of an ion exchange column, adsorbent column and borosilicate glass still. It is essential to have ion free water to prevent erroneous results from being obtained on the ion chromatograms.

Calibration and testing solutions were prepared fresh daily from sodium cyanide and sodium hydroxide (pH = 11). A 1000 ppm NaCN stock solution was prepared and solutions for analysis were prepared from this immediately prior to the analysis.

A 0.05 N sodium acetate buffer (pH = 5.0) was prepared from glacial acetic acid and concentrated sodium hydroxide.

The iodine solution was prepared daily by dissolving sufficient solid iodine in 95% ethanol to make a 0.1 N solution. To prevent the decomposition of the solution, the container was wrapped in tin foil and stored in the dark.

A column containing the Amberlite XAD-4 resin was made in a 12 cm glass tube fitted with a glass frit. The resin is a polymeric adsorbent which can be used to remove hydrophobic solutes from relatively polar solvents. It is a crosslinked polystyrene type polymer with a very high surface area and excellent physical durability. Samples were injected on to the top of the column and allowed to elute by gravity so that sufficient time to absorb the excess iodine was possible.

A 0.05 N nitric acid solution was prepared in acetone for the purpose of removing the absorbed iodine from the XAD-4 resin.

Standard solutions of other common anions (such as Cl^- , NO_2^- , NO_3^- , and $\text{SO}_4^{=}$) were prepared by dissolving their corresponding sodium salts in water.

Apparatus

Ion chromatographic separation was carried out on a 4.1 mm i.d., 250 mm long ion exchange column (Hamilton, high resolution PRP-X100 column (8)). The packing was a rigid macroporous poly(styrene-divinylbenzene) co-polymer, chemically bound with trimethyl ammonium groups to provide exchange capabilities for anion IC. The eluent used was o-phthalic acid (aqueous, 2.5 mmol) buffered to pH 6.0 with sodium hydroxide. The eluent was delivered to the column at a flow rate of 1.50 mL/min using a Spectra Physics SP8700 pump. Samples were introduced using a Rheodyne 7010 valve and 7001 Auto injector fitted with a 200 μL loop. The separated anions leaving the column were detected using a Vydac 6000CD conductivity detector. A Hewlett Packard Reporting Integrator Model 3390A was connected to the detector and was used to record the ion chromatographs.

*Some commercial equipment is identified in this paper to adequately specify the experimental procedure. Such identification does not imply recommendation or endorsement by the National Research Council, nor does it imply that the equipment identified is the best for the purpose.

PROCEDURE

Liquid Samples

Samples for analysis should be prepared just prior to the analysis from the stock solution of sodium cyanide. This prevents the loss of cyanide by hydrolysis of cyanide ion to hydrogen cyanide.

Pipette accurately 40 mL of the cyanide sample (in pH 11 NaOH) into a 50 mL volumetric flask. To the flask add 1 mL of the 0.05 N sodium acetate buffer and shake well. Using a microsyringe add 0.6 mL* of the ethanolic iodine solution to the flask and dilute to volume with water. Shake well and then allow the solution to stand for at least 10 to 15 minutes. From the 50 mL flask take a 10 mL aliquot and pass it through the XAD-4 precolumn. This process not only removes the excess iodine but also removes the water soluble organic gases. The effluent from the precolumn containing the anions of NO_2^- , NO_3^- , I^- and others is then chromatographically separated for quantification. A calibration plot was prepared by analyzing several standards and plotting the area of the respective peak as a function of the cyanide concentration.

In between samples the excess iodine was removed from the precolumn using 10 mL of the nitric acid acetone mixture. Sufficient quantities (50 mL) of water were passed through the column to ensure that all the nitrate ions are removed from the packing. This is an important step since nitrate is one of the ions that is of prime interest in the analysis of fire gases by IC.

Fire Gas Samples

A 5 L glass volumetric flask was evacuated. For obtaining a fire gas sample a piece of Orlon cloth (a polyacrylonitrile based fabric) was burned under controlled conditions in an oxygen index apparatus. The fire gases evolved on combustion of the material were collected in the flask by releasing the vacuum and drawing them into the flask. To the flask inject with a syringe through a rubber fitting 100 mL of 0.001 N sodium hydroxide. Shake the flask well to absorb all the fire gases in the alkaline media. Release the vacuum and then shake the flask again. Let the flask sit for at least 10 minutes and then pour the solution from the flask into a clean beaker. Pipette 40 mL of the sample solution into a 50 mL volumetric flask and process and analyze in the same fashion as the calibration solutions. From the calibration plot determine the level of cyanide in the sample and (correcting for dilutions) the amount of HCN in the original fire gas.

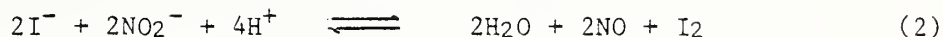
If after addition of iodine to the sample a yellow colour is not observed, the sample may require a dilution to fit the linear range of quantitative analysis (see discussion).

*0.6 mL of the iodine solution is enough to give a two-fold excess at a cyanide concentration of 20 ppm. For samples less than 10 ppm CN^- , 0.3 mL of the iodine solution is sufficient for at least a two-fold excess. The amount of iodine added also affects the sensitivity of the method, as discussed later.

RESULTS AND DISCUSSION

The conductometric detection of iodide ion is much more sensitive than that of cyanide ion. Iodide chromatographs well under the conditions used and has a retention time of about 14 minutes. A linear range for iodide quantitation was established from 1 ppm to greater than 100 ppm. A possible expansion of the method would be to use an amperometric detector for low level cyanide solutions. This type of detector would broadly increase the dynamic range for analysis as it is sensitive to iodide at the sub-ppb level.

Iodide appears to chromatograph well in the presence of other common anions such as nitrite, nitrate and sulphate. A chromatogram of a fire gas sample from burning Orlon cloth is shown in Fig. 1. The retention times were for sulphate about 8 minutes; for nitrate 5.5 minutes; for nitrite 3.8 minutes and for chloride 3.1 minutes. Note that retention times vary depending on the IC conditions and also vary slightly with a change in sample concentration. The initial peak, which is always present in single column IC, results from the difference in conductances of the eluent and the injected sample. The large negative dip after the initial peak results from the acetate ions introduced just prior to the reaction of cyanide with iodine. Initially this negative peak caused problems in the simultaneous analysis of nitrite, nitrate and cyanide. That is, the peak corresponding to the nitrite ions was too early in the chromatograph and thus not observed (Compare with the small peak for Cl^- in Fig. 1. This level of Cl^- is about 15 ppm and the area response is not representative of the correct amount of Cl^- (see Fig. 2 at about 4 mins)). By lowering the eluent concentration and decreasing the pH, the retention times of all anions increase. For example, a chromatogram of Cl^- , NO_2^- , NO_3^- and $\text{SO}_4^{=}$ was obtained using a 1 mmol o-phthalic acid (pH 6.0), as shown in Fig. 2. On this chromatogram chloride elutes at greater than 4 minutes, which should be sufficient to avoid the negative acetate peak. Further experimentation is required to establish the best conditions for the analysis. Note that the eluent concentration should not be lowered too much since the dynamic range for that analysis would be decreased substantially (i.e., the maximum concentration that can be quantitated is lowered). The pH should be kept as close to 6 as possible. According to DuVal et al (1), the iodide peak height remains relatively constant between pH 4 to pH 6. At pH values greater than 6 the peak height and thus area increases rapidly. As well in alkaline media the potential exists for iodine to oxidize other compounds and produce further errors in iodide quantitation. At lower PH nitrite can react with the released nitrite according to the reaction shown below (Eq. 2):



Despite the possible interferences, the present experimental procedure is suitable for the simultaneous analysis of NO_x and HCN in fire gases.

The reaction between cyanide and iodine appeared to be quantitative over the range of 1 ppm to 20 ppm in solution. An experimental calibration curve is shown in Fig. 3. It appears from the calibration curve that the background level of iodide ion is quite high (about 15000 area units). When only 0.3 mL of iodine was added to the reacting solution the background level was much lower (about 1200 area units). The sensitivity was much better under these conditions, but the linear range decreased to a maximum

of just greater than 10 ppm cyanide in solution (see Fig. 4). The calibration curve tailed off at 12 to 15 ppm for the latter case and at about 25 ppm for the former case.

In fire gases the gas phase concentration of HCN is usually of the order of 10 ppm to 300 ppm. With the present experimental procedure the resulting solution of the dissolved gases would contain cyanide in solution in the range of 0.6 ppm to 19 ppm. This range of concentrations fits the linear dynamic range of the method quite well. Another advantage of the method is that the nitrite and nitrate ions do not present any observable interferences. Both NO_2^- and NO_3^- can be quantified over the 1 ppm to 100 ppm range while simultaneously cyanide is quantified as iodide.

CONCLUSION

Ion chromatography is not a continuous monitoring method for fire gases but it has the distinct advantage of being able to quantify a variety of inorganic fire gases simultaneously. In particular, a method suitable for the simultaneous analysis of HCN and NO_x was developed. Future research about IC conditions and possible interferences should help to further strengthen the method.

ACKNOWLEDGEMENTS

One of the authors (R. Curtis) extends his thanks to the IRC for giving him the opportunity to pursue this research project. The authors would like to thank Brian Stewart and Mike Clermont for the help along the way.

REFERENCES

1. DuVal, D.L., Fritz, J.S., and Gjerde, D.T., Indirect Determination of Cyanide by Single Column Ion Chromatography, *Analytical Chemistry*, 54, 830, 1982.
2. Bond, A.M., Heritage, I.D., and Wallace, G.G., Simultaneous Determination of Free Sulfide and Cyanide by Ion Chromatography with Electrochemical Detection, *Analytical Chemistry*, 54, 582, 1982.
3. Okada, T., and Kuwamoto, T., Potassium Hydroxide Eluent for Nonsuppressed Anion Chromatography of Cyanide, Sulfide, Arsenite and Other Weak Acids, *Analytical Chemistry*, 57, 829, 1985.
4. Tsuchiya, Y., Ion Chromatography for the Analysis of Fire Gases, Prepared for submission to the 4th expert meeting of Canada-Japan-USA Trilateral Cooperative Study on Fire Gas Toxicity, Division of Building Research, National Research Council of Canada, Montreal Road Campus, Ottawa, Ontario, April 1985.
5. Koch, W.F., The Determination of Trace Levels of Cyanide by Ion Chromatography with Electrochemical Detection, *Journal of Research of the National Bureau of Standards*, 88, No. 3, May-June 1983.
6. Treadwall, F.P., and Hall, W.T., *Analytical Chemistry*, Volume 1, 6th ed., John Wiley and Sons Inc., p. 330-337, 1930.
7. Beran, P., and Bruckenstein, S., Pneumatoamperometric Determination of Nanogram Amounts of Cyanide, *Analytical Chemistry*, 52, 1183, 1980.
8. Lee, D.P., A New Anion Exchange Phase for Ion Chromatography, *Journal of Chromatographic Science*, 22, 327, August 1984.

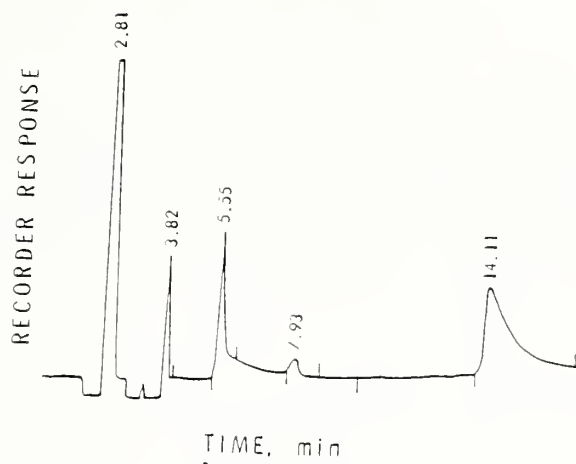


FIGURE 1
 ION CHROMATOGRAM OF FIRE GASES
 RESULTING FROM BURNING OF ORLON CLOTH

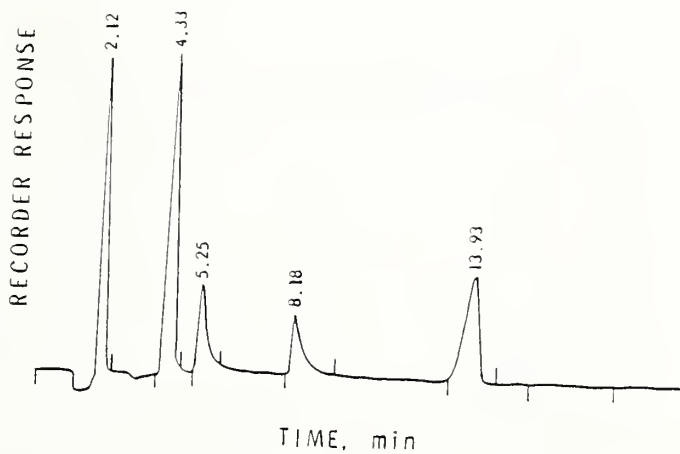


FIGURE 2
 ION CHROMATOGRAM USING A DILUTED
 ELUENT - 1 mmol O-PHTHALIC ACID (PH 6.0)

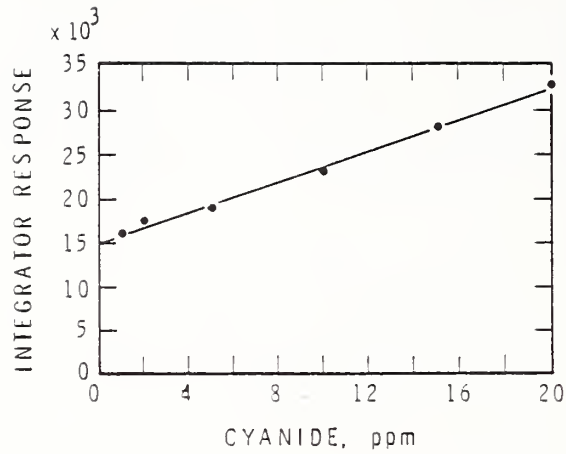


FIGURE 3
 STANDARD CALIBRATION CURVE
 FROM 1 TO 20 ppm CYANIDE ($r = 0.986$)

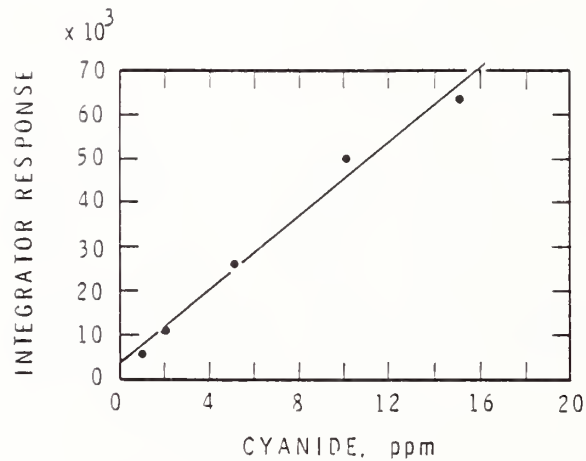


FIGURE 4
 STANDARD CALIBRATION CURVE
 USING ONLY 0.3 ml OF THE IODINE
 SOLUTION ($r = 0.986$)

A PROPOSED METHOD FOR THE SIMULTANEOUS ANALYSIS OF HCN AND NO_x IN FIRE GASES
R. Curtis and Y. Tsuchiya, National Research Council of Canada

GANN: What is the cycle time for running samples?

TSUCHIYA: Running time is about this, but before that, there is treatment of the samples each time. In the first stage we collected for combustion gas in glass flasks. We found that NOX goes through the wall of the bags, so we now use glass bottles for collecting NOX gas, mixed with oxygen and oxidized to NO₃. NO₂ doesn't dissolve in water. We have to combat NO₂ through NO₃. Then we dissolve the gas in an aqueous solution and filter that solution to remove organic material. It takes about 2 hours.

GANN: Including the iodine treatment?

TSUCHIYA: I don't know the time for the iodine treatment.

EVALUATION OF COMBUSTION TOXICITY FROM
VARIOUS MATERIALS USING A NEW TESTING APPARATUS

by

Shyuitsu YUSA

Building Research Institute, Ministry of Construction
1 Tatehara, Oho-Machi, Tsukuba-Gun
Ibaraki Prefecture, JAPAN

(For Ninth U.S.-Japan Natural Resources Panel Meeting
On Fire Research And Safety, Factory Mutual Research Corporation
Norwood, Massachusetts 02062 U.S.A.)

May 1987

EVAUATION OF COMBUSTION TOXICITY FROM VARIOUS MATERIALS
USING A NEW TESTING APPARATUS

by

Shyuitsu YUSA

Building Research Institute, Ministry of Construction
1 Tatehara, Oho-Machi, Tsukuba-Gun
Ibaraki Prefecture, JAPAN

ABSTRACT

The Building Research Institute is developing an apparatus for toxicity test of building materials. The toxicity of combustion products of typical materials are evaluated by animal exposure tests using the new apparatus. The weights of the materials when generating combustion products sufficient to cause incapacitation of mice under given exposure conditions (steady - state) are obtained and combined with the time to incapacitation. It is shown that the relative degrees of toxicities of combustion products of materials may be expressed by those values (ECT).

1. INTRODUCTION

The new apparatus for testing combustion toxicity was developed at Building Research Institute, Ministry of Constraction in Japan around 1983. It has been developed in the research program of the United States - Canada - Japan Trilateral Research Group on Toxicity of Combustion Products from Building Materials and Iuterior Goods (from 1982 FY to 1986 FY). The apparatus is designed to supply air or N₂ mixture in furnace, and to simulate the condition to which the materials are exposed in real fire.

2. METHODS

The materials used for testing were those indicated Table 1. They were made into specimens 10cm in diameter, dried in an oven at temperatures of 45 to 55

°C for at least 24 hours, then left in a desiccator containing silica gel for more than 24 hours, upon which they were testes.

The testing apparatus comprises combustion device and an exposure chamber as shown in Figure 1. The cone quartz combustion tube is held inside a cone radiative electric furnace. The mass loss of the samples during the tests is measured continuously by the load cell. From the bottom of quartz tube and around the sample, air is supplied to continue the combustion. At the top the cone quartz tube, the gasket is set up to make the time to introduce the products arbitrary so that a selected part of combustion could be introduced to the exposure chamber. The exposure chamber is designed to produce a square wave (Steady - State) exposure condition to the animals.

Specifications of the apparatus are described in the following:

(1) The combustion system

:heating system ----- electric radiation heater (cone furnace of ISO type)
:furnace ----- cone shaped quartz tube (40 mm in inner diameter at the upper part, 164 mm in inner diameter at the lower part, 3 mm thick)
:air supply system --- mechanical supply (air, air + N₂ mixture), air temperature control system
:test sample ----- commercial products, horizontal orientation

(2) The exposure system

:exposure method ----- static, whole body exposure, 15-30 minutes of exposure, square wave exposure
:animal ----- species : mouse (dd strain weight 20 +2g) number : 6

(3) Measurements

:mass loss ----- continuous measurement during the test
:chamber atmosphere -- continuous measurement of the concentrations of O₂, CO₂, CO, and temperature
: concentrations of HCN and HCl at a fixed time interval
:effect to animals --- time to incapacitation, etc.

The combustion products generated from flaming combustion or non flaming combustion are introduced into the exposure chamber for the several duration to make various concentrations of products. The animal cover is pulled up following the constant concentration of the products, and the exposure to 6 animals in revolving cages starts. The conditions of mine causing the cages to revolve are recorded as electrical pulses by proximity switches. The incapacitation time to incapacitation is defined as the length of time from start of exposure until the point that a mouse could no longer make its cage revolve. External radiation levels were mainly 2.5 w/cm^2 , and partially 3.5 and 4.5 w/cm^2 . The air supply rates are selected by which the flaming mode is sustained in the minimum rates. However the non flaming mode appeared partially.

The gas concentration inside the exposure chamber is measured by a magnetic type analyzer for O_2 , and by an infrared ray analyzer for CO_2 and CO . To determine the concentration of hydrogen cyanide in exposure chamber 100 ml of sample gas was collected every two minutes into a syringe barrel and absorbed in an $0.1 \text{ N} - \text{NaOH}$ solution, and then analyzed by 10n cheomatography. To determine the concentration of hydrogen chloride in combustion gases 200 ml of sample gas was collected every two or three minutes into a syringe barrel with approximately 20 ml of alkaline absorption (0.1N NaOH) and analyzed by an ion chromatography. The CO , CO_2 , and O_2 data and temperature measurements at the animal exposure position were collected by an on - line computer every 6 seconds as were the weight of the sample. The COHb value in the blood of mouse is determined by the IL282 CO-OXIMETER , although not for all the case.

3. Results and Considerations

Though the combustion of tested materials was almost near steady state, there were some materials which had both flaming and non flaming mode in one test run. These were MRIS, Acrylic, and Modacrylic. In the case of PVC, there was some scatter in formation of flame. The test results of the various materials are indicated in Table 2.

The exposure method used in this study is, as mentioned above, intended the square wave exposure. However, although the steady state was obtained in the case of O_2 , CO_2 , and CO , the difficulty in maintaining HCl concentraton con-

stant was shown at the last UJNR meeting¹⁾. In the case of HCN, Fig. 2 shows that the concentration falls by degrees but not so much as is the case of HCl.

With regard to the test results of various materials, the relationship between mass concentrations (mass loss/chamber volume;mg/l) and average times to incapacitation of mice, and also average concentrations of gases indicated in Figs 3 through 9. In the Fig. 3 the result when oxygen partial pressure is varied is also indicated. It might be learned that low oxygen concentration increased CO generation from the material and resulted in shortening the times to incapacitation of mice. However, the difference between the two is not so much that there needs more detailed study for clear conclusion.

Wood based materials such as Lauan, INSLBD, and PATCBD combusted relatively stabilized so that correlation between the mass concentration and gas concentration is good. And it can explain the the variation of the time to incapacitation. Compared with those materials, synthetic materials and wool show some scatter in combustion. Among these, FPU shows relatively clear results as indicated in Fig. 6. With regard to the PTFE, it did not decompose at the 2.7 w/cm² heating while decomposed at 3.8 w/cm² (NF) and 4.8 w/cm² (F). In any case there need further consideration on combustion.

In the combustion toxicity field the LC₅₀ is commonly used and LCT₅₀ (mg/l·min) is used to compare materials. In this study, using the concept, the ECT which is obtained by multiplying mass concentration by time to incapacitation is shown in Table 2 and indicated in Fig. 10. As a matter of course, it may not be possible to compare with LCT directly. However, it is thought the method in this present study, although approximate, is fairly effective in comparison of materials.

References

- 1) S. Yusa, Toxicity testing of fire effluents, Proceedings of the 8th UJNR Panel on Fire Research and Safety, 13-21 May, 1985

Table 1. Materials Tested

Material	Form	Thickness (mm)	Density (g/cm ³)
Lauan	Board	9.8	0.50 0.53
Insulation board	Board	9.0	0.26
Particle board	Board	12.5	0.61 0.68
Melamine resin-impregnated sheet	Rigid sheet	1.5	1.12
Acrylic	Carpet	10	
Polyamide(Nylon)	Carpet	10	
Wool	Felt	10	0.20
Flexible Polyurethane	Flexible foam	10	0.02
Polyvinyl chloride	Board	3	1.38
Modacrylic	Fiber		
PTFE	Flexible sheet		

Table 2. Results for animal exposure test

Material	\dot{q}_e	Air (l/min)	Comb. Time mode to Ig (sec)	Mass content (mg/l)	Ave. CO (%)	HCN (ppm)	HCl (ppm)	CO / CO ₂	Ave. time to incapacitation (min)	ECT (mg/l.min)	COHb (%)	Mortality
Lauan	2.50	8.0	F 35	81.80	0.72	-	-	0.19	4.64 ±1.29	379.37	-	3/6
			F 35	144.24	1.24	-	-	0.20	2.03 ±0.42	292.81	-	6/6
			F 35	72.96	0.68	-	-	0.19	4.82 ±1.59	351.67	-	6/6
			F 45	56.24	0.45	-	-	0.18	9.06 ±4.16	509.53	-	1/6
		6.0+	F 40	115.76	1.26	-	-	0.33	1.94 ±0.33	224.57	-	6/6
		5.6N ₂	F 30	62.80	0.64	-	-	0.26	4.43 ±0.76	278.20	-	6/6
			F 30	45.60	0.47	-	-	0.25	12.50 ±4.92	572.74	-	3/6
			F 5	86.24	1.00	-	-	0.39	3.99 ±0.71	344.10	-	6/6
			F 10	54.80	0.65	-	-	0.37	5.50 ±1.04	301.40	-	5/6
			F 10	46.00	0.42	-	-	0.39	12.61 ±3.54	580.06	-	2/6
INSLBD	2.52	10.0	F 10	106.96	0.45	-	-	0.08	6.61 ±1.80	707.01	-	6/6
	2.59		F 15	86.96	0.34	-	-	0.08	15.83 ±6.54	1376.58	-	3/6
	2.60	8.0	F 15	98.72	0.85	-	-	0.20	2.98 ±0.37	294.20	-	6/6
	2.65		F 15	102.24	0.96	-	-	0.24	3.17 ±0.01	324.10	-	6/6
	2.72		F 10	111.60	1.01	-	-	0.24	2.97 ±0.41	331.50	-	6/6
	2.5	10	F -	105.80	1.24	-	-	0.35	1.18 ±0.17	124.84	-	6/6
			F 50	88.70	1.01	-	-	0.29	1.03 ±0.19	91.36	-	6/6
			F 60	41.92	0.54	-	-	0.30	2.95 ±0.83	123.66	-	6/6
			F 50	19.92	0.36	-	-	0.27	7.09 ±3.15	141.23	-	6/6
			F 55	15.76	0.25	-	-	0.26	10.88 ±4.87	171.47	-	6/6
PTCBD	2.72		F 50	33.76	0.22	41	-	0.27	19.70 ±2.86	665.07	45.62	0/6
	2.75		F 50	65.00	0.75	195	-	0.28	2.44 ±0.63	158.60	55.00	6/6
	2.57		F 60	40.40	0.43	105	-	0.26	5.79 ±1.44	233.92	67.02	6/6
	2.27	6.0	NF+F (45)	50.20	0.91	159	-	1.27	2.13 ±0.33	106.93	64.80	6/6
MRIS	2.59		F 45	62.50	0.34	46	-	0.53	11.22 ±3.25	701.25	62.90	4/6
	2.89		NF -	43.90	0.56	135	-	0.65	4.15 ±0.98	182.19	64.90	6/6

Table 2. Results for animal exposure test

Material	\dot{q}_e (l/min)	Comb. Time mode to Ig (sec)	Mass concent (mg/l)	Ave. concent of gases			CO / CO ₂	Ave. time to incapacitation (min)	ECT (mg/l·min)	COHb %	Mortality		
				CO	HCN (ppm)	HCl (ppm)							
Acrylic	2.64	6.0	F+NF	10	10.40	0.06	231	-	0.23	3.41 ±1.17	35.46	17.60	6/6
	2.62	6.0	F	10	14.60	0.09	342	-	0.20	1.45 ±0.27	21.23	5.90	6/6
	2.80	6.0	F	10	17.00	0.09	351	-	0.25	1.52 ±0.14	25.84	9.20	6/6
	2.72	6.0	F	10	12.20	0.08	244	-	0.28	1.85 ±0.28	22.57	-	6/6
Nylon	2.74	6.0	F	60	45.00	0.28	343	-	0.27	2.34 ±0.91	105.30	27.50	6/6
	2.64	6.0	F	80	27.80	0.19	184	-	0.23	3.78 ±2.09	105.10	29.80	1/6
	2.52	6.0	F	58	28.80	0.18	244	-	0.19	1.99 ±0.55	57.30	27.50	6/6
	2.70	6.0	F	75	23.80	0.16	238	-	0.19	2.03 ±0.04	48.30	36.40	4/6
	2.79	6.0	F	75	23.40	0.13	133	-	0.19	6.73 ±1.32	157.50	20.20	1/6
Wool	2.60	10.0	F	0	36.60	0.09	312	-	0.06	2.29 ±0.75	83.80	3.30	6/6
	2.87	10.0	F	10	13.20	0.04	185	-	0.06	5.00 ±1.88	66.00	12.00	2/6
	2.95	10.0	F	7	13.50	0.07	304	-	0.10	2.05 ±1.09	27.70	4.50	6/6
	2.69	10.0	F	5	58.70	0.11	306	-	0.07	1.68 ±1.09	98.60	7.50	6/6
FPU	2.72	6.0	F	0	13.76	0.20	61	-	0.21	14.68 ±4.64	202.00	47.10	0/6
	2.64	6.0	F	0	26.00	0.41	110	-	0.34	5.97 ±1.86	155.20	65.10	6/6
	2.75	6.0	F	0	35.92	0.60	174	-	0.37	2.34 ±0.58	84.10	61.40	6/6
PVC	2.34	15.0	F	90	108.00	0.31	-	5800	0.22	10.66 ±3.70	115.30	-	6/6
	2.44	15.0	F	85	96.00	0.35	-	9750	0.27	5.95 ±1.59	505.80	-	6/6
	2.50	15.0	F	80	71.20	0.33	-	12250	0.35	5.24 ±1.36	373.10	-	6/6
	2.60	15.0	F	75	36.00	0.16	-	5800	0.41	15.22 ±7.96	547.90	-	6/6
Methacrylic	2.67	6.0	F	25	16.72	0.03	117	-	0.06	3.62 ±1.98	60.50	7.10	2/6
	2.62	6.0	F+NF	40	15.04	0.03	397	-	0.08	1.24 ±0.22	18.70	1.00	6/6
	2.57	6.0	F+NF	40	16.00	0.03	382	-	0.08	1.21 ±0.24	19.40	0.70	6/6
	2.54	6.0	NF	-	20.40	0.02	526	-	0.23	1.22 ±0.11	24.40	0.00	6/6
PTFE	2.74	6.0	-	-	-	-	-	-	-	-	-	0.00	0/6
	4.77	6.0	F	30	5.60	0.01	-	-	-	24.26 ±2.86	135.90	-	0/6
	3.84	6.0	NF	-	6.67	0.02	-	-	-	9.72 ±2.39	64.80	0.70	5/6

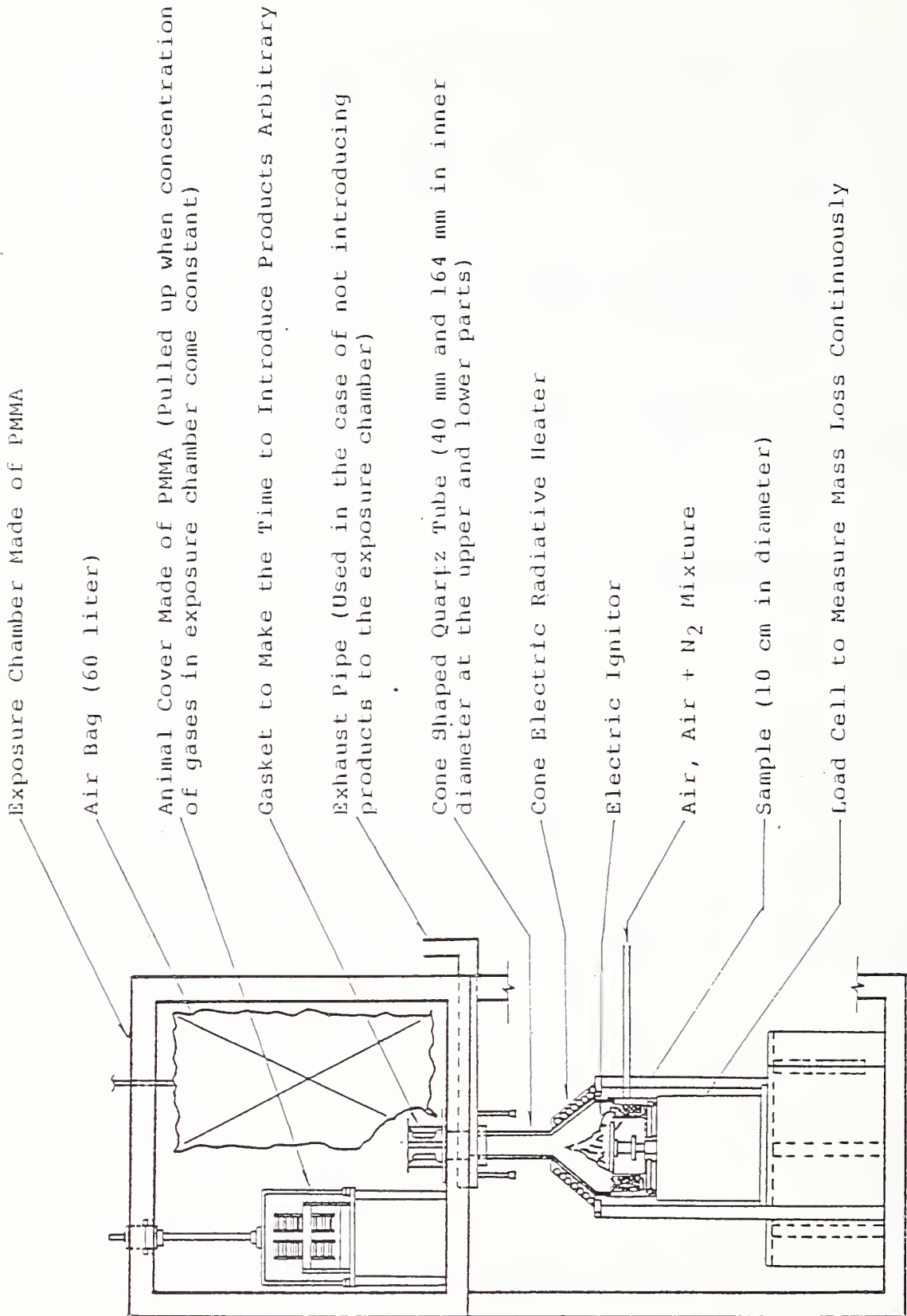


Figure 1. Test apparatus

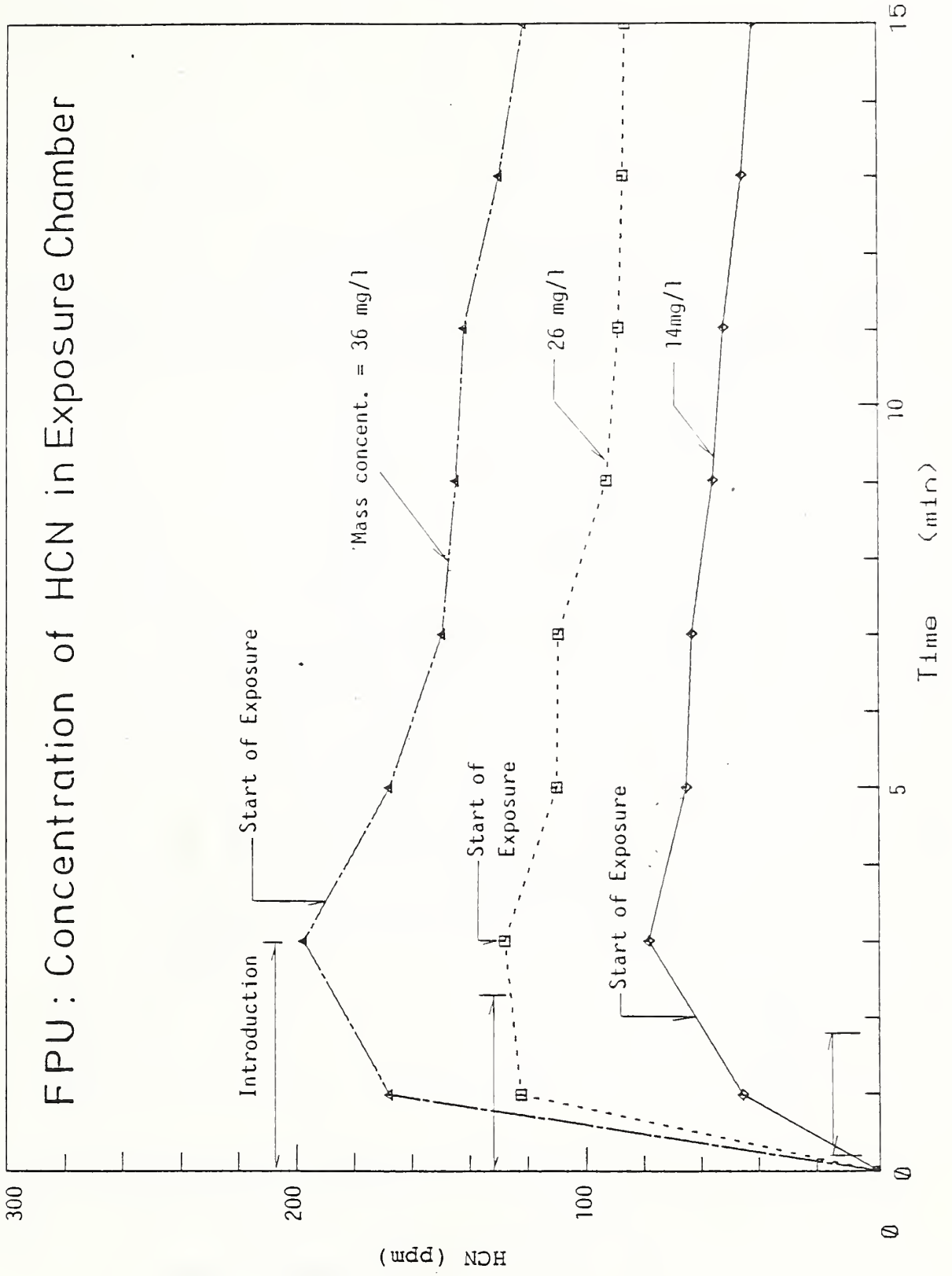


Fig. 2

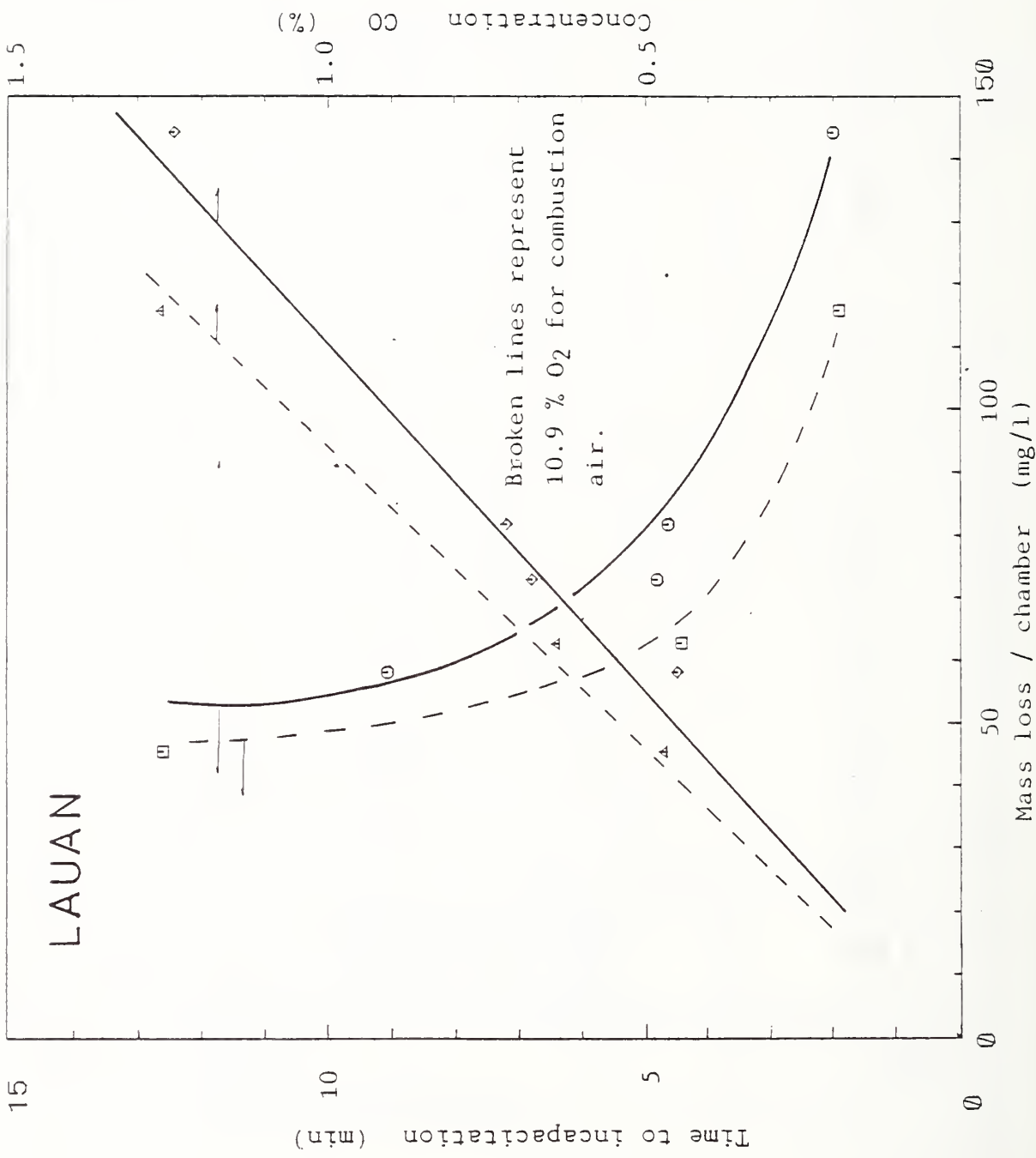


Fig. 3 Result on animal exposure test for lauan.

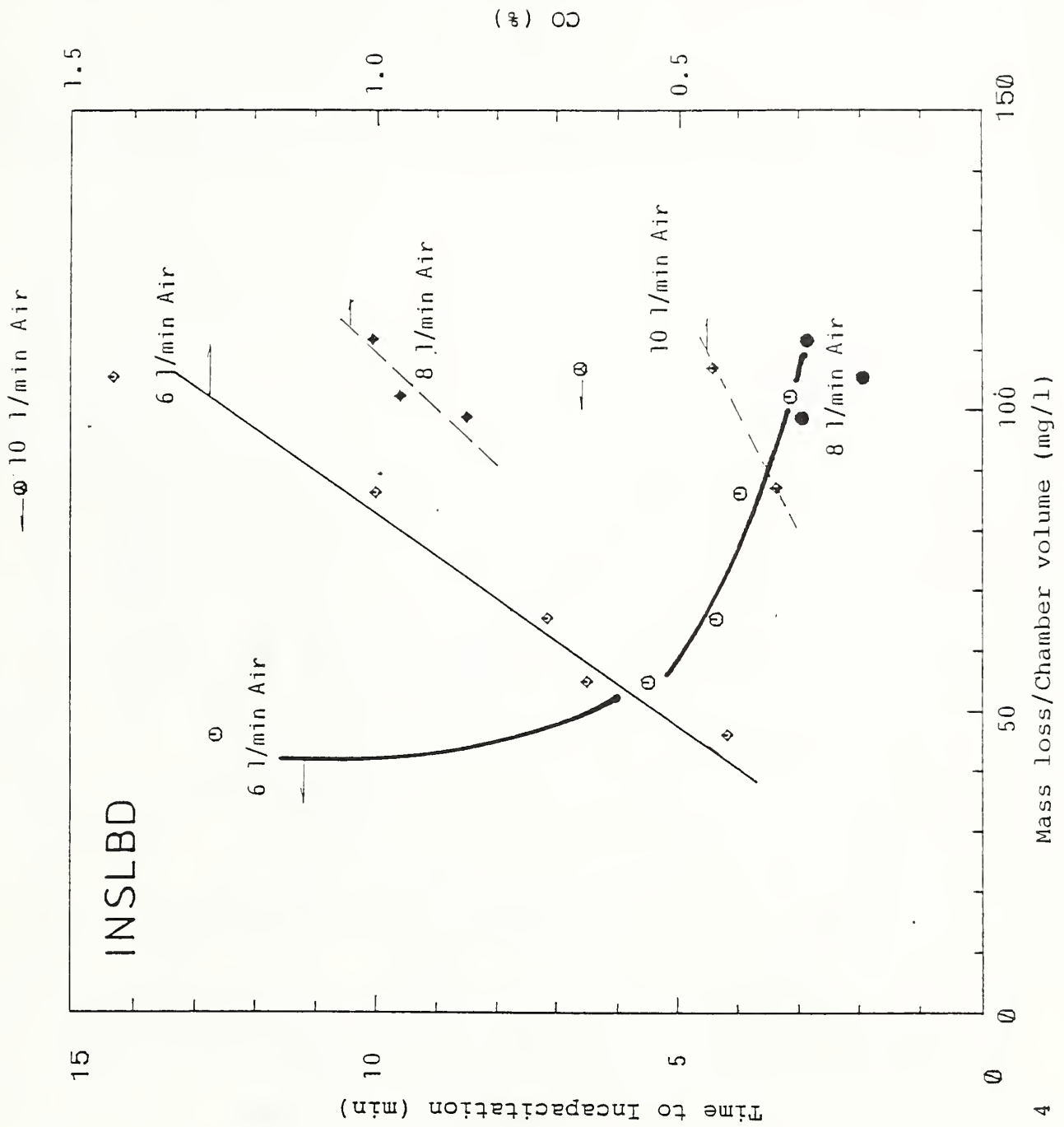


Fig. 4

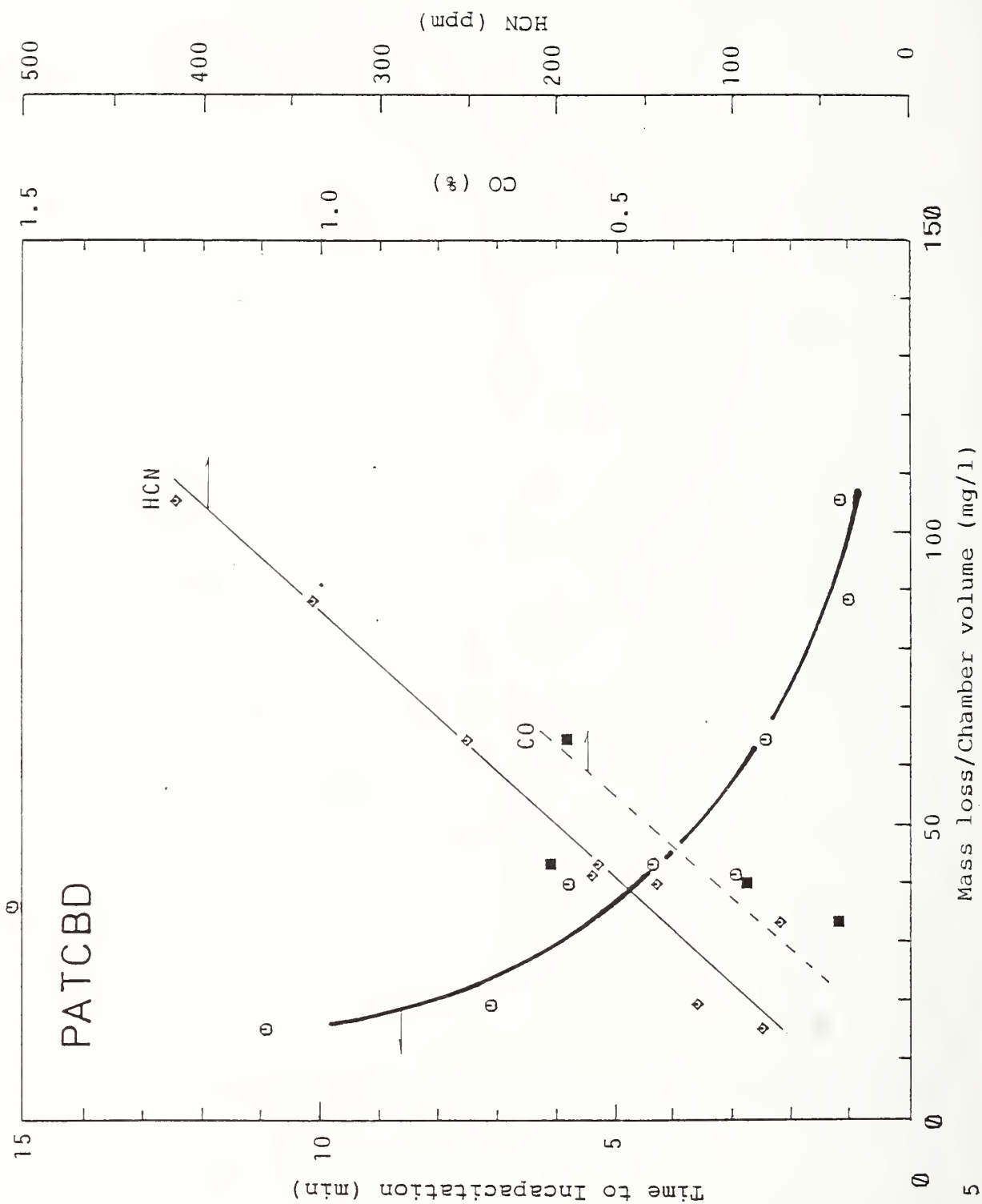


Fig. 5

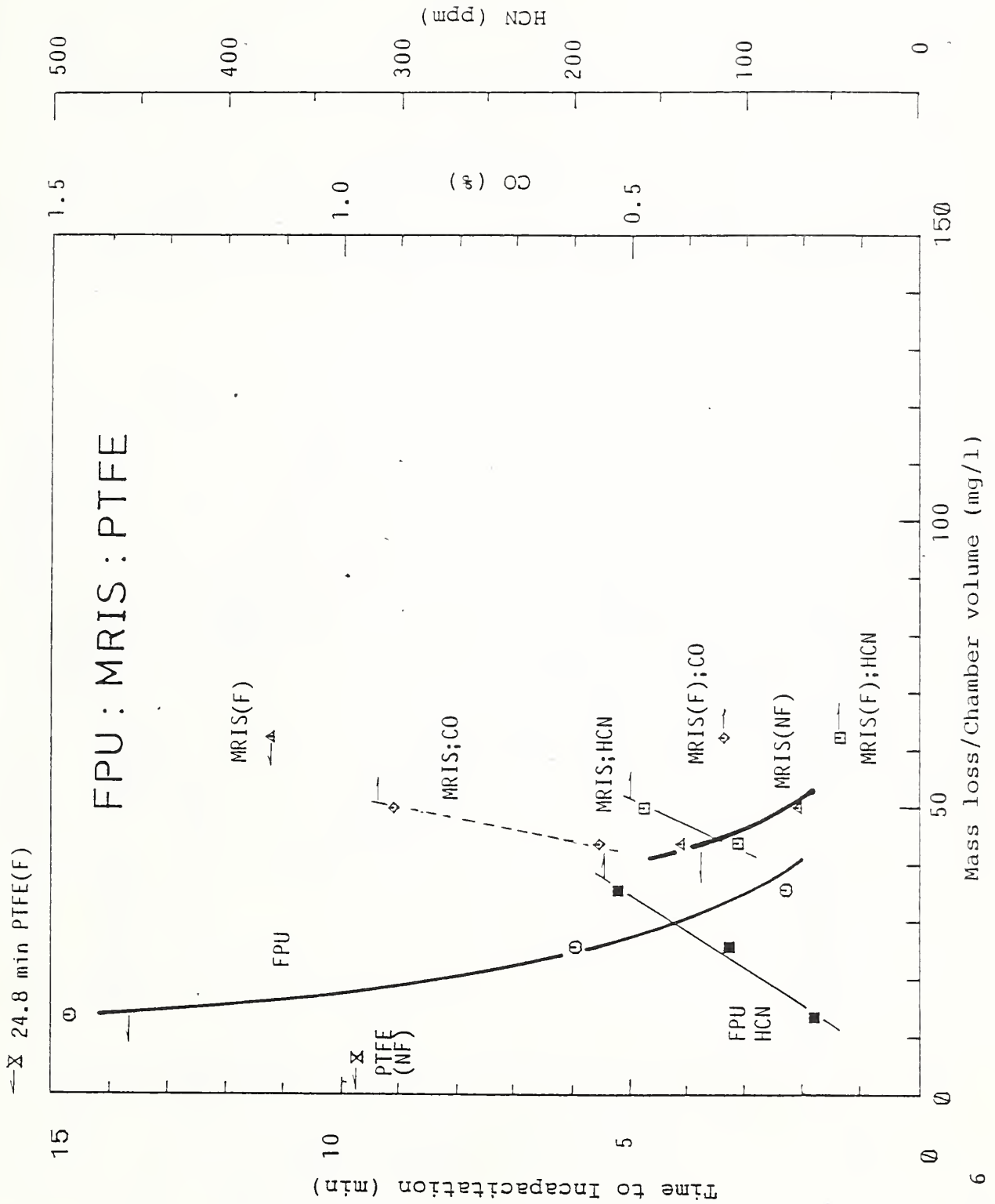


Fig. 6

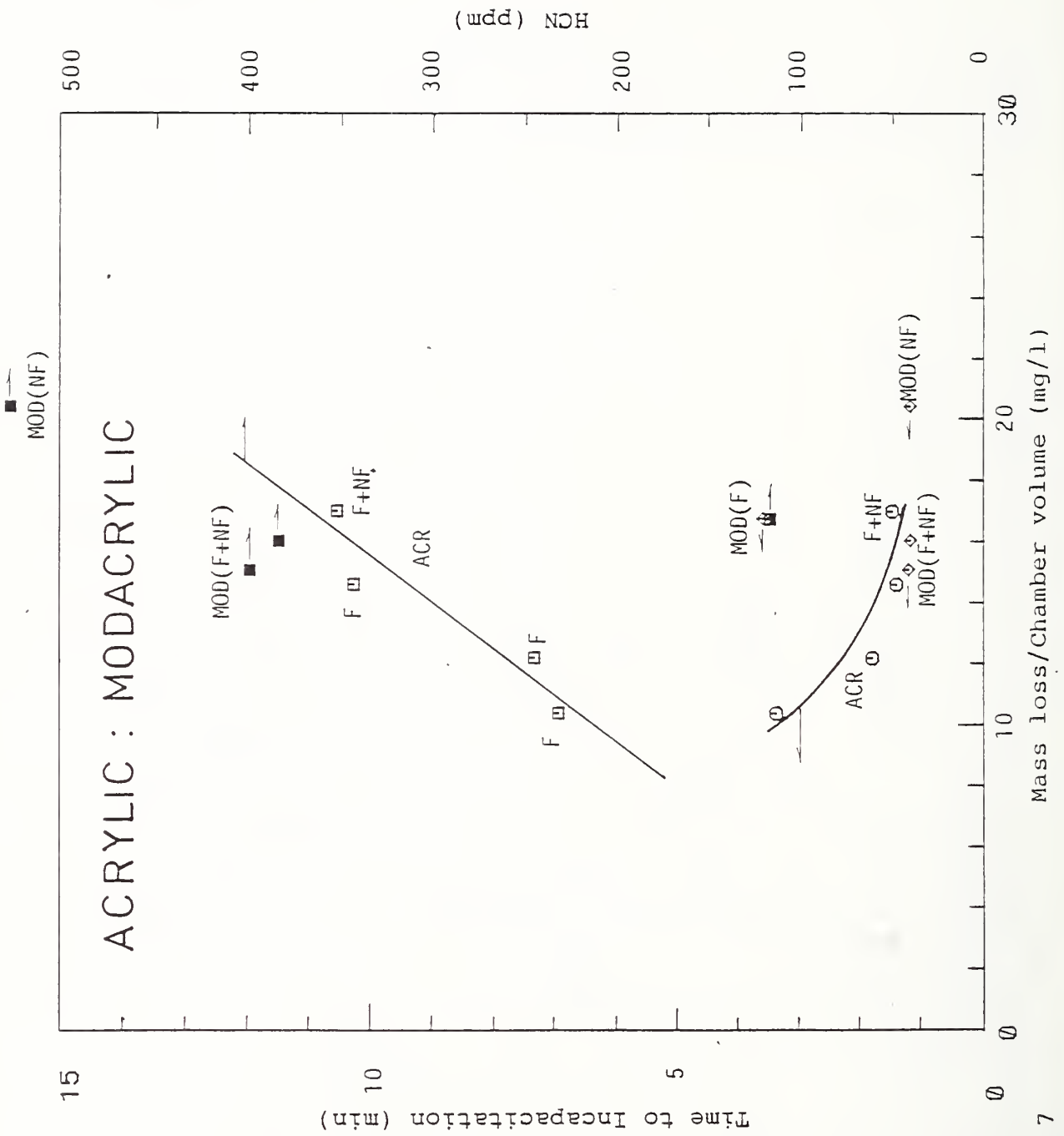


Fig. 7

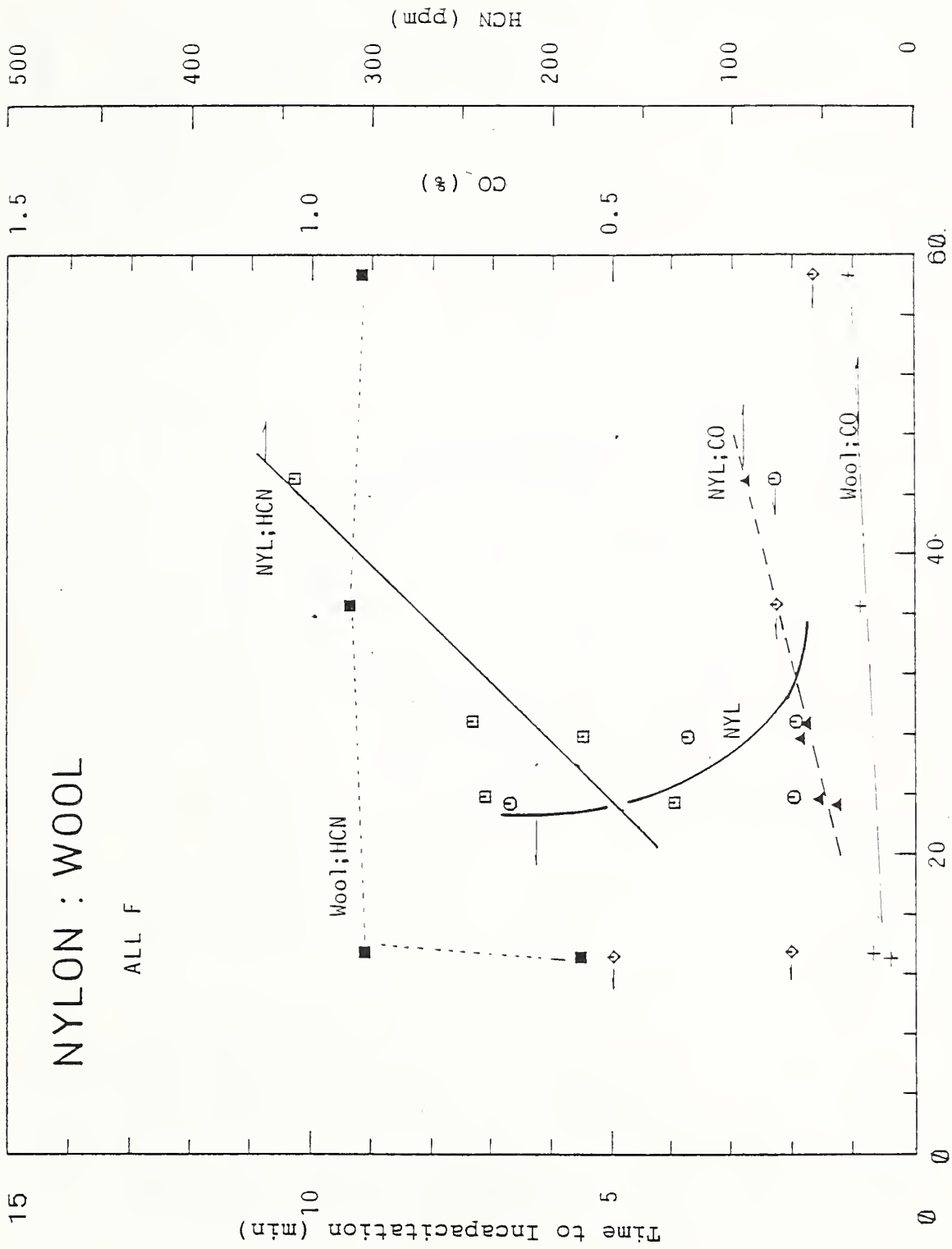
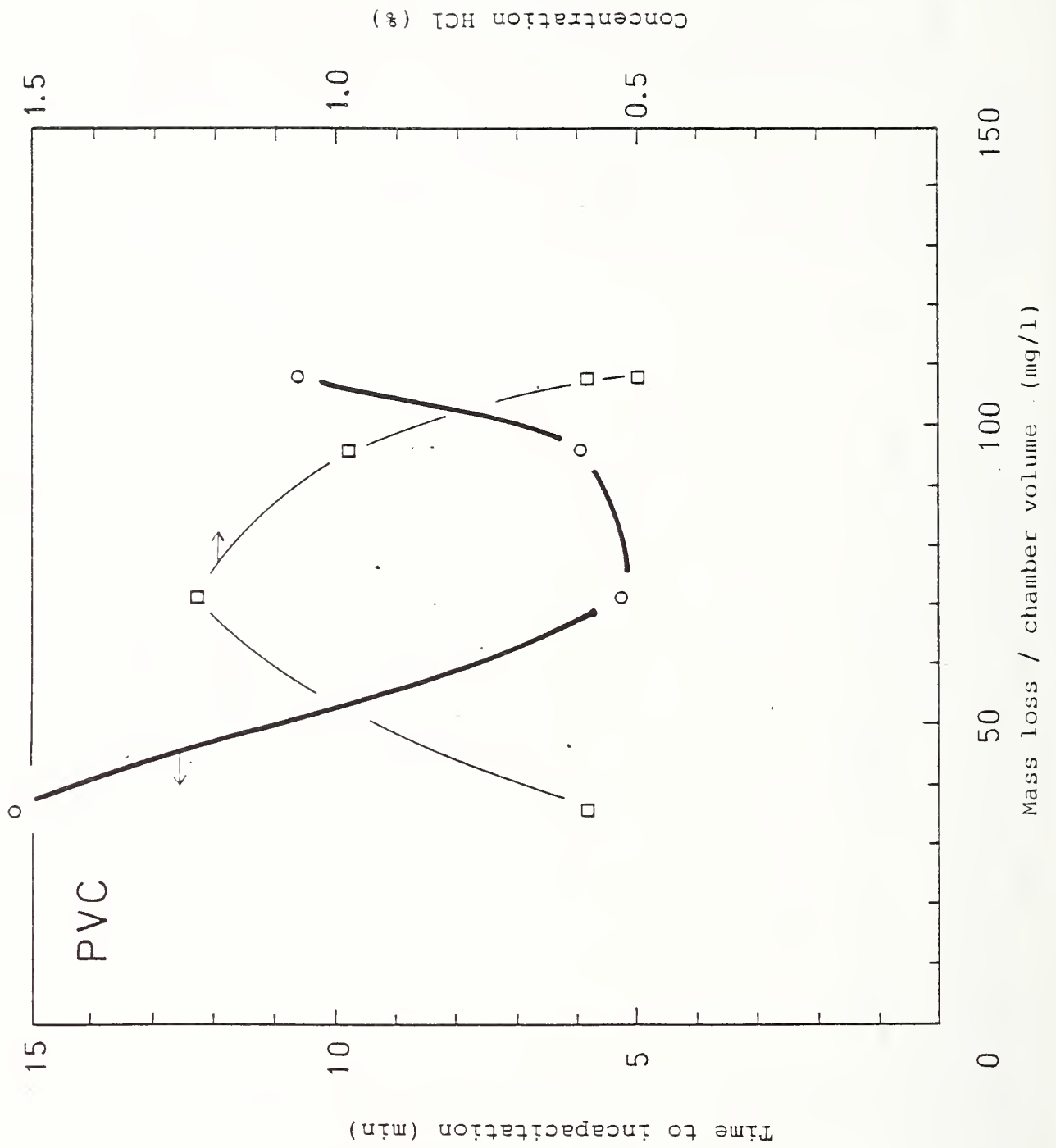


Fig. 8



Concentration HCl (%)

1.5

1.0

0.5

150

100

50

Mass loss / chamber volume (mg/l)

PVC

15

10

5

0

Time to incapacitation (min)

Fig. 9 Result on animal exposure test for PVC

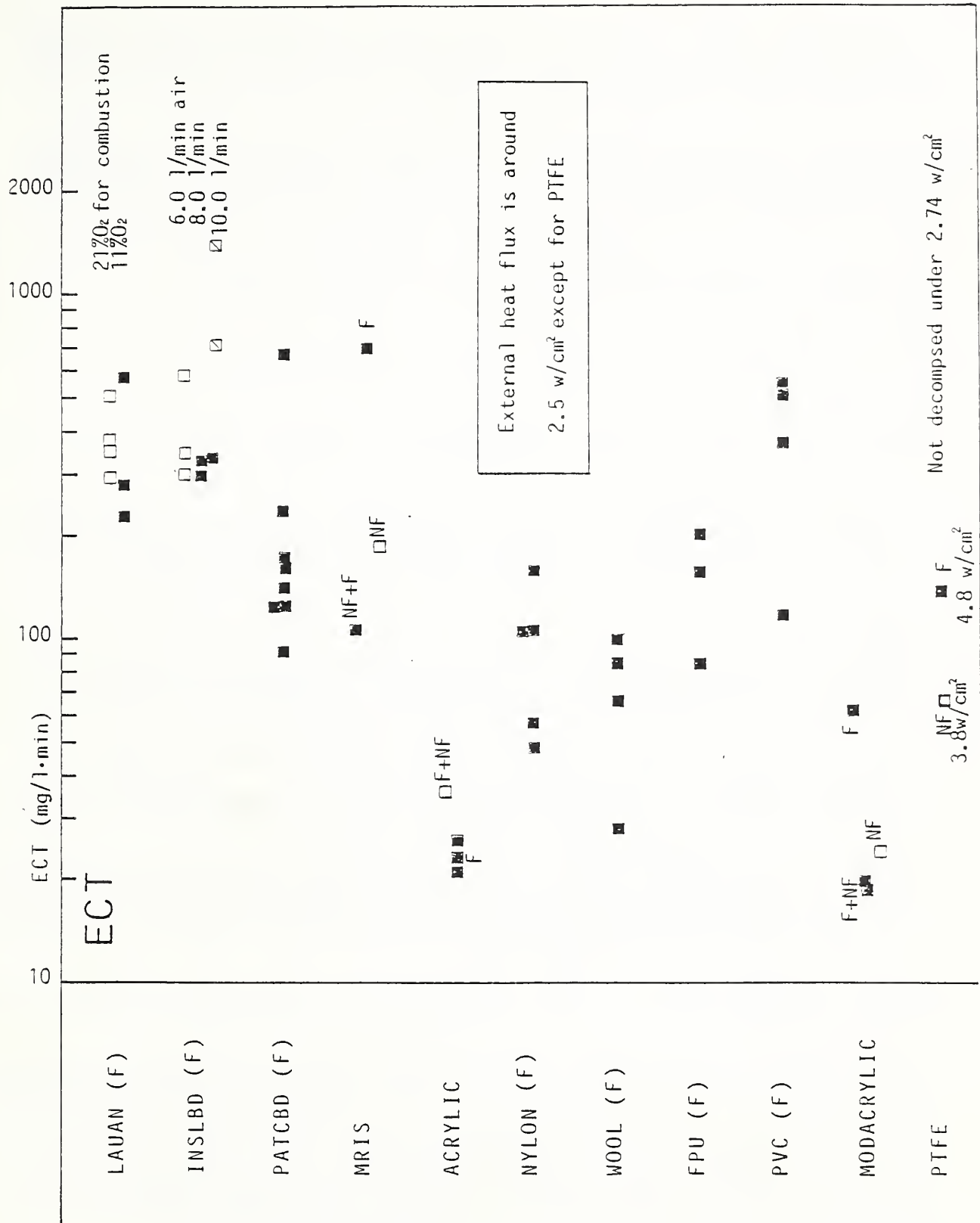


Fig. 10

EVALUATION OF COMBUSTION TOXICITY FROM VARIOUS MATERIALS BY NEWLY DEVELOPED APPARATUS

S. Yusa, Building Research Institute, Japan

TEWARSON: In the charts that you are showing, grams per liter, this is the concentration?

SUSUKI: Yes.

TEWARSON: Basically you are measuring this potential yield?

SUZUKI: Yes.

TEWARSON: Because you must have a density per grams of CO per gram of the mass loss rate.

SUZUKI: Yes, it is the yield of the products. Yield was divided by the size of the room.

TEWARSON: But the interesting part of the data is that as you change the air flow, you are changing the fire ventilation which, in turn, is changing the constraint, which, in turn, is effecting the targeted capacitacion possibility.

SUZUKI: Yes.

TEWARSON: Therefore, this is the first time that the toxicity method is taking into consideration the importance of fire ventilation.

SUZUKI: I appreciate your comment. Mr. Yusa will be happy to learn of it.

TEWARSON: However, you also may have to do some other plots where you could put the fire ventilation versus the effect on animals.

SUZUKI: At this moment, we do not have enough data, we only have enough data to see the tendencies, but I think time will solve these shortcomings. When we were developing this new apparatus we referenced Mr. Tewarson's apparatus a lot, so I'd like to acknowledge it here.

LEVIN: In your Figure 9, I don't understand why, as the mass increases, the HCl is accurate.

SUZUKI: Regarding the result of the CO and the CO₂, we have quite accurate data. However, regarding HCl, the data seems varied and not the steady result we can get here. At this moment, we can say we lack good data for HCl. We still have to gather more HCl data so that we will have more exactness. One more thing, at BRI, we have been measuring HCl by certain time intervals. However, at Factory Mutual, when we visited, they seemed to have the measuring apparatus constantly checking HCl. Perhaps we should adopt that type of instrument in Japan too for this kind of continuous experiment.

TSUCHIYA: About this HCl concentration, I suspect that HCl in the sample is mainly consumed at the maximum point of the concentration curve.

SUZUKI: May I ask you a question? What do you think, is it that things are burnt in a short time, or that a certain amount of burning things is taking a long time to burn, and so HCl can be absorbed by the wall or some other things?

TSUCHIYA: I don't know the answer to your question. Is your question related to the pyrolysis reaction of PVC? After the first stage of pyrolysis, HCl goes up first; then carbon further decompose. You measure these two stages of reaction. I don't think this is caused by absorption.

A REVIEW OF THE FIVE-YEAR COOPERATIVE PROGRAM ON SMOKE TOXICITY
by R. Gann, H. Suzuki, and Y. Tsuchiya

Presentation by Richard Gann

The five-year period is drawing to a close and we have just finished the 6th Expert Panel Meeting. In reviewing the accomplishments of this group, I am very encouraged by the amount of work that has been performed. And yet we still are not quite at the end point. Let me briefly summarize what I see as some of the principal accomplishments.

Over this five-year period, we have apparently reached a consensus that the use of mixed gas data is an excellent way to represent the toxicity of fire smokes. To this end a sizable amount of new data and analysis of data have been performed in all countries. We are now well on the way to using this as a basis for reducing the dependence on animal testing. At the same time, this data is highly usable as input for fire hazard and risk modeling. The second observation that I would make is that we are finally beginning to do the proper experiments at real scale to allow us to determine the relevance of the various bench-scale toxicity measurement methods. I don't think that the fact that we are just doing this now is a mistake on our part. Much of the knowledge that allows us to do relevant testing today has come from the prior five years of research. The third area I would like to comment on is the animal end point that we are using. While most of the data that we are taking is still neither on animal deaths or on very serious impairment of the animals, we are just starting to get some data on the threshold for abnormal behavior as a result of smoke inhalation. If we understand the concentrations of smoke that barely produce effects and, at the other end of the spectrum, the concentrations that produce animal deaths, we then are in a position to assess realistically the kinds of safety factors that need to be used. I think we need to do far more work on this threshold measurement, such has been performed by Professor Alarie and reported at the last Expert Meeting.

Those are the major accomplishments I see. I now would like to spend a moment on where we have not yet been. Five years ago we set a very ambitious goal for ourselves; that was the development and testing of a single test method for smoke toxicity. This was, in fact, a quite proper goal. However, it was far too ambitious for the amount of resources we have been able to develop. I feel meeting this goal is, in fact, possible and that if we don't set aggressive goals for ourselves, we would not have achieved what we have over the last five years.

I will conclude by stating that I hope this cooperative effort will continue, that significant effort will continue to be expended on the multiple gas approach, that both experimental and analytical efforts will be spent on validating small-scale test methods, and that we will indeed be able to define the proper criteria for a bench-scale data generator.

Presentation by Hiroaki Suzuki

I appreciate the fact that Dr. Gann and Dr. Tsuchiya attended the first Tripartite Meeting on toxicity and contributed to the progress of the study on toxicity. One of the difficulties in studying the toxicity issue is that we cannot find the definitive fixed criteria for the exposure conditions. Therefore, we had to conduct bench-scale tests and then we had to find out the relevance of these bench-scale tests to large scale. We had to find a correlation between the two experiments. Our next task was to implement the apparatus design and gather data. Then we had to come up with some sort of a criterion for prediction. So these are the tasks for the scientists. On the slide, I have listed five major objectives. We have achieved quite a bit on the objectives. Also, there are certain cases where, even though an excellent test method was developed, this test method was not necessarily applicable to the situation. For instance, if we were to use certain measurements for a test method, we might come up with the kind of data that indicates low level or high level toxicity. However, when you report the results and conditions in the actual situation, as often is the case, we tend to forget about the conditions. For instance, the experimental data we gathered under the certain conditions cannot necessarily predict toxicity of the certain toxicants or predict the toxicity level. As scientists we should be able to evaluate the toxicity of the materials even if the evaluation of the combustible material is not necessarily in harmony with commercial bias. As a scientist I feel that it is important to find the basic conditions and also the basic principles for explaining toxicity. We have so far experimented with the toxicity level by using animals such as mice; however, if we are to experiment with that kind of toxicity on human beings, that seems to be rather cruel. Yesterday the medical doctor showed slides where the dead, grotesque body, caused by fire, was really a horrible sight. Therefore, we must prevent that type of casualty at all costs by finding out the scientific facts. Since we cannot experiment on a human being at the toxicity level, but, after the fact, we can examine the dead body and gather data from that, then we can use that data for preventing that kind of casualty. Even though we have almost completed the five-year project, our research activity must continue. In the future we should continue the trilateral research cooperation. We may not be able to have this kind of meeting on a regular basis but, with the cooperation of the UJNR, we should have a Expert Meeting such as this as often as we can. We also need help from the research organizations throughout the world.

Presentation by Yoshi Tsuchiya

I would like to review our activities in this Tripartite cooperation on fire gas toxicity. Incidentally, I am the only person who has witnessed the development from the beginning. This cooperation officially started in 1982. In June 1982, there was a director's meeting in Ottawa. At that meeting the three countries agreed to cooperate in the fire gas toxicity study. Prior to the Tripartite cooperation there was a bilateral cooperation between Canada and Japan, starting in 1980. This cooperation was a little bit different from the present Tripartite cooperation. The cooperation was on a much narrower subject and there was much closer cooperation. Discussions started with Dr. Saito of BRI and myself. At that time BRI already had expertise in animal testing. We had no experience, even today, in animal testing but we had expertise in analysis of fire gases. We helped the Japanese group by giving our expertise in chemical analysis and we were helped by the Japanese group with their knowledge of animal testing. We exchanged only information, but we ran experiments together. I proposed to use the Ohio State University heat release rate apparatus for the generation of combustion gases. We had one at that time and BRI built one. We studied the components of combustion gases by burning various materials in this apparatus at the same conditions of combustion and in Japan they burned the same materials and determined the effect on animals. That was the start of bilateral cooperation. Before that, about 18 years ago, I proposed to run animal tests at our institution. At that time not many research institutions were running animal tests. I proposed a study of fire gases using animals, but our director did not give us approval for that. The possible reason was that we were not biologists or physiologists, but chemists. The positive reason was that we had some expertise in analysis at that time. After the cooperation started, we had a good reason to develop our analytical expertise. We have developed analytical facilities since this cooperation started. Now we are one of the best equipped laboratories as far as fire gas analysis is concerned. In these cooperative activities we worked in three areas. One is the development of analytical techniques. We have GCMS with which we can analyze organic components of fire gases. We have APCIMS and with it we can analyze fire gases in real time. Also, we have ICHPLC with which we can analyze inorganic gases and aldehydes. In regard to analytical information, our function in the cooperative program is disseminating information to other countries. The second area is mathematical analysis of fire gas toxicity. In this area we developed mathematical equations in cooperation with members of BRI. For necessary data to input into this equation, we used animal data built by many groups, for example, Dr. Saito, Mr. Sakurai of Japan and Dr. Hartzell and many other groups in the United States. At this moment we can predict incapacitation time or lethal time in a given toxic gas atmosphere. In this area, I believe this cooperation has had very fruitful results. Our future area is full-scale tests. This is just my review of the cooperation. In the future even this official cooperation may terminate, but actual research will proceed.

PANEL DISCUSSION: A REVIEW OF THE FIVE YEAR COOPERATIVE PROGRAM ON SMOKE TOXICITY

R. Gann, H. Suzuki, and Y. Tsuchiya

HARTZELL: I would like to go along with those remarks made by Dr. Gann and Dr. Tsuchiya, in that I feel amazing progress has been made in the last five years for being able to predict toxicological effects. Certainly, as far as rodents are concerned, and with some additional information, I think we can go a long way towards predicting those effects for humans. In some ways, it's a shame that so many of our resources have been spent in the last few years on test method development, and not into this type of thing. Unfortunately, in this country this is still true that many of our resources are being spent, I think, in the wrong direction.

The second comment, in the nature of test methodology, I'd like to say that I am more impressed all the time with the test method under development by Dr. Yusa. I've been involved for a number of years with the work of ISO TC92 FC3, and I must say that I feel that Dr. Yusa's method probably satisfies more of the criteria being developed in ISO than any of the other test methods currently in use or being considered. I commend the Japanese and Dr. Yusa.

TEWARSON: Where would we find the data from the Ohio State University?

TSUCHIYA: Unfortunately, these results will not be published. We found that, in most cases, animals are not necessary. In this study, a very narrow range was used to determine very accurate information to determine the effect on living animals. In most cases, under normal fire conditions, all of the animals died or did not die. Therefore, in most cases, after fire conditions, animals aren't necessary.

TEWARSON: If I requested the data, will I be able to get it?

TSUCHIYA: No, I don't think so; the analysis is not complete.

TANAKA: This is not a question, but I would like to express my greatest appreciation for the American and Canadian scholars' cooperation in achieving the results.

Since the analysis we are all experts involved with the toxicity study, some of you might have questions about the Tripartite Cooperative in this effort. To be honest with you, when we initiated this topic, we asked for help from Canada and the United States. For this cooperative joint project, we received a rather larger sum of funds from the Japanese Science and Technology Agency. Because of this large sum of funds, we could study effectively the toxicity of the materials and could provide the necessary data.

The major benefits obtained from this project to the Tripartite Cooperative were that the American and Canadian researchers contributed to Japan, in terms of philosophy and methodology and data on toxicity. In Japan, as you know, the Japanese building code specifies the toxicity test method. Therefore, we need to upgrade the existing toxicity test method. In this sense, this meeting was very meaningful in terms of learning about upgrading the test methods. Because of the funds received from the fire and technology agencies,

we could establish many research institutes, laboratories, facilities, and what not. In addition to that, we could establish the research group. Therefore, we want to continue this kind of research activity from now on, and we also will need your help in the future.

OPEN TECHNICAL SESSION (CONT.)

Characterization Of Flame Spread Over PMMA Using Holographic Interferometry Sample Orientation Effects

Akihiko Ito¹ and Takashi Kashiwagi
Center For Fire Research
National Bureau Of Standard
Gaithersburg, MD 20899

ABSTRACT

Flame spread over a thermally thick slab of PMMA at several angles of sample orientation from $\theta = -90^\circ$ (vertically downward flame spread) to $\theta = +90^\circ$ (vertically upward flame spread) in air was investigated by measuring temperature distributions within the PMMA sample in the vicinity of the leading edge of the flame front using holographic interferometry. Samples with widths of 0.32, 0.47, 1.0, and 2.5 cm, a thickness of 2.5 cm and a length of 30 cm were used. The measured net heat flux from the gas phase to the sample surface at the vaporization front of the sample is about 7 W/cm^2 for downward flame spread ($\theta < 0^\circ$), 6.5 W/cm^2 at $\theta = +10^\circ$ and 2.8 W/cm^2 at $\theta = +90^\circ$. However, the total net heat transfer rate increases with an increase in the angle of sample orientation, because the characteristic heating length, defined as the distance from the adiabatic point on the sample surface to the vaporization point, increases with an increase in the orientation angle of the sample. The total net heat transfer rate into the sample from the gas phase is about 56% of the total net heat transfer input to the sample at $\theta = -90^\circ$, 78% at $\theta = 0^\circ$, 87% at $\theta = +10^\circ$, and 99% at $\theta = +90^\circ$. Therefore, heat transfer from the gas phase into the unburnt fuel ahead of the vaporization point is the dominant heat transfer path for all angles of orientation. This was clearly demonstrated by the net heat flow vector patterns within the sample. The conductive heat transfer rate through the sample decreases with an increase in flame spread rate (increase in the sample orientation angle) due to insufficient time being available for the slow thermal wave to travel through the sample.

1. INTRODUCTION

In the initial stages of building fires, flame spread over the surface of combustible solid materials such as a floor covering, a wall or interior furnishings is the key determinant of the rate of the fire growth. The controlling mechanism of flame spread appears to differ with the surrounding conditions, such as the ambient oxygen concentration or the gas flow velocity.^(1,2) The flame spread rate in air is controlled by the rate of thermal energy feedback from the flame to the unburned fuel surface.^(3,4) This heat feedback rate differs significantly with the direction of flame spread relative to the direction of the gas flow.⁽⁵⁾ Since upward flame spread rate over a PMMA surface is one or two orders of magnitude faster than downward flame spread,⁽⁶⁻⁸⁾ it is expected that the heat feedback rate differs significantly with the sample orientation angle. In practical

¹Guest worker from Oita University, Oita Japan.
Current address: Oita University, 700 Dannoharu, Oita Japan.

application, flame spread over various furnishings occurs at many different orientation angles.

In order to determine heat feedback rates from the flame to the unburnt fuel surface, one needs the detailed temperature profiles in the gas phase and also in the condensed phase. For this reason, Fernandez-Pello *et al.*⁽⁷⁾ Hirano *et al.*,⁽⁸⁾ and Ray *et al.*⁽⁹⁾ measured the temperature distributions using thermocouples in the gas and the condensed phases for downward vertical or horizontal flame spread on PMMA. Saito *et al.*⁽¹⁰⁾ measured the surface temperature histories for upward flame spread over a PMMA surface. However, when using thermocouples, it is difficult to measure the temperature distribution with sufficient spatial resolution within the critical thin thermal layer in the vicinity of the traveling flame front. Therefore, heat feedback rates calculated from the measured temperature distribution using thermocouples do not have high accuracy, particularly at the sample surface due to the steep temperature gradient at the surface.

The present authors recently applied a holographic interferometry technique for determining the temperature distribution within a transparent solid such as PMMA by measuring changes in refractive index of the material.⁽¹¹⁾ A high spatial resolution, 30 μm , in the temperature distribution measurement is obtained by this technique. Therefore, the heat flux distribution can be determined very accurately. In our previous paper,⁽¹²⁾ the temperature distributions in a thick slab of PMMA during vertically downward flame spread were measured by this technique. In this study, the same technique was applied to flame spread over a PMMA sample in air at several angles of orientation from $\theta = -90^\circ$ (vertically downward flame spread) to $+90^\circ$ (vertically upward flame spread). The results of temperature and net heat flux distributions in the PMMA sample are presented, and the effects of the sample orientation angle on the net heat feedback rates and the heat transfer process in the sample are discussed in this paper.

2. EXPERIMENTAL PROCEDURE AND APPARATUS

Since the detailed description of the relationship between temperature and the fringe number and also the detailed discussion of the technique were described elsewhere,⁽¹¹⁾ only a brief description is presented in this paper. The relationship between the temperature and the fringe number, N , can be expressed as⁽¹¹⁾

$$B \int_{T_\infty}^T (dn_p/dT)dT + \alpha B(T - T_\infty) \left[\int_{T_\infty}^T (dn_p/dT)dT + n_{p_\infty} - n_{a_\infty} \right] = \lambda(2N - 1)/2$$

where B is the width of the sample. The term dn_p/dT is the thermo-optic coefficient of the material, α is the linear thermal expansion coefficient, n_{p_∞} is the refractive index of the material at the ambient temperature, n_{a_∞} is the refractive index of air at the ambient temperature, and λ is the wavelength of the light. The thermo-optic coefficient and the linear thermal expansion coefficient of PMMA have been recorded up to a little over the glass transition temperature (about 105°C).⁽¹³⁾ Above the glass transition temperature, accurate data for these coefficients are not currently available. Therefore, the surface temperature history measured with a fine thermocouple was used as the reference temperature to analyze interference fringes above the glass transition temperature.

Since the refractive index change of PMMA due to temperature change is much larger than those of gases, the fringe number is more sensitive to temperature for PMMA than for gases. Therefore, a short path length through the sample is required to be able to resolve each fringe. However, a wide sample is needed to insure that temperature distributions in the gas phase and in the condensed phase are two dimensional. This condition is necessary because the technique used in this study is based on the integral of the change in refractive index along the sample width. The experimental configuration was arranged to satisfy the above two conflicting requirements.⁽¹²⁾ Two thin sheets of quartz with a 0.09 cm thickness were installed at both sides of the PMMA sample with a small clearance. This clearance is close to a quenching distance, about 0.15-0.17 cm, which prevents flames passing over both sides of the sample and insures two-dimensional flame spread. These sheets of quartz hardly affect the fringe shift because their thermo-optic coefficient and thermal expansion coefficient are much less than those of PMMA and also their thickness is much less than that of the sample. A PMMA sample was supported by an aluminum holder to form many different orientation angles with respect to the horizontal plane as shown in Fig. 1. For the recording of holograms, the double exposure method⁽¹⁴⁾ was employed for the experiments in which steady or near steady flame spread was observed. However, the real time method⁽¹⁴⁾ was used for the experiment with unsteady accelerating flame spread which was observed in the vertically upward mode. The optical setup and the holographic procedure were described in our previous paper.⁽¹²⁾

A 25 μm wire diameter chromel-alumel thermocouple was used to measure the history of the surface temperature of the sample during the flame approaching period. To assure good contact between the thermocouple and the PMMA surface, the thermocouple was heated electrically and pressed onto the surface prior to the test. The surface temperature measurement by the thermocouple was conducted simultaneously with the interferometric measurement. Cast slabs of Lucite L (E.I. du Pont de Nemours & Co.)² with widths of 0.32, 0.47, 1.0 and 2.5 cm, a thickness of 2.5 cm and a length of 30 cm were used as samples in this study. The selection of Lucite L was based on its cleaner burning than previously studied Plexiglas G.⁽¹⁵⁾

3. RESULTS AND DISCUSSION

3.1 FLAME SPREAD RATE

The observed steady flame spread rate at $\theta = -90^\circ$ (vertically downward) was 5.8×10^{-3} cm/s for a sample width, B, of 0.32 cm, 5.5×10^{-3} cm/s for B = 0.47 cm and 5.0×10^{-3} cm/s for B \geq 1.0 cm. The results on flame spread rate for the sample 0.47 cm wide, 2.5 cm thick and 30 cm long at various angles of the orientation are shown in Fig. 2; they are compared with the results reported in previous studies^(7,8) using different PMMA samples. The comparison indicates that flame spread rates measured in this study are slightly higher than those previously reported at $-90^\circ = \theta \leq 0^\circ$ but they become slightly slower than those reported at $\theta \geq +10^\circ$. Since it was reported that flame spread rate over Plexiglas G was slightly slower than

²Certain materials are identified in this paper in order to adequately specify the experimental procedure. Such identification does not imply that the material is necessarily the best available for the purpose.

that over Lucite L at $\theta = -90^\circ$,⁽¹⁵⁾ this slight difference in flame spread rate shown in Fig.2 might be due to the difference in material. The vaporization front was a straight line across the sample surface perpendicular to the direction of downward flame spread. Therefore, it is assumed here that the specific experimental configuration shown in Fig.1 and described in the previous section did provide the two-dimensional flame spread comparable to a large width sample at $\theta \leq 0^\circ$.

For vertically upward flame spread ($\theta = +90^\circ$), the initial short flame is laminar and blue. After the flame travels about 10 cm from the ignition line, the blue flame changes to a yellow flame with some fluctuation. The temperature distribution was measured at 20 cm from the ignition line. Although the flame is yellow and unstable, it appears to be in the transition regime and may not be a fully developed turbulent flame. Flame spread is accelerating and it is difficult to measure its rate accurately. Although the measured flame spread rate and the temperature distribution which will be described in the next section are not universal values at $\theta = +90^\circ$, the observed trends are very clear compared with those at other sample orientation angles.

3.2 TEMPERATURE AND HEAT FLUX DISTRIBUTIONS

Typical interferograms are shown in Fig. 3. Since a condensed fuel must supply evolved combustible products to the gas phase to form a flame, the vaporization front of the sample surface is defined at $x = 0$ in this study where x is the coordinate parallel to the sample surface and it increases with downstream distance. The visible flame front extends further forward from the vaporization front. This overhang distance of the flame increases with an increase in the angle of the sample orientation.

In these interferograms, it is noted that the fringe pattern sometimes behaves abnormally. This is caused by the glass transition in the PMMA sample. The thermo-optic coefficient of PMMA decreases with an increase in temperature (negative value), but the thermal expansion coefficient increases with an increase in temperature.⁽¹¹⁾ Near the glass transition temperature, about 105°C , the term including these coefficients becomes close to zero. Therefore, the fringe pattern appears to be at a singular point at the glass transition temperature of PMMA. Except for the glass transition layer, however, the fringes shown in Fig. 3 correspond to isotherms.

Fig.3(a) shows that the surface temperature at $\theta = -90^\circ$ starts to increase from about $x \approx -1$ cm, and the adiabatic condition at the surface is reached at about -0.34 cm, where the fringe is normal to the surface. The sample surface slightly loses heat to the gas phase at $x < -0.34$ cm because the interior temperature of the sample is slightly higher than the surface temperature. The number of fringes gradually increases until the glass transition layer and it increases significantly within the distance of 0.2 cm from the glass transition layer to the vaporization front indicating a steep temperature increase. In the distance between the adiabatic point and the vaporization front, net heat is transferred from the gas phase into the sample. A "characteristic length for flame spread", l , can be defined as this distance. This characteristic length increases with the increase in the angle of the sample orientation. For the vertically upward flame spread shown in Fig.3(b), the adiabatic condition is not found in this figure

because this point is located well ahead of the vaporization front, about at $x = -5$ cm.

Surface temperature histories measured by a thermocouple at various sample orientation angles are shown in Fig. 4. The results show that the surface temperature at the vaporization front ($x = 0$) is about 380°C at the angles of -90° , -30° and 0° . However, this vaporization temperature tends to decrease with an increase in the angle of the sample orientation for upward flame spread, for example, about 375°C at $\theta = +10^\circ$ and about 365°C at $\theta = +90^\circ$. The difference in vaporization temperature between upward and downward flame spread must be due to the difference in heating rate. For vertically downward flame spread, the sample is rapidly heated from ambient temperature to the vaporization temperature within a short time. On the other hand, since the flame front in upward flame spread extends further ahead of the vaporization front, the sample is slowly heated over a long time.

The temperature distributions within the condensed phase were calculated from the interferograms using the surface temperatures measured by a thermocouple above the glass transition temperature region. By taking the spatial derivative of the temperature distributions, conductive heat fluxes in the direction normal to the surface, q_y , are calculated. The results for the conductive heat flux at the surface, q_{y0} , are plotted in Fig. 5. Ahead of the vaporization front, the meaning of q_{y0} can be defined from the energy balance at the surface which can be expressed as

$$q_{y0} = \lambda_s (\partial T/\partial y)_{y=-0} = \lambda_g (\partial T/\partial y)_{y=+0} + Q_{rf} - \epsilon_s \sigma (T_s^4 - T_a^4) \quad \text{at } y = 0 \quad (2)$$

where λ_s and λ_g are the thermal conductivities of the sample and gas, respectively, Q_{rf} is the radiative flux from flame, ϵ_s is the emissivity of the sample, σ is the Stefan-Boltzman constant, T_s is the surface temperature of the sample and T_a is an ambient temperature. The first term of the right hand side of Eq.(2) represents the convective/conductive heat flux from the gas phase. The third term represents the radiative heat loss from the surface to surroundings. Therefore, q_{y0} is the net heat flux from the gas phase at the sample surface. The results shown in Fig. 7 indicate that the value of q_{y0} at $\theta = -90^\circ$ increases sharply from 0 to about 7 W/cm^2 within a short characteristic distance of about 0.34 cm. The value of q_{y0} at $x = 0$ for downward flame spread ($\theta < 0^\circ$) does not change significantly with the sample orientation angle and it remains at around 7 W/cm^2 . However, it tends to decrease with an increase in the angle of the sample orientation for upward flame spread. Especially for vertically upward flame spread ($\theta = +90^\circ$), the value of q_{y0} increases gradually from about 5 W/cm^2 at a distance of 5 cm ahead of the vaporization front, and its value does not change significantly within a distance of 2 cm from the vaporization front. The value of q_{y0} reaches to about 2.8 W/cm^2 at the vaporization front. The main reason for this difference between 2.8 W/cm^2 at $x = 0$ for vertically upward flame spread and 7 W/cm^2 for vertically downward flame spread is considered to be accounted for by the observation that the upward spreading flame is far away from the sample surface; therefore, the conductive/convective heat flux from the flame is much smaller than that of the downward spreading flame. Although the experimental condition is significantly different from this study, a value of 2.5 W/cm^2 was reported for a steady wall burning study.⁽¹⁷⁾

Conductive heat fluxes in the direction parallel to the sample surface, q_x , were calculated from the measured temperature distributions similarly to q_y . The results for heat flux conducted through the sample at $x = 0$, Q_{x0} , are plotted in Fig. 6. This figure indicates that the value of q_{x0} decreases significantly with an increase in the sample orientation angle, for example, from about 3.2 W/cm^2 at $\theta = -90^\circ$ to about 0.1 W/cm^2 at $\theta = +90^\circ$. Since the value of q_{x0} decreases in spite of increasing in flame spread rate with an increase in θ , the contribution of conductive heat transfer through the sample to the overall energy balance for flame spread decreases with the increase in the sample orientation angle. Further detailed discussion of the overall energy balance will be given later.

3.3 FLAME SPREAD MECHANISM

Isotherm contours and heat flux vectors (determined from the values of q_y and q_x) in the sample in the vicinity of the flame front were obtained to examine the heat flow path in the sample. The typical results are shown in Fig. 7(a) at $\theta = -90^\circ$ and 7(b) at $\theta = +90^\circ$. Broken lines in these figures are isotherms and arrows are heat flux vectors which indicate the magnitude of the heat flux and the direction of heat flow. For vertically downward flame spread, heat flows into the sample at relatively steep angles and large magnitudes especially near the vicinity of the vaporization front. The magnitude of the heat flux decreases rapidly with the distance away from the vaporization front. At about 0.4 cm ahead of the vaporization front, the direction of the heat flow is nearly parallel to the sample surface and beyond 0.4 cm the heat starts to flow toward the surface from the inside of the sample. The overall heat flow pattern at $\theta = 0^\circ$ is similar to that at $\theta = -90^\circ$. On the other hand, for vertically upward flame spread shown in Fig. 7(b), the direction of the heat flow over the entire figure is almost normal to the sample surface. This indicates that heat conduction through the sample in the direction parallel to the surface is negligible for the vertical upward flame spread mode.

The temperature and heat flux distributions were used to construct an energy balance in the condensed phase. The control volume is the layer from $x = 0$ to $-\infty$ and $y = 0$ to $-L$ (L is the depth of the sample). Then, the net heat transfer rate into the control volume from the gas phase is

$$Q_g = \int_{-\infty}^0 \lambda \frac{\partial T}{s \partial y} \Big|_{y=0} dx = \int_{-\infty}^0 q_{y0} dx, \quad (3)$$

and the amount of heat conducted into the control volume through the plane of $x = 0$ is

$$Q_c = \int_{-L}^0 \lambda \frac{\partial T}{s \partial x} \Big|_{x=0} dy = \int_{-L}^0 q_{x0} dy. \quad (4)$$

The rate of heat loss from the rear sample surface is

$$Q_L = \int_{-\infty}^0 \lambda_s \frac{\partial T}{\partial y} \Big|_{y=-L} dx \quad (5)$$

Then, the net heat accumulated in the control volume is

$$Q_T = Q_g + Q_c - Q_L \quad (6)$$

This must be equal to the net flow of thermal enthalpy

$$Q = \int_{-L}^0 \rho_s V \left(\int_{T_\infty}^T c_s dT \right)_{x=0} dy \quad (7)$$

The following thermal properties were used to calculate the above integrals; thermal conductivity of the sample $\lambda_s = 2.1 \times 10^{-3} \text{ J/cm s K}$,⁽¹⁸⁾ density $\rho_s = 1.19 \text{ g/cm}^3$, and values of specific heat C_s based on the results of ref.(19). The calculated values of Q_g , Q_c , Q_T , and Q for each angle of the sample orientation are shown in Table 1. The results show that the net heat transfer rate from the gas phase into the control volume, Q_g , increases with an increase in the sample orientation angle, but the conductive heat transfer rate through the sample across the plane of $x = 0$, Q_c , decreases with an increase in the angle. The net heat accumulated in the control volume, Q_T , also increases with an increase in the angle and its change with the angle is roughly proportional to a change in flame spread rate. The values of Q_T are about 3-7% larger than those of the net flow of thermal enthalpy, Q . This difference is mainly due to heat loss by surface reradiation from the sides of the sample, which is not counted in the energy balance. The fraction of Q_g in the total net heat transfer rate, Q_T , as described by Eq.(6) is about 56% at $\theta = -90^\circ$, 70% at $\theta = -30^\circ$, 78% at $\theta = 0^\circ$, 87% at $\theta = +10^\circ$ and 99% at $\theta = +90^\circ$. Therefore, the heat transfer from the gas phase into the sample surface ahead of the vaporization front is the dominant heat transfer path for all angles of orientation of thermally thick PMMA samples. This does not necessarily mean that heat conduction through the sample in the direction parallel to the surface is negligible. This is particularly true for flame spread at from $\theta = -90^\circ$ to $\theta = 0^\circ$.

The isotherm contours and heat flow vectors shown in Figs.7 indicate that the high temperature region is located only in the vicinity of the flame front, i.e., there is a "critical zone" defined by the two length scales l and δ in the x and y directions, respectively. The characteristic length l can be defined as the distance between the vaporization front and the location where the adiabatic condition is attained at the surface. Then the characteristic time for the non-vaporizing sample to be exposed to the heat from the gas phase, τ , can be expressed as

$$\tau = l / V$$

The thermal wave penetration depth, δ , during this characteristic time period can be expressed as

$$\delta = \sqrt{a\tau}$$

where a is the thermal diffusivity of the sample material. The values of l were determined from the temperature distributions and τ can be calculated from the values of l and V . Then, using the previously described thermal properties of the material, the values of δ were calculated. The results are listed in Table 2. It indicates that τ and δ do not change significantly with change in the sample orientation angle, although l changes significantly as discussed previously. Therefore, the thermal wave velocity, δ/τ , of the sample material is also independent of the angle. The thermal wave has two components; one is in the direction normal to the sample surface, normal heat conduction, and the other is in the direction parallel to the surface, streamwise heat conduction. It appears that the normal heat conduction is nearly independent with a change in the sample orientation angle due to a nearly constant value of τ as shown in Table 2. However, since the flame spread velocity becomes much larger than the thermal wave velocity, δ/τ , for upward flame spread, the effects of the streamwise heat conduction become less significant with an increase in the angle.

4. Conclusions

(1) The surface temperature of PMMA at the vaporization front is about 380°C for downward flame spread. However, it tends to become lower with an increase in the sample orientation angle, such as 375°C at $\theta = +10^\circ$ and 365°C at $\theta = +90^\circ$. This is due to the difference in heating rate.

(2) The net heat flux from the gas phase at the vaporization front is about 7 W/cm² for the downward flame spread ($\theta < 0^\circ$). It decreases with an increase in the sample orientation angle and reaches about 2.8 W/cm² for vertically upward flame spread.

(3) The total net heat transfer rate from the gas phase into the sample ahead of the vaporization front increases with an increase in the sample orientation angle and its fraction of the total net heat transfer rate into the control volume increases from 56% at $\theta = -90^\circ$, 78% at $\theta = 0^\circ$ to 99% at $\theta = +90^\circ$. Therefore, the heat transfer from the gas phase into the sample ahead of the vaporization front is the dominant heat transfer path at all angles of sample orientation. The role of streamwise heat conduction through the sample decreases with an increase in flame spread rate due to insufficient time being available for the slow thermal wave to conduct sufficient energy through the sample.

(4) The characteristic length, l , defined as the distance between the vaporization front and the location where the adiabatic condition is attained at the surface, increases significantly with an increase in the sample orientation angle. However, the thermal wave penetration depth, δ , and characteristic time, τ , are nearly independent of the sample orientation angle.

5. REFERENCES

1. Magee, R. S. and McAlevy III, R.F., J. Fire and Flammability, 2, 217 (1971).
2. Ray, S. R. and Glassman, I., Combust. Sci. Tech. 32,33 (1983).
3. Williams, F. A., Sixteenth Symposium (International) on Combustion, The Combustion Institute, 1281 (1977).

4. Fernandez-Pello, A. C. and Hirano, T., Combust. Sci. Tech. 32, 1 (1983).
5. Ito, A., " Flame Spread Over Thin Combustible Solid", Ph. D Thesis, Tokyo Institute of Technology, Tokyo, Japan (1979).
6. Orloff, L., de Ris, J., and Markstein, G.H., Fifteenth Symposium (International) on Combustion, The Combustion Institute, 183 (1975).
7. Fernandez-Pello, A. C., and Williams, F. A., Fifteenth Symposium (International) on Combustion, The Combustion Institute, 217 (1975).
8. Hirano, T., Koshida, T., and Akita, K., Bullet. Japan Assoc. Fire Sci. Eng. 27, 33 (1977).
9. Ray, S. R., " Flame Spread over Solid Fuels", Ph. D. Thesis, Princeton Univ. (1981).
10. Saito, K., Quintiere, J. and Williams, F. A., Fire Safety Science- Proceedings of the First International Symposium, Hemisphere Publishing Co., 75 (1986).
11. Ito, A and Kashiwagi, T., " Measurement Technique for Determining the Temperature Distribution in a Transparent Solid Using Holographic Interferometry", (in press) Applied Optics.
12. Ito, A. and Kashiwagi, T., "Temperature Measurements in PMMA During Downward Flame Spread in Air Using Holographic Interferometry", Twenty First Symposium (International) on Combustion, (in press).
13. Brandrup J., and Immergut, E.H. Ed. " Polymer Handbook", John Wiley & Sons, New York, v-56, 1975.
14. Vest, C.M. " Holographic Interferometry ", Wiley, New York, chapt. 6, 1979.
15. Kashiwagi, T., Inaba, A., and Brown, J. E., Fire Safety Science - Proceedings of the First International Symposium, Hemisphere Pub. Co., 483 (1986).
16. Waxler, R. M., Horowitz, D., and Feldman, A., Applied Optics 18, 101 (1979).
17. Quintiere, J., Harkleroad, M., and Hasemi, Y., Combust. Sci. Tech., 48, 191 (1986).
18. Hand, S.D. and Horsfall, F., J. Physics E. Scientific Instruments 8, 687 (1975).
19. Bares, V. and Wunderlich, B., J. Polymer Sci. 11, 861 (1973).

Table 1. Net heat transfer rates and net flow of thermal enthalpy.

θ	V (cm/s)	Q_g (W/cm)	Q_c (W/cm)	Q_T (W/cm)	Q (W/cm)
-90°	5.5×10^{-3}	0.52	0.42	0.93	0.89
-30°	6.0×10^{-3}	0.71	0.33	1.02	0.94
0°	7.4×10^{-3}	1.0	0.29	1.3	1.2
+10°	9.5×10^{-3}	1.3	0.22	1.5	1.5
+90°	8.3×10^{-2}	(8.2)	(0.13)	(8.3)	

() means not the steady state value.

Table 2. Characteristic lengths and characteristic time

θ	V (cm/s)	l (cm)	τ (s)	δ (cm) at $x=0$	δ/τ (cm/s)
-90°	5.5×10^{-3}	0.34	62	0.24	3.9×10^{-3}
-30°	6.0×10^{-3}	0.36	60	0.23	3.8×10^{-3}
0°	7.4×10^{-3}	0.44	60	0.23	3.9×10^{-3}
$+10^\circ$	9.5×10^{-3}	0.48	51	0.21	4.1×10^{-3}
$+90^\circ$	8.3×10^{-2}	5.0	60	0.22	3.7×10^{-3}

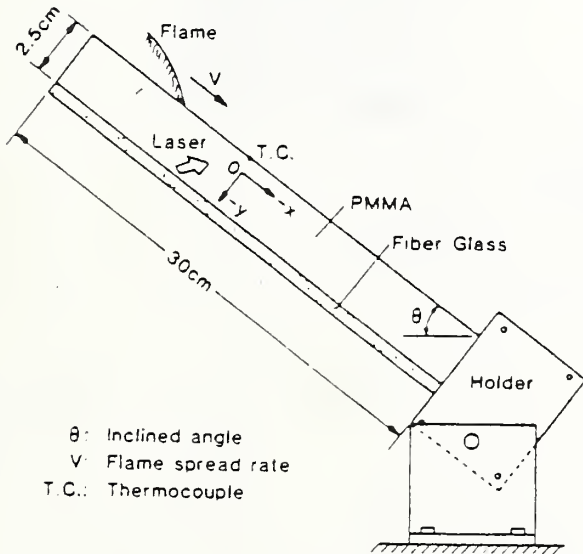


Fig.1. Schematic illustration of the experimental apparatus.

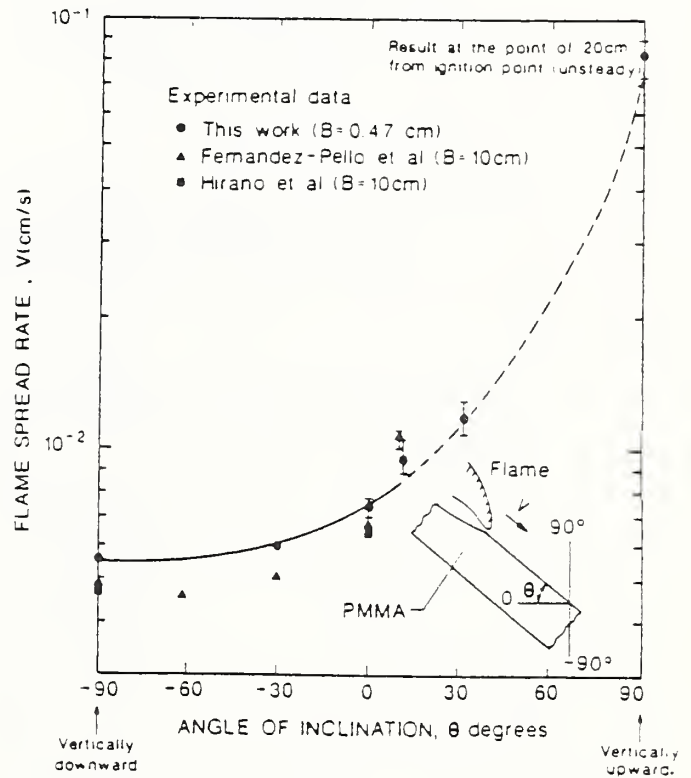
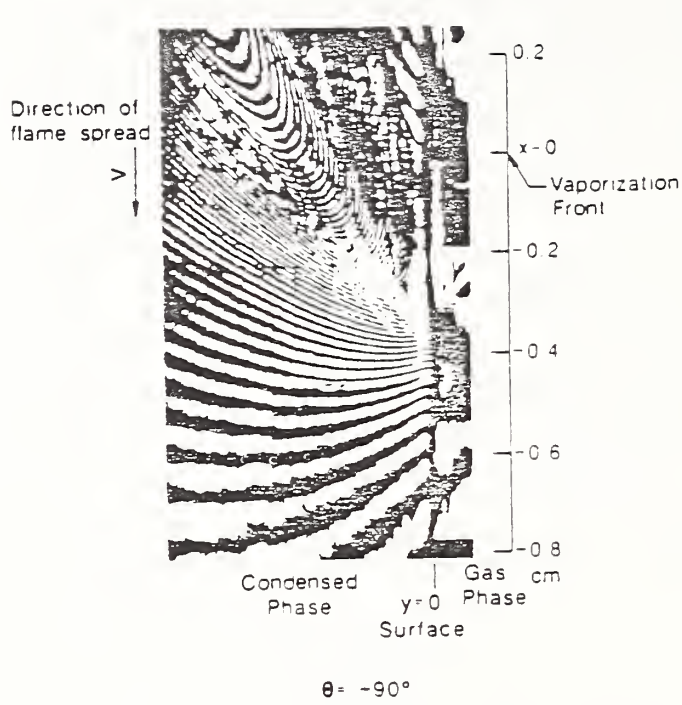
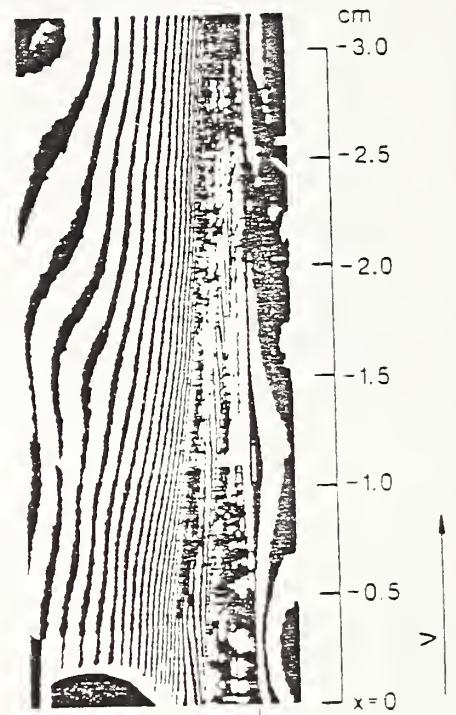


Fig.2. Relation between flame spread rate and the sample orientation angle.



$\theta = -90^\circ$



$y=0$

$\theta = -90^\circ$

Fig.3. Typical interferogram pictures at various sample orientation angles, (a) $\theta = -90^\circ$, and (b) $\theta = +90^\circ$.

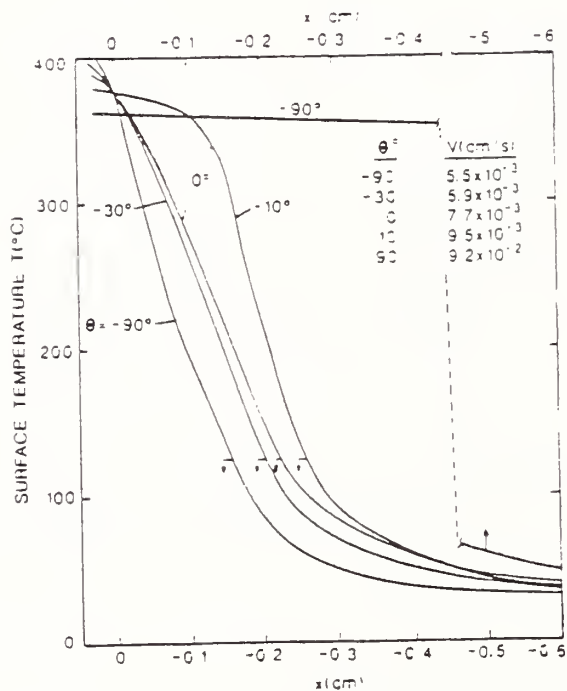


Fig.4. Surface temperature distributions ahead of the vaporization front ($x = 0$ at the vaporization front) at various sample orientation angles.

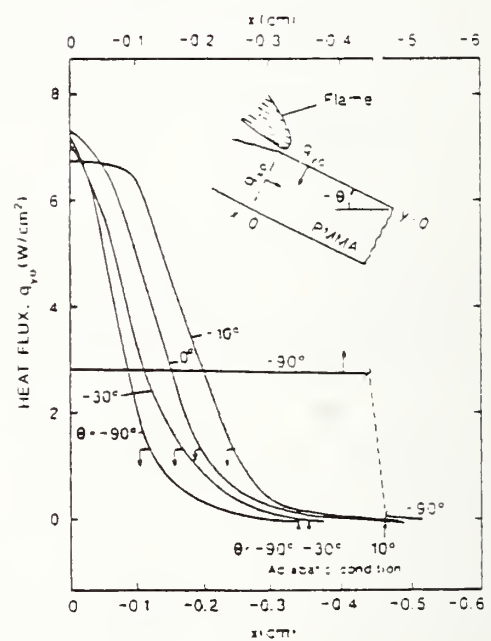


Fig.5. Distributions of normal heat flux at the surface along the distance ahead of the vaporization front.

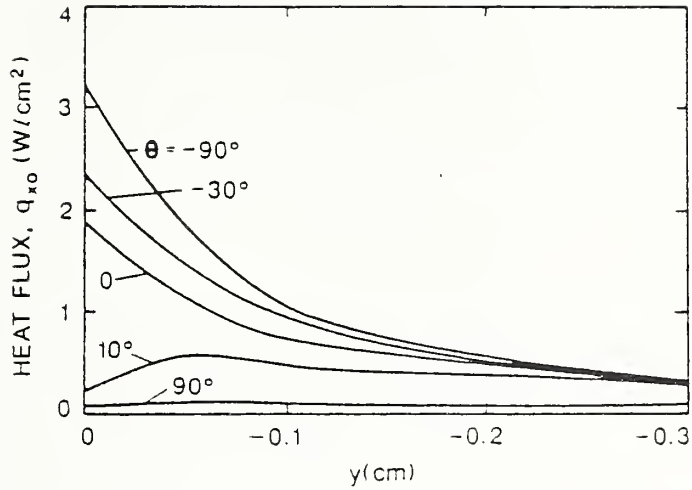


Fig. 6. Distributions of streamwise heat flux at $x = 0$ plane with the sample depth.

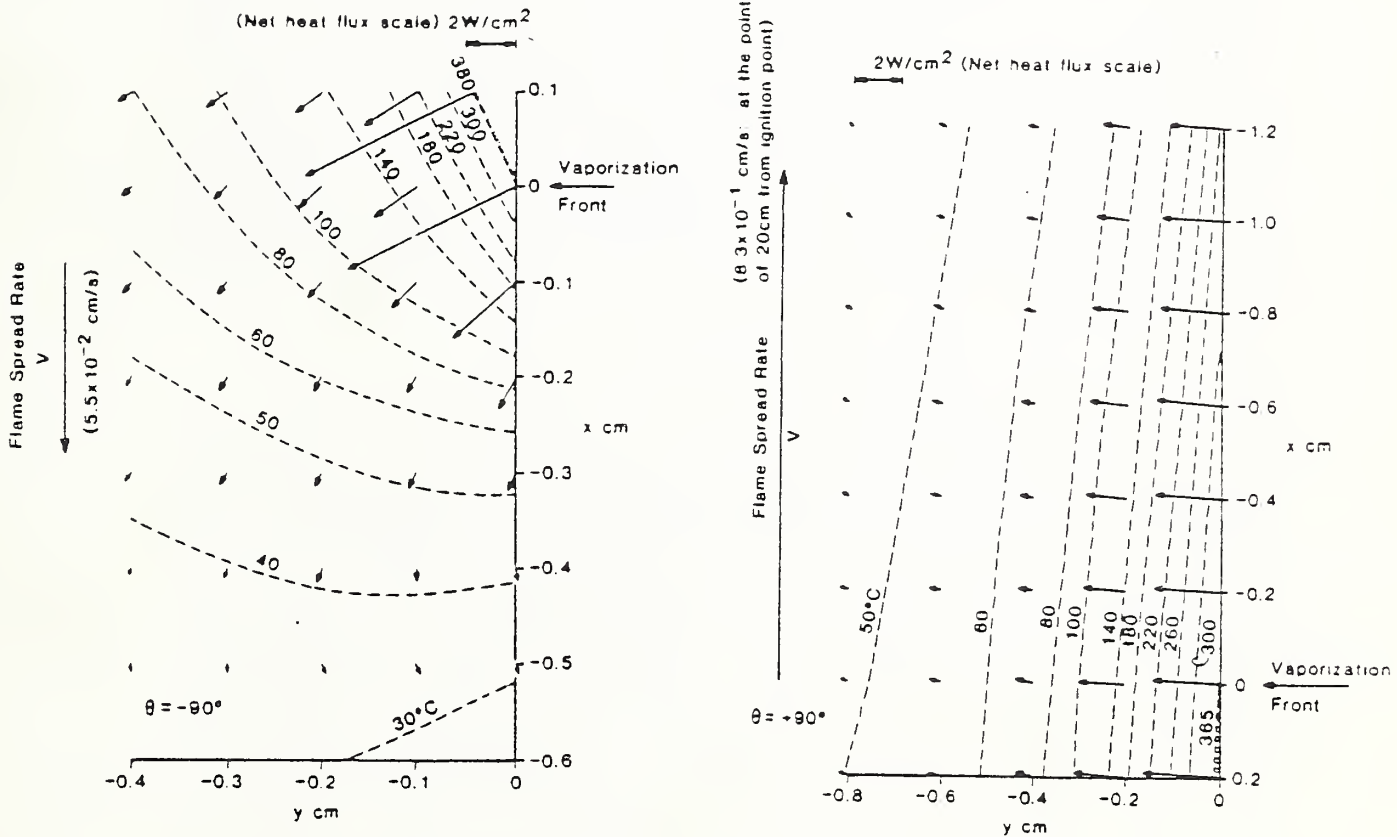


Fig. 7. Isotherm contours (dashed lines) and heat flow vectors (arrows) at various sample orientation angles, (a) $\theta = -90^\circ$, and (b) $\theta = +90^\circ$.

CHARACTERIZATION OF FLAME SPREAD OVER PMMA USING HOLOGRAPHIC INTERFEROMETRY
SAMPLE ORIENTATION EFFECTS

A. Ito and T. Kashiwagi, National Bureau of Standards, USA

JIN: He's asking a question of whether the heat loss from or to sides of the sample was important or not, or whether the thing was taken only on a two-dimensional plane.

KASHIWAGI: There was a barrier (a fused silicon plate) spaced between the samples so there would be no heat overflow to the side. Although the flame was against the sample, there was a certain amount of heat loss to the sides. But they were able to measure the difference of heat loss around the sample and the barrier. However, it was so insignificant that they did not put it on the chart. In order to get a more accurate reading, they would have to install sensors on an order of magnitude much greater than what they did in order to get an accurate reading, otherwise, it's just an academic exercise in indicating that there had been some heat loss.

The barriers which prevent the flame from going to the side were not directly attached to the samples per se, because by doing that you have a misreading because there's a heat loss through both the barrier and the sample. It was close but not touching.

QUINTIERE: Do you have any explanation as to why the characteristics of time is apparently a constant for all those orientations?

KASHIWAGI: In this case, it comes down to applications. If you heat so, a kind of ghostly thermal pressure conduction of the normal side is about the same because ventilation comes out the same. Then as you go into the sampling, it's about the same. So, whatever is happening, total energy is about the same. It could be a very long time for a low spot, or a high spot in a shorter time.

QUINTIERE: Vaporization temperature is the same for all cases?

KASHIWAGI: Very constant.

QUINTIERE: So, if I interpret this, due to the particular distribution of heat flux, the distance somehow the integral of that distance --

KASHIWAGI: Right, it doesn't matter how you do it.

QUINTIERE: It's the same?

KASHIWAGI: Right.

A NUMERICAL STUDY OF PERIODIC ALTERNATING FLOW OF FIRES

Kohyu Satoh

Fire Research Institute of Japan
3-14, Nakahara, Mitaka, Tokyo 181

ABSTRACT

It is pointed out that large-scale turbulence can accelerate combustion due to surface and bulk mechanism. This suggests that fluctuations of fires based on turbulence may play a significant role in fire growth. The author et al. have numerically studied regular oscillatory flows caused by turbulence. It was found in those studies that the frequencies of oscillatory flows depend upon the 1/3rd power of heating rate, similarly to experiments. Recently it has been revealed that numerical calculations can reproduce turbulent flows extremely similar to the actual dynamic fluid flows (particularly in case of the wake behind a circular cylinder). So-called computer fluid dynamics are generally being applied in designing aircrafts. In the future numerical fire simulations corresponding to a "numerical wind tunnel" may be available in designing fire safety systems. Currently the author has investigated the dynamic behavior of both a plume above a heat source and a turbulent jet from a nozzle, relevant to a "dynamic numerical fire". The objective of the present report is to discuss the periodic oscillatory behavior of fire flows due to vortices, based on the numerical results calculated by the author and by the other investigators. In these results calculated, numerous vortices are periodically created near the stream and cause the periodic fluctuations of flows, growing up in the downstream. The present two-dimensional calculations showed the existence of vortices appearing alternately on opposite sides of both a plume and a turbulent jet axis. These periodic fluctuations are essentially the same as the Karman-vortex street in the wake behind a circular cylinder.

1. INTRODUCTION

A characteristic feature of actual fires is the dynamic motion accompanying combustion. Oscillatory flows due to turbulence may play a significant role in fire growth. Frank-Kamenetskii¹ and Williamson et al.² pointed out that large-scale turbulence can accelerate combustion, that is, the energy release from the flames may be accelerated. Two possible mechanisms, surface and bulk mechanism, are suggested. Thus the investigation of turbulent flow of fires should be important to analyse fire growth. The author et al.³⁻¹⁰ have numerically investigated oscillatory flows due to turbulence, using a finite difference computer code UNSAFE¹¹. The flows in some cases calculated were very regularly oscillating. In particular the venting flow from floor to ceiling caused by a central heat source on the floor in an enclosure was highly periodic. The oscillatory frequencies of flows depended upon the 1/3rd power of the heating rate. The relationship was quite similar to the one in experiments as shown in Fig.1-A. The two-dimensional oscillating flows depicted by velocity vectors and isotherms are shown in Fig.1-B, where the air outflow rate is maximum at $t=36.50$ sec (t :time after heating) and minimum at $t=37.00$ to 37.25 sec. The same phase as at $t=36.5$ sec appears

at $t=37.75$ sec, i.e. the frequency is 0.8 Hz for the heating rate 10 kW.

It has recently been revealed that numerical calculations can reproduce turbulent flows extremely similar to the actual dynamic fluid flows. In particular the turbulence near the wake of a circular cylinder or a rectangular block located in a uniform flow has very precisely been calculated¹²⁻¹⁴. It is well-known that the Karman vortex street near the wake behind a block located in a uniform flow shows a periodic oscillation. The so-called computer fluid dynamics (or "numerical wind tunnel") is now being applied in designing aircrafts. Hence in the future a "numerical fire room" corresponding to a "numerical wind tunnel" may be available in designing fire safety systems. Currently the author has investigated the dynamic behavior of both a plume above a heat source and a turbulent jet from a nozzle, relevant to a "dynamic numerical fire". Time-dependent oscillatory flows due to a localized heat source have recently been calculated by some other researchers, too. These oscillatory flows must be based on the same origin. The objective of the present report is to discuss the periodic oscillatory behavior of fire flows due to vortices, based on the numerical results calculated by the author and by the researchers in different fields of fluid mechanics.

2. NUMERICAL RESULTS OF PERIODIC MOTION OF A PLUME ABOVE A HEAT SOURCE AND A TURBULENT JET

Two oscillatory flows calculated here are first represented, since they are typical of oscillatory flow behaviors. Calculations are conducted using the two-dimensional finite difference UNDSAFE computer code which is based on a micro control-volume method. Detailed procedures for calculations are not shown here, but are described in the previous reports¹⁵⁻¹⁶. The original code has, however, been largely refined.

2.1 Swaying motion of a plume

Forstrom et al.¹⁷ first measured the natural swaying motion of a plume above a line heat source, although the flow was very slow and laminar. Noto et al.¹⁹ experimentally investigated the relationship between swaying frequency and heating rate, using a fine electrically-heated wire as a heat source in an enclosure (0.8 x 0.8 x 1.0 m (height)). The author has studied the flow behavior by two-dimensional calculations, since the motion of flows is reported to be in a two-dimensional plane and to be quite regular. For calculations the flow domain is mainly divided into about 10000 grids, e.g. nonuniform 103 x 110 and uniform 30 x 100 grid.

A line heater is located at 0.4 m from the left side wall and 0.4 m above the floor. The heating rate varies from 10 to 120 watts/m. A small disturbance (by dislocating the heat source to an adjacent grid briefly) is numerically added to a plume to accelerate the commencement of swaying motion. The plume above the line heat source, however, began to sway spontaneously, even without the disturbance to the plume. And a longer time was required for the swaying motion to begin spontaneously in the calculations. The swaying period was almost constant and the frequency depends upon the heating rate of a line heater. Fig.2-A shows the relationship between the frequency and the heating rate, from experimental measurements by Noto et al. and present numerical calculations. The dynamic motion of a plume calculated is shown in Fig.2-B, in which the swaying motion of a plume and vortices along a plume can be seen. The thermal conditions at the walls had a quite large effect upon the

swaying frequency, that is, cooling of the ceiling reduces the frequency of swaying motion.

The relationship in the experiments was expressed as $Re = 0.33 Ra^{1/3}$, where Re is the Reynolds number defined by $Re = f \cdot L^2 / \nu$ and the Rayleigh number $Ra = L^3 \cdot g \cdot \beta \cdot Q / \lambda \cdot \nu^2$ (f : frequency, L : reference length, ν : kinematic viscosity, g : gravitational acceleration, Q : heating rate, λ : heat conductivity). A close relationship was given by the present numerical calculations as shown in Fig.2-A.

At the initial stage before swaying motion began, nearly symmetric pressure distribution was shown at both sides of the plume. The pressure imbalance at the both corners of enclosure was, however, made accompanying the swaying motion of plume. A small vortex was alternately created at each side of the plume and grows moving upwards with swaying motion.

2.2 Turbulent free jet

Antonia et al.¹⁹ studied a flag-like flapping motion of a two-dimensional turbulent free jet. It is suggested that the motion can be represented by a two-dimensional von Karman vortex-street pattern. Shimizu²⁰ and Hasegawa et al.²¹ studied the jet numerically by the so-called discrete-vortex method, but the maximum time after the ejection of a jet and the maximum distance from a nozzle investigated were quite limited. The present study investigates the jet motion using a two-dimensional finite difference method. The regimens studied by the three researchers are shown as follows in dimensionless and dimensional forms:

	Shimizu ²⁰	Hasegawa et al. ²¹	Present study
Maximum distance from nozzle	30(15 cm)	10(10cm)	400(400 cm)
Maximum time after ejection	160(.01s)	60(.06 s)	150(.15 s)
Reynolds number	26700	6667	6667
Reference speed	(80 m/s)	(10 m/s)	(10 m/s)
Reference length	(0.5 cm)	(1 cm)	(1 cm)

Temperature and density of the flow are fixed constant in the present calculations. Figs.3-A and B show the behavior of vortices and isobaric lines along the jet, calculated by dividing the numerical domain into nonuniform 111 x 117 grid. In this calculation a short-time disturbance was added to the jet (by dislocating the nozzle to one adjacent grid briefly), in order to accelerate the initiation of the flapping. Even without the disturbance the flapping of a jet began spontaneously in this calculation. The vortices appeared alternately on opposite sides of the jet. The bending locations of a flapping jet coincided with the locations of vortices. The frequency of the periodic flapping motion of a jet depends upon the initial speed of the jet from the nozzle, i.e. Reynolds number. Due to the flapping motion of the jet, the half-width of the jet increases and the maximum velocity decreases along the jet axis as shown in Figs.3-A and B, based on the time-averaged velocity distributions.

3. Examples of other oscillatory flows calculated numerically

The two flows (mentioned above) calculated by the author definitely display periodic oscillations. Recently time-dependent flows have widely been investigated by numerical calculations. Examples of other oscillatory flows calculated by several investigators are:

3.1 Unsteady wake behind a circular cylinder or a rectangular block

Numerous numerical studies solving the unsteady Navier-Stokes equations have been concerned with the unsteady features of the wake behind a circular cylinder or a rectangular block placed in a uniform flow. It is considered as a very convenient test case for fluid-dynamic computations. Hence some numerical results calculated are extremely precise.

For example, Braza et al.¹² studied the initiation mechanism for vortex shedding in the range of the Reynolds number of 100 - 1000. Fig.5-A shows the alternating vortices calculated, where the loss of symmetry was initiated by a numerical perturbation (by adding a brief rotation to the cylinder artificially). The periodic flow pattern was extremely similar to that in experiments, although the numerical perturbation was not always the same as the physically existing perturbations in the experiments. Further, Ogawa et al.¹³ investigated the vortex shedding characteristics, too. The unsteady flow pattern in the wake, with the Reynolds number of 400000, was extremely precise as shown in Fig.5-B, displaying a periodic alternating behavior. A number of small vortices regularly leaving the surface of a circular cylinder are observed. In this calculation no particular perturbation was reported as having been used to initiate the vortex shedding.

These alternating flows in the wake behind a block must be common with the oscillatory flows of turbulent jet mentioned above. Cantwell et al.¹⁴ reported contours for mean Reynolds stress in the wake behind a circular cylinder as shown in Fig.5-C, which displays a similar structure shown in Fig.3-B for a turbulent jet.

3.2 Unsteady thermal convection caused by a localized heat source

Kuwahara et al.²² attempted to investigate periodic motions of thermal convection due to a ring-type heat source, with the intent of eventually studying firewhirls. The size of the ring was 0.5 km for the inner radius and 2.5 km for the outer one. Numerical calculations were based on axisymmetric cylindrical co-ordinates with the Boussinesq approximation.

The isotherms above a heat source were highly time-dependent as shown in Fig.6. Profiles at 6600, 10800 and 15600 seconds belong to the same phase. A vortex is periodically created near the ring-type heat source. Three-dimensional calculations will additionally give three-dimensional twisting flows around the plume axis. This author²³ studied the thermal convection between two circular plates, using axisymmetric cylindrical coordinates, as shown in Fig.7. The flow was weakly oscillatory. Matubara²⁴ studied the merging and oscillatory flows of buoyant plumes above two line heat sources as shown in Fig.8.

Kou et al.²⁵ calculated periodic variations of smoke concentration around an aircraft fuselage in a crosswind near the ground, as shown in Fig.9. Kuwahara et al.²⁶ numerically studied the time-dependent flow in a channel with a partially heated floor. The flow pattern is highly oscillatory as shown in Fig.10. These oscillatory flows must be based on vortices created periodically around a heat source.

Nakamura et al.²⁷ attempted to computationally determine the coupling between flame size, the speed of the induced (combustion) air, and the burning rate. Fig. 11 represents a steady state flame of a Bunzen burner. A weakly oscillating temperature profile around the top of a flame is suggested. Baum et al.²⁹ studied the plume pulsations in a cubic enclosure, as shown in Fig.12 where an artificial disturbance was added.

In these oscillatory flows periodically created vortices are suggested.

4. DISCUSSION

Numerous vortices around flows are commonly created in buoyant flows shown in Figs. 2 and 5 and forced cool flows shown in Fig. 6. In two-dimensional flows, vortices are alternatively created in each side of main stream, where pressure imbalances are determined by the von Karman vortex-street. In three-dimensional calculations such as by Baum et al., too, numerous vortices should be created and grow to cause pulsations.

The thermal plume will be stable if there are perfectly no disturbance around the plume. However, even very careful experiments can not be free from physically existing disturbances. Likewise, if there are perfectly no truncation errors in calculations, the plume above a heat source will not oscillate. The oscillations in the wake calculated by Ogawa et al. must be initiated by small truncation errors accompanying calculations. Thus, an increase in numerical precision will delay the commencement of oscillations. Perturbations added to the plume accelerate the commencement of oscillations. However, these effects in calculations will not greatly affect the natural oscillatory frequency itself, but affect the time oscillations commence. An artificial perturbation and small truncation errors in calculations are only a trigger in initiating the oscillatory flows. Hence the natural oscillatory flows calculated as above reflect the physical phenomena.

Vortices created around buoyant flows and turbulent jets play a significant role in the turbulent flows. Thus combustions, or fires, must be greatly affected by the oscillatory flows.

5. CONCLUSION

The present two-dimensional calculations showed the existence of vortices appearing alternately on opposite sides of both a plume and a turbulent jet axis. In these results calculated, numerous vortices are periodically created near the stream and cause the periodic fluctuations of flows. These periodic fluctuations are essentially the same as the Karman-vortex street in the wake behind a circular cylinder, which has been simulated well by many investigators.

The origin initiating oscillatory flows between numerical calculations and experiments differs each other, but they only play as a trigger to initiate the periodic flows, that is, they only affect the time oscillations commence. Oscillatory behavior of flows in some numerical examples mentioned above are quite common and are very similar to the actual fluid flows. Thus the natural oscillatory flows calculated as above reflect the physical phenomena.

Vortices created around buoyant flows and turbulent jets play a significant role in the turbulent flows. Thus combustions, or fires, must be greatly affected by the oscillatory flows.

REFERENCES

- 1) Frank-Kamenetskii, D.A.: Diffusion and Heat Transfer in Chemical Kinetics, 2nd edition Tr. by J. P. Appleton, Plenum Press, New York, p.560(1969)
- 2) Williamson, R.B. et al.: "Observations of Large Scale Turbulence in Corner Wall Experiments", Combustion Science and Technology, Vol.41, p.83(1984)
- 3) Satoh, K. et al.: "A Numerical and Experimental Study of the Relationship between Periodic Temperature Variations of Outflowing Air and Heating

- Rate in an Enclosure", Proc. 16th Conf. Fluid Mech. (Japan), p.154(1984)
- 4) Satoh, K. et al.: "A Numerical Finite-Difference Study of the Oscillatory Behavior of Vertically Vented Compartments", Numerical Properties and Methodologies in Heat Transfer, Hemisphere Publishing Co., p.517(1981)
 - 5) Satoh, K., et al.: "Flow and Temperature Oscillations of Fire in a Cubic Room with Ceiling and Floor Vents (Part 3 Relationship between Frequency and Heat Source Strength)", Rep. Fire Res. Inst., No.57, p.79(1984)
 - 6) Satoh, K. et al.: "Flow and Temperature Oscillations of Fire in a Cubic Enclosure with Ceiling and Floor Vents (Part 1 Oscillatory Behaviors & Heat Source Strength)", ibid., No.55, p.31(1983)
 - 7) Satoh, K.: "A Numerical Study of Swaying Motion of Fire Plume (in Japanese)", Proc. 23rd Japanese Symposium of Heat Transfer, p.424(1986)
 - 8) Satoh, K.: "A Numerical Finite Difference Study of Natural Swaying Motion of Plume above a Heated Line Source", Proc. the 2nd ASME-JSME Thermal Engineering Joint Conference, Honolulu, Vol.4, p.41(1987)
 - 9) Satoh, K.: "A Numerical Study of Two-Dimensional Free-Jet" (in Japanese), Proc. 18th Conference of Fluid Mechanics (Japan), p.42(1986)
 - 10) Satoh, K. et al.: "Three-Dimensional Numerical Simulation of Aircraft Cabin Fires", Proc. 24th Aircraft Symposium (Japan), p.326(1986)
 - 11) Liu, V. et al.: "UNSAFE-II, A Computer Code for Buoyant Turbulent Flow in an Enclosure with Thermal Radiation", Tech. Rep. of the Department of Aerospace and Mech. Eng. of Univ. of Notre Dame, TR-79002-78-3(1978)
 - 12) Braza, M. et al.: "Numerical Study of the Pressure and Velocity Fields in the Near Wake of a Circular Cylinder", J. Fluid Mech., Vol.165, p.79(1986)
 - 13) Ogawa, S. et al.: "Flow around a Circular Cylinder (in Japanese)", Proc. 17th Conference of Fluid Mechanics (Japan), p.22(1985)
 - 14) Cantwell, B. et al.: "An Experimental Study of Transport in the Turbulent near Wake of a Circular Cylinder", J. Fluid Mech., Vol. 136, p.321(1983)
 - 15) Ku, A.C. et al.: "Numerical Modeling of Unsteady Buoyant Flows Generated by Fire in a Corridor", 16th Symp. (Int.) on Comb., p.1373(1977)
 - 16) Patankar, S.W.: Numerical Heat Transfer and Fluid Flow, McGraw-Hill(1980)
 - 17) Forstrom, R.J. et al.: "Experiments on the Buoyant Plume above a Heated Horizontal Wire", Int. J Heat Mass Transfer, Vol.10, p.321(1967)
 - 18) Noto et al.: "Swaying Motion in Thermal Plume above a Heat Source", Bull. Japan Soc. Mech. Eng. (Ser. B), Vol.50, No.457, p.2179(1984)
 - 19) Antonia, R.A. et al.: "On the Organized Motion of a Turbulent Plane Jet", J. Fluid Mech., Vol.134, p.49(1983)
 - 20) Shimizu, S.: "Numerical Analysis of Two-Dimensional Jet by a Discrete-Vortex Method", Bull. Japan Soc. Mech. Eng. (Ser. B), No.472, p.3852(1985)
 - 21) Hasegawa, T. et al.: "Numerical Simulation of Two-Dimensional Jet by a Discrete-Vortex Method", ibid., Vol.52, No.476, p.1451(1986)
 - 22) Kuwahara, K. et al.: "Thermal Convection caused by Ring-Type Heat Source", J. Physical Soc. Japan, Vol.51, No.11, p.3711(1982)
 - 23) Satoh, K.: "A Numerical Study and Experimental Verifications of Air Entrainment by Fire Plume", Fire Sci. & Tech., Vol.2, No.2, p.127(1982)
 - 24) Matubara, "A Consideration of the Oscillatory Behavior of Flame of Pool Fire", Proc. 1986 Conf. Japan Soc. Fire Sci. and Eng., p.111(1986)
 - 25) Kou, H.S. et al.: "Turbulent Buoyant Flow and Pressure Variations around an Aircraft Fuselage in a Cross Wind near the Ground", Fire Safety Science-Proceedings of the First International Symposium, p.173(1985)
 - 26) Kuwahara, K.: "Computation of Thermal Convection with a Large Temperature Difference", Proc. 4th Int. Conf. Applied Num. Modeling, p.565(1984)
 - 27) Nakamura, S.: "A Computational Model for Fire Research", Proceedings of International Symposium on Computational Fluid Dynamics, p.678(1985)
 - 28) Baum, H.: "Calculations of Three Dimensional Buoyant Plumes in Enclosure" Combustion Science and Technology, Vol.4., p.55(1984)

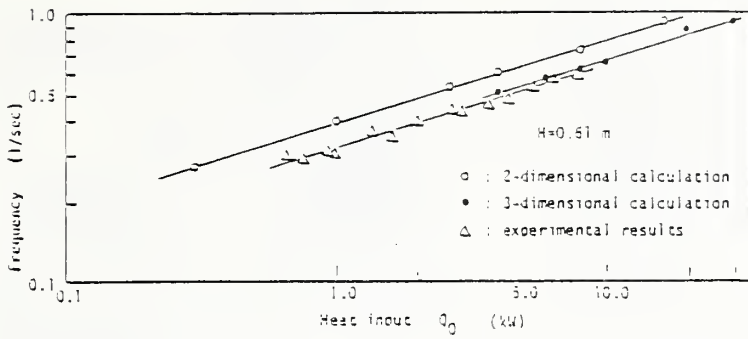


Fig. 1-A Oscillatory frequency of buoyant plume vs. heating rate of central volumetric heat source in a vertically vented room.

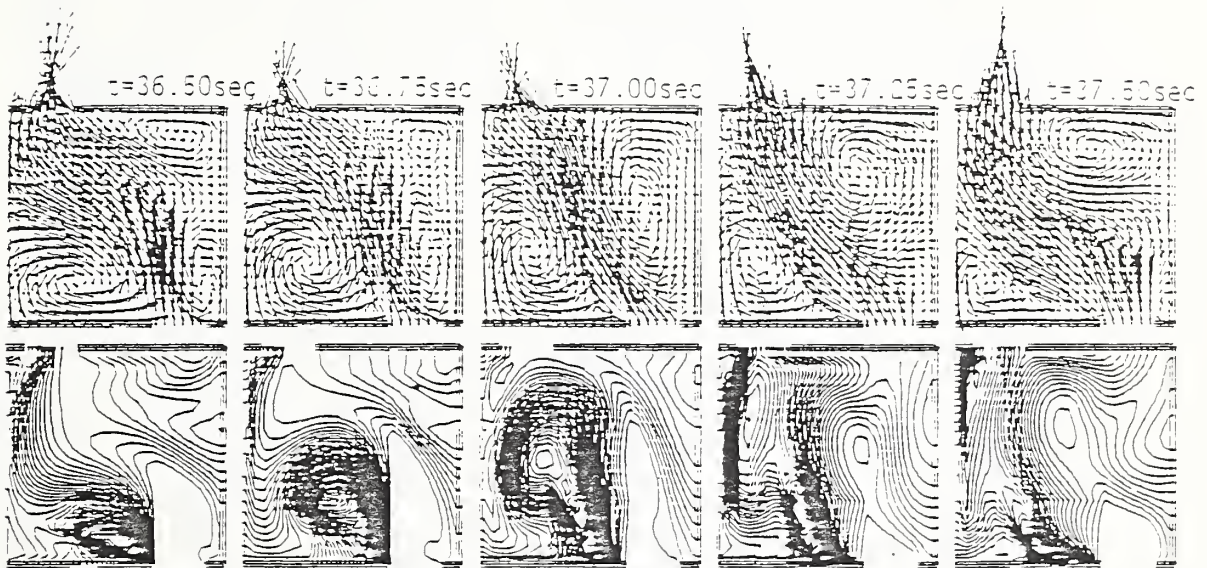


Fig. 1-B Velocity vectors and temperature contours. Heating rate $Q=10$ kW, enclosure dimensions : 61 x 61 cm.

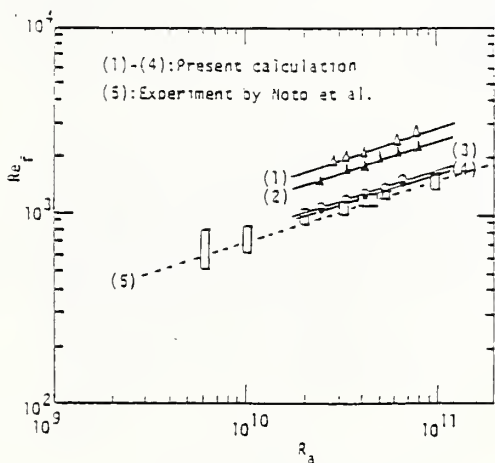


Fig. 2-A Reynolds number on frequency of swaying plume vs. Rayleigh number. Enclosure dimensions : 80 x 100 cm. Lines (1) to (4) depend on boundary conditions (details are found in Ref.(3)).

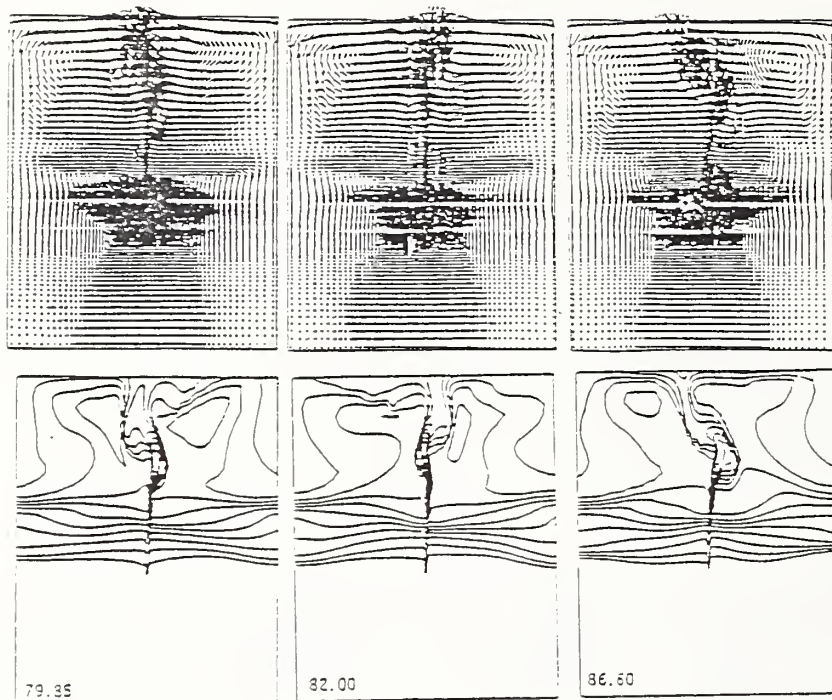


Fig.2-B (right)
Swaying motion
of plume depicted by
velocity vectors (upper)
and isotherms (lower).
Heating rate $Q=120$ kW/m.
Calculated by nonuniform
 103×110 grid.

Fig.3-A (middle left)
Flapping motion of jet
depicted by velocities.
 $Re=6667$.

Fig.3-B (middle right)
Isobaric contours.

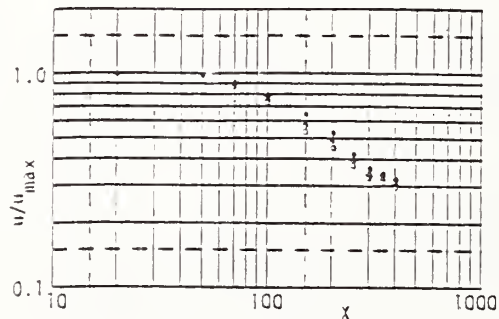
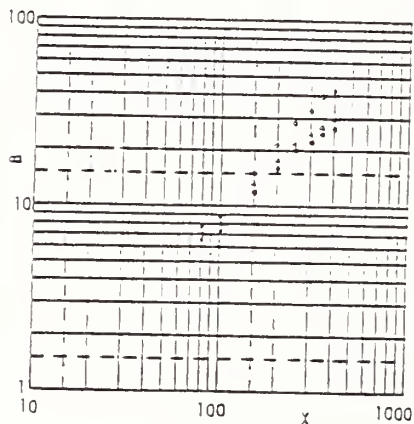
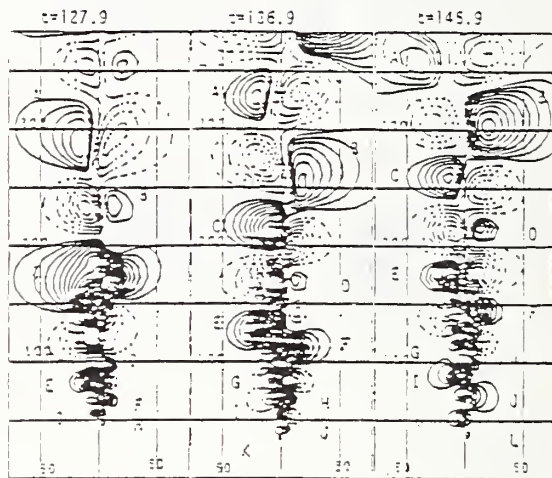
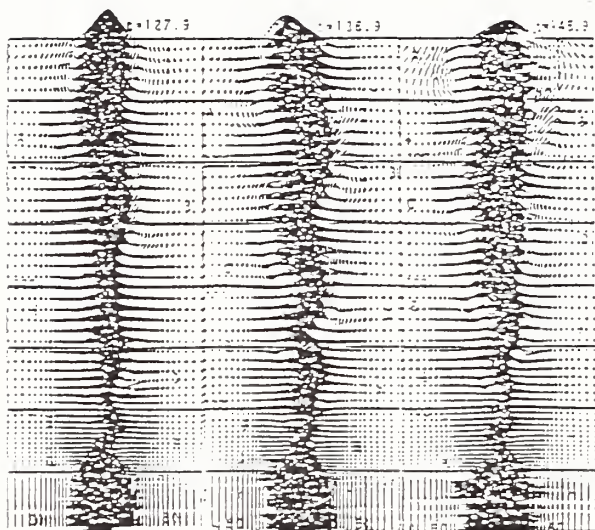


Fig.4-A (bottom left) Half width of velocity distribution
along jet axis (x).

Fig.4-B (bottom right)
Maximum velocity
along jet axis.

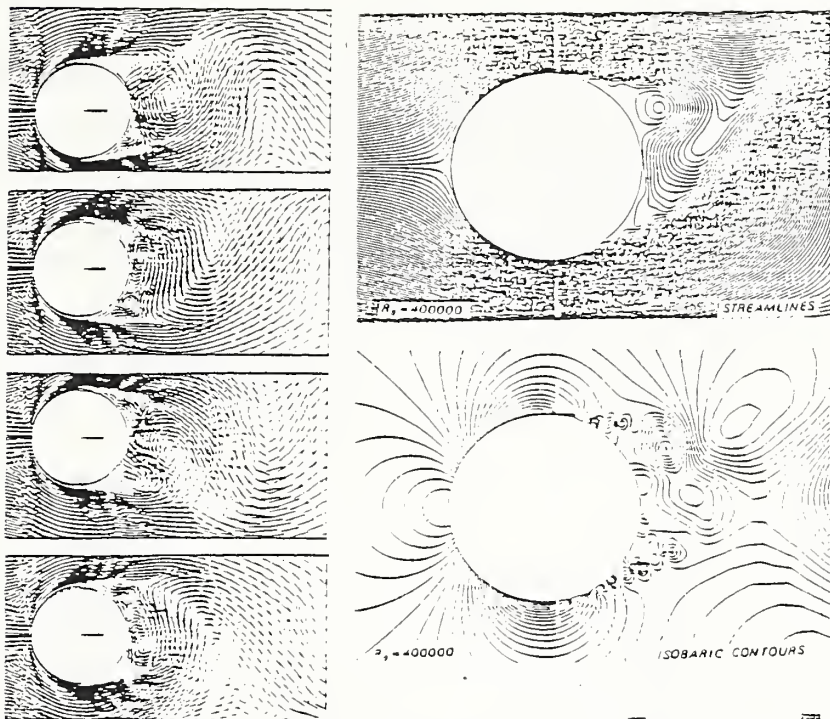


Fig. 5-B Vortex shedding for $Re=40000$.
(By Ogawa et al. ¹³)

Fig. 5-A Oscillatory motion of wake behind a circular cylinder.
(By Braza et al. ¹²)

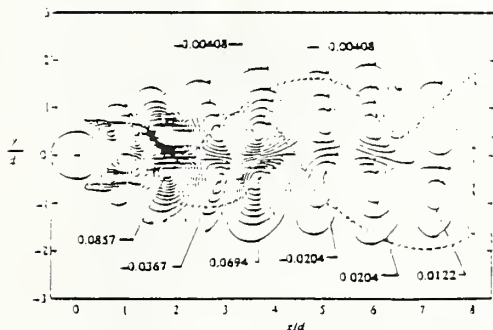


Fig. 5-C Contours for mean Reynolds shearing stress.
(By Cantwell et al. ¹⁴)



Fig. 6 Thermal convection caused by ring-type heat source. (By Kuwahara et al. ²²)

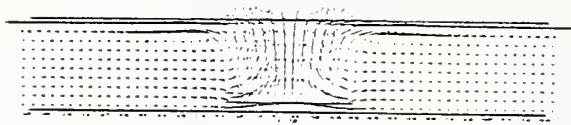


Fig. 7 Buoyant plume above a circular plate-type heat source. Weak oscillation was observed. Cylindrical coordinates were employed. (By the present author ²³)

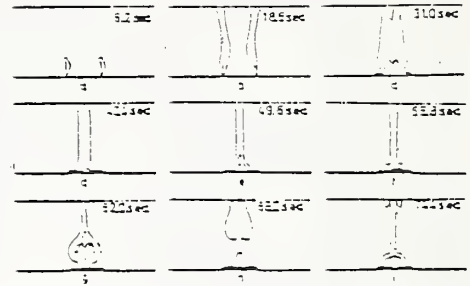


Fig. 8 Merging of plumes above two line heat sources. (By Matubara ²⁴)

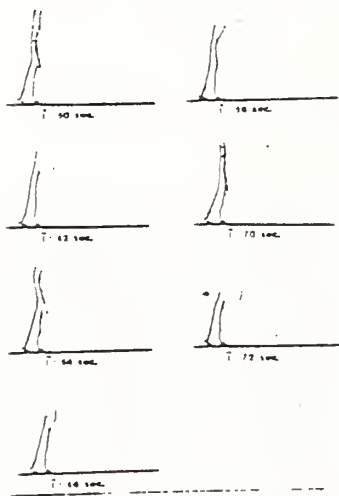


Fig. 9 Oscillatory buoyant plume due to fire located closely to an aircraft fuselage. (By Kou et al. ²⁵)

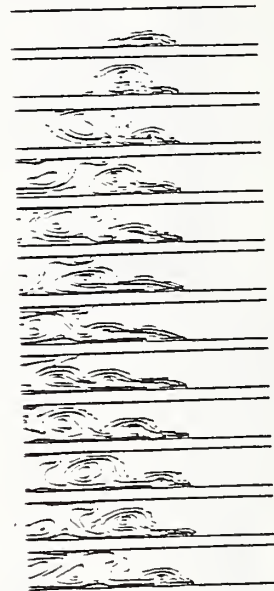


Fig. 10 Thermal convective flow in a channel with partially heated floor. (By Kuwahara et al. ²⁶)

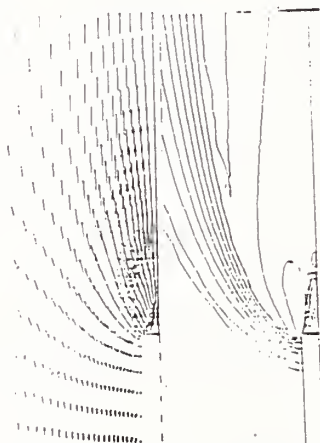


Fig. 11 Slow diffusion flame. The fuel gas mixture was ignited just after the opening of a gas valve. (By Nakamura et al. ²⁷)

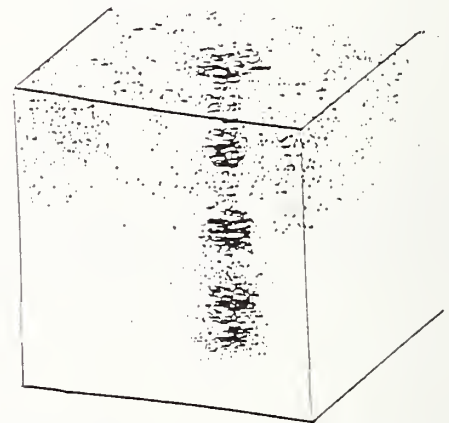


Fig. 12 Three dimensional buoyant plume in a cubic enclosure. (By Baum et al. ²⁸)

CLOSING CEREMONIES

CLOSING CEREMONIES

JIN: We would like to begin our formal closing ceremonies. When the Japanese delegation arrived in Boston, our impression was that this was the end of the winter season. In the one week that we have been privileged to be here, we have seen the magnolia bushes begin to blossom and the maple trees begin to put on their red leaves as they start to flower. We have the definite impression that spring has finally arrived. They have told us that the New England spring is a very short lived one. We have found that this also applies to this particular conference. It has already begun and ended in a matter of moments that we have been conscious of its existence. It has been customary, and I believe I, as the visitor, have the privilege of beginning the closing ceremonies.

There are many very important items in the resolution. Four individuals, Dr. Pagni as the lead, participated in the formulation of the final resolution. Specifically, I must say that they began their work last night and finalized it this morning. There is a reason for Dr. Pagni's passion in assisting us in this regard. The reason being that if we get too involved in arguments over these resolutions, Dr. Pagni will miss his airplane, so I would like to request everybody's cooperation in passing the resolutions post haste.

I would like to request that Dr. Pagni start off by reading the English version of the resolution.

PAGNI: We left the fate of the fat mice out of the resolutions.

The resolutions follow Mr. Chairman:

The members of the United States-Japan Natural Resources Board on Fire Research and Safety are quite pleased with the results of the 9th Joint Meeting, held in Boston, Massachusetts, May 3rd through 8th, 1987. We wish to thank the National Bureau of Standards, the National Fire Protection Association, and especially Factory Mutual Research Corporation, for the New England hospitality we have all enjoyed. We also are grateful for the insights provided by Professor Hottel from MIT and Professor Emmons from Harvard University. We note again that each time we meet, the quality and quantity of our technical communication improves. The four workshops on special topics proved informative and stimulating for all participants.

The toxicology discussions held jointly with Canadian representatives showed good progress. We hope this Tripartite Cooperative will continue.

The following resolutions summarize the consensus reached:

It is hereby resolved that:

Resolution 1: The objectives of the meetings of this Panel remain to:

- A. Exchange the latest technical information.
- B. Promote cooperative research on fire safety science.
- C. Encourage the innovation necessary for the development of new testing methods, designs and standards.

- D. Form a multinational consensus in the field of computer-based fire modeling.
- E. Explore the possibility of developing performance fire codes.

Resolution 2: The 10th Meeting of the UJNR Panel on Fire Research and Safety will be held in June of 1988 in Tokyo or Tsukuba, Japan.

Resolution 3: The same format as the 9th Meeting is proposed for the 10th Meeting, with shorter sessions to accommodate attendance of panel members and associates at the Second International Symposium on Fire Safety Science.

Resolution 3A: Agenda Topics:

- 1. Fire and smoke physics.
- 2. Fire and toxicity chemistry.
- 3. Risk, hazard and evacuation.
- 4. Open technical session.

Resolution 3B: The discussion of each topic should begin with an outline of progress made in each field between meetings by both Japan and the United States.

Resolution 4: Cooperative fire research programs should be continued. These are especially valuable where the facilities are somewhat different in our two countries. It is suggested that joint research programs be organized on:

- 1. The structure of large, buoyant diffusion flame plumes.
- 2. Smoke movement and fire growth computer modeling.
- 3. Fire retardant and combustion product chemistry.
- 4. The proper definition of risk and risk analysis.
- 5. Other topics at the discretion of the Chairman.

In addition, the exchange of working personnel should continue to be pursued vigorously. During the past two years, Dr. D. Evans, an NBS employee, spent a valuable month in Japan. Dr. A. Sekizawa of FRI, Mr. Y. Yamauchi of Hochici Corporation, Professor A. Ito of Ohita University and Mr. H. Otani of IHI have conducted useful research projects in the United States.

Resolution 5: Panel members are encouraged to exchange information of interest through the respective Chairmen between meetings. Research reports issued in each country should be exchanged every three months. The titles of these reports will be sent to the Panel members in each country who can identify the ones they would like to receive from their Chairman.

It is important that all the relevant reports for the next meeting be sent in time to be received in the other country at least one month before the 10th Meeting.

Mr. Chairman, those are the resolutions.

TAKAHASHI: I was told that both resolutions would be read in their respective languages, so Mr. Jin will read the Japanese version of the resolutions.

JIN: Prior to the reading of the resolutions, I'd like to make a comment to just the Japanese delegation. The resolutions were made in such haste that perhaps the translation may not be as accurate as desired. Therefore, I'm asking the Japanese delegation to rely on the English version as final.

TAKAHASHI: I believe, after reading over the resolutions, that there were three main points of quite high importance in my mind. One important issue is the statement that refers to the toxicity studies, and the recommendations that these studies be conducted under a Tripartite Cooperative System. The second is that there is a need to decide at this Session that the 10th Panel Meeting to be held either at Tokyo or at Scuba. I would prefer that the decision on this particular site be delayed if that is possible.

The third important point is, I believe, the addition of sub-items 3 and 4 in the 4th resolution, which called for additional studies. I believe it is a very good thing for this type of Panel to have their sights set on as wide and as broad a spectrum as possible.

Are there any questions or discussions that anybody might have concerning this resolution?

SNELL: For my part, I'd simply like to say I agree with your three points and observations: that the Tripartite continue, that the decision on location be deferred based on your situation in Japan, and thirdly, I too think of some other topics that we might wish to pursue on cooperative projects and look forward to discussing those with you later.

JIN: Thank you very much for your comments. Then would it be all right to assume that we have accepted the resolutions?

In deference to Dr. Pagni's very tight schedule, we seem to all have agreed that the resolutions are acceptable.

I'd like to proceed on to the next item on the agenda and call on Dr. Gann to summarize his views on the current meeting.

GANN: Good morning again. It is a pleasure to be asked to summarize the value of this meeting. Unfortunately, I was unable to attend the Risk, Hazard and Evacuation session because we were holding parallel meetings. However, I have read those papers, and I plan to include some discussion of them in my remarks.

In my opinion, this is easily the best of the UJNR meetings that I've attended. There were some research areas in which remarkable, innovative progress has been made. There are some other areas in which the progress can best be described as incremental. I think the mixture of these two is healthy, but I think that in the future, we should reconsider the spacing of the meetings so that we can have major progress to report in virtually all of the areas.

There is an aspect of maturity about the technical nature of this Panel. We've all now known each other for many years, and the exchange of ideas seems to be far more fluid. In many of the projects that were reported here during the last week, it's obvious that ideas that have contributed to those projects

have come from both countries. Since this is the essence of holding these kinds of meetings, I think we should applaud ourselves for taking advantage of it.

In thinking about the sessions and the papers on fire and smoke physics, I consider that this is by far the most mature, the most well-developed of the disciplines discussed this week. Because of this large technical base and experience, it is not surprising that there are remarkable advances each time we meet, both in the understanding of the physical phenomena of fire, and in the mathematical modeling. We've just spent the last hour or so discussing the accomplishments of the Toxicity Tripartite Group over the last five years. Suffice it to say that this year, as in each of the prior years, the amount of progress, the evolution of our thinking, and the wholesale generation of data is extremely encouraging. The most gratifying and most rapid progress has been made in the area of risk and hazard evaluation. Perhaps the youngest of the fire disciplines is the true fire chemistry field. For decades, we have been making analytical measurements of the products of combustion and the history of how materials fall apart during fires. However, there are still very few papers on the true chemistry of how those processes occur.

First of all, as the hosts of the prior UJNR meetings in the United States, I and my colleagues from the National Bureau of Standards greatly appreciate the excellent hosting job provided by Factory Mutual Research. In particular, Ms. Madeline Anderson has been an excellent resource.

In addition, the opportunity to tour laboratories that many of us have not seen before, or certainly not recently, allows us to visualize the kinds of apparatus and where the results come from. I also think we should provide a round of applause for our interpreters who have made a fairly significant language barrier disappear this week.

I would now like to make a few brief announcements on procedure. As in the past, we will be preparing proceedings from this meeting. We hopefully have tape recordings of the discussions from the various papers and will be transcribing it. We have the original copies, I believe, of virtually all the papers. As in the past, we allow about a one-month period after the meeting for those of you who would like to submit revised versions. If you send the revised version to NBS within the next four to six weeks, we will be happy to use it in place of the original. If not, we'll just go ahead and use the paper you provided prior to the meeting.

Next, I'm going to preempt Dr. Snell, who normally has the pleasure of presenting some sort of parting souvenir for the attendees at the meeting. As I recall, approximately two years ago in Tsukuba, we were presented small models of a traditional Japanese fire standard from years past. In fact, I still have mine sitting on my desk. This year, we have another totally unique parting gift for all participants. The National Fire Protection Association has published a special commemorative facsimile version of the very first Fire Protection Handbook. For those of you who are familiar with the current version, it is extremely large and thick and contains almost everything you need to know about fire. This is the same version of that book 90 years ago. In the carton in the second row, there are copies for everybody. For those people whom already have left the meeting, we ask that people please take copies back to them.

And last, after the closing ceremonies are over, we would like to take a photograph of all the people who are still here. Please go out the back door and find a suitable location. This should only take a moment or two and you will still be able to catch your flight.

SNELL: My remarks will be very brief because the efficient Dr. Gann has stated most of them already and has presented them very well. I too am impressed with the quality of this meeting, as distinct from our previous meetings that I've observed. Even though I missed the important heat transfer experiments Wednesday night, I am pleased the Red Sox not only won the game but saw to it that nobody became ill.

More seriously, after reading the papers and hearing your discussions of them, I think that the time has come for us to begin working on a new type of cooperative project. A number of years ago, Professor Emmons challenged us to develop the pieces for predicting fire hazard and safety. Reflecting on the comments of Professors Hottel and Emmons this week, it seems that we now are in a position to confront how to bring these pieces together. It's a problem bigger than either of us can solve separately, so I propose we go at it collectively. Dr. Tanaka has noted the success the Japanese have had in obtaining resources for cooperative efforts. I think the time has come for us to try to work the same game the other way, so you might expect us coming to you to ask for similar help in the near future.

I am pleased that the experiment of holding this meeting outside of Washington has been so successful, and warmly support Dr. Gann's comments concerning the hospitality of our New England friends. In sitting right here, one observes the youthful energetic appearance of the current Japanese delegation. Dr. Gann called it maturity; maybe there are other words that come to your mind when you observe the other side. Be that as it may, we shall continue to do our best effort to stay the course.

Now, and on behalf of the U.S. Panel, and our hosts at NFPA and Factory Mutual Research Corporation, we wish you all a safe journey back home.

TAKAHASHI: We have finally reached the end and I too would like to make a few words of comment. Many people have already stated this, but I would like to repeat and add my thanks to the very kind and helpful reception given to us by the NBS, and particularly by FMRC and NFPA. Judging from your warm reception, we were able to gather from the warmth of the feelings that were addressed to us from the American side. And one more word of appreciation. I would like to comment on the Tripartite Cooperation between Japan, the United States and Canada. We talked of success of these joint meetings but joint meetings cannot succeed unless there is a meeting of minds of very important and respected participants. Therefore, I hope that the 9th Meeting will lead to the 10th, 11th, and infinitum, and that as many participants as possible will continue for as long as possible. I also would like to express my thanks to the people who were backstage in this particular conference. We cannot disregard the tremendous part that was played by Ms. Madeline Anderson in making this conference both memorable and good in feeling.

This is not part of the agenda but I would like to present her with a memorial.

ANDERSON: Thank you very much.

TAKAHASHI: She is not here today but there is one other very important person in these meetings and that is Ms. Debbie Cramer. She was the one responsible for wading through the voluminous papers that was exchanged prior to the meetings. I would like to ask Dr. Snell to present this to her in my place.

SNELL: I would be honored to do so.

TAKAHASHI: I don't believe there was any more difficult situation and I'd also like to thank the interpreters.

We have now reached the end and I'd like to say that this will close the meeting. I hope to see you in June 1988 in Japan.



AUTHOR INDEX

A

Apostolakis, G., 146
Atreya, A., 24

B

Babrauskas, V., 100
Baier, L., 368
Baum, H., 50
Brandyberry, M., 146
Bukowski, R., 219

C

Carrier, G., 305
Curtis, R., 461

D

de Ris, J., 83

E

Emmons, H., 24
Evans, D., 325

G

Gann, R., 235, 490
Grand, A., 405
Gurman, J., 368

H

Hall, J., 131
Harmathy, T., 238
Hartzell, G., 405
Hasemi, Y., 4, 41
Henzel, V., 100
Hirano, T., 73, 397
Hirata, T., 417
Holt, T., 368
Hotta, H., 357

I

Ito, A., 496

J

Jin, T., 189, 294
Joh, T., 63

K

Kashiwagi, T., 496
Kawamoto, S., 417
Kim, A., 428

L

Levin, B.C., 368
Levin, B.M., 280

M

Mashige, J., 63
Morikawa, T., 443
Mulholland, G., 100

N

Nakamura, K., 113
Nakaya, I., 397
Nelson, H., 157
Nishihata, M., 41
Nishimaru, Y., 455
Nishina, T., 443

O

Ohlemiller, T.J., 13
Oka, Y., 357

P

Paabo, M., 368
Parker, W., 257

R

Rehm, R., 50

S

Saito, F., 336
Sakurai, T., 386
Satoh, K., 509
Sekizawa, A., 189
Sugawa, O., 63, 357
Suzuki, H., 232, 491
Switzer, W., 405

T

Takahashi, K., 203
Tanaka, T., 136, 172, 203, 240
Tewarson, A., 267
Tsuchiya, Y., 428, 461, 492
Tsuda, Y., 455
Tsujimoto, M., 139

Y

Yamada, T., 294
Yanai, E., 443
Yao, C., 314
Yoshida, M., 336
Yoshikawa, T., 63
Yusa, S., 470

Z

Zukoski, E., 8, 111

U.S. DEPT. OF COMM. BIBLIOGRAPHIC DATA SHEET (See instructions)		1. PUBLICATION OR REPORT NO. NBSIR 88-3753	2. Performing Organ. Report No.	3. Publication Date April 1988
4. TITLE AND SUBTITLE 9TH JOINT PANEL MEETING OF THE UJNR PANEL ON FIRE RESEARCH AND SAFETY PROCEEDINGS				
5. AUTHOR(S) Nora H. Jason and Barbara A. Houston, Editors				
6. PERFORMING ORGANIZATION (If joint or other than NBS, see instructions) NATIONAL BUREAU OF STANDARDS U.S. DEPARTMENT OF COMMERCE GAITHERSBURG, MD 20899			7. Contract/Grant No.	8. Type of Report & Period Covered
9. SPONSORING ORGANIZATION NAME AND COMPLETE ADDRESS (Street, City, State, ZIP)				
10. SUPPLEMENTARY NOTES <input type="checkbox"/> Document describes a computer program; SF-185, FIPS Software Summary, is attached.				
11. ABSTRACT (A 200-word or less factual summary of most significant information. If document includes a significant bibliography or literature survey, mention it here) The 9th Joint Panel Meeting of the United States-Japan Panel on Fire Research and Safety was held jointly with the Combustion Toxicity and 6th Expert Meeting of the U.S.-Japan-Canada Cooperative Research Group on Toxicity of Combustion Products from Building Materials and Interior Goods at the Factory Mutual Research Corporation, Norwood, MA. Technical sessions were in the areas of: Fire and Smoke Physics; Risk, Hazard and Evacuation; and Fire Toxicity and Evacuation. Progress reports were presented in each area, in addition to state-of-the-art papers. The next conference will be held in Japan in June 1988.				
12. KEY WORDS (Six to twelve entries; alphabetical order; capitalize only proper names; and separate key words by semicolons) building fires; evacuation; fire hazards; fire models; human behavior; risk analysis; smoke; smoldering combustion; sprinklers; toxicity; wood.				
13. AVAILABILITY <input checked="" type="checkbox"/> Unlimited <input type="checkbox"/> For Official Distribution. Do Not Release to NTIS <input type="checkbox"/> Order From Superintendent of Documents, U.S. Government Printing Office, Washington, D.C. 20402. <input checked="" type="checkbox"/> Order From National Technical Information Service (NTIS), Springfield, VA. 22161			14. NO. OF PRINTED PAGES 547	
			15. Price \$42.95	

